

**Some pages of this thesis may have been removed for copyright restrictions.**

If you have discovered material in Aston Research Explorer which is unlawful e.g. breaches copyright, (either yours or that of a third party) or any other law, including but not limited to those relating to patent, trademark, confidentiality, data protection, obscenity, defamation, libel, then please read our [Takedown policy](#) and contact the service immediately (openaccess@aston.ac.uk)

# **The effect of green tea extract compounds on regulation of glucose homeostasis in insulin-sensitive and breast cancer cells**

Sattar AL-Shaeli  
Doctor of Philosophy

Aston University  
March 2017

©Sattar AL-Shaeli, 2017

Sattar AL-Shaeli asserts his moral right to be identified as the author of  
this thesis

This copy of the thesis has been supplied on condition that anyone who consults it is understood to recognise that its copyright rests with its author and that no quotation from the thesis and no information derived from it may be published without proper acknowledgement.

**Aston University**

**The effect of green tea extract compounds on regulation of glucose homeostasis in insulin-sensitive and breast cancer cells**

Sattar AL-Shaeli

Doctor of Philosophy

March 2017

**Thesis summary**

Green tea and its active constituents possess numerous health promoting properties, including regulation of glucose homeostasis and anti-cancerous effects. However, the molecular mechanisms underpinning these properties are poorly understood. This study investigated the effects of green tea extracts on glucose metabolism in insulin-sensitive and breast cancer cells, and C57/BL mice. Glucose uptake in the presence and absence of protein kinase B (Akt) and adenosine 5'-monophosphate-activated protein kinase (AMPK) inhibitors, hepatic glycogenesis, triglyceride content, the rate of lipolysis, metabolic gene expression, and Akt and AMPK phosphorylations were assessed in mouse skeletal myotubes, adipocytes and hepatocytes. Epigallocatechin gallate (EGCG), epicatechin (EC), epicatechin gallate (ECG), quercetin, and combinations of these compounds selectively increased glucose uptake in these cell lines, and specific dose and time points of ECG and quercetin stimulated AML12 glycogenesis. EGCG, EC, and ECG suppressed adipocyte adipogenesis and lipolysis. These effects were mediated via AMPK in myotubes and Akt in adipocytes/hepatocytes cells. In mice fed a normal or glucose rich diet alongside decaffeinated green tea extract (DGTE), EGCG, and commercial green tea extract (GTE), markers related to glucose and lipid metabolism, body and tissues mass, and ingestion behaviour were assessed. DGTE and EGCG significantly reduced fasting glucose by 45.5% and 33.9% in a glucose fed mice. EGCG increased insulin level and accordingly increased measured of insulin resistance and beta cell function in normal fed mice, whilst, EGCG and GTE significantly increased insulin levels only in glucose-fed mice. Interestingly, selected extracts of green tea raised all adipose tissue masses. The significant increase in triglyceride contents were seen in mice fed a normal diet with DGTE and EGCG, and only EGCG with glucose diet. In breast cancer cells, cell viability, apoptosis, 2-NBDG uptake, lactate production, cellular migration, and phosphorylation of Akt and AMPK markers were explored. EGCG, experiment catechins, and quercetin significantly decreased cell viability, and induced apoptosis, whilst EGCG and quercetin showed reduced cell migration. EGCG and quercetin significantly decreased MCF7 and MDA-MB-231 glucose uptake associated with marked decrease in lactate production. To conclude, selected green tea compounds have significant potential anti-glycaemic, anti-diabetic, and anti-tumour properties, and exert their effects at least in part through Akt and AMPK signalling pathways.

**Keywords:** green tea, EGCG, breast cancer, insulin-sensitive cells, glucose metabolism.

**Dedication**

*To my beloved*

*Iraq*

*With Peace & Hope*

## **Acknowledgements**

In the name of Allah, most gracious, most merciful, the first who deserves all thanks and appreciation for granting me with the will, strength and help to complete this work.

As no such a work could be done without financial funding, therefore I would like to express my gratitude to Ministry of Higher Education and Scientific Research of Iraq, Iraqi Cultural Attaché London, and Wasit University for their funding and supporting role during this study.

Of course, I am deeply indebted and grateful to my supervisor Dr James Brown for affording me with such a wonderful opportunity to work with him and for his supervision as he is always providing me with valuable advice and critical observations during laboratory works and writing my thesis. Therefore, I will never forget his beautiful friendship, and I will be in touch with him forever.

I would like to express my special appreciations and thanks to Dr Adam Watkins who spend more than two months of works on mice research, and I appreciated for his great help during that time. Extended thanks to Aston Research Centre for Healthy Ageing Advanced Imaging Facility and particularly to Ms Charlotte Bland for her assistant and training me on the CellIQ imaging system and fluorescent microscopy. Also, I would like to express my appreciations and thanks to Life and Health Sciences Research office staff and senior international officer Yuliya Whitem for their essential role at some point.

I would like to thanks, all members of my family especially my wife and my brother Jasim AL-Shaeli for their continuous support. Extended thanks to my respected colleagues and treasured friends Dr Karan Rana, Dr Mohammad Arif, Mr Mahmood Jasim, Ms Ibteasam AL-Delfi, Mr Khaled Alghareeb, Mr Ali Hussein for their friendship and support. Moreover, also my thanks to all staff and students in the Labs MB334 and MB634C and offices MB645, MB436.

## List of contents

Thesis summary .....	2
Dedication .....	3
Acknowledgements .....	4
List of contents .....	5
List of tables .....	11
List of figures .....	12
Abbreviations .....	18
1 Introduction .....	23
1.1 Glucose homeostasis .....	24
1.1.1 The role of liver in glucose homeostasis .....	26
1.1.2 The role of skeletal muscle in glucose homeostasis .....	27
1.1.3 The role of adipose tissue in glucose homeostasis .....	27
1.2 Glucose metabolism .....	28
1.3 Signalling pathways involved in glucose metabolism .....	31
1.3.1 The PI3K/Akt molecular pathway .....	32
1.3.2 The AMPK signalling pathway .....	33
1.4 Diabetes mellitus .....	36
1.4.1 Type 2 diabetes mellitus .....	36
1.4.2 Aetiology of type 2 diabetes mellitus .....	36
1.4.2.1 Pancreatic beta-cell dysfunction .....	36
1.4.2.2 Insulin resistance .....	38
1.4.2.2.1 Obesity .....	38
1.4.2.2.1.1 Obesity and the role of genetics, diet, and lifestyle .....	40
1.4.2.2.2 Mitochondrial dysfunction .....	41
1.5 Cancer .....	42
1.6 Breast cancer .....	43
1.6.1 Classification of breast cancer .....	44
1.6.2 Metastasis .....	45
1.7 The association between obesity, T2D and breast cancer .....	47
1.7.1 Insulin/ insulin growth factors (IGFs) connection .....	48
1.8 Glucose metabolism in cancer cells .....	50
1.9 Tea .....	53
1.9.1 Green tea .....	54
1.9.1.1 Composition of green tea .....	54
1.9.1.2 Bioactivity of green tea .....	55

1.10	Aims and hypotheses .....	57
2	Materials and methods.....	58
2.1	Cell line studies .....	59
2.1.1	Cell culture .....	59
2.1.1.1	Mouse hepatocyte (AML12) cell line.....	59
2.1.1.2	Mouse myoblast (C2C12) cell line .....	59
2.1.1.2.1	C2C12 cell line differentiation .....	60
2.1.1.3	Mouse embryonic fibroblast (3T3-L1) cells.....	60
2.1.1.3.1	3T3-L1 cell differentiation .....	60
2.1.1.4	Breast adenocarcinoma (MCF7) cell line .....	61
2.1.1.5	Breast adenocarcinoma (MDA-MB-231) cell line .....	62
2.1.2	Green tea compound preparation.....	62
2.1.3	Cell line cryopreservation.....	62
2.1.4	Cell counting.....	62
2.1.5	Determination of glucose in culture media of insulin-sensitive cell lines .....	63
2.1.6	2-(N-(7-Nitrobenz-2-oxa-1,3-diazol-4-yl)Amino)-2-Deoxyglucose (2-NBDG) uptake .....	64
2.1.6.1	Insulin-sensitive cell 2-NBDG uptake.....	64
2.1.6.2	Breast cancer cell 2-NBDG uptake.....	64
2.1.7	Cell viability assays .....	65
2.1.7.1	PrestoBlue® cell viability assay .....	65
2.1.7.2	Neutral red cell viability assay .....	65
2.1.8	Analysis of glycogen content in AML12 cells .....	66
2.1.9	Estimation of free glycerol release from mature 3T3-L1 cells.....	66
2.1.10	Mature 3T3-L1 Triglyceride Oil red O staining .....	67
2.1.11	Estimation of cellular triglyceride content in mature 3T3-L1 cells.....	67
2.1.12	Cellular lactate assay .....	68
2.1.13	Caspase 3/7 apoptosis assay .....	68
2.1.14	Cellular migration assays.....	69
2.1.14.1	Wound scratch classic microscopic imaging assay .....	69
2.1.14.2	Wound scratch cell IQ® migratory assay.....	69
2.1.15	Total RNA extraction and reverse transcription.....	70
2.1.16	Real-time Polymerase Chain Reaction (qPCR) .....	70
2.1.17	Analysis of cell signalling .....	72
2.1.17.1	Protein isolation.....	72
2.1.17.2	Protein quantification .....	72
2.1.17.3	Sodium dodecyl sulphate-polyacrylamide gel electrophoresis (SDS-PAGE).....	73
2.1.17.4	Western blotting .....	73

2.2	Analysis of green tea consumption in mice .....	74
2.2.1	Animal care and housing .....	74
2.2.2	Experimental design and treatment .....	74
2.2.3	Blood sampling and tissue harvesting .....	75
2.2.4	Glucose tolerance test (GTT).....	75
2.2.5	Measurement of circulating insulin .....	77
2.2.6	Calculation of homoeostasis model assessment (HOMA) .....	77
2.2.7	Measurements of weight gain, food and water consumption .....	78
2.2.8	Circulating lipid profile .....	78
2.2.9	Total RNA extraction and reverse transcription .....	79
2.2.10	Real-time polymerase chain reaction (PCR) .....	79
2.3	Statistical analysis.....	79
3	The effect of active compounds of green tea extract on glucose and lipid metabolism in insulin-sensitive cell lines.....	80
3.1	Introduction .....	81
3.2	Materials and methods.....	82
3.3	Results .....	83
3.3.1	Selected compounds of green tea increased glucose uptake in C2C12 cells.....	85
3.3.2	Selected compounds of green tea increased glucose uptake in 3T3-L1 cells.....	85
3.3.3	Selected compounds of green tea increased glucose uptake in AML12 cells .....	85
3.3.4	The role of AMPK and Akt in enhanced glucose uptake in C2C12 cells by green tea compounds.....	91
3.3.5	The role of AMPK and Akt in enhanced glucose uptake in 3T3-L1 cells by green tea compounds.....	91
3.3.6	The role of AMPK and Akt in enhanced glucose uptake in AML12 cells by green tea compounds.....	92
3.3.7	Green tea compounds increased 2-NBDG uptake in C2C12 cells .....	103
3.3.8	Green tea compounds increased 2-NBDG uptake in 3T3-L1 cells.....	103
3.3.9	Green tea compounds increased 2-NBDG uptake in AML12 cells.....	104
3.3.10	Role of AMPK and Akt on green tea induced 2-NBDG uptake in C2C12 cells .....	106
3.3.11	Role of AMPK and Akt on green tea induced 2-NBDG uptake in 3T3-L1 cells .....	106
3.3.12	Role of AMPK and Akt on green tea induced 2-NBDG uptake in AML12 cells .....	106
3.3.13	The effect of green tea compounds on cell viability.....	110
3.3.14	Selected green tea compounds increased glycogen formation in AML12 cells .....	110
3.3.15	Lipid accumulation in differentiated 3T3-L1 cells .....	112
3.3.16	Selected green tea compounds decreased triglyceride contents in 3T3-L1 cells.....	113
3.3.17	Selected green tea compounds reduced lipolysis in 3T3-L1 cells .....	113

3.3.18	Effect of green tea compounds on the level of glucose and lipid metabolism gene expression.....	116
3.3.19	Effect of green tea compounds on AMPK phosphorylation in C2C12 cells.....	120
3.3.20	Effect of green tea compounds on phosphorylation of Akt in 3T3-L1 cells.....	120
3.3.21	Effect of green tea compounds on phosphorylation of Akt in AML12 cells.....	120
3.4	Discussion.....	124
4	The effect of green tea extract on glucose homoeostasis in high glucose fed mice.....	128
4.1	Introduction.....	129
4.2	Materials and methods.....	130
4.3	Results.....	131
4.3.1	Effect of green tea extracts and EGCG on total weight and weight gain.....	131
4.3.2	Effect of green tea extracts and EGCG on food and water intake.....	131
4.3.3	Effect of green tea extract on insulin-sensitive tissue mass.....	136
4.3.4	Effect of green tea extracts on glucose tolerance test (GTT).....	136
4.3.5	Selected green tea extracts reduced mice fasting blood glucose (FBG).....	145
4.3.6	Selected green tea extracts increased the levels of fasting insulin in serum.....	145
4.3.7	Homoeostasis model assessment (HOMA).....	145
4.3.8	Selected green tea extracts reduced circulating total cholesterol (TC).....	150
4.3.9	Selected green tea extract increased circulating triglyceride (TG) levels.....	150
4.3.10	Effect of green tea extract on the level of high-density lipoprotein (HDL).....	151
4.3.11	Selected green tea extracts decreased the level of calculated low-density lipoprotein (cLDL).....	151
4.3.12	Effect of green tea extract on glucose metabolism gene expression in liver.....	156
4.3.13	Effect of green tea extract on glucose metabolism gene expression in skeletal muscle.....	156
4.3.14	Effect of green tea extract on glucose and lipid metabolism gene expression in adipose tissue.....	156
4.4	Discussion.....	161
5	The effect of active compounds of green tea extracts on glucose metabolism in breast cancer cell lines.....	169
5.1	Introduction.....	170
5.2	Materials and methods.....	171
5.3	Results.....	172
5.3.1	Selected green tea compounds reduced MCF7 cell viability measured using PrestoBlue®.....	172
5.3.2	Selected green tea compounds reduced MDA-MB-231 cell viability measured using PrestoBlue®.....	172
5.3.3	Selected green tea compounds decreased MCF7 cell viability measured using neutral red.....	176

5.3.4	Selected green tea compounds decreased MDA-MB-231 cell viability measured using neutral red.....	176
5.3.5	Selected compounds of green tea does not alter BC cell viability after 6h .....	180
5.3.6	Akt inhibition further reduced MCF7 cell viability alongside green tea compounds.....	181
5.3.7	AMPK inhibition further reduced MCF7 cell viability alongside green tea compounds ...	181
5.3.8	Sodium pyruvate suppressed reduced MCF7 cell viability induced by green tea compounds.....	181
5.3.9	Akt inhibition further reduced MDA-MB-231 cell viability alongside green tea compounds.....	181
5.3.10	AMPK inhibition further reduced MDA-MB-231 cell viability alongside green tea compounds.....	182
5.3.11	Sodium pyruvate suppressed reduced MDA-MB-231 cell viability induced by green tea compounds.....	182
5.3.12	Impact of green tea compounds on phosphorylation of Akt and AMPK .....	182
5.3.13	Selected green tea compounds induced apoptosis in BC cell lines .....	188
5.3.14	Effect of selected compounds of green tea on BC cell apoptotic gene expression.....	188
5.3.15	Selected green tea compounds decreased BC cell lactate production after 24h .....	191
5.3.16	Sodium pyruvate suppressed green tea reduced BC cell lactate production after 24h .....	191
5.3.17	Selected compounds of green tea decreased BC cell lactate production after 6h.....	191
5.3.18	Sodium pyruvate does not alter green tea reduced BC lactate production after 6h.....	192
5.3.19	Selected compounds of green tea decreased 2-NBDG uptake in BC cells.....	192
5.3.20	Akt and AMPK inhibition unaltered green tea compounds-induced decrease BC cell 2-NBDG uptake .....	192
5.3.21	Selected compounds of green tea reduced MCF7 cellular migration .....	200
5.3.22	Selected compounds of green tea reduced MDA-MB-231 cellular migration .....	200
5.4	Discussion.....	207
6	Discussion, conclusion, and future studies.....	212
6.1	Discussion.....	213
6.2	Future studies.....	223
6.3	Conclusions .....	225
7	References .....	227
8	Appendices .....	248
8.1	Appendix 1; Amplification and disassociation curves of glucose and lipid metabolism gene expression in insulin-sensitive cell lines.....	249
8.1.1	Amplification and disassociation curves of glucose metabolism gene expression in C2C12 cells.....	249

8.1.2	Amplification and disassociation curves of glucose and lipid metabolism gene expression in 3T3L1 cells.....	252
8.1.3	Amplification and disassociation curves of glucose metabolism gene expression in AML12 cells.....	257
8.2	Appendix 2; Amplification and disassociation curves of glucose and lipid metabolism gene expression in mice insulin-sensitive tissues .....	262
8.2.1	Amplification and disassociation curves of glucose metabolism gene expression in mice liver.....	262
8.2.2	Amplification and disassociation curves of glucose metabolism gene expression in mice skeletal muscle.....	266
8.2.3	Amplification and disassociation curves of glucose and lipid metabolism gene expression in mice adipose tissue .....	269
8.3	Appendix 3; Amplification and disassociation curves of pro and anti-apoptotic gene expression in BC cells .....	273
8.3.1	Amplification and disassociation curves of pro and anti-apoptotic gene expression in MCF7 cell.....	273
8.3.2	Amplification and disassociation curves of pro and anti-apoptotic gene expression in MDA-MB-231 cell.....	276

## List of tables

Table 2.1 Primer sequences of metabolic and BC cell lines. ....	71
Table 3.1 Effect of green tea compounds on glucose metabolism mRNA expression in C2C12 cells. .....	116
Table 3.2 Effect of green tea compounds on glucose and lipid metabolism mRNA expression in 3T3-L1 cells. ....	117
Table 3.3 Effect of green tea compounds on glucose metabolism mRNA expression in AML12 cells. .....	118
Table 4.1 Effect of green tea extracts on glucose metabolism mRNA expression in the liver of mice fed normal or glucose-rich diet. ....	157
Table 4.2 Effect of green tea extracts on glucose metabolism mRNA expression in the skeletal muscle of mice fed normal or glucose-rich diet. ....	158
Table 4.3 Effect of green tea extracts on glucose metabolism mRNA expression in the adipose tissue of mice fed normal or glucose-rich diet. ....	159
Table 5.1 Effect of green tea compounds on some pro and anti-apoptotic mRNA expression in MCF7 cell. ....	190
Table 5.2 Effect of green tea compounds on some pro and anti-apoptotic mRNA expression in MDA- MB-231 cell. ....	190

## List of figures

Figure 1.1 The cell cycle.....	24
Figure 1.2 Glucose homoeostasis process.....	26
Figure 1.3 Skeletal muscle glucose uptake. ....	28
Figure 1.4 Steps involve in glycolysis. ....	30
Figure 1.5 Fates of pyruvate.....	31
Figure 1.6 Insulin signalling pathway (PI3K/Akt).....	33
Figure 1.7 AMPK signalling pathway. ....	35
Figure 1.8 Glucose stimulates insulin secretion.....	37
Figure 1.9 Insulin resistance. ....	40
Figure 1.10 Tumour development stages. ....	43
Figure 1.11 Cancer cells metastasis mechanism. ....	47
Figure 1.12 Association between obesity, T2D and initiation of cancer. ....	49
Figure 1.13 Factors involved in the alteration of cancer cells metabolism.....	53
Figure 1.14 Chemical structure of active constitues in green tea.....	56
Figure 2.1 3T3-L1 cell line differentiation medium. ....	61
Figure 2.2 Cells counted using haemocytometer. ....	63
Figure 2.3 Mice experimental design.....	76
Figure 3.1 Mouse myoblast (C2C12) cell line differentiation. ....	83
Figure 3.2 Mouse pre-adipocyte (3T3-L1) cell line differentiation. ....	84
Figure 3.3 Green tea compounds and glucose uptake in C2C12 cells. ....	86
Figure 3.4 Selected green tea compounds increase glucose uptake in C2C12 cells. ....	87
Figure 3.5 Selected green tea compounds increase glucose uptake in C2C12 cells. ....	87
Figure 3.6 Green tea compounds and glucose uptake in 3T3-L1 cells. ....	88
Figure 3.7 Selected green tea compounds increase glucose uptake in 3T3-L1 cells. ....	88
Figure 3.8 Selected green tea compounds increase glucose uptake in 3T3-L1 cells. ....	89
Figure 3.9 Selected green tea compounds increase glucose uptake in AML12 cells.....	89
Figure 3.10 Green tea compounds and glucose uptake in AML12 cells.....	90
Figure 3.11 Selected green tea compounds increase glucose uptake in AML12 cells.....	90
Figure 3.12 AMPK and Akt inhibitors reduce EGCG induced glucose uptake in C2C12 cells. ....	93
Figure 3.13 AMPK and Akt inhibitors reduce EC induced glucose uptake in C2C12 cells.....	94
Figure 3.14 AMPK and Akt inhibitors reduce ECG induced glucose uptake in C2C12 cells.....	95
Figure 3.15 Akt inhibitor reduces EGCG induced glucose uptake in 3T3-L1 cells.....	96
Figure 3.16 Akt inhibitor reduces EC induced glucose uptake in 3T3-L1 cells. ....	97
Figure 3.17 Akt inhibitor reduces ECG induced glucose uptake in 3T3-L1 cells. ....	98
Figure 3.18 Akt inhibitor reduces ECG induced glucose uptake in AML12 cells.....	99

Figure 3.19 Akt inhibitor reduces EC induced glucose uptake in AML12 cells.....	99
Figure 3.20 Akt inhibitor reduces ECG induced glucose uptake in AML12 cells.....	100
Figure 3.21 Akt inhibitor reduces green tea combination induced glucose uptake in AML12 cells. ..	101
Figure 3.22 Akt inhibitor reduces quercetin induced glucose uptake in AML12 cells.....	102
Figure 3.23 Akt inhibitor reduces quercetin induced glucose uptake in AML12 cells.....	103
Figure 3.24 Selected green tea compounds increase 2-NBDG uptake in C2C12 cells.....	104
Figure 3.25 Selected green tea compounds increase 2-NBDG uptake in 3T3-L1 cells.....	105
Figure 3.26 Selected green tea compounds increase 2-NBDG uptake in AML12 cells. ....	105
Figure 3.27 AMPK inhibition reduces green tea compounds induced C2C12 2-NBDG uptake. ....	107
Figure 3.28 Akt inhibition reduces green tea compounds induced 3T3L-1 2-NBDG uptake.....	108
Figure 3.29 Akt inhibition reduces green tea compounds induced AML12 2-NBDG uptake. ....	109
Figure 3.30 ECG increases glycogen content in AML12 cells. ....	111
Figure 3.31 Quercetin increases glycogen contents in AML12 cells.....	111
Figure 3.32 Oil red O triglyceride staining of 3T3-L1 cells during differentiation. ....	112
Figure 3.33 Selected green tea compounds decrease triglyceride level in 3T3-L1 cells. ....	114
Figure 3.34 Selected green tea compounds reduce glycerol release from 3T3-L1 cells.....	115
Figure 3.35 Effect of selected green tea compounds on pAMPK expression in C2C12 cells. ....	121
Figure 3.36 Effect of selected green tea compounds on pAkt expression in 3T3-L1 cells.....	122
Figure 3.37 Effect of selected green tea compounds on pAkt expression in AML12 cells. ....	123
Figure 4.1 GTE increases body weight at week one in mice fed normal or glucose-rich diet.....	132
Figure 4.2 Selected green tea extracts reduce weight gain in mice fed normal diet. ....	133
Figure 4.3 DGTE reduces diet intake in mice fed normal diet.....	134
Figure 4.4 DGTE reduces water intake in mice fed normal diet.....	135
Figure 4.5 EGCG increases liver mass in mice fed normal diet. ....	137
Figure 4.6 Green tea extracts do not alter skeletal muscle mass in all mice groups. ....	138
Figure 4.7 Selected green tea extracts increase SAT mass in mice fed normal or glucose-rich diet. ..	139
Figure 4.8 Selected green tea extracts increase VAT mass in mice fed normal or glucose-rich diet. .	140
Figure 4.9 Selected green tea extracts increase BAT mass in mice fed normal or glucose-rich diet...	141
Figure 4.10 Glucose levels during GTT in all mice received green tea extracts.....	142
Figure 4.11 Green tea extracts do not reduce gAUC in mice fed normal or glucose-rich diet. ....	143
Figure 4.12 Green tea extracts do not increase glucose clearance during GTT in all mice. ....	144
Figure 4.13 Selected green tea extracts decrease FBG levels in mice fed glucose-rich diet. ....	146
Figure 4.14 Selected green tea extracts increase insulin levels in mice fed normal or glucose-rich diet. ....	147
Figure 4.15 EGCG increases HOMA-IR value in mice fed normal diet. ....	148
Figure 4.16 EGCG increases HOMA-B value in mice fed normal diet.....	149
Figure 4.17 Green tea extracts do not alter HOMA-S in mice fed glucose-rich diet. ....	150

Figure 4.18 Selected green tea extracts decrease TC levels in mice fed normal or glucose-rich diet..	152
Figure 4.19 Selected green tea extracts increase TG levels in mice fed normal or glucose-rich diet. .	153
Figure 4.20 Green tea extracts do not alter HDL levels in mice fed normal or glucose-rich diet.....	154
Figure 4.21 Selected green tea extracts decrease cLDL levels in mice fed normal or glucose-rich diet. .....	155
Figure 5.1 Selected green tea compounds decrease MCF7 cell viability after 24h intervention. ....	173
Figure 5.2 Selected green tea compounds decrease MCF7 cell viability after 48h intervention. ....	173
Figure 5.3 Selected green tea compounds decrease MCF7 cell viability after 72h intervention. ....	174
Figure 5.4 Selected green tea compounds decrease MDA-MB-231 cell viability after 24h intervention. .....	174
Figure 5.5 Selected green tea compounds decrease MDA-MB-231 cell viability after 48h intervention. .....	175
Figure 5.6 Selected green tea compounds decrease MDA-MB-231 cell viability after 72h intervention. .....	175
Figure 5.7 Selected green tea compounds reduce MCF7 cell viability after 24h intervention. ....	177
Figure 5.8 Selected green tea compounds reduce MCF7 cell viability after 48h intervention. ....	177
Figure 5.9 Selected green tea compounds reduce MCF7 cell viability after 72h intervention. ....	178
Figure 5.10 Selected green tea compounds decrease MDA-MB-231 cell viability after 24h intervention. .....	178
Figure 5.11 Selected green tea compounds decrease MDA-MB-231 cell viability after 48h intervention. .....	179
Figure 5.12 Selected green tea compounds decrease MDA-MB-231 cell viability after 72h intervention. .....	179
Figure 5.13 Selected compounds of green tea do not alter BC cell viability after 6h intervention. ....	180
Figure 5.14 Akt inhibitor increases reduced MCF7 cell viability by green tea compounds. ....	183
Figure 5.15 AMPK inhibitor increases reduced MCF7 cell viability by green tea compounds. ....	183
Figure 5.16 Sodium pyruvate suppresses reduced MCF7 cell viability by green tea compounds.....	184
Figure 5.17 Akt inhibitor increases reduced MDA-MB-231 cell viability by green tea compounds. .	184
Figure 5.18 AMPK inhibitor increases reduced MDA-MB-231 cell viability by green tea. ....	185
Figure 5.19 Sodium Pyruvate suppresses reduced MDA-MB-231 cell viability by green tea. ....	185
Figure 5.20 Effect of selected green tea compounds on pAkt & pAMPK expression in MCF7 cell...	186
Figure 5.21 Effect of selected green tea compounds on pAkt & pAMPK expression in MDA-MB-231 cell.....	187
Figure 5.22 Selected green tea compounds induce apoptosis in BC cell. ....	189
Figure 5.23 Selected green tea compounds decrease BC cell lactate production after 24h intervention. .....	193

Figure 5.24 Sodium pyruvate suppresses green tea reduced BC cell lactate release after 24h intervention.	194
Figure 5.25 Selected green tea compounds reduce BC cell lactate production after 6h intervention.	195
Figure 5.26 Sodium pyruvate does not alter BC cell lactate release after 6h intervention.	196
Figure 5.27 Selected compounds of green tea reduce BC cell 2-NBDG uptake.	197
Figure 5.28 Akt and AMPK inhibitors do not alter green tea reduced BC 2-NBDG uptake after 4h intervention.	198
Figure 5.29 Akt and AMPK inhibitors do not alter green tea reduced BC 2-NBDG uptake after 8h intervention.	199
Figure 5.30 Effect of selected green tea compounds on MCF7 cell migration (microscope images).	201
Figure 5.31 Effect of selected green tea compounds on MCF7 cell migration (CellIQ®) images.	202
Figure 5.32 Selected compounds of green tea reduce MCF7 cell migration.	203
Figure 5.33 Effect of selected green tea compounds on MDA-MB-231 cell migration (microscope images).	204
Figure 5.34 Effect of selected green tea compounds on MDA-MB-231 cell migration (CellIQ®) images.	205
Figure 5.35 Selected compounds of green tea reduce MDA-MB-231 cell migration.	206
Figure 8.1 C2C12 SYBR® Green Rt. PCR analysis of actin gene expression.	249
Figure 8.2 C2C12 SYBR® Green Rt. PCR analysis of IR gene expression.	249
Figure 8.3 C2C12 SYBR® Green Rt. PCR analysis of HK1 gene expression.	250
Figure 8.4 C2C12 SYBR® Green Rt. PCR analysis of Glut4 gene expression.	250
Figure 8.5 C2C12 SYBR® Green Rt. PCR analysis of PDK4 gene expression.	251
Figure 8.6 C2C12 SYBR® Green Rt. PCR analysis of PGC1 $\alpha$ gene expression.	251
Figure 8.7 C2C12 SYBR® Green Rt. PCR analysis of Gys1 gene expression.	252
Figure 8.8 3T3-L1 SYBR® Green Rt. PCR analysis of actin gene expression.	252
Figure 8.9 3T3-L1 SYBR® Green Rt. PCR analysis of IR gene expression.	253
Figure 8.10 3T3-L1 SYBR® Green Rt. PCR analysis of HK1 gene expression.	253
Figure 8.11 3T3-L1 SYBR® Green Rt. PCR analysis of Glut4 gene expression.	254
Figure 8.12 3T3-L1 SYBR® Green Rt. PCR analysis of C/EBP $\alpha$ gene expression.	254
Figure 8.13 3T3-L1 SYBR® Green Rt. PCR analysis of LPL gene expression.	255
Figure 8.14 3T3-L1 SYBR® Green Rt. PCR analysis of FASN gene expression.	255
Figure 8.15 3T3-L1 SYBR® Green Rt. PCR analysis of FABP4 gene expression.	256
Figure 8.16 3T3-L1 SYBR® Green Rt. PCR analysis of SREBP1c gene expression.	256
Figure 8.17 3T3-L1 SYBR® Green Rt. PCR analysis of PPAR $\gamma$ gene expression.	257
Figure 8.18 AML12 SYBR® Green Rt. PCR analysis of actin gene expression.	257
Figure 8.19 AML12 SYBR® Green Rt. PCR analysis of IR gene expression.	258
Figure 8.20 AML12 SYBR® Green Rt. PCR analysis of HK1 gene expression.	258

Figure 8.21 AML12 SYBR® Green Rt. PCR analysis of Glut2 gene expression.....	259
Figure 8.22 AML12 SYBR® Green Rt. PCR analysis of Gys1 gene expression. ....	259
Figure 8.23 AML12 SYBR® Green Rt. PCR analysis of G6Pase gene expression. ....	260
Figure 8.24 AML12 SYBR® Green Rt. PCR analysis of PEPCCK gene expression. ....	260
Figure 8.25 AML12 SYBR® Green Rt. PCR analysis of CPT1 $\alpha$ gene expression. ....	261
Figure 8.26 AML12 SYBR® Green Rt. PCR analysis of ACSL gene expression. ....	261
Figure 8.27 Liver SYBR® Green Rt. PCR analysis of actin gene expression.....	262
Figure 8.28 Liver SYBR® Green Rt. PCR analysis of IR gene expression. ....	262
Figure 8.29 Liver SYBR® Green Rt. PCR analysis of Glut2 gene expression. ....	263
Figure 8.30 Liver SYBR® Green Rt. PCR analysis of Gys1 gene expression. ....	263
Figure 8.31 Liver SYBR® Green Rt. PCR analysis of G6Pase gene expression. ....	264
Figure 8.32 Liver SYBR® Green Rt. PCR analysis of PEPCCK gene expression. ....	264
Figure 8.33 Liver SYBR® Green Rt. PCR analysis of CPT1 $\alpha$ gene expression. ....	265
Figure 8.34 Liver SYBR® Green Rt. PCR analysis of FASN gene expression. ....	265
Figure 8.35 Skeletal muscle SYBR® Green Rt. PCR analysis of actin gene expression. ....	266
Figure 8.36 Skeletal muscle SYBR® Green Rt. PCR analysis of IR gene expression.....	266
Figure 8.37 Skeletal muscle SYBR® Green Rt. PCR analysis of Glut4 gene expression.....	267
Figure 8.38 Skeletal muscle SYBR® Green Rt. PCR analysis of Gys1 gene expression.....	267
Figure 8.39 Skeletal muscle SYBR® Green Rt. PCR analysis of PDK4 gene expression.....	268
Figure 8.40 Skeletal muscle SYBR® Green Rt. PCR analysis of PGC1 $\alpha$ gene expression.....	268
Figure 8.41 Adipose tissue SYBR® Green Rt. PCR analysis of Actin gene expression.....	269
Figure 8.42 Adipose tissue SYBR® Green Rt. PCR analysis of IR gene expression.....	269
Figure 8.43 Adipose tissue SYBR® Green Rt. PCR analysis of SREBP1c gene expression.....	270
Figure 8.44 Adipose tissue SYBR® Green Rt. PCR analysis of PPAR $\gamma$ gene expression.....	270
Figure 8.45 Adipose tissue SYBR® Green Rt. PCR analysis of FASN gene expression. ....	271
Figure 8.46 Adipose tissue SYBR® Green Rt. PCR analysis of Glut4 gene expression.....	271
Figure 8.47 Adipose tissue SYBR® Green Rt. PCR analysis of C/EBP $\alpha$ gene expression.....	272
Figure 8.48 Adipose tissue SYBR® Green Rt. PCR analysis of FABP4 gene expression.....	272
Figure 8.49 Adipose tissue SYBR® Green Rt. PCR analysis of LPL gene expression.....	273
Figure 8.50 MCF7 SYBR® Green Rt. PCR analysis of hYWHAZ gene expression. ....	273
Figure 8.51 MCF7 SYBR® Green Rt. PCR analysis of Bcl2 gene expression.....	274
Figure 8.52 MCF7 SYBR® Green Rt. PCR analysis of Bax gene expression.....	274
Figure 8.53 MCF7 SYBR® Green Rt. PCR analysis of Myc gene expression.....	275
Figure 8.54 MCF7 SYBR® Green Rt. PCR analysis of P53 gene expression. ....	275
Figure 8.55 MDA-MB-231 SYBR® Green Rt. PCR analysis of hYWHAZ gene expression.....	276
Figure 8.56 MDA-MB-231 SYBR® Green Rt. PCR analysis of Bcl2 gene expression.....	276
Figure 8.57 MDA-MB-231 SYBR® Green Rt. PCR analysis of Bax gene expression.....	277

Figure 8.58 MDA-MB-231 SYBR® Green Rt. PCR analysis of Myc gene expression. ....277  
Figure 8.59 MDA-MB-231 SYBR® Green Rt. PCR analysis of P53 gene expression. ....278

## Abbreviations

ACC	Acetyl-CoA carboxylase
ADH	Atypical ductal hyperplasia
ADP	Adenosine diphosphate
Akt	Protein kinase B
ALH	Atypical lobular hyperplasia
AMPK	5' adenosine monophosphate-activated protein kinase
ANOVA	Analysis of variance
aPKC	Atypical protein kinase C
AS160	Akt substrate 160
ASCL	Acyl-CoA Synthase (Long-Chain)
ATM	Ataxia-Telangiectasia Mutated
ATP	Adenosine triphosphate
BAT	Brown adipose tissue
Bax	Apoptosis regulator Bax
BC	Breast Cancer
BC12	B-cell lymphoma
BMI	Body mass index
BRCA1	Breast cancer one gene
BSA	Bovine serum albumin
BUB2	Mitotic checkpoint protein
C	Catechin
C/EBP $\alpha$	CCAAT-enhancer-binding protein alpha
CaMKKB	Calcium/calmodulin-dependent protein kinase kinase B
cDNA	Complementary DNA
CG	Catechin gallate
ChREBP	Carbohydrate response element binding protein
cLDL	Calculated low-density lipoprotein
COX2	Cyclooxygenase-2
CPT1	Carnitine-palmitoyl transferase1
CRTC2	Element (CRE)-binding protein regulated transcription coactivator2
DAG	Diacylglycerol
DCIS	Noninvasive ductal carcinoma in situ
DGTE	Decaffeinated green tea extract
DMEM	Dulbecco's modified Eagle medium
DMSO	Dimethyl sulphoxide

E1	Estrone
E2	Estradiol
E3	Estriol
EC	Epicatechin
ECG	Epicatechin gallate
ECL	Enhanced Chemiluminescence
EGC	Epigallocatechin
EGCG	Epigallocatechin gallate
EMT	Epithelial-to-mesenchymal transition
ER	Oestrogen receptor
FABP4	Fatty acid binding protein 4
FASN	Fatty acid synthase
FBG	Fasting blood glucose
FBS	Foetal bovine serum
FDH	Fumarate dehydrogenase
FFA	Free fatty acid
FOXO1	Forkhead box O1
G1	Gap phase 1
G6Pase	Glucose 6 phosphatase
gAUC	Glucose area under the curve
GC	Gallocatechin
GCG	Gallocatechin gallate
Gluts	Glucose transporters
GS	Glycogen synthase
GSIS	Glucose stimulate insulin secretion
GSK-3	Glycogen synthase kinase-3
GT	Green tea
GTC	Green tea catechins combination
GTE	Green tea extract
GTP	Green tea polyphenol
GTT	Glucose tolerance test
Gys1	Glycogen synthase 1
HBSS	Hank's balanced salt solution
HCl	Hydrochloric acid
HDL	High-density lipoprotein
HIF-1 $\alpha$	Hypoxia-inducible factor 1-alpha
HK	Hexokinase

HMG-CoA	3-hydroxy-3-methylglutaryl coenzyme A
HOMA	Homeostasis model assessment
HRP	Horseradish peroxidase
HSL	Hormone-sensitive lipase
IBMX	3-isobutyl-1-methylxanthine
IDH	Isocitrate dehydrogenase
IGF	Insulin growth factor
IGFBP	Insulin growth factor binding protein
I $\kappa$ B-kinase	I-kappa-B kinase
IL	Interleukin
IL-1R1	Interleukin1 receptor 1
IR	Insulin receptor
IRS-1	Insulin receptor substrate 1
ITS	Insulin Transferrin Selenium
JNK	Jun N-terminal kinase
LC-CoA	Long-chain fatty acetyl CoA
LCIS	Lobular carcinoma in situ
LDHA	Lactate dehydrogenase A
LG	L-Glutamine
LKB1	Liver kinase B1
LOX	Lysyl oxidase
LPL	Lipoprotein lipase
MCP-1	Monocyte chemoattractant protein
mRNA	Messenger ribonucleic acid
mtDNA	Mitochondrial DNA mutation
mTOR	Mammalian target of rapamycin
NADH	Nicotinamide adenine dinucleotide
NEFA	Nonesterified fatty acid
NR	Neutral red
P/S	Penicillin/Streptomycin
P53	Tumour Suppressor p53
PAGE	Polyacrylamide gel electrophoresis
PAI-1	Plasminogen activator inhibitor 1
PAS	Phospho-Akt Substrate
PBS	Phosphate-buffered saline
PDK	Pyruvate dehydrogenase kinase
PEPCK	Phosphoenolpyruvate carboxykinase

PGC1 $\alpha$	Peroxisome proliferator-activated receptor gamma coactivator1 $\alpha$
PI3K	Phosphoinositide 3-kinase
PKD	3-phosphoinositide dependent protein kinase
PPAR $\gamma$	Peroxisome proliferator-activated receptor gamma
PR	Progesterone Receptor
qPCR	Real-time polymerase chain reaction
RCF	Relative centrifugal force
RIPA	Radio-Immunoprecipitation Assay
RNA	Ribonucleic acid
ROS	Reactive oxygen species
SASP	Senescence-associated secretory phenotype
SAT	Subcutaneous adipose tissue
SCO2	Cytochrome C oxidase
SDH	Succinate dehydrogenase
SDS	Sodium dodecyl sulphate
SEM	Standard error mean
SHBG	Sex hormone binding globulin
SREBP1c	Sterol regulatory element binding protein 1c
T2D	Type 2 diabetes
TAK1	Transforming growth factor-B activated protein kinase 1
TBS	Tris-buffered saline
TBST	Tris Buffered Saline Tween 20
TC	Total cholesterol
TCA	Tricarboxylic acid cycle
TDLU	Terminal ductal lobular unit
TG	Triglyceride
TIGAR	TP53-inducible glycolysis and apoptosis regulator
TNF- $\alpha$	Tumour necrosis factor alpha
TP53	Tumour suppressor 53 Gene
Tre-2/USP6	Ubiquitin-specific protease 6
TSC2	Tuberous sclerosis 2
UK	United Kingdom
USA	United States of America
VAT	Visceral adipose tissue
VEGF	Vascular endothelial growth factor
VLDL	Very low-density lipoprotein
WAT	White adipose tissue

# **Chapter One**

## **Introduction**

## 1 Introduction

The understanding of the molecular and genetic basis of human biology has developed rapidly to improve our knowledge of many life-threatening diseases. The evolution of biomedical science has contributed to significant improvements in human life through more efficient diagnosis and treatment of the main human diseases. Despite this, there remain numerous fatal diseases which act to limit human lifespan and quality of life. The mechanisms of these diseases are as yet not well understood, and a fundamental understanding of them through continuous research is necessary.

The human body consists of some interconnected, complex physiological systems which work together to maintain homeostasis throughout life. Fundamentally, the human body develops from a single fused cell which undergoes proliferation, development, and differentiation to form many differentiated cells, tissues, and organs. The total number of cells in the human body is thought to be between  $10^{12}$  and  $10^{16}$ . However, the estimated number could be  $3.72 \times 10^{13}$  (Bianconi, *et al.*, 2013). All physiological processes are controlled by the protein coding genes of the human genome, the total number of which is still under debate. Estimations of the total number of genes are varied with ranges of 26,000 and 30,000 (Lander, *et al.*, 2001), 20,000-25,000 (Collins, *et al.*, 2004). It is likely, however, that 19,000 might be an accurate number of genes that exist in the human body (Ezkurdia, *et al.*, 2014).

Many eukaryotic cells undergo mitotic cell division in which a single cell produces two daughter cells holding the same genetic components as the progenitor. All cells are systematically organised through a cell cycle which consists of two gap phases (G1 and G2), a synthesis phase (S), and a mitotic phase (M) (Figure 1.1) (Krafts, 2010). Cells actively start their journey from a G1 phase in which the cells are growing and metabolically active, subsequently passing to S phase to completely replicate DNA. These cells then pass on to G2 phase to complete protein synthesis and prepare for mitosis, followed by mitotic division in the M phase, however, some cells become quiescent but still metabolically active when they moved from G1 to G0 (Kumar, *et al.*, 2010).

The cells, tissues, and organs in the human body exhibit homeostasis process which enable the maintenance of a constant internal environment. Cell, tissue, and organ homeostasis, therefore, contribute to the various systems that support homeostasis at the level of the whole body (Guyton and Hall, 2006). Clearly, disruption of the main cellular functions in the body due to illness or injury may affect tissue, organ, and whole body function and essentially leads to disorder and disease. Of vital importance to the present study is dysregulated glucose metabolism, which can contribute to many disorders including hyperglycaemia, hyperinsulinemia, insulin resistance, and increase the risk of type 2 diabetes (T2D) (Bano, 2013). Furthermore, disruption in the balance of cellular homeostasis between proliferation and apoptosis can cause either development of cancer due to the free rate of proliferation

or degeneration due to a counter state (Elmore, 2007). As the rapid growth of cancer cells requires high energy to maintain proliferation, survival and biosynthesis, this energy can be obtained from accelerating aerobic glucose metabolism (Vander Heiden, *et al.*, 2009). Therefore, targeting cancer cell glucose metabolism may provide possible therapeutic resolution.

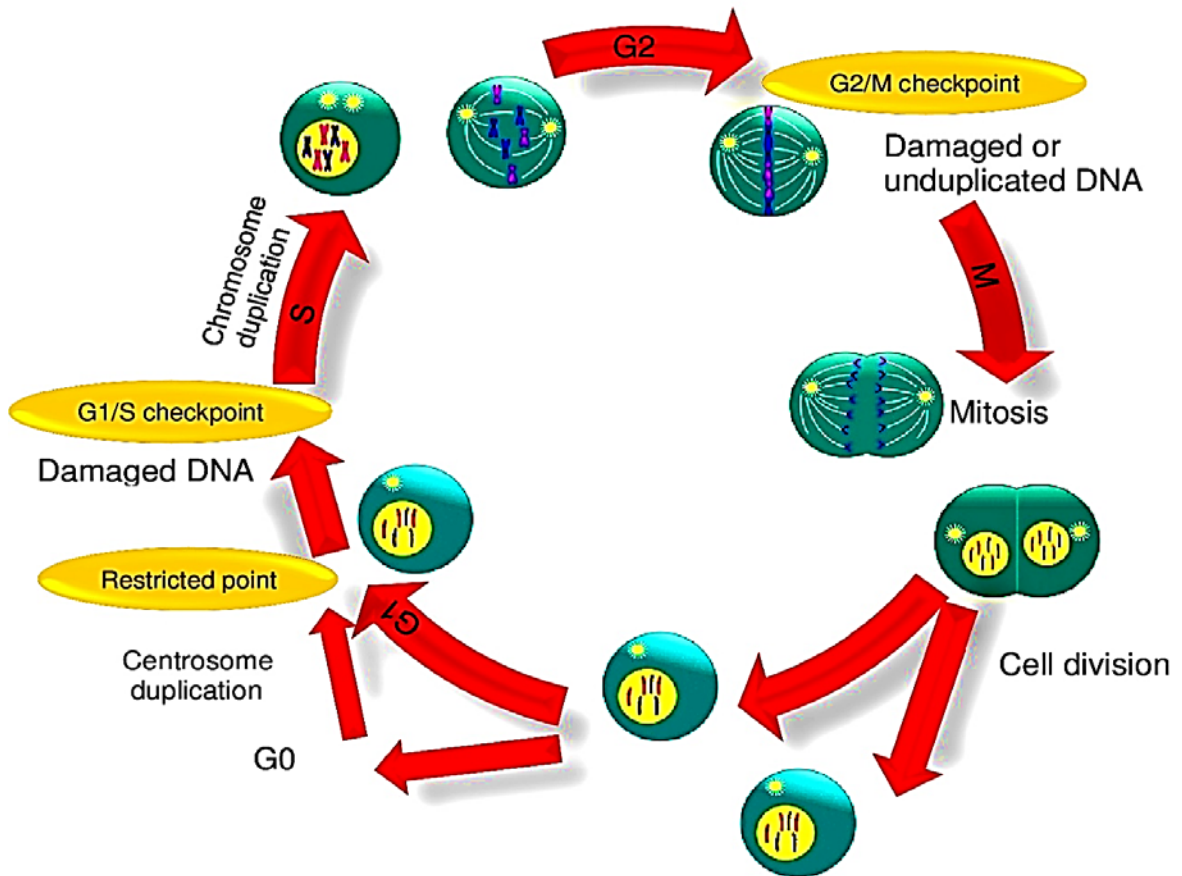


**Figure 1.1** The cell cycle.

### 1.1 Glucose homeostasis

Glucose is a common metabolic substrate and necessary form of energy which provides cells and organs with a substrate from which they can produce vital energy to perform their normal functions. Under normal physiological circumstances, cellular glucose is metabolised throughout the body to generate adenosine triphosphate (ATP), a coenzyme that acts as a key mediator of cellular energy in many cells including the brain and nervous system (Thorens and Mueckler, 2010). Almost all living cells continuously utilise glucose as a primary source of energy for performing their regular functions. The main sources of glucose in the body are from ingested food, as well as glucose released into the blood from stores of glycogen in the liver (referred to as glycogenolysis) and glucose converted from amino acids and lactate (gluconeogenesis) (Gong and Muzumdar, 2012). The levels of circulating glucose, therefore, depend on the amount of glucose entering and leaving the blood (Gerich, 2000).

After a meal or prolonged fasting the levels of glucose may either rise or fall and the body, therefore, needs to respond to maintain glucose at its physiological set point of 4 and 6 mmol/l (Saltiel and Kahn, 2001). The sharp decrease in blood glucose levels may lead to seizures, unconsciousness, and death while chronically high concentrations may result in blindness, vascular diseases, and renal damage (Szablewski, 2011). Thus, maintaining constant levels of blood glucose concentration is a fundamental process known as glucose homeostasis (DeFronzo, 1988).

Insulin and glucagon are the major hormones that control the levels of glucose in the circulation and therefore regulate glucose homeostasis. Insulin is an essential anabolic hormone which regulates energy and glucose metabolism (Pessin and Saltiel, 2000; Szablewski, 2011). It is synthesised and released directly into the bloodstream from pancreatic beta-cells in response to stimuli including increased glucose and amino acid concentrations in the blood after a meal. The major function of insulin is suppression of glucagon secretion and hepatic glucose production (Sesti, 2006). Furthermore, insulin can facilitate glucose uptake in skeletal muscle and adipose tissue via translocation of glucose transporters through activating insulin receptor (Bano, 2013). Glucagon is secreted from pancreatic alpha-cells in response to decreased blood glucose levels and can restore normoglycaemia by targeting glycogen in the liver and increasing glucose release by glycogenolysis (Mayo, *et al.*, 2003), and increasing gluconeogenesis (Landau, *et al.*, 1996). Therefore, glucagon counteracts the glucoregulatory function of insulin (Drucker, 2005). Thus, insulin and glucagon in addition to insulin-sensitive tissues are essential in maintaining normal glucose homeostasis (Figure 1.2).

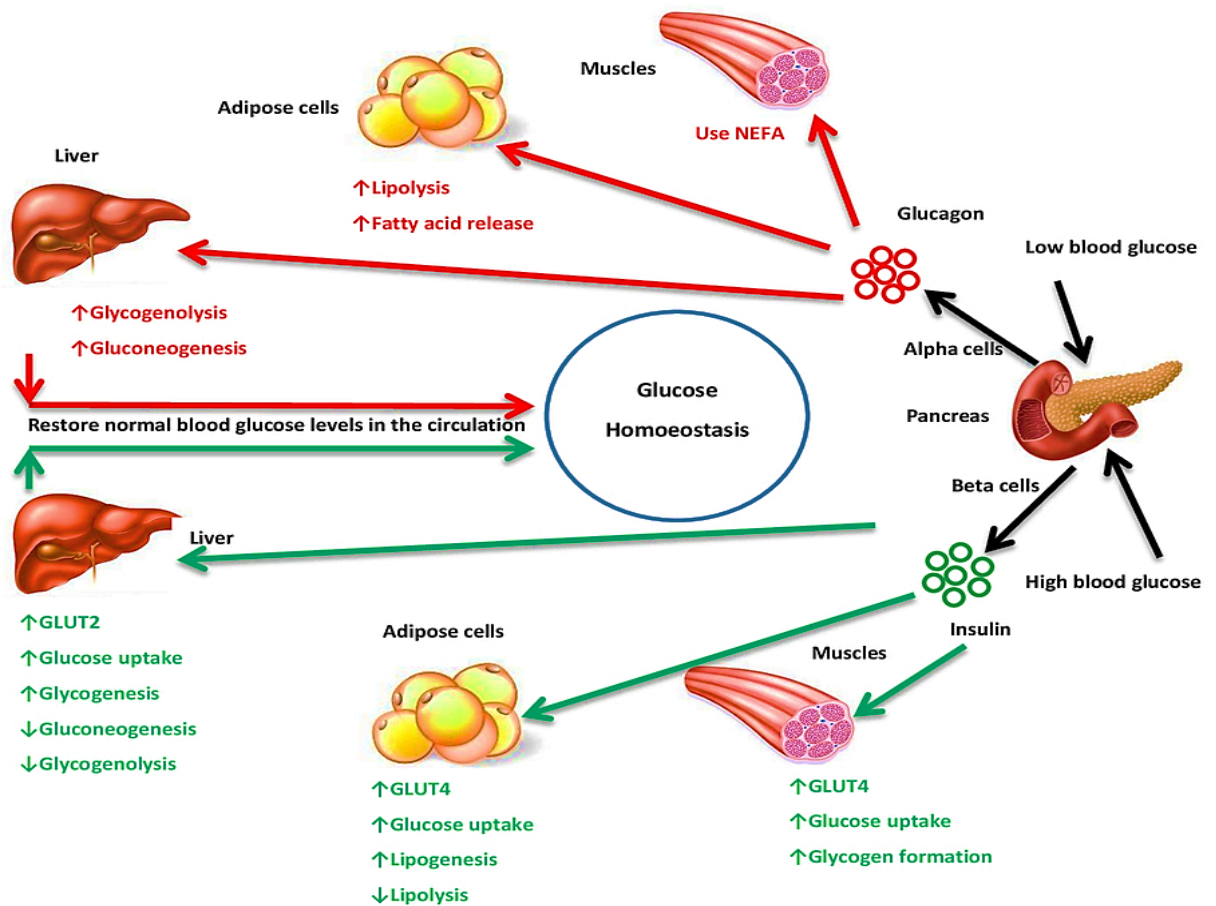


**Figure 1.2 Glucose homeostasis process.**

High blood glucose stimulates pancreatic beta-cells to secrete insulin which targets insulin-sensitive tissues including adipose, hepatic, and skeletal muscle to maintain normal glucose level through increasing glucose uptake, glycogenesis, lipogenesis, and suppression of lipolysis, glycolysis and hepatic glucose production. Whereas, low blood glucose stimulates pancreatic alpha-cells to secrete glucagon which acts to increase hepatic glucose production, lipolysis and glycolysis to restore normal blood glucose levels.

### 1.1.1 The role of liver in glucose homeostasis

The liver has a crucial role in maintaining blood glucose levels by providing a balance between glucose production and uptake. In the normal physiological state, after a meal, the level of blood glucose is increased, and accordingly insulin secretion is increased. In this circumstance, the liver acts to neutralise blood glucose levels through minor changes in glucose uptake and glycogen storage in hepatocytes (Figure 1.2) (Edgerton, *et al.*, 2009). Furthermore, the liver can convert glucose into lipids in the form of very low-density lipoprotein (VLDL) after glycogen deposits are full, and this lipid is transported to adipose tissue (Vidal-Alabró, *et al.*, 2012). In the prolonged fasting state, the level of blood glucose is low, and this stimulates glucagon release. The following acts directly on the liver to release glucose and compensate low level of glucose. This glucose is released firstly by breaking down the stored glycogen into glucose via glycogenolysis and secondly, through gluconeogenesis after

glycogen levels are depleted in an extended period of fasting (Edgerton, *et al.*, 2009). The liver is responsible for releasing 80% of glucose into the blood circulating in fasting condition (Cano, 2002). Therefore, insulin resistance and prevalence of T2D can impair hepatic glucose metabolism and increase hepatic glucose production.

### **1.1.2 The role of skeletal muscle in glucose homoeostasis**

Skeletal muscle is the major tissue for post-prandial glucose disposal in the body and as such plays a pivotal role in maintaining glucose metabolism. The normal function (contraction and relaxation) of skeletal muscle required energy which is continuously obtained; the principle sources of energy in skeletal muscle are glucose and lipids (Frayn, 2003). In the fed state, blood glucose and insulin levels are increased, and therefore insulin stimulates the skeletal muscle to increase glucose uptake through insulin receptor-mediated glucose transporter translocation (Figure 1.3) (Tremblay, *et al.*, 2003). Furthermore, glucose that is absorbed by muscle can be converted into glycogen and stores within the skeletal muscle tissue (Saltiel and Kahn, 2001). Whereas, in the fasted state, the levels of glucose and insulin are reduced, and therefore skeletal muscle uses non-esterified fatty acids (NEFA) as a source of energy.

### **1.1.3 The role of adipose tissue in glucose homoeostasis**

Adipose tissue is a connective tissue that plays a major role in the regulation of energy homoeostasis including glucose and lipid homoeostasis. Two main types of adipose tissue are distributed in the body; the most abundant is white adipose tissue (WAT), and the second is brown adipose tissue (BAT). WAT is comprised of 35-75% adipocytes with the remainder comprising cell types including pericytes, blood cells, endothelial cells and others (Cinti, 2009). Interestingly, WAT has dual functions. First, it assists in maintaining blood glucose by storing glucose and lipids within adipocytes as triglyceride in the fed state and releasing glycerol and lipids in the fasted state. Secondly, it secretes adipokines which are known to be heavily involved in glucose and lipid metabolism ((Bays, *et al.*, 2008;Gaidhu, *et al.*, 2011). In the fed state, insulin promotes glucose uptake and inhibits lipolysis in adipocytes, and increases NEFA uptake by activating lipoprotein lipase (Campbell, *et al.*, 1992).

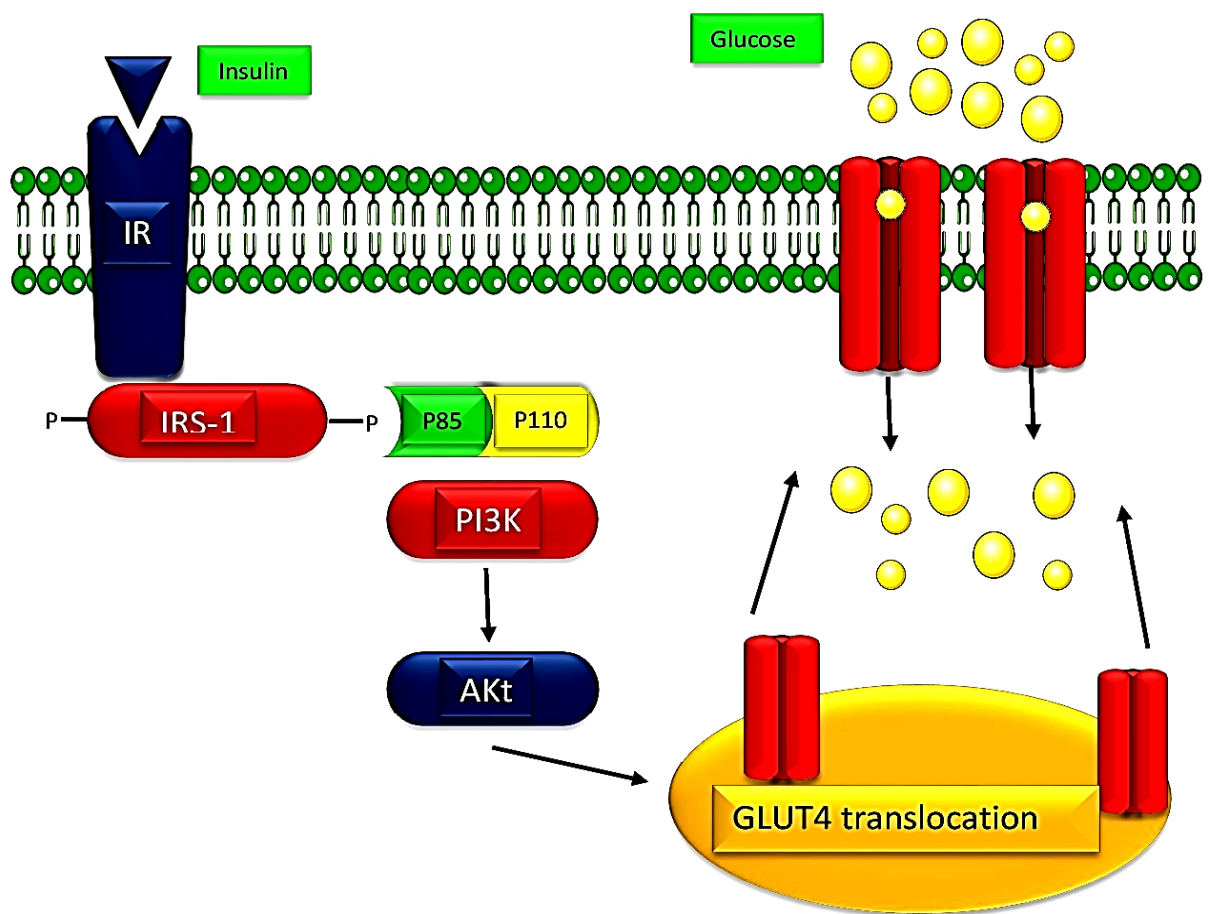


**Figure 1.3 Skeletal muscle glucose uptake.**

Insulin stimulates the skeletal muscle to increase glucose uptake based on insulin signalling that promotes activation of PI3K/Akt which eventually causes Glut4 translocation and expression leading to increased glucose uptake.

## 1.2 Glucose metabolism

Metabolism is a multi-chemical process that leads to production or consumption of energy during various physiological states. Glucose is a basic and important molecule which is considered the largest source of energy fuels to most organisms. The glucose is transported into the cells by facilitating diffusion through glucose transporters proteins (Gluts) that are expressed on cell surface membranes (Thorens and Mueckler, 2010). Based on physiological status, the entering glucose molecules undergo either anabolic processes to form glycogen and triglycerides by glycogenesis and lipogenesis respectively or catabolic processes to generate energy by glycolysis. Glycolysis is a series of chemical reactions of glucose molecule metabolism that liberates chemical energy. This process is composed of 10 enzymatic reactions classified into two stages (Figure 1.4). The energy investment phase is the first of five reactions, and the next five reactions are called the energy generation phase (Harvey and Ferrier, 2011).

In the first stage, glucose is phosphorylated by the enzyme hexokinase to form glucose-6-phosphate which is unable to be transported out of cells. Isomerization of this molecule by phosphoglucose isomerase leads to the formation of fructose-6-phosphate which undergoes phosphorylation to form fructose 1,6-bisphosphate by the action of the enzyme phosphofructokinase. Subsequently, aldolase acts to split 1,6-bisphosphate molecule into glyceraldehyde 3-phosphate and dihydroxyacetone phosphate; the latter is then isomerised by triosephosphate isomerase to form two molecules of glyceraldehyde 3-phosphate. This stage is accomplished by consuming two molecules of ATP rather than generating energy whereas the end products of the second stage are two molecules of pyruvate and four of ATP (Harvey and Ferrier, 2011). The second stage starts with oxidative-reduction of glyceraldehyde 3-phosphate by an enzyme called glyceraldehyde 3-phosphate dehydrogenase to form 1,3-bisphosphoglycerate which is catalysed by phosphoglycerate kinase to synthesis 3-phosphoglycerate. The phosphate group in the latter molecule is switched to the 2<sup>nd</sup> position by phosphoglycerate mutase to produce 2-phosphoglycerate which undergoes dehydration by enolase to form phosphoenolpyruvate that is subsequently catalysed to liberate pyruvate by the function of pyruvate kinase enzyme (Mckee and Mckee, 2013).

Fundamentally, the end product of glycolysis, pyruvate, could be used to generate more energy through the process of oxidative phosphorylation or be converted to lactate or ethanol by lactic acid and alcoholic fermentation (Figure 1.5). In anaerobic conditions, lactate dehydrogenase stimulates the process of pyruvate reduction by NADH to produce lactate or pyruvate decarboxylase converts pyruvate to acetaldehyde which is subsequently converted to ethanol by alcohol dehydrogenase without producing any additional ATP from both fates and this pathway is called anaerobic glycolysis (Gatenby and Gillies, 2004). In aerobic conditions, pyruvate dehydrogenase stimulates oxidative decarboxylation of pyruvate to form acetyl-Coenzyme A in mitochondria which subsequently enters the tricarboxylic acid (TCA) cycle. This process is called aerobic glycolysis (oxidative respiration), and the end products of this process are CO<sub>2</sub>, H<sub>2</sub>O, and 32 ATP molecules (Harvey and Ferrier, 2011).

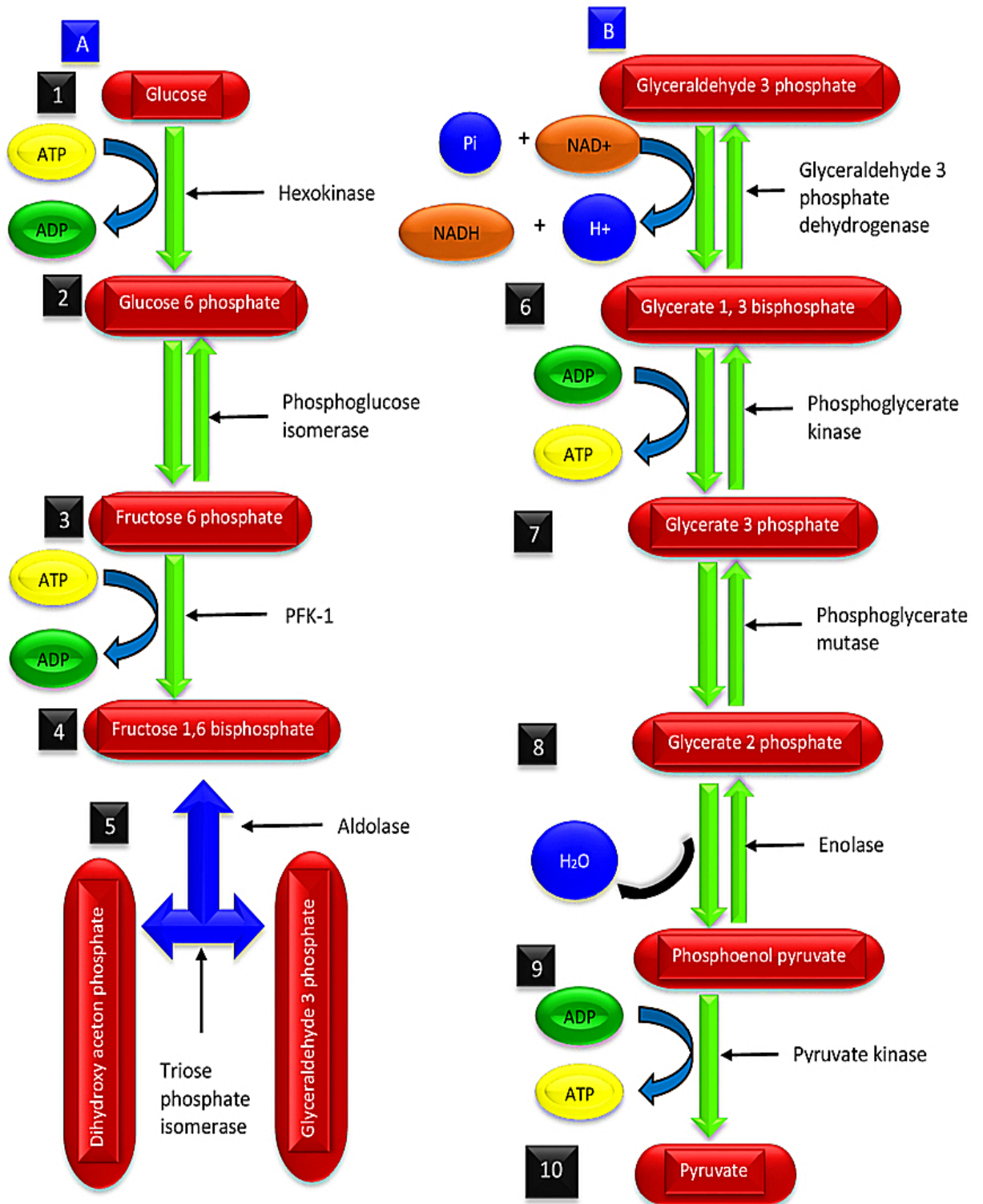


**Figure 1.4 Steps involve in glycolysis.**

The investment stage (A) starts with the first phase through oxidation of entering glucose by hexokinase and ends with the fifth step, the formation of glyceraldehyde-3-phosphate and dihydroxyacetone phosphate. This stage consumes two molecules of ATP and is promoted by the action of 5 enzymes. The energy generating stage (B) which starts with oxidative-reduction of glyceraldehyde 3-phosphate by the enzyme glyceraldehyde 3-phosphate dehydrogenase and produces two molecules of pyruvate and four molecules of ATP at the end. This stage is mediated by the action of 5 enzymes.

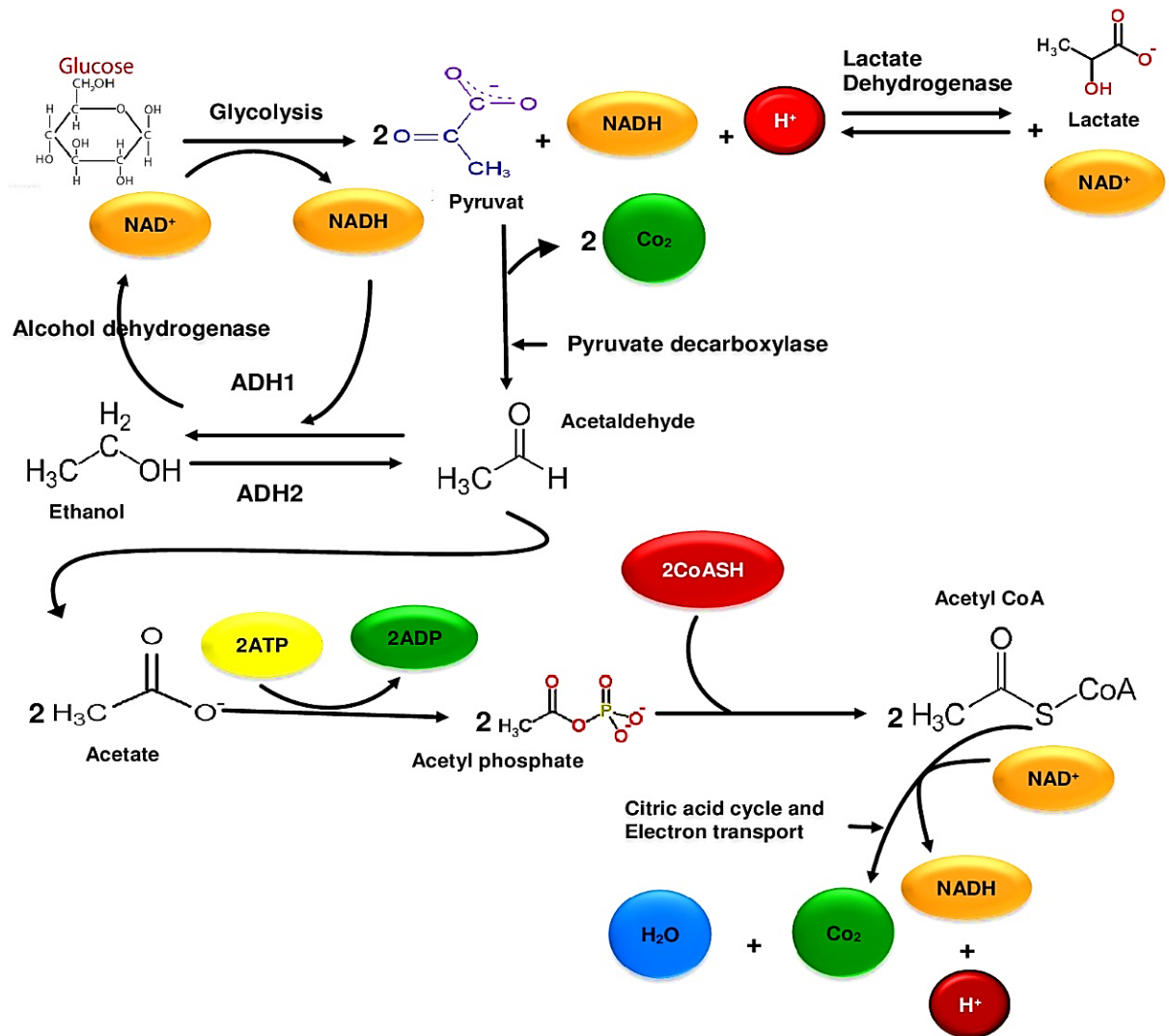


**Figure 1.5 Fates of pyruvate.**

Pyruvate can undergo anaerobic fermentation to form lactate by the action of lactate dehydrogenase, or ethanol-mediated by pyruvate decarboxylase and alcohol dehydrogenase enzymes. Whereas, in the presence of oxygen, pyruvate undergoes oxidative phosphorylation to acetyl CoA and the latter enters TCA and electron transport system to produce carbon dioxide, water, and ATPs.

### 1.3 Signalling pathways involved in glucose metabolism

Multiple signalling pathways are thought to participate in the regulation of glucose homeostasis. Insulin-dependent phosphoinositide 3-kinase/protein kinase B (PI3K/Akt) is one of the main pathways which plays a critical role in maintaining glucose metabolism. This role occurs by increasing glucose uptake, glycogen and triglyceride formation, and suppressing hepatic glucose production in response to insulin (DeFronzo and Tripathy, 2009; Lanner, *et al.*, 2006; Sesti, 2006). Adenosine 5'-monophosphate-activated protein kinase (AMPK) is another metabolic regulator which is believed to be a major insulin-independent signalling pathway that is responsible for maintaining glucose homeostasis (Carling, 2004; Kemp, *et al.*, 2003).

### 1.3.1 The PI3K/Akt molecular pathway

PI3K/Akt is a major and classical molecular pathway of metabolic actions of insulin (Figure 1.6) (Cho, *et al.*, 2001). PI3K class I is a member of three categories (I-III) of lipid kinase family based on lipid affinity substrate and structure domain (Engelman, *et al.*, 2006; Vanhaesebroeck, *et al.*, 2010). This class is well characterised and plays a vital role in insulin signalling to mediate glucose homeostasis (Rameh and Cantley, 1999). PI3K is heterodimer protein which is composed of the regulatory subunits P85, and P110 a catalytic subunit (Foster, *et al.*, 2003).

The activation of this signalling pathway depends on the ability of insulin to bind to its receptor. The binding occurs at the level of extracellular  $\alpha$ -subunit of the insulin receptor that is located on the surface of many cell types including hepatocytes, myocytes, and adipocytes (Khan and Pessin, 2002). Furthermore, tyrosine residue auto-phosphorylation at the level of intracellular  $\beta$ -subunit leads to phosphorylation of the insulin receptor substrate (IRS) (Sesti, *et al.*, 2001). Subsequently, IRS 1 and 2 binds with PI3K at the P85 regulatory subunit causing activation of the P110 catalytic subunit (Schultze, *et al.*, 2012). Once PI3K is activated, the phosphorylation of ptdlns (4,5) p2 on the cell surface membrane leads to the formation of ptdlns (3,4,5) p3, subsequently activating 3-phosphoinositide dependent protein kinase (PDK) which is responsible for activation of Akt and atypical protein kinase C (aPKC).

Akt is a Ser/Thr protein kinase which is responsible for regulating a wide variety of cellular functions, including regulation of glucose metabolism (Whiteman, 2002). Akt consists of an N-terminal PH domain, a C-terminal tail PH domain, and a kinase domain located between them. Three types of encoding Akt are expressed in mammalian tissues, Akt1/PKB $\alpha$ , Akt2/PKB $\beta$ , and Akt3/PKB $\gamma$  (Manning and Cantley, 2007; Schultze, *et al.*, 2011). Insulin sensitive tissues expressed Akt isoforms 1 and 2, whereas isoform 3 is only expressed in the brain, testes, pancreatic islets, and adipose tissue (Buzzi, *et al.*, 2010; Yang, *et al.*, 2003). Phosphorylation of PKB on Thr 308 and Ser 473 leads to activate Akt to enhance insulin action via translocation of glucose transporters to increase glucose uptake in insulin-sensitive cells (Leney and Tavaré, 2009). In addition to inactivation of glycogen synthase kinase-3 (GSK-3) and activation of glycogen synthase gene to promote glycogen synthesis, and fatty acid synthase gene to enhance lipogenesis (Lanner, *et al.*, 2006; Schultze, *et al.*, 2012). This pathway regulates suppression of hepatic glucose production through downregulating phosphoenolpyruvate carboxykinase (PEPCK) and glucose 6 phosphatase (G6Pase) transcriptional genes by inhibiting the activity of forkhead box O1 (FOXO1) factor (Figure 1.6) (O-Sullivan, *et al.*, 2015).

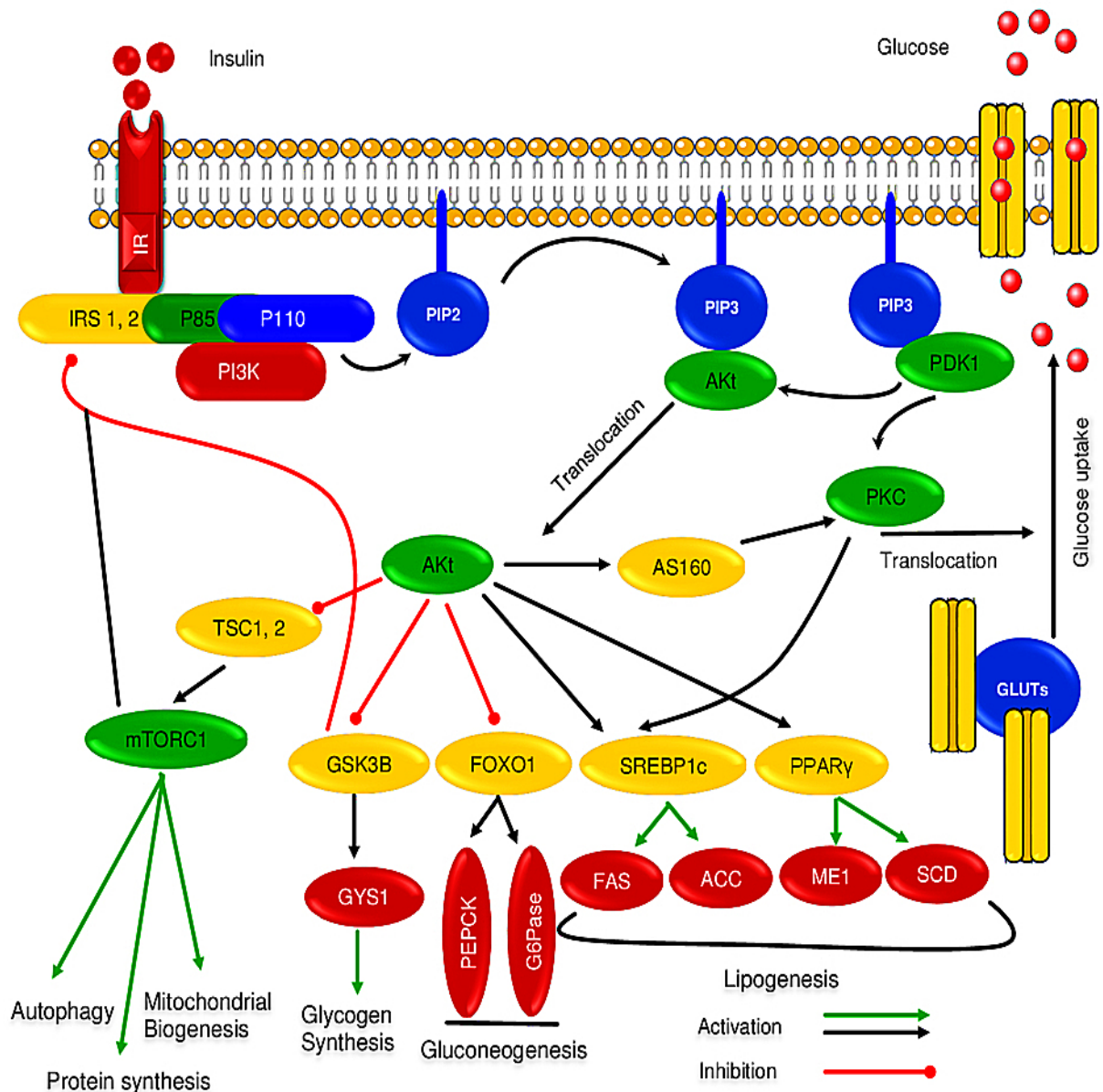


**Figure 1.6 Insulin signalling pathway (PI3K/Akt).**

The signalling pathway is initiated by binding insulin with the extracellular  $\alpha$ -subunit of its receptor which leads to activating PI3K and then Akt. This activation leads to increased glucose uptake through Gluts translocation, increased glycogenesis through phosphorylation of GSK-3, and increased lipogenesis through increased transcriptional genes of SREBP-c and PPAR $\gamma$ . Furthermore, the pathway suppresses hepatic glucose production by inhibiting FOXO1 which decreases the expression of PEPCK and G6Pase, and activation mTORC1 through inhibiting TSC1, 2.

### 1.3.2 The AMPK signalling pathway

AMPK is a major energy sensor which plays a central role in lipid and glucose metabolism to regulate the balance between energy generation and expenditure at both cellular and whole organism levels (Carling, 2004;Hardie, 2004;Kemp, *et al.*, 2003). AMPK is a serine/threonine kinase heterotrimeric protein composed of three encoding subunits. One catalytic  $\alpha$ -subunit which displays two isoforms  $\alpha 1$  and  $\alpha 2$  as well as two regulatory ( $\beta$  and  $\gamma$ ) subunits in two and three isoforms ( $\beta 1$ ,  $\beta 2$  and  $\gamma 1$ ,  $\gamma 2$ , and  $\gamma 3$ )

respectively. These isoforms are expressed in specific tissues and could form 12 heterotrimeric combinations (Mahlapuu, *et al.*, 2004). Isoform one from each of three subunits ( $\alpha$ 1,  $\beta$ 1, and  $\gamma$ 1) is expressed in most cells while the other isoforms are expressed specifically in skeletal muscles and myocardium (Carling, 2005; Wong and Lodish, 2006).

Activation of AMPK is controlled and mediated by three distinct upstream kinases. Stimulation of these kinases leads to the phosphorylation of a threonine residue (Thr-172) on the current T-loop of the  $\alpha$ -subunit (Birnbaum, 2005). An energy depleted state in response to an increase in AMP/ATP ratio causes activation of first upstream kinase tumour suppressor liver kinase B1 (LKB1) to induce AMPK activation through an AMP-dependent pathway (Kahn, *et al.*, 2005; Lizcano, *et al.*, 2004; Woods, *et al.*, 2003). Calcium/calmodulin-dependent protein kinase kinase B (CaMKKB) is another upstream regulator which is stimulated by increasing intracellular  $Ca^{+2}$  to mediate phosphorylation of Thr-172 and activation of AMPK (Birnbaum, 2005; Hawley, *et al.*, 2005; Woods, *et al.*, 2005). A third regulator is transforming growth factor-B activated protein kinase 1 (TAK1) which when upregulated leads to the activation of AMPK (Hawley, *et al.*, 2005) and increases cellular protection against apoptosis by TNF (Herrero-Martin, *et al.*, 2009). Once AMPK activation occurs, many cellular processes can be activated in various metabolic tissues to regulate glucose and lipid metabolism through stimulation of multiple downstream pathways (Figure 1.7).

In skeletal muscle, activation of AMPK through physiological or pharmacological signals enhances glucose uptake by increasing translocation of Glut4 (Mu, *et al.*, 2003; Wright, *et al.*, 2005). The proposed molecular mechanism of this action is phosphorylation of phospho-Akt substrate (PAS, AS160)/ (TBC1D1) tre-2/USP6, BUB2, cdc16 domain family member 1 (Frosig, *et al.*, 2010; Funai and Cartee, 2009). Also, AMPK increases fatty acid oxidation in muscles and liver through inhibition of Malonyl-CoA (fatty acid uptake inhibitor). This inhibition is mediated by phosphorylation and inactivation of acetyl-CoA carboxylase 2 (ACC2) (Malonyl-CoA creator) and regulation of carnitine-palmitoyl transferase1 (CPT1) (Dean, *et al.*, 2000; Zhou, *et al.*, 2001). Alternatively, direct inactivation of acetyl-CoA carboxylase 1 (ACC1) suppresses fatty acid synthesis (Saha and Ruderman, 2003). Furthermore, decreased cholesterol synthesis is also seen through inhibition of 3-hydroxy-3-methylglutaryl coenzyme A (HMG-CoA) which is main cholesterol synthesis regulator (Pallottini, *et al.*, 2004).

In the hepatocytes, activation of AMPK can directly phosphorylate and inhibit glycogen synthase 2 and 1 (GS) in the hepatocytes and myocytes respectively, causing decreased glycogen synthesis (Bultot, *et al.*, 2012; Jorgensen, *et al.*, 2004). However, there is a suggestion that AMPK activity could be inhibited by glycogen due to the binding site between them on the  $\beta$ -subunit (McBride, *et al.*, 2009). Moreover, activation of AMPK has been implicated in the regulation of gluconeogenesis by inhibiting hepatic glucose production through downregulation of PEPCK and G6Pase gene (Cool, *et al.*, 2006).

The molecular mechanisms that may be involved in the suppression of hepatic glucose output are inactivation of c-AMP response element (CRE)-binding protein regulated transcription coactivator2 (CRTC2) and FOXO1 (Liu, *et al.*, 2008b). Also decrease transcriptional activity of c-AMP response elements (CRE) by inhibiting GSK-3B (Horike, *et al.*, 2008).

In adipocytes, AMPK and its specific downstream pathways can regulate lipid metabolism. In addition to decreased fatty acid synthesis and increased oxidation, AMPK phosphorylation inactivates hormone sensitive lipase (HSL) and suppresses its translocation to lipid droplets as well as inhibiting its action on isoproterenol leading to inhibition of lipolysis (Daval, *et al.*, 2005). Furthermore, AMPK inhibits lipogenesis and triglyceride formation through decreasing the activity of glycerol acyl transferase (triglyceride synthesis) (Daval, *et al.*, 2006). Also inhibiting the expression of transcriptional lipogenesis factors including sterol regulatory element binding protein 1c (SREBP-1c) (Zhou, *et al.*, 2001), carbohydrate response element binding protein (ChREBP), and FOXO1 (Orci, *et al.*, 2004).

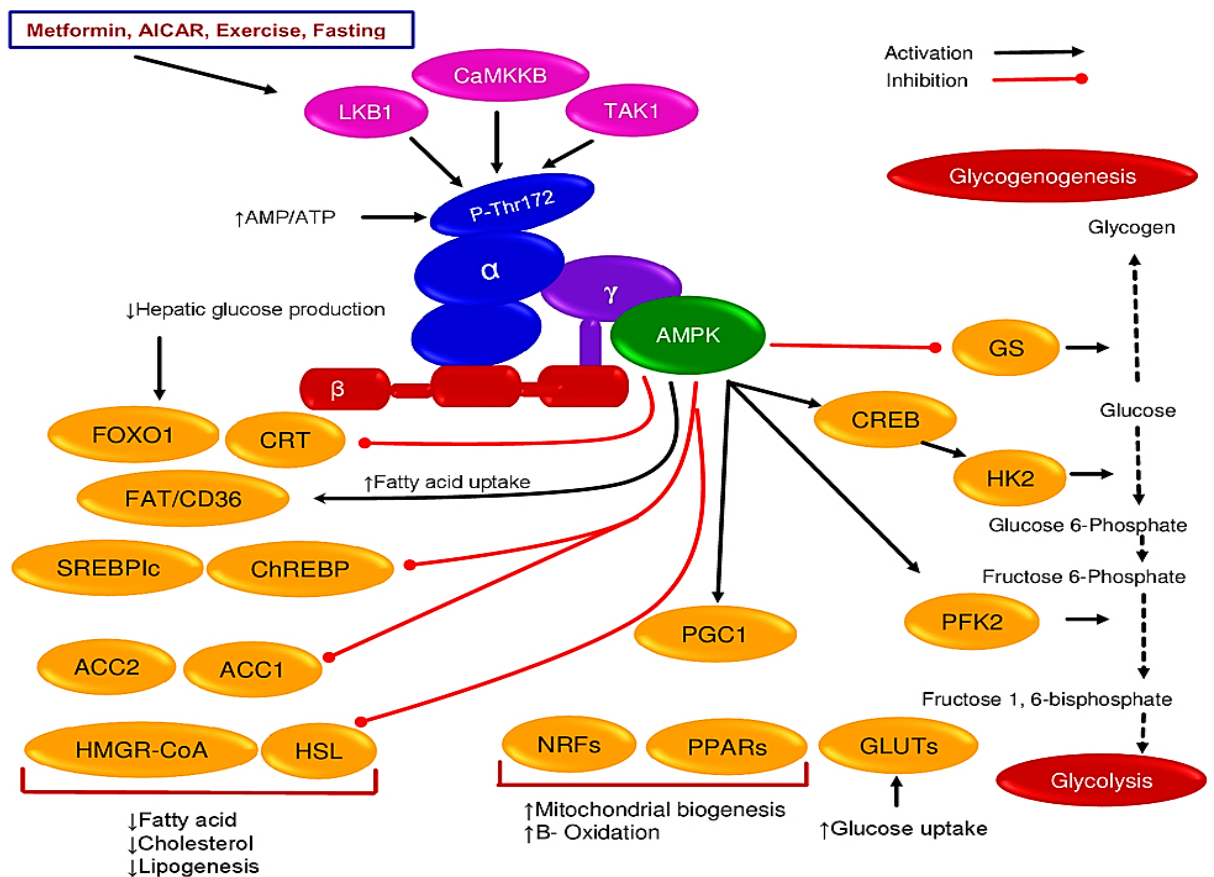


**Figure 1.7 AMPK signalling pathway.**

Phosphorylation of Thr 172 and activation of AMPK is mediated by three signals included LKB1, CaMKKB, and TAK-1 associated with increased AMP: ATP ratio. Once activation is promoted, AMPK acts to regulate glucose metabolism in hepatic, muscular, and adipose tissues. These are increased glucose and fatty acid uptake through increasing expression of Gluts, increase mitochondrial biogenesis, and inhibits fatty acid and cholesterol synthesis, increasing fatty acid oxidation and inhibiting lipogenesis, and decrease hepatic glucose production.

## **1.4 Diabetes mellitus**

Diabetes is a common metabolic disorder characterised by elevating blood glucose levels due to defects in carbohydrate metabolism associated with absent or insufficient insulin and decreased insulin sensitivity. According to IDF (2015), there are currently 415 million people who suffer from diabetes mellitus worldwide. Of these there 153.2 million in the Western Pacific, 78.3 million in South East Asia, 59.8 million in Europe, 44.3 million in North America and the Caribbean, 35.4 million in the Middle East and North Africa, 29.6 million in South and Central America, and finally 14.2 million in Africa. The incidence of this disease will likely increase, and the global incidence is expected to reach 642 million by 2040. Despite global efforts, the prevalence of diabetes is increasing due to some factors including obesity, poor diet, sedentary behaviour and also genetic predispositions (Muoio and Newgard, 2008). There are several classifications of diabetes mellitus including type 1, type 2, gestational diabetes and maturity onset diabetes of the young (MODY). Type 2 diabetes (T2D) is by far the most prevalent form of these categories and has historically been associated with increasing age and adiposity.

### **1.4.1 Type 2 diabetes mellitus**

T2D is the most common form of diabetes and occurs primarily due to a dual defect of insulin resistance and beta cell dysfunction. Despite hyperinsulinaemia due to the pancreatic beta-cells produced insulin, plasma glucose concentrations still rise due to decreased insulin sensitivity, and when the pancreas can no longer counteract this insulin resistance, a diagnosis of diabetes is usually made (Bano, 2013; Kahn, *et al.*, 2006). The prevalence of T2D is increased in older people, therefore; it is a major health problem (IDF, 2015).

### **1.4.2 Aetiology of type 2 diabetes mellitus**

Despite the global efforts to elucidate the causes and predisposing factors so that T2D may be better prevented and treated, the morbidity and mortality rates are still increasing (IDF, 2015). A complex combination of factors exists which enhances the risk of T2D, and these causes are either related to insufficient insulin secretion and/or insulin action.

#### **1.4.2.1 Pancreatic beta-cell dysfunction**

Recently, it has been suggested that the key aetiology involved in the onset of T2D is a failure of pancreatic beta-cells to produce sufficient insulin to overcome peripheral insulin resistance (Dunmore and Brown, 2013). The pancreas is a mixed gland which contains two main portions; an exocrine portion which forms the majority of the pancreas, while the smaller element is the endocrine portion which secretes hormones directly into the bloodstream (Persaud, *et al.*, 2012). Islets of Langerhans have exhibited at least five different endocrine cells including alpha, beta, delta, gama, and epsilon cells (Int

Veld and Marichal, 2010). The beta-cell secretes insulin as a result of elevated blood glucose levels through glucose-stimulated insulin secretion (GSIS), whereby glucose is transported into the beta-cell by Glut2 and oxidised by glucokinase to produce ATP. The ATP/ADP ratio is altered and induces ATP-sensitive K (KATP) channel closure at the cell membrane. The latter leads to depolarization of the plasma membrane which facilitates the influx of extracellular  $Ca^{+2}$  stimulating insulin exocytosis (Figure 1.8) (Gong and Muzumdar, 2012). Even in the face of constant high plasma glucose concentration, the beta-cell can rapidly act to compensate the demand of insulin to maintain glucose homoeostasis in the body. Therefore, prolonging the action of beta-cells can lead to an eventual loss of their sensation and function to produce insulin through impairment of GSIS, which finally leads to the development of diabetes (Hou, *et al.*, 2009;Ohtsubo, *et al.*, 2005).

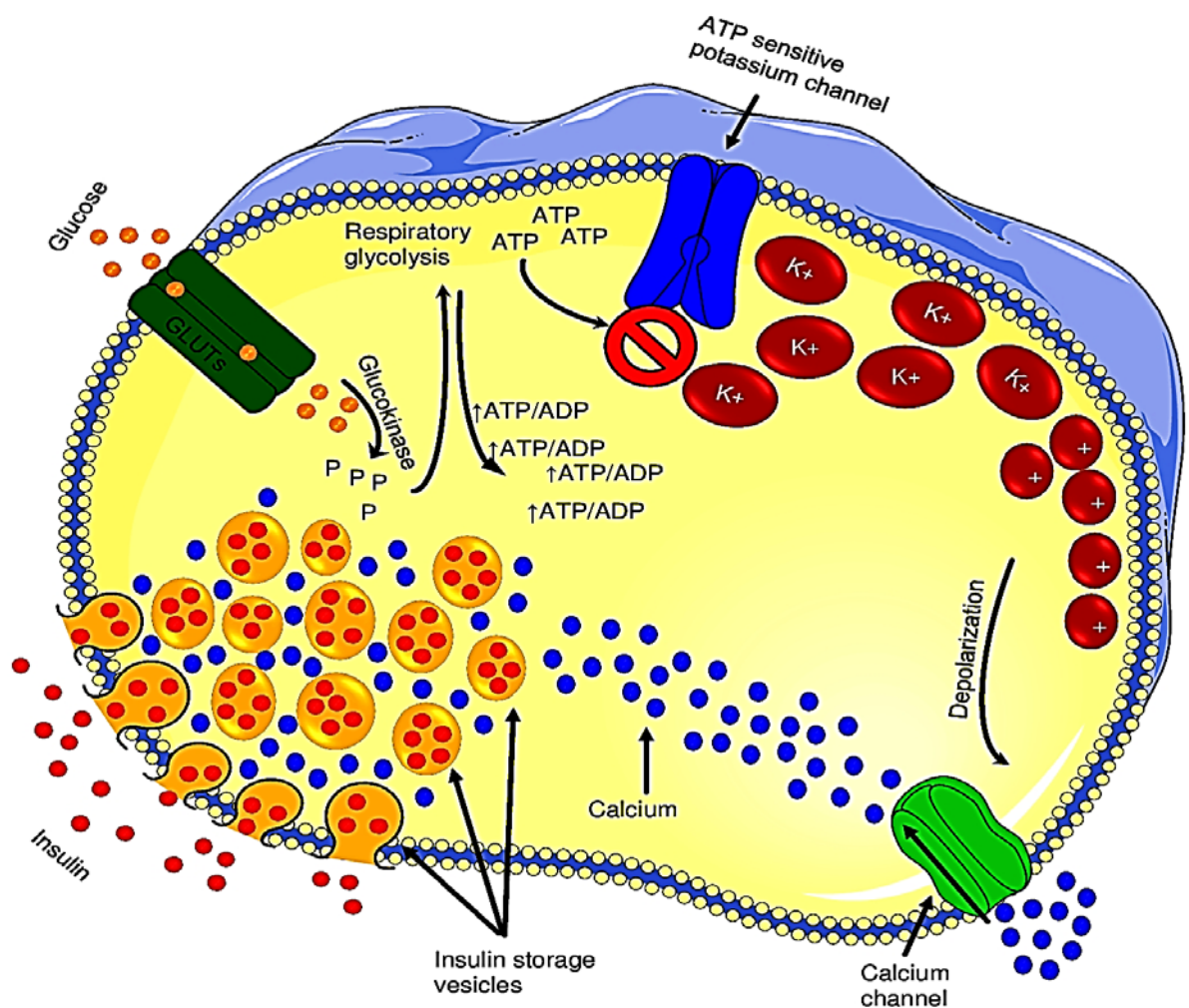


**Figure 1.8 Glucose stimulates insulin secretion.**

Diagram of insulin release from pancreatic beta-cells. Insulin is secreted in response to elevated glucose concentration. The process initiation by transporting glucose into beta-cell through Glut2 and oxidised by glucokinase to produce ATP. Increase ATP/ADP ratio and induced ATP-sensitive K (KATP) channel closure the cell surface. As a result of that, depolarization of plasma membrane is take placed which facilitate the extracellular  $Ca^{+2}$  influxes into beta-cell which subsequently triggers cytosolic insulin granules and release it by exocytosis.

### 1.4.2.2 Insulin resistance

Insulin resistance is an abnormal condition which leads to loss of sensitivity of metabolic cells (hepatocytes, adipocytes, and myocytes) to insulin while beta cells still produce insulin to neutralise the hyperglycaemia. It is often associated therefore with hyperinsulinaemia and increases the risk of developing T2D (IDF, 2006). Failure of insulin to activate the signalling pathways through binding with its receptor leads to the development of insulin resistance (Pessin and Saltiel, 2000). Furthermore, inhibition of tyrosine phosphorylation of IRS-1 concomitant with decreased activity of PI3K can cause impairment of insulin function in peripheral tissues and insulin resistance (Figure 1.9) (Petersen and Shulman, 2006). Over the past decade, the research in this field has developed rapidly and focused on mechanisms of insulin resistance to create a therapeutic agent targeting this mechanism to increase insulin sensitivity. However, progress has been slow (Savage, *et al.*, 2005).

#### 1.4.2.2.1 Obesity

Obesity is one of the major public health concerns worldwide due to implications and consequences accompanied it. Simply, it can be defined as an abnormal excessive accumulation of adipose tissue. More specifically, it is a term which describes an imbalance between energy consumption and expenditure (WHO, 1998). Those who are obese and/or overweight are assessed by using body mass index (BMI) which is individual body weight in kilograms divided by the square of the height in meters ( $\text{kg}/\text{m}^2$ ). The WHO (2003) has set the parameters of this phenotypic measurement with overweight individuals having a BMI greater than  $25\text{kg}/\text{m}^2$  BMI and obese individuals greater than  $30\text{kg}/\text{m}^2$  BMI. Other methods exist, including skinfold thickness and waist circumference (Bano, 2013). Globally, there are more than one billion overweight adults and approximately 300 million individuals described as being clinically obese (WHO, 2003), whereas the global overweight or obese children are estimated 42 million in 2013 and by 2025 could reach to 70 million between infants and young children (WHO, 2014a).

Obesity has been well studied and is known to play a fundamental role in the pathogenesis of insulin resistance and development of T2D (Figure 1.9) (Item and Konrad, 2012; Kahn, *et al.*, 2006). Adipose tissue has a significant endocrine function in addition to its distinct storage role, where secreted molecules including adipokines have been shown to be strongly linked to glucose homeostasis (Ginter and Simko, 2010). Dysfunction of adipose tissue in obesity and overweightedness can include abnormal accumulation of lipid as well as adipocyte hypertrophy (Castro, *et al.*, 2014). This adipose tissue tends to release a relatively high amount of non-esterified fatty acid (NEFA) due to increased lipolysis, in addition to adipokines and inflammatory cytokines (Abel, 2010; Makki, *et al.*, 2013). Circulating NEFA can target skeletal muscle tissue and promote insulin resistance through impairment of insulin-stimulated glucose uptake by increasing long-chain fatty acetyl-CoA (LC-CoA) accumulation and

formation of diacylglycerol (DAG) and ceramide. The latter caused activation of protein kinase C (PKC), I-kappa-B kinase (IKB-kinase-B), and Jun N-terminal kinase (JNK) and causes serine phosphorylation of IRS-1 (Morino, *et al.*, 2006). The phosphorylation reduces the ability of IRS-1 to activate PI3K and downstream pathways (Snel, *et al.*, 2012). Similarly, NEFA promotes insulin resistance in the liver and therefore prevents glucose uptake and glycogen synthesis (Snel, *et al.*, 2012).

Some of the adipokines that are released by adipose tissue are strongly linked to obesity, insulin resistance, and development of T2D. A wide array of adipokines, chemokines, and cytokines are released from adipose tissue, and their levels can change with progression towards obesity (Fain, 2010;Fain, 2012;Fantuzzi, 2005;Trayhurn, *et al.*, 2006). Dysfunction of adipose tissue can lead to dysregulated fatty acid metabolism due to excess energy, which in turn can cause alteration of adipokines secretion and development of inflammation (McArdle, *et al.*, 2013). Adipokines related to obesity and insulin resistance including pro-inflammatory interleukin-1 $\alpha$  and  $\beta$  (IL-1 $\alpha$ ,  $\beta$ ), inflammatory interleukin 6 (IL-6), tumour necrosis factor alpha (TNF $\alpha$ ), monocyte chemoattractant protein (MCP-1), plasminogen activator inhibitor 1 (PAI-1). In addition to leptin, resistin, and adiponectin (Fain, 2012;Rasouli and Kern, 2008). Increased circulating levels of IL-1 $\beta$  and IL-1receptor 1 (IL-1R1) are also associated with obesity and insulin resistance (Juge-Aubry, *et al.*, 2003). These cytokines can impair insulin signalling through serine phosphorylation of IRS-1 due to activation of many serine kinases like JNK and I $\kappa$ B kinase (IKK) (Gual, *et al.*, 2005). The impaired insulin signalling reduced the activation of PI3K and thereafter decreased the expression of Gluts and glucose uptake (Juge-Aubry, *et al.*, 2003;McArdle, *et al.*, 2013;Schenk, *et al.*, 2008).



The hypothalamus plays a central role in maintaining the balance between energy intake and expenditure in the body as it contains several nuclei which receive regulatory information through hormonal and neuronal signals (Xu, *et al.*, 2003). The arcuate nucleus plays a key role in the regulation of energy balance; it contains two sets of neurones. The first set is orexigenic and the second anorexigenic. Stimulation of orexigenic neurones leads to increased food intake and decreased energy expenditure, while activation of anorexigenic neurones induces energy expenditure and inhibits food intake (Barsh and Schwartz, 2002). Insulin is responsible for glucose and lipid homeostasis that has an anorexigenic impact (Air, *et al.*, 2002). In addition, a primary adiposity indicator leptin has a similar effect to insulin (Friedman and Halaas, 1998). Furthermore, ghrelin secreted as a result of an empty stomach acts to regulate energy balance by stimulating orexigenic set (Kohno, *et al.*, 2003). Moreover, the distal part of the gastrointestinal tract secretes peptide YY (PYY) which suppresses orexigenic neurones set (Calle, *et al.*, 2003).

The lifestyle factors that interact with the other factors are essential for progression of individual obesity. According to WHO (2003), the prevalence of obesity is increased due to high consumption of low nutrient food with high energy associated with a lack of physical activity. Obviously, sedentary behaviour, eating habits, and increased consumption of high-calorie food due to low price and availability is highly associated with the prevalence of obesity and weight gain (Kelly, *et al.*, 2008; Maffeis, 2000). There is a strong relationship between lifestyle with physical activity and weight gain (Swinburn, *et al.*, 2004). Recently, several studies have evidenced a strong link between energy intake and sedentary behaviour in the prevalence of obesity and weight gain (Papas, *et al.*, 2007). Gortmaker, *et al.* (1996) and Robinson (2001) identified the effects of watching TV on child obesity, and the results showed a strong relationship between watching television and the onset of obesity in children.

#### **1.4.2.2.2 Mitochondrial dysfunction**

Dysregulation of normal mitochondrial function has been associated with the development of insulin resistance and the increased onset of obesity and T2D. Mitochondria are a key cellular organelle that regulates cellular energy balance through facilitating the production of ATP from glucose and lipid metabolism (Turner and Heilbronn, 2008). Mitochondrial oxidative phosphorylation produces ATP which in turn is consumed by cells based on need. However, the process is considered efficient when high levels of ATP are produced (Mogensen and Sahlin, 2005). High energy demand stimulates mitochondrial biogenesis so that mitochondrial numbers can adapt to match this requirement (Alam and Rahman, 2014). Mitochondrial dysfunction is mediated by alteration of several markers including levels of protein, mRNA, and oxidation activity of mitochondrial enzymes (Heilbronn, *et al.*, 2007). Also alteration in the number, size, shape, content and oxidative phosphorylation activity (Montgomery and

Turner, 2015;Ritov, *et al.*, 2005). Mitochondrial function can be impaired with reduced biogenesis, oxidative protein content and activity, and fatty acid oxidation (Montgomery and Turner, 2015).

## 1.5 Cancer

Cancer is a common and potentially fatal disease which is considered as the second greatest cause of death globally after cardiovascular diseases. It is believed that the disruption of the balance of normal cellular proliferation/apoptosis is responsible for cancer initiation (Elmore, 2007). Globally there were 14.1 million new cases diagnosed and 8.2 million deaths in 2012 (WHO, 2014b). The prevalence of cancer is expected to increase by 2030 to up to 22.2 million new cases annually (Bray, *et al.*, 2012) and the mortality rate is also projected to increase from 8.2 million to 12.6 million cases (WHO, 2014b). The term 'cancer' was first used by Hippocrates, the great Greek physician in around 460-370BC, and the terms cancerous, and carcinoma has been used from that time to describe non-ulcer and ulcer-forming tumours (American Cancer Society, 2014). However, cancer has been discovered in ancient Egypt mummies when the evidence of bone cancer was displayed (Sudhakar, 2009). The first recorded case that described cancer is detected in ancient Egyptian manuscripts which back to 1600BC and called Edwin Smith papyrus which referred to an American Egyptologist Edwin Smith (ACS, 2014).

At the cellular level, cancer is a multi-step process initiated from one single cell or a small number of cells. These steps were proposed in 1947 as pre-carcinogenic, epi-carcinogenic, and meta-carcinogenic (Berenblum and Shubik, 1947). However, many studies have since been carried out to investigate these cancer development stages. The process of tumorigenesis is thought to consist of three major phases (Figure 1.10) which are an initiation, promotion, and progression (Cooper, 2000). In the first step, a normal cell is transformed into a neoplastic cell which is subsequently stimulated to enter the promotion phase via an increased rate of proliferation as well as increases in the size of the tumour followed by excess mutations to promote progression (Devi, 2004). Several categorizations are applied to recognise the type of cancer. Based on the cell type in which the tumour originated, three groups are identified, and these are carcinomas, sarcomas, and leukaemias or lymphomas which could be either benign or malignant according to their behaviour and response to treatment (Cooper, 2000). Furthermore, a widely used classification is based on the type of tissue in which cancer was developed for instance: breast, lung, pancreatic, liver, prostate, and more (Cooper, 2000).



**Figure 1.10 Tumour development stages.**

Three stages can be recognised in tumour development; these are an initiation, promotion, and progression. In these stages, single or cluster of cells acquired genetic mutation and altered their proliferation behaviour, the cells then increased their proliferation rate leading to excessive accumulation of genetic mutation. The cells then entered promotion stage followed by progression stage. This figure reproduced from(Hardin, *et al.*, 2012).

**1.6 Breast cancer**

Breast cancer (BC) is a term that describes heterogeneous tumours formed from breast tissue that is commonly diagnosed in females. Globally, BC is considered the leading cause of women cancer death and is the second leading cause of overall cancer death after lung cancer (Steward and Wild, 2014). According to IARC (2013), there were 1.7 million new cases of BC recorded in 2012 worldwide which represented 25% of all cases of female cancer diagnosis, the mortality rate was 14.7% of all female cancer death cases, with about 521,907 death cases being recorded. In the UK, the recorded new cases of female BC in 2011 were 50,285 with 11,643 death cases in 2012 (Cancer Research UK, 2012). In the USA, there were 232,670 new female diagnosed with BC which account 29% from all diagnosis types of cancer in woman whereas mortality rate was 15% about 40.000 death cases (Siegel, *et al.*, 2014). Therefore, BC in the UK and USA is considered the second most common cause of female death.

Cancer, including breast cancer (BC), is a multifactorial disease and several predisposing factors are thought to be involved in its initiation. These are genetics, lifestyle, related diseases, and other factors including ageing, ethnicity, menarche and menopause, the density of breast tissue, radiation, previous cancer or BC. Also birth control, hormonal replacement therapy, breastfeeding, in addition to controversial factors like bras, induced abortion, breast implants, and antiperspirants (American Cancer Society, 2014). In the UK, statistics have shown that modification of poor lifestyle including cessation of smoking, eating healthy food, decreased consumption of alcohol, reduced hormonal replacement therapy associated with increased breastfeeding. Also increased physical activity and reduction in body mass, decreased exposure to sunlight and radiation can be involved in prevention of 174,200 general cancer cases and 15,000 BC cases each year (Cancer Research UK, 2014).

### **1.6.1 Classification of breast cancer**

During puberty, lactation, and pregnancies the breast epithelial stem cells undergo rapid proliferation and morphogenesis to develop breast tissue (Visvader, 2009). These stem cells may be exposed to carcinogenic agents which can cause genetic mutation leading to uncontrolled proliferation to form atypical hyperplasia which then develops to in situ carcinoma and is followed by invasive carcinoma (Allred, *et al.*, 2001). Atypical hyperplasia is considered to be a pre-invasive lesion which contains some abnormal mutant cells without displaying invasive properties and which is known as atypical ductal hyperplasia (ADH) when located in the ductal portion or atypical lobular hyperplasia (ALH) when located in a lobular portion (Allred, *et al.*, 2001). Further proliferation of abnormal cells in ADH and ALH leads to the development of non-invasive ductal carcinoma in situ (DCIS) and lobular carcinoma in situ (LCIS). The risk of development invasive BC is increased in patients diagnosed with DCIS and LCIS (Li, *et al.*, 2006a).

To date, several classifications of BC have been used and developed to improve treatment and predicting clinical outcomes. The first classification is based on tumour size, lymph node and metastatic status in addition to histological type and grade (Elston and Ellis, 1991;Schnitt, 2010). BC can also be classified into biological and clinical subtypes (Taherian-Fard, *et al.*, 2015). In the late 1980s, a new classification landed which depends on an expression of molecular biomarkers including oestrogen receptor (ER), progesterone receptor (PR), and human epidermal growth factor receptor 2 (HER2) (Leong and Zhuang, 2011). Based on this BC can be categorised into eight subtypes including ER+/PR+/HER2+, ER+/PR+/HER2-, ER+/PR-/HER2+, ER+/PR-/HER2-, ER-/PR+/HER2-, ER-/PR-/HER2+, ER-/PR+/HER2+, and ER-/PR-/HER2- or triple-negative (Parise and Caggiano, 2014). Molecular gene expression profiles identified four major molecular subtypes including; luminal-like, basal-like, HER2+, and normal like (Perou, *et al.*, 2000), and then became five categories including luminal A, luminal B, HER2+, basal-like, and normal like (Sorlie, *et al.*, 2003). These subtypes were

correlated with biomarkers (ER, PR, HER2, Ki-67, and cytokeratin) to identify broad categories of BC (Joensuu, *et al.*, 2013;Parise and Caggiano, 2014). These are luminal A (ER+/PR+/HER2-/lowKi-67), luminal B (ER weaker+/PR+ or -/HER2+ or -/Ki-67+ high), HER2 enriched (ER-/PR-/HER2+), basal-like (ER-/PR-/HER2-/CK5/6+/EGFR+), and normal like (ER- or +/PR unknown/HER2-/CK5/6+/EGFR+) (Rosa, 2015;Weigelt, *et al.*, 2010).

### 1.6.2 Metastasis

Metastasis is a series of complex biological steps in which cancerous cells are transported from their origin site to a new secondary organ in the body. Due to heterogeneity, BC cells have the ability to develop metastatic behaviour and invade distant organs through the lymphatic and vascular systems (Weigelt, *et al.*, 2005). The major metastatic sites of BC are bone, liver, lung, brain, and distant nodal (Kennecke, *et al.*, 2010). In general, approximately 90% of all cancer mortality is related to metastatic behaviour (Spanoa, *et al.*, 2012), whereas metastasis is responsible for around 25%-50% of death in patients diagnosed with BC (Kozlowski, *et al.*, 2015). Furthermore, the poor survival outcomes of some BC subtypes like a triple negative (ER-/PR-/HER2-) are strongly associated with rapid tumour development and metastasis (Lorusso and Ruegg, 2012).

The increase in research into metastasis of tumourigenic cells has seen the development of several theories on the mechanisms underpinning metastasis. The relationship between metastasis and target tissue was first mentioned in “Das sarkomdes Uvealtradius” by the Austrian ophthalmologist Ernst Fuchs in 1882 (Piris and Mihm, 2007). This observation inspired English surgeon Stephen Paget, and after seven years he published a paper with the title ‘The distribution of secondary growths in cancer of the breast’ which held the first concept on cancer metastasis. This theory referred to ‘seed and soil’ which proposed that primary cancer cells with metastatic behaviour (seed) have the ability to spread to the other organs which provided an appropriate environment for these ‘seeds’ to grow (Paget, 1989). Since published, this theory was debated by other researchers for several years and was finally accepted as the main theory contributing to the field of cancer and which was subsequently supported by many studies later on.

There exist two different spatial-temporal models responsible for tumour cell dissemination to other organs and tissues (Klein, 2009;Pantel and Brakenhoff, 2004). The first states that metastasis is time dependent and that its development occurs with continuous time (Kozlowski, *et al.*, 2015). Due to the rapid accumulation of mutant genes, primary cancer cells progressively proliferate and expand during the time, and some of these cells acquire metastatic capability and escape from the primary lesion and invade distant organs (Fidler, 2003;Pantel and Brakenhoff, 2004). This type of metastasis is called the linear model of cancer (Kozlowski, *et al.*, 2015). The second model is known as the parallel model and

opposes the linear model and suggests that tumour cells, especially breast carcinomas, have the ability to spread from a pre-malignancy primary site to other organs in the early stages of progression (Klein, 2009).

Simply put, BC metastasis is a multi-step biological event that occurs as a result of excessive genomic modification leading to increased cellular proliferation and alteration of behaviour during tumour progression. These complex steps include angiogenesis, local migratory and systemic invasion, and specific organ cloning (Figure 1.11) (Kozlowski, *et al.*, 2015). All tumour cells including BC cells have the ability to create new blood vessels from pre-existing vasculature via angiogenesis through an angiogenic factor called hypoxia-inducible factor 1 (HIF-1) as a result of hypoxia which is a proper condition for survival and growth of tumour cells (Harris, 2002). This factor targets several key genes responsible for survival and induces organ-specific metastasis like vascular endothelial growth factor (VEGF) and chemokine receptor (CXCR4) (Kozlowski, *et al.*, 2015). Furthermore, increased expression of a collagen remodelling factor called lysyl oxidase (LOX) in BC has been involved in increase metastasis (Erler, *et al.*, 2006).

After the formation of new blood vessels, cancer cells migrate from the primary tumour in the form of single or grouped cells through disruption of cell-to-cell adhesion by attenuating the expression of E-Cadherin and increasing epithelial-to-mesenchymal transition (EMT) (Hennessy, *et al.*, 2009). These detached cells are motile and locally intravasate newly formed blood vessels through the actions of markers including TGF $\beta$ , notch and hedgehog, transcription regulators Twist and Snail (SNA, SNA11), MAP-Kinases, and Wnt which stimulate cells to undergo EMT (Tse and Kalluri, 2007). In the circulation, the cells adapt to their new environment and increase their survival through interacting with blood platelets and using them as a protective shield whilst in the circulation (Gupta and Massague, 2006). Once again, these migratory cells at some point in the circulation act to break down the vasculature wall and escape out by extravasation facilitated by L or P-selectins, expression of NAGPTL4 gene, and targeting tissue chemokines (Kozlowski, *et al.*, 2015). The cells in new tumour site either enter the dormancy state and lose their ability to colonise the target organ while remaining viable and invasive, or they adapt to the new environment and promote growth and survival (Gupta and Massague, 2006).



**Figure 1.11 Cancer cells metastasis mechanism.**

This figure illustrates the mechanism of cancer cell metastasis started from excess mutation of proliferating cells to invade distinct organs. This figure reproduced from (Gupta and Massague, 2006).

**1.7 The association between obesity, T2D and breast cancer**

Obesity, insulin resistance, and T2D are the major factors which have been confirmed to have a positive correlation with the incidence of most types of cancer including BC (Cohen and LeRoith, 2012; Ghose, *et al.*, 2015; Lipscombe, *et al.*, 2015). It is believed that individuals who are overweight or obese are more likely to develop cancer (Park, *et al.*, 2014). Furthermore, the mortality rate of cancer is increased by 52% and 62% in obese men and women with BMIs  $> 40\text{kg/m}^2$  which suggests a strong relationship between obesity and the prevalence of cancer (Calle, *et al.*, 2003). A recent meta-analysis of large cohort studies identified that increased BMI is associated with increased incidence of breast and other types of cancer (Reeves, *et al.*, 2007). Pre-menopausal BC has been found to have an inverse

relationship with obesity (Stephenson and Rose, 2003). This effect is thought to be due to relatively low concentrations of oestrogen in an obese pre-menopausal woman (Abrahamson, *et al.*, 2006). Despite obese pre-menopausal woman exhibiting a relatively reduced risk of BC, many observations have suggested that they express high levels of oestrogen receptors which can lead to malignancy (Daling, *et al.*, 2001).

Several meta-analyses including case-control and cohort studies have been conducted to determine the relative risk factors for BC in patients who were diagnosed with T2D. Indeed evidence appears to show that the prevalence of T2D increases the development of many types of cancer including liver, pancreatic, and endometrial cancers with about 200% relative risk. Whereas relative risks for colon, rectum, breast, and bladder cancers were 120% - 150% (Giovannucci, *et al.*, 2010). Furthermore, diabetic patients are more likely to develop cancer at any site with approximately 74% higher risk compared with non-diabetic patients (Tsilidis, *et al.*, 2015). Specifically, several studies confirmed that BC is increased in diabetic patients by 20%, 22%, and 23% higher risk compared to non-diabetic patients (Hardefeldt, *et al.*, 2012; Larsson, *et al.*, 2007; Liao, *et al.*, 2011). A cohort study showed that diabetes increases the risk of developing stages II, III, IV of BC by 14%, 21%, and 33% respectively compared to stage I (Lipscombe, *et al.*, 2015). Due to the different status of pre- and post-menopausal risk, a meta-analysis has shown that diabetes increases the risk of developing post-menopausal BC compared to non-diabetic, whereas no association with premenopausal BC was seen (Bowker, *et al.*, 2011; Boyle, *et al.*, 2012).

Molecularly and biologically, several mechanisms are thought to be involved in the association between obesity, insulin resistance, T2D and increased incidence of cancer, including BC. These mechanisms may include oestrogen bioavailability, insulin and insulin-like growth factors (IGFs), and chronic inflammatory cytokines alteration (Figure 1.12) (Joung, *et al.*, 2015).

### **1.7.1 Insulin/ insulin growth factors (IGFs) connection**

Increased circulation of endogenous insulin and IGFs have been identified to be involved in tumorigenesis processes in BC (Cohen and LeRoith, 2012). High levels of these peptides are related to different metabolic disorders including hyperinsulinemia, obesity, insulin resistance, and T2D. IGFs are insulin related peptides consisting of IGF-1 and IGF-2 isoforms which are secreted mainly by the liver in response to growth hormone (Lann and LeRoith, 2008). Most circulating IGFs are bounded to IGFbps which act to regulate IGF bioavailability (Laron, 2001). It has been reported that the metabolic syndrome is strongly associated with high levels of free IGF-1 due to inhibition of IGFbp production (van Kruijsdijk, *et al.*, 2009). Both insulin and IGF-1 receptors are heterotetrameric structures that exhibit high homology to each other (Lann and LeRoith, 2008). The function of both is mediated by binding to

their receptors leading to the activation of signalling pathways including PI3K/Akt/mTOR, Ras/MAPK and NF- $\kappa$ B nuclear translocation (Rose and Vona-Davis, 2012). Therefore, high circulating levels of insulin and IGF-1 target cellular homeostasis and can promote cellular proliferation concomitant with suppression of apoptosis which leads to increased prevalence of cancer.

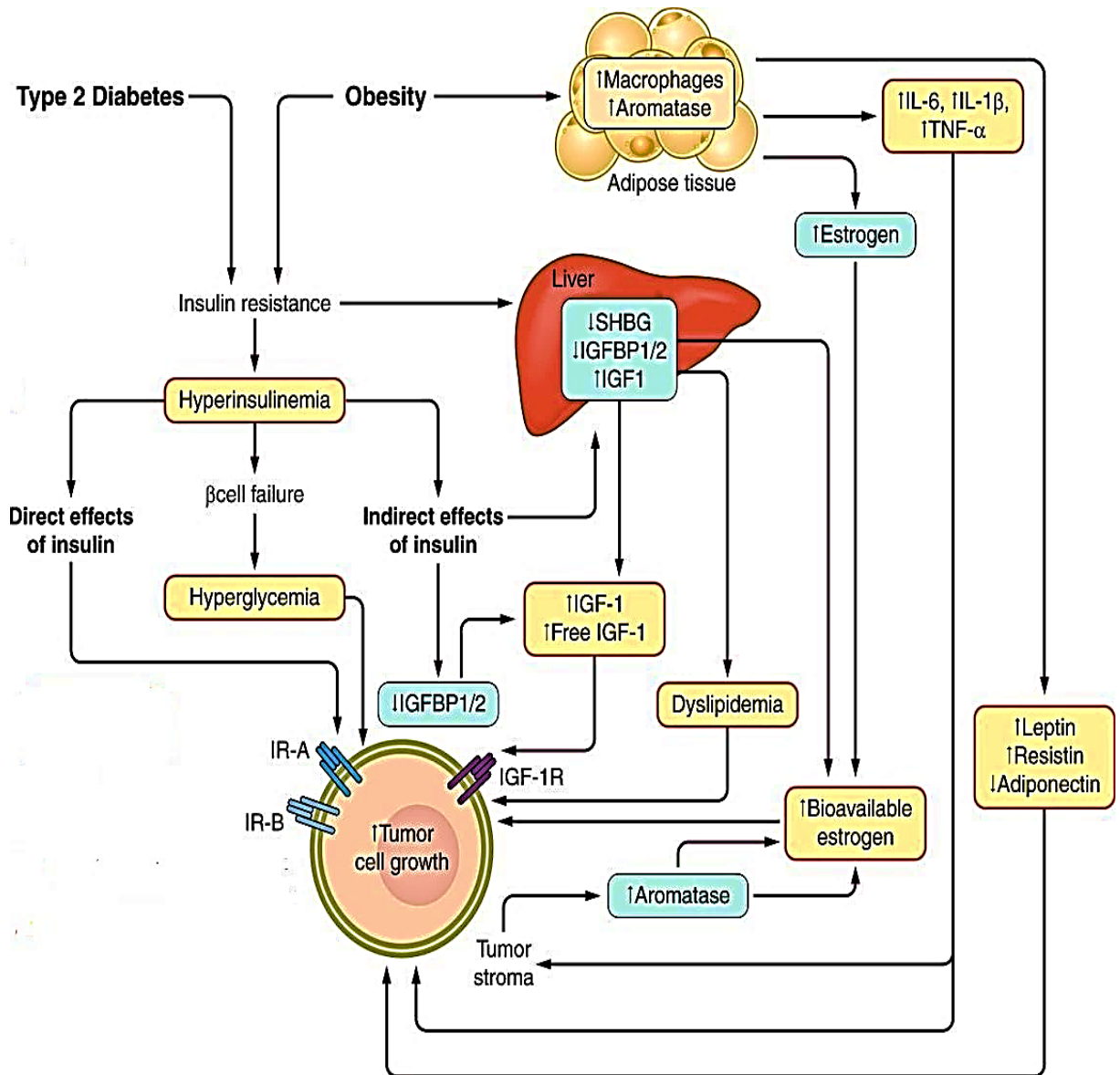


**Figure 1.12 Association between obesity, T2D and initiation of cancer.**

Three mechanisms may be involved in the development of cancer in obese and diabetic patients. These are insulin/IGFs, oestrogen/SHBG, chronic inflammation/cytokines, and adipokines connections. Obesity and diabetes cause insulin resistance which increases Insulin and IGF-1 availability and decreases GFBP1/2 and SHBG. In addition to increased inflammatory cytokines (TNF $\alpha$ , IL-6, IL-1 $\beta$ ), and dysregulated adipokines secretion (increased leptin, decreased adiponectin and resistin). Furthermore, increased bioavailability of oestrogen due to the high activity of the aromatase enzyme may also occur. All these factors together target cellular homeostasis and dysregulate the balance between cellular proliferation and apoptosis which leads to cancer initiation. Figure adapted from (Gallagher and LeRoith, 2015).

## 1.8 Glucose metabolism in cancer cells

The process of cellular metabolism consists of a vast number of chemical reactions regulated by a network of specific enzymes and detectors that can sense nutrients in the surrounding microenvironment to produce the chemical energy required for proliferation and survival. As mentioned earlier, the pyruvate produced from glycolysis undergoes oxidative decarboxylation in the presence of oxygen to form acetyl coenzyme A (acetyl-CoA) which enters the TCA cycle and is completely oxidised by the respiratory chain to generate 36 ATP molecules (Seo, *et al.*, 2014). The other fate of pyruvate is to be converted to lactate through a fermentation process by the activity of lactate dehydrogenase during anaerobic conditions without generating any additional ATP molecules (Lunt and Vander Heiden, 2011). Glucose can be metabolised to produce a high quantity of lactate even in the presence of oxygen, and this process is referred to as 'aerobic glycolysis' or the 'Warburg effect' (Lunt and Vander Heiden, 2011; Vander Heiden, *et al.*, 2009). Due to the inefficiency of this process to generate ATP, the process of aerobic glycolysis occurs rapidly to produce more energy to meet the cellular demand for proliferation (Ganapathy-Kanniappan and Geschwind, 2013). This rapid proliferation rate under hypoxic and less vascularised conditions which is associated with massive consumption of glucose as a source of energy are recognised in cancer cells. The accelerated metabolism via the aerobic glycolysis pathway provides energy for survival, proliferation, and biosynthesis (Li, *et al.*, 2011a). This metabolism is a fundamental discovery presented in the 1920s by German physiologist and medical doctor Otto Heinrich Warburg, awarded medical Nobel Prize in 1931 for this discovery and later on supported works. The second process provides glucose as a source of energy consumed by cancer cells for proliferation and survival is Cori cycle (Goodwin, *et al.*, 2014). This gluconeogenesis process is provided energy required by cancer cells through converting lactate to glucose in the liver (Tisdale, 2009). The hypothesis behind the alteration of metabolism of the cancer cells from oxidative phosphorylation (more efficient) to aerobic glycolysis (less efficient) is disruption of cancer cells mitochondria which cause switching of the metabolic pathway (Koppenol, *et al.*, 2011).

Despite the uncertain origin of tumour cell metabolic change which is proposed by many studies that investigated Warburg phenomenon, aerobic glycolysis is considered one of the main hallmarks of cancer cells (Hsu and Sabatini, 2008). Previous studies have investigated the precise mechanisms which could be responsible for metabolic modification of cancer cells that are present in Warburg effect. As previously mentioned, the Warburg effect is thought to be due to a mitochondrial defect; however research has identified that the mitochondrial disruption may be an incorrect hypothesis to explain the alteration of metabolism from oxidative phosphorylation to aerobic glycolysis (Weinhouse, 1976). Furthermore, studies have shown that cancer cell metabolism is a complex process and many factors could be involved in shifting metabolism including the availability of nutrients and microenvironmental hypoxia, mitochondrial DNA (mtDNA) mutations, tumour suppressor genes, and oncogenes (Figure

1.13) (Jang, *et al.*, 2013b). Moreover, it has been suggested that genetic mutations leading to alterations in some signalling molecule pathways and enzymes which are involved in glucose utilisation and uptake as well as in cellular proliferation and survival may also be involved in metabolism (Cairns, *et al.*, 2011; Vander Heiden, *et al.*, 2009).

The first of these potential factors is the tumour microenvironment (Hsu and Sabatini, 2008). Tumour hypoxia conditions promote activation of HIF-1 which subsequently regulates many genes and enzymes responsible for angiogenesis, glycolysis, and pyruvate converted to lactate including increased expression of VEGF, Glut1, and lactate dehydrogenase A (LDHA) (Semenza, 2010). Furthermore, activation of HIF-1 leads to a reduction in oxidative phosphorylation via prevention of pyruvate entering the TCA cycle through increased activation of (PDKs) concomitant with inhibition of pyruvate dehydrogenase (Kim, *et al.*, 2006a; Papandreou, *et al.*, 2006). In addition to hypoxia, normoxia conditions can promote stabilisation of HIF-1 through various mechanisms like the oncogenic PI3K/Akt/mTOR pathway (Cairns, *et al.*, 2011).

Increased mtDNA mutation is another marker potentially responsible for reducing oxidative phosphorylation in cancer cells which increase aerobic glycolysis to compensate for the energy required for proliferation (Kroemer, 2006). These mutations can directly dysregulate enzymes implicated in the oxidative process including succinate dehydrogenase (SDH), isocitrate dehydrogenase (IDH), and fumarate dehydrogenase (FDH) (Wallace, 2012). Accumulation of succinate, fumarate, 2-hydroxyglutrate and other oncometabolite in cancer cell mitochondria can lead to modification of cellular metabolism (Adam, *et al.*, 2014). Obviously, generation of mitochondrial ROS is constantly responsible for mediating mtDNA mutation in tumour cells (Li, *et al.*, 2011a).

Additionally, oxidative stress and generation of cellular ROS can lead to genomic instability, dysregulated tumour suppressor gene function (including P53) which interacts with cellular metabolism of tumour cells (Liu, *et al.*, 2008a; Vousden and Ryan, 2009). The main functions of transcriptional factor P53 are regulating cell cycle, promoting DNA repair, and regulating apoptosis process (Vousden and Ryan, 2009). However, it is believed that the P53 plays an important role in cellular metabolism through upregulation of TP53-induced glycolysis and apoptosis regulator (TIGAR) which in turn dephosphorylates fructose-2,6-bisphosphatase (Fru-2,6-P2) and directly suppresses glycolysis (Bensaad, *et al.*, 2006). Also, P53 promotes the expression of cytochrome C oxidase (SCO2) which is an essential assembly gene in the mitochondrial electron transport chain that leads to the activation of glucose metabolism through oxidative phosphorylation (Matoba, *et al.*, 2006). Furthermore, P53 cooperates with transcriptional factor OCT1 to regulate metabolism and provide a balance between oxidative phosphorylation and glycolysis (Shakya, *et al.*, 2009). Therefore, dysfunction of P53 leads to altered cellular metabolism from oxidative respiration to a high glycolysis rate and lactate production.

Alteration of oncogenic signalling pathways including PI3K/Akt/mTOR and LKB1/AMPK are involved in tumour cell proliferation, survival, and metabolic modification. The activity of PI3K in tumour cells is controlled by tumour suppressor gene PTEN which is subsequently regulated by P53 gene (Stambolic, *et al.*, 2001). Activation of PI3K leads to activation of the downstream pathway Akt which in turn activates glycolysis through increasing the activity of glycolytic enzymes such as phosphofructokinase 2 and hexokinase (Elstrom, *et al.*, 2004; Robey and Hay, 2009). Furthermore, Akt promotes activation of mTOR through inhibiting tuberous sclerosis 2 (TSC2) (Robey and Hay, 2009), and increasing expression of HIF-1 in both hypoxic and normoxic conditions (Cairns, *et al.*, 2011). Thus, dysfunction of P53 leads to deregulated PTEN which promotes PI3K activation and subsequently stimulate glycolysis. Similarly, activation of the energy sensor AMPK through the expression of the upstream LKB1 promotes activation of AMPK which in turn activates mTOR and switches cancer cell metabolism towards aerobic glycolysis.

Dysregulation of the Ras/Raf/MAPK pathway has been identified in tumourigenesis as an oncogenic alteration which occurs due to Ras and Raf mutations (Dhillon, *et al.*, 2007). Activation of mutant Ras is mediated through stimulating receptor tyrosine kinases (RtKs) as a result of binding of growth factors to generate specific binding sites called growth factor receptor-bound protein 2 (GRB2) which induce the nucleated exchange factor son of sevenless (SOS) (Santarpia, *et al.*, 2012). Once Ras is activated, the further activation of downstream pathways takes place including Raf, MEK1 and 2, and ERK1 and 2 that leads to increased cellular proliferation and survival in cancer cells (Kim and Choi, 2010).

MYC is pro-oncogene transcriptional factor acting as a regulator of cell proliferation and metabolism. Activation and overexpression of MYC have been confirmed to be involved in the alteration of many factors including glucose and glutamine metabolism, lipid synthesis, mitochondrial biogenesis, and cell-cycle progression, which increase tumorigenesis and alter metabolism (Dang, 2013). Decreased expression of MYC in T-cells causes inhibition of cellular glycolysis and glutaminolysis (Wang, *et al.*, 2011). Furthermore, dysregulated MYC has been shown to cooperate with HIF-1 to mediate glycolysis through activation of several factors including hexokinase 2, pyruvate dehydrogenase kinase 1, and VEGF, as well as activation of Glut1 and lactate dehydrogenase A (Dang, *et al.*, 2008; Kim, *et al.*, 2007). Finally, alteration of all these markers promotes modification of cancer cell metabolism to glycolysis instead of oxidative phosphorylation.

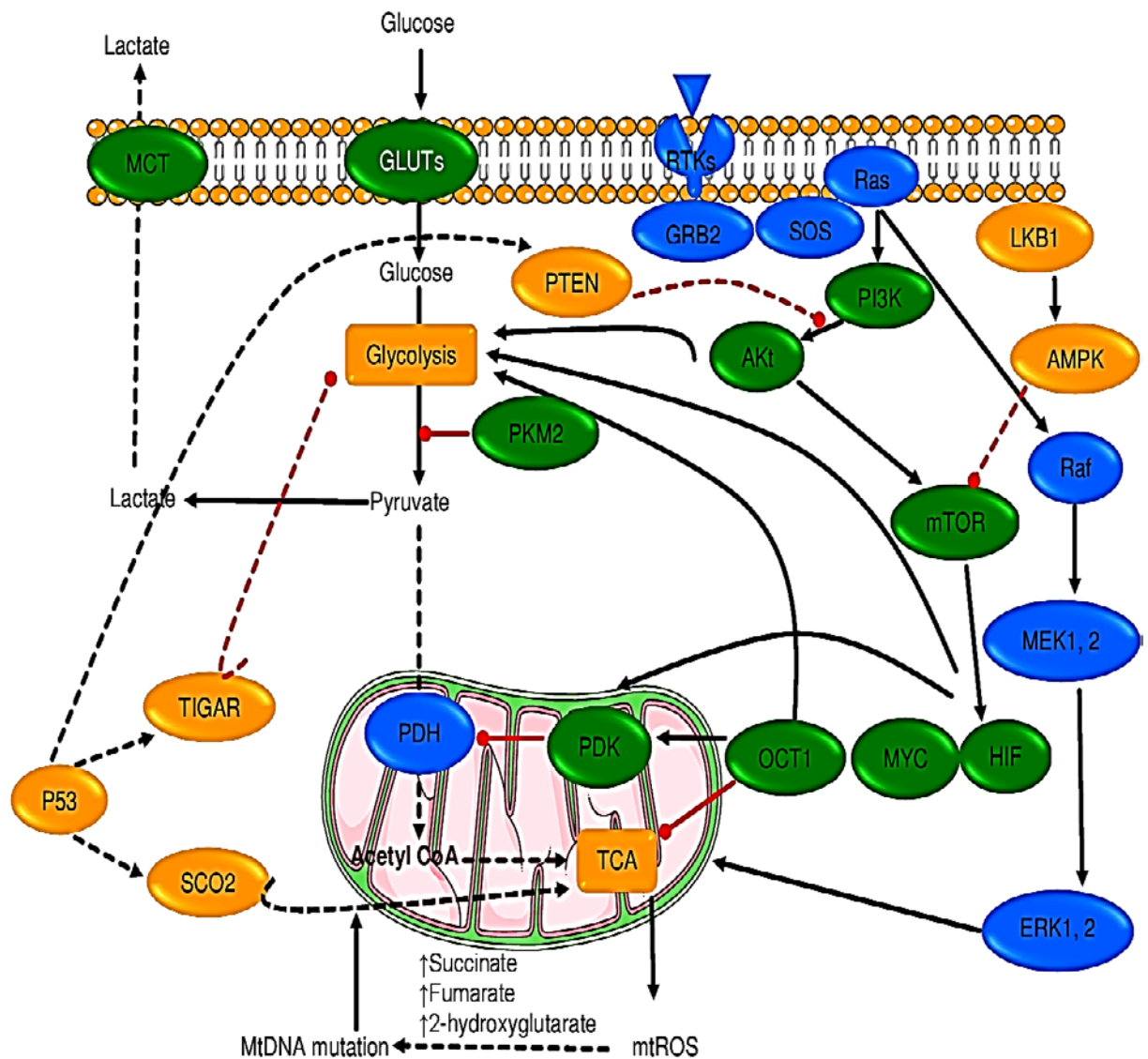


**Figure 1.13 Factors involved in the alteration of cancer cells metabolism.**

Several factors involved in aerobic glycolysis of cancer cells. Hypoxia stimulates glycolysis by increasing expression of HIF-1, Glut, VEGF, LDHA and PDK associated with inhibition of PDH. Secondly, mtDNA mutation and accumulation of succinate, fumarate, and 2-hydroxyglutarate in mitochondrion. Dysfunction of P53 causes deregulation of TIGAR, SCO2, OCT1 and PTEN which activates PI3K/Akt/mTOR to increased glycolysis. Mutant LKB1 mediated deactivate of AMPK which activates mTOR and interacts with glycolysis. Activation of Ras/Raf/MEK1,2/ERK1,2 or Ras/PI3K/Akt/mTOR due to mutant Ras or/and Raf increases cellular proliferation and cancer initiation. Overexpression of MYC is increased glycolysis and glutaminolysis by cooperating with HIF-1 to promote glycolysis.

## 1.9 Tea

Tea is an ancient natural beverage which is believed to be the second most consumed drink in the world after water (Cheng, 2004; Jian, *et al.*, 2004; Peres, *et al.*, 2011; Vuong, *et al.*, 2010). The different types of tea originate from the leaves that grow in a superior bud above the shoots of the plant which belong to the Aceae family of the *Camellia Sinensis* plant (Gutman and Ryu, 1996). There are three

different types of tea based on fermentation status which are; black fully fermented, oolong partially fermented, and green unfermented tea (Cheng, 2004). However, more types of tea have been identified additionally including yellow, white, and Pu-Erh (Cheng, 2006;Vuong, 2014). The consumption of these types of tea varies based on some factors including country and culture. The global consumption of black, green, and oolong teas is estimated at 75%, 23%, and 2% respectively (McKay and Blumberg, 2002). Another study suggested similar findings, reporting that the world consumption of a black, green, and another type of teas are 78%, 20%, and 2% respectively (Vuong, 2014). The most popular tea consumed in India, Europe, and many other countries is black tea (Chung, *et al.*, 2003;McKay and Blumberg, 2002) whilst Asian countries, especially China and Japan prefer green tea as well as oolong tea (Cheng, 2004;Koo and Cho, 2004).

### **1.9.1 Green tea**

Green tea is considered the second most popular tea consumed around the world after black tea (Vuong, 2014). Green tea is thought to contain more ingredients potentially responsible for health benefits compared with black tea due to its unfermented production through direct steaming of tea leaves which allow the enzymes responsible for changing colour to break down and preserve active compounds (Chacko, *et al.*, 2010;Senanayake, 2013). Historically, this popular type of tea is mainly produced in China and Japan (Willson, 1999;Zuo, *et al.*, 2002). The bitter taste of green tea is assigned to high contents of polyphenol (Willson, 1999).

#### **1.9.1.1 Composition of green tea**

The composition of tea varies due to several factors including the type of tea, geographic origin, harvested season, the age of the leaves, environmental conditions, and the level of fermentation or manufacturing method (Chacko, *et al.*, 2010;Fraser, *et al.*, 2013). The unfermented production process of tea leaves produces a green tea that preserves active compounds due to this process. Polyphenols are a major constituent of phytochemicals which are present in many fruits and vegetables including green tea which makes up between 45-90% (w/w) (Chacko, *et al.*, 2010). Green tea polyphenols can be divided into phenolic acid (not polyphenol), non-flavonoid polyphenol, and flavonoids and these subclasses are further divided into many subcategories (Ganguly, 2003). Flavonoids are an interesting subclass because they exhibit some compounds that have been reported to have health benefits. The backbone of this family contains two aromatic rings (A and B) which are connected by C ring. This family can be subdivided depending on the position of attachment between B and C ring, the position of hydroxyl groups on the rings, and general structure into flavan-3-ols, flavanones, flavonols, anthocyanidins, flavones and isoflavones (Beecher, 2003).

Most common effects of green tea are assigned to catechins which are the most abundant members of the flavan-3-ol subfamily and represent around 25-35% of the dry weight (w/w) of green tea extract (Abdel-Rahman, *et al.*, 2011). Green tea catechins contain several active ingredients possessing different chemical structures (Figure 1.14). These are catechin (C) which represents around 6% (w/w), epicatechin (EC; 11%, w/w), epicatechin gallate (ECG; 14%, w/w), epigallocatechin (EGC; 23%, w/w), and epigallocatechin gallate (EGCG; 41%, w/w). In addition to caffeine which represents around 5% (w/w) (El-Shahawi, *et al.*, 2012). Furthermore, galocatechin (GC), catechin gallate (CG), and galocatechin gallate (GCG) are types of catechins that have been identified in green tea (Dalluge and Nelson, 2000). While the flavonols are thought to be less potent than catechins and contain mainly quercetin, myricetin, and kaempferol which represent 2-3% (v/v) of the water soluble solids (Wang and Helliwell, 2000). Chemically, green tea extract consists of (w/w) 15-20% protein, 4% amino acid, 26% fibre. Also 7% carbohydrate, 7% lipid, 2% pigment, 5% minerals, and 30% phenolic compounds (mainly EC, EGC, ECG, and EGCG) (Chacko, *et al.*, 2010).

#### **1.9.1.2 Bioactivity of green tea**

In recent decades, several *in vivo* and *in vitro* studies have been carried out to investigate the role of green tea in a broad range of common diseases. The potentially powerful positive impact of green tea is typically assigned to one of the phenol groups in its content. Nevertheless, the underlying mechanism behind any health benefits of consuming green tea or its active compounds is still poorly understood. Importantly, green tea extract is thought to have the ability to scavenge oxygen and nitrogen free radicals that result from cell and tissue oxidative stress. This ability occurs by utilising the radicals through its phenol group, suggesting that consumption of green tea may prevent some pathological processes (Cabrera, *et al.*, 2006; Mak, 2012; Zhang, *et al.*, 2013b).

The health benefits of consuming green tea have been demonstrated in different fields including oxidation (Koo and Cho, 2004) and inflammation (Cavet, *et al.*, 2011). Also in reducing the onset and ameliorating the effect of cardiovascular disease (Chacko, *et al.*, 2010; Zheng, *et al.*, 2011). In addition, green tea has been reported to have a positive effect on weight loss and regulation of adipose tissue accumulation in the body (Park, *et al.*, 2011; Rains, *et al.*, 2011; Richard, *et al.*, 2009). Also benefits in neurodegenerative diseases (Mandel, *et al.*, 2004). Furthermore, green tea and its polyphenolic active compounds have been shown to have the ability to regulate glucose homeostasis and improve diabetic condition (Babu, *et al.*, 2013; Hininger-Favier, *et al.*, 2009; Roghani and Baluchnejadmojarad, 2010). These effects are mediated by increasing cellular glucose uptake of insulin-sensitive cells through increasing expression of Gluts and decreasing hepatic glucose output through suppressing gluconeogenesis genes (PEPCK and G6Pase). These effects are thought to be achievable by different signalling pathway including activation of AMPK and/or PI3K/Akt (Babu, *et al.*, 2013; Collins, *et al.*,

2007;Hininger-Favier, *et al.*, 2009;Zhang, *et al.*, 2010). Moreover, green tea and several of its active ingredients possess anti-tumourigenic effects including reduced cell viability via increasing apoptosis, inhibition of cell growth and cell cycle arrest (Adhami, *et al.*, 2003;Baliga, *et al.*, 2005;Carvalho, *et al.*, 2010). Many molecular pathways are potentially implicated in green tea's anti-cancer activity including targeting cell signalling and metabolic enzymes like PI3K/Akt, MAPK, JAK/STAT, Wnt and Notch, COX, and NFκB (Singh, *et al.*, 2011).

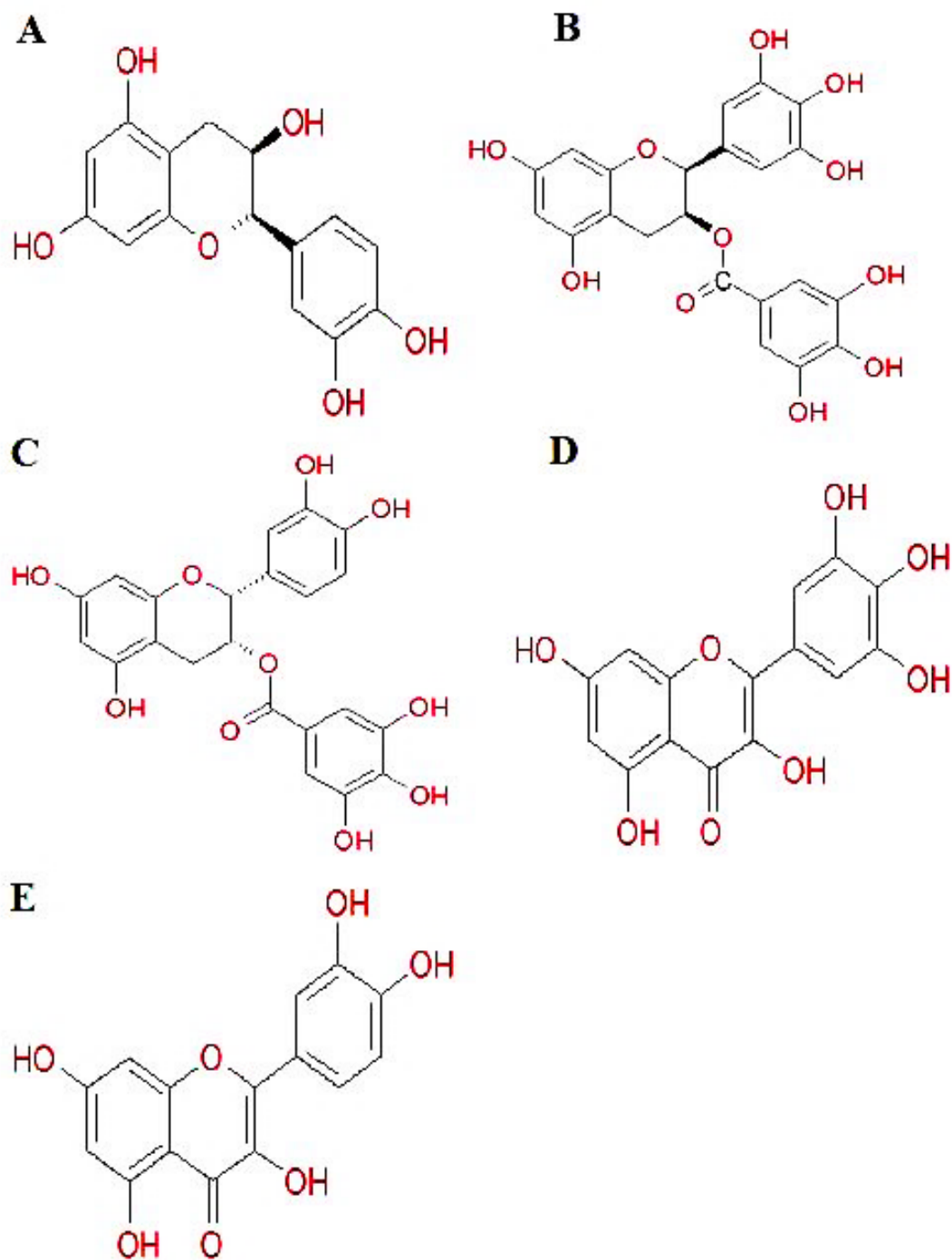


**Figure 1.14 Chemical structure of active constituents in green tea.**

Chemical structures of the main active ingredients in green tea, epicatechin EC (A), epigallocatechin gallate EGCG (B), epicatechin gallate ECG (C), quercetin (D), and myricetin (E).

## 1.10 Aims and hypotheses

The comprehensive purpose of this study was to identify the effect of green tea extract on glucose homeostasis and metabolism using *in vitro* and *in vivo* models, as well as to investigate the impact of green tea on breast cancer (BC) cells *in vitro*. Bearing in mind the well-defined dysregulation of glucose homeostasis including glucose and lipid metabolism and related progression of diseases including T2D and BC, the hypotheses of this study were:

- The active compounds of green tea extract have the ability to maintain glucose homeostasis through regulating glucose and lipid metabolism by increasing glucose uptake in insulin-sensitive cells and stimulated glycogenesis and lipogenesis associated with decreased lipolysis by activation of AMPK or Akt pathway.
- These compounds play a major role in decreasing progression of breast cancer through reducing viable cells and induced apoptosis by alteration of cellular glucose metabolism through a direct effect on AMPK or Akt pathway.
- Whole green tea extract and EGCG act to prevent obesity, increase insulin sensitivity, and prevent diabetes in mice either consuming high glucose solution or normal drinking water through regulating glucose and lipid metabolism.
- Activation of AMPK and/or Akt and downstream signalling pathways could be the potential mechanism of these compounds to promote anti-obesity and anti-diabetic effects through expression markers related to glucose and lipid metabolism in essential mouse insulin-sensitive tissues.

As a result of these hypotheses the defined aims of this study were stated as follow:

- To investigate the impact of most abundant active ingredients of green tea extract on regulation glucose and lipid metabolism in insulin-sensitive cells through assessing several metabolic markers like glucose uptake, glycogenesis, lipogenesis, lipolysis, and metabolic genes expression.
- To identify the role of these compounds on Akt and AMPK signalling pathways.
- To determine the ability of these active compounds to mediate toxic effect on BC cells to reduce cell viability through promoting apoptosis.
- To investigate the role of these compounds on BC glucose metabolism and their relationship with Akt and AMPK signalling pathways.
- To demonstrate the potential effect of whole green tea extract and EGCG on maintaining glucose homeostasis, weight gain, adiposity and lipid metabolism, and insulin sensitivity in mice consuming normal water or challenging with high glucose water to induce obesity and insulin resistance.
- To elucidate the mechanisms underlying the effect of these naturally occurring compounds as glucose homeostasis regulators, anti-obesity and anti-diabetic agents.

# **Chapter Two**

## **Materials & Methods**

## **2.1 Cell line studies**

### **2.1.1 Cell culture**

#### **2.1.1.1 Mouse hepatocyte (AML12) cell line**

Mouse hepatocytes (AML12) cell were purchased from American Type Culture Collection (ATCC® CRL2254™), the vial containing cells was thawed at 37°C by using a water bath, and this process was carried out for one to two minutes until only a small piece of ice remained in the vial. The vial was moved to tissue culture cabinet after rinsing it with 70% ethanol. Total vial contents were transferred to a 25 cm<sup>2</sup> Corning tissue culture flask (TC) (Appleton Woods, UK) containing 6 ml of complete growth medium (1:1 Dulbecco's Modified Eagle's Medium and Ham's F12, Gibco®, Life Technologies, UK). The medium supplemented with 0.005 mg/ml insulin, 0.005 mg/ml transferrin, 5 ng/ml selenium (ITS) (Gibco®, Life Technologies, UK), and 40 ng/ml dexamethasone (Sigma Aldrich, UK), in addition to 50:500ml (v/v) Foetal Bovine Serum (FBS) (Gibco®, Life Technologies, UK) and 2mM/ml L-Glutamine (LG) 5:500ml (v/v) (Gibco®, Life Technologies, UK), and 100 unit/ml penicillin and 0.1mg/ml streptomycin (P/S) 5:500ml (v/v) (Sigma Aldrich, UK). The flask was transferred to a tissue culture incubator and incubated at 37°C and 5% CO<sub>2</sub> humidified air atmosphere. Cells were subcultured when 80-90% confluent. Briefly, flasks containing cells were removed from the incubator and placed inside a tissue culture cabinet, media were removed and cells were washed once with 5ml of 1x Phosphate Buffer Saline pH 7.4 (PBS) (Gibco®, Life Technologies, UK). The washing buffer was aspirated, and the cells were exposed to 1ml of 1x 0.5% trypsin, 0.2% EDTA (Sigma Aldrich, UK) and placed in the incubator for 5 minutes to allow all cells to detach. 1ml of complete media was added to the cell suspension to neutralise the action of trypsin. The cell suspension was then transferred to a centrifuge tube, and cell pellets were collected after five minutes of centrifugation at 500 RCF. The cells were resuspended in 2ml complete cell culture medium and subsequently transferred to a 75 cm<sup>2</sup> TC flask containing 15ml complete medium and placed in a tissue culture incubator under the standard condition. The cell culture was maintained through replenishing the cell culture media every 2 to 3 days.

#### **2.1.1.2 Mouse myoblast (C2C12) cell line**

Mus Musculus (mouse) myoblast (C2C12) cell was obtained from American Type Culture Collection (ATCC® CRL1772™). The cells were cultured in 25 cm<sup>2</sup> TC flask containing 6ml of completed growth media a Dulbecco's Modified Eagle's Medium (DMEM) containing 4.5 g/L glucose and 4mM LG with phenol red (Gibco®, Life Technologies, UK). The media supplemented with 50:500ml (v/v) FBS in addition to 5:500ml (v/v) penicillin/streptomycin equal 100 unit/ml penicillin and 0.1mg/ml streptomycin. The cells were then incubated in the same incubation conditions mentioned previously. The subculturing procedure was similar to the method stated above, and the media were replenished every 2 to 3 days to maintain culture.

#### **2.1.1.2.1 C2C12 cell line differentiation**

Mouse myoblasts are primary myocyte characterised by specific a morphology that is distinct from mature myocyte morphology. The myoblasts cells were exposed to a specific differentiation medium for a limited time, and the cells become fully differentiated (myocytes). The differentiation media is mostly similar to the proliferation and maintaining media (PM) except the supplementation of serum, where instead of using 50:500ml (v/v) of FBS a 10:500ml (v/v) horse serum (Gibco, Life Technologies, UK) is used to induce differentiation. The differentiation process is variable but normally takes around 4-5 days in early passage cells and 7-9 days from passage 15 and over. Clear morphological alteration could be seen after two days of the differentiation process. The clearest morphological changes after full differentiation include that the cells became tubular, elongated, and multinuclear.

#### **2.1.1.3 Mouse embryonic fibroblast (3T3-L1) cells**

3T3-L1 cell was obtained from Zenbio Inc., Cambridge Bioscience, UK (Zenbio® SP-L1-F). Cells were cultured to proliferate in 25 cm<sup>2</sup> TC flask containing 6ml of completed proliferation media (BM), a Dulbecco's Modified Eagle's Medium (DMEM) containing 4.5 g/L glucose and 4mM LG with phenol red and without sodium pyruvate (Corning®, 10-017-CV, Appleton Woods, UK). The media supplemented with 50:500ml (v/v) FBS in addition to 100 unit/ml penicillin and 0.1mg/ml streptomycin 5:500ml (v/v). The cells were then incubated in the same incubation conditions mentioned previously for culturing AML12 and C2C12 cells. Cells were then subcultured into 75 cm<sup>2</sup> TC flask containing complete proliferation media described above by using the same procedure for sub-culturing AML12 and C2C12 cell lines. Finally, the cells were incubated in 5% carbon dioxide humidified atmosphere at 37°C temperature. The culture media was replenished every 2-3 days to maintain healthy proliferating conditions.

##### **2.1.1.3.1 3T3-L1 cell differentiation**

3T3-L1 cells are pre-adipocytes originating from clonal murine Swiss mouse fibroblasts. This cell line is commonly used in basic science research focussed on obesity and metabolism due to its ability to readily differentiate into mature adipocytes when exposed to a special cocktail to stimulate adipogenesis and lipid droplet formation. Pre-adipocyte cells were cultured into TC flask or in microwell plates containing complete proliferation media and incubated at 37°C temperature in a humidified atmosphere with 5% CO<sub>2</sub>. Culture medium was replaced every 2-3 days with fresh proliferation medium until the cells reached confluency. Before induced differentiation, the cells were incubated for additional 48 hours in proliferation media. Differentiation was initiated by removing proliferating media and replacing it with differentiation media (DM), Dulbecco's Modified Eagle's Medium/Ham's F12 (50:50) mixture with L-glutamine and phenol red and without sodium pyruvate. The media supplemented with 50ml FBS, 100 unit/ml Penicillin and 0.1mg/ml Streptomycin which equivalent 5ml and several

differentiation agents. These agents including 1µg/ml insulin, 0.25µM of dexamethasone, 0.5mM of 3-isobutyl-1-methylxanthine (IBMX, Sigma Aldrich, UK), 3.3µM of biotin (Sigma Aldrich, UK), 2µM of rosiglitazone (Santa Cruz Biotechnology, USA), and 0.17µM of pantothenate (Sigma Aldrich, UK). The cells were then incubated for three days in the conditions mentioned previously to induce differentiation by stimulating adipogenesis and lipid droplets formation which increased in number and size with time. Differentiation media was aspirated after three days of incubation, and the cells were then exposed to maintaining media (MM) which consisted of Dulbecco's Modified Eagle's Medium/Ham's F12 (50:50) mixture with L-glutamine. Complemented with 50ml FBS, 5ml penicillin/streptomycin, and many important agents for stimulating and maintaining the cells and lipid droplets formation which included 1µg/ml insulin, 0.25µM of dexamethasone, 3.3µM of biotin, and 0.17µM of pantothenate. The maintaining media was replenished on days 6, 9, and 12. The differentiating cells displayed varying numbers and sizes of lipid droplets in day 15 when they were considered fully differentiated. A detailed description of media used in 3T3-L1 cells differentiation is summarised in (Figure 2.1).

<b>Basic media</b>	<b>Differentiated media</b>	<b>Maintaining media</b>
<ul style="list-style-type: none"> <li>• DMEM high glucose with L-Glutamine</li> <li>• 50ml FBS</li> <li>• 5ml P/S</li> </ul>	<ul style="list-style-type: none"> <li>• DMEM Ham's F12 (50:50) with LG</li> <li>• 50ml FBS</li> <li>• 5ml P/S</li> <li>• 1µg/ml Insulin</li> <li>• 0.25µM Dexamethasone</li> <li>• 0.5mM IBMX</li> <li>• 3.3µM Biotin</li> <li>• 2µM Rosiglitazone</li> <li>• 0.17µM of Panthothenate</li> </ul>	<ul style="list-style-type: none"> <li>• DMEM Ham's F12 (50:50) with LG</li> <li>• 50ml FBS</li> <li>• 5ml P/S</li> <li>• 1µg/ml Insulin</li> <li>• 0.25µM Dexamethasone</li> <li>• 3.3µM Biotin</li> <li>• 0.17µM of Panthothenate</li> </ul>

**Figure 2.1 3T3-L1 cell line differentiation medium.**

#### **2.1.1.4 Breast adenocarcinoma (MCF7) cell line**

The MCF7 cell line was obtained from American Type Culture Collection (ATCC® HTB-22™). Cells were grown and maintained in Dulbecco's Modified Eagle's Medium (DMEM) containing 4.5 g/L glucose and 4 mM LG with phenol red and without sodium pyruvate supplemented with 50:500ml (v/v) FBS and 100 unit/ml penicillin and 0.1mg/ml streptomycin, 5:500ml (v/v). Cells were incubated at 37°C in a humidified atmosphere containing 5% CO<sub>2</sub> and media was replenished every 2-3 days. The cells were subcultured after reaching confluence by using a similar process for sub-culturing described earlier.

### **2.1.1.5 Breast adenocarcinoma (MDA-MB-231) cell line**

The MDA-MB-231 cells were purchased from American Type Culture Collection (ATCC® HTB-26™). The cells were grown in RPMI 1640 containing phenol red, LG and 100 unit/ml penicillin and 0.1mg/ml streptomycin which is equivalent to 5:500ml (v/v), and supplemented with 50:500ml (v/v) FBS. The culture was incubated at 37°C in a 5% CO<sub>2</sub> humidified atmosphere. Subculturing was performed when the cells reach confluence by using the same protocol mentioned earlier.

### **2.1.2 Green tea compound preparation**

All green tea compounds were purchased from Sigma Aldrich, UK unless otherwise stated. Epigallocatechin gallate (EGCG), epicatechin gallate (ECG), epicatechin (EC) were dissolved in sterile deionized water at 1mM concentration whereas, myricetin and quercetin were dissolved in dimethyl sulfoxide (DMSO) at 1mM concentration. The stock solution was aliquot and stored at -20°C until used.

### **2.1.3 Cell line cryopreservation**

All cell lines used in this study were cryopreserved in liquid nitrogen in-between uses and therefore required freezing and thawing procedures. Briefly, media was aspirated from 75 cm<sup>2</sup> TC flask containing cell culture and subsequently washed with 10ml of PBS. The PBS was removed and cells were detached using trypsin as detailed earlier. Detached cells were subsequently centrifuged at 500 RFC to form a cell pellet. Pellets were resuspended in cryopreserving solution which is 10% (v/v) of cryoprotectant DMSO in complete cell culture media, and then 1ml of the cell suspension was transferred into a cryovial. The vial was stored for 24 hours at -80°C in cell freezing box and then moved into liquid nitrogen bank.

### **2.1.4 Cell counting**

Trypan blue dye is widely used regarding counting cells by using haemocytometer to identify living and dying cells. The assay is based on living cells excluding uptake of the dye and non-viable cells then being stained dark blue. The assay was performed to count cells of all cell lines that have been used in this study. The cells were routinely trypsinized and neutralised with complete medium, and cell suspensions were then transferred to centrifuge tubes and spun down for 5 minutes at 500 RFC followed by discarding the supernatant and resuspension of the cell pellet with 1ml of complete medium. Subsequently, 100µl of cell suspension was transferred to new Eppendorf tube, and an equal volume of 0.4% (v/v) trypan blue was added, followed by pipetting up and down to enhance mixing. A 10µl of the mixture was loaded on one side of haemocytometer chamber, and the cells were examined under a microscope. The living unstained cells were counted, whereas stained dying cells were excluded in 4 squares located at the corner and one big central square in the middle of haemocytometer field (Figure 2.2). The equation display to calculate the number of the live cells in one millilitre was [(living cell numbers in 5 squares/ 5) x diluent factor (2) x 10<sup>4</sup>].

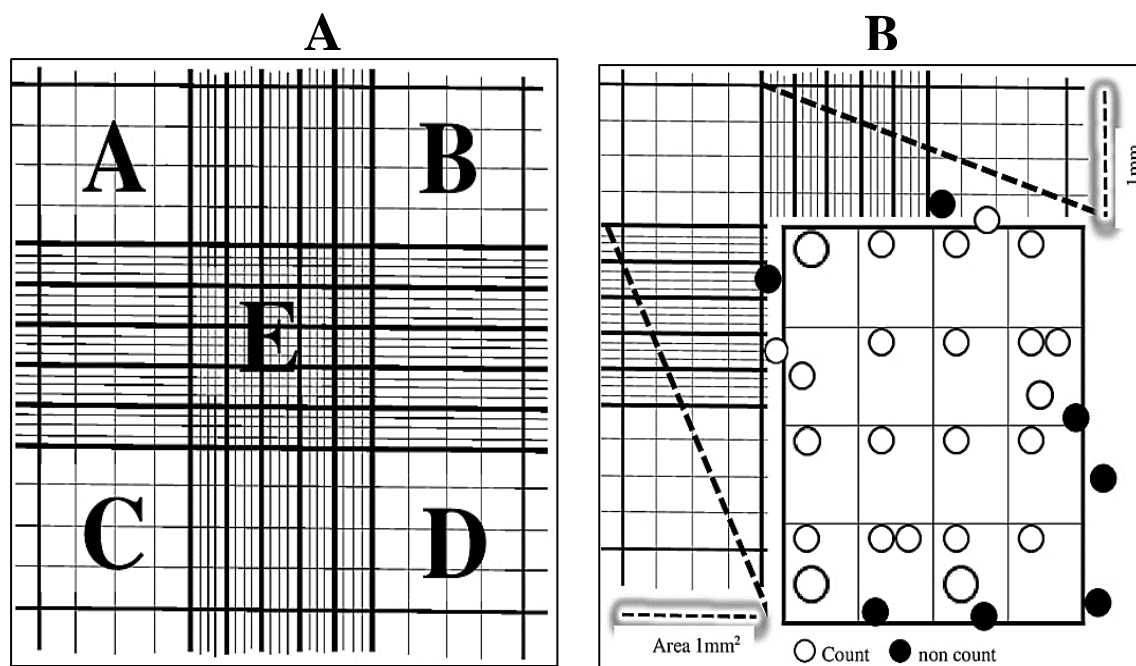


**Figure 2.2 Cells counted using haemocytometer.**

Haemocytometer field is showing counting area which is represented by four squares at the corners of the field and one square located in the middle (A). Haemocytometer counting area. (B). One square calculated area is showing counting process.

### 2.1.5 Determination of glucose in culture media of insulin-sensitive cell lines

Measuring glucose concentration in cell supernatant is a widely used indirect technique to estimate cellular glucose uptake (Drira and Sakamoto, 2013). However, this method is less accurate as it measures the concentration of glucose remain in the medium which could contain glucose resulting from gluconeogenesis and glycogenolysis. Insulin-sensitive cell lines including C2C12, 3T3-L1, and AML12 cells were seeded into 24 well plates at density of  $2 \times 10^5$  and maintained in the standard conditions mentioned previously until reach confluency. C2C12 and 3T3-L1 were routinely differentiated following the differentiation protocol described earlier. All cells were starved in serum-free medium for 2h and then treated with 0.1, 1, and  $10 \mu\text{M}$  active compounds of green tea (EGCG, EC, ECG, myricetin, quercetin, and combinations of these compounds) in various time points including 24, 48, 72 hours. The  $20 \mu\text{M}$  concentration of all compounds was tested only in AML12 in addition to other doses. The cells were treated with and without  $10 \mu\text{M}$  of selective AMPK (Dorsomorphin dihydrochloride, Tocris, UK) and selective Akt (10-[4'-(N, N-Diethylamino)butyl]-2-chlorophenoxazine hydrochloride, Tocris, UK) inhibitor molecules. These treatments were in addition to green tea active compounds in concentration and time points where significant results had previously been established when the cells were treated only with green tea compounds. The medium was collected at each time point, centrifuged and the amount of glucose in the medium was measured using a commercially available glucose oxidase/peroxidase assay kit (GAGO20, Sigma Aldrich, UK) with an amendment for use in 96 well plates. This kit depends on an enzymatic reaction in which glucose is oxidised to gluconic acid and

hydrogen peroxide by the action of glucose oxidase. The existence of peroxidase generates a brown colour of oxidised o-dianisidine that resulted from the reaction between hydrogen peroxide and colourless o-dianisidine. This colour will then be converted to a solid pink colour by the reaction between oxidised o-dianisidine and sulfuric acid. The assay was performed in all treated metabolic cell line culture medium using 96 well plates. Briefly, the glucose standard was prepared in 5 points including 0, 10, 20, 30, and 40µg/ml respectively by using glucose standard supplied with the kit (1mg/ml). All metabolic cells culture media were diluted between 1/100 and 1/150 by using deionized water. A 50µl/well of standard and sample were transferred into 96 well plates in duplicated followed by adding 100µl/well of glucose assay reagent. The plate was protected from light by using aluminium foil, and the reaction was initiated by placing the plate in an incubator at 37°C for 30 minutes. After completed incubation period, a 100µl/well of 12N H<sub>2</sub>SO<sub>4</sub> was added to stop the reaction. The intensity absorbance was measured at 540nm using Multiscan (Thermo Scientific®) plate reader.

## **2.1.6 2-(N-(7-Nitrobenz-2-oxa-1,3-diazol-4-yl)Amino)-2-Deoxyglucose (2-NBDG) uptake**

### **2.1.6.1 Insulin-sensitive cell 2-NBDG uptake**

AML12, myoblast (C2C12), and preadipocytes (3T3-L1) cells were seeded into 96 well plates at a density of 10<sup>4</sup> cells/well in 100µl complete media and incubated overnight. C2C12 and 3T3-L1 cells were differentiated before measuring 2-NBDG uptake. All cells were supplemented with low glucose serum free medium up to 2h before treatment, and subsequently, the cells (C2C12 and 3T3-L1) were treated with 1 and 10µM of EGCG, EC, and ECG. Whereas AML12 treated with 1 and 10µM of EC, ECG, combination, and 1, 10, 20µM of quercetin in addition to the 100µM final concentration of 2-NBDG in 100µl/well completed low glucose media in triplicated. The cells were then incubated for 6h followed by washing 3x with pre-cold HBSS and leaving the last wash solution. Subsequently, fluorescence intensity was measured at 465/540 Excitation/Emission (Ex/Em) using fluorescence microplate reader SpectraMAX GeminiXS (Molecular Devices, UK) and SoftMaxPro software.

### **2.1.6.2 Breast cancer cell 2-NBDG uptake**

MCF7 and MDA-MB-231 BC cells were plated in 96 well plates at a density of 10<sup>4</sup> cells/well in 100µl completed media and incubated overnight. Subsequently, cells were serum starved in DMEM low glucose medium for 2h, followed by treatment with green tea compounds that caused reduced lactate concentration in previous experiments in addition to the 100µM final concentration of 2-NBDG in 100µl/well complete low glucose media in triplicate. MCF7 cells were treated with 100µM and 150µM of EGCG in addition to 150µM quercetin, whereas MDA-MB-231 cells are treated same as MCF7 in addition to 100µM and 150µM of combination catechins (EGCG, EC, and ECG). The cells of both cell lines were incubated 4h in the incubator, and 2-NBDG uptake was measured following the method mentioned previously.

## **2.1.7 Cell viability assays**

### **2.1.7.1 PrestoBlue® cell viability assay**

The proliferative/cytotoxic effects of various compounds of green tea at specific used concentrations and incubation times were investigated in all insulin-sensitive and BC cell lines used. PrestoBlue® cell viability reagent (Life Technologies, UK) was used to measure proliferation/viability of cells. The assay is based on the conversion of blue resazurin to red resorufin by the metabolic activity of viable cells. Briefly, all cell lines were seeded in 96 well plates at a cell density of  $5 \times 10^3$  in 100  $\mu$ l/well final volume of complete medium and incubated overnight to allow cells to attach. Insulin-sensitive cell lines were differentiated prior to treatment with various concentrations of green tea compounds over a range of times. 1 and 10  $\mu$ M of EGCG, EC, ECG, myricetin, quercetin, and the combination of all compounds were used to treat C2C12 and 3T3-L1 cells, whereas AML12 cells were treated with same doses and compounds in addition to 20  $\mu$ M for 24, 48, and 72h. Both BC cell lines were treated with 1, 10, 50, 100, and 150  $\mu$ M of EGCG, EC, ECG, a combination of these compounds, myricetin, and quercetin for 24, 48, and 72h. After desired treatment periods had been complete, cell culture medium was aspirated, and the cells were rinsed in 90  $\mu$ l of completed fresh medium. Subsequently, 10  $\mu$ l of PrestoBlue was added to cell culture in addition to control wells that did not contain any cells in triplicate; then the plate was incubated for 4 hours at 37°C and 5% CO<sub>2</sub> incubator. When the incubation period was finished, the cell culture medium containing PrestoBlue was transferred to 96 fluorescence microplate, and the fluorescence was measured at 353/615nm (Ex/Em) by using fluorescence microplate reader SpectraMAX GeminiXS (Molecular Devices, UK) and SoftMaxPro software.

### **2.1.7.2 Neutral red cell viability assay**

Neutral red (NR) is another reagent widely used to measure cell viability. The assay was used to determine live cells in both BC cell lines in addition to PrestoBlue® in order to confirm the effect of test compounds. NR solution (0.33% in DPBS) was purchased from Sigma Aldrich, UK. The principle action of NR is based on dye incorporation and liberation, in other words, live cells in culture will absorb the vital dye by active transport, and it is incorporated in lysosomes then this dye will liberate from lysosomes in the presence of an acidophilic solution.  $5 \times 10^3$  cells were seeded in clear 96 well plates and incubated in the standard conditions overnight, then the test compounds were applied for the desired period, and cell viability was measured after the complete treatment time in triplicate wells. Briefly, the treated medium was removed and 10  $\mu$ l of NR reagent in 90  $\mu$ l fresh completed medium was added to cell culture. The plate was incubated for 4 hours at 37°C temperature and humidified atmosphere containing 5% CO<sub>2</sub> to allow the vital dye to incorporate. After that, the dye solution was aspirated carefully, and the cells were quickly fixed by using neutral red fixative solution (0.1% CaCl<sub>2</sub> in 0.5% formaldehyde, w/v) for two minutes, extended fixation time will lead to bleach the dye. The fixative was removed after two minutes, and 100  $\mu$ l of solubilization solution (1% acetic acid in 50% ethanol,

v/v) was added and incubated at room temperature for 10 minutes to allow dye liberation. The plate was then placed on a horizontal shaker for 1 minute to enhance dye mixing. The absorbance was measured at 540nm and 690nm using Multiscan (Thermo Scientific®) plate reader.

### **2.1.8 Analysis of glycogen content in AML12 cells**

To determine the concentration of glycogen in AML12 cells a proprietary glycogen assay kit was obtained from BioAssay Systems, UK (EnzyChrom™Glycogen Assay Kit, Cat#E2GN-100). The assay is enzymatic based that measures glucose which results in the final step from the breakdown of glycogen. Cells were cultured in 24 well plates in 1ml complete media and allowed to be 80-90% confluent, followed by serum starvation for up to 2h before being exposed to the treatment. Cells were supplemented with green tea compounds that previously showed increased glucose uptake (1µM EC, 1 and 10µM ECG, 1, 10, 20µM quercetin, and 1 and 10µM combination for 72h, in addition to 10µM ECG for 24h). Then the cells were subsequently harvested, and the glycogen assay was performed following the manufacturer's protocol. Briefly, cells were homogenised in an ice bath by adding 25µl of homogenization solution which is a mixture of 25mM citrate and 2.5g/L NaF with pH= 4.2. The samples were centrifuged for 5 minutes at 14000 RFC, and the clear supernatant was collected and diluted 1/100 for assay. A glycogen standard was prepared in 4 concentrations in addition to the blank (200, 150, 100, 50, and 0µg/ml) by using the standard solution supplied with this kit. 10µl of standards and samples were transferred to clear 96 well plates in duplicated. Subsequently, 90µl of assay reagent (90µl assay buffer, 1µl enzyme A, 1µl enzyme B, and 1µl dye) was added, the plate was tapped to enhance mixing and incubated for 30 minutes at room temperature. The intensity of the colour that results from the reaction was measured at 570nm using Multiscan (Thermo Scientific®) plate reader.

### **2.1.9 Estimation of free glycerol release from mature 3T3-L1 cells**

Measurement of the amount of glycerol produced from adipose tissue is indicative of the rate of lipolysis which is the process of breakdown of triglyceride into free fatty acid and glycerol due to energy demand. Pre-adipocytes cells were plated into 24 well plates in full proliferation media mentioned earlier and incubated in a CO<sub>2</sub> incubator at 37°C until the cells were become 100% confluent, followed by incubation for an additional two days before initiating differentiation. Differentiation was induced as described previously. Mature adipocytes were serum starved for 2h and subsequently treated with test compounds in dose and time points that increased glucose uptake previously (1 and 10µM of EGCG, EC, and ECG) for 48 and 72h. Cell culture supernatant was collected and glycerol content was detected using a commercial free glycerol reagent kit from Sigma Aldrich, the UK based on the protocol provided with the kit with minor modification to use it with 96 well plates instead of a cuvette. The detection of glycerol in this methodology depends on several enzymatic reactions, first adenosine-5'-triphosphate (ATP) phosphorylation of glycerol to form glycerol-1-phosphate (G-1-P) and adenosine-5'-diphosphate

(ADP) by the catalysed action of glycerol kinase (GK). Then glycerol phosphate oxidase subsequently oxidises glycerol-1-phosphate to produce dihydroxyacetone phosphate (DHAP) and hydrogen peroxide ( $H_2O_2$ ), and the latter reacts with sodium N-ethyl-N-(3-sulfopropyl)-anisidine (ESPA) and 4-aminoantipyrine (4-AAP) to produce quinonimine dye by the effect of peroxidase (POD). Finally, dye absorbance is measured. Briefly, glycerol standard was prepared in 8 points serial dilution from 260 $\mu$ g/ml to 0 $\mu$ g/ml, then the standard and samples were plated in duplicate well of 96 clear well plates in a volume of 2.5 $\mu$ l/ well followed by adding 200 $\mu$ l/ well free glycerol reagent to initiate the reaction. Subsequently, the plate was incubated at room temperature and protected from light by aluminium foil for 10-15 minutes. The dye absorbance was measured at 540nm using Multiscan (Thermo Scientific®) plate reader.

#### **2.1.10 Mature 3T3-L1 Triglyceride Oil red O staining**

Pre-adipocytes (3T3-L1) cells were seeded into 24 well plates in completed media and incubated in  $CO_2$  incubator till they reached 100% confluence. Differentiation was induced following the protocol mentioned previously. Cells were washed twice with PBS and subsequently fixed by adding 10% (v/v) isotonic formaldehyde solution for 30 minutes at 37°C. The fixative solution was discarded and cells were again washed twice with dH<sub>2</sub>O followed by a five-minute room temperature incubation in 60% (v/v) isopropanol. This solution was aspirated, and the cells were rinsed with an appropriate volume of oil red O working solution (Sigma Aldrich, UK) for 15 minutes at 37°C. Oil red O solution was removed carefully, and then the cells were washed several times with dH<sub>2</sub>O and subsequently examined and photographed under a fluorescence microscope (Leica DMI4000 B inverted microscope).

#### **2.1.11 Estimation of cellular triglyceride content in mature 3T3-L1 cells**

3T3-L1 cells were seeded into 24 well plates and differentiated following the protocol mentioned previously. Mature adipocytes were then treated with green tea compounds (1 and 10 $\mu$ M of EGCG, EC, and ECG for 48 and 72h). Cellular triglycerides were extracted directly by using 5% (v/v) of 100x triton (Fisher Scientific, UK). Briefly, media were removed, and the cells were washed with PBS followed by addition of 100 $\mu$ l/well of 5% (v/v) of 100x triton solution. Cells were then scraped from the surface of their well plates. The suspensions were collected and slowly heated from 80°C-100°C for 5 minutes and subsequently slowly cooled down to room temperature. The heating and cooling were repeated once again, and samples were then centrifuged at 14,000 RCF for 10 minutes. The supernatant was transferred to new tubes for assay. A proprietary triglyceride assay kit was obtained from BioAssay Systems, UK (EnzyChrom™ Triglyceride Assay Kit, Cat#ETGA-200). This assay is based on measuring colour intensity that resulted from dye oxidation during triglyceride hydrolysis and glycerol capture. The assay was performed according to the manufacturer's protocol. Briefly, a triglyceride standard was prepared in 4 points started from 1.0 mmol/L (1, 0.6, 0.3, 0 mmol/L) using the standard reagent supplied with the

kit. A 10  $\mu$ l/well of standard and diluted samples (1:10) were placed in 96 well plates in duplicate, followed by the addition of 100 $\mu$ l/well of working reagent which included 100 $\mu$ l assay buffer, 2 $\mu$ l enzyme mix, 5 $\mu$ l lipase, 1 $\mu$ l ATP, and 1 $\mu$ l dye reagent. Then the plate was tapped and incubated for 30 minutes at room temperature, and subsequently, the absorbance was measured at 570nm using Multiscan (Thermo Scientific®) plate reader.

#### **2.1.12 Cellular lactate assay**

Amplite™ Fluorimetric L-Lactate Assay Kit was purchased from AAT Bioquest® (Cat# 13814). This assay depends on coupled enzymatic activity to detect the amount of lactate by measuring the amount of fluorogenic NADH that is formed in the final step which is related to the amount of lactate, and the assay was performed following the manufacturer protocol. Briefly, MCF7 and MDA-MB-231 BC cell lines were seeded into 24 well plates at a cell density of  $3 \times 10^4$  /well in 1ml complete media. The cells were cultured overnight and subsequently serum starved for 2h with serum free media before being exposed to active compounds of green tea in 1ml complete media for 6 and 24h with and without 1mM sodium pyruvate. The cell culture medium was collected and stored directly at -80°C or immediately underwent deproteinization to inactivate all enzymes especially lactate dehydrogenase. To perform deproteinization cell culture medium was heated up for 15 minutes at 80°C and subsequently centrifuged at 8000 RCF for 10 minutes. The supernatant was collected for assay and stored at -20°C. Before the start of the test, the L-lactate standard that was supplied with the assay kit was prepared in 8 concentrations starting from 1mM - 0 $\mu$ M. The assay was initiated by adding 50 $\mu$ l/well of standard and samples into black 96 well plates in duplicate. 50 $\mu$ l of lactate assay mixture solution was added to each well. The reaction was completed by incubating the plate for 2h at room temperature away from light. Fluorescence intensity was measured at 540/590 Ex/Em with 570 cut off point using fluorescence microplate reader SpectraMAX GeminiXS (Molecular Devices, UK) and SoftMaxPro software.

#### **2.1.13 Caspase 3/7 apoptosis assay**

The CellEvent® Caspase-3/7 Green Ready Probes® Reagent (cat no R 37111) was purchased from Thermofisher Scientific, UK. This assay is based on detection of the activation of caspase 3/7 during apoptosis which promotes DEVD cleavage allowing a nucleic acid dye to bind with DNA and generate a fluorescent signal. The assay was performed following the manufacturer's protocol. Briefly, MCF7 and MDA-MB-231 cells were plated into 96 well plates at a cell density of  $5 \times 10^3$  cells/well and incubated for 24h at standard incubation environment. MCF7 cells were treated with 100, 150 $\mu$ M EGCG and 150 $\mu$ M quercetin with and without 1mM sodium pyruvate for 24h in 100 $\mu$ l complete media. MDA-MB-231 cells were treated with 100 and 150 $\mu$ M of EGCG and combination of green tea catechin in addition to 150 $\mu$ M quercetin with and without 1mM sodium pyruvate for 24h. Cell culture medium was aspirated, and cells were exposed to 100 $\mu$ l/well of fresh medium containing CellEvent reagent (2

drops/1ml media). The cells were incubated for 60 minutes in a standard cell culture incubator, and subsequently, emission of fluorescence was measured at 502/530 Ex/Em using fluorescence microplate reader SpectraMAX GeminiXS (Molecular Devices, UK).

#### **2.1.14 Cellular migration assays**

Scratch assay is conventional, well developed, and economical method which has been used widely to track *in vitro* cell migration, matrix remodelling, and cellular polarisation (Liang, *et al.*, 2007). Simply, the assay is based on monitoring cellular movement from both edges of artificial scratch that is made in confluent monolayer cell toward the gap until newly cellular contact is established (Liang, *et al.*, 2007). The disruption of the cell to cell contact during scratch assay causes increased growth factors concentration at the margins which stimulate wound healing through proliferation and migration (Yarrow, *et al.*, 2004). Cellular migrations of both BC cell lines (MCF7 and MDA-MB-231) have been assessed using wound scratch healing assay. A classic microscopic imaging and automated cell-IQ® were used to determine migration process based on the ability of cells to migrate and close the artificial gap.

##### **2.1.14.1 Wound scratch classic microscopic imaging assay**

Cellular migration of MCF7 and MDA-MB-231 was investigated using traditional standard wound scratch assay. Briefly, cells were seeded into 24 well plates in 1ml complete media and were incubated at 37°C and 5% CO<sub>2</sub> atmosphere until they became 100% confluent. Cells were then exposed to 5µg/ml of mitomycin C in serum-free media for 2h before treatment and initiation of the assay to inhibit cellular proliferation (Carretero, *et al.*, 2008). A cross shape scratch was performed in each well of monolayer cell using a sterile 20µl pipette tip, and subsequently, cells were washed with HBSS to remove all detachable cells. The MCF7 cells were then treated with 50µM of EGCG and quercetin, whereas MDA-MB-231 cells were treated with EGCG, a combination of green tea catechin (GTC), and quercetin in 1ml complete media and wound healing was monitored at two-time points (0 and 24h). Images were captured at 0, and 24h using Leica DMI4000 B inversion microscope and % of wound closure was analysed using free TScratch software developed by Koumoutsakos's group (CSE Lab, ETH, Zurich) (Geback, *et al.*, 2009).

##### **2.1.14.2 Wound scratch cell IQ® migratory assay**

Confirmation of MCF7 and MDA-MB-231 cell migration in response to green tea treatments was determined using an automated image capture system called Cell IQ® (CM Technologies, Finland). Cells were cultured in 24 well plates in 1ml complete media and incubated in standard condition until they reached 100% confluence. Prior to introduction to the Cell-IQ system, the cellular proliferation was inhibited by exposing both cultured cell lines to 5µg/ml of mitomycin C in serum-free media for 2h. The

cell monolayer was scratched along the vertical axis using a sterile 20µl pipette tip, and washing was applied to remove any free cells using HBSS. The MCF7 and MDA-MB-231 cells were then treated with treatments mentioned above, and plates were placed in the Cell IQ® system, and two interested regions were chosen for each well of both cell lines. The captured images were selected every six hours over 24 hour treatment. A percent of wound closure was calculated by analysing images using Cell-IQ® analyser™ software based on comparing initially scratched area and new closure area during time points that were selected previously.

### **2.1.15 Total RNA extraction and reverse transcription**

Total RNA of both metabolic and cancer cell lines was isolated using Ambion/RNA Trizol® Reagent (Life Technologies, UK). Briefly, all cell lines were seeded into 12 well plates and incubated at standard conditions for 24h. The metabolic cells including C2C12 and 3T3-L1 were differentiated before treatment as mentioned previously. C2C12 and 3T3-L1 cells were treated with 10µM EGCG, EC, and ECG; whereas AML12 has been processed with 10µM of EC, ECG, quercetin, whole experiment green tea compounds, also, to control containing 0.1% (v/v) DMSO as a vehicle for 24h. While, MCF7 and MDA-MB-231 were treated with 100µM of EGCG and quercetin, and EGCG, GTC, quercetin respectively in addition to 1% (v/v) DMSO control as a vehicle for 24h. The cells were then lysed directly using 1ml of Trizol® reagent per 10 cm<sup>2</sup>, which means 1ml/3 wells of 12 well plates and the total RNA was isolated following the manufacturer's protocol. Subsequently, purified RNAs were quantified using NanoDrop1000 spectrophotometer (Thermofisher Scientific, UK), and RNA concentration was recorded by measuring absorbance at 260/280nm. 1µg of total RNA from each sample of all cell lines was reverse transcribed using cDNA synthesis kit containing oligo dT primer (Primer design, UK) except 3T3-L1 cells in which total RNA was used at a concentration of 100ng in 20µl final volume. Synthesis of cDNA was performed following manufacturer's instruction by initiation reaction for 20 minutes at 55°C and then heat inactivation for 15 minutes at 75°C using a programmed thermocycler. The cDNAs obtained from this synthesis were diluted one in 10 using PCR water and stored at -20°C until required for amplification.

### **2.1.16 Real-time Polymerase Chain Reaction (qPCR)**

Specific mouse metabolic genes and human cancer apoptotic genes were amplified using 5µl diluted cDNA in 20µl final volume reaction by performing SYBR® Green qPCR. Specific mouse metabolic and human apoptotic primers were purchased from Thermofisher Scientific as well as selected housekeeping primers (Invitrogen, UK). These primers are insulin receptor (IR), hexokinase 1 (HK1), Glut2, Glut4, Gys1, pyruvate dehydrogenase kinase 4 (PDK4), Peroxisome proliferator-activated receptor gamma coactivator 1-alpha (PGC1α), G6Pase, PEPCCK, carnitine palmitoyltransferase 1alpha (CPT1α), Acyl-CoA Synthase (Long-Chain) (ACSL), C/EBPα, SREBP1c. Furthermore, lipoprotein lipase (LPL), fatty

acid synthase (FASN), fatty acid binding protein 4 (FABP4), peroxisome proliferator-activated receptor gamma (PPAR $\gamma$ ), B-cell lymphoma 2 (BCL2), apoptosis regulator Bax (Bax), oncogene Myc (Myc), and tumour suppressor p53 (P53). The forward and reverse sequence of primers and normalising housekeeping gene primers that have been used for each cell line of mouse metabolic and human cancer apoptosis are listed in Table 2.1. 20 $\mu$ l of final volume reaction (5 $\mu$ l diluted sample and 15 $\mu$ l master mix containing SYBR green with forward and reverse interested primers) were placed in each well of 96 PCR well plates in duplicated and subsequently sealed. The plate was transferred to Stratagene MX3000P™ thermal cycler (Stratagene, UK). The thermocycling conditions were one activation cycle of 95°C for 10 minutes, 40 cycles of 95°C for 15 seconds and 60°C for one minute, and one cycle of 95°C for 30 seconds followed by 60°C for one minute and the 95°C for 30 seconds. The cycle threshold (C<sub>t</sub>) value is the point at which fluorescence in each well begins to increase exponentially, and this was obtained for housekeeping genes and interesting genes. The average value of C<sub>t</sub> was used to calculate the value of  $\Delta$ C<sub>t</sub> by subtracting average C<sub>t</sub> value of housekeeping gene from average C<sub>t</sub> value of responsive genes. The relative level of gene expression was calculated using equation  $2^{-\Delta\Delta C_t}$  whereas  $\Delta\Delta C_t$  is the average  $\Delta C_t$  value of control reference subtracted from the  $\Delta C_t$  value of the interested gene.

**Table 2.1 Primer sequences of metabolic and BC cell lines.**

No	Cell lines	Primer	Forward and Reverse sequences
1	C2C12	mActin	F/ CCTCCCTGGAGAAGAGCTATG R/ TTACGGATGTCAACGTCACAC
		mIR	F/ AATGGCAACATCACACTACC R/ CAGCCCTTTGAGACAATAATCC
		mHK1	F/ GACCGAGGCATCTTCGA R/ AGCAGCGGTAATCGGTCACT
		mGLUT4	F/ ACATACCTGACAGGGCAAGG R/ CGCCCTTAGTTGGTCAGAAG
		mGys1	F/ TATCGCTGGCCGCTATGAGTT R/ CACTAAAAGGGATTCATAGAG
		mPDK4	F/ GATTGACATCCTGCCTGACC R/ CATGGAAGTCCACCAAATCC
		mPGC1 $\alpha$	F/ GAGTCTGAAAGGGCCAAGC R/ GTAAATCACACGGCGCTCTT
2	AML12	mActin	F/ CCTCCCTGGAGAAGAGCTATG R/ TTACGGATGTCAACGTCACAC
		mIR	F/ AATGGCAACATCACACTACC R/ CAGCCCTTTGAGACAATAATCC
		mHK1	F/ GACCGAGGCATCTTCGA R/ AGCAGCGGTAATCGGTCACT
		mGLUT2	F/ TGTGCTGCTGGATAAATTCGCCTG R/ AACCATGAACCAAGGGATTGGACC
		mGys1	F/ TATCGCTGGCCGCTATGAGTT R/ CACTAAAAGGGATTCATAGAG
		mG6Pase	F/ AACGCCTTCTATGTCCTCTTTC R/ GTTGCTGTAGTAGTCGGTGTCC
		mPEPCK	F/ CTTCTCTGCCAAGGTCATCC R/ TTTGGGGATGGGCAC

		<b>mCPT1<math>\alpha</math></b>	F/ ACGGAGTCCTGCAACTTTGT R/ GTACAGGTGCTGGTGCTTTTC
		<b>mACSL</b>	F/ CAGAACATGTGGGTGTCCAG R/ GTTACCAACATGGGCTGCTT
<b>3</b>	<b>3T3L1</b>	<b>mActin</b>	F/ CCTCCCTGGAGAAGAGCTATG R/ TTACGGATGTCAACGTCACAC
		<b>mIR</b>	F/ AATGGCAACATCACACTACC R/ CAGCCCTTTGAGACAATAATCC
		<b>mHK1</b>	F/ GACCGAGGCATCTTCGA R/ AGCAGCGGTAATCGGTCACT
		<b>mGLUT4</b>	F/ ACATACCTGACAGGGCAAGG R/ CGCCCTTAGTTGGTCAGAAG
		<b>mCEBP<math>\alpha</math></b>	F/ TGGATAAGAACAGCAACGAG R/ TCACTGGTCAACTCCAACAC
		<b>mSREBP1c</b>	F/ CAACGCTGGCCGAGATCTAT R/ TCCCATCCACGAAGAAACG
		<b>mPPAR<math>\gamma</math></b>	F/ GTCACGTTCTGACAGGACTGTGTGAC R/ TATCACTGGAGATCTCCGCCAACAGC
		<b>mLPL</b>	F/ TGGATGAGCGACTCCTACTTCA R/ CGGATCCTCTCGATGACGAA
		<b>mFASN</b>	F/ GGCTCTATGGATTACCCAAGC R/ CCAGTGTTTCGTTCTCGGA
		<b>mFABP4</b>	F/ TCACCATCCGGTCAGAGAGTA R/ GCCATCTAGGGTTATGATGCTC
<b>4</b>	<b>MCF7 &amp; MDA-MB-231</b>	<b>hYWHAZ</b>	F/ ACTTTTGGTACATTGTGGCTTCAA R/ CCGCCAGGACAAACCAGTAT
		<b>hBCI2</b>	F/ AGGAAGTGAACATTTCCGGTGAC R/ GCTCAGTTCAGGACCAGGC
		<b>hBax</b>	F/ TGCTTCAGGGTTTCATCCAG R/ GGCGGCAATCATCCTCTG
		<b>hMyc</b>	F/GGCAAAAGGTCAGAGTCTGG R/ GTGCATTTTCGGTTGTTGC
		<b>hP53</b>	F/ CTGGCCCCTGTCATCTTCTG R/ CCGTCATGTGCTGTGACTGC

## 2.1.17 Analysis of cell signalling

### 2.1.17.1 Protein isolation

Cells were lysed using 1x Radio-Immunoprecipitation Assay (RIPA) buffer (Millipore, Watford, UK) containing phosphatase and complete protease inhibitor cocktail C (Santa Cruz Biotechnology, Germany). Briefly, treated cells were washed two times with 1x cold Tris-buffered saline (TBS) (20mM Tris and 150mM NaCl), and an appropriate volume of complete RIPA buffer was added. Subsequently, the cell layer was scraped and all content was transferred into a microcentrifuge tube and incubated in an ice bath for 15 minutes to complete cell lysis. The content was centrifuged at 10,000RCF for 10 minutes at 4°C to remove all debris followed by collecting supernatant into the new microcentrifuge tube and storing at -80°C.

### 2.1.17.2 Protein quantification

The concentration of the total protein in the samples was quantified using Bio-Rad DC™ Protein Assay (Bio-Rad, UK). The principle of this assay is similar to Lowry assay with only reducing

measurement time. The assay is based on reduced folin reagent by copper-treated protein that resulted from reaction between protein and copper in an alkaline medium. The absorbance of the final generated blue colour is then measured at 750nm. Briefly, bovine serum albumin was dissolved in 1x RIPA buffer as standard ranging from (0.25-1.5mg/ml) in addition to diluent buffer RIPA as a 0ng/ml. Samples were diluted in 1x RIPA buffer (1:4). 5µl of standard and samples were transferred to each well of 96 well plates in triplicate. 25µl of working reagents A and B (50:1) were added to each well followed by adding 200µl/well reagent B. The plate was incubated 15 minutes at room temperature, and subsequently, absorbance was read at 750nm using a Multiscan (Thermo Scientific®) plate reader. Protein concentration was calculated from plotting a standard curve from the data obtained and using the equation of the line.

### **2.1.17.3 Sodium dodecyl sulphate-polyacrylamide gel electrophoresis (SDS-PAGE)**

Samples were denatured in 5x Laemmli sample buffer (deionized water, 60mM Tris-HCl pH 6.8, 10% (v/v) glycerol, 2% (v/v) SDS, 0.01% (v/v) bromophenol blue and 5% (v/v) β-mercaptoethanol) for 5 minutes at 95°C. Gels were prepared according to standard manufacturer recipes using 1mm thick glass plates. 4% (v/v) protogel stacking buffer and 12% (v/v) of 4x protogel resolving buffer (National Diagnostics, Geneflow, UK) were prepared and casted, and a comb was inserted on the top of stacking gel to make wells for loading samples. 20µg of total protein from 3T3-L1, AML12, MCF7, and MDA-MB-231, and 25µg of total protein from C2C12 were loaded into each well in addition to 5µl molecular weight marker as a protein ladder PageRuler™ Plus (Fisher Scientific, UK). Samples then underwent electrophoresis in 1x running buffer Novex® Tris-Glycine SDS running buffer (Life Technologies, UK) to separate protein by size and charge using SDS-PAGE which performed by using Mini Protean® 3 Cell (Bio-Rad Laboratories Ltd., UK). Gels were run at 40mA for more than 1 hour or until the stain reached the bottom of the gel.

### **2.1.17.4 Western blotting**

The tank and all equipment required to perform transfer were prepared, and foam pads, filter papers, and nitrocellulose hybond ECL membranes (Amersham GE Healthcare, UK) were soaked into 1x Novex Tris-Glycine Transfer Buffer (Life Technologies, UK) for 15 minutes prior to transfer cassette assembly. After protein being separated by SDS-PAGE, the gel containing separated protein was removed carefully from the glass plate and placed into 1x transfer buffer for 5 minutes. The transfer sandwich was built from negative to positive charge. The foam pad has been put on a first layer followed by two pieces of Whatman chromatography filter paper, the SDS-PAGE gel was then placed and subsequently, nitrocellulose membrane positioned above, two pieces of Whatman chromatography filter paper formed the 5<sup>th</sup> layer, and foam pad formed the 6<sup>th</sup> layer. The cassette was closed and placed in mini trans-blot electrophoretic transfer cell (Bio-Rad Laboratories Ltd, UK) with an ice pack to keep transfer process

cool. The tank was filled with transfer buffer and run at 100V for one hour. After protein had been moved to nitrocellulose membrane, the latter was washed with 1x TBS and blocked overnight with 3% (v/v) BSA in Tris Buffered Saline Tween 20 (0.1% (v/v) Tween) (TBST) at 4°C. The membrane was then washed three times with 1x TBS for 5 minutes each and subsequently incubated with primary antibody diluted in TBST containing 0.5% (v/v) BSA for 1.5 hours at room temperature. The primary antibodies used are Akt 1/2/3 mouse monoclonal (1:500), AMPK $\alpha$  1/2 mouse monoclonal (1:500), pAkt 1/2/3 mouse monoclonal (1:250), and pAMPK $\alpha$  1/2 Thr172 rabbit polyclonal (1:250) (Santa Cruz Biotechnology Inc., Germany). Following that the membrane was washed five times with TBST 5 minutes each and one time with TBS for 5 minutes. Incubation with secondary antibody was performed for one hour at room temperature using goat anti-mouse IgG-HRP (1:5000) for all mouse monoclonal primary antibodies, and goat anti-rabbit IgG-HRP (1:5000) for rabbit polyclonal primary antibody (all purchased from Santa Cruz Biotechnology Inc., Germany). After incubation with the secondary antibody, the membrane was washed with TBST five time for five minutes each and one time with TBS for five minutes. The excess wash solution was removed and an equal volume of reagent A and B of Enhanced Chemiluminescence substrate (ECL) (Geneflow, UK) were mixed and applied to cover the membrane (0.1ml/cm<sup>2</sup>) for 5 minutes in a dark room. The excess ECL substrate was drained and the membrane was developed and visualised using a G-box transilluminator (Syngene). Protein bands intensity were quantified using Image J software (ImageJ, NIH). The analysed data were normalised to total Akt 1/2/3 and total AMPK $\alpha$  1/2 band intensity.

## **2.2 Analysis of green tea consumption in mice**

### **2.2.1 Animal care and housing**

48 male C57BL/6J mice aged 6-8 weeks were purchased from Charles River, UK, and housed in an animal unit of Aston University, School of Life and Health Sciences. All experiments were conducted under research ethics regulations and approved by Aston University Ethics Committee, Birmingham, UK, and the project licence reference is PPL30/3253. Mice were maintained under standard conditions 12:12 h light/dark cycle, 20°C  $\pm$  1°C temperature, and 50%  $\pm$ 10% humidity. Mice were allowed to adapt to the new environment for five days before any treatment with free access to tap water and chow (Rat and Mouse No 3 Breeding (RM3), Special Dietary Services (SDS), UK).

### **2.2.2 Experimental design and treatment**

After five days of acclimatisation, mice were separated into two main groups of 24 for experiments one and two. Following that, mice of each main group were then randomly divided into four groups with each group containing six mice housed in two separate cages. For experiment one (1), all four groups had free access to standard chow and controlled access to water containing the treatment compounds for four weeks. The groups were control group (C) which received only vehicle (1% (v/v) DMSO, Fisher

Scientific, UK) with drinking water, decaffeinated green tea extract group (DGTE) received 50mg/kg/day decaffeinated green tea extract (Sigma Aldrich, UK originally from U.S. Pharmacopeial Convention, USA) with drinking water. EGCG group received 10mg/kg/day EGCG (Tocris Bioscience, UK), and green tea extract (GTE) group received 100mg/kg/day commercial green tea extract (Blackburn distributions, UK). For experiment two (2), all four groups had similarly free access to chow and controlled access to glucose supplemented water containing treatment for four weeks. The groups of experiment 2 were treated the same as treatment provided to groups of experiment 1 except the drinking water in experiment 2 containing 30% (w/v) D-glucose (Sigma Aldrich, UK) to produce a hypercaloric diet. Mice distribution and treatment for this work appears in Figure 2.3.

### **2.2.3 Blood sampling and tissue harvesting**

At the end of the experiment, mice were fasted overnight and sacrificed by cervical dislocation. Blood was collected for all groups and subjected to clot, centrifuge and serum obtained for measuring insulin and total cholesterol. Organs and tissues including liver, heart, brain, kidneys, skeletal muscle, visceral adipose tissue, subcutaneous adipose tissue, and intra-scapular adipose tissue were dissected carefully by Adam Watkins. All organs and tissues weight were measured and stored at -80°C.

### **2.2.4 Glucose tolerance test (GTT)**

A glucose tolerance test (GTT) was performed for all mice at days 0 and 28 days. Briefly, mice were fasted overnight (16h) before a bolus of 2g/kg of D-glucose solution was injected intraperitoneally (IP). The blood glucose levels were measured using GlucoRx nexus blood glucose monitor kit TD 4277 (pharmacy link, UK) at time 0 before glucose injected (fasting blood glucose) and at 15, 30, 60, and 120 minutes after glucose solution injection by sampling blood from the tip of the tail of all mice. Fasting blood glucose (FBG), glucose area under the curve (gAUC), and the level of blood glucose after 2h of GTT were recorded, calculated, and analysed for all mice groups. The test was performed by Adam Watkins.

### Mouse work experimental design

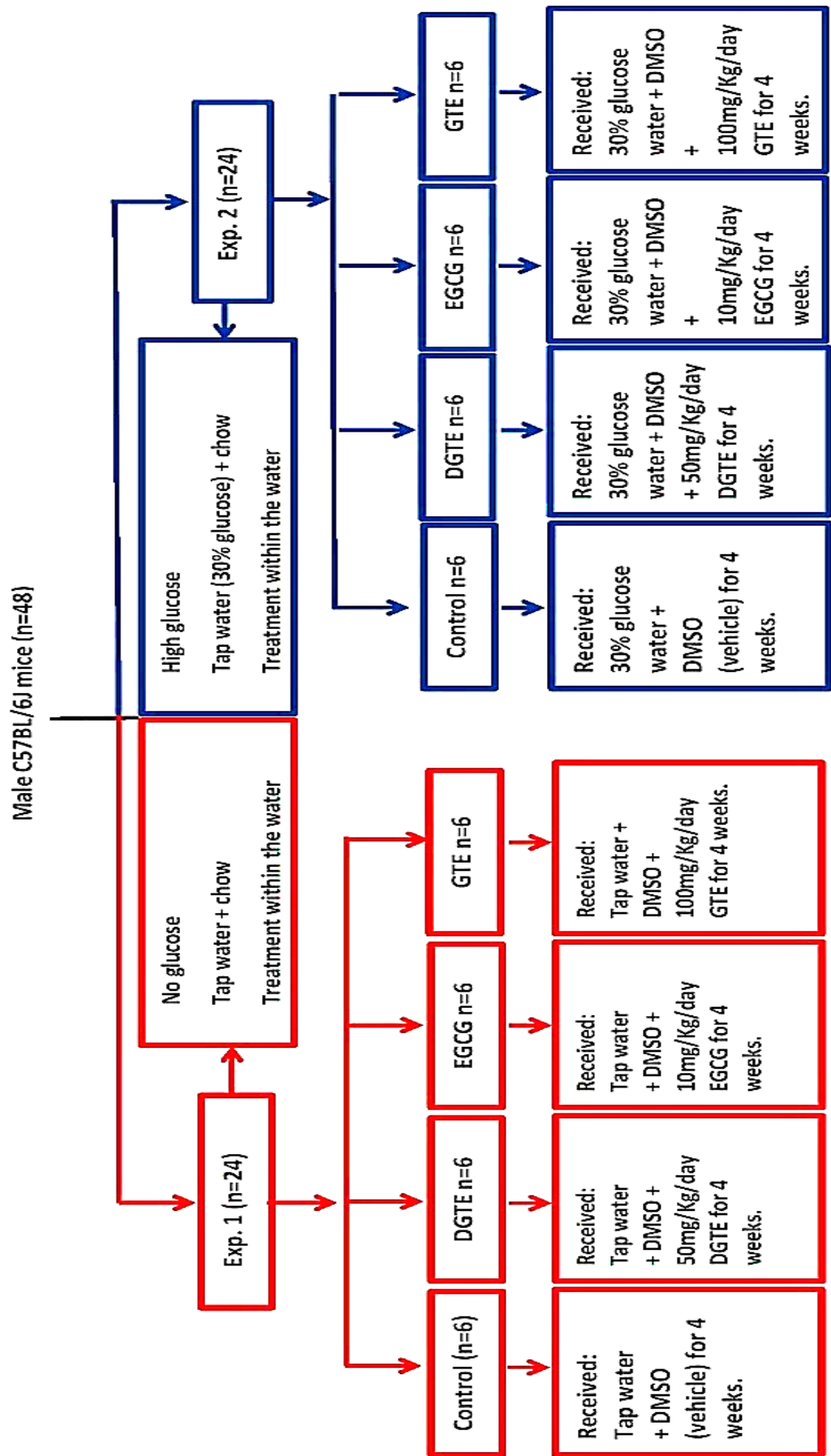


Figure 2.3 Mice experimental design.

### **2.2.5 Measurement of circulating insulin**

This study was designed to investigate circulating insulin levels alongside the level of glucose during GTT at day 0 and 28 days after treatment for all mice groups. However, it was difficult to obtain a sufficient volume of blood from the tip of the tail for both glucose and insulin (Bowe, *et al.*, 2014). Thus, the level of insulin was measured for all groups only at the end of the experiment. Mice fasted overnight, and blood was collected from them after sacrifice. Blood samples were allowed to clot and quickly centrifuged at 2000 RCF for 10 minutes at 4°C. A clear serum supernatant was aspirated and stored at -80°C. Subsequently, the concentration of fasting serum insulin was assayed in the samples using a mouse insulin ELISA kit (Mercodia, Sweden) according to the manufacturer's protocol. This sandwich enzymatic immunoassay is a colorimetric-based assay which detects insulin molecules in the samples through direct sandwich ELISA technique. Briefly, the insulin in the sample reacts with peroxidase conjugated mouse monoclonal anti-insulin enzyme which is conjugated with anti-insulin antibodies that bounded to wells surfaces. An unbounded enzyme that labelled antibodies was removed by washing followed by initiating the reaction to detect bounded conjugate through additional 3,3',5,5'-tetramethylbenzidine (TMB) substrate. Acid was used to stop this reaction followed by optical density measurement at 450nm. Briefly, 1x of enzyme conjugate reagent was prepared by mixing one part of enzyme conjugate 11x with ten parts of enzyme conjugate buffer, which were all supplied with the kit. 1x of washing buffer was also prepared through diluted 21x wash solution that was supplied with the kit using doubled distilled water. The standard reagents supplied with the kit are ready to use, and the concentrations are 0, 0.2, 0.5, 1.5, 3, and 6.5µg/l. 10µl/well of standards and samples were transferred to a special plate coated with mouse monoclonal anti-insulin in duplicate. 100µl/well of 1x enzyme conjugate solution was added, and the plate was sealed and incubated for 2h at room temperature on plate shaker 800 rpm. After incubation, the plate was washed six times using 350µl/well washing buffer, then 200µl/well of TMB substrate was added, and the plate was incubated for 15 minutes at room temperature. The reaction was stopped after 15 minutes through applying 50µl/well of 0.5M of H<sub>2</sub>SO<sub>4</sub> stopping solution followed by shaking the plate for 5 seconds to enhance mixing, and the optical density was read at 450nm using Multiscan (Thermo Scientific®) plate reader.

### **2.2.6 Calculation of homoeostasis model assessment (HOMA)**

Homeostatic modelling including homoeostasis model assessment-insulin resistance (HOMA-IR), homoeostasis model assessment-beta cell function (HOMA-B), and homoeostasis model assessment-insulin sensitivity (HOMA-S) were calculated from data obtained from fasting glucose and insulin for all mice after 28 days of treatment. These homeostatic models have been calculated using computerised HOMA calculator two software version 2.2.3 (Oxford University, Diabetes Trial Unit, Oxford Centre for Diabetes, Endocrinology and Metabolism, UK). HOMA is a simple, inexpensive, and reduced time consuming model compared to euglycemic clamp test. The model is developed by Matthews in 1985 to

measure insulin sensitivity in human clinical cases based on strong correlation between the levels of insulin and glucose in fasting status. Several studies validated this model to measure insulin sensitivity and beta cell function in human (Chang, *et al.*, 2006), with limited study showed accurate using this model to calculate insulin sensitivity in rodent, however the limitation is due to the metabolic differences between human and rodent (Antunes, *et al.*, 2016).

### **2.2.7 Measurements of weight gain, food and water consumption**

The body weight of mice in all eight groups was measured before intervention (week 0), and every week during the experiment. Total body weight gain of each group (control and treated) was calculated at the end of the experiment by subtracting body weight at week 0 from body weight at week 4. Similarly, consumption of chow and water containing treatment were measured and recorded each week during the intervention for all groups. The average mouse chow and water consumption were calculated each week for each group. As treatments were administrated with drinking water, and due to the inherent lack of control on the water volume consumed, the proposed treatments concentration that has been used were inaccurate. Therefore, the actual average concentration of treatments (DGTE, EGCG, and GTE) for each mouse was calculated based on the mean volume of water consumed by mouse per day.

### **2.2.8 Circulating lipid profile**

The original design of the experiment was proposed to determine lipid profile of all mouse groups before treatment and 28 days after administrated treatment. However, due to the limited blood volume obtainable from the tip of the tail of each mouse, the measurement of lipid profile was assessed only after 28 days of treatment. Mice fasted overnight, the level of triglyceride (TG) and high-density lipoprotein (HDL) were determined in obtained blood using CardioChek® P.A analyser and lipid PTS panels (RedMed™, Poland). Briefly, the panel chip and lipid panel test strips were attached to their places on the analyser. A 50µl blood sample was loaded onto the test strip, and after 2 minutes the measurements were displayed. Total cholesterol (TC) in mice serum samples was detected separately by using the EnzyChrom™ Cholesterol Assay Kit (BioAssay System, Universal Biologicals Ltd., UK). This colorimetric assay is based on measurement the density of reduced form of Nicotinamide adenine dinucleotide (NAD) which is NADH. First, cholesterol esters are hydrolyzed to free cholesterol by cholesterol esterase; then cholesterol dehydrogenase catalysed free cholesterol to cholest-4-ene-3-one which reduced NDA to form NADH which is proportional to total cholesterol in the sample. Finally, the calculated Low-Density Lipoprotein (cLDL) was calculated from the existing data obtained (total cholesterol, TG, and HDL) using Friedewald formula (FF) which is  $cLDL = TC - HDL - TG/5$  LDL (Friedewald, *et al.*, 1972;Knopfholz, *et al.*, 2014).

### **2.2.9 Total RNA extraction and reverse transcription**

Total RNA of mouse liver, adipose tissue, and skeletal muscle was extracted using Ambion/RNA Trizol® Reagent (Life Technologies, UK) following the manufacturer's protocol. Briefly, more than 100mg of tissue (liver, adipose tissue, and skeletal muscle) were homogenised in 1ml Trizol reagent in an ice bath using IKA® T10 basic homogenizer (IKA® WERKE GMBH & CO. KG., Germany). The homogenised samples were centrifuged at 12,000RCF for 10 minutes at 4°C to remove all insoluble materials. The supernatant which contains RNA was aspirated and placed in 1.5ml PCR microcentrifuge tube, and RNA was isolated following the procedure mentioned previously in section 2.1.15. RNA was then quantified, all samples were treated with RNase-free DNase (Qiagen, UK) to remove genomic contamination. Reverse transcription was performed as mentioned previously and 500ng for liver and skeletal muscle, and 100ng for adipose tissue RNA samples were used for cDNA synthesis.

### **2.2.10 Real-time polymerase chain reaction (PCR)**

SYBR® Green qPCR was performed for liver, skeletal muscle, and adipose tissue cDNA samples following the protocol mentioned in section 2.1.16. The specific target genes are mouse IR, Gys1, Glut2, G6Pase, PEPCK, CPT1 $\alpha$ , and FASN for the liver. Also IR, Glut4, Gys1, PDK4, and PGC1 $\alpha$  for skeletal muscle, and IR, Glut4, SREBP1c, C/EBP $\alpha$ , PPAR $\gamma$ , FABP4, FASN, and LPL, in addition to Actin. The sequences of these primers are mentioned in Table 2.1.

### **2.3 Statistical analysis**

Statistical analysis was performed using Graph Pad Prism version 6 software (Inc., USA). All data were presented as means  $\pm$  standard error of the mean (SEM) in triplicate of 3 independent experiments. The statistical analysis between experimental statuses of all presented data was determined by one-way analysis of variance (ANOVA) followed by Tukey's post-hoc test for multiple comparisons unless otherwise states. The differences were considered significant at p values < 0.05 as specified by \*, p values < 0.01 are specified by \*\*, p values < 0.001 are specified by \*\*\*, and p values < 0.0001 are specified by \*\*\*\*.

## **Chapter Three**

**The effect of active compounds  
of green tea extract on glucose  
and lipid metabolism in insulin-  
sensitive cell lines**

### 3.1 Introduction

The human body can maintain blood glucose within the normal physiological levels through balancing glucose entering the circulation and removing excess glucose from the circulation during various conditions including fed and fast states. This homeostatic process is under tight hormonal control under normal circumstances, specifically relying on insulin and glucagon in addition to insulin and glucagon sensitive tissues including hepatic, skeletal muscles, and adipose tissue, as well as insulin insensitive tissues like stomach, gut, brain, and pancreas (Aronoff, *et al.*, 2004). After a meal, elevated circulatory blood glucose levels stimulate pancreatic beta-cells to secrete insulin into the bloodstream through a process called GSIS (Gong and Muzumdar, 2012). Once insulin is released, the metabolically sensitive tissues accelerate glucose uptake and reduce endogenous glucose output to restore the normal blood glucose level. This cellular glucose can be converted to glycogen which is stored in hepatic tissue and consumed in skeletal, muscular tissue due to daily energy requirements, whereas adipose tissue metabolises glucose and stores it in the form of triglyceride (Aronoff, *et al.*, 2004; Saltiel and Kahn, 2001).

Disruption of glucose homeostasis either due to inadequate insulin secretion and/or insulin insensitivity leads to metabolic disturbance and eventually T2D. It is well known that this disease is characterised by hyperglycaemia associated with or without hyperinsulinaemia due to insulin resistance and continuous glucose released from the liver and adipose tissue (Gerich, 2000; Zhang, *et al.*, 2013a). Although significant research into the fundamental biology of T2D has been performed in recent decades, it is still poorly understood and ‘incurable’ and considered a common and major health concern.

There exist several different types of anti-diabetic drug that have been developed and approved to managed hyperglycaemia in diabetic conditions. These include sulfonylureas, biguanides,  $\alpha$ -glucosidase inhibitors, thiazolidinediones, meglitinides, amylin analogues, and dipeptidyl peptidase 4 (DPP4) inhibitors (Distefano and Watanabe, 2010). However, metformin is the most commonly prescribed drug which has been used to manage high blood glucose levels primarily via suppression of hepatic glucose output in diabetic patients (Zhou, *et al.*, 2001). Green tea and its active compounds have been reported to have a broad range of health benefits, including claims of anti-diabetic properties (Babu, *et al.*, 2013). Like agents that sensitise to insulin, green tea and its ingredients appear to possibly regulate glucose homeostasis through increasing glucose uptake that is enhanced by expression of Glut2 and 4 in insulin-sensitive tissues (Hanhineva, *et al.*, 2010). Furthermore, they regulate glucose utilisation in hepatic tissue by inhibiting glucose production through a direct effect on PEPCK and G6Pase, as well as increased insulin sensitivity (Babu, *et al.*, 2013). This anti-diabetic action of green tea could be promoted by activation of the AMPK or/and PI3K signalling pathways (Zhang, *et al.*, 2010).

The aims of the research described in this chapter are

- To investigate the effect of individual active compounds of green tea including EGCG, EC, ECG, myricetin, quercetin, and combination of all these compounds together on glucose and lipid metabolism *in vitro*.
- To investigate the regulation of metabolic gene expression by active compounds of green tea including EGCG, EC, ECG, myricetin, quercetin, and combination of all these compounds together
- To identify the potential role of the AMPK and Akt signalling pathways in any effects that are caused by exposure to active compounds of green tea.

### **3.2 Materials and methods**

All materials and methods of three insulin-sensitive cell lines included AML12, C2C12, and 3T3L1 related to *in vitro* study were mentioned in detail in chapter two (Materials and Methods). These are glucose assay, cellular fluorescence glucose analogue uptake (2-NBDG), Rt. PCR, SDS-PAGE, and cell viability assay for all cell lines, in addition to glycogen assay of AML12 cell line only, free glycerol released, Oil red O staining, triglyceride assay for mature 3T3-L1.

### 3.3 Results

Both C2C12 and 3T3-L1 are undifferentiated cell lines and therefore require differentiation before they are suitable to study glucose metabolism. Thus, these cells were differentiated before any experimental work commenced. The process of differentiation of C2C12 may take four to eight (or nine) days, following the process described in chapter two. This process was observed under a light microscope and was based on morphological changes including cellular elongation and tubular formation (Figure 3.1). Alternatively, 3T3-L1 pre-adipocyte differentiation takes approximately 15 days, the process of which is also described in chapter two. Accumulation of lipid droplets was observed during the differentiation process until the cells expressed increased in number and size of lipid droplets (Figure 3.2).

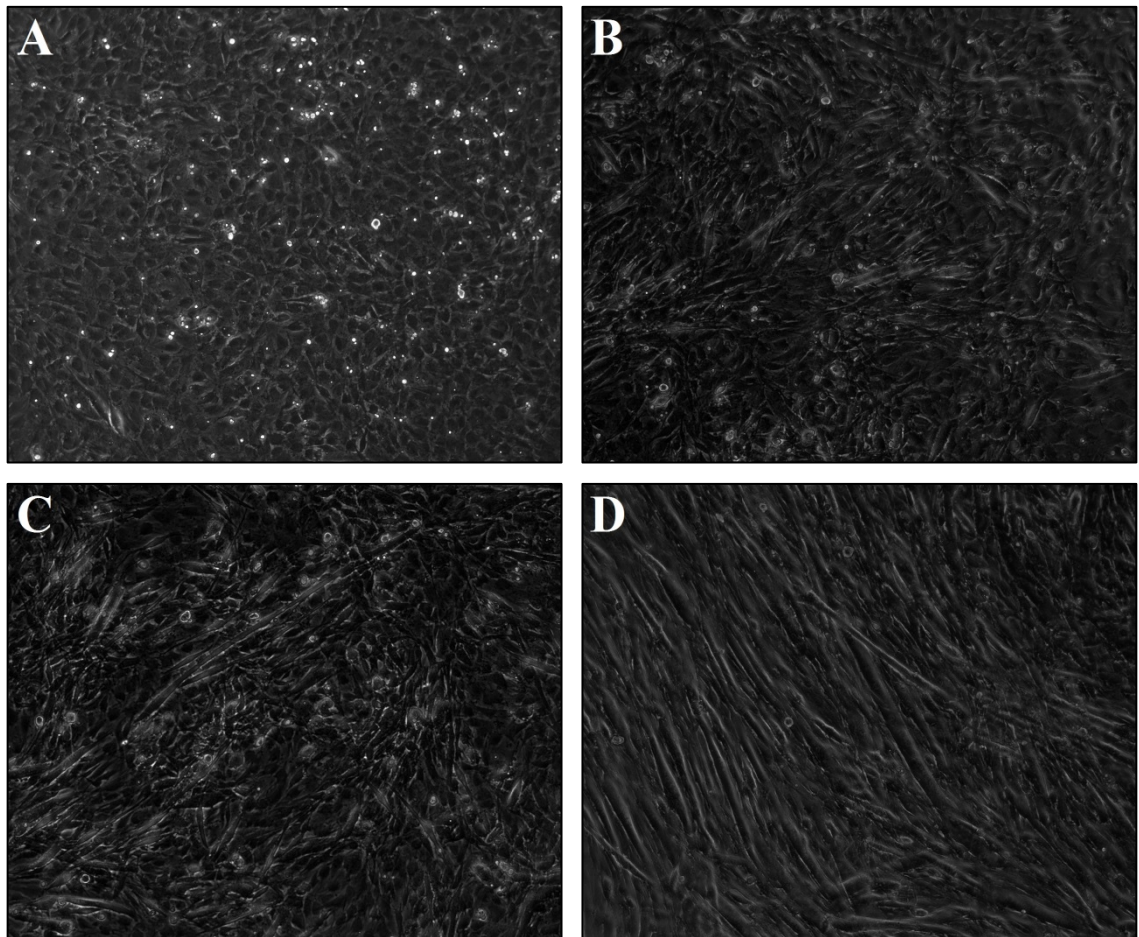


**Figure 3.1 Mouse myoblast (C2C12) cell line differentiation.**

Differentiation of C2C12 cells was performed as mentioned previously in tissue culture materials and methods before any experiment to study the effect of green tea active compounds on glucose metabolism. (A) C2C12 cells at day 0. (B) Day 3 of differentiation. (C) Day 5 of differentiation. (D) Day 8 of differentiation. The images were captured using Leica DMI4000 B inversion microscope at 100x magnification.

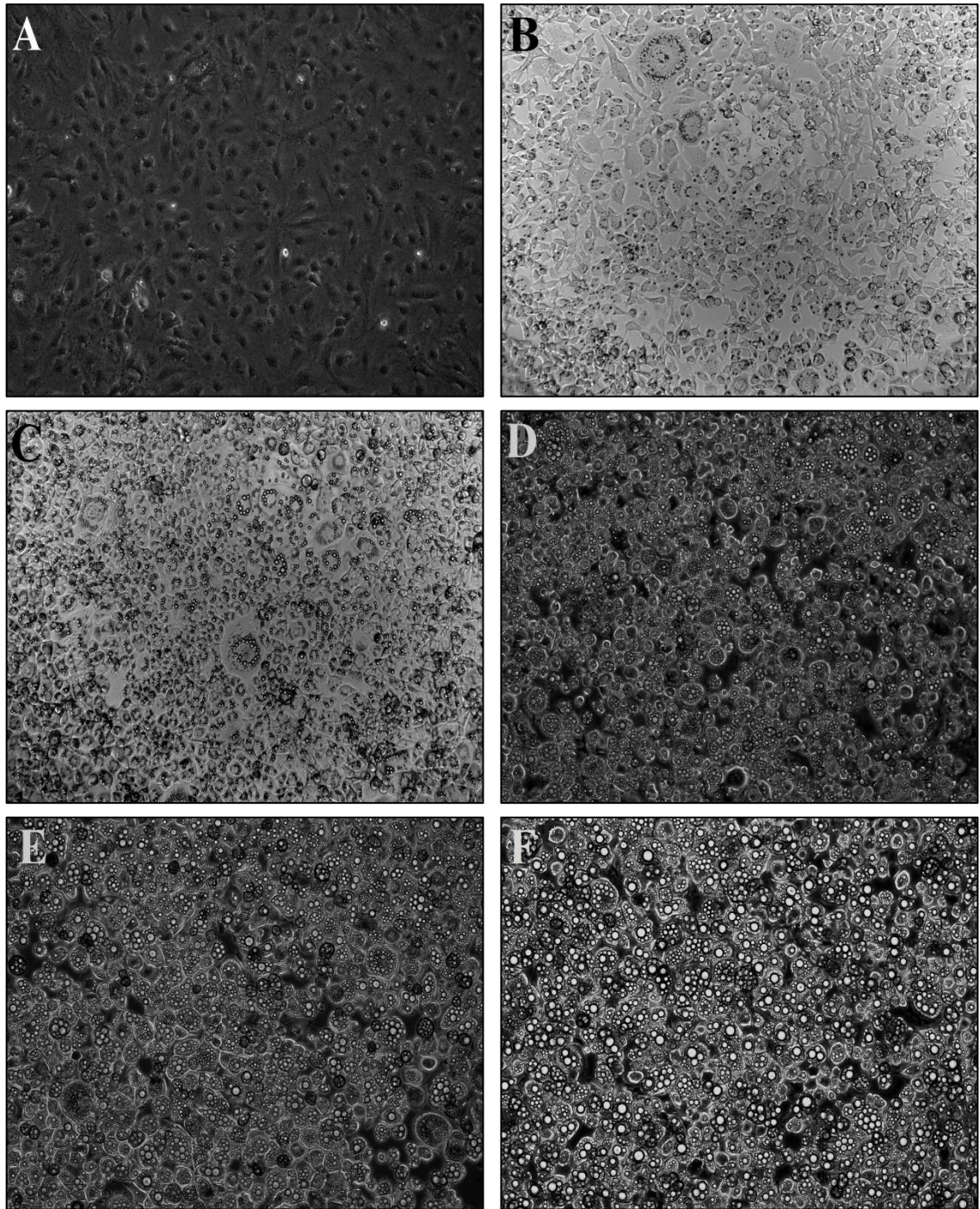


**Figure 3.2 Mouse pre-adipocyte (3T3-L1) cell line differentiation.**

Differentiation process of 3T3-L1 cells was performed as mentioned previously in tissue culture materials and methods before any experiment to study the effect of green tea active compounds on glucose and lipid metabolism. (A) Day 0 of differentiation. (B) Day 3 of differentiation, some cells show visible small lipid droplets. (C) Day 6 of differentiation, the numbers and sizes of lipid droplet is increased. (D) Day 9 of differentiation, the cells showed an increase in the size of lipid droplets. (E, F) Day 12, 15 of the differentiation process. The images were captured using Leica DMI4000 B inversion microscope at 100x magnification.

### 3.3.1 Selected compounds of green tea increased glucose uptake in C2C12 cells

Measurement of glucose concentration in cell supernatant is indirect technique used to estimate cellular glucose uptake, with decreased glucose concentration in supernatant being indicative of an increase in cellular glucose uptake (Drira and Sakamoto, 2013). Regulation of glucose uptake in differentiated C2C12 cells was investigated. Cells were treated with several active compounds of green tea including EGCG, EC, ECG, myricetin, quercetin, and the combination of (EGCG, EC, ECG, myricetin, and quercetin) at various concentrations (0.1, 1, and 10 $\mu$ M) at specified time points (24, 48, and 72h). The results showed that EGCG, EC, and ECG at 1 and 10 $\mu$ M induced significant increases of glucose uptake by 36.47% $\pm$ 4.3% (p=0.0191), 37.30% $\pm$ 2.2% (p=0.0150), 38.33% $\pm$ 4.5% (p<0.0001), 41% $\pm$ 3.58% (p<0.0001), 47.26% $\pm$ 5.16% (p<0.0001), 47.58% $\pm$ 5.17% (p<0.0001) respectively after 48h (Figure 3.4) and 45.14% $\pm$ 8.81% (p<0.0001), 55.70% $\pm$ 13.93% (p<0.0001), 56.77% $\pm$ 6.57% (p<0.0001), 46.12% $\pm$ 2.38% (p<0.0001), 51.74% $\pm$ 5.66% (p<0.0001), 48.76% $\pm$ 6.37% (p<0.0001) respectively after 72h (Figure 3.5) compared to control. Cellular glucose uptake was unaffected by myricetin, quercetin, and combination of green tea compounds at all concentrations and time points. Neither green tea compounds nor concentrations caused any significant effect on glucose uptake after 24h of intervention (Figure 3.3).

### 3.3.2 Selected compounds of green tea increased glucose uptake in 3T3-L1 cells

The impact of several active compounds of green tea on glucose uptake in adipose cells was investigated by exposing the differentiated 3T3-L1 cells to 0.1, 1, and 10 $\mu$ M of EGCG, EC, ECG, myricetin, quercetin, and the combination of these compounds for 24, 48, 72h. Cells showed significant response and increased glucose uptake by 38.2% $\pm$ 3.46% (p=0.0001), 37.7% $\pm$ 6.81% (p=0.0002), 37.86% $\pm$ 6.1% (p=0.0002), 34% $\pm$ 6.95% (p=0.0013), 49.72% $\pm$ 16% (p<0.0001), 41.57% $\pm$ 6.5% when treated with only 1 and 10 $\mu$ M of EGCG, EC, and ECG after 48h respectively (Figure 3.7) and by 57.9% $\pm$ 13.43% (p<0.0001), 54.7% $\pm$ 13.16% (p<0.0001), 55.4% $\pm$ 13% (p<0.0001), 51.76% $\pm$ 10.63% (p<0.0001), 56.87% $\pm$ 11.6% (p<0.0001), 48.41% $\pm$ 10% (p<0.0001) after 72h respectively compared to control (Figure 3.8). No effects were mediated by myricetin, quercetin, and the combination of green tea compounds at all concentrations during the same incubation periods. Similarly, no effect of all green tea compounds on glucose uptake was observed after 24h incubation (Figure 3.6).

### 3.3.3 Selected compounds of green tea increased glucose uptake in AML12 cells

The role of green tea active ingredients on indirect cellular glucose uptake in AML12 was determined by treating the cells with 0.1, 1, 10, 20 $\mu$ M of EGCG, EC, ECG, myricetin, quercetin, and the combination of these compounds for 24, 48, 72h. After 24h incubation only, insulin and ECG at 10 $\mu$ M significantly increased glucose uptake by 23.4% $\pm$ 2.7% (p<0.0001) and 23.3% $\pm$ 4% (p<0.0001) (Figure 3.9). Whilst no effect of all green tea compounds on glucose uptake was observed after 48h, except

insulin increased glucose uptake by 29.7%±1% (p=0.0078) compared to control and 30.2%±2.1% (p=0.0055) compared to DMSO (Figure 3.10). Significant effects were exhibited after 72h intervention, ECG and combination of green tea compounds at 1 and 10µM elevated glucose uptake by 35%±1.1% (p<0.0001), 33.4%±3.55% (p<0.0001), 33.6%±0.9% (p<0.0001), and 37.7%±1.25% (p<0.0001) respectively. Similar effects were mediated by quercetin at 1, 10, and 20µM which caused 62.8%±6% (p<0.0001), 44.3%±3.5% (p<0.0001), and 43.2%±5.55% (p<0.0001) increases in glucose uptake respectively compared to control. EC at only 1µM increased glucose uptake by 34.4%±5.6% (p<0.0001) compared to control (Figure 3.11).

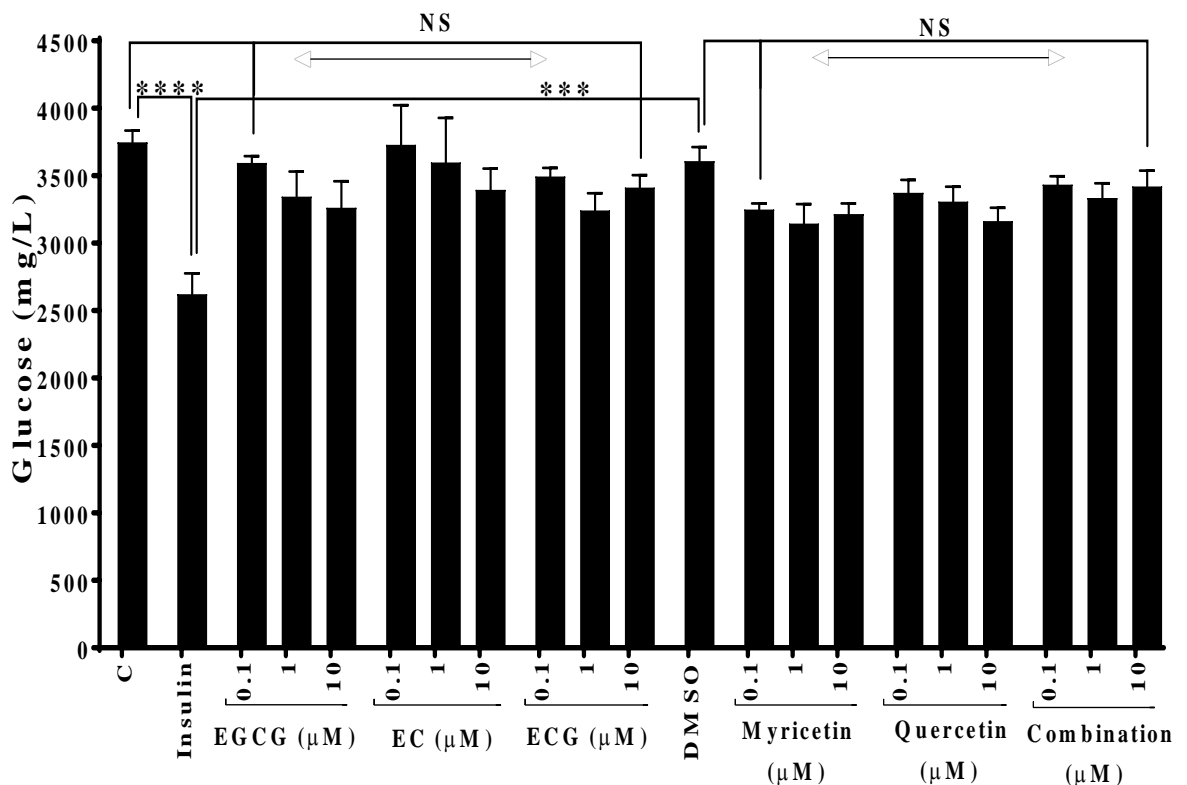


**Figure 3.3 Green tea compounds and glucose uptake in C2C12 cells.**

C2C12 cells were seeded in 24 well plate at density  $2 \times 10^5$  and incubated in standard conditions until reached 80% confluency. Differentiation was induced, and the cellular glucose uptake was assessed by measuring amount of glucose remained in culture media after treated cells with different concentrations and compounds of green tea for 24h. No effect of these compounds on glucose uptake was observed compared to control. Data presented mean  $\pm$  SEM, \*\*\*p<0.001, \*\*\*\*p<0.0001, n=3.

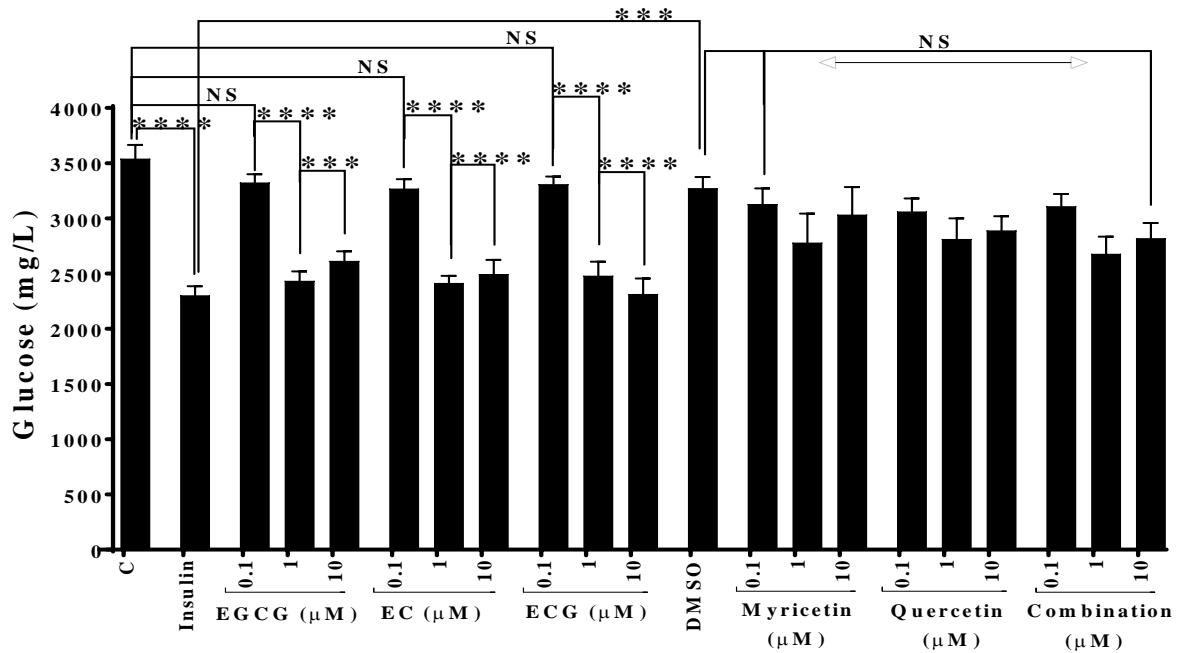


**Figure 3.4 Selected green tea compounds increase glucose uptake in C2C12 cells.**

C2C12 cells were seeded in 24 well plate at density  $2 \times 10^5$  and incubated in standard conditions until reached 80% confluency. Differentiation was induced, and cellular glucose uptake was assessed by measuring amount of glucose remained in culture media after cells treated with different concentrations and compounds of green tea for 48h. EGCG, EC, and ECG significantly increased cellular glucose uptake compared to control. Data presented mean  $\pm$  SEM, \*\*\* $p < 0.001$ , \*\*\*\* $p < 0.0001$ ,  $n = 3$ .

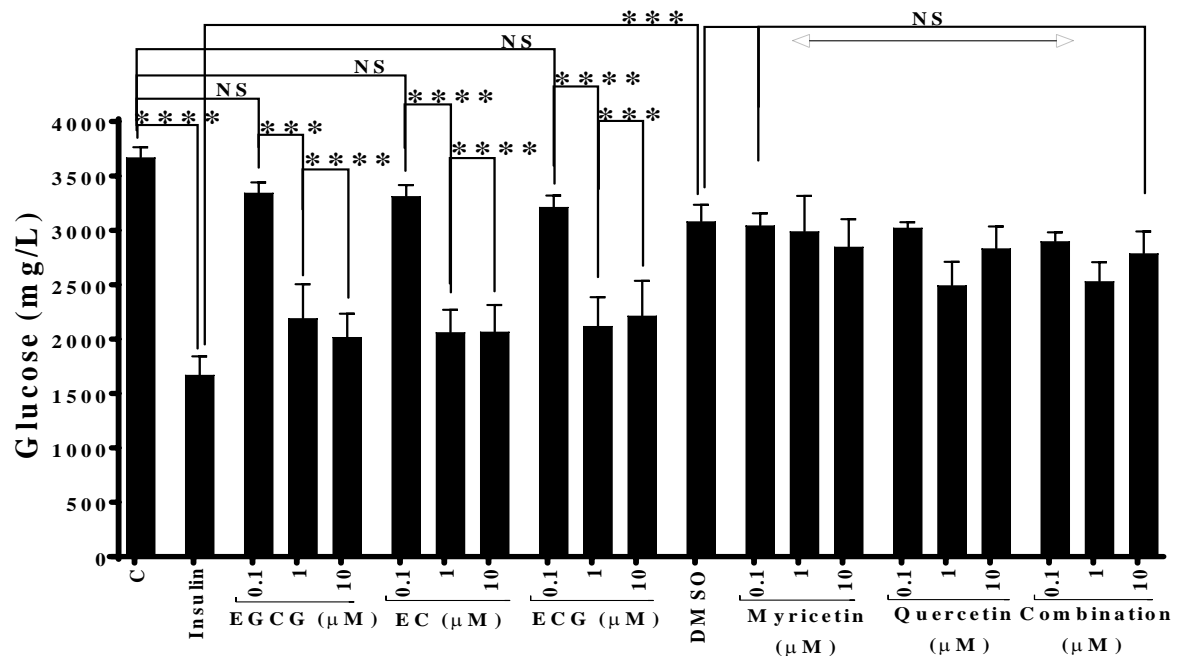


**Figure 3.5 Selected green tea compounds increase glucose uptake in C2C12 cells.**

C2C12 cells were seeded in 24 well plate at density  $2 \times 10^5$  and incubated in standard conditions until reached 80% confluency. Differentiation was induced, and cellular glucose uptake was assessed by measuring amount of glucose remained in culture media after treated cells with different concentrations and compounds of green tea for 72h. EGCG, EC, and ECG significantly increased cellular glucose uptake compared to control. Data presented mean  $\pm$  SEM, \*\*\* $p < 0.001$ , \*\*\*\* $p < 0.0001$ ,  $n = 3$ .

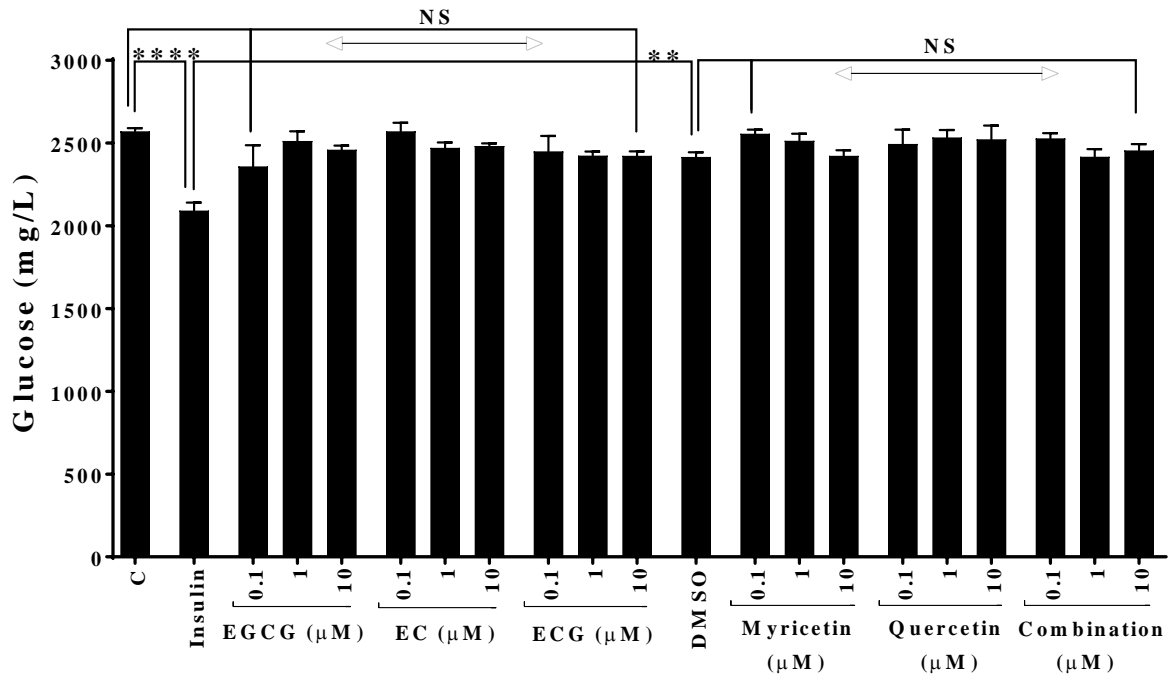


**Figure 3.6 Green tea compounds and glucose uptake in 3T3-L1 cells.**

3T3L1 cells were seeded in 24 well plate at density  $1.5 \times 10^4$  and incubated in standard conditions until completed confluency. Differentiation was induced, and cellular glucose uptake was assessed by measuring amount of glucose remained in culture media after exposed cells to different concentrations and compounds of green tea for 24h. No effect of these compounds on glucose uptake was observed compared to control. Data presented mean  $\pm$  SEM, \*\* $p < 0.01$ , \*\*\*\* $p < 0.0001$ ,  $n = 3$ .

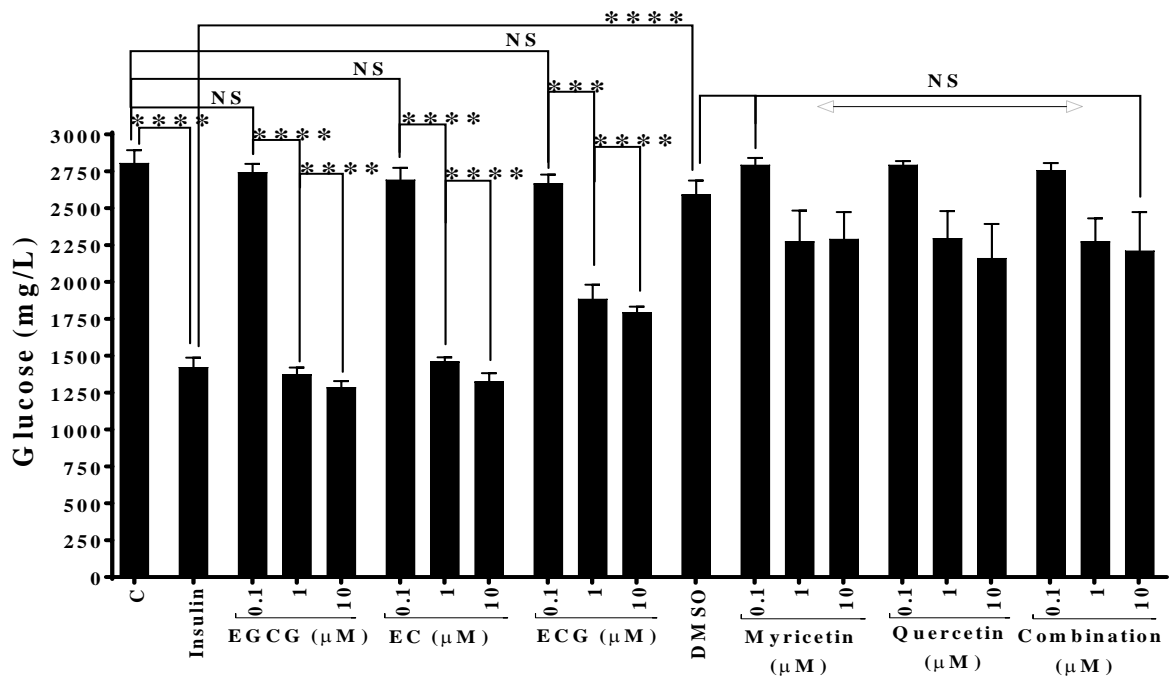


**Figure 3.7 Selected green tea compounds increase glucose uptake in 3T3-L1 cells.**

3T3L1 cells were seeded in 24 well plate at density  $1.5 \times 10^4$  and incubated in standard conditions until completed confluency. Differentiation was induced, and cellular glucose uptake was assessed by measuring amount of glucose remained in culture media after exposed cells to different concentrations and compounds of green tea for 48h. EGCG, EC, and ECG significantly increased cellular glucose uptake compared to control. Data presented mean  $\pm$  SEM, \*\*\* $p < 0.001$ , \*\*\*\* $p < 0.0001$ ,  $n = 3$ .

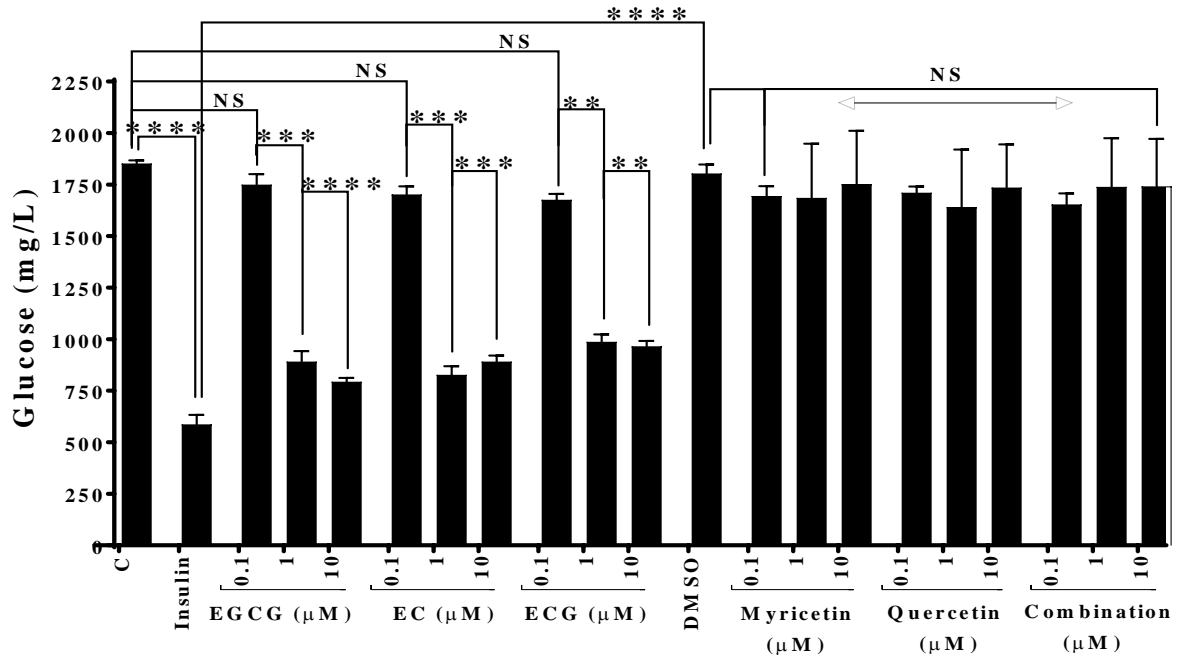


**Figure 3.8 Selected green tea compounds increase glucose uptake in 3T3-L1 cells.**

3T3L1 cells were seeded in 24 well plate at density  $1.5 \times 10^4$  and incubated in standard conditions until completed confluency. Differentiation was induced, and cellular glucose uptake was investigated by measuring amount of glucose remained in culture media after exposed cells to different concentrations and compounds of green tea for 72h. EGCG, EC, and ECG significantly increased cellular glucose uptake compared to control. Data presented mean  $\pm$  SEM, \*\* $p < 0.01$  \*\*\* $p < 0.001$ , \*\*\*\* $p < 0.0001$ ,  $n = 3$ .

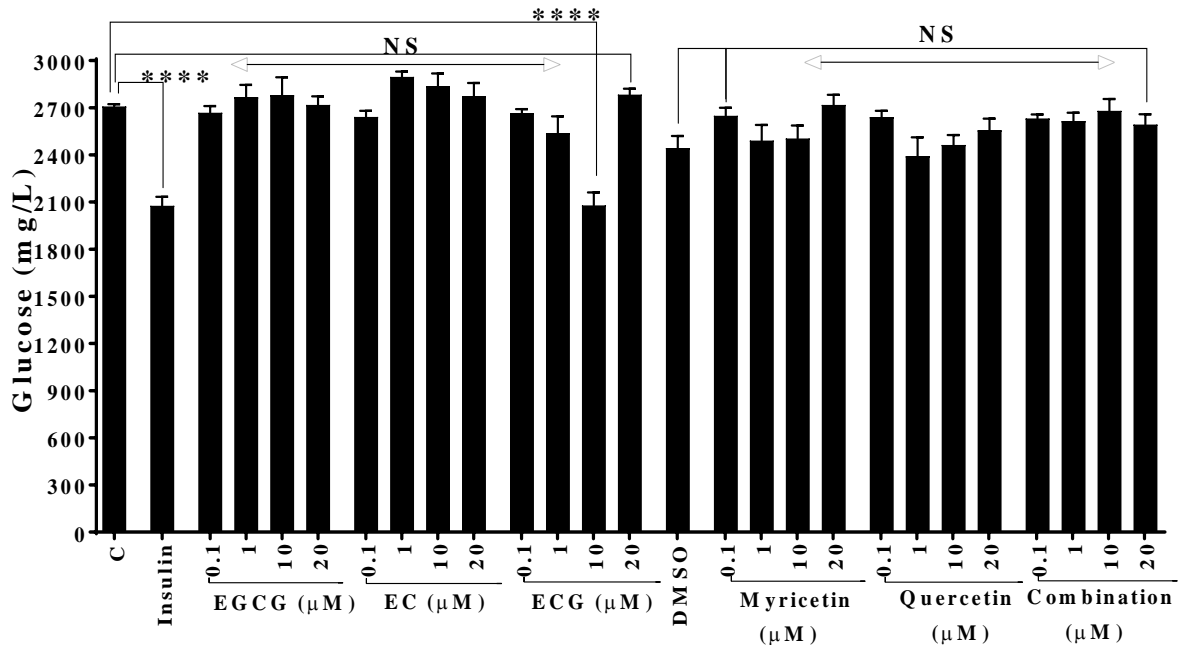


**Figure 3.9 Selected green tea compounds increase glucose uptake in AML12 cells.**

AML12 cells were seeded in 24 well plate at density  $2 \times 10^5$  and incubated in standard conditions until completed confluency. Cellular glucose uptake was investigated by measuring the amount of glucose remained in culture media after exposed cells to different concentrations and compounds of green tea for 24h. Only ECG at  $10 \mu\text{M}$  significant increased cellular glucose uptake compared to control. Data presented mean  $\pm$  SEM, \*\*\*\* $p < 0.0001$ ,  $n = 3$ .

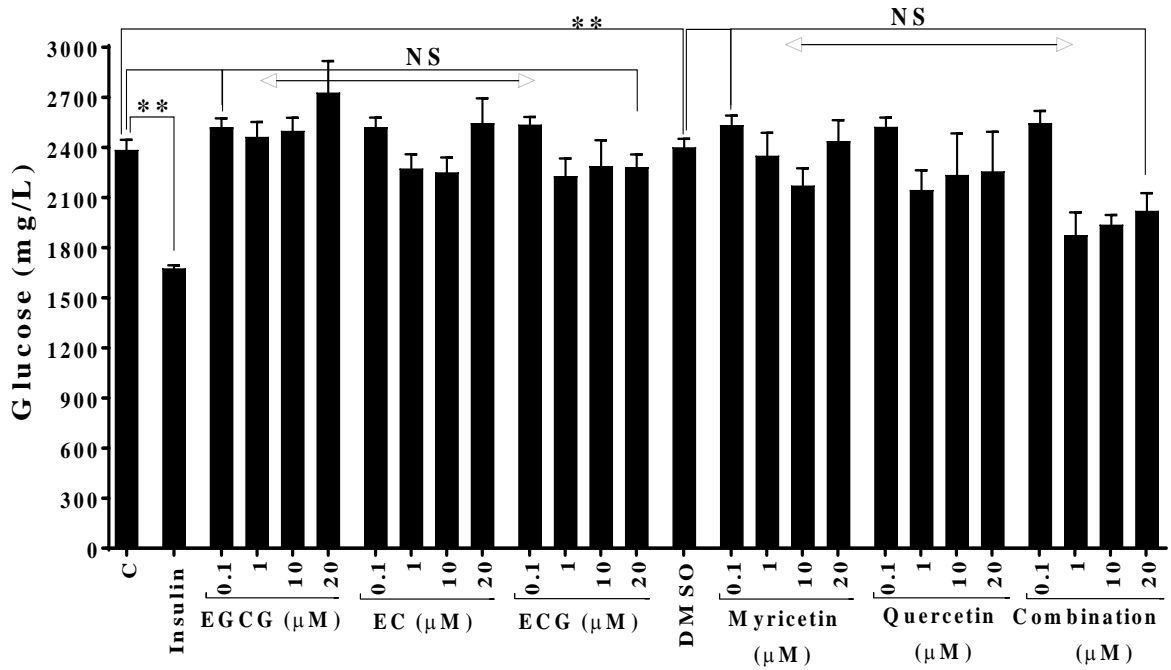


**Figure 3.10 Green tea compounds and glucose uptake in AML12 cells.**

AML12 cells were seeded in 24 well plate at density  $2 \times 10^5$  and incubated in standard conditions until completed confluency. Cellular glucose uptake was assessed by measuring amount of glucose remained in culture media after exposed cells to different concentrations and compounds of green tea for 48h. No effect of these compounds on glucose uptake was observed compared to control. Data presented mean  $\pm$  SEM, \*\* $p < 0.01$ ,  $n = 3$ .

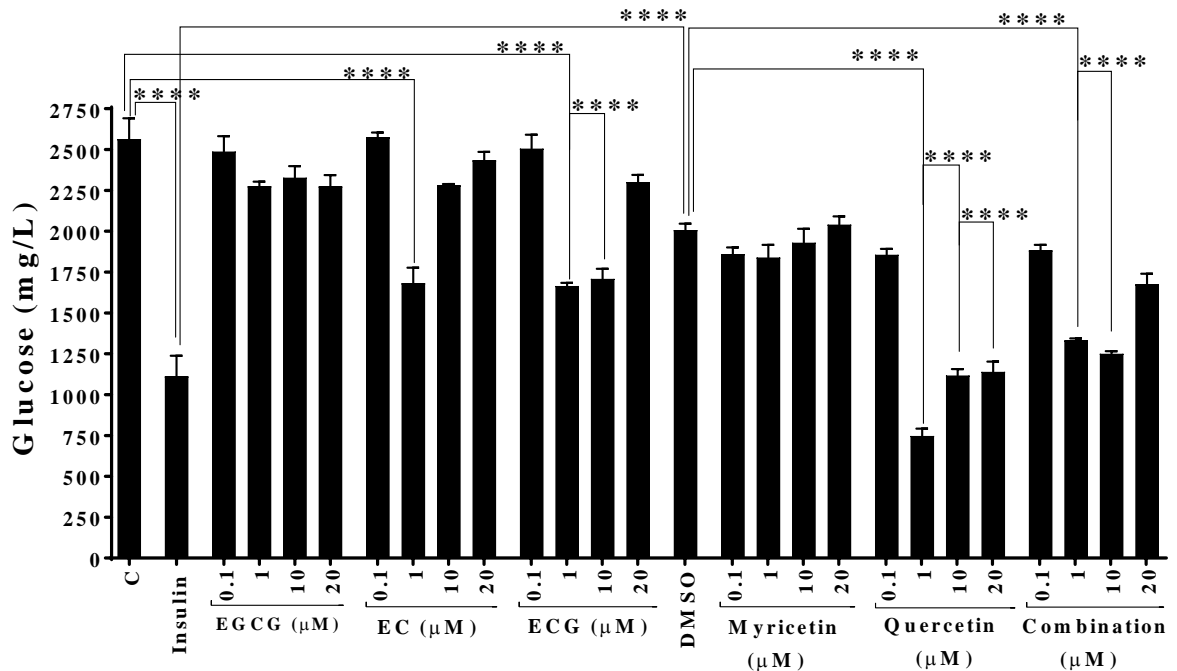


**Figure 3.11 Selected green tea compounds increase glucose uptake in AML12 cells.**

AML12 cells were seeded in 24 well plate at density  $2 \times 10^5$  and incubated in standard conditions until completed confluency. Cellular glucose uptake was investigated by measuring the amount of glucose remained in culture media after exposed cells to different concentrations and compounds of green tea for 72h. The result showed a significant increase of cellular glucose uptake responding to EC, ECG, quercetin, and combination compared to control. Data presented mean  $\pm$  SEM, \*\*\*\* $p < 0.0001$ ,  $n = 3$ .

### 3.3.4 The role of AMPK and Akt in enhanced glucose uptake in C2C12 cells by green tea compounds

The role of the AMPK and Akt signalling pathways in the gluco-regulatory effects of selected green tea compounds that increased glucose uptake in C2C12 cells were investigated by co-incubating cells with specific AMPK or Akt inhibitor molecules in addition to green tea compounds. Differentiated C2C12 cells were treated with 1 and 10 $\mu$ M of EGCG, EC, and ECG with and without AMPK or Akt inhibitor molecules for 48 and 72h. 1 and 10 $\mu$ M EGCG increased glucose uptake by 36.5% $\pm$ 4.3% ( $p=0.0069$ ), 37.3% $\pm$ 2.2% ( $p=0.0051$ ) after 48h and 45.14% $\pm$ 4.8% ( $p<0.0001$ ), 55.7% $\pm$ 14% ( $p<0.0001$ ) after 72h. Co-incubation with AMPK or Akt inhibitors alongside 1 and 10 $\mu$ M EGCG for 48h produced significant reductions of glucose uptake compared to EGCG alone, in response to AMPK inhibition. The recorded reductions were: 48.6% $\pm$ 13% ( $p<0.0001$ ) and 73% $\pm$ 11.7% ( $p=0.0002$ ) (Figure 3.12 A). Both AMPK and Akt inhibitors incubated alongside 1 and 10 $\mu$ M EGCG significantly decreased glucose uptake after 72h incubation. These decreases were: 65.9% $\pm$ 5.3% ( $p <0.0001$ ) and 124.2% $\pm$ 5.1% ( $p<0.0001$ ) by AMPK inhibitor, 40.6% $\pm$ 3.4% ( $p=0.0242$ ) and 49.7% $\pm$ 4.7% ( $p=0.0273$ ) by Akt (Figure 3.12 B). EC at 1 and 10 $\mu$ M significantly elevated glucose uptake by 38.33% $\pm$ 6.5% ( $p<0.0001$ ) and 41% $\pm$ 3.6% respectively ( $p<0.0001$ ) after 48h, and by 56.8% $\pm$ 6.6% ( $p<0.0001$ ) and 46.1% $\pm$ 2.4% ( $p<0.0001$ ) after 72h. These increases were inhibited by 74.3% $\pm$ 12.6% ( $p<0.0001$ ) and 56.5% $\pm$ 2.6% ( $p=0.0003$ ) through inhibition AMPK for 48h (Figure 3.13 A), whereas both AMPK and Akt inhibitors significantly suppressed glucose uptake by 123.8% $\pm$ 6.4% ( $p<0.0001$ ) and 100.4% $\pm$ 6.5% ( $p<0.0001$ ), 60.9% $\pm$ 5.2% ( $p=0.0031$ ), and 39.3% $\pm$ 1.9% ( $p=0.0413$ ) after 72h respectively (Figure 3.13 B). Similarly, 1 and 10 $\mu$ M ECG mediated 47.3% $\pm$ 5.2% ( $p<0.0001$ ), 47.6% $\pm$ 5.2% ( $p <0.0001$ ), 51.7% $\pm$ 5.7% ( $p<0.0001$ ), and 48.8% $\pm$ 6.4% ( $p<0.0001$ ) increases in glucose uptake after 48 and 72h. Inhibition of AMPK suppressed these increases in glucose uptake by 103.3% $\pm$ 9.7% ( $p<0.0001$ ) and 63.8% $\pm$ 3.2% ( $p<0.0001$ ) after 48h (Figure 3.14 A), while both AMPK and Akt inhibitors caused 87% $\pm$ 6.2% ( $p<0.0001$ ), 122.8% $\pm$ 5.4% ( $p<0.0001$ ), 59.8% $\pm$ 15.5% ( $p=0.0171$ ), and 55% $\pm$ 2.4% ( $p=0.00224$ ) decrease in glucose uptake compared to treatment alone after 72h intervention (Figure 3.14 B).

### 3.3.5 The role of AMPK and Akt in enhanced glucose uptake in 3T3-L1 cells by green tea compounds

The role of AMPK and Akt was also examined in adipocyte glucose uptake in response to selected green tea active compounds. Mature 3T3-L1 cells were co-cultured with 10 $\mu$ M of AMPK or Akt selective inhibitor molecules alongside 1 and 10 $\mu$ M of EGCG, EC, and ECG that increased glucose uptake previously for 48 and 72h. EGCG at 1 and 10 $\mu$ M caused 38.2% $\pm$ 3.5% ( $p<0.0001$ ), 37.8% $\pm$ 6.8% ( $p<0.0001$ ), 57.9% $\pm$ 13.4% ( $p<0.0001$ ), and 54.7% $\pm$ 13.2% ( $p<0.0001$ ) increases in glucose uptake compared to control after 48 and 72h respectively. These increases were significantly inhibited by the Akt inhibitor only and estimated reductions were 45.5% $\pm$ 5.9% ( $p=0.0041$ ), 49.5% $\pm$ 1.5% ( $p=0.0010$ ),

117.8%±13.5% ( $p<0.0001$ ), and 90.5%±8.4% ( $p=0.0022$ ) after 48 and 72h incubation respectively (Figure 3.15). A similar effect was observed when the cells were treated with 1 and 10µM of EC. These compounds caused 37.9%±6.1% ( $p<0.0001$ ), 34%±7% ( $p=0.0012$ ), 55.4%±13% ( $p<0.0001$ ), and 51.8%±10.6% ( $p<0.0001$ ) increases in glucose uptake after 48 and 72h incubation. These increases in glucose uptake were suppressed by 57.5%±6.7% ( $p=0.0005$ ), 57.6%±7.2% ( $p=0.0002$ ), 102.2%±11% ( $p<0.0001$ ), and 72.9%±7.9% ( $p=0.0032$ ) when the cells were exposed to the Akt inhibitor after 48 and 72h incubation respectively (Figure 3.16). Furthermore, 1 and 10µM ECG significantly increased glucose uptake by 49.7%±15.9% ( $p<0.0001$ ), 41.6%±6.5% ( $p<0.0001$ ), 59.2%±12.4% ( $p<0.0001$ ), and 60.6%±10.3% ( $p<0.0001$ ) after 48 and 72h incubation compared to control. Co-incubation with the Akt inhibitor significantly reduced glucose uptake compared to treatment alone, with reductions of 59.6%±7.5% ( $p=0.0104$ ), 49%±6.3% ( $p=0.0179$ ), 86.6%±7.3% ( $p=0.0084$ ), and 95%±8.4% ( $p=0.0039$ ) after 48 and 72h respectively being recorded (Figure 3.17). Alternately, co-incubation with an AMPK inhibitor alongside green tea treatments for 48 and 72h did not significantly change glucose uptake rates.

### **3.3.6 The role of AMPK and Akt in enhanced glucose uptake in AML12 cells by green tea compounds**

The role of AMPK and Akt signalling pathways on selected compounds of green tea that enhanced glucose uptake in AML12 cells were explored through co-incubating cells with 10µM of selective AMPK or Akt inhibitor molecules in the presence of green tea compounds that previously produced significant increases glucose uptake. The impact of EC, ECG, quercetin, and combination of experimental green tea compounds in AML12 cells was only apparent after 72h treatment with no significant effect displayed before that, except ECG at 10µM after 24h. The latter compound significantly increased glucose uptake by 16.8%±1.95% ( $p=0.0009$ ), and this amount was suppressed by adding an Akt inhibitor, which reduced glucose uptake by 16.4%±4% ( $p=0.0135$ ) (Figure 3.18). EC at 1µM for 72h significantly increased glucose uptake by 32.4%±7.4% ( $p=0.0086$ ), which was reduced by 48.5%±9.5% by the action of the Akt inhibitor molecule ( $p=0.0076$ , Figure 3.19). Also, 1 and 10µM of ECG increased glucose uptake by 30.2%±7.3% ( $p=0.0011$ ) and 29.9%±5.6% ( $p=0.0021$ ) respectively after 72h, and Akt inhibition suppressed this by 37%±5.3% ( $p=0.0087$ ) and 42%±6.6% ( $p=0.0027$ ) respectively (Figure 3.20). A combination of green tea compounds increased glucose uptake at 1 and 10µM up to 38.2%±4.8% ( $p=0.0002$ ) and 35.75%±3.6% ( $p=0.0005$ ) after 72h incubation respectively. Again the Akt pathway seemed to be involved in this effect by suppressing glucose uptake by 45.8%±9.8% ( $p=0.0040$ ) and 52.8%±9.8 ( $p=0.0011$ ) respectively, compared to treatment alone (Figure 3.21). Furthermore, quercetin at 1, 10, and 20µM caused 34.3%±5.6% ( $p=0.0005$ ), 41.8%±2.8% ( $p=0.0008$ ), and 34.2%±5.6 ( $p=0.0008$ ) increases in glucose uptake after 72h incubation respectively, whilst Akt inhibition significantly decreased this by 45.8%±7.9% ( $p=0.0033$ ), 67%±12.6% ( $p=0.0022$ ), and 53.4%±7.3% ( $p=0.0004$ ) respectively (Figure 3.22 and Figure 3.23).

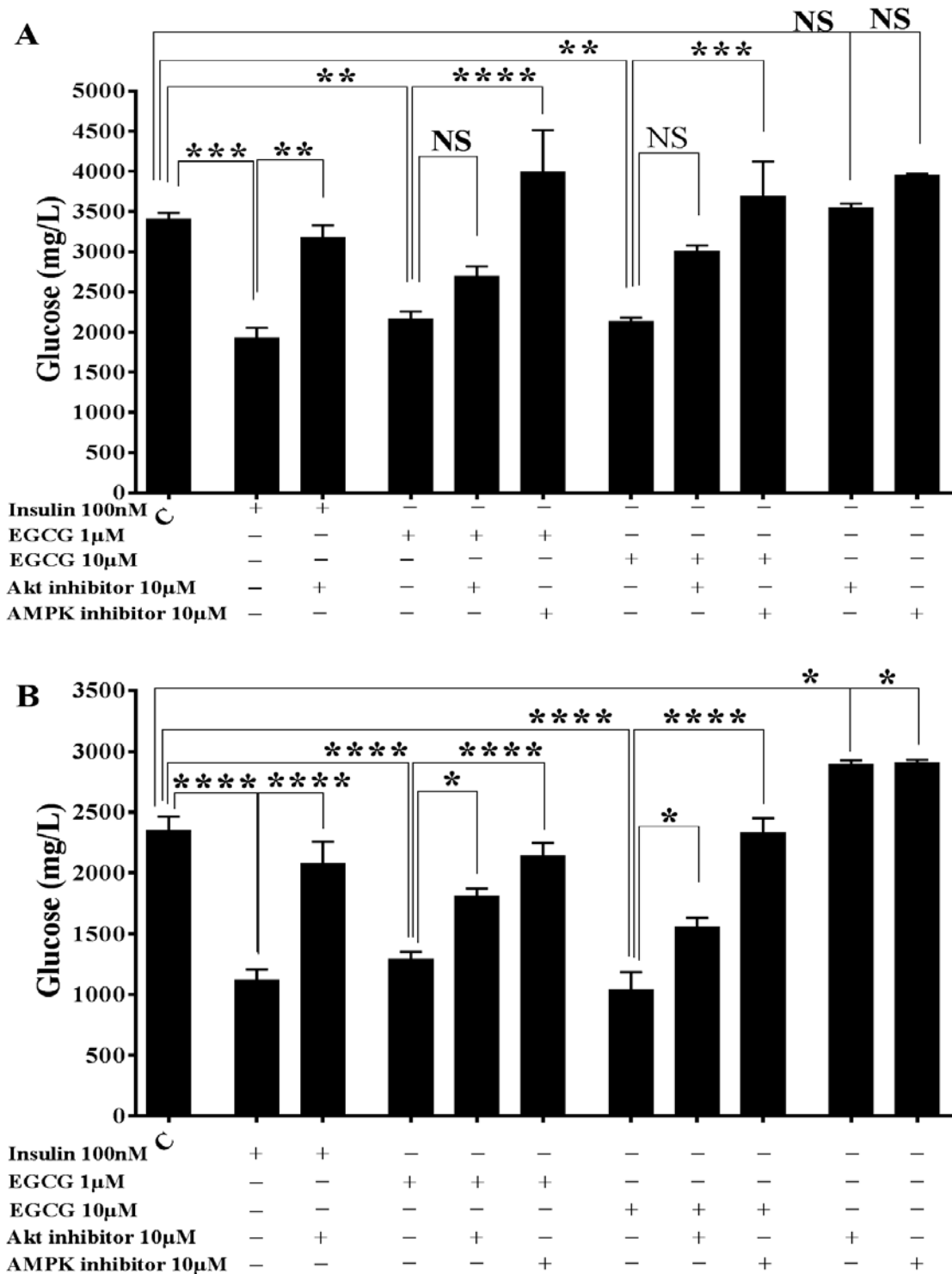


**Figure 3.12 AMPK and Akt inhibitors reduce EGCG induced glucose uptake in C2C12 cells.**

C2C12 cells were seeded in 24 well plate at density  $2 \times 10^5$  and incubated in standard conditions until reached 80% confluency. Differentiation was induced, and cells were treated with EGCG in presence and absence AMPK or Akt inhibitor, followed by estimating glucose uptake through measuring glucose remained in the media. (A) EGCG significantly increased glucose uptake compared to control, and this effect was significantly inhibited by AMPK inhibitor after 48h. (B) EGCG significantly increased glucose uptake compared to control, and this effect was significantly inhibited by AMPK and Akt inhibitors after 72h, and strongest effect mediated by AMPK inhibitor. Data presented mean  $\pm$  SEM, \* $p < 0.05$ , \*\* $p < 0.01$ , \*\*\* $p < 0.001$ , \*\*\*\* $p < 0.0001$ ,  $n = 3$ .

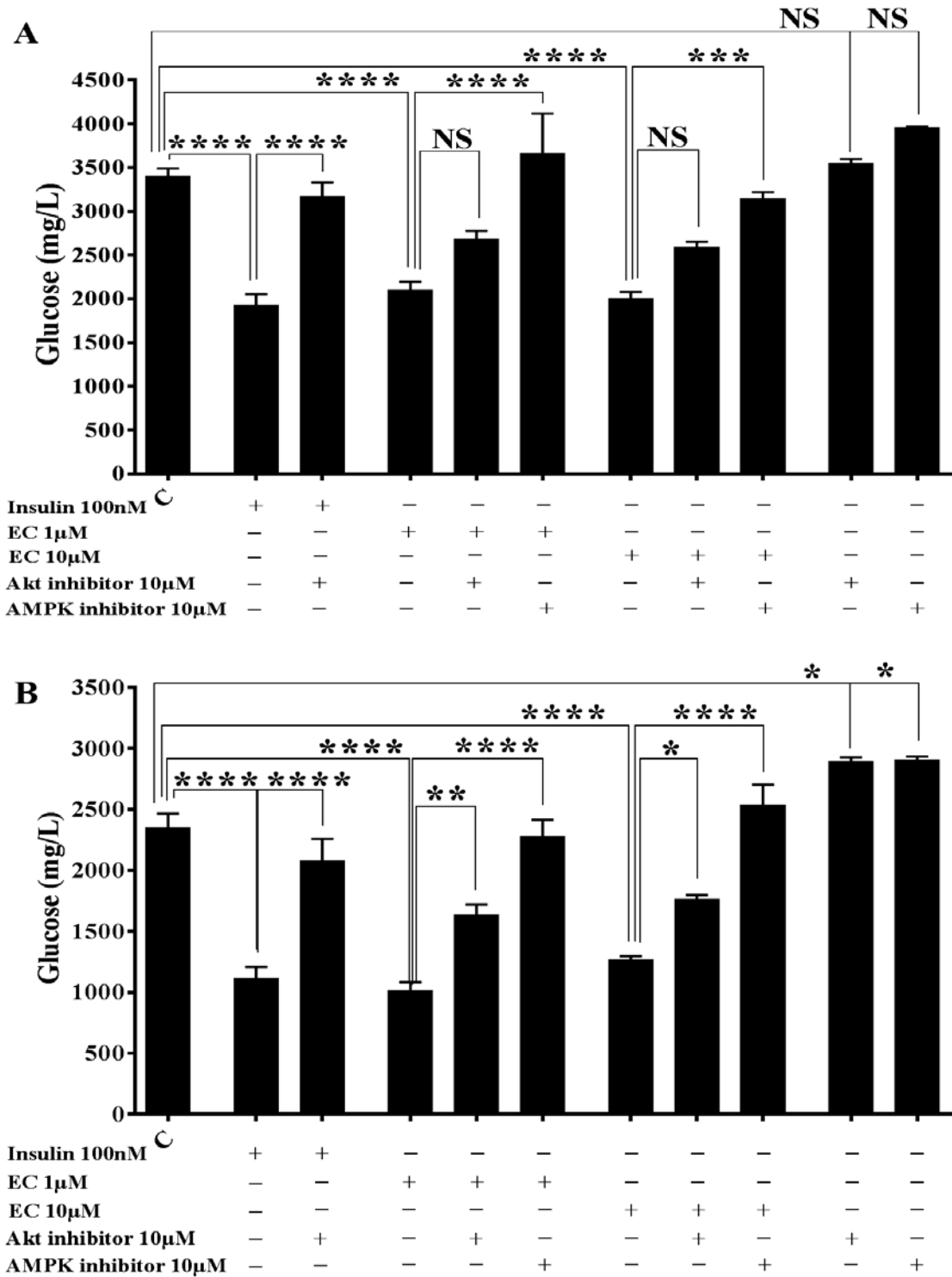


**Figure 3.13 AMPK and Akt inhibitors reduce EC induced glucose uptake in C2C12 cells.**

C2C12 cells were seeded in 24 well plate at density  $2 \times 10^5$  and incubated in standard conditions until reached 80% confluency. Differentiation was induced, and cells were treated with EC in presence and absence AMPK or Akt inhibitor, followed by estimating glucose uptake through measuring glucose remained in the media. (A) EC significantly increased glucose uptake compared to control, and this effect was significantly inhibited by AMPK inhibitor after 48h. (B) EC significantly increased glucose uptake compared to control, and this effect was significantly inhibited by AMPK and Akt inhibitors after 72h, and strongest effect mediated by AMPK inhibitor. Data presented mean  $\pm$  SEM, \* $p < 0.05$ , \*\* $p < 0.01$ , \*\*\* $p < 0.001$ , \*\*\*\* $p < 0.0001$ ,  $n = 3$ .

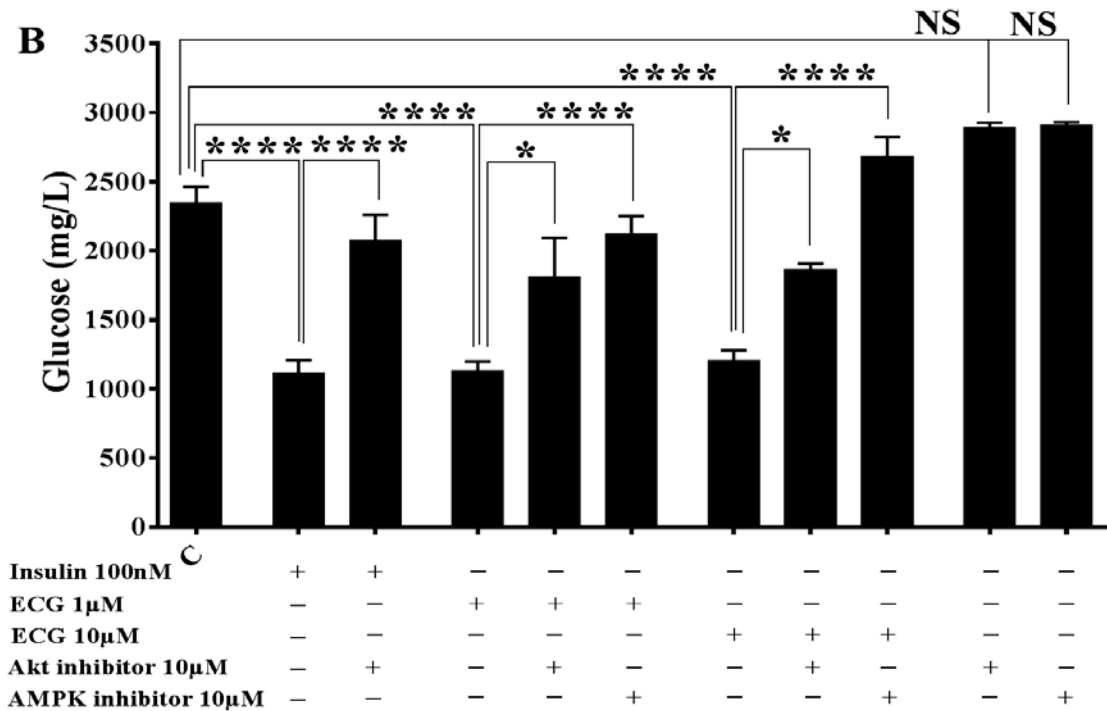
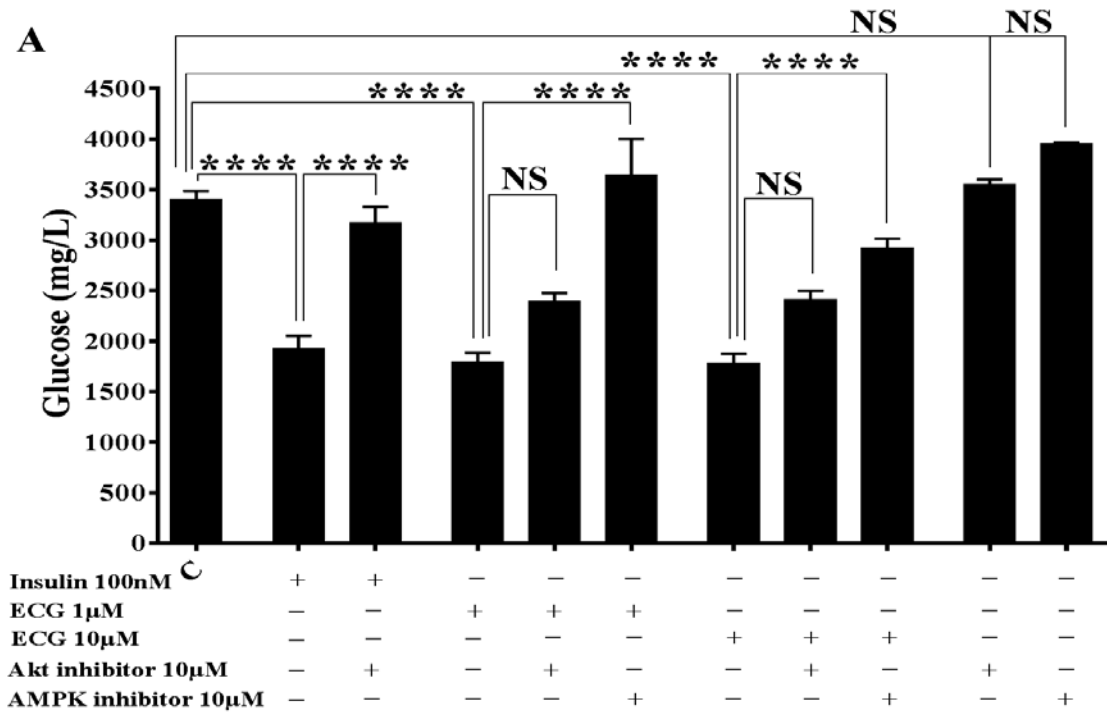


**Figure 3.14 AMPK and Akt inhibitors reduce ECG induced glucose uptake in C2C12 cells.**

C2C12 cells were seeded in 24 well plate at density  $2 \times 10^5$  and incubated in standard conditions until reached 80% confluency. Differentiation was induced, and cells were treated with ECG in presence and absence AMPK or Akt inhibitor, followed by estimating glucose uptake through measuring glucose remained in the media. (A) ECG significantly increased glucose uptake compared to control, and this effect was significantly inhibited by AMPK inhibitor after 48h. (B) ECG significantly increased glucose uptake compared to control, and this effect was significantly inhibited by AMPK and Akt inhibitors after 72h, and strongest effect mediated by AMPK inhibitor. Data presented mean  $\pm$  SEM, \* $p < 0.05$ , \*\*\*\* $p < 0.0001$ ,  $n = 3$ .

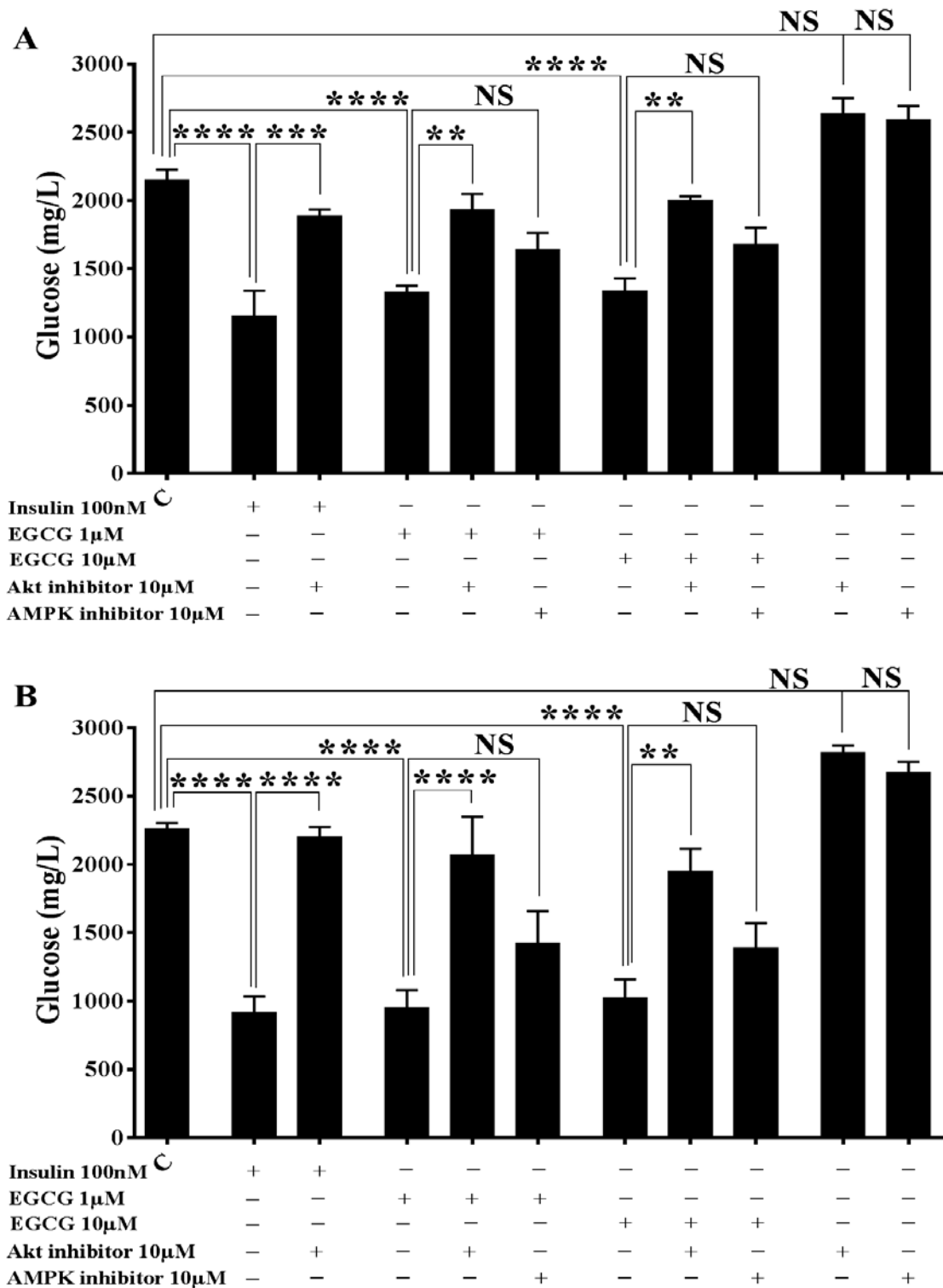


**Figure 3.15 Akt inhibitor reduces EGCG induced glucose uptake in 3T3-L1 cells.**

3T3L1 cells were seeded in 24 well plate at density  $1.5 \times 10^4$  and incubated in standard conditions until completed confluency. Differentiation was induced, and cells were treated with EGCG in presence and absence AMPK or Akt inhibitor, followed by estimating glucose uptake through measuring glucose remained in the media. (A) EGCG significantly increased glucose uptake compared to control, and this effect was significantly inhibited by AMPK inhibitor after 48h. (B) EGCG significantly increased glucose uptake compared to control, and this effect was significantly inhibited by AMPK inhibitor after 72h. Data presented mean  $\pm$  SEM, \*\* $p < 0.01$ , \*\*\* $p < 0.001$ , \*\*\*\* $p < 0.0001$ ,  $n = 3$ .

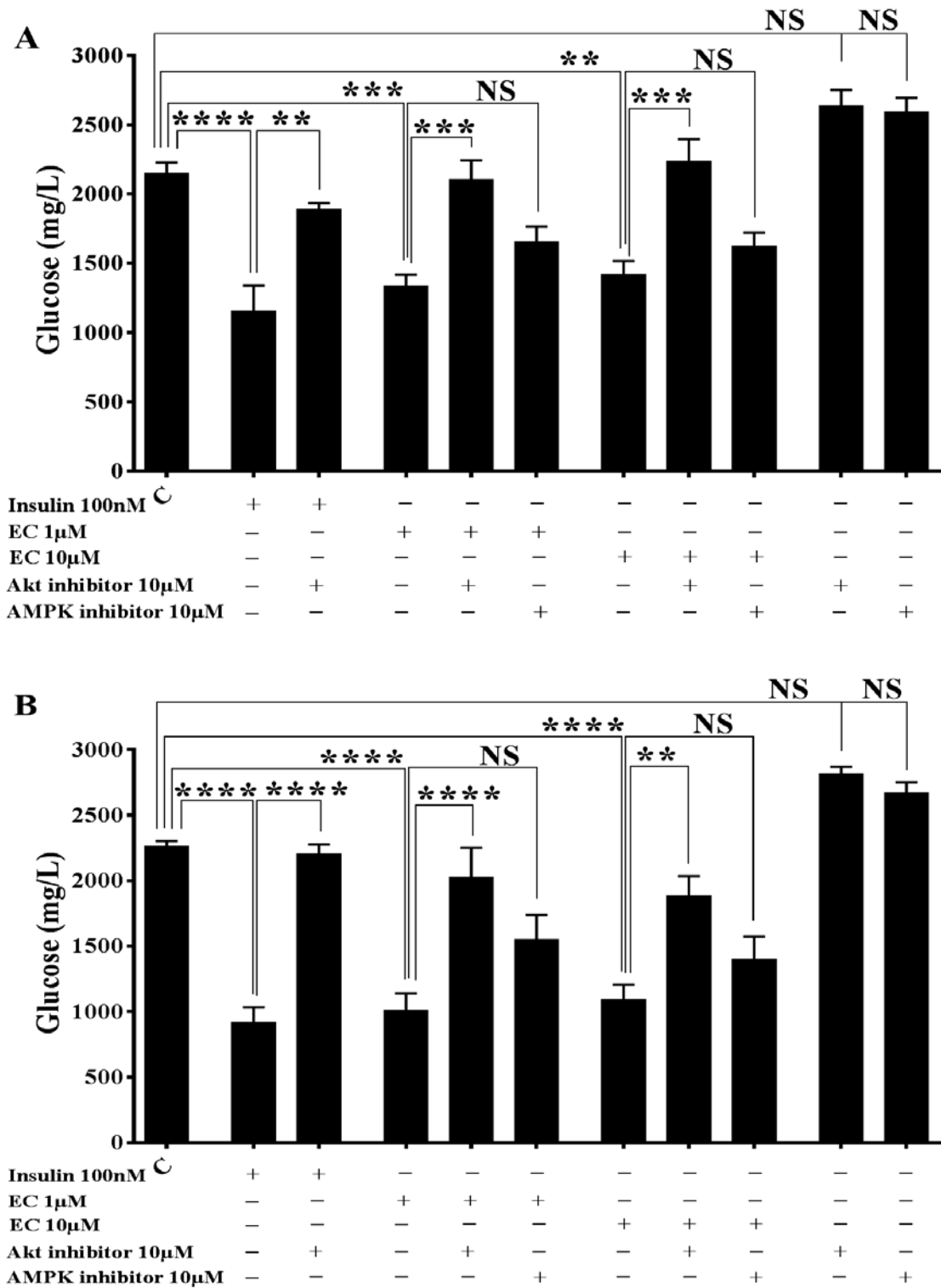


**Figure 3.16 Akt inhibitor reduces EC induced glucose uptake in 3T3-L1 cells.**

3T3L1 cells were seeded in 24 well plate at density  $1.5 \times 10^4$  and incubated in standard conditions until completed confluency. Differentiation was induced, and cells were treated with EC in presence and absence AMPK or Akt inhibitor, followed by estimating glucose uptake through measuring glucose remained in the media. (A) EC significantly increased glucose uptake compared to control, and this effect was significantly inhibited by AMPK inhibitor after 48h. (B) EC significantly increased glucose uptake compared to control, and this effect was significantly inhibited by AMPK inhibitor after 72h. Data presented mean  $\pm$  SEM, \*\* $p < 0.01$ , \*\*\* $p < 0.001$ , \*\*\*\* $p < 0.0001$ ,  $n = 3$ .

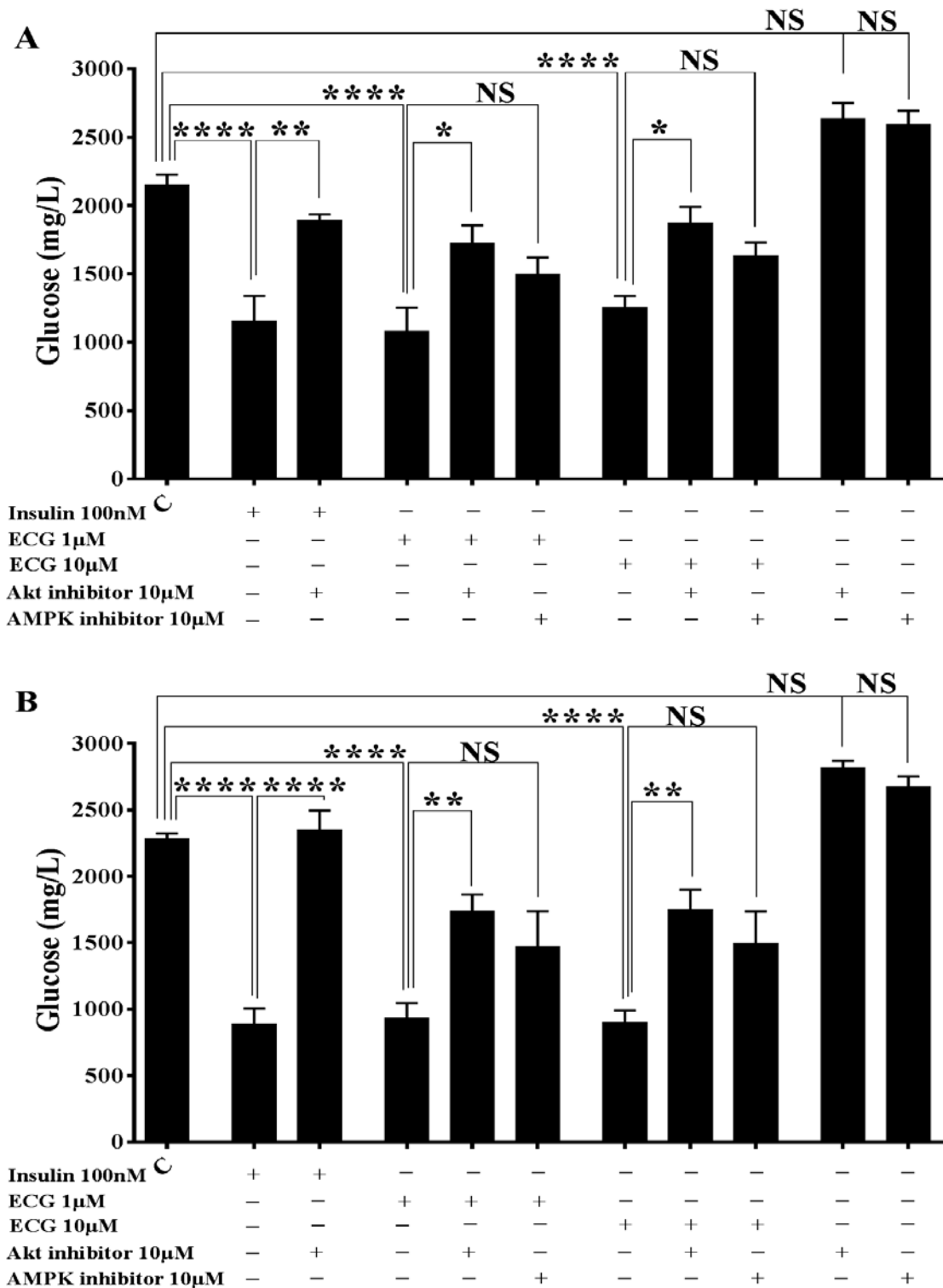


**Figure 3.17 Akt inhibitor reduces ECG induced glucose uptake in 3T3-L1 cells.**

3T3L1 cells were seeded in 24 well plate at density  $1.5 \times 10^4$  and incubated in standard conditions until completed confluency. Differentiation was induced, and cells were treated with ECG in presence and absence AMPK or Akt inhibitor, followed by estimating glucose uptake through measuring glucose remained in the media. (A) ECG significantly increased glucose uptake compared to control, and this effect was significantly inhibited by AMPK inhibitor after 48h. (B) ECG significantly increased glucose uptake compared to control, and this effect was significantly inhibited by AMPK inhibitor after 72h. Data presented mean  $\pm$  SEM, \* $p < 0.05$ , \*\* $p < 0.01$ , \*\*\*\* $p < 0.0001$ ,  $n = 3$ .

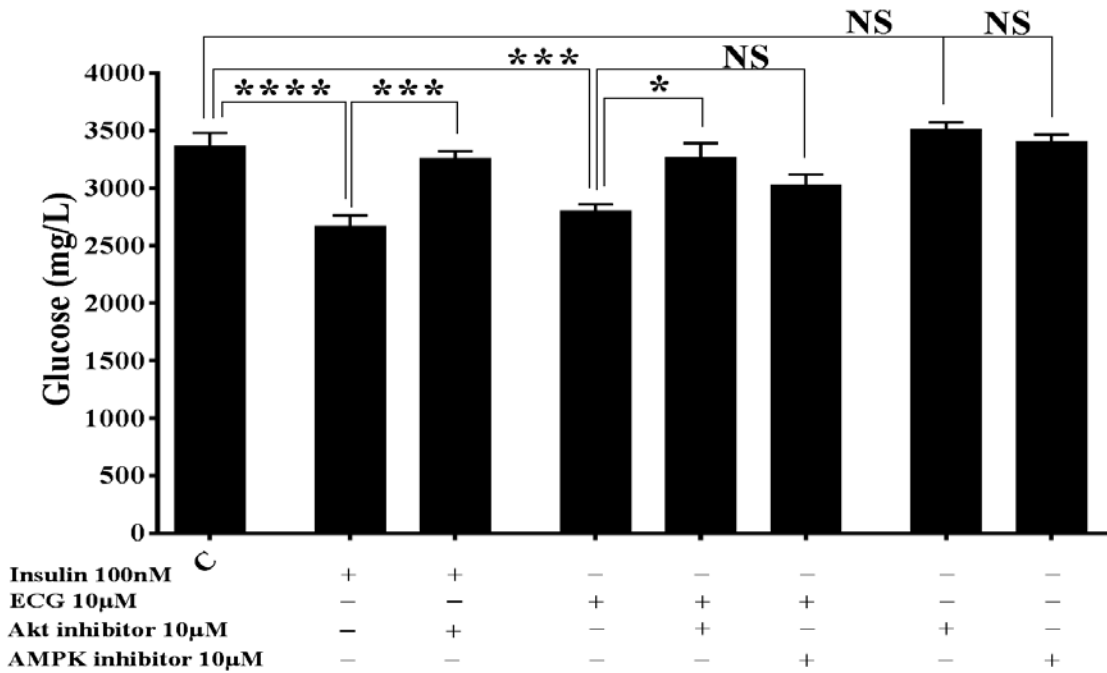


**Figure 3.18 Akt inhibitor reduces ECG induced glucose uptake in AML12 cells.**

AML12 cells were seeded in 24 well plate at density  $2 \times 10^5$  and incubated in standard conditions until completed confluency. Cells were treated with ECG in presence and absence AMPK or Akt inhibitor, followed by estimating glucose uptake through measuring glucose remained in the media. ECG significantly increased glucose uptake after 24h compared to control, and this increase was significantly suppressed by Akt inhibitor. Data presented mean  $\pm$  SEM, \* $p < 0.05$ , \*\*\* $p < 0.001$ , \*\*\*\* $p < 0.0001$ ,  $n = 3$ .

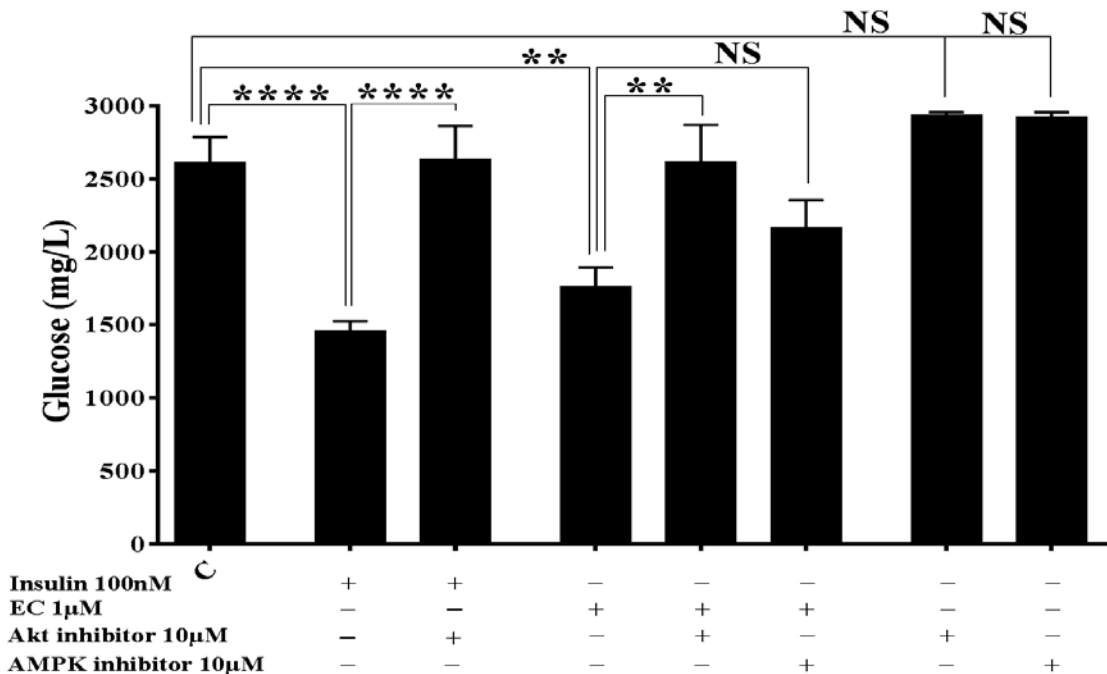


**Figure 3.19 Akt inhibitor reduces EC induced glucose uptake in AML12 cells.**

AML12 cells were seeded in 24 well plate at density  $2 \times 10^5$  and incubated in standard conditions until completed confluency. Cells were treated with EC in presence and absence AMPK or Akt inhibitor, followed by estimating glucose uptake through measuring glucose remained in the media. EC significantly increased glucose uptake after 72h compared to control, and this increase was significantly suppressed by Akt inhibitor. Data presented mean  $\pm$  SEM, \*\* $p < 0.01$ , \*\*\*\* $p < 0.0001$ ,  $n = 3$ .

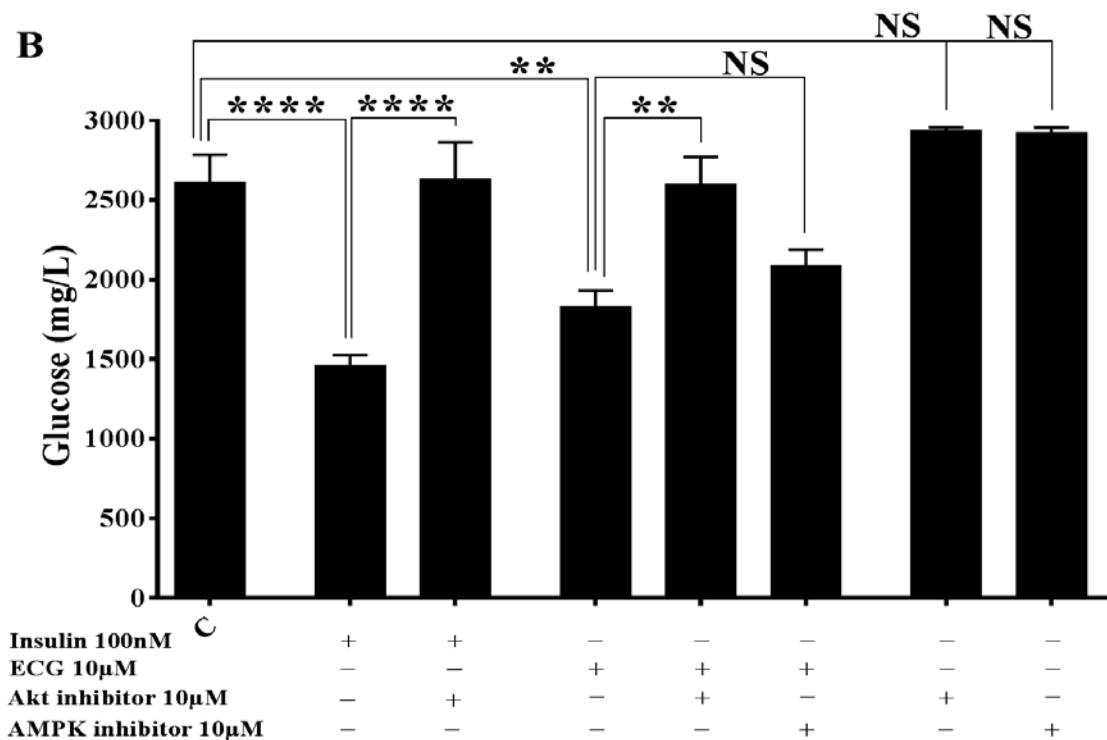
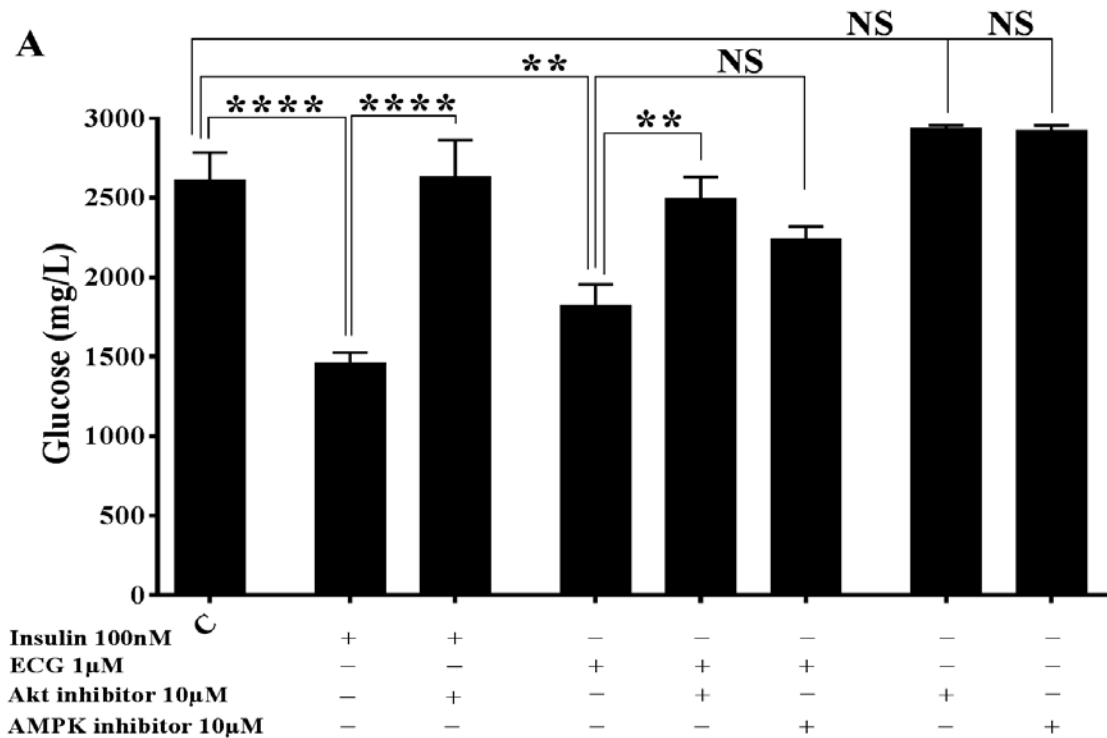


**Figure 3.20 Akt inhibitor reduces ECG induced glucose uptake in AML12 cells.**

AML12 cells were seeded in 24 well plate at density  $2 \times 10^5$  and incubated in standard conditions until completed confluency. Cells were treated with ECG in presence and absence AMPK or Akt inhibitor, followed by estimating glucose uptake through measuring glucose remained in the media. (A, B) ECG at 1 and  $10 \mu\text{M}$  significantly increased glucose uptake after 72h compared to control, and this increase was significantly suppressed by Akt inhibitor. Data presented mean  $\pm$  SEM, \*\* $p < 0.01$ , \*\*\*\* $p < 0.0001$ ,  $n = 3$ .

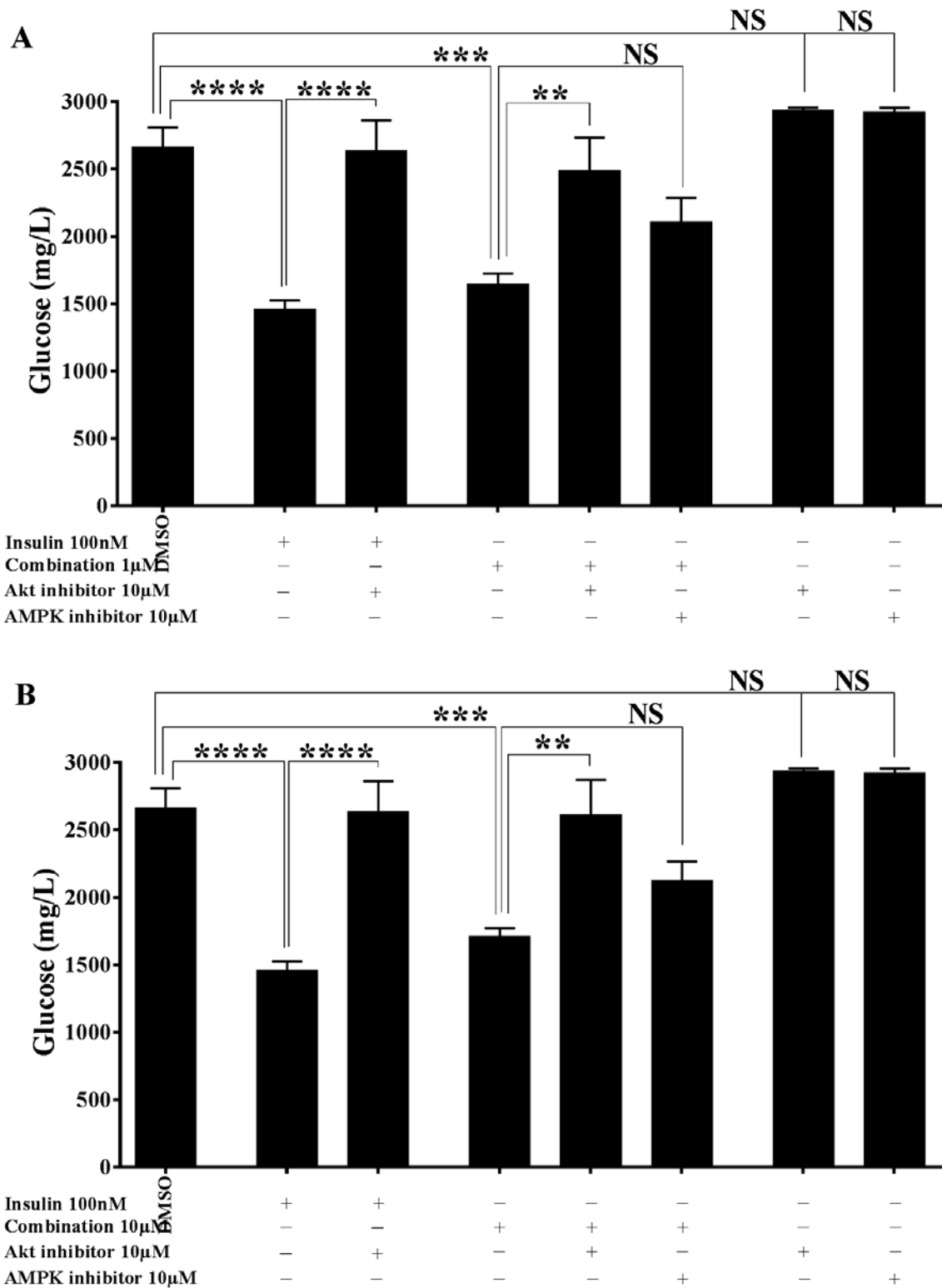


**Figure 3.21 Akt inhibitor reduces green tea combination induced glucose uptake in AML12 cells.**

AML12 cells were seeded in 24 well plate at density  $2 \times 10^5$  and incubated in standard conditions until completed confluency. Cells were treated with combination of green tea compounds in presence and absence AMPK or Akt inhibitor, followed by estimating glucose uptake through measuring glucose remained in the media. (A, B) Green tea combination at 1 and  $10 \mu\text{M}$  significantly increased glucose uptake after 72h compared to control, and this increase was significantly suppressed by Akt inhibitor. Data presented mean  $\pm$  SEM,  $**p < 0.01$ ,  $***p < 0.0001$ ,  $n=3$ .

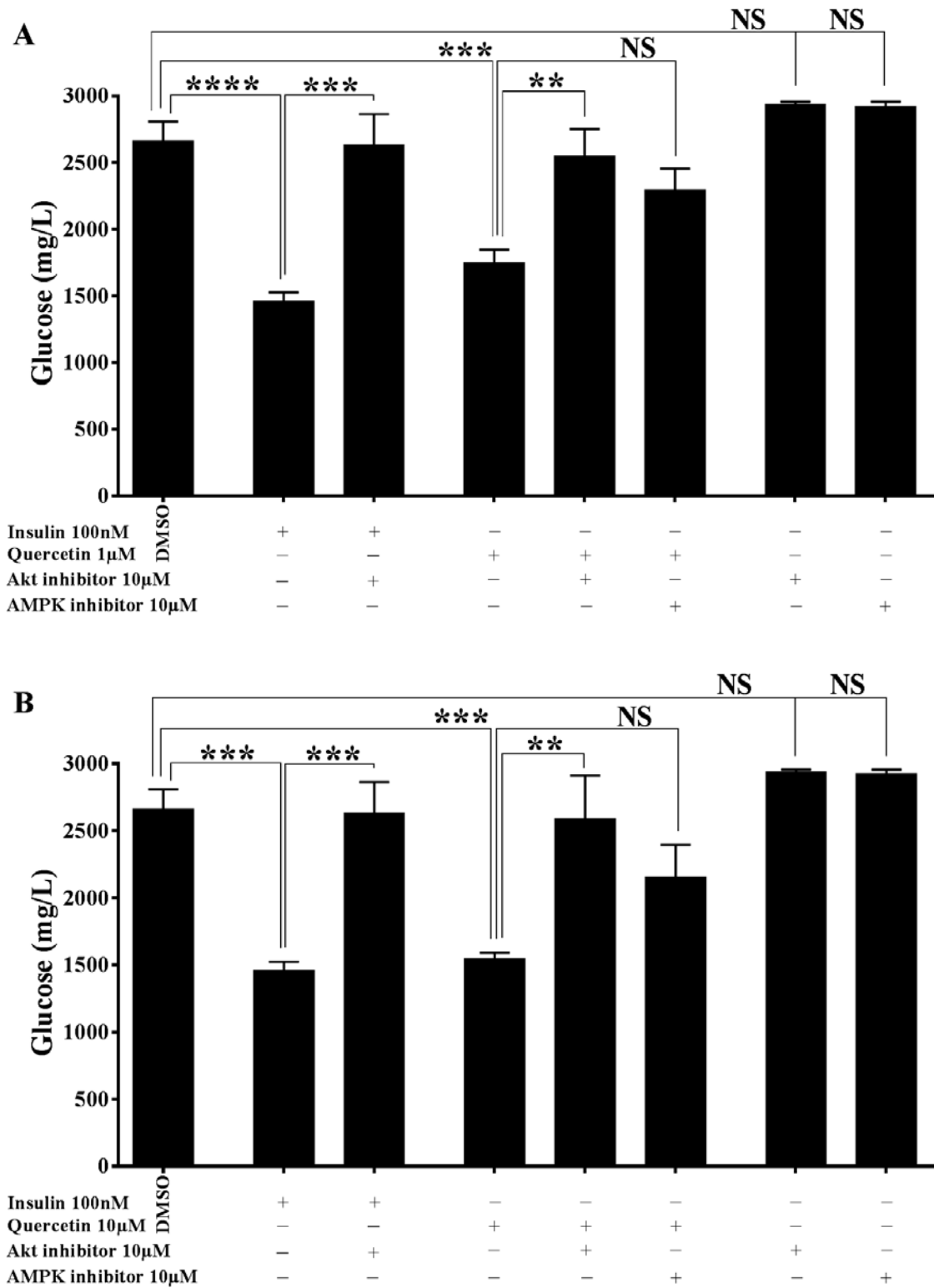


**Figure 3.22 Akt inhibitor reduces quercetin induced glucose uptake in AML12 cells.**

AML12 cells were seeded in 24 well plate at density  $2 \times 10^5$  and incubated in standard conditions until completed confluency. Cells were treated with quercetin in presence and absence AMPK or Akt inhibitor, followed by estimating glucose uptake through measuring glucose remained in the media. (A, B) Quercetin at 1 and 10μM significantly increased glucose uptake after 72h compared to control, and this increase was significantly suppressed by Akt inhibitor. Data presented mean  $\pm$  SEM, \*\*p<0.01, \*\*\*p<0.001, \*\*\*\*p<0.0001, n=3.

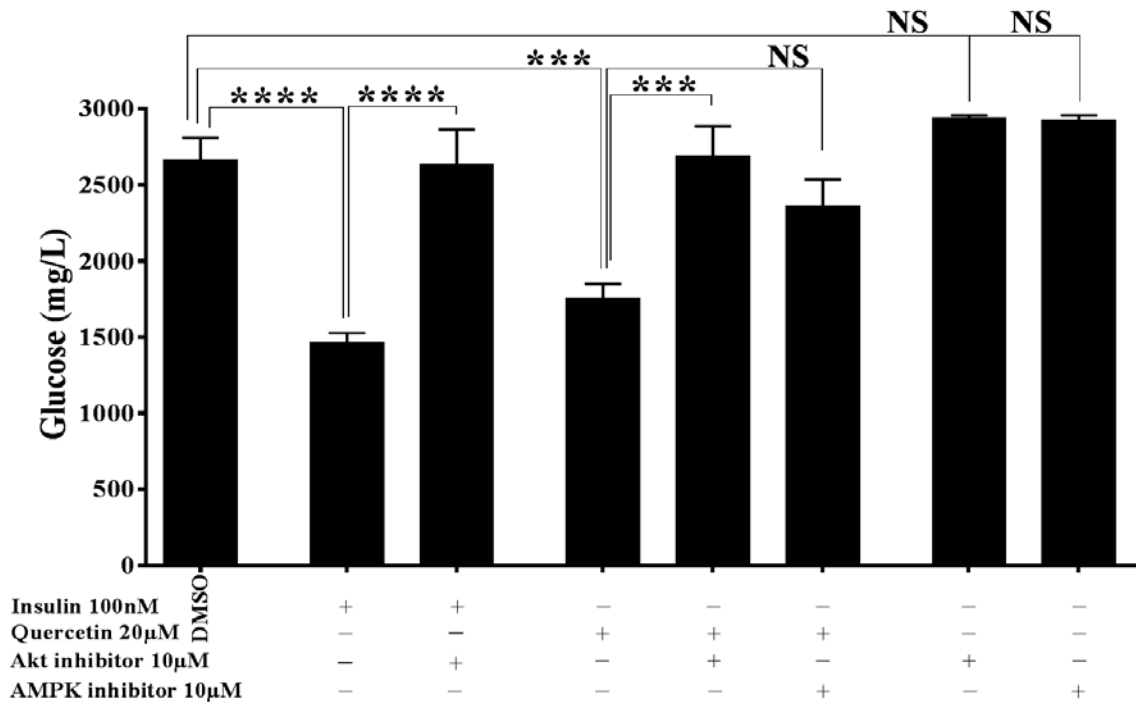


**Figure 3.23 Akt inhibitor reduces quercetin induced glucose uptake in AML12 cells.**

AML12 cells were seeded in 24 well plate at density  $2 \times 10^5$  and incubated in standard conditions until completed confluency. Cells were treated with  $20 \mu\text{M}$  of quercetin in presence and absence AMPK or Akt inhibitor, followed by estimating glucose uptake through measuring glucose remained in the media. Quercetin significantly increased glucose uptake after 72h compared to control, and this increase was significantly suppressed by Akt inhibitor. Data presented mean  $\pm$  SEM, \*\*\* $p < 0.001$ , \*\*\*\* $p < 0.0001$ ,  $n = 3$ .

### 3.3.7 Green tea compounds increased 2-NBDG uptake in C2C12 cells

2-NBDG is a fluorescent glucose analogue which has been successfully used to determine the rate of cellular glucose uptake in various cell lines (O'Neil, *et al.*, 2005). The 2-NBDG uptake was assessed in differentiated C2C12 cells after incubation with selected compounds of green tea that had previously shown a significant increase in glucose uptake. Treatment was performed for 6h to provide a shorter-term analysis of glucose movement. Results showed that 1 and  $10 \mu\text{M}$  EGCG, EC, and ECG significantly increased cellular 2-NBDG uptake in treated cells compared to control, however the increases are very small which contrast with glucose uptake measured by estimating amount of glucose remain in the media (Figure 3.24). The increases in the amount of fluorescence related to 2-NBDG uptake were recorded as:  $16.7\% \pm 2.4\%$  ( $p = 0.0001$ ),  $17.6\% \pm 2\%$  ( $p < 0.0001$ ),  $17.15 \pm 1.9\%$  ( $p < 0.0001$ ),  $18.28\% \pm 1.7\%$  ( $p < 0.0001$ ),  $17.18\% \pm 1.8\%$  ( $p < 0.0001$ ), and  $19.06\% \pm 2.2\%$  ( $p < 0.0001$ ) compared to control respectively.

### 3.3.8 Green tea compounds increased 2-NBDG uptake in 3T3-L1 cells

The 2-NBDG uptake was investigated in mature 3T3-L1 cells in response to selected compounds of green tea that showed a significant increase in glucose uptake previously for 6h. The results showed that 1 and  $10 \mu\text{M}$  EGCG, EC, and ECG significantly boosted cellular 2-NBDG uptake in treated cells

compared to control (Figure 3.25). Increases in fluorescence of  $21.15\pm 1.77\%$  ( $p<0.0001$ ),  $25.46\pm 1.76\%$  ( $p<0.0001$ ),  $24.12\pm 2\%$  ( $p<0.0001$ ),  $26.75\pm 2\%$  ( $p<0.0001$ ),  $22.14\pm 1.85\%$  ( $p<0.0001$ ), and  $26.30\pm 1.45\%$  ( $p<0.0001$ ) respectively were observed. These modest but significant glucose uptake are difference from amount of glucose uptake that measured by indirect estimated level of glucose remain in the media.

### 3.3.9 Green tea compounds increased 2-NBDG uptake in AML12 cells

Similarly, 2-NBDG uptake was investigated in AML12 when cultured with selected compounds of green tea that previously showed a significant increase in cellular glucose uptake. 1 and  $10\mu\text{M}$  of EC, ECG, and combination of green tea compounds, in addition to 1, 10,  $20\mu\text{M}$  of quercetin significantly increased 2-NBDG uptake (Figure 3.26). Percentage increases were:  $14.60\pm 1.33\%$  ( $p<0.0001$ ),  $17.23\pm 2\%$  ( $p<0.0001$ ),  $18.62\pm 1.64\%$  ( $p<0.0001$ ),  $18.96\pm 1.75\%$  ( $p<0.0001$ ),  $22.29\pm 1.43\%$  ( $p<0.0001$ ),  $25.44\pm 0.95\%$  ( $p<0.0001$ ),  $33.56\pm 0.87\%$  ( $p<0.0001$ ),  $25.63\pm 1.83\%$  ( $p<0.0001$ ), and  $23.89\pm 1.79\%$  ( $p<0.0001$ ) for EC, ECG, quercetin, and combination of green tea compared to control respectively. As previously mentioned, these little but significant elevated in glucose uptake are contradict from the indirect uptake that measured level of glucose remain in the media.

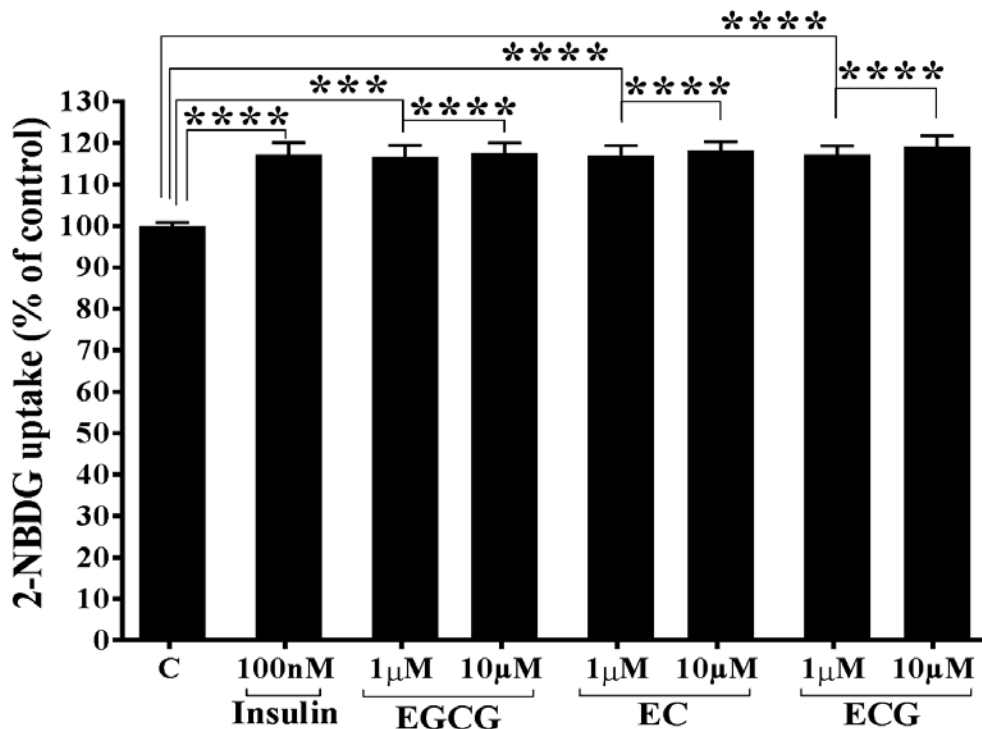


**Figure 3.24 Selected green tea compounds increase 2-NBDG uptake in C2C12 cells.**

C2C12 cells were seeded in 96 well plate at density  $10^4$  and incubated in standard conditions for 24h. Differentiation was induced, and the cells were then serum starved for 2h followed by treating with EGCG, EC, and ECG in low glucose media containing  $100\mu\text{M}$  2-NBDG for 6h. Cellular fluorescence was measured, and the result showed that green tea compounds significantly increased 2-NBDG uptake compared to control. Data presented mean  $\pm$  SEM, \*\*\* $p<0.001$ , \*\*\*\* $p<0.0001$ ,  $n=3$ .

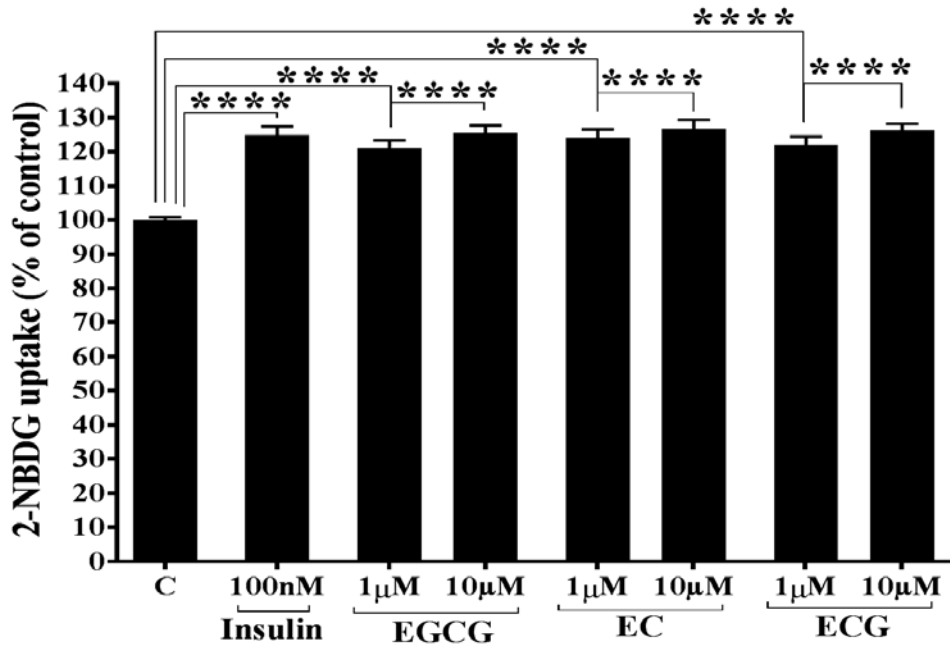


**Figure 3.25 Selected green tea compounds increase 2-NBDG uptake in 3T3-L1 cells.**

3T3L1 cells were seeded in 96 well plate at density  $10^4$  and incubated in standard conditions until reach confluency. Differentiation was induced, and the cells were serum starved for 2h followed by treating with EGCG, EC, and ECG in low glucose media containing  $100\mu\text{M}$  2-NBDG for 6h. Cellular fluorescence was measured, and the result showed that green tea compounds significantly increased 2-NBDG uptake compared to control. Data presented mean  $\pm$  SEM, \*\*\*\* $p < 0.0001$ ,  $n=3$ .

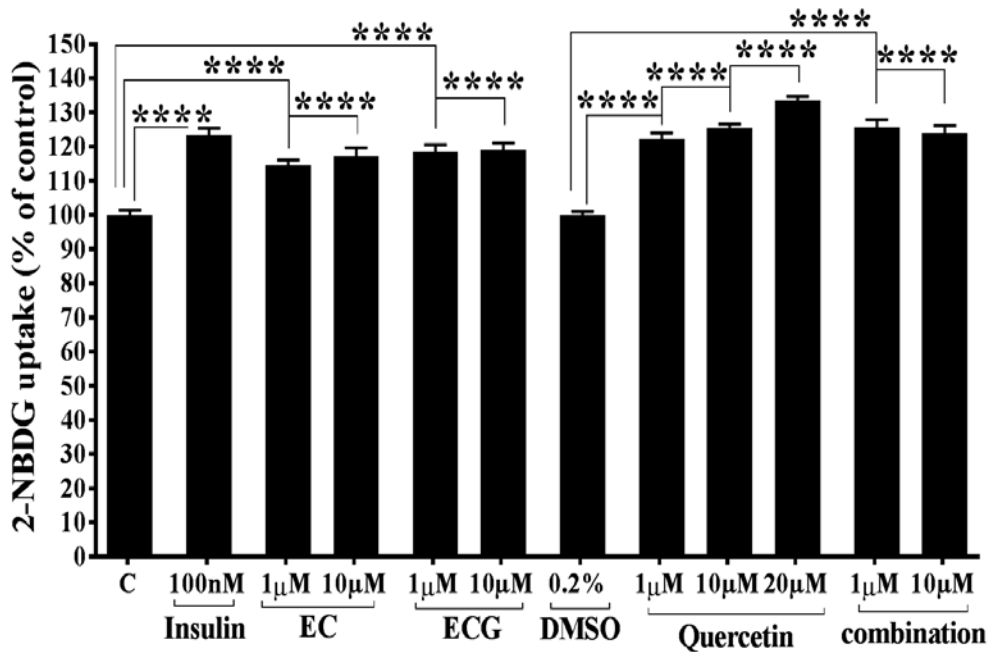


**Figure 3.26 Selected green tea compounds increase 2-NBDG uptake in AML12 cells.**

AML12 cells were seeded in 96 well plate at density  $10^4$  and incubated in standard conditions for 24h. Cells were then serum starved for 2h followed by treating with EC, ECG, quercetin, and combination in low glucose media containing  $100\mu\text{M}$  2-NBDG for 6h. Cellular fluorescence was measured, and the result showed that green tea compounds significantly increased 2-NBDG uptake compared to control. Data presented mean  $\pm$  SEM, \*\*\*\* $p < 0.0001$ ,  $n=3$ .

### **3.3.10 Role of AMPK and Akt on green tea induced 2-NBDG uptake in C2C12 cells**

The impact of AMPK and Akt inhibitors on the cellular 2-NBDG uptake in C2C12 cells was investigated. Cells were exposed to these compounds at 10 $\mu$ M in addition to 1 $\mu$ M of EGCG, EC, and ECG that previously showed a significant increase in 2-NBDG uptake for 6 and 12h. A significant increase of 2-NBDG uptake was observed after 6h in response to green tea compounds, and this uptake was unaffected by AMPK or Akt inhibitors (Figure 3.27A). In contrast, after 12h of treatment, the cells showed significant elevation in 2-NBDG uptake by 21.2% $\pm$ 0.9% ( $p$ <0.0001), 20.3% $\pm$ 0.3% ( $p$ <0.0001), and 20.4% $\pm$ 0.7% ( $p$ <0.0001) respectively, which significantly decreased by 11% $\pm$ 0.8% ( $p$ <0.0001), 10.3% $\pm$ 0.75% ( $p$ <0.0001), and 10.2% $\pm$ 0.8% ( $p$ <0.0001) respectively when the cells were co-incubated with selective AMPK inhibitor molecules alongside these green tea compounds (Figure 3.27 B).

### **3.3.11 Role of AMPK and Akt on green tea induced 2-NBDG uptake in 3T3-L1 cells**

To identify the effect of AMPK and Akt on increased 2-NBDG uptake that was mediated by selected compounds of green tea in 3T3-L1 cells, mature cells were co-incubated with selective 10 $\mu$ M AMPK or Akt inhibitors alongside 1 $\mu$ M of EGCG, EC, and ECG for 6 and 12h. Green tea compounds caused increases in 2-NBDG uptake after 6h without any effect of AMPK or Akt inhibitors on this uptake (Figure 3.28 A). After 12h, however, green tea compounds increased 2-NBDG uptake by 22.3% $\pm$ 0.8% ( $p$ <0.0001), 20.2% $\pm$ 1.3% ( $p$ <0.0001), and 19.5% $\pm$ 1.6% ( $p$ <0.0001) respectively, and this increases was reduced by 13.9% $\pm$ 1.1% ( $p$ <0.0001), 14.5% $\pm$ 1.3% ( $p$ <0.0001), and 13.7% $\pm$ 1.1% ( $p$ <0.0001) in response to the Akt inhibitor only (Figure 3.28 B).

### **3.3.12 Role of AMPK and Akt on green tea induced 2-NBDG uptake in AML12 cells**

The role of AMPK and Akt inhibitor molecules were examined on the cellular 2-NBDG uptake in AML12 cells through supplementing the culture cells to these inhibitors in addition to green tea compounds that had previously shown significant increases in 2-NBDG uptake (EC, ECG, quercetin, and catechins combination) for 6 and 12h. Cells showed a significant increase in 2-NBDG uptake after 6h in response to green tea compounds with no effect of Akt or AMPK inhibitors in reducing 2-NBDG uptake (Figure 3.29 A). Cells after 12h of exposure to selected green tea compounds exhibited significant increases of 2-NBDG uptake by 26.6% $\pm$ 1.5% ( $p$ <0.0001), 29.6% $\pm$ 3.15% ( $p$ <0.0001), 27.2% $\pm$ 1.7% ( $p$ <0.0001), and 25.7% $\pm$ 1.1% ( $p$ <0.0001) respectively, and these increases were reduced markedly by 18.4% $\pm$ 1.1% ( $p$ <0.0001), 13.7% $\pm$ 1.6% ( $p$ <0.0001), 16.8% $\pm$ 1% ( $p$ <0.0001), and 16.8% $\pm$ 1.1% ( $p$ <0.0001) respectively in response to the Akt inhibitor (Figure 3.29 B).

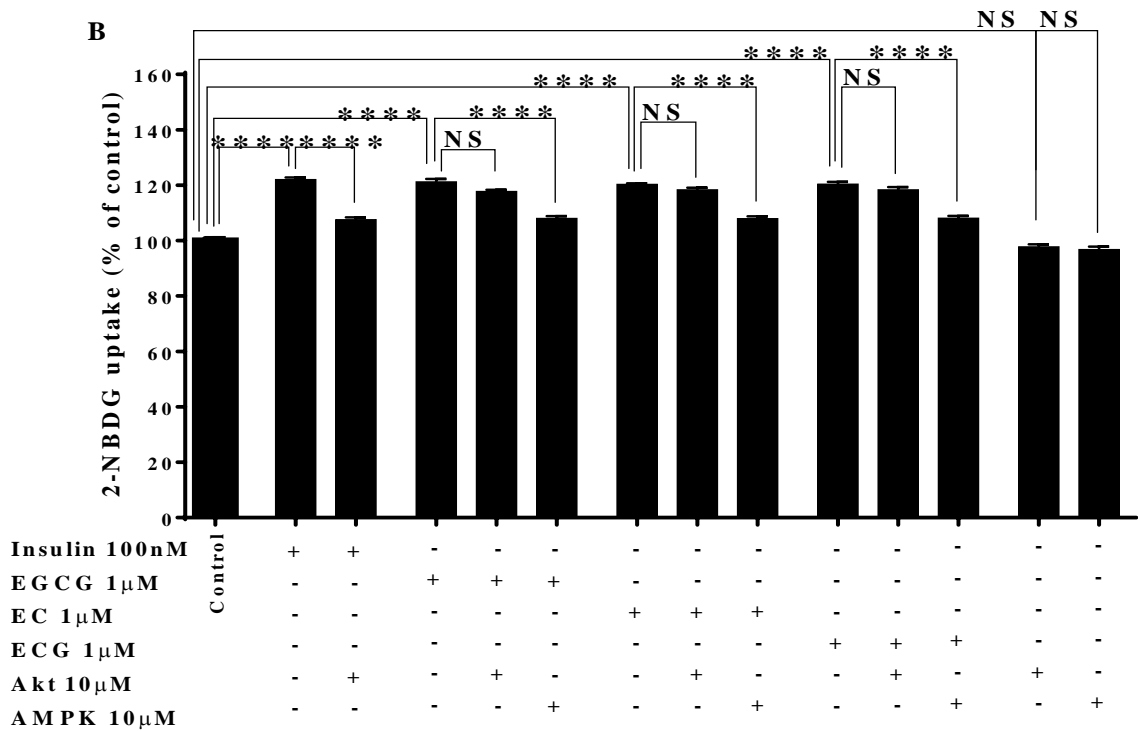
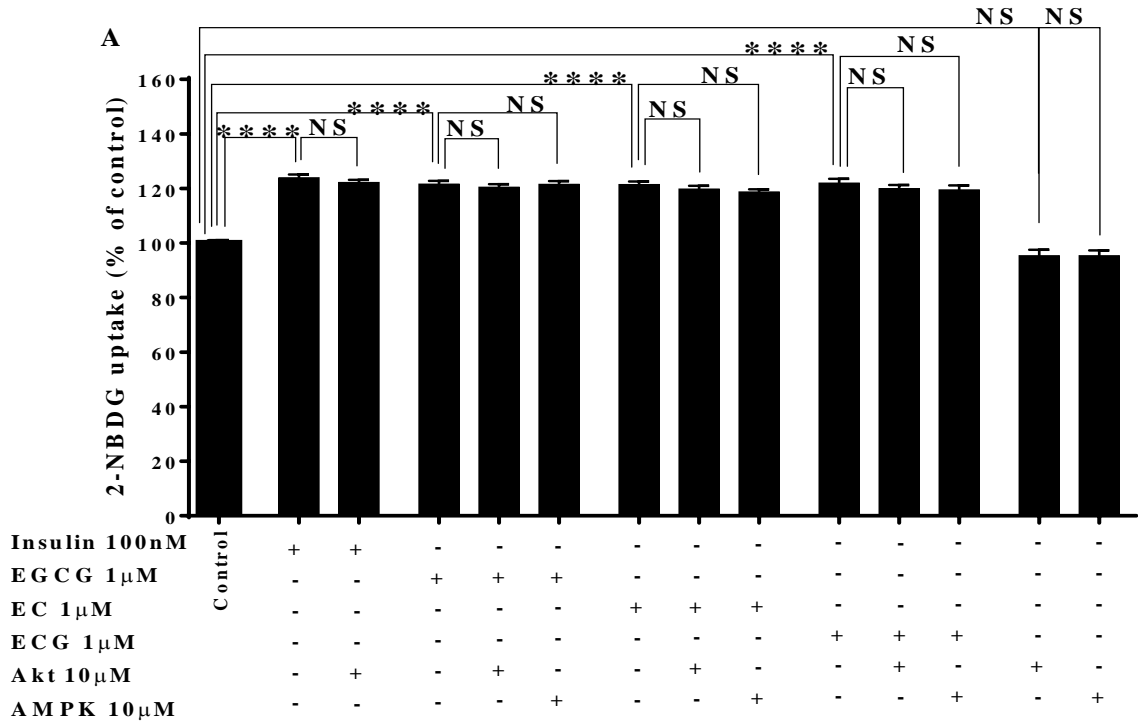


**Figure 3.27 AMPK inhibition reduces green tea compounds induced C2C12 2-NBDG uptake.**

C2C12 cells were seeded in 96 well plate at density  $10^4$  and incubated in standard conditions for 24h. Differentiation was induced, and the cells were then serum starved for 2h followed by treating with EGCG, EC, and ECG with and without AMPK or Akt inhibitor in low glucose media containing  $100\mu\text{M}$  2-NBDG. (A) Six hours co-incubation, green tea compounds increased 2-NBDG uptake without any effect of both inhibitors. (B) 12h co-incubation, green tea compounds increased 2-NBDG uptake, and the increases were significantly reduced by AMPK inhibition. Data presented mean  $\pm$  SEM, \*\*\*\* $p < 0.0001$ ,  $n = 3$ .

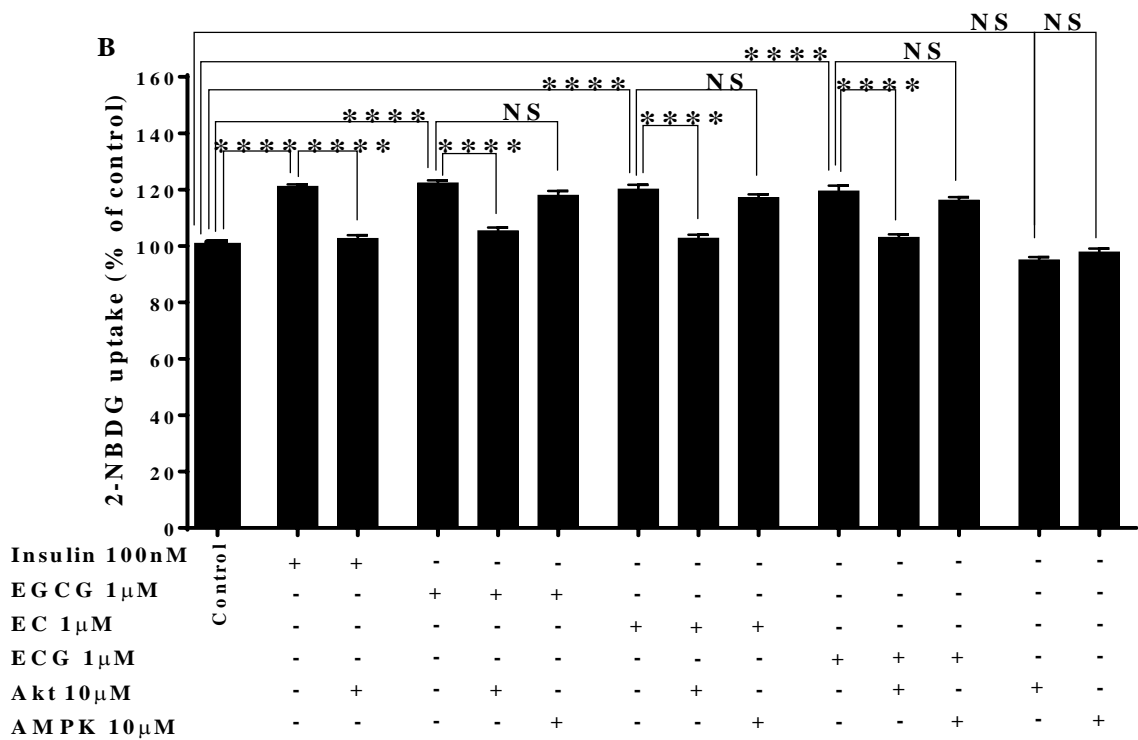
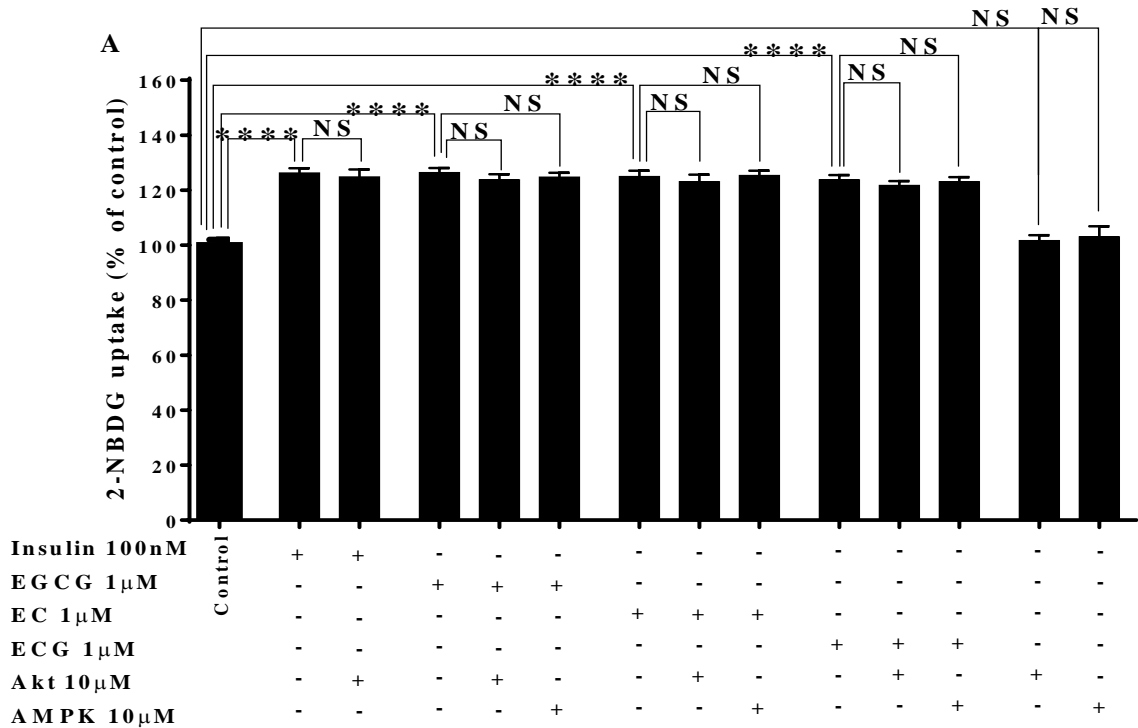


**Figure 3.28 Akt inhibition reduces green tea compounds induced 3T3L-1 2-NBDG uptake.**

3T3L1 cells were seeded in 96 well plate at density  $10^4$  and incubated in standard conditions until reach confluency. Differentiation was induced, and the cells were then serum starved for 2h followed by treating with EGCG, EC, and ECG with and without AMPK or Akt inhibitor in low glucose media containing  $100\mu\text{M}$  2-NBDG. (A) Six hours co-incubation, green tea compounds increased 2-NBDG uptake without any effect of both inhibitors. (B) 12h co-incubation, green tea compounds increased 2-NBDG uptake, and the increases were significantly reduced by Akt inhibition. Data presented mean  $\pm$  SEM, \*\*\*\* $p < 0.0001$ ,  $n = 3$ .

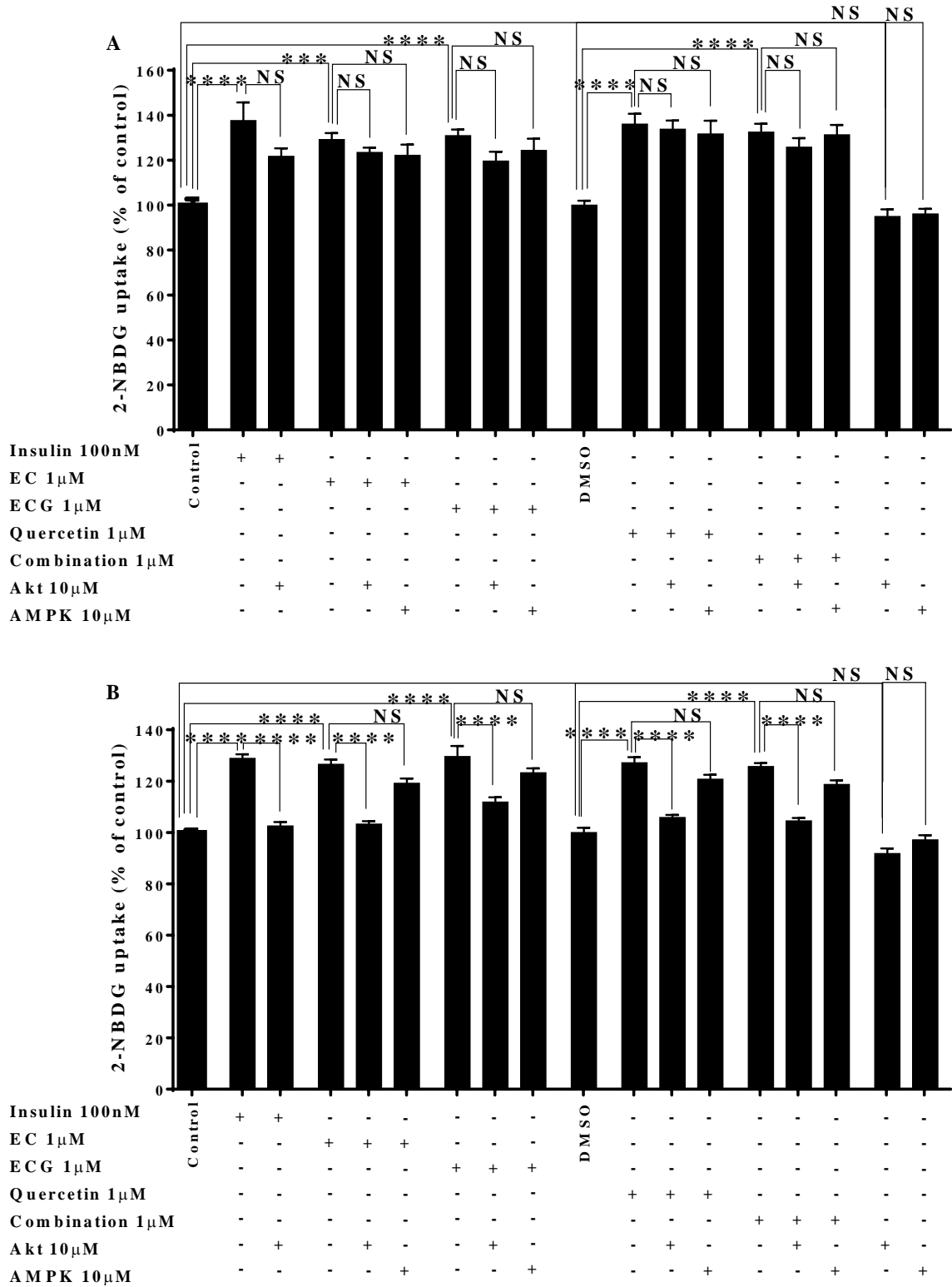


**Figure 3.29 Akt inhibition reduces green tea compounds induced AML12 2-NBDG uptake.**

AML12 cells were seeded in 96 well plate at density  $10^4$  and incubated in standard conditions for 24h. Cells were serum starved for 2h followed by treating with EC, ECG, quercetin, and combination with and without AMPK or Akt inhibitor in low glucose media containing  $100\mu\text{M}$  2-NBDG. (A) Six hours co-incubation, green tea compounds increased 2-NBDG uptake without any effect of both inhibitors. (B) 12h co-incubation, green tea compounds increased 2-NBDG uptake, and the increases were significantly reduced by Akt inhibition. Data presented mean  $\pm$  SEM, \*\*\*\* $p < 0.0001$ ,  $n = 3$ .

### 3.3.13 The effect of green tea compounds on cell viability

The cell viability of insulin-sensitive cell lines including AML12, differentiated C2C12, and 3T3-L1 was assessed to ensure that changes in nutrient utilisation were not due to changes in cell viability. Also to fully clarify the understanding of the link between the effects of active constituents of green tea and the significant increases of cellular glucose and 2-NBDG uptake that had previously been displayed. The assay was performed as described in chapter two. Differentiated C2C12 cells were exposed to 1 and 10 $\mu$ M EGCG, EC, ECG, myricetin, quercetin, and the combination of these compounds for 24, 48, and 72h. Neither concentrations nor different time points affected cell viability (data not shown). Similarly, mature 3T3-L1 treated with the same compounds at the same incubation times revealed cell viability was unchanged in response to treatment at any time points (data not shown). AML12 cells were cultured with the same compounds above, but at 1, 10, and 20 $\mu$ M, and again all compounds at all concentrations did not affect cell viability (data not shown).

### 3.3.14 Selected green tea compounds increased glycogen formation in AML12 cells

Glycogen content was determined in AML12 cells that had exhibited significant increases in glucose and 2-NBDG uptake previously in response to selected green tea compounds. Cells were exposed to 10 $\mu$ M ECG for 24h, 1 and 10 $\mu$ M of ECG and combination of green tea compounds, 1 $\mu$ M EC, and 1, 10, and 20 $\mu$ M quercetin for 72h followed by measuring the amount of glycogen stored in the cells. No significant differences in glycogen content were observed in cells treated with 1 $\mu$ M EC, 1 $\mu$ M and 10 $\mu$ M ECG for 72h compared to control (**Error! Reference source not found.**). Whereas, exposure to 10 $\mu$ M ECG for 24h caused a significant increase in cellular glycogen content (59.24% $\pm$ 12%,  $p=0.0284$ ), as shown in Figure 3.30. Quercetin treatment at 1 and 10 $\mu$ M for 72h did not elicit any significant change in cellular glycogen content, whilst 20 $\mu$ M significantly increased cellular glycogen content to 157.4% $\pm$ 13.9% ( $p=0.0245$ ) compared to control group (Figure 3.31). Combined green tea compounds did not significantly alter glycogen content, with measurements of up to 94.1% $\pm$ 12.1% ( $p=0.0875$ ) and 142.7% $\pm$ 15.94% ( $p=0.0531$ ) for 1 and 10 $\mu$ M compared to control respectively (Figure 3.31).

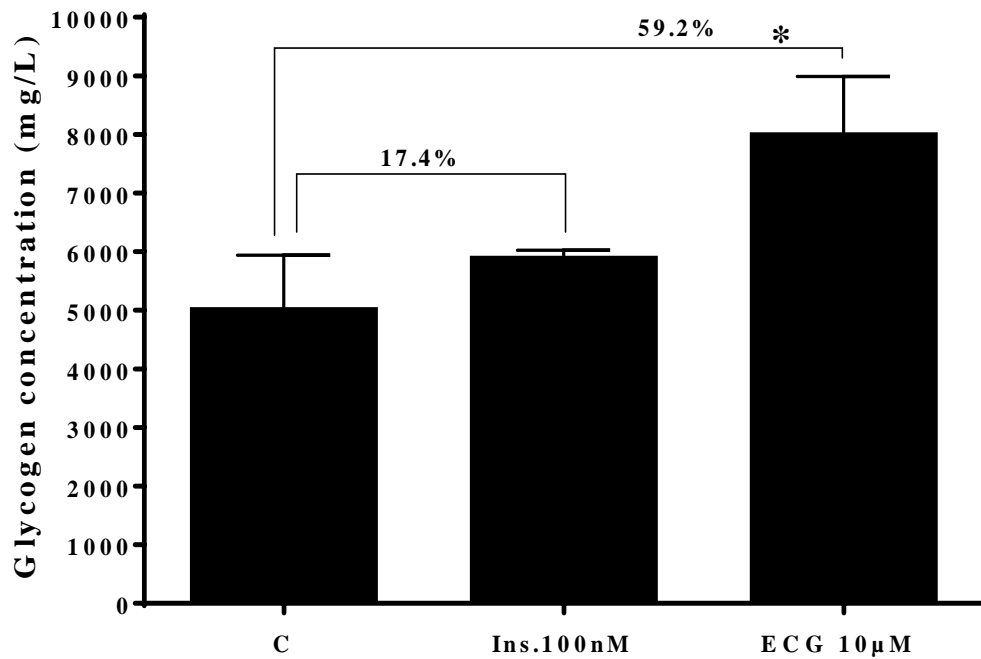


**Figure 3.30 ECG increases glycogen content in AML12 cells.**

AML12 cells were seeded in 24 well plate at density  $2 \times 10^5$  and incubated in standard conditions until completed confluency. Cells were serum starved for 2h, and treated with  $10 \mu\text{M}$  ECG for 24h, then cells were homogenised, and glycogen content was investigated. The result showed ECG significantly increased glycogen content compared to control. Data presented mean  $\pm$  SEM, \* $p < 0.05$ ,  $n = 3$ .

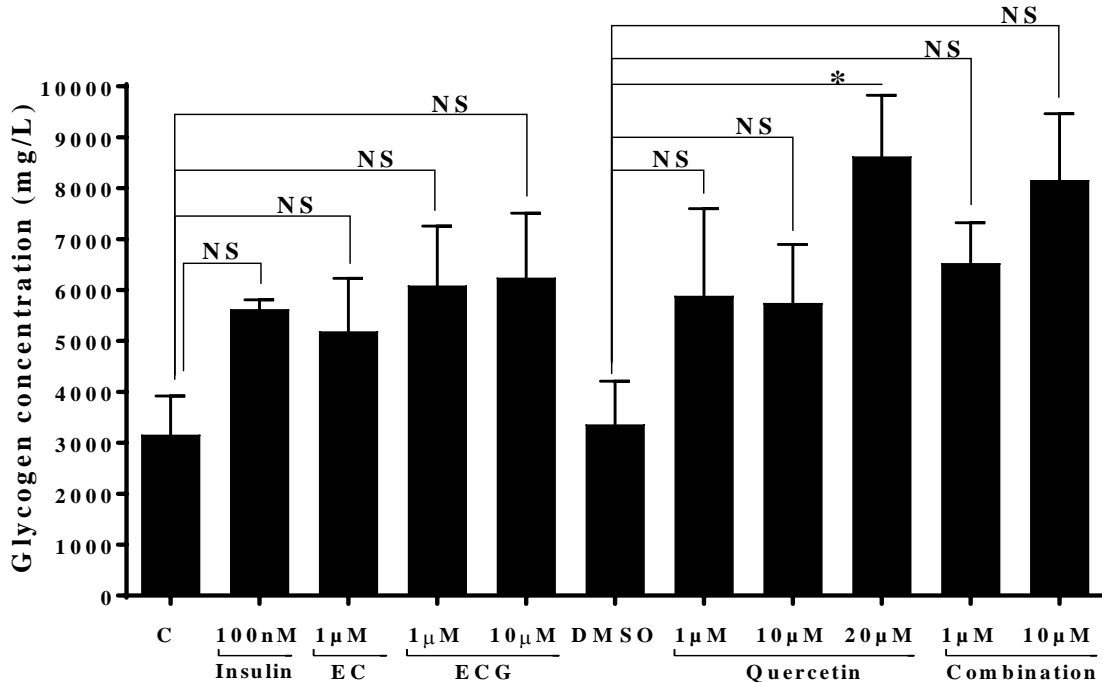


**Figure 3.31 Quercetin increases glycogen contents in AML12 cells.**

AML12 cells were seeded in 24 well plate at density  $2 \times 10^5$  and incubated in standard conditions until completed confluency. Cells were serum starved for 2h, and treated with indicated concentration of EC, ECG, quercetin, and green tea compounds combination for 72h, then cells were homogenised, and glycogen content was investigated. Only  $20 \mu\text{M}$  quercetin increased glycogen content compared to DMSO. Data presented mean  $\pm$  SEM, \* $p < 0.05$ ,  $n = 3$ .

### 3.3.15 Lipid accumulation in differentiated 3T3-L1 cells

Oil red O staining was used to assess lipid accumulation in differentiating 3T3-L1 cells during various time points of differentiation. The cells accumulated noticeable lipid droplets at days 6, 9, 12 and 15 from initiation of differentiation, and both the size and number of lipid droplets increased with advances in time (Figure 3.32).

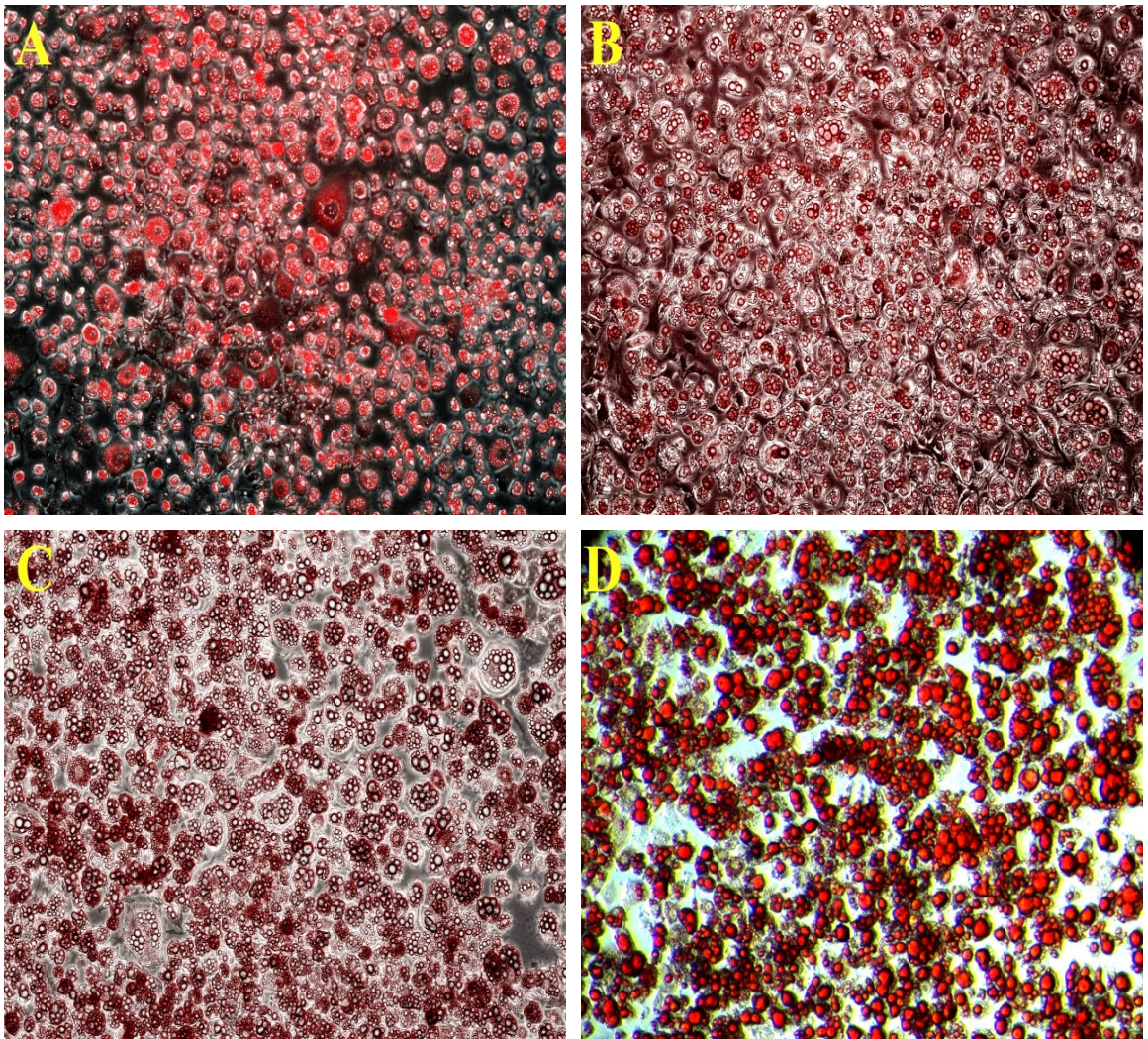


**Figure 3.32 Oil red O triglyceride staining of 3T3-L1 cells during differentiation.**

3T3L1 cells were seeded in 6 well plate at density  $6 \times 10^5$  and incubated in standard conditions until completed confluency. Differentiation was induced as mentioned in materials and methods, and the cells were stained with oil red O during differentiation process. (A) Cells were stained at day 6 of differentiation demonstrating small and numerous lipid droplets appearing red in colour. (B) Staining at day 9 shows an increased number and size of lipid droplets. (C) Lipid droplets become larger than before at day 12 of differentiation. (D) Red stained larger lipid droplets formed by day 15 of differentiation. The images were captured using Leica DMI4000 B inversion microscope and Ceti Inverso TC100 inverted microscope at 100x magnification.

### 3.3.16 Selected green tea compounds decreased triglyceride contents in 3T3-L1 cells

The effect of green tea compounds on lipid homeostasis in adipocytes was investigated by measuring triglyceride content of mature 3T3-L1 after exposed to selected compounds of green tea at concentrations and time points that had previously shown significant increases in glucose and 2-NBDG uptake. Cells were treated with EGCG, EC, and ECG at 1 and 10 $\mu$ M for 48 and 72h and subsequently assayed triglyceride content as described in chapter two. The results showed significant reduction of cellular triglyceride content in cells treated with selected compounds of green tea after 48 and 72h compared to control (Figure 3.33). Reductions of 74.11% $\pm$ 4% ( $p$ <0.0001), 77% $\pm$ 10.8% ( $p$ <0.0001), 39.91% $\pm$ 19.7% ( $p$ =0.0170), 51.9% $\pm$ 16.8% ( $p$ =0.0014), 43.5% $\pm$ 21.25% ( $p$ =0.0081), and 48% $\pm$ 1.5% ( $p$ =0.0031) respectively were observed after 48h, in addition to 95% $\pm$ 26.2% ( $p$ <0.0001) and 36.8% $\pm$ 0.6% ( $p$ = 0.0173) decreases of triglyceride level caused by 10 $\mu$ M isoprenaline and 100nM insulin respectively compared to control. After 72h the reductions in triglyceride levels were 62.75% $\pm$ 20.62% ( $p$ <0.0001), 52% $\pm$ 13.56% ( $p$ =0.0001), 32.8% $\pm$ 4.4% ( $p$ =0.0178), 60.24% $\pm$ 13.43% ( $p$ <0.0001), 50.86% $\pm$ 7% ( $p$ =0.0002), and 53.17% $\pm$ 20.76% ( $p$ =0.0001) respectively, whereas isoprenaline and insulin caused a 61.7% $\pm$ 12.6% ( $p$ <0.0001) and 28.6% $\pm$ 4.6% ( $p$ = 0.0496) reduction in triglyceride compared to control (Figure 3.33). Surprisingly, the cells exposed to insulin for 48 and 72h show significant reduction in triglyceride which is a unique and unlikely effect as the proper effect is to stimulate lipogenesis.

### 3.3.17 Selected green tea compounds reduced lipolysis in 3T3-L1 cells

The amount of glycerol released from differentiated 3T3-L1 cells is an indirect measure of cellular lipolysis. Glycerol release was measured for treatment concentrations that had previously shown an increase in glucose and 2-NBDG uptake associated with a decrease in triglyceride content. Cells were incubated with 1 and 10 $\mu$ M EGCG, EC, and ECG for 48 and 72h, and glycerol release was measured in the cell culture media. The results showed that treatment with EGCG, EC, and ECG for 48 and 72h significantly reduced the amount of glycerol released from 3T3-L1 cells compared to control (Figure 3.34). Reductions in glycerol release in compared to control were: 38.8% $\pm$ 9.5% ( $p$ =0.0003), 38.9% $\pm$ 10.1% ( $p$ =0.0002), 29.4% $\pm$ 7.6% ( $p$ =0.0110), 41.3% $\pm$ 7.4% ( $p$ <0.0001), 36.3% $\pm$ 9.1% ( $p$ =0.0007), and 39.1% $\pm$ 7.9% ( $p$ =0.0002) for 48h respectively, whereas 10 $\mu$ M isoprenaline as a positive control increased glycerol release by 37.6% $\pm$ 1.2% ( $p$ =0.0002) compared to control. After 72h, decreases of glycerol release were 36.5% $\pm$ 8.7% ( $p$ =0.0002), 32.4% $\pm$ 10% ( $p$ =0.0012), 42.5% $\pm$ 8.8% ( $p$ <0.0001), 45% $\pm$ 9.7% ( $p$ <0.0001), 42.7% $\pm$ 10.3% ( $p$ <0.0001), and 37.7% $\pm$ 5.8% ( $p$ =0.0001) respectively, whilst isoprenaline elevated glycerol release by 28.6% $\pm$ 1.5% ( $p$ =0.0033) compared to control.

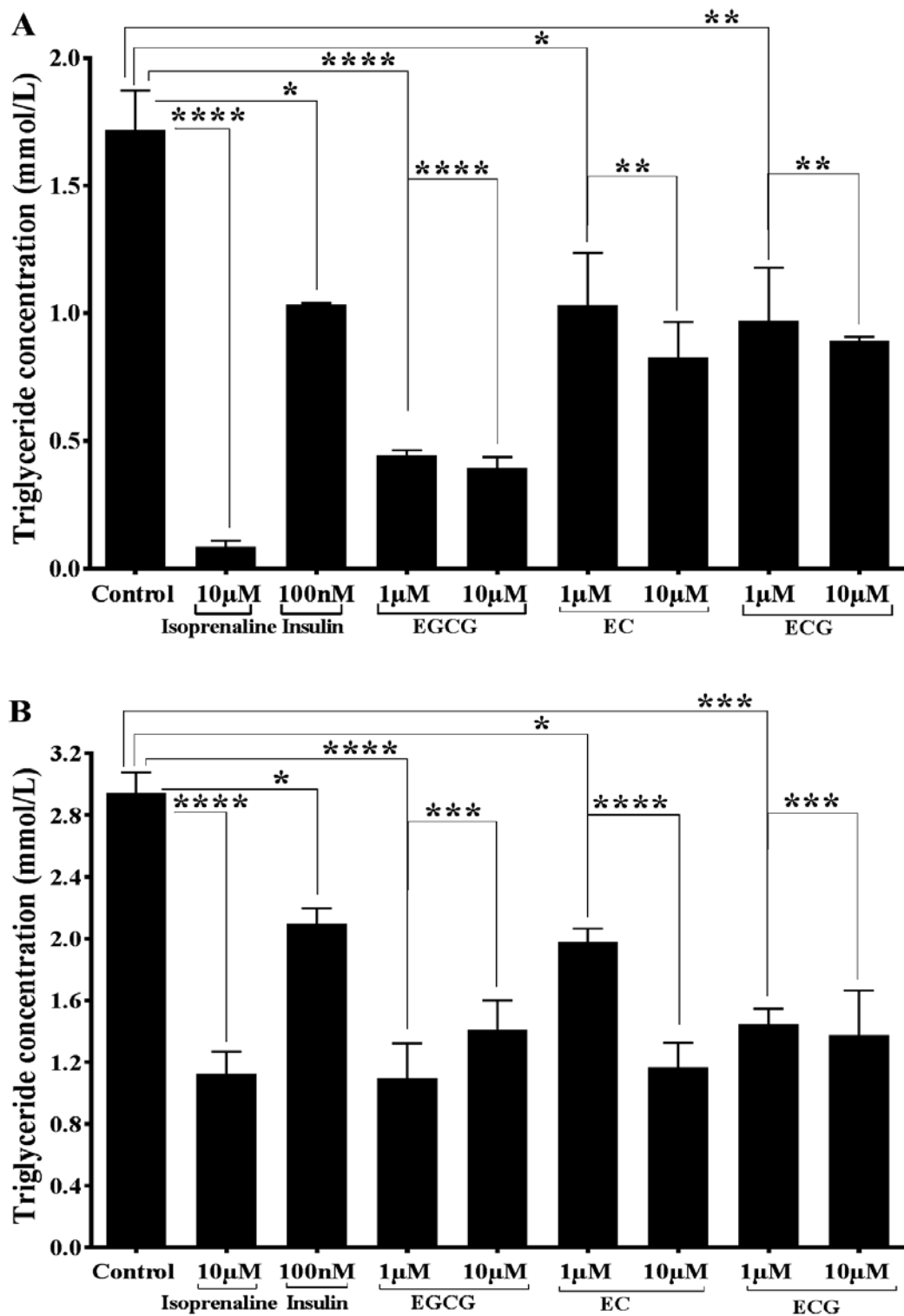


**Figure 3.33 Selected green tea compounds decrease triglyceride level in 3T3-L1 cells.**

3T3L1 cells were seeded in 24 well plate at density  $1.5 \times 10^4$  and incubated in standard conditions until completed confluency. Differentiation was induced, and the cells were serum starved for 2h, and treated with EGCG, EC, and ECG for 48 and 72h. Triglyceride was extracted and quantified. (A) Significant decreases of cellular triglyceride were observed in treated cells compared to control after 48h. (B). Treated cells exhibited significant reductions in triglyceride content after 72h incubation compared to control. Data presented mean  $\pm$  SEM, \* $p < 0.05$ , \*\* $p < 0.01$ , \*\*\* $p < 0.001$ , \*\*\*\* $p < 0.0001$ ,  $n = 3$ .

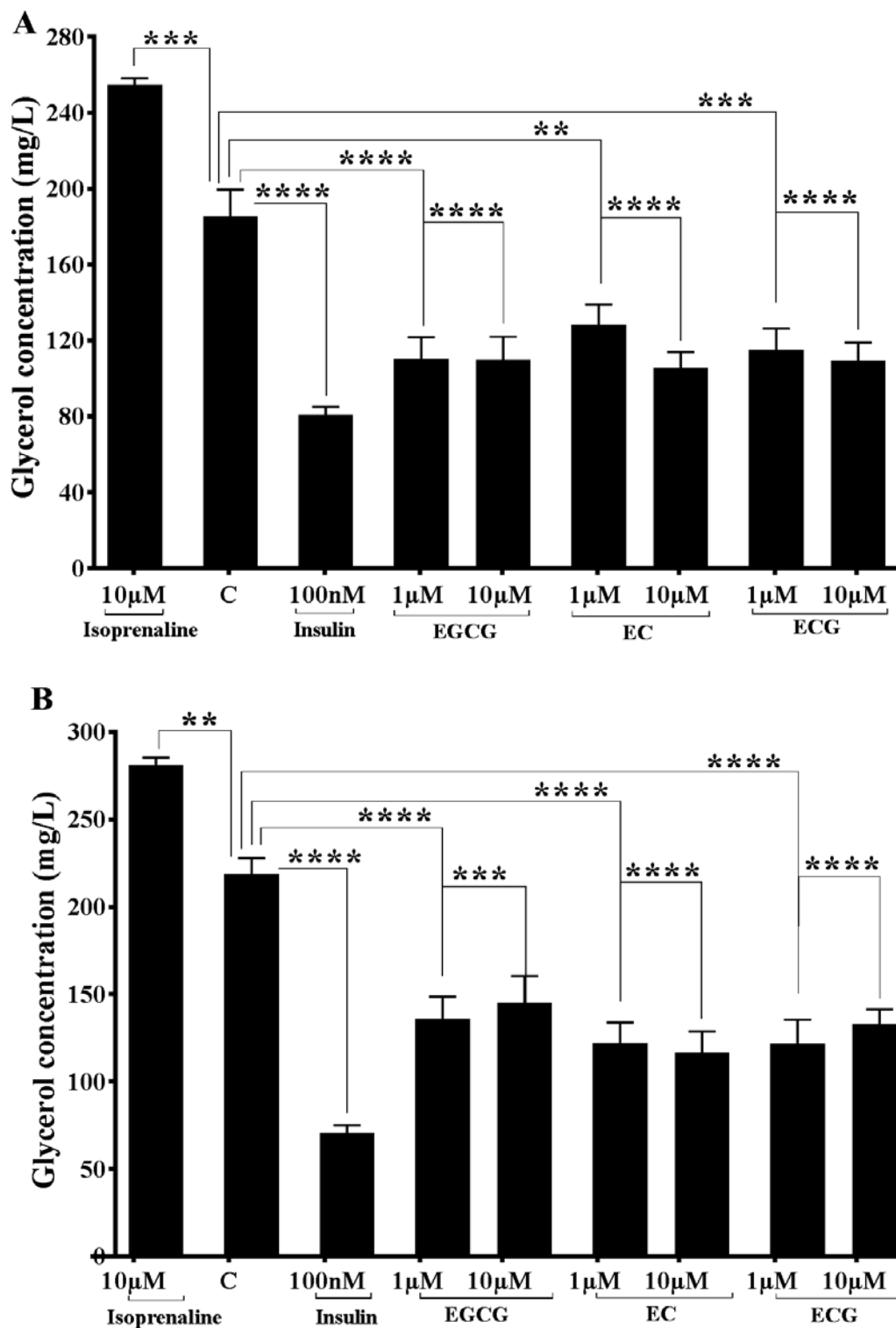


**Figure 3.34 Selected green tea compounds reduce glycerol release from 3T3-L1 cells.**

3T3L1 cells were seeded in 24 well plate at density  $1.5 \times 10^4$  and incubated in standard conditions until completed confluency. Differentiation was induced, and the cells were serum starved for 2h, and treated with EGCG, EC, and ECG for 48 and 72h. The level of glycerol releases from cells was quantified in culture media. (A) Significant reduction of glycerol concentration was observed in treated cell culture media compared to control after 48h. (B). Treated cells culture media exhibited significant reduce in glycerol levels after 72h incubation compared to control. Data presented mean  $\pm$  SEM, \*\* $p < 0.01$ , \*\*\* $p < 0.001$ , \*\*\*\* $p < 0.0001$ ,  $n = 3$ .

### 3.3.18 Effect of green tea compounds on the level of glucose and lipid metabolism gene expression

The effects of active green tea compounds that previously showed significant effects on nutrient homeostasis on gene expression of metabolic genes were investigated using qRT-PCR. The genes tested were IR, HK1, Glut4, PDK4, PGC1a, and Gys1 for C2C12 cells. Also IR, HK1, Glut2, Gys1, G6Pase, PEPCCK, ACSL, CPT $\alpha$ 1 in AML12 cells and IR, HK1, Glut4, C/EBP $\alpha$ , LPL, FASN, FABP4, SREBP1c, and PPAR $\gamma$  in 3T3-L1 cells. The relative mRNA expression of these genes was calculated using equation  $2^{-\Delta\Delta C_t}$  (Livak and Schmittgen, 2001) after gene expression was normalised to a housekeeping gene (Actin). The result showed that the level of mRNA expression of metabolic genes in C2C12 was not significantly altered by any of the treatments (Table 3.1). Similarly, EGCG, EC, and ECG did not alter the level of metabolic gene expression in 3T3L1 cells compared to control (Table 3.2). Furthermore, no significant change in metabolic genes expression were observed in treated AML12 cells compared to control (Table 3.3).

**Table 3.1 Effect of green tea compounds on glucose metabolism mRNA expression in C2C12 cells.**

C2C12 cells were seeded in 12 well plate at density  $4 \times 10^5$  and incubated in standard conditions until reached 80% confluency. Differentiation was induced, cells were starved for 2h and then were treated with  $10 \mu\text{M}$  of EGCG, EC, and ECG for 24h. RNA was isolated and reverse transcriptased, followed by quantifying amplification of selected glucose metabolism mRNA by using qPCR. No significant differences between green tea treatments and control of all tested gene were seen. Data displayed as relative fold of gene expression normalised to housekeeping gene. Data presented mean  $\pm$  SEM, n=3.

mRNA	Treatment	$\uparrow\downarrow$ Fold of control	P value
IR	Insulin	$0.7225 \pm 0.1607$	0.8968
	EGCG	$0.9104 \pm 0.1584$	0.9980
	EC	$1.296 \pm 0.4067$	0.8873
	ECG	$0.7591 \pm 0.1858$	0.9340
HK1	Insulin	$0.9279 \pm 0.2694$	0.9952
	EGCG	$1.600 \pm 0.4044$	0.9014
	EC	$0.9197 \pm 0.5066$	0.9944
	ECG	$0.8396 \pm 0.3577$	0.9812
Glut4	Insulin	$1.369 \pm 0.09037$	0.8790
	EGCG	$1.450 \pm 0.2536$	0.7845
	EC	$1.504 \pm 0.3905$	0.7120
	ECG	$1.374 \pm 0.3988$	0.8739
PDK4	Insulin	$1.052 \pm 0.2113$	> 0.9999
	EGCG	$1.194 \pm 0.08041$	> 0.9999
	EC	$1.389 \pm 0.4891$	0.9908
	ECG	$1.687 \pm 0.7814$	0.8850

<b>PGC1<math>\alpha</math></b>	<b>Insulin</b>	1.049 $\pm$ 0.09195	> 0.9999
	<b>EGCG</b>	0.6439 $\pm$ 0.1376	0.3476
	<b>EC</b>	0.5368 $\pm$ 0.1943	0.1656
	<b>ECG</b>	0.4297 $\pm$ 0.01285	0.0733
<b>Gys1</b>	<b>Insulin</b>	1.229 $\pm$ 0.3843	0.9929
	<b>EGCG</b>	1.212 $\pm$ 0.5074	0.9948
	<b>EC</b>	0.8237 $\pm$ 0.3283	0.9956
	<b>ECG</b>	0.8745 $\pm$ 0.3953	0.9987

**Table 3.2 Effect of green tea compounds on glucose and lipid metabolism mRNA expression in 3T3-L1 cells.**

3T3-L1 cells were seeded in 12 well plate at density  $3 \times 10^5$  and incubated in standard conditions until completed confluency. Differentiation was induced, cells were starved for 2h and then were treated with 10 $\mu$ M of EGCG, EC, and ECG for 24h. RNA was isolated and reverse transcribed, followed by quantifying amplification of selected glucose and lipid metabolism mRNA by using qPCR. No significant differences between green tea treatments and control of all tested gene were seen. Data displayed as relative fold of gene expression which normalised to housekeeping gene. The data presented mean  $\pm$  SEM, n=3.

<b>mRNA</b>	<b>Treatment</b>	<b><math>\uparrow\downarrow</math> Fold of control</b>	<b>P value</b>
<b>IR</b>	<b>Insulin</b>	0.8526 $\pm$ 0.1703	0.9642
	<b>EGCG</b>	0.7121 $\pm$ 0.1036	0.7805
	<b>EC</b>	1.012 $\pm$ 0.3244	> 0.9999
	<b>ECG</b>	0.6547 $\pm$ 0.1224	0.6695
<b>HK1</b>	<b>Insulin</b>	1.144 $\pm$ 0.4587	> 0.9999
	<b>EGCG</b>	2.529 $\pm$ 1.562	> 0.9999
	<b>EC</b>	3.860 $\pm$ 2.633	> 0.9999
	<b>ECG</b>	34.31 $\pm$ 31.40	0.4966
<b>Glut4</b>	<b>Insulin</b>	0.5101 $\pm$ 0.08767	0.9548
	<b>EGCG</b>	1.261 $\pm$ 0.4688	0.9987
	<b>EC</b>	0.6888 $\pm$ 0.1649	0.9893
	<b>ECG</b>	1.857 $\pm$ 1.115	0.8416
<b>C/EBP<math>\alpha</math></b>	<b>Insulin</b>	0.8030 $\pm$ 0.1598	0.9913
	<b>EGCG</b>	1.076 $\pm$ 0.08899	0.9998
	<b>EC</b>	1.296 $\pm$ 0.1898	0.9669
	<b>ECG</b>	2.434 $\pm$ 0.6798	0.0687
<b>LPL</b>	<b>Insulin</b>	0.5314 $\pm$ 0.1204	0.9997
	<b>EGCG</b>	4.989 $\pm$ 1.468	0.6566
	<b>EC</b>	1.155 $\pm$ 0.5874	> 0.9999
	<b>ECG</b>	6.559 $\pm$ 4.238	0.3665

<b>FASN</b>	<b>Insulin</b>	0.6635 ± 0.1479	0.9590
	<b>EGCG</b>	1.885 ± 0.1188	0.9103
	<b>EC</b>	1.580 ± 0.3627	0.9887
	<b>ECG</b>	2.883 ± 1.129	0.2983
<b>FABP4</b>	<b>Insulin</b>	0.6989 ± 0.1674	0.9919
	<b>EGCG</b>	3.245 ± 0.9062	0.2867
	<b>EC</b>	1.660 ± 0.6312	0.9820
	<b>ECG</b>	3.257 ± 1.063	0.2823
<b>SREBP1c</b>	<b>Insulin</b>	0.7561 ± 0.06438	0.9662
	<b>EGCG</b>	0.7484 ± 0.1120	0.9628
	<b>EC</b>	1.385 ± 0.1669	0.9304
	<b>ECG</b>	2.090 ± 0.6413	0.2021
<b>PPAR<math>\gamma</math></b>	<b>Insulin</b>	0.4943 ± 0.08012	0.6540
	<b>EGCG</b>	1.117 ± 0.2819	0.9977
	<b>EC</b>	1.853 ± 0.1615	0.2217
	<b>ECG</b>	1.795 ± 0.4757	0.2755

**Table 3.3 Effect of green tea compounds on glucose metabolism mRNA expression in AML12 cells.**

AML12 cells were seeded in 12 well plate at density  $4 \times 10^5$  and incubated in standard conditions until completed confluency. Cells were starved for 2h and then were treated with  $10 \mu\text{M}$  of EC, ECG, quercetin, and combination for 24h. RNA was isolated and reverse transcriptased, followed by quantifying amplification of selected glucose metabolism mRNA by using qPCR. No significant differences between green tea treatments and control of all tested gene were seen. Data displayed as relative fold of gene expression which normalised to housekeeping gene. The data presented mean  $\pm$  SEM, n=3.

<b>mRNA</b>	<b>Treatment</b>	<b><math>\uparrow\downarrow</math> Fold of control</b>	<b>P value</b>
<b>IR</b>	<b>Insulin</b>	1.675 ± 0.9192	>0.9999
	<b>EC</b>	8.615 ± 3.918	0.1498
	<b>ECG</b>	2.897 ± 0.1303	0.9914
	<b>Quercetin</b>	2.359 ± 0.8495	0.9997
	<b>Combination of GT</b>	4.113 ± 2.961	0.9400
<b>HK1</b>	<b>Insulin</b>	4.158 ± 3.087	0.5755
	<b>EC</b>	1.606 ± 0.1642	0.9998
	<b>ECG</b>	2.28 ± 0.2419	0.9888
	<b>Quercetin</b>	2.482 ± 0.8616	0.9940
	<b>Combination of GT</b>	1.364 ± 0.2924	>0.9999

<b>Glut2</b>	<b>Insulin</b>	3.354 ± 1.906	0.9568
	<b>EC</b>	6.011 ± 2.345	0.4419
	<b>ECG</b>	4.719 ± 1.572	0.7393
	<b>Quercetin</b>	2.168 ± 0.6923	0.9997
	<b>Combination of GT</b>	3.921 ± 3.003	0.9221
<b>Gys1</b>	<b>Insulin</b>	3.071 ± 1.473	0.5464
	<b>EC</b>	2.143 ± 0.4149	0.9442
	<b>ECG</b>	3.276 ± 0.5819	0.4437
	<b>Quercetin</b>	3.266 ± 1.007	0.4649
	<b>Combination of GT</b>	2.31 ± 0.7633	0.9096
<b>G6Pase</b>	<b>Insulin</b>	4.371 ± 4.069	0.9036
	<b>EC</b>	3.146 ± 0.6884	0.9897
	<b>ECG</b>	1.759 ± 0.4488	>0.9999
	<b>Quercetin</b>	2.207 ± 1.379	0.9996
	<b>Combination of GT</b>	4.26 ± 2.916	0.9092
<b>PEPCK</b>	<b>Insulin</b>	6.897 ± 5.82	0.6857
	<b>EC</b>	6.43 ± 2.543	0.7564
	<b>ECG</b>	4.097 ± 0.7925	0.9766
	<b>Quercetin</b>	1.92 ± 0.6199	>0.9999
	<b>Combination of GT</b>	3.577 ± 2.361	0.9940
<b>CPT<math>\alpha</math></b>	<b>Insulin</b>	3.455 ± 2.244	0.5044
	<b>EC</b>	2.611 ± 0.427	0.8623
	<b>ECG</b>	2.665 ± 0.1158	0.8439
	<b>Quercetin</b>	1.378 ± 0.5809	>0.9999
	<b>Combination of GT</b>	1.44 ± 0.2106	>0.9999
<b>ACSL</b>	<b>Insulin</b>	3.537 ± 2.387	0.9845
	<b>EC</b>	8.671 ± 4.06	0.2773
	<b>ECG</b>	3.8 ± 0.6926	0.9744
	<b>Quercetin</b>	3.293 ± 1.033	0.9958
	<b>Combination of GT</b>	5.089 ± 3.368	0.8976

### **3.3.19 Effect of green tea compounds on AMPK phosphorylation in C2C12 cells**

Previous results showed the inhibitory effect of selective AMPK inhibitor molecule on glucose uptake in C2C12 cells mediated by selective green tea compounds including EGCG, EC, and ECG. Based on that, the AMPK pathway is likely implicated in the effect of selected green tea compounds in glucose homeostasis regulation. Phosphor-specific Western blotting was used to detect the levels of phosphorylated AMPK (pAMPK) protein expression in C2C12 cell lysate after exposed cells to green tea compounds for 15 and 30 minutes. As this experiment was performed on two occasions only, which cannot be taken as a final result, the data did not show statistically significant differences between green tea treatments and control (Figure 3.35).

### **3.3.20 Effect of green tea compounds on phosphorylation of Akt in 3T3-L1 cells**

Based on the result shown previously that co-incubating mature 3T3-L1 cells with selective Akt inhibitor molecule alongside selected green tea compounds significantly suppresses glucose and 2-NBDG uptake, Akt could be involved in the effect of these selected compounds of green tea in regulating glucose homeostasis. This signalling pathway was determined in 3T3-L1 cells through measuring of expression of specific Akt protein in cell lysate by phosphor-specific Western blotting after 15 and 30 minutes post-treatment with selected compounds of green tea. This experiment was also only performed twice and therefore cannot be considered in drawing final conclusions. However, the analysed data displayed no significant differences in phosphorylation of Akt protein between treatments and control (Figure 3.36).

### **3.3.21 Effect of green tea compounds on phosphorylation of Akt in AML12 cells**

Looking at Akt expression in AML12, based on the result expressed previously, showed that Akt inhibition significantly reduced cellular glucose and 2-NBDG uptake in AML12 when the cells were co-cultured with selected green tea compounds in addition to selective Akt inhibitor molecules. Accordingly, Akt could be a potential pathway of the effect of selected green tea compounds to regulate glucose homeostasis. Phosphor-specific Western blotting was performed to identify the levels of phosphorylated Akt (pAkt) proteins in AML12 cell lysate post-treatment with EC, ECG, and quercetin for 15 and 30 minutes. Similarly, this experiment was conducted twice which therefore cannot use to make any final conclusion. However, the result showed no significant differences between treatments and control in the expression level of pAkt (Figure 3.37).

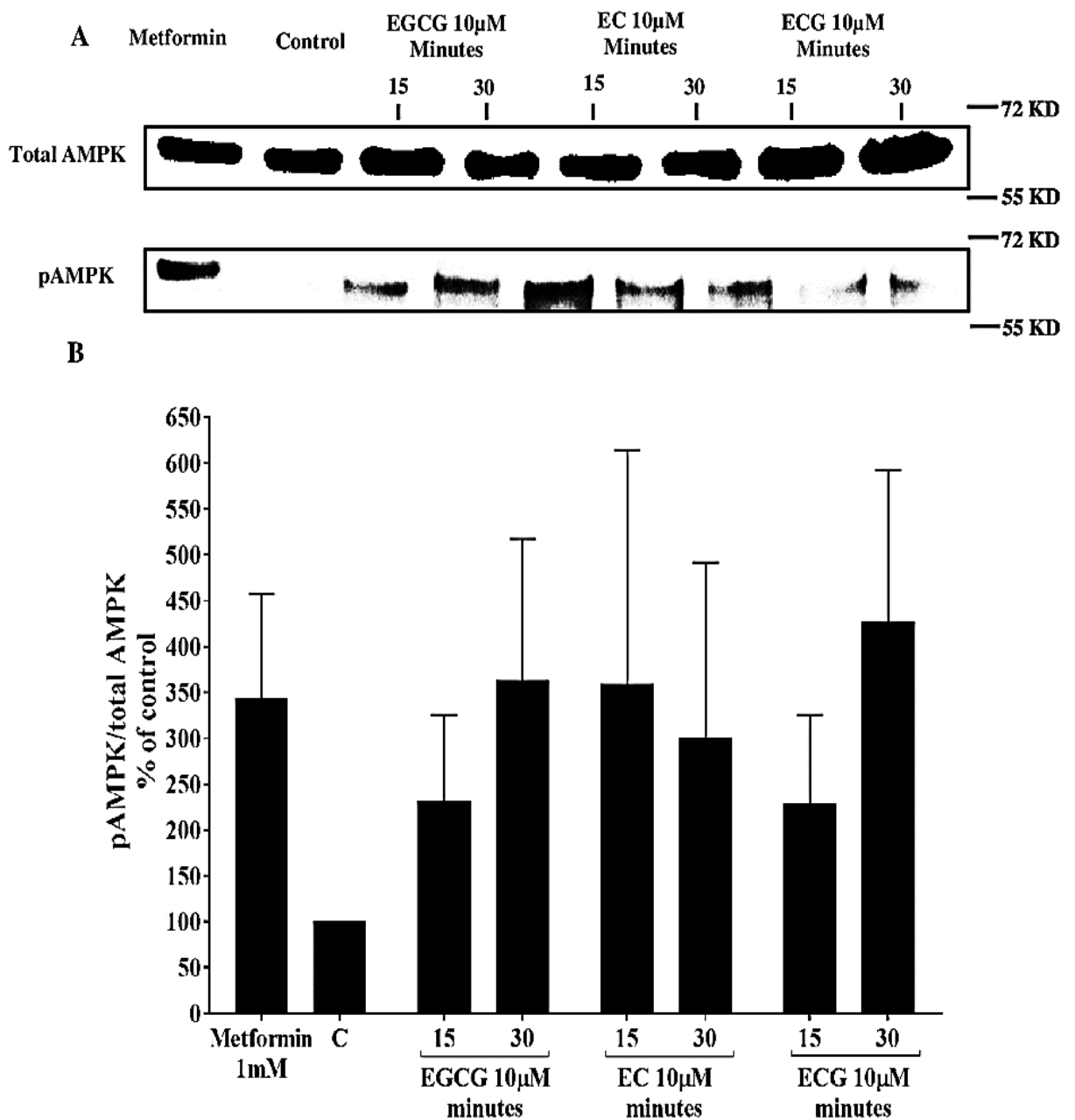


**Figure 3.35 Effect of selected green tea compounds on pAMPK expression in C2C12 cells.**

C2C12 cells were seeded in 6 well plate at density  $8 \times 10^5$  and incubated in standard conditions until reached 80% confluency. Differentiation was induced, and the cells were serum starved for 2h, and then were treated with 10 $\mu$ M of EGCG, EC, and ECG for 15 and 30 minutes. Total protein was isolated and quantified, and phosphor western blotting was performed to identify the leve of pAMPK. (A). Total and phosphorylation levels of AMPK protein bands represented one experiment. (B) Analysed band intensity of pAMPK expression. Due to the experiment was performed in two occasion, therefore, no final conclusion can be drawn and more independent experiment is needed. The data displayed as a % of control which normalised to total AMPK expression. Bands intensity were quantified using Image J software. Data presented as n=2.

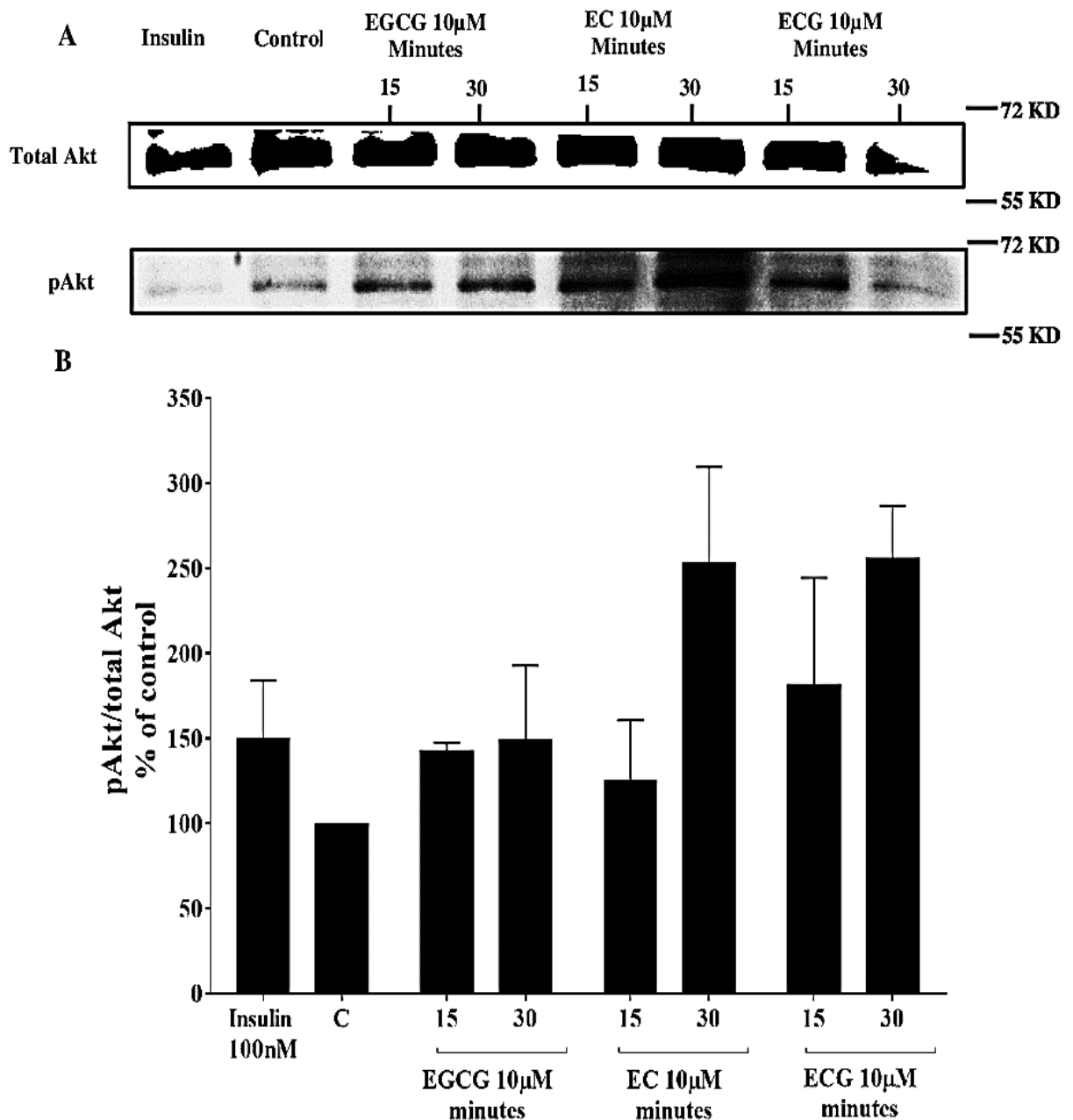


**Figure 3.36 Effect of selected green tea compounds on pAkt expression in 3T3-L1 cells.**

3T3-L1 cells were seeded in 6 well plate at density  $6 \times 10^5$  and incubated in standard conditions until completed confluency. Differentiation was induced, and the cells were serum starved for 2h, and then were treated with 10 $\mu$ M of EGCG, EC, and ECG for 15 and 30 minutes. Total protein was isolated and quantified, and phosphor western blotting was performed to identify the leve of pAkt. (A). Total and phosphorylation levels of Akt protein bands represented one experiment. (B) Analysed band intensity of pAkt expression. Due to the experiment was performed in two occasion, therefore, no final conclusion can be drawn and more independent experiment is needed. The data displayed as a % of control which normalised to total Akt expression. Bands intensity were quantified using Image J software. Data presented as n=2.

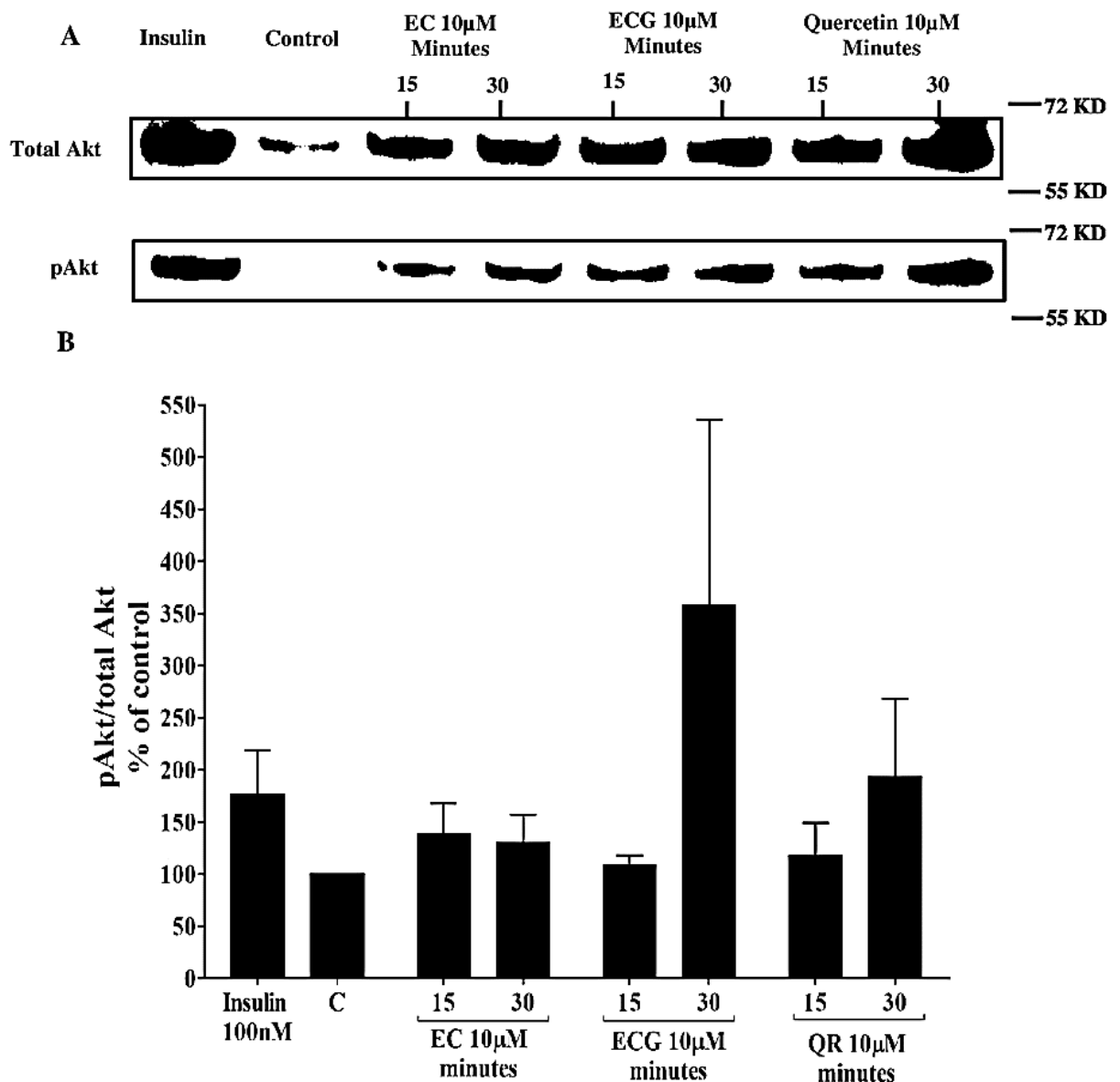


**Figure 3.37 Effect of selected green tea compounds on pAkt expression in AML12 cells.**

AML12 cells were seeded in 6 well plate at density  $8 \times 10^5$  and incubated in standard conditions until completed confluency. The cells were serum starved for 2h, and then were treated with  $10 \mu\text{M}$  of EC, ECG, and quercetin for 15 and 30 minutes. Total protein was isolated and quantified, phosphor western blotting was performed to identify the leve of pAkt. (A). Total and phosphorylation levels of Akt protein bands represented one experiment. (B) Analysed band intensity of pAkt expression. Due to the experiment was performed in two occasion, therefore, no final conclusion can be drawn and more independent experiment is needed. The data displayed as a % of control which normalised to total Akt expression. Bands intensity were quantified using Image J software. Data presented as  $n=2$ .

### 3.4 Discussion

Normal cellular glucose homeostasis contributes significantly towards the maintenance of normal blood glucose levels between 4 and 6mmol/L in the circulation (DeFronzo, 1988;Saltiel and Kahn, 2001) and therefore to regular metabolic health. During ageing, or changes in diet or physical inactivity, this process can be disrupted, causing unsustainably high amounts of glucose in the circulation. Prolonged hyperglycaemia together with elevated secretion of insulin eventually leads to decreased insulin sensitivity and a reduction in the ability of metabolic cells to respond to insulin action; a phenomenon referred to as insulin resistance which leads to an increased risk of developing T2D. Therefore, seeking a natural compound that possesses robust properties is essential and can be successfully involved in prevention and/or improving impaired glucose homeostasis including glucose and lipid metabolism. As alternative herbal medicine has been excessively used to protect and cure some diseases, green tea has shown potent properties against wide pathogenic processes, including dysregulation of glucose and lipid metabolism, although the signalling pathway of this impact is not yet completely understood. Therefore, this study was designated to determine the ability of several active compounds of green tea to regulate glucose metabolism and the possible pathway of this effect *in vitro*.

The glucose uptake data presented in this study shows that insulin-sensitive cell lines selectively respond to some compounds of green tea and thus increases cellular glucose and 2-NBDG uptake (Figure 3.3 to Figure 3.11 and Figure 3.24 to Figure 3.26). These increases were produced by different green tea compounds that varied in their effect according to cell type and time of exposure, however small but significant uptake was seen when glucose uptake was measured directly using 2-NBDG compared to amount of glucose uptake that measured by estimating the level of glucose remained in the media. These effect of green tea compounds on glucose uptake in both methods of measuring were not dose dependent, and the effect of some compounds particularly in AML12 cells (Figure 3.9 and Figure 3.11) showed U-shaped doses response. This phenomenon is widely seen, as the low dose promoted effect without affected biological system until the high dose reached threshold which inhibited compounds effect due to saturation (Reynolds, 2010) Therefore, the study suggests that some of these effective compounds produce their effects specific to metabolic cell type. As the green tea compounds can boost glucose uptake in some metabolic cells (Yan, *et al.*, 2012), this is often enhanced through the function of Gluts, particularly class I (Zhao and Keating, 2007). The present study result is partially consistent with recent work which showed green tea, and some of its compounds can increase glucose uptake in hepatocytes (Cordero-Herrera, *et al.*, 2014), myocytes (Deng, *et al.*, 2012), and in adipocytes (Ueda, *et al.*, 2010) through Gluts translocation. However, the current study presents some unique data in AML12 cells. Despite previous contradictory data regarding the level of Glut2 and 4 mRNA expression (Table 3.1 to Table 3.3), the results are suggestive of the effects being mediated via translation regulation of Gluts. Although the results were statistically insignificant, increasing the

number of independent observations might clarify any effect of green tea on Gluts expression. Additionally, due to limitations in budget, it was not possible to investigate protein expression or trafficking of Gluts, so the possibility of green tea compounds regulating glucose homeostasis via translation or post-translational regulation of Gluts exists. Collectively, the study suggests that consumption of some compounds of the green tea could manage high levels of circulating glucose and therefore might be supported pre-diabetic and existing diabetic conditions.

Cellular glucose uptake and metabolism are mainly regulated through the major molecular pathways PI3K and AMPK. Due to the accumulation evidence that identified the green tea compounds can increase glucose uptake and regulate metabolism through activation of the AMPK pathway, the present study considered the role of both Akt and AMPK in the effect of selected green tea compounds that had induced glucose uptake previously. Firstly, this was performed through inhibiting either Akt or AMPK in the insulin-sensitive cell lines that were exposed to selected green tea compounds. The result showed that inhibiting AMPK in C2C12 cells suppressed glucose uptake in response to selected green tea compounds, whilst inhibiting Akt suppressed green tea compounds from inducing glucose uptake in 3T3-L1 and AML12 cells (Figure 3.12 to Figure 3.23). Secondly, based on these results, the activity of pAkt and pAMPK proteins was assessed in insulin-sensitive cell lines in response to green tea compounds to confirm signalling pathway. As this experiment was repeated only twice, the displayed results (Figure 3.35 to Figure 3.37) cannot be used to build a conclusion and therefore further independent experiments are required. These results, however, do not fully correspond with the majority of previous work that has identified several compounds of green tea capable of increasing skeletal muscle cell glucose uptake. This uptake occurs through activating AMPK, which was confirmed by increasing expression of the pAMPK protein (Deng, *et al.*, 2012;Ding, *et al.*, 2012;Li, *et al.*, 2011b;Zhang, *et al.*, 2010). However, Akt could be responsible for this uptake (Jung, *et al.*, 2008). Regulation of glucose uptake and metabolism in adipocyte and hepatocyte using green tea compounds is believed to be through increasing activation of pAMPK (Collins, *et al.*, 2007;Hwang, *et al.*, 2005;Murase, *et al.*, 2009). However, Akt might be involved in this effect of green tea (Ueda, *et al.*, 2010). Regardless of the previously published results, the current study presents some unique data that describes the regulatory effect of some specific compounds of green tea in 3T3-L1 and AML12 through activating Akt signalling. The study, therefore, suggesting that selected green tea compound-induced glucose uptake may selectively activate either PI3K/Akt and/or AMPK pathways depending on insulin-sensitive cell type. A further study encompassing this aspect is, however, needed to understand this further.

The hepatic tissue is play crucial role in maintaining glucose homeostasis under different physiological conditions. Hepatic cellular glucose is usually converted to glycogen in an insulin-dependent manner, together with the activity of specific genes related to glycogen synthesis. In T2D this

is often impaired, which leads to reducing glycogen formation due to decreased glucose uptake, secondary to insulin insensitivity and decreased activity of glycogenic genes. This impairment occurs alongside increased hepatic glucose production through glycogenolysis and gluconeogenesis. The present study attempted to identify the level of glycogen, the activity of glycogen synthesis gene, and activity of genes that directly regulate glucose production in response to selected compounds of green tea. Whilst some green tea compounds failed to induce a significant change in glycogen concentration, ECG after 24h and quercetin after 72h did cause an increase in glycogen storage (Figure 3.30 and Figure 3.31). Alongside this data, analysis of mRNA expression of the glycogen synthase (GS) gene, G6Pase and PEPCCK showed no significant changes in expression (Table 3.3). The effect of green tea compounds on glycogen activity and hepatic glucose production have been recently investigated with contradictory findings being reported. Supplementing green tea to diabetic rats caused an increase in activity of the GS gene and, therefore, increased hepatic glycogen formation compared with non-treated rats, whilst no effect of green tea was found on hepatic glycogen content in rats fed on a high-fat diet (Sundaram, *et al.*, 2013). Furthermore, green tea active constituents play a critical role in the liver gluconeogenic process through regulating key genes, including G6Pase and PEPCCK, and eventually leading to suppressed hepatic glucose production (Collins, *et al.*, 2007; Waltner-Law, *et al.*, 2002; Yasui, *et al.*, 2011). The data regarding gene expression, however, did not support the previous positive effect of green tea compounds, as measuring mRNA does not always provide a proper indication. The amount of protein phosphorylation, which was not considered in this study due to the cost, is therefore required to understand this further. A possible reason for the data on mRNA expression could be due to the poor performance of the primers used to detect the expression of these genes (Figure 8.18 to Figure 8.26), or methodological error due to insufficient independent experiment. While a possible reason for the glycogen result is that the cells did not express an increase in glycogen storage which may have exhibited an increase in glucose oxidation; the cells are removing more glucose from their environment but not storing any extra glycogen. As the insulin also did not induced any significant effect on glycogen content, the possible reason for that could be insensitive assay kit or methodology error and more independent experiment is required. Despite the present study results and previously published results, the study identified the metabolic effect of some green tea compounds on the AML12 cell line for the first time. Therefore any data presented is considered unique.

Adipose tissue is a major site of energy storage which can metabolise glucose into triglycerides through the multistep process of lipogenesis in an insulin-dependent manner. Also, lipolysis, a process of catabolism of triglyceride into glycerol and free fatty acid, is inhibited by insulin (Duncan, *et al.*, 2007). Insulin resistance and diabetes cause an increase in lipolysis rate which increases glycerol and free fatty acid release from adipose tissue stores. It is widely accepted that the green tea extracts can regulate glucose metabolism in adipose tissue importantly through suppressed lipolysis and therein FFA releases. The present study investigates these impacts in mature 3T3-L1 cells. As the results show, the

selected green tea compounds reduced triglyceride levels (Figure 3.33) and glycerol release (Figure 3.34). The study did not, however, detect any significant differences in mRNA levels of adipogenic and lipolytic genes (Table 3.2). These insignificant expressions of mRNA could be due to insufficient independent experiment, or unspecific primer binding (Figure 8.8 to Figure 8.17). This data fits with previous study results which have demonstrated the ability of green tea extracts to prevent fat formation (Cunha, *et al.*, 2013; Lee, *et al.*, 2009a; Mochizuki and Hasegawa, 2004), and to reduce lipolysis by decreasing the amount of glycerol released (Kim, 2014). These effects are enhanced through alteration of some adipogenic and lipolytic key genes including C/EBP- $\alpha$ , PPAR- $\gamma$ , SREBP-1c, FABP4, LPL and FAS by downregulating expression levels of their mRNA (Lee, *et al.*, 2009b). Based on all of these results together, the study suggests that EGCG, EC, and ECG possess anti-obesity effects by altering the levels of lipogenesis/lipolysis through an as yet unexplored mechanism. As only the levels of mRNA were measured with no significant result, it was difficult to draw a mechanism and measurement of protein activities are therefore needed to explore this further. Despite the previously published results, the data presented here is very pertinent as the study used mature cells that closely exhibited the normal physiological functions seen in the human body. Accordingly, early and regular consumption of green tea compounds could prevent more triglyceride accumulation and suppress FFA release, which might protect from developing obesity and T2D, or could manage them if they already exist.

Ultimately, the study has identified that several active compounds of green tea including EGCG, EC, ECG, quercetin, and a combination of these compounds, could regulate cellular glucose and lipid metabolism in insulin-sensitive cell lines. The regulatory effects of these compounds are firstly through increasing cellular glucose uptake, which induced selectively based on compounds and cell type. Some of these compounds in addition to increased glucose uptake, stimulated firstly used AML12. Furthermore, in addition to well-known regulatory effect of EGCG in adipose cells, EC and ECG showed potent effect to regulate lipogenesis/lipolysis including suppressed more triglyceride accumulation and FFA release, this observation is important as obesity is encompassed releases of FFA which both involved in development insulin resistance. All these effects are in part mediated by selective activation of either AMPK in skeletal muscle cells or Akt hepatic and adipose cells, and this result suggests selective effect of green tea compounds according to cell type. However, the signalling pathway of these effects are not yet confirmed and specific studies to investigate this further are required. These compounds could, however, potentially be therapeutic agents to regulate glucose and lipid metabolism in individuals with metabolic disease or disorders like obesity and T2D.

## **Chapter Four**

# **The effect of green tea extract on glucose homoeostasis in high glucose fed mice**

## 4.1 Introduction

A cluster of risk factors has been shown to have a critical role in dysregulation body glucose homeostasis and increase the incidence of several disorders and diseases related to impairment glucose and lipid metabolism (Lebovitz, 2006;Martín-Timón, *et al.*, 2014;Rossner, 2002). Obesity associated with insulin resistance, dyslipidaemia, and glucose intolerance are the major metabolic dysfunction referred to as 'metabolic syndrome' that increases the risk of type 2 diabetes (T2D) (Batsis, *et al.*, 2007;Flier, 2004;Kahn, *et al.*, 2006). Excessive caloric intake is the main factor involved in the development of individual obesity which is linked to insulin resistance that precedes to T2D (Hill, *et al.*, 2012;Pang, *et al.*, 2014). In this case, there is an increased glucose influx concomitant with elevated hepatic glucose production that causes continuous hyperglycaemia which is a characteristic feature of T2D (Inzucchi, *et al.*, 2012;Nathan, *et al.*, 2009).

Rodents, particularly mice and rats, are widely used as a model to study dysregulated of glucose and lipid metabolism including conditions such as obesity, insulin resistance, and T2D. The diet-induced obesity and insulin resistance in rodents is gaining attention as a tool to investigate the role and composition of the diet in the induction of obesity (Barbosa-da-Silva, *et al.*, 2014;Islam and Loots du, 2009). In addition to impairment of glucose metabolism (Bowe, *et al.*, 2014), and development of novel anti-diabetic treatments (King, 2012). The effect of high-fat diet on C57BL/6 mice was firstly reported in 1988 (Surwit, *et al.*, 1988). Mice that consumed a high-fat diet developed obesity, impaired of glucose tolerance, dysregulated of glucose homeostasis and insulin resistance (Ahren, 1999;Winzell and Ahren, 2004). Furthermore, this impairment can be achieved by inducing a positive energy balance via supplementing other nutrients. These nutrients could be the carbohydrates sucrose and fructose either in diet or drinking water (Lim, *et al.*, 2010;Schultz, *et al.*, 2013;Sumiyoshi, *et al.*, 2006;Tran, *et al.*, 2009;Wagoner, *et al.*, 2015).

The beneficial effects of green tea extract and/or some of its main active constituents on the regulation of glucose and lipid metabolism has previously been studied in animal models (Chen, *et al.*, 2011;Haidari, *et al.*, 2012), and in human trials (Mackenzie, *et al.*, 2007;Suliburska, *et al.*, 2012;Venables, *et al.*, 2008;Zhang, *et al.*, 2012). The green tea extract or EGCG can improve glucose tolerance in rodent fed high fat, high fructose and sucrose diet induced obesity, and in induced diabetes (Chen, *et al.*, 2009;Tang, *et al.*, 2013;Wolfram, *et al.*, 2005;Wu, *et al.*, 2004b). Secondly, consumption of these compounds caused reduction of high fasting blood glucose that resulted from dysregulation of glucose and lipid metabolism in obesity and diabetes (Alam, *et al.*, 2014;Bose, *et al.*, 2008;Tsuneki, *et al.*, 2004;Wu, *et al.*, 2004a). In addition, green tea compounds can reduce accumulation of fat in various body regions, as well as reduce body weight and weight gain (Chen, *et al.*, 2009;Cunha, *et al.*, 2013;Klaus, *et al.*, 2005;Park, *et al.*, 2011). Furthermore, decreased the level of circulating insulin,

ameliorated insulin resistance and increased insulin sensitivity in obese and pre-diabetic subjects (Bose, *et al.*, 2008;Nomura, *et al.*, 2015;Tang, *et al.*, 2013;Wu, *et al.*, 2004a;Wu, *et al.*, 2004b). Moreover, these compounds show the ability to regulate impaired lipid metabolism by decreasing the levels of circulating cholesterol and triglyceride (Axling, *et al.*, 2012;Bose, *et al.*, 2008;Sugiura, *et al.*, 2012).

The aims of the research described in this chapter are:

- To explore the impact of green tea extract and its abundant active compound (EGCG) on body weight and weight gain, subcutaneous, visceral, and intra-scapular fat weight, feeding and drinking behaviour in mice fed normal chow and drinking either water or high glucose supplemented water.
- To investigate the effect of these natural compounds on measures of glucose metabolism including fasting glucose, glucose tolerance, insulin sensitivity, beta-cell function, and markers of lipid metabolism including measurement of total cholesterol (TC), triglyceride (TG), high-density lipoprotein (HDL), and low-density lipoprotein (LDL) in both normal and glucose fed mice.
- To determine the role of these compounds to regulate genes expression related to glucose and lipid metabolism in the main metabolic insulin-sensitive tissues (hepatic, skeletal muscle, and adipose tissues).

## 4.2 Materials and methods

All material and methods that have been used to investigate the effects of green tea extracts and its main compound EGCG on glucose homeostasis *in vivo* were mentioned in details in chapter two. These methods including measurement the level of glucose during tolerance test (GTT), fasting blood glucose (FBG) using glucose meter, calculated glucose area under the curve (gAUC). In addition to estimate the level of fasting serum insulin through ELISA kit, and calculating homeostasis model assessment including insulin resistance, beta cell function, and insulin sensitivity (HOMA-IR, B, and S) based on FBG and insulin data in fasting state using computerised HOMA calculator two software. Furthermore, food and water consumption, total weight gain, fat pads mass (visceral, subcutaneous, intra-scapular), and organs weight, as well as lipid profile including TC, HDL, TG, and cLDL. TG and HDL were measured by using CardioChek<sup>®</sup> P.A analyser, and the level of TC was estimated by colorimetric assay, whereas, cLDL was calculated by using Friedewald equation based on the levels of TC, TG, and HDL. Moreover, expressions of some genes that involved in regulation of glucose and lipid metabolism in insulin-sensitive tissue were measured by using qPCR. All data were analysed using one way ANOVA followed by Tukey's post-hoc test for multiple comparisons unless otherwise stated.

## 4.3 Results

### 4.3.1 Effect of green tea extracts and EGCG on total weight and weight gain

Total body weight and therefore weight gain were monitored weekly in the control and three treatment groups decaffeinated green tea extract (DGTE), EGCG, and commercial green tea extract (GTE) of mice that had water supplemented with or without glucose. Whole body weight of mice showed no significant differences between treatment and control in all groups, except GTE fed mice, which displayed a significant increase body weight of 11% ( $p=0.0392$ ) and 12.25% ( $p=0.0247$ ) at week one only in both main groups respectively (Figure 4.1). Mice that received treatments without glucose showed significantly less weight gain compared to control, with DGTE fed mice having  $40.8\% \pm 8\%$  less weight gain ( $p=0.0070$ ), and EGCG fed mice having  $31\% \pm 4.5\%$  less weight gain ( $p=0.0471$ ) (Figure 4.2 A). However, GTE fed mice did not show a significant decrease in weight gain. No significant effect of green tea extracts on weight gain were seen in mice receiving treatment with a high glucose diet compared to control mice (Figure 4.2 B).

### 4.3.2 Effect of green tea extracts and EGCG on food and water intake

Diet and water consumption were measured weekly during the treatment period. The average food consumed (mouse/day) in mice treated without glucose was: 3.79g (control), 3.39g (DGTE), 3.57g (EGCG), and 3.88g (GTE). From this, only DGTE caused a significant decrease food intake by  $10.4\% \pm 3.2\%$  ( $p=0.0007$ ) compared to control (Figure 4.3 A), whereas no significant differences in food intake were recorded between treatment and control groups that received 30% (w/v) of glucose alongside green tea extracts. The average food intake (mouse/day) of these groups were: 2.041g (control), 1.863g (DGTE), 2.32g (EGCG), and 1.9g (GTE) (Figure 4.3 B). These data do however show that supplementation of water with glucose reduced the amount of food consumed in all groups. Water intake (mouse/day) was calculated in (control, DGTE, EGCG, and GTE) groups fed normal and a glucose diet, and the average intakes were; 5.776mls, 4.149mls, 4.797mls, and 6.252mls and 8.155mls, 9.578mls, 8.79mls, and 9.037mls respectively. Based on analysed data, there were no significant differences between treatment and control of all groups except DGTE, which caused a significant decrease water intake by  $28.2\% \pm 4\%$  ( $p=0.0382$ ) in mice fed a normal diet (Figure 4.4). According to water consumption data, the actual doses of treatment were calculated for each group. These doses were 39.555, 13.943, and 89.036mg/kg/day for groups receiving DGTE, EGCG, and GTE without glucose respectively, and for those fed with high glucose, the doses were 56.628, 11.748, and 83.759 mg/kg/day respectively.

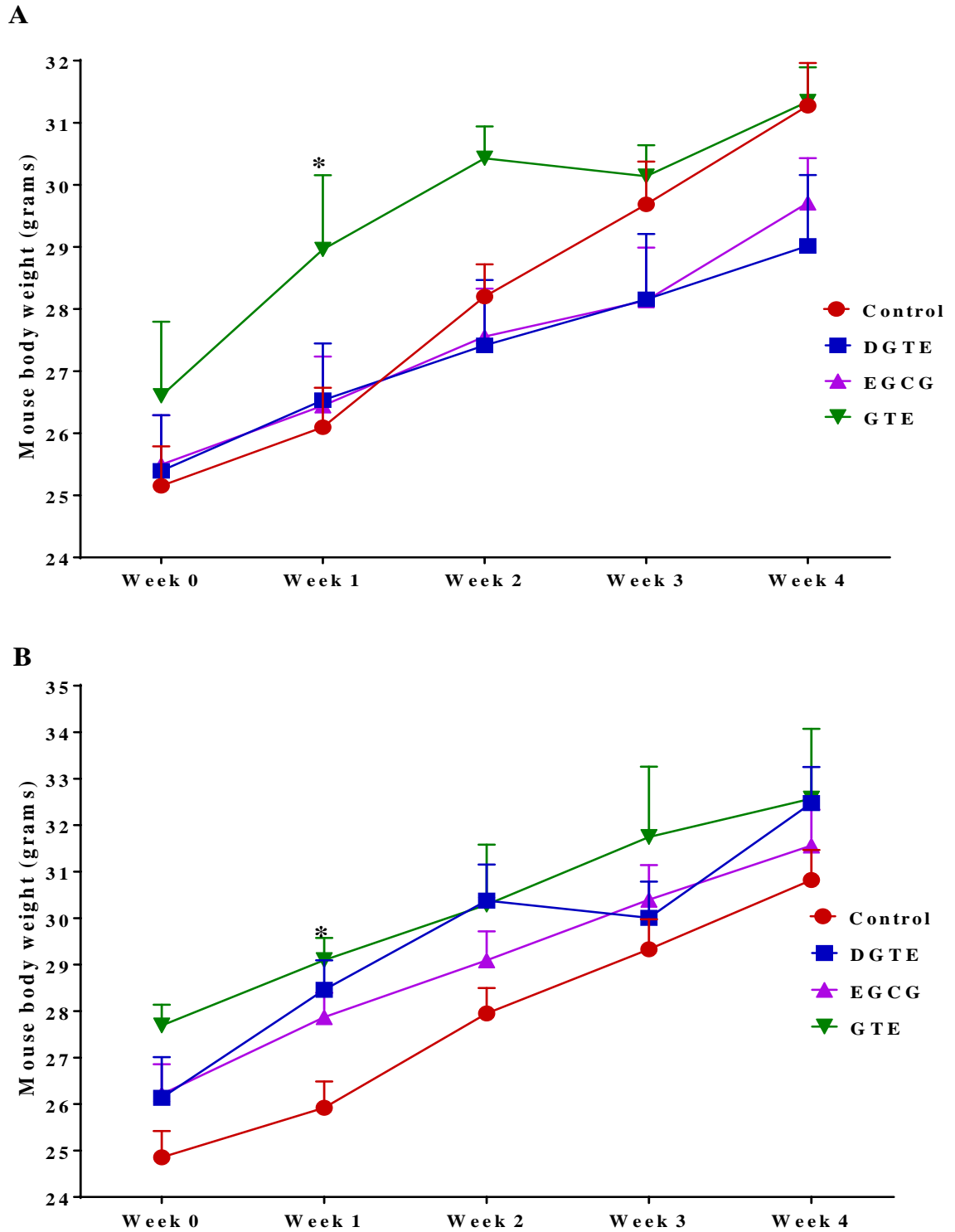


**Figure 4.1 GTE increases body weight at week one in mice fed normal or glucose-rich diet.**

Mice fed DGTE, EGCG, and GTE for 28 days in drinking water supplemented with or without 30% (w/v) of glucose. Mice weight was measured weekly and average weight was then calculated every week during experiment. (A) Body weight of mice fed green tea compounds without glucose diet, only GTE at week one increased body weight compared to control. (B) Body weight of mice fed green tea compounds alongside glucose diet, only GTE at week one increased body weight compared to control. Data presented mean  $\pm$  SEM, \* $p < 0.05$ ,  $n = 6$ .

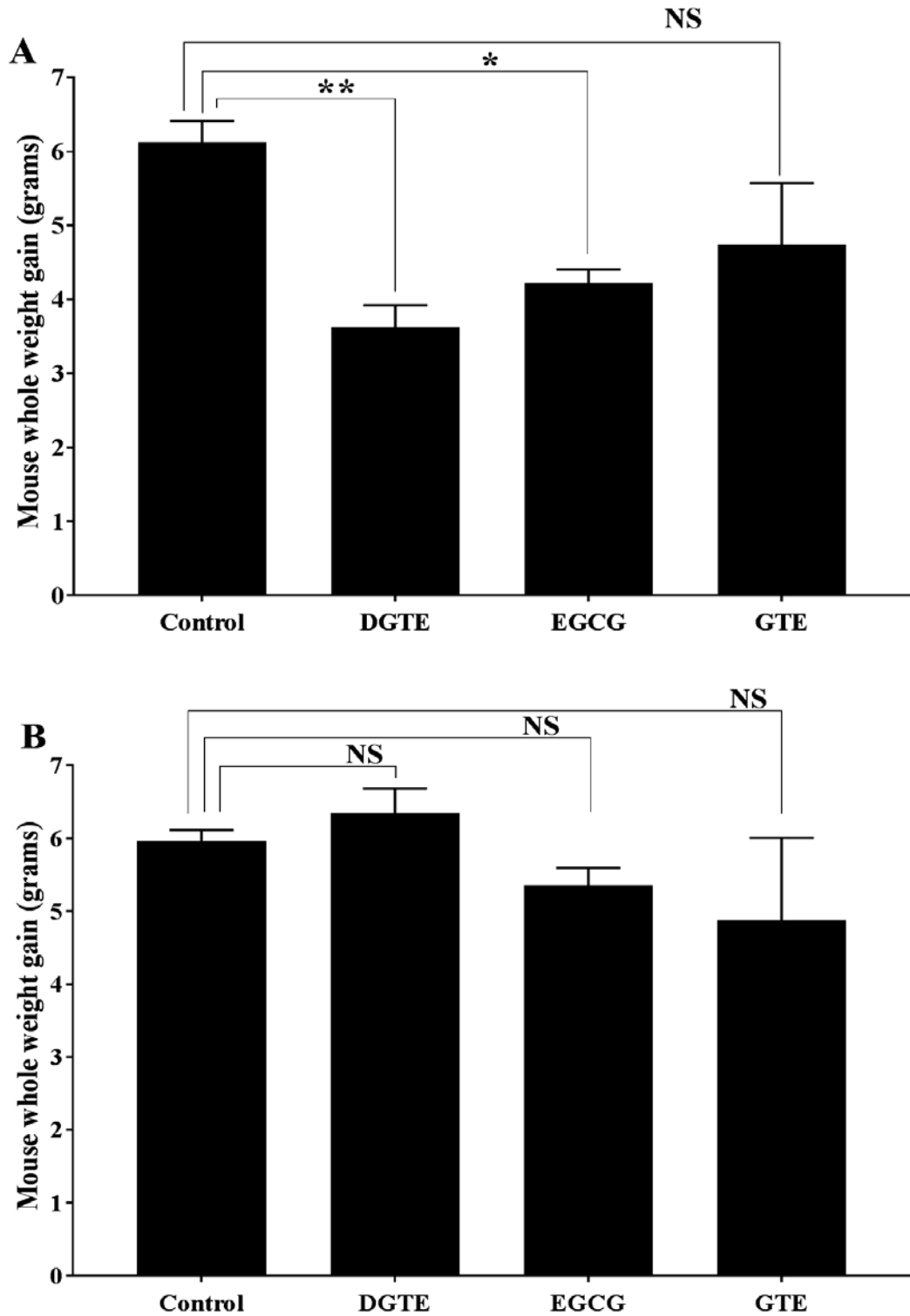


**Figure 4.2 Selected green tea extracts reduce weight gain in mice fed normal diet.**

Mice fed DGTE, EGCG, and GTE for 28 days in drinking water supplemented with or without 30% (w/v) of glucose. Mice weight was measured weekly and average weight gain was then calculated at the end of experiment. Mice body weight gain was calculated based on the differences between the recorded weight of mice at day 0 and day 28 post treatment with green tea extracts. (A) DGTE and EGCG significantly decreased weight gain in mice fed normal diet compared to control. (B) All treatments showed no significant effect to reduce weight gain in mice supplemented with glucose diet. Data presented mean  $\pm$  SEM, \* $p < 0.05$ , and \*\* $p < 0.01$ ,  $n = 6$ .

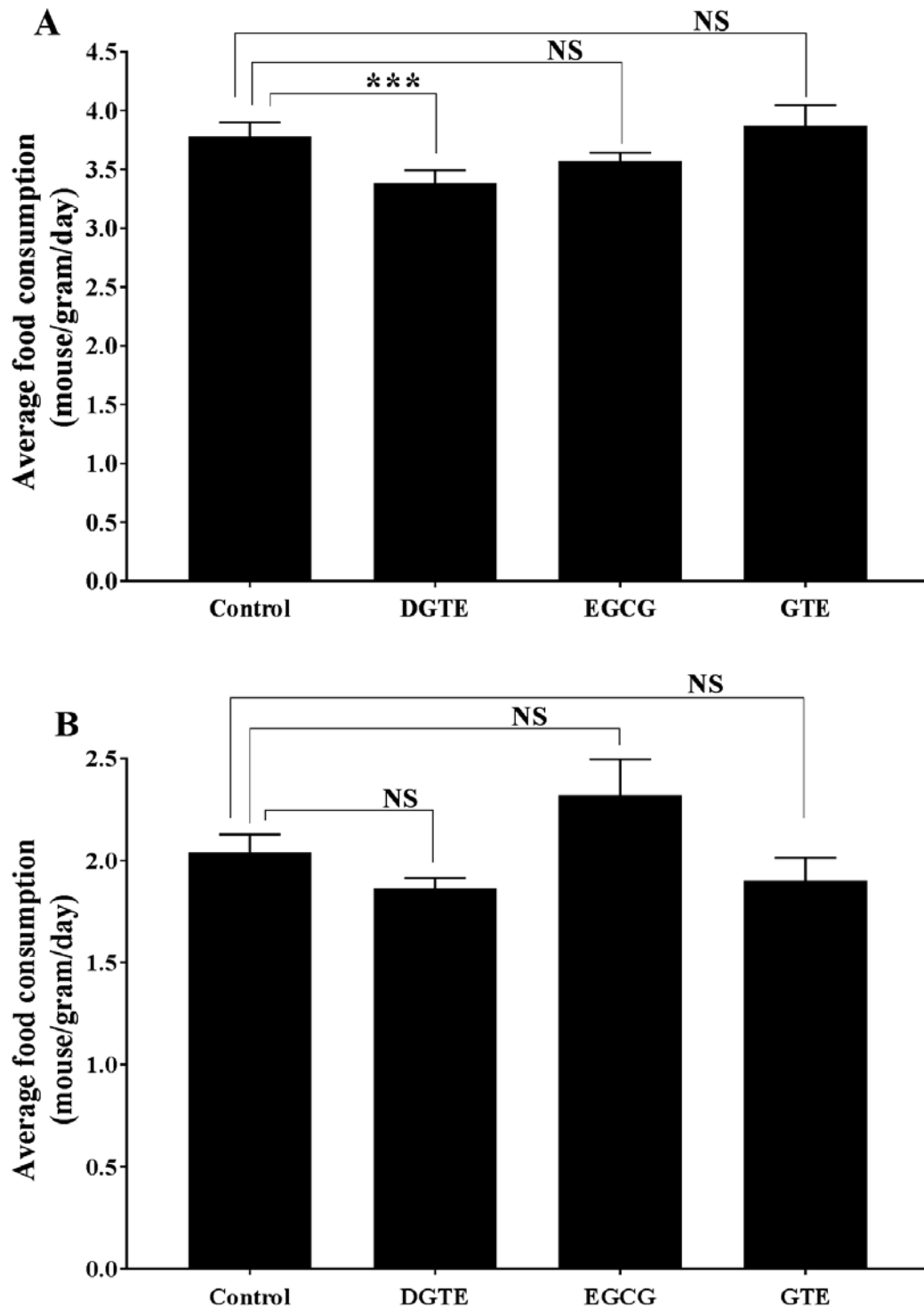


**Figure 4.3 DGTE reduces diet intake in mice fed normal diet.**

Mice fed DGTE, EGCG, and GTE for 28 days in drinking water supplemented with or without 30% (w/v) of glucose. Mice food intake was measured twice a week and average chow intake was then calculated at the end of experiment. (A). Diet consumption of mice received treatments without glucose diet; only DGTE decreased diet intake compared to control. (B). Diet consumption of mice received treatments with glucose diet, no effect of all treatments on food intake compared to control. However, mice received 30% (w/v) of glucose in drinking water showed decreases diet intake compared to mice received normal water. Data presented mean  $\pm$  SEM, \*\*\* $p < 0.001$ ,  $n = 6$ .

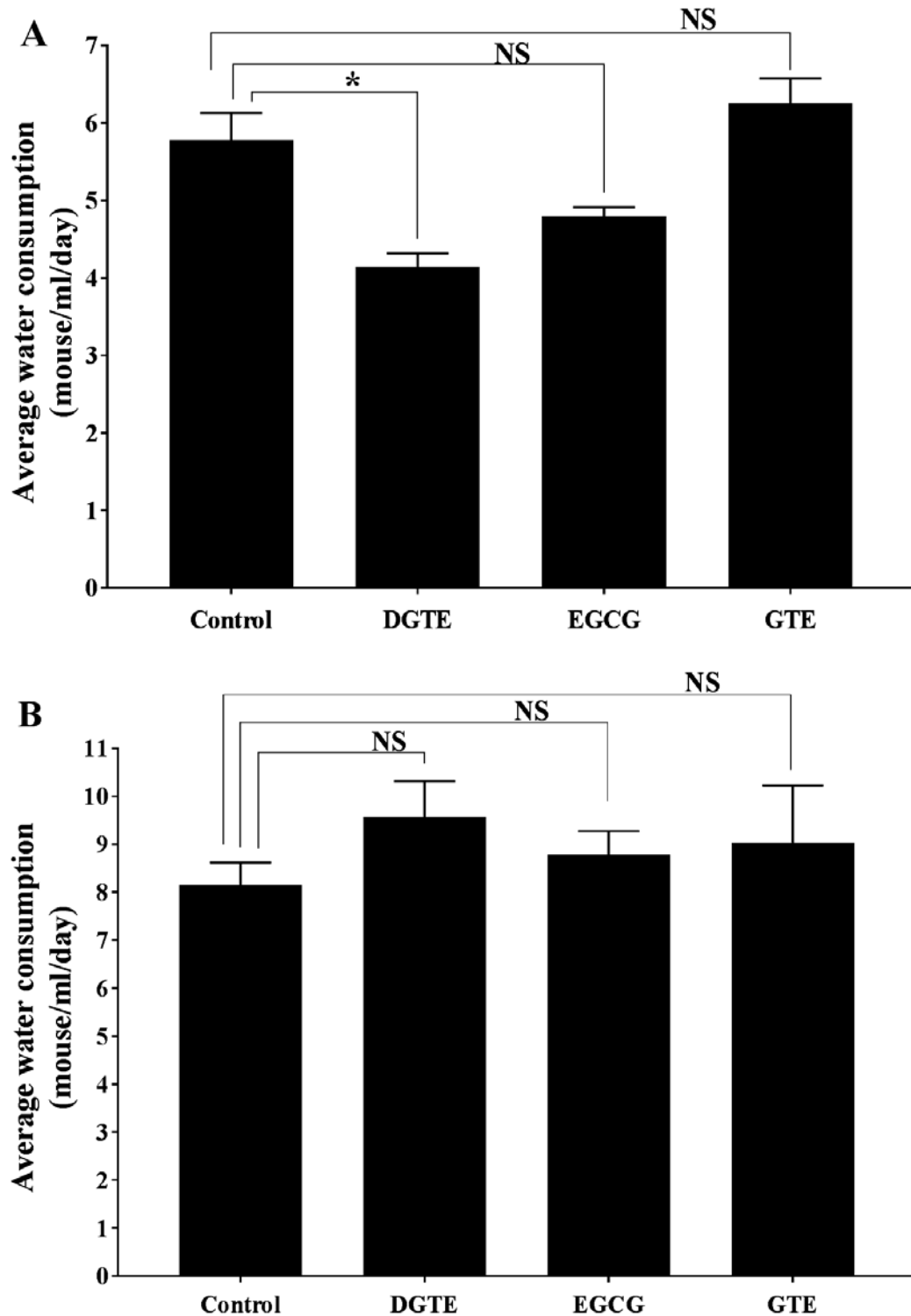


**Figure 4.4 DGTE reduces water intake in mice fed normal diet.**

Mice fed DGTE, EGCG, and GTE for 28 days in drinking water supplemented with or without 30% (w/v) of glucose. Mice water intake was measured twice a week and average water intake was then calculated at the end of experiment. (A). Average water consumptions of mice received treatments without glucose water; only DGTE decreased water intake compared to control. (B). Water consumption of mice received treatments with glucose-rich diet, no effect of all treatments on water intake compared to control. However, mice fed 30% (w/v) of glucose water showed increases water intake compared to mice fed normal water. Data presented mean  $\pm$  SEM, \* $p < 0.05$ ,  $n = 6$ .

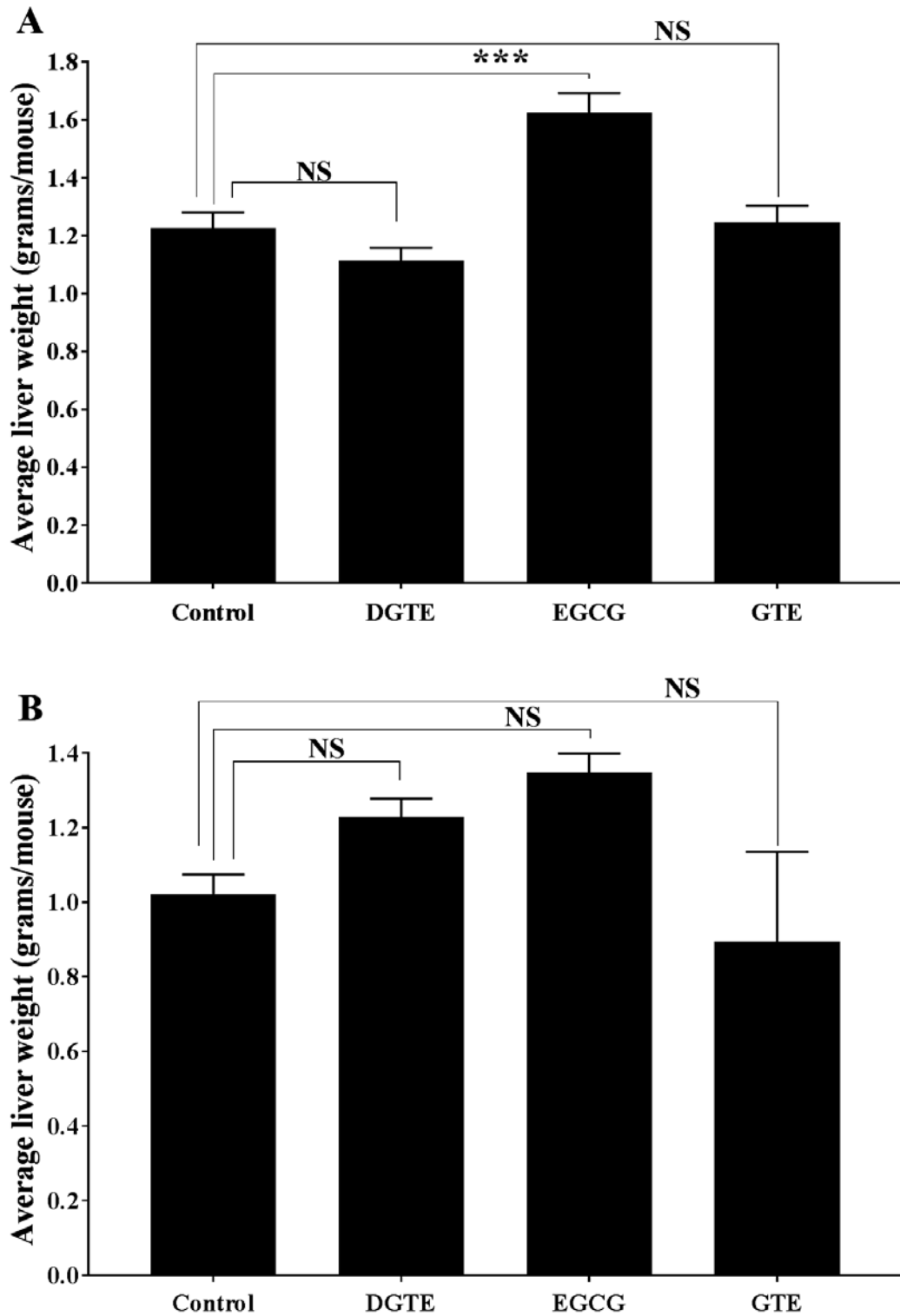
#### 4.3.3 Effect of green tea extract on insulin-sensitive tissue mass

Liver, skeletal muscle, subcutaneous adipose tissue (SAT), visceral adipose tissue (VAT), and intrascapular brown adipose tissue (BAT) were harvested and weighted after 28 days of treatment with DGTE, EGCG, and GTE supplementation with or without high glucose diet. Only EGCG significantly increased liver mass ( $32.6\% \pm 4.1\%$ ,  $p=0.0004$ ) compared to control in mice fed a normal diet (Figure 4.5 A). All green tea treatments supplemented with a high glucose diet did not alter liver mass compared to control (Figure 4.5 B). All green tea extracts provided to mice without and with a glucose diet did not affect skeletal muscle mass compared to control (Figure 4.6).

Mice supplemented with 30% (w/v) of glucose in their drinking water for 28 days showed no significant changes in fat depots mass compared to mice received only water except SAT weight was significantly increased ( $p=0.0375$ ). SAT mass was significantly increased in mice receiving DGTE and EGCG without glucose supplementation compared to control. These increases in mass were  $88.7\% \pm 14\%$  ( $p=0.0186$ ) and  $192.2\% \pm 8.1\%$  ( $p<0.0001$ ) (Figure 4.7 A). SAT mass in mice supplemented with green tea extracts alongside glucose diet appeared to be higher than control, however only DGTE and GTE promoted significant increases. The recorded increases of SAT mass were  $88.6\% \pm 12\%$  ( $p=0.0116$ ) and  $82.5\% \pm 13.7\%$  ( $p=0.0197$ ) respectively (Figure 4.7 B). Only EGCG treatment significantly altered VAT mass with an increase of  $121.6\% \pm 7.8\%$  ( $p<0.0001$ ) being recorded in mice fed a normal diet compared to control (Figure 4.8 A). DGTE and GTE significantly increased VAT mass by  $91.5\% \pm 12.7\%$  ( $p=0.0145$ ) and  $85.4\% \pm 14\%$  ( $p=0.0237$ ) compared to control in mice fed a glucose-rich diet (Figure 4.8 B). In mice fed a normal diet only, EGCG caused a significant increase in BAT mass by  $76.5\% \pm 6.9\%$  ( $p<0.0001$ ) compared to control (Figure 4.9 A). Mice supplemented with a high glucose diet alongside green tea treatments DGTE, and GTE increased BAT mass by  $79.7\% \pm 6.4\%$  ( $p=0.0082$ ) and  $101\% \pm 8.8\%$  ( $p=0.0009$ ) compared to control (Figure 4.9 B).

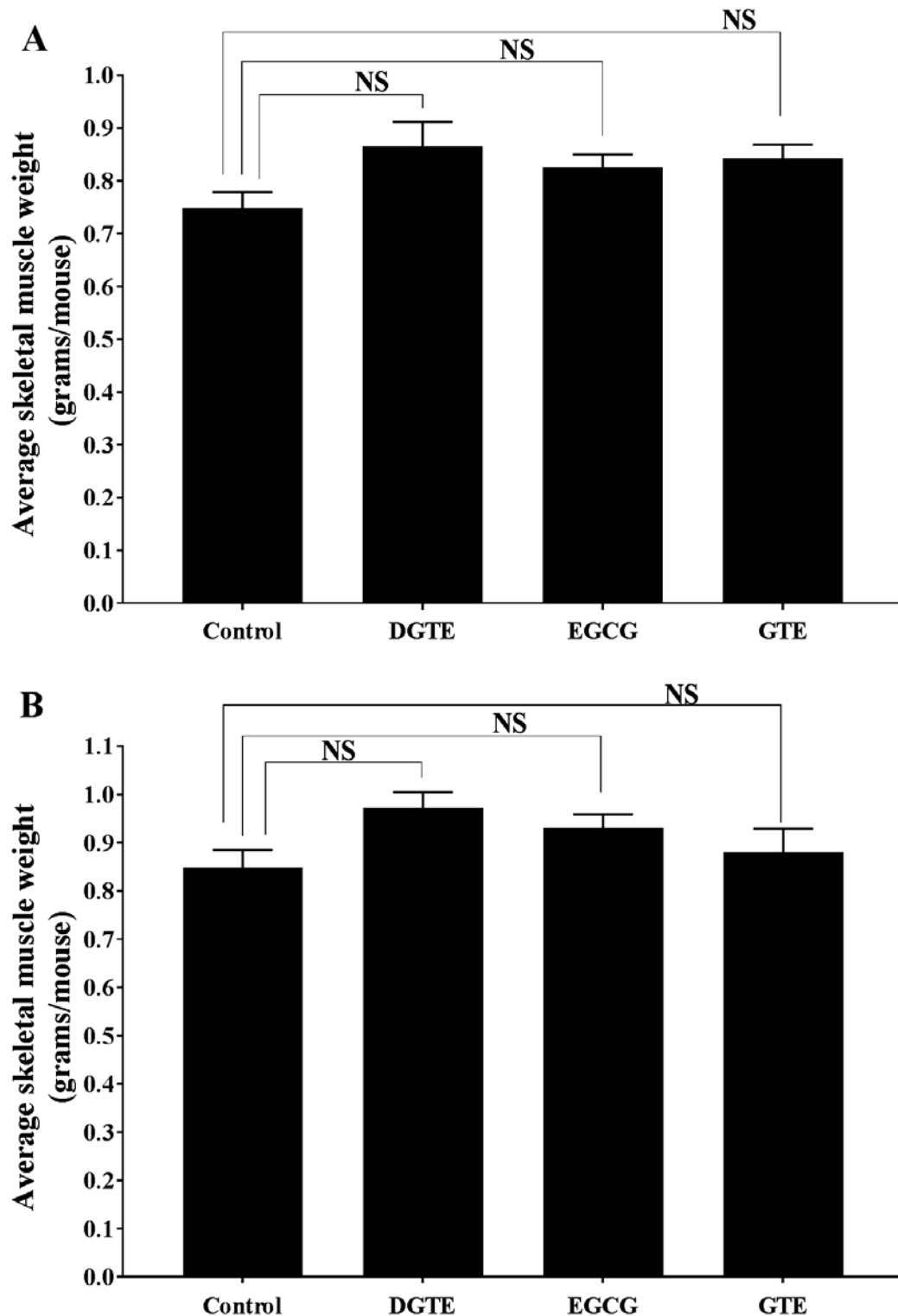
#### 4.3.4 Effect of green tea extracts on glucose tolerance test (GTT)

The GTT was performed before and after treatment with DGTE, EGCG, and GTE with and without glucose supplementation for 28 days. The level of blood glucose was monitored at set time points (0 – 2h) during GTT (Figure 4.10). From obtained data, glucose area under the curve (gAUC) was calculated, and the result showed no differences between green tea extract treatments and control in all groups (Figure 4.11). The level of glucose after 2h was recorded to identify the ability of the body to dispose of glucose. In all groups, those who administered green tea extracts without or with a glucose diet showed no significant differences in blood glucose concentration between treatment and control which indicated that green tea extract did not increase glucose clearance (Figure 4.12). Furthermore, Glucose supplemented to mice for 28 days did not significantly impair glucose tolerance compared to glucose tolerance at day 0 as the gAUC and glucose clearance were not significantly changed.



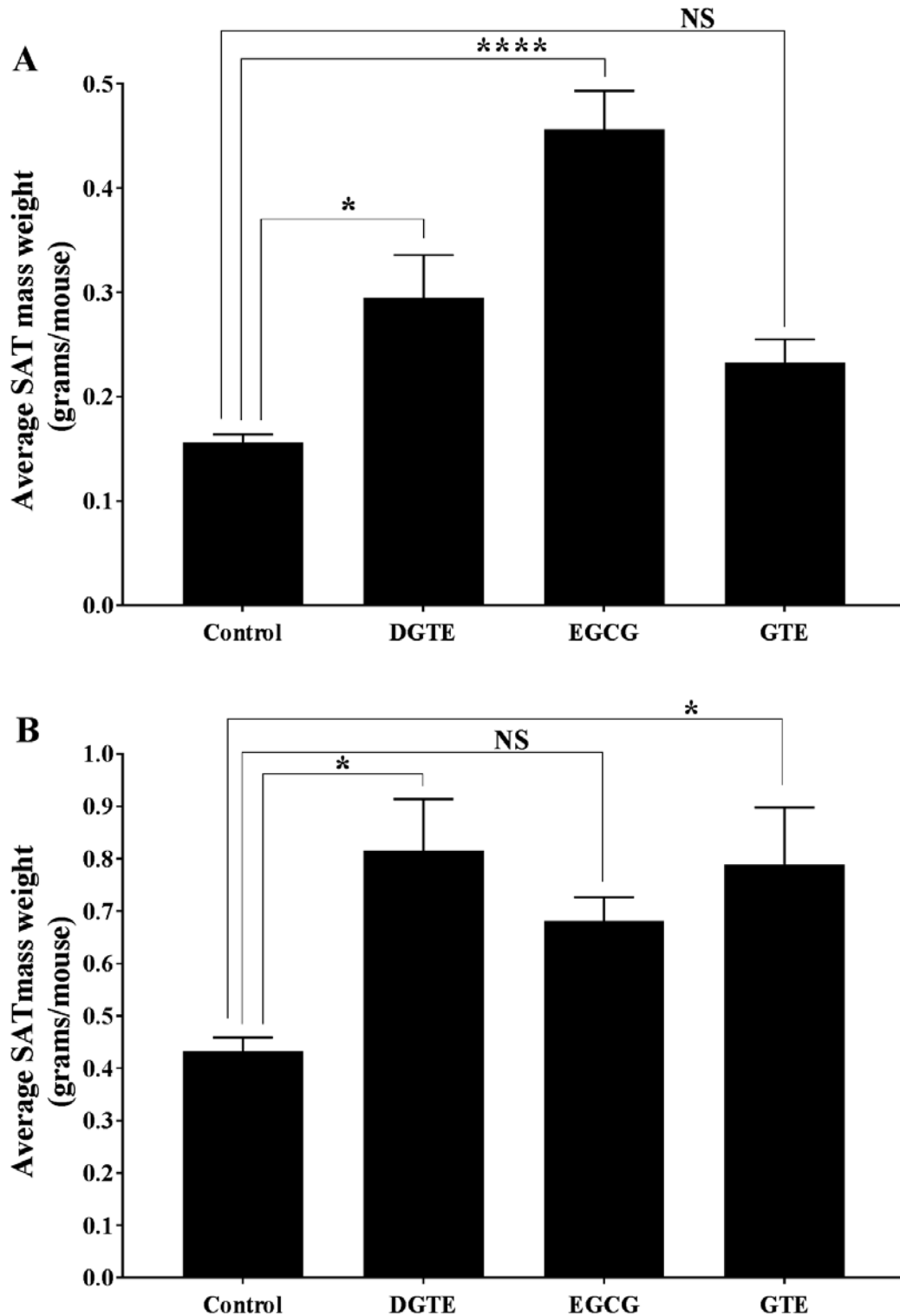
**Figure 4.5 EGCG increases liver mass in mice fed normal diet.**

Mice fed DGTE, EGCG, and GTE for 28 days in drinking water supplemented with or without 30% (w/v) of glucose. At the end of experiment, fasted mice were sacrificed, and the liver was dissected and weighted, and then average weight was calculated. (A). Liver mass of mice fed a normal diet with green tea extracts; only EGCG increased liver weight compared to control. (B). Liver mass of mice fed glucose rich diet with green tea extracts; all treatments did not change liver mass compared to control. Data presented mean  $\pm$  SEM, \*\*\* $p < 0.001$ ,  $n = 6$ .



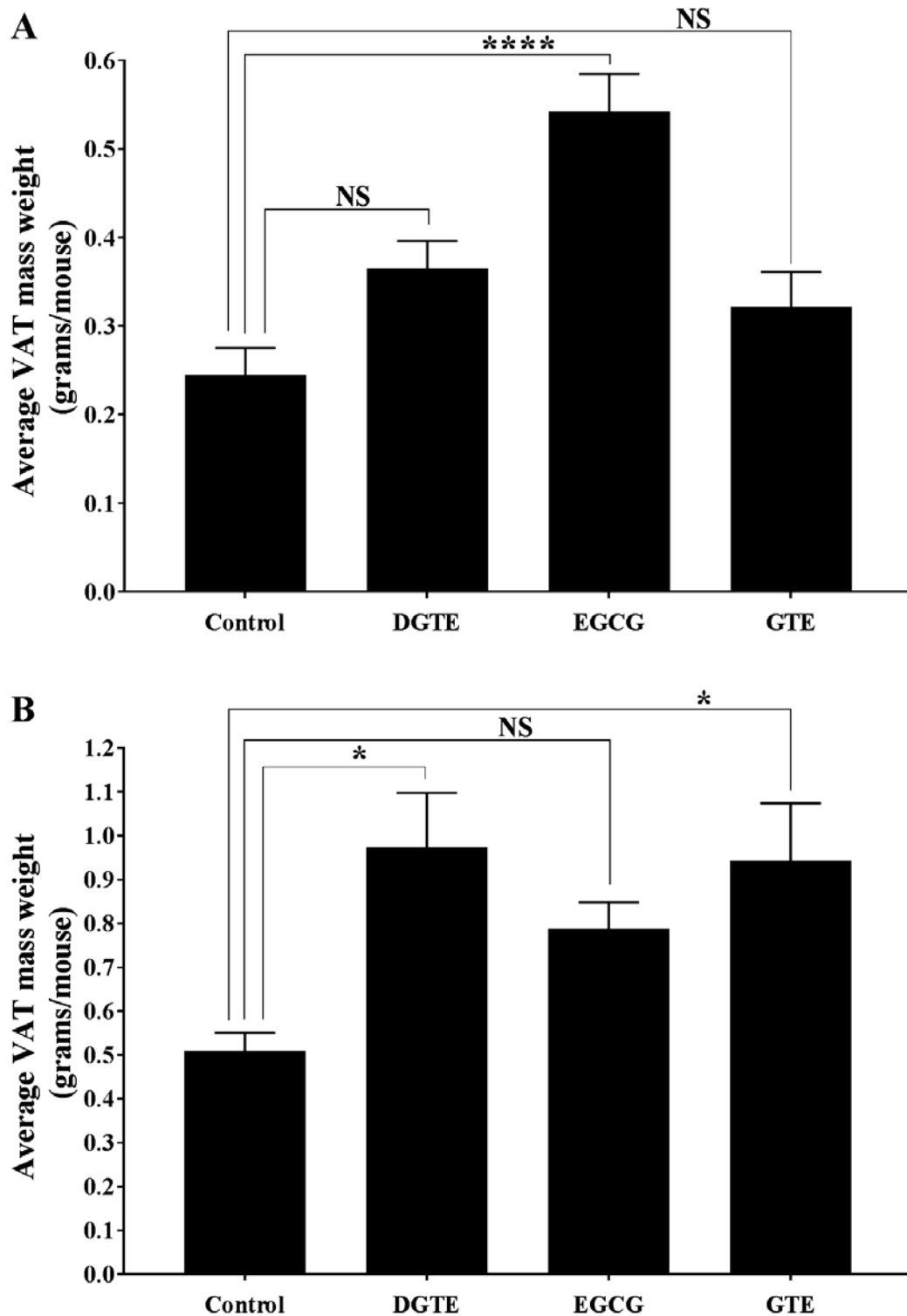
**Figure 4.6 Green tea extracts do not alter skeletal muscle mass in all mice groups.**

Mice fed DGTE, EGCG, and GTE for 28 days in drinking water supplemented with or without 30% (w/v) of glucose. At the end of experiment, fasted mice were sacrificed, and the skeletal muscles were dissected and weighted, and then average weight was calculated. (A). The skeletal muscle mass of mice fed a normal diet with green tea extracts showed no differences between treated and control group. (B). The skeletal muscle mass of mice fed glucose rich diet with green tea extracts showed no differences between treated and control group. Data presented mean  $\pm$  SEM, n=6.



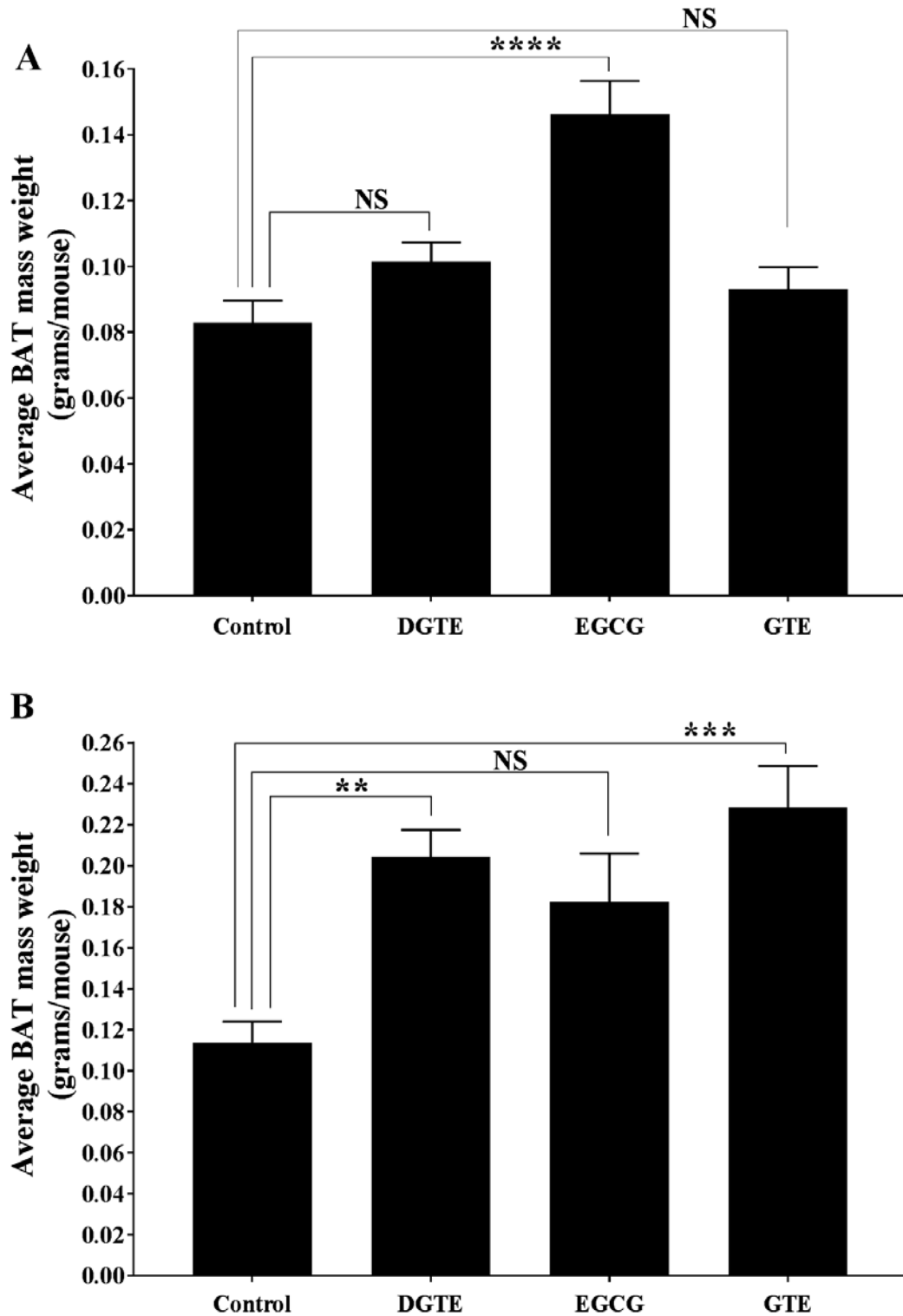
**Figure 4.7 Selected green tea extracts increase SAT mass in mice fed normal or glucose-rich diet.**

Mice fed DGTE, EGCG, and GTE for 28 days in drinking water supplemented with or without 30% (w/v) of glucose. At the end of experiment, fasted mice were sacrificed, and the SAT was dissected, weighted, and the average weight was calculated. Mice fed glucose diet showed significant increased SAT weight compared to normal mice. (A). SAT mass of mice fed a normal diet with green tea extracts, DGTE and EGCG increased SAT mass compared to control. (B). SAT mass of mice fed glucose diet with green tea extracts, DGTE and GTE increased SAT mass compared to control. Data presented mean  $\pm$  SEM, \* $p < 0.05$  and \*\*\*\* $p < 0.0001$ ,  $n = 6$ .



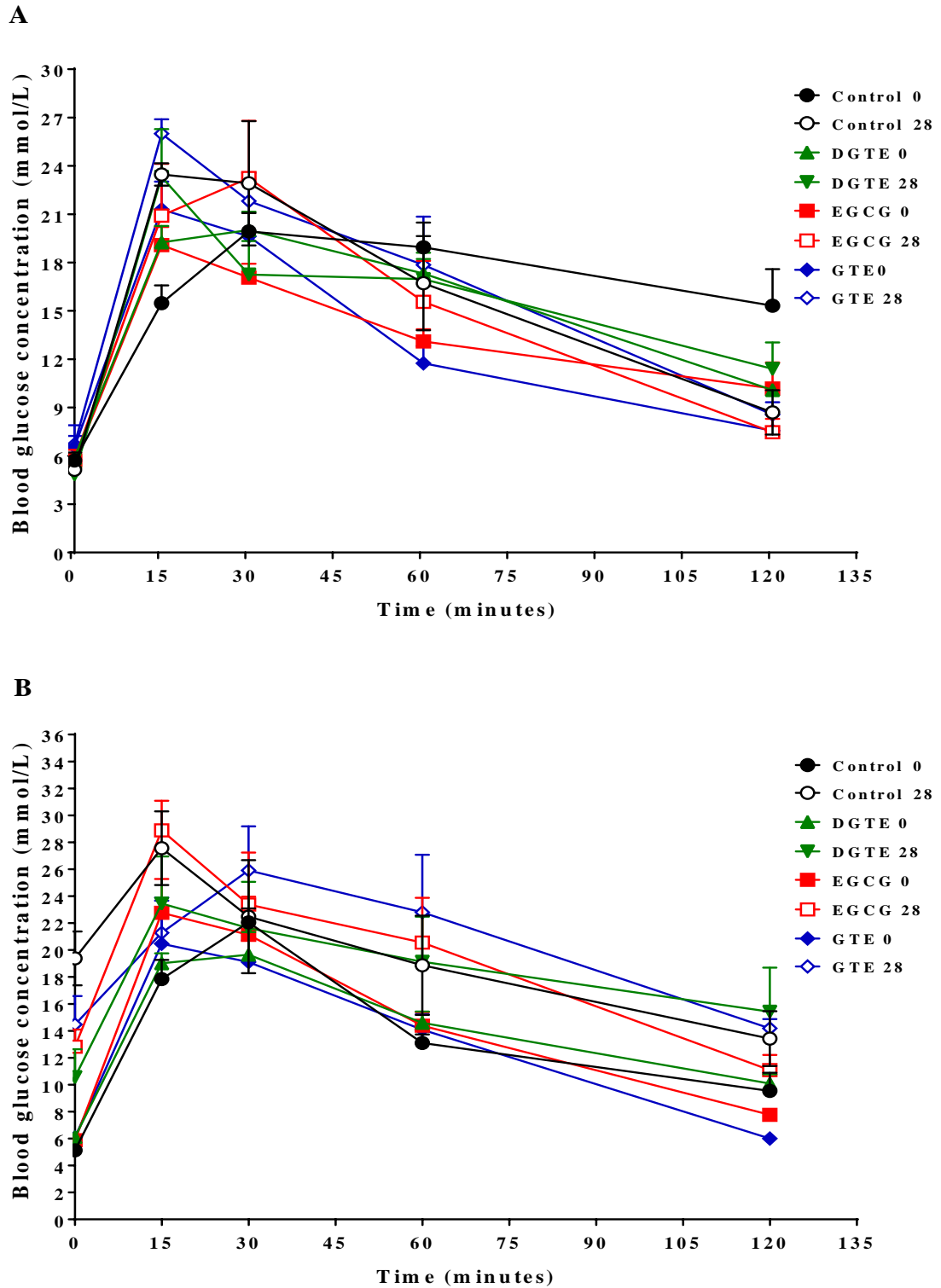
**Figure 4.8 Selected green tea extracts increase VAT mass in mice fed normal or glucose-rich diet.**

Mice fed DGTE, EGCG, and GTE for 28 days in drinking water supplemented with or without 30% (w/v) of glucose. At the end of experiment, fasted mice were sacrificed, and the VAT was dissected, weighted, and the average weight was calculated. Mice fed glucose diet showed no significant of VAT weight compared to normal mice. (A). VAT mass of mice fed a normal diet with green tea extract, EGCG increased VAT mass compared to control. (B). VAT mass of mice fed glucose rich diet with green tea extracts, DGTE and GTE increased VAT mass compared to control. Data presented mean  $\pm$  SEM, \* $p < 0.05$ , \*\*\*\* $p < 0.0001$ ,  $n = 6$ .



**Figure 4.9 Selected green tea extracts increase BAT mass in mice fed normal or glucose-rich diet.**

Mice fed DGTE, EGCG, and GTE for 28 days in drinking water supplemented with or without 30% (w/v) of glucose. At the end of experiment, fasted mice were sacrificed, and the BAT was dissected, weighted, and the average weight was calculated. Mice fed glucose diet showed no significant of VAT weight compared to normal mice. (A). BAT mass of mice fed a normal diet with green tea extracts, EGCG increased BAT mass compared to control. (B). BAT mass of mice fed glucose rich diet with green tea extracts, DGTE and GTE increased BAT mass compared to controls. Data presented mean  $\pm$  SEM, \*\* $p < 0.01$ , \*\*\* $p < 0.001$ , \*\*\*\* $p < 0.0001$ ,  $n = 6$ .



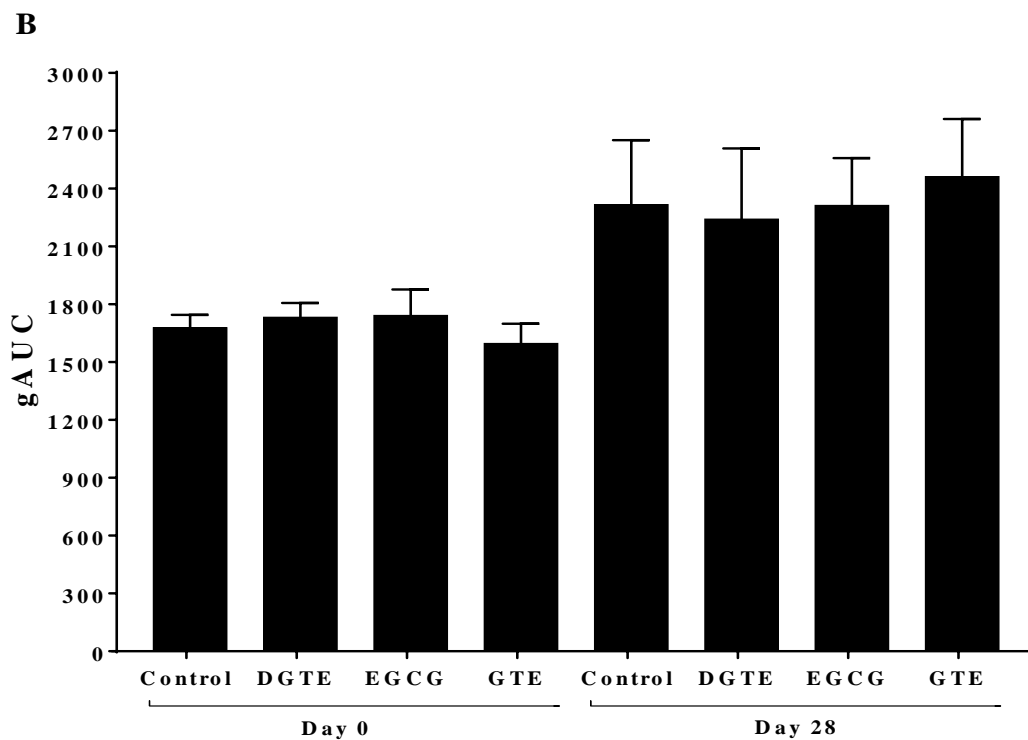
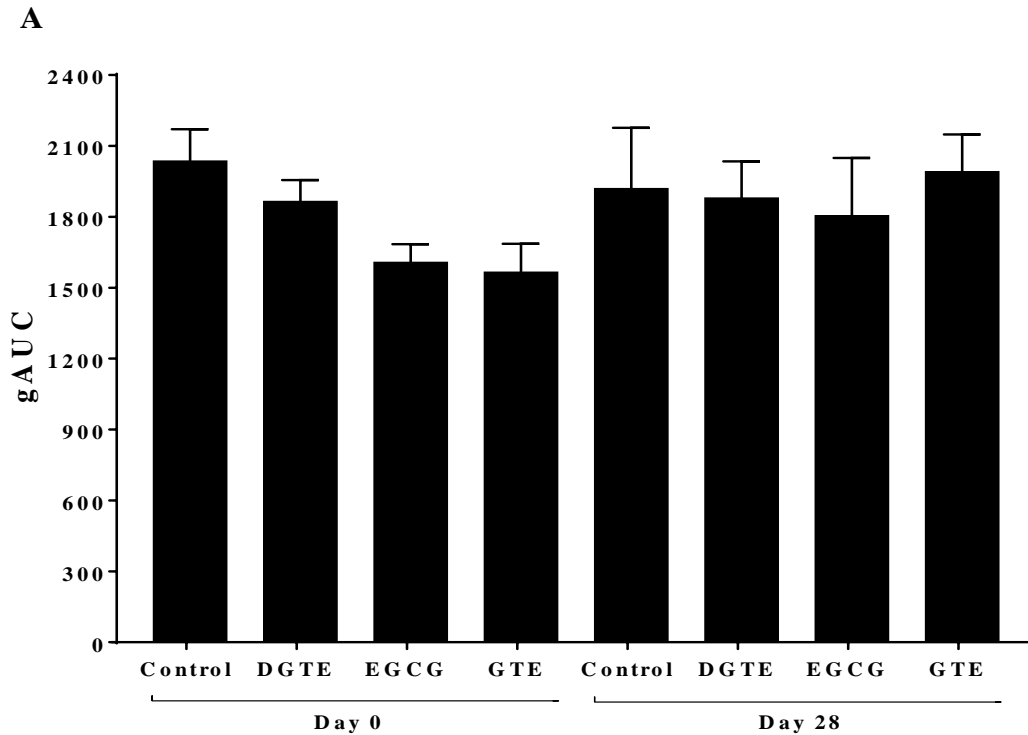


**Figure 4.11 Green tea extracts do not reduce gAUC in mice fed normal or glucose-rich diet.**

Mice fed DGTE, EGCG, and GTE for 28 days in drinking water supplemented with or without 30% (w/v) of glucose. Glucose levels were measured during GTT at day 0 and 28, and glucose area under the curve was calculated. Mice fed glucose diet for 28 days showed no significant reduction of gAUC compared to gAUC in mice at day 0. (A). The gAUC of mice fed a normal diet with green tea extracts, no effect of treatments to reduce gAUC compared to control. (B). The gAUC of mice fed glucose rich diet with green tea extracts; all treatments did not reduce gAUC compared to control. The data presented mean  $\pm$  SEM, n=6.

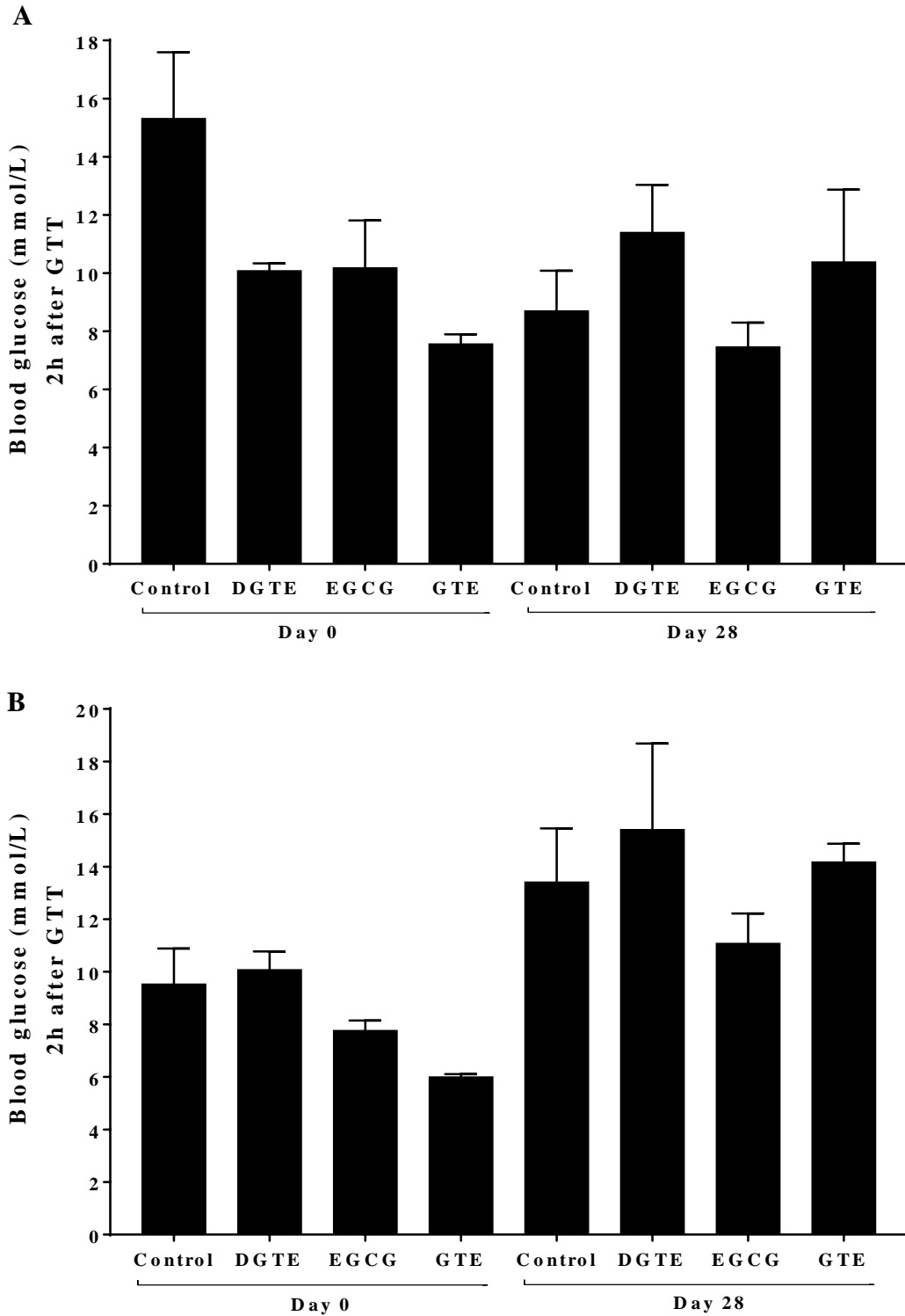


**Figure 4.12 Green tea extracts do not increase glucose clearance during GTT in all mice.**

Mice fed DGTE, EGCG, and GTE for 28 days in drinking water supplemented with or without 30% (w/v) of glucose. Glucose levels at 120 minutes during GTT at 0 and 28 days was obtained and glucose clearance was then analysed. Mice fed glucose diet showed no significant effect to reduce glucose clearance compared to mice at day 0. (A). A glucose level of mice fed a normal diet with green tea extracts, no effect of all treatments to dispose of glucose compared to control. (B). A glucose level of mice fed glucose rich diet with green tea extracts, no effect of all treatments to increase disposal blood glucose compared to control. Data presented mean  $\pm$  SEM, n=6.

#### **4.3.5 Selected green tea extracts reduced mice fasting blood glucose (FBG)**

FBG was measured before GTT was performed as a baseline of glucose concentration for mice that received treatments without and with glucose rich diet. The FBG levels in mice fed a normal diet with DGTE, EGCG, and GTE were unchanged compared to control (Figure 4.13 A,  $p > 0.9999$ ,  $0.9939$ , and  $0.5797$  respectively). Alternatively, supplementation of glucose to the control group for 28 days significantly increased FBG level ( $277.6\% \pm 10.4\%$  ( $p < 0.0001$ )) compared to the control group at day 0. Only DGTE and EGCG reduced the high level of FBG by  $45.5\% \pm 19.7\%$  ( $p = 0.0011$ ) and  $33.9\% \pm 10\%$  ( $p = 0.0296$ ) compared to control (Figure 4.13 B).

#### **4.3.6 Selected green tea extracts increased the levels of fasting insulin in serum**

The levels of fasting insulin were determined in serum of all mice groups after 28 days of treatment with DGTE, EGCG, and GTE either without or with a glucose supplemented diet. Mice treated with green tea only, DGTE, and GTE showed no significant effect on the level of insulin ( $77.3\% \pm 34.2\%$ ,  $p = 0.8707$  and  $49\% \pm 57.3\%$ ,  $p = 0.9434$ ). EGCG, however, caused a significant elevation in the level of insulin by  $443.8\% \pm 20.7\%$  ( $p = 0.0009$ ) compared to control (Figure 4.14 A). Mice treated with these extracts in addition to a glucose diet expressed high levels of insulin compared to control, with only EGCG and GTE significantly increased insulin concentrations by  $194.5 \pm 17.3\%$  ( $p = 0.0022$ ) and  $149.8\% \pm 13.9\%$  ( $p = 0.0175$ ) (Figure 4.14 B).

#### **4.3.7 Homoeostasis model assessment (HOMA)**

HOMA including IR, B, and S were calculated based on the glucose and insulin levels in fasting condition. HOMA-IR and B were measured in all mice groups, whereas HOMA-S was determined only in mice receiving green tea extracts with a high glucose diet. The latter was due to the levels of insulin in groups receiving treatments without a glucose-rich diet being low. Therefore, ineligible for use in calculating HOMA S. DGTE and GTE did not cause any significant effect on insulin resistance ( $p = 0.5255$  and  $p = 0.9684$ ), while EGCG significantly increased insulin resistance by  $411.3\% \pm 13.7\%$  ( $p < 0.0001$ ) compared to control in mice fed a normal diet (Figure 4.15 A). All treatments in mice supplemented with a glucose diet did not show any differences in insulin resistance compared to control (Figure 4.15 B,  $p = 0.2836$ ),  $p = 0.4398$ , and  $p = 0.3955$ ). In mice fed a normal diet alongside green tea extracts, only EGCG significantly increased pancreatic beta-cell function by  $548.4\% \pm 27.9\%$  ( $p = 0.0066$ ) (Figure 4.16 A). No statistically significant increases in beta-cells function were seen in mice supplemented with green tea extracts alongside a glucose-rich diet, with values of  $653\% \pm 38\%$ ,  $p = 0.0629$ ,  $511\% \pm 24.2\%$ ,  $p = 0.1815$ , and  $375\% \pm 20.4\%$ ,  $p = 0.4202$  compared to control (Figure 4.16 B). Moreover, unchanged levels of insulin sensitivity were observed between all treatment and control mice that had consumed a high glucose diet (Figure 4.17,  $p = 0.1593$ ,  $0.9859$ , and  $0.9998$ ).

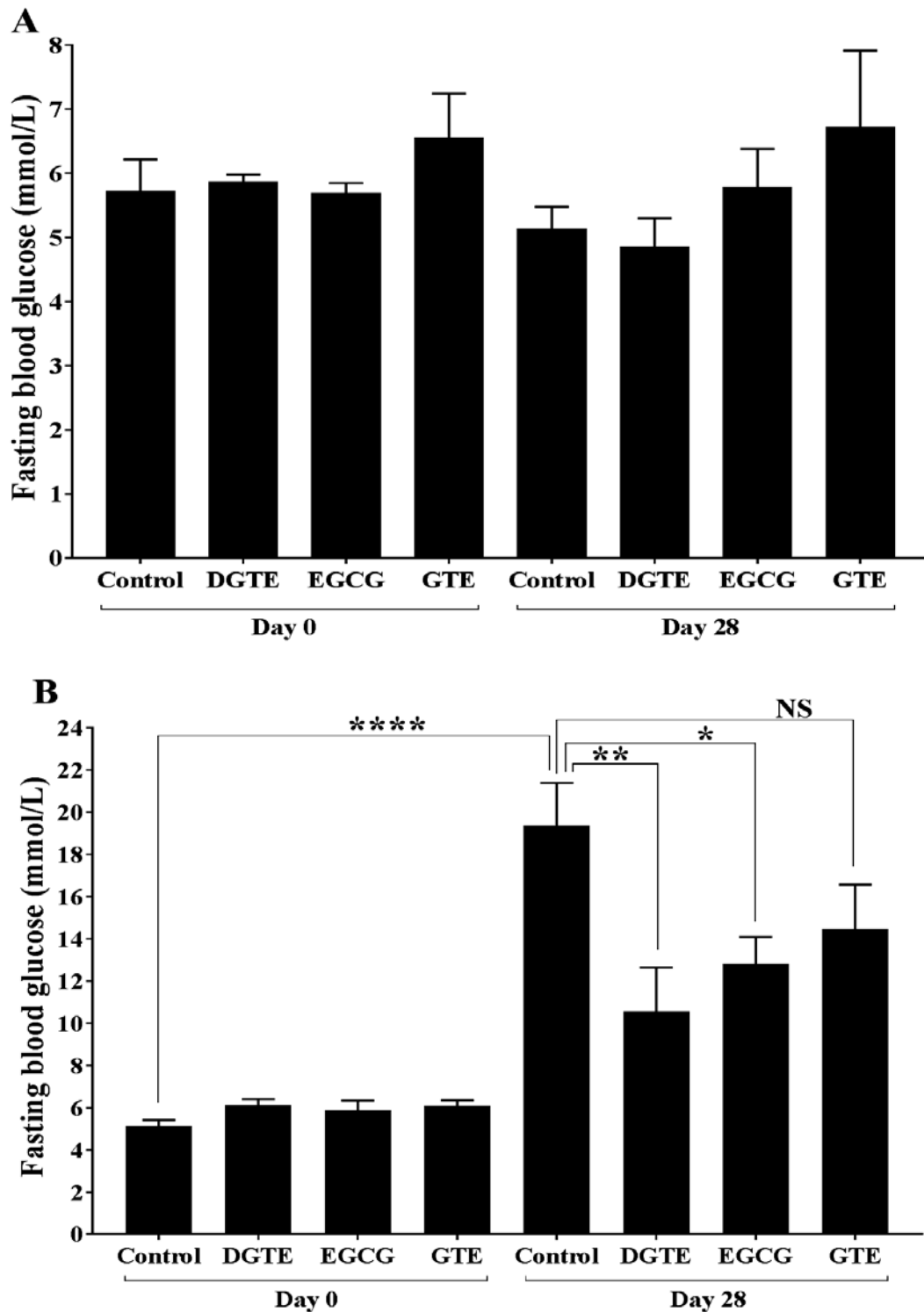


**Figure 4.13 Selected green tea extracts decrease FBG levels in mice fed glucose-rich diet.**

Mice fed DGTE, EGCG, and GTE for 28 days in drinking water supplemented with or without 30% (w/v) of glucose. Fasting blood glucose level was measured at day 0 and 28 after treatment with selected green tea extract using glucose meter. Mice fed glucose diet for 28 days showed impairment of FBG which was significantly increased compared to its level at day 0. (A). FBG levels of mice fed a normal diet with green tea extracts, no effect of all treatments to reduce FBG compared to control. (B). FBG levels of mice fed glucose rich diet with green tea extracts, DGTE and EGCG significantly reduced high level of FBG compared to control. Data presented mean  $\pm$  SEM, \* $p$ <0.05 \*\* $p$ <0.01, and \*\*\*\* $p$ <0.0001,  $n$ =6.

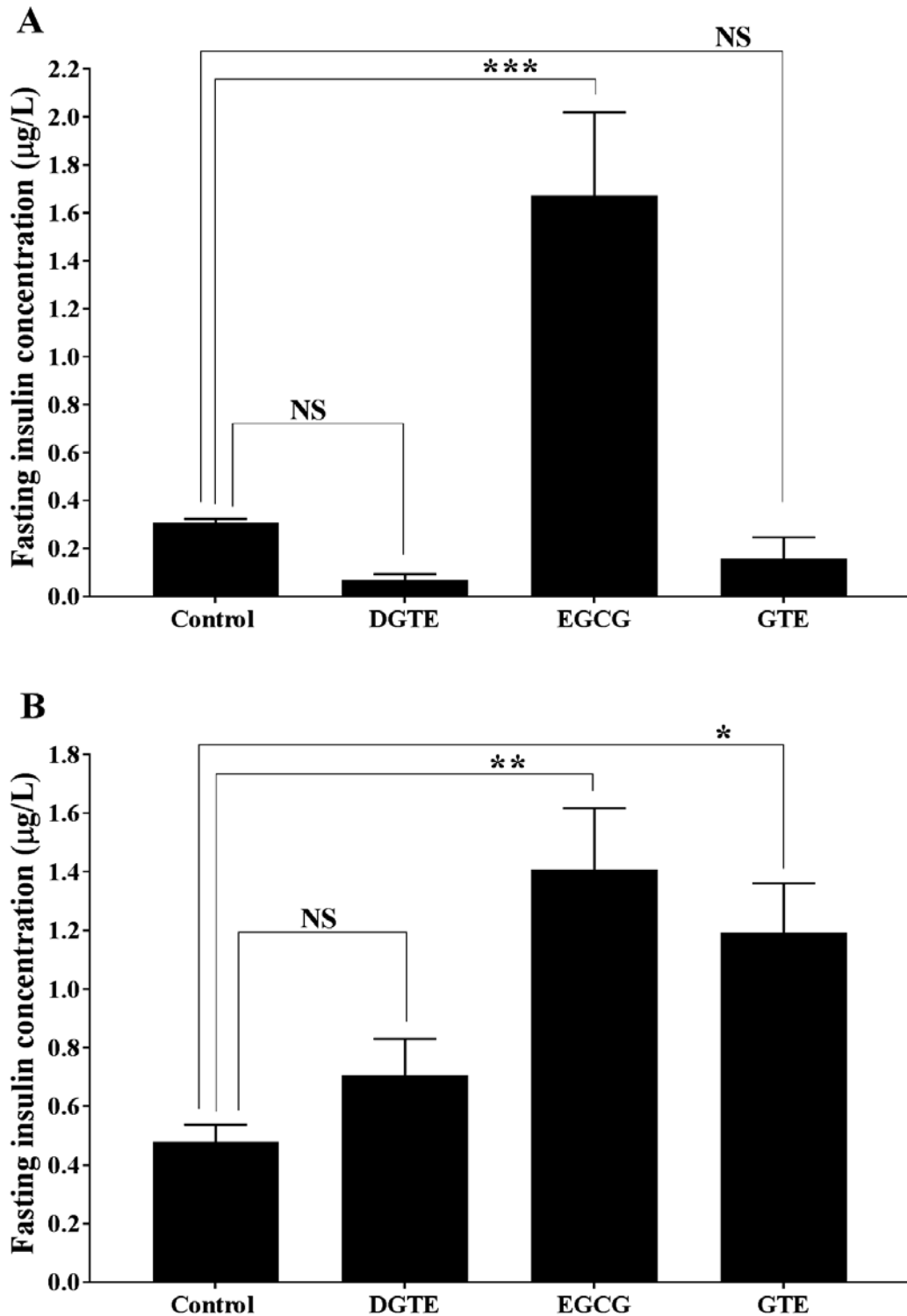


**Figure 4.14 Selected green tea extracts increase insulin levels in mice fed normal or glucose-rich diet.**

Mice fed DGTE, EGCG, and GTE for 28 days in drinking water supplemented with or without 30% (w/v) of glucose. At the end of experiment, blood was collected from fasted mice and subjected to serum process. Fasting serum insulin levels were measured specific ELISA kit. (A). Insulin level of mice fed a normal diet with green tea extracts; only EGCG increased insulin level compared to control. (B). Insulin level of mice fed glucose rich diet with green tea extracts, EGCG and GTE increased insulin level compared to control. Data presented mean  $\pm$  SEM, \* $p$ <0.05 \*\* $p$ <0.01, \*\*\* $p$ <0.001,  $n$ =5.

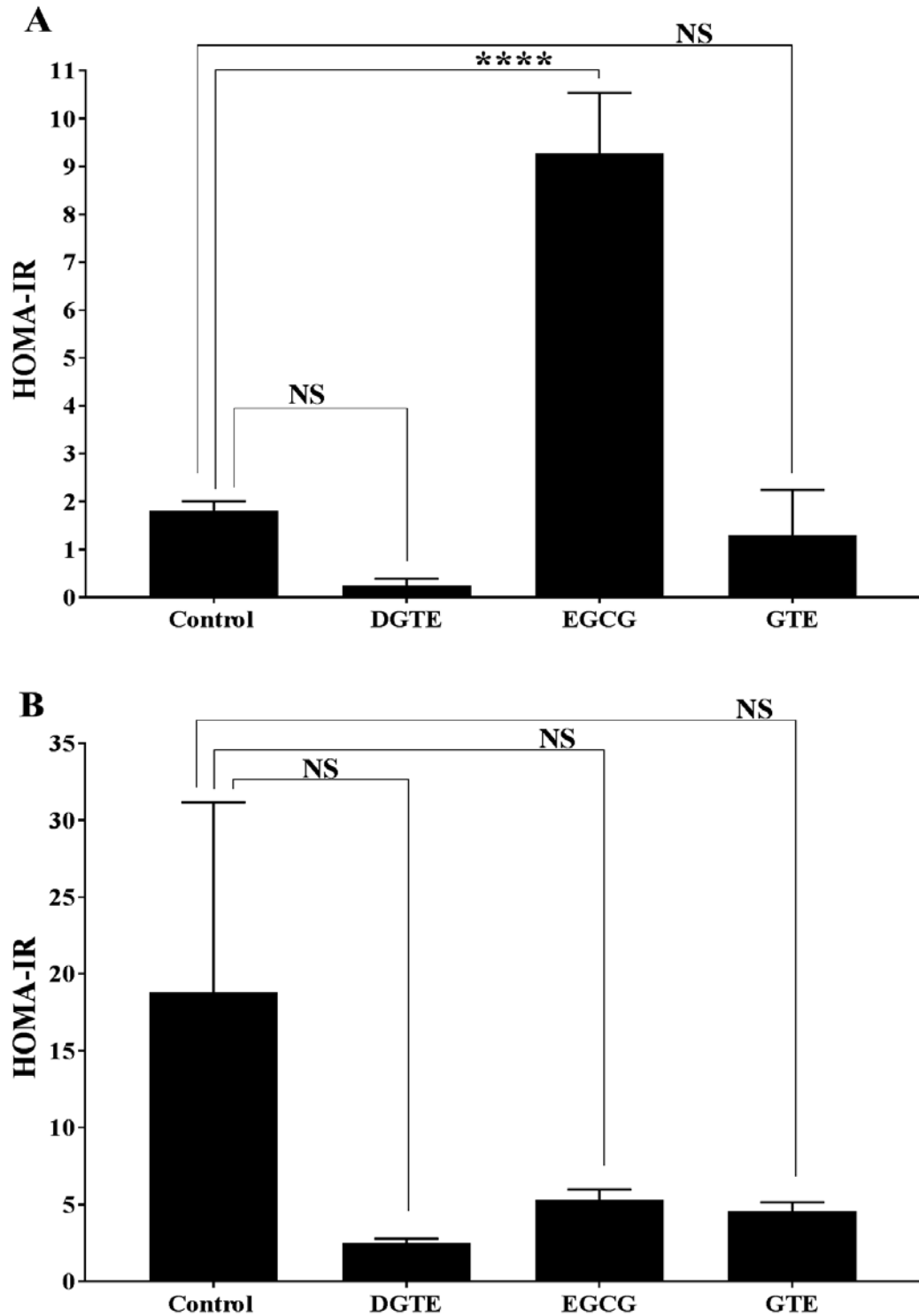


**Figure 4.15 EGCG increases HOMA-IR value in mice fed normal diet.**

Mice fed DGTE, EGCG, and GTE for 28 days in drinking water supplemented with or without 30% (w/v) of glucose. At the end of experiment, fasting glucose and insulin were measured, and then HOMA-IR was calculated. (A). HOMA-IR of mice fed a normal diet with green tea extracts; only EGCG increased insulin resistance compared to control. (B) HOMA-IR of mice fed glucose rich diet with green tea extracts, no significant effect of all treatments on insulin resistance compared to control. Data analysed by using computerised HOMA calculator 2 software (Oxford University, Diabetes Trial Unit, UK). Data presented mean  $\pm$  SEM, \*\*\*\* $p$ <0.0001,  $n$ =5.

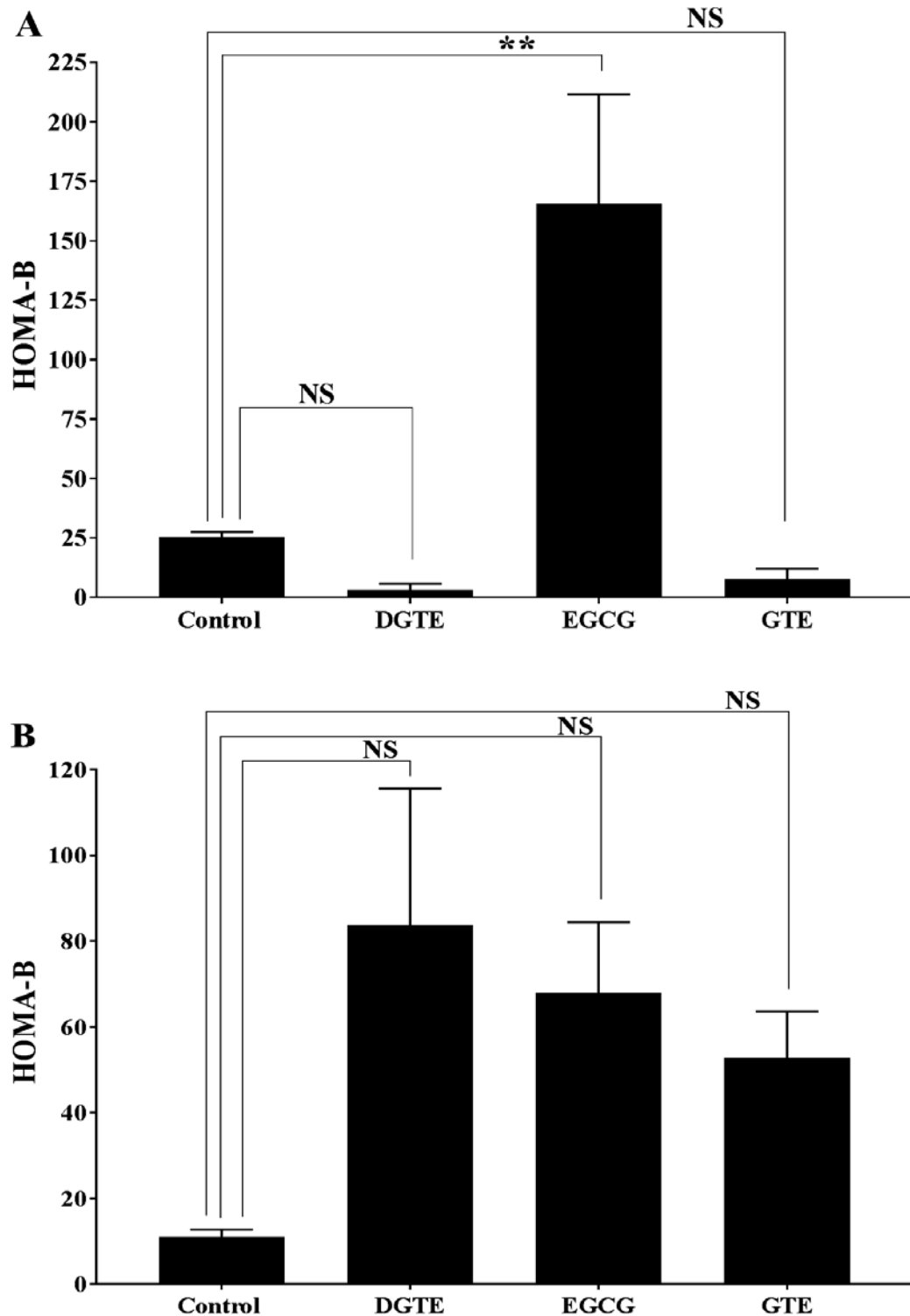


**Figure 4.16 EGCG increases HOMA-B value in mice fed normal diet.**

Mice fed DGTE, EGCG, and GTE for 28 days in drinking water supplemented with or without 30% (w/v) of glucose. At the end of experiment, fasting glucose and insulin were measured, and then HOMA-B was calculated. (A). HOMA-B of mice fed a normal diet with green tea extracts; only EGCG increased of beta-cell function compared to control. (B) HOMA-B of mice fed glucose rich diet with green tea extracts, no significant effect of all treatments on beta-cell function compared to control. Data analysed by using computerised HOMA calculator 2 software (Oxford University, Diabetes Trial Unit, UK). Data presented mean  $\pm$  SEM, \*\* $p < 0.01$ ,  $n = 5$ .

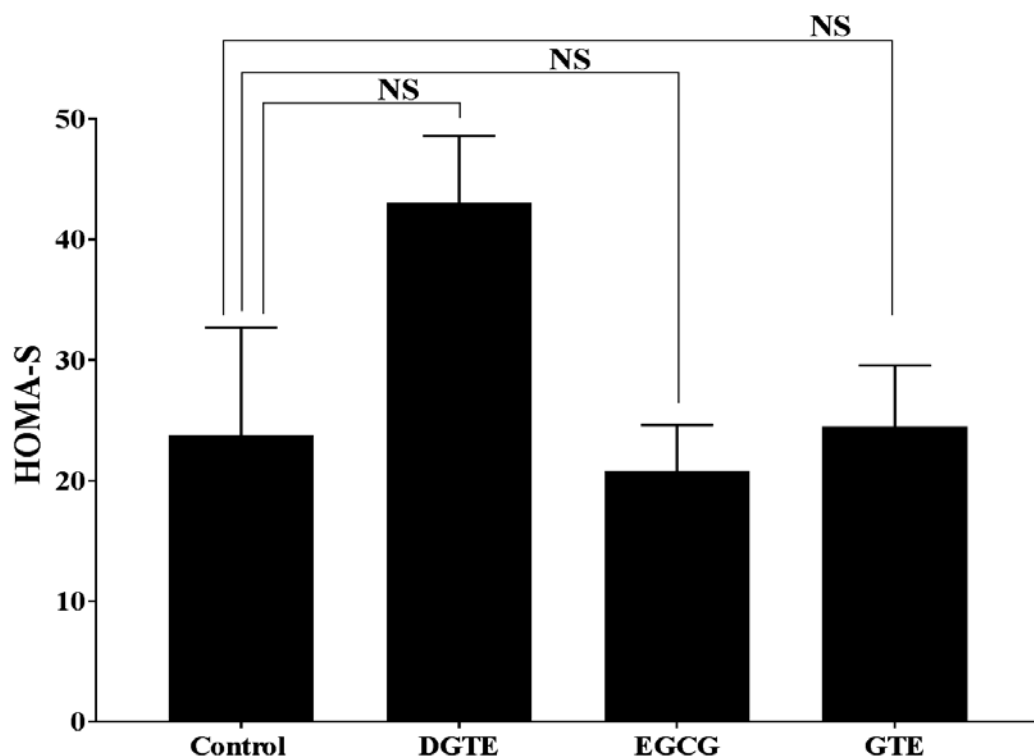


**Figure 4.17 Green tea extracts do not alter HOMA-S in mice fed glucose-rich diet.**

Mice fed DGTE, EGCG, and GTE for 28 days in drinking water supplemented with or without 30% (w/v) of glucose. At the end of experiment, fasting glucose and insulin were measured, and then HOMA-S was calculated only in mice fed glucose diet. No significant effect of all treatments on insulin sensitivity compared to control. Data analysed by using computerised HOMA calculator 2 software (Oxford University, Diabetes Trial Unit, UK). Data presented mean  $\pm$  SEM, n=5.

#### **4.3.8 Selected green tea extracts reduced circulating total cholesterol (TC)**

The levels of TC were investigated in mice after 28 days of treatment with DGTE, EGCG, and GTE with or without glucose supplementation. Mice treated with EGCG and GTE compounds without high glucose showed no significant reduction in the levels of TC ( $p=0.0656$  and  $p=0.4653$ ) compared to control, however only DGTE significantly decreased the level of TC by  $44.4\% \pm 3.7\%$  ( $p=0.0014$ ) (Figure 4.18 A). All green tea extract treatments in mice supplemented with glucose caused significant decreases in the level of TC compared to control (Figure 4.18 B). The recorded percentage of these reductions were:  $52.2\% \pm 10\%$  ( $p<0.0001$ ),  $51.5\% \pm 3.3\%$  ( $p<0.0001$ ), and  $53.2\% \pm 6.9\%$  ( $p<0.0001$ ) respectively.

#### **4.3.9 Selected green tea extract increased circulating triglyceride (TG) levels**

The concentration of TG was measured in all groups after 28 days of treatment with DGTE, EGCG, and GTE with or without glucose supplementation. The result showed that the level of TG was significantly increased by  $123.2\% \pm 4.7\%$  ( $p<0.0001$ ) and  $64\% \pm 8.3\%$  ( $p=0.0004$ ) in mice that received

DGTE and EGCG without a high glucose diet compared to control, with no significant effect of GTE ( $p=0.9968$ ) (Figure 4.19 A). EGCG treatment alongside a glucose supplemented diet caused a  $62.2\% \pm 6.9\%$  ( $p < 0.0001$ ) increase of TG compared to control without significant effect of DGTE ( $p=0.4630$ ) and GTE ( $p=0.9010$ ) (Figure 4.19 B).

#### **4.3.10 Effect of green tea extract on the level of high-density lipoprotein (HDL)**

The level of HDL was determined in mice after 28 days post-treatment with DGTE, EGCG, and GTE that were supplemented with or without a glucose diet. The result showed that there were no significant differences between treatments and control regarding HDL concentration in mice fed a normal diet (Figure 4.20 A,  $p=0.8699$ ,  $0.2460$ , and  $0.7694$  respectively). Similarly, mice given green tea extracts alongside a glucose-rich diet did not express statistically significant increases in HDL level compared to control (Figure 4.20 B,  $p=0.1414$ ,  $0.0541$ , and  $0.7863$  respectively).

#### **4.3.11 Selected green tea extracts decreased the level of calculated low-density lipoprotein (cLDL)**

The level of cLDL was measured in mice after 28 days of treatment with DGTE, EGCG, and GTE that received treatment alone or with a high glucose diet based on obtained lipid profile data, including TC, TG, and HDL. The levels of cLDL were significantly decreased by  $72.5\% \pm 10.5\%$  ( $p=0.0008$ ) and  $53.5\% \pm 35.9\%$  ( $p=0.0126$ ) when mice were treated with DGTE and EGCG alone compared to control, whereas GTE statistically failed to decrease cLDL level ( $p=0.3541$ ) (Figure 4.21 A). Mice were given DGTE, EGCG, and GTE alongside a glucose rich diet expressed significant reduction in the level of cLDL compared to control. These decreases were:  $81.8\% \pm 46.8\%$  ( $p < 0.0001$ ),  $86.3\% \pm 20\%$  ( $p < 0.0001$ ), and  $76.8\% \pm 12.7\%$  ( $p < 0.0001$ ) respectively (Figure 4.21 B).

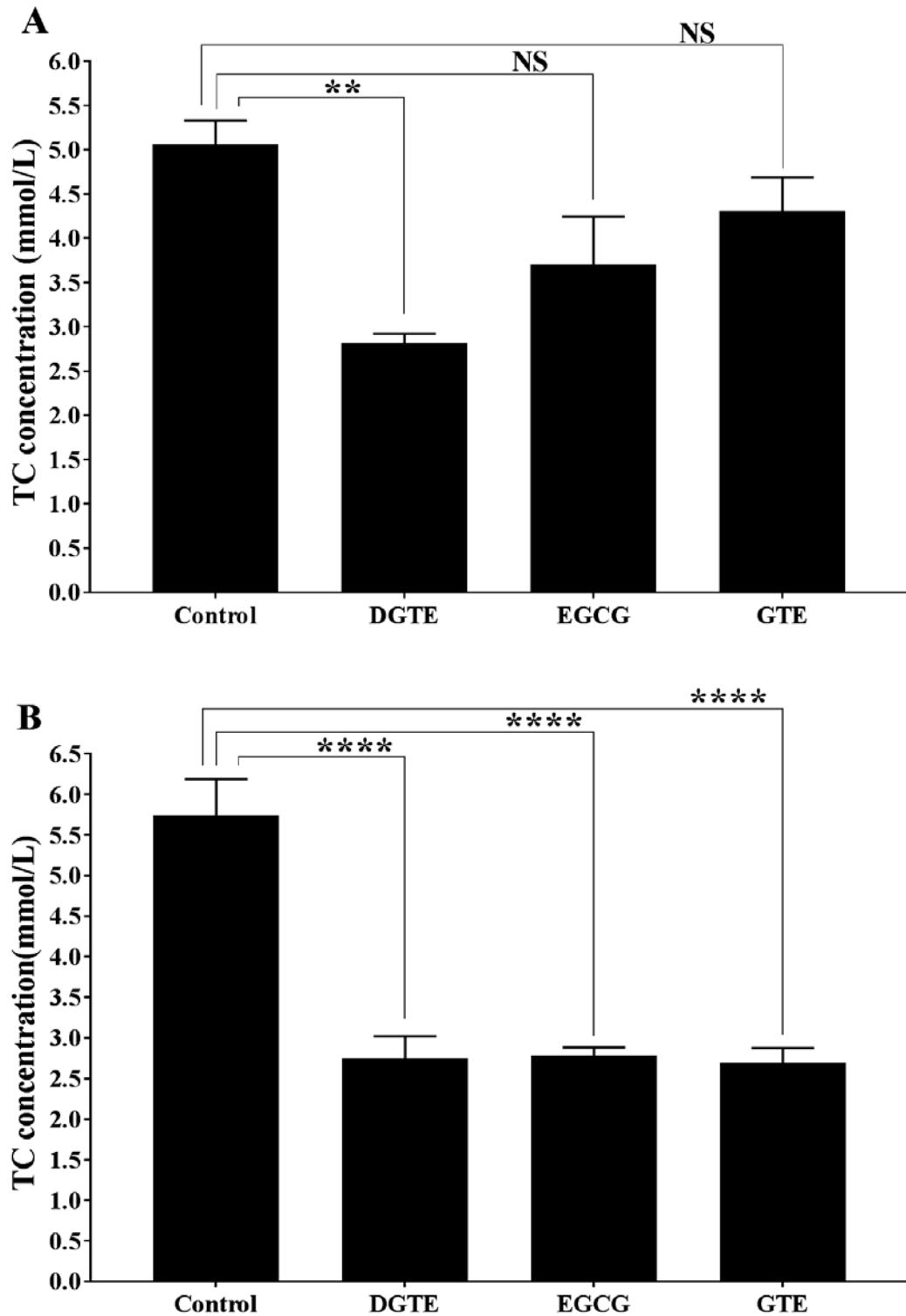


**Figure 4.18 Selected green tea extracts decrease TC levels in mice fed normal or glucose-rich diet.**

Mice fed DGTE, EGCG, and GTE for 28 days in drinking water supplemented with or without 30% (w/v) of glucose. At the end of experiment, fasted mice were sacrificed, and blood was collected and subjected to serum process. The level of circulating total cholesterol was measured by using colorimetric assay kit. (A). TC levels of mice fed a normal diet with green tea extracts, DGTE decreased the level of TC compared to control (B). TC level of mice fed glucose rich diet with green tea extracts, all treatments decreased TC level compared to controls. Data presented mean  $\pm$  SEM, \*\* $p < 0.01$ , \*\*\*\* $p < 0.0001$   $n = 6$ .

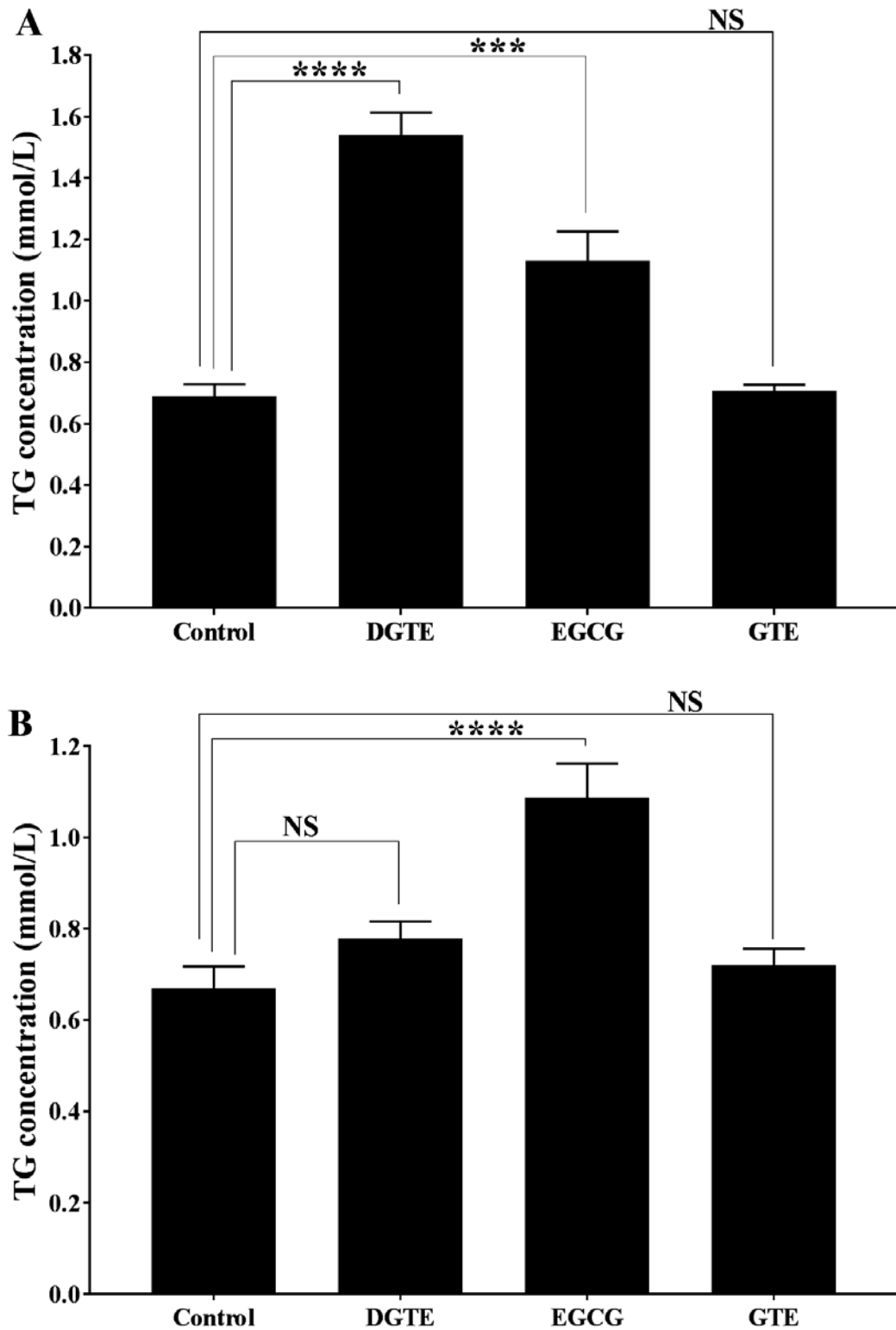


**Figure 4.19 Selected green tea extracts increase TG levels in mice fed normal or glucose-rich diet.**

Mice fed DGTE, EGCG, and GTE for 28 days in drinking water supplemented with or without 30% (w/v) of glucose. At the end of experiment, the level of circulating triglyceride was measured in fasted mice by using CardioChek® P.A analyser with lipid PTS panels. (A). TG levels of mice fed a normal diet with green tea extracts, DGTE and EGCG increased of TG level compared to control. (B). TG levels of mice fed glucose rich diet with green tea extracts, only EGCG increased the level of TG compared to control. Data presented mean  $\pm$  SEM, \*\*\* $p$ <0.001, \*\*\*\* $p$ <0.0001,  $n$ =6.

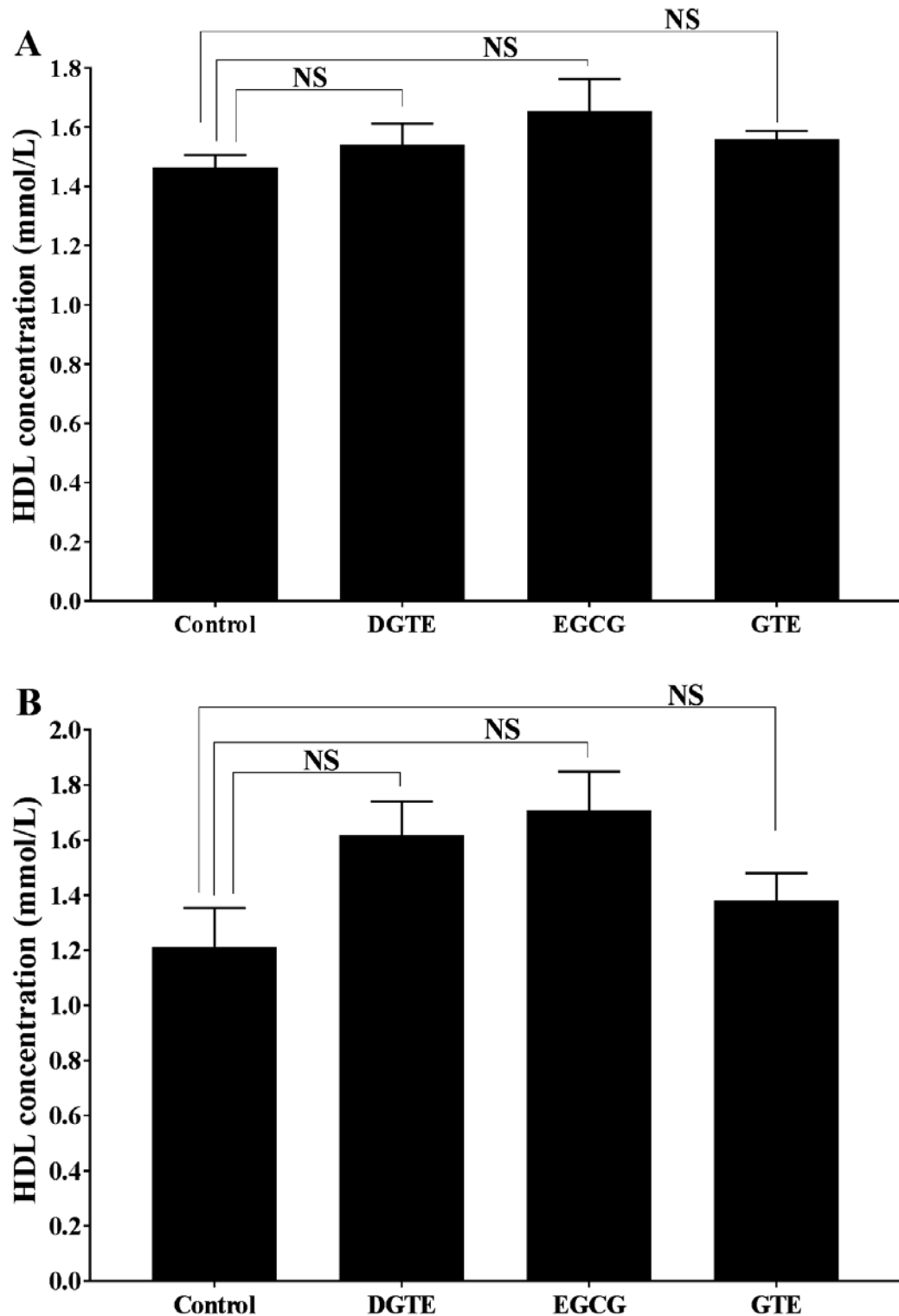


**Figure 4.20 Green tea extracts do not alter HDL levels in mice fed normal or glucose-rich diet.**

Mice fed DGTE, EGCG, and GTE for 28 days in drinking water supplemented with or without 30% (w/v) of glucose. At the end of experiment, the level of circulating high density lipoprotein was measured in fasted mice by using CardioChek<sup>®</sup> P.A analyser with lipid PTS panels. (A). HDL levels of mice fed a normal diet with green tea extracts, no effect of all treatments on the level of HDL was observed compared to control. (B). HDL levels of mice fed glucose rich diet with green tea extract, no effect of all treatments on the level of HDL was observed compared to control. Data presented mean  $\pm$  SEM, n=6.

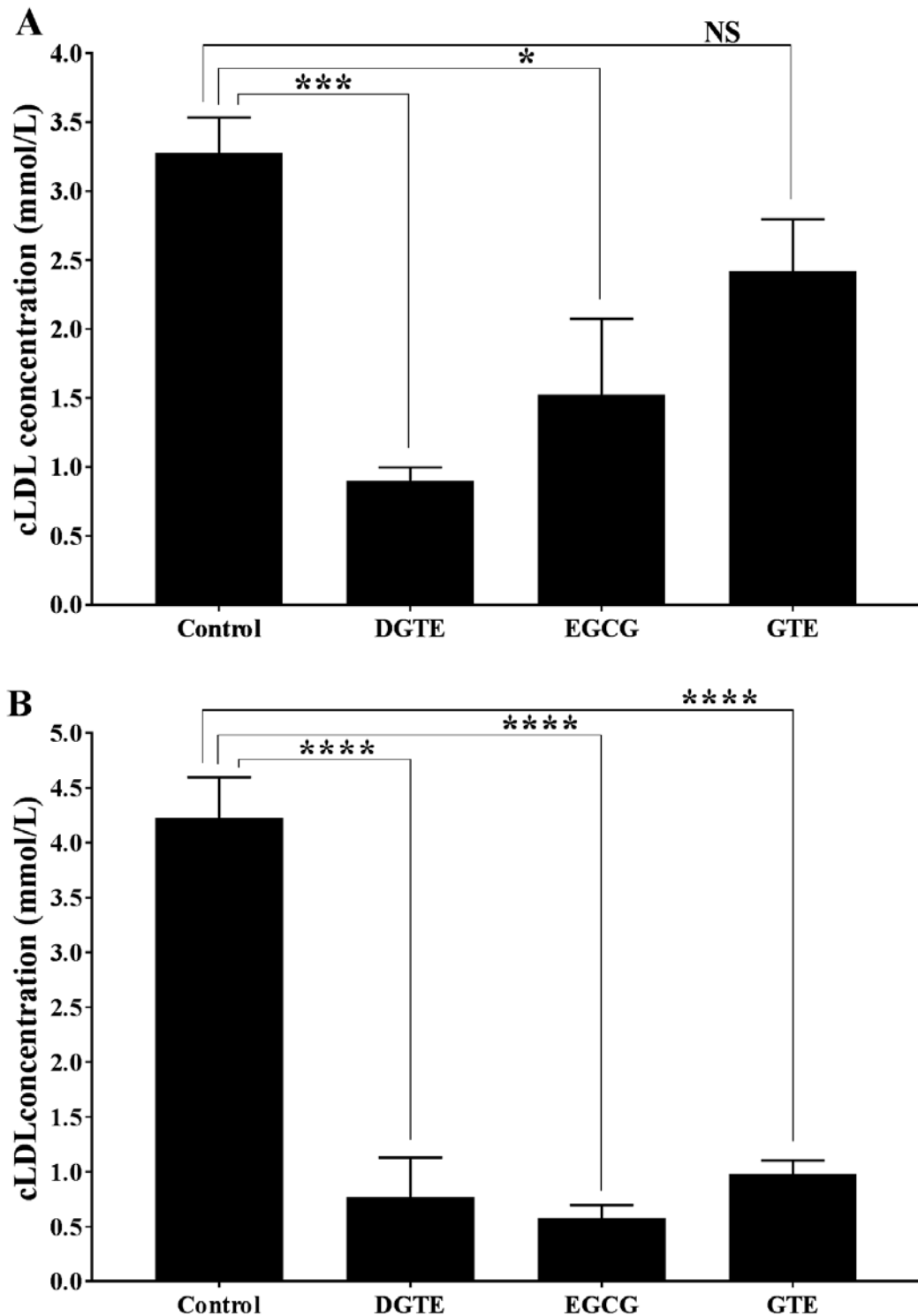


**Figure 4.21 Selected green tea extracts decrease cLDL levels in mice fed normal or glucose-rich diet.**

Mice fed DGTE, EGCG, and GTE for 28 days in drinking water supplemented with or without 30% (w/v) of glucose. At the end of experiment, the level of circulating low density lipoprotein was calculated by using Friedewald formula based on obtained lipid profile data row (A). The cLDL levels of mice fed a normal diet with green tea extracts, DGTE and EGCG decreased the level of cLDL compared to control. (B). The cLDL levels of mice fed glucose rich diet with green tea extracts, all treatments decreased the level of cLDL compared to control. Data presented mean  $\pm$  SEM, \* $p < 0.05$ , \*\*\* $p < 0.001$ , \*\*\*\* $p < 0.0001$ ,  $n = 6$ .

#### **4.3.12 Effect of green tea extract on glucose metabolism gene expression in liver**

Expression of mRNA related to glucose regulation and metabolism were examined in the liver of mice supplemented with DGTE, EGCG, and GTE with or without a rich glucose diet after 28 days of treatment. Expression of IR, Glut2, Gys1, G6Pase, PEPCK, CPT1 $\alpha$  and FASN were assessed. The results of both main groups revealed that mice treated without and with a glucose diet showed no differences in expression of those genes between treatments and control, except EGCG in the high glucose diet group, which significantly downregulated expression of PEPCK mRNA, and all gene expression data can be seen in Table 4.1.

#### **4.3.13 Effect of green tea extract on glucose metabolism gene expression in skeletal muscle**

The mRNA expression of glucose metabolism genes including IR, Glut4, Gys1, PDK4, and PGC1 $\alpha$  were determined in skeletal muscle of mice that received green tea extracts with or without a high glucose diet after 28 days of treatment. Green tea extracts did not mediate any differences in expression of these genes in all groups. Only EGCG and GTE gave to mice with a high glucose diet caused significant downregulation of PDK4 mRNA by 92% $\pm$ 34.25%,  $p=0.0131$  and 93% $\pm$ 7.4%,  $p=0.0122$  compared to control, and all gene expression data can be seen Table 4.2.

#### **4.3.14 Effect of green tea extract on glucose and lipid metabolism gene expression in adipose tissue**

The level of mRNA expression of glucose and lipid metabolism genes expression including IR, Glut4, SREBP1c, C/EBP $\alpha$ , PPAR $\gamma$ , FASN, FABP4, and LPL were investigated in mice adipose tissue. Green tea extracts did not alter the expression of IR, SREBP1c, PPAR $\gamma$ , and FASN mRNA in all mice (Table 4.3). Green tea extracts supplemented to mice fed a normal diet did not change the level of Glut4 expression (Table 4.3). DGTE and GTE significantly downregulated Gult4 mRNA expression by 68.4% $\pm$ 40.75%,  $p=0.0124$  and 65.9% $\pm$ 17.2%,  $p=0.0153$  in mice fed a glucose-rich diet. (Table 4.3). DGTE and GTE combined with a calorie-rich diet significantly downregulated C/EBP $\alpha$  mRNA by 87.6% $\pm$ 38.9%,  $p=0.0282$  and 79% $\pm$ 44.75%,  $p=0.0459$  compared to control. (Table 4.3). No differences in expression level of C/EBP $\alpha$  mRNA between treatments and control in mice fed a normal diet were seen. Furthermore, DGTE, EGCG, and GTE significantly decreased expression of FABP4 by 77.6% $\pm$ 46.9%,  $p=0.0032$ , 85.9% $\pm$ 20.8%,  $p=0.0017$ , and 49.6% $\pm$ 30.3%,  $p=0.0386$  in mice fed a normal diet, and by 89.3% $\pm$ 62%,  $p=0.0098$ , 75% $\pm$ 24.1%,  $p=0.0252$ , and 67.2% $\pm$ 32.4%,  $p=0.0427$  in mice fed a high glucose (Table 4.3). LPL mRNA was significantly downregulated by 81% $\pm$ 31.2%,  $p=0.0016$ , 78.7% $\pm$ 47.9%,  $p=0.0019$ , and 46.2% $\pm$ 7%,  $p=0.0427$  in response to DGTE, EGCG, and GTE in mice fed a normal diet. Whereas no statistically significant differences in LPL expression in response to DGTE were seen in mice fed a glucose-rich diet (Table 4.3).

**Table 4.1 Effect of green tea extracts on glucose metabolism mRNA expression in the liver of mice fed normal or glucose-rich diet.**

Mice fed DGTE, EGCG, and GTE for 28 days in drinking water supplemented with or without 30% (w/v) of glucose. At the end of experiment, fasted mice were sacrificed and the liver was dissected. RNA was isolated and reverse transcriptased, followed by quantifying amplification of selected glucose metabolism mRNA by using qPCR. No significant differences between green tea treatments and control of all tested genes were seen except EGCG supplemented to mice with glucose significantly downregulated PEPCCK mRNA leve compared to control. Data displayed as relative fold of gene expression which normalised to housekeeping gene. The data presented mean  $\pm$  SEM, n=3.

<b>mRNA</b>	<b>Mice treatment</b>	<b><math>\uparrow\downarrow</math> Fold of control <math>\pm</math> SEM</b>	<b>P value</b>
<b>IR</b>	<b>DGTE</b>	1.488 $\pm$ 0.8094	0.9639
	<b>DGTE with glucose</b>	6.007 $\pm$ 3.402	0.2486
	<b>EGCG</b>	1.411 $\pm$ 1.17	0.9779
	<b>EGCG with glucose</b>	0.3412 $\pm$ 0.04296	0.9907
<b>Glut2</b>	<b>GTE</b>	0.8031 $\pm$ 0.1628	0.9969
	<b>GTE with glucose</b>	0.8626 $\pm$ 0.3526	0.9998
	<b>DGTE</b>	1.245 $\pm$ 0.7747	0.9954
	<b>DGTE with glucose</b>	7.954 $\pm$ 4.692	0.2709
<b>Gys1</b>	<b>EGCG</b>	1.792 $\pm$ 1.068	0.8503
	<b>EGCG with glucose</b>	2.555 $\pm$ 1.591	0.9696
	<b>GTE</b>	1.305 $\pm$ 0.1774	0.9907
	<b>GTE with glucose</b>	1.541 $\pm$ 0.2099	0.9987
<b>G6Pase</b>	<b>DGTE</b>	0.8558 $\pm$ 0.3334	>0.9999
	<b>DGTE with glucose</b>	54.24 $\pm$ 26.84	0.0883
	<b>EGCG</b>	15.18 $\pm$ 14.91	0.5635
	<b>EGCG with glucose</b>	0.7416 $\pm$ 0.2109	>0.9999
<b>PEPCK</b>	<b>GTE</b>	0.7586 $\pm$ 0.1532	>0.9999
	<b>GTE with glucose</b>	0.7472 $\pm$ 0.08106	>0.9999
	<b>DGTE</b>	0.5731 $\pm$ 0.3303	0.8303
	<b>DGTE with glucose</b>	1.145 $\pm$ 0.1539	0.8855
<b>PEPCK</b>	<b>EGCG</b>	0.9426 $\pm$ 0.6006	0.9992
	<b>EGCG with glucose</b>	0.6194 $\pm$ 0.07095	0.2640
	<b>GTE</b>	0.6069 $\pm$ 0.105	0.8603
	<b>GTE with glucose</b>	1.154 $\pm$ 0.2	0.8661
<b>PEPCK</b>	<b>DGTE</b>	0.716 $\pm$ 0.3643	0.9229
	<b>DGTE with glucose</b>	0.6626 $\pm$ 0.2196	0.2962
	<b>EGCG</b>	0.2242 $\pm$ 0.1087	0.4014
	<b>EGCG with glucose</b>	0.2402 $\pm$ 0.05387	0.0113*
<b>PEPCK</b>	<b>GTE</b>	1.456 $\pm$ 0.4756	0.7818
	<b>GTE with glucose</b>	0.537 $\pm$ 0.1013	0.1139

<b>CPT1<math>\alpha</math></b>	<b>DGTE</b>	0.3487 $\pm$ 0.2785	0.8249
	<b>DGTE with glucose</b>	11.09 $\pm$ 7.078	0.2637
	<b>EGCG</b>	1.106 $\pm$ 1.003	0.9989
	<b>EGCG with glucose</b>	0.303 $\pm$ 0.1073	0.9988
<b>FASN</b>	<b>GTE</b>	0.6815 $\pm$ 0.08612	0.9735
	<b>GTE with glucose</b>	0.9237 $\pm$ 0.6349	>0.9999
	<b>DGTE</b>	0.2884 $\pm$ 0.2178	0.9511
	<b>DGTE with glucose</b>	3.955 $\pm$ 1.707	0.4262
<b>FASN</b>	<b>EGCG</b>	3.045 $\pm$ 1.957	0.5186
	<b>EGCG with glucose</b>	3.358 $\pm$ 1.126	0.5973
	<b>GTE</b>	0.5641 $\pm$ 0.1129	0.9869
	<b>GTE with glucose</b>	4.225 $\pm$ 1.603	0.3589

**Table 4.2 Effect of green tea extracts on glucose metabolism mRNA expression in the skeletal muscle of mice fed normal or glucose-rich diet.**

Mice fed DGTE, EGCG, and GTE for 28 days in drinking water supplemented with or without 30% (w/v) of glucose. At the end of experiment, fasted mice were sacrificed and the skeletal muscle was dissected. RNA was isolated and reverse transcriptased, followed by quantifying amplification of selected glucose metabolism mRNA by using qPCR. No significant differences between green tea treatments and control of all tested genes were seen except EGCG and GTE supplemented to mice with glucose significantly downregulated PDK4 mRNA leve compared to control. Data displayed as relative fold of gene expression which normalised to housekeeping gene. The data presented mean  $\pm$  SEM, n=3.

<b>mRNA</b>	<b>Mice treatment</b>	<b><math>\uparrow\downarrow</math> Fold of control <math>\pm</math> SEM</b>	<b>P value</b>
<b>IR</b>	<b>DGTE</b>	3.766 $\pm$ 1.891	0.3789
	<b>DGTE with glucose</b>	0.9502 $\pm$ 0.1348	0.9923
	<b>EGCG</b>	0.5352 $\pm$ 0.1317	0.9905
	<b>EGCG with glucose</b>	0.5171 $\pm$ 0.09557	0.1347
<b>Glut4</b>	<b>GTE</b>	2.881 $\pm$ 1.266	0.6656
	<b>GTE with glucose</b>	0.3921 $\pm$ 0.05978	0.0546
	<b>DGTE</b>	2.158 $\pm$ 0.8696	0.9387
	<b>DGTE with glucose</b>	2.423 $\pm$ 1.192	0.4119
<b>Gys1</b>	<b>EGCG</b>	0.9123 $\pm$ 0.2169	>0.9999
	<b>EGCG with glucose</b>	0.6245 $\pm$ 0.033	0.9650
	<b>GTE</b>	3.345 $\pm$ 2.71	0.6681
	<b>GTE with glucose</b>	0.4442 $\pm$ 0.1525	0.9039
<b>Gys1</b>	<b>DGTE</b>	8.396 $\pm$ 7.428	0.5331
	<b>DGTE with glucose</b>	1.077 $\pm$ 0.3249	0.9984
	<b>EGCG</b>	0.9202 $\pm$ 0.08099	>0.9999
	<b>EGCG with glucose</b>	1.928 $\pm$ 0.5771	0.2889

	<b>GTE</b>	1.403 ± 0.1515	0.9999
	<b>GTE with glucose</b>	0.636 ± 0.1486	0.8703
<b>PDK4</b>	<b>DGTE</b>	2.738 ± 1.16	0.3970
	<b>DGTE with glucose</b>	0.4075 ± 0.1715	0.0995
	<b>EGCG</b>	0.03981 ± 0.01105	0.7800
	<b>EGCG with glucose</b>	0.08186 ± 0.02804	0.0131*
	<b>GTE</b>	2.197 ± 0.8704	0.6747
	<b>GTE with glucose</b>	0.07029 ± 0.005224	0.0122*
<b>PGC1<math>\alpha</math></b>	<b>DGTE</b>	5.76 ± 4.181	0.5067
	<b>DGTE with glucose</b>	1.354 ± 0.3336	0.6709
	<b>EGCG</b>	1.674 ± 0.6686	0.9967
	<b>EGCG with glucose</b>	0.6666 ± 0.1058	0.6963
	<b>GTE</b>	3.12 ± 1.9	0.9146
	<b>GTE with glucose</b>	0.5895 ± 0.1989	0.5552

**Table 4.3 Effect of green tea extracts on glucose metabolism mRNA expression in the adipose tissue of mice fed normal or glucose-rich diet.**

Mice fed DGTE, EGCG, and GTE for 28 days in drinking water supplemented with or without 30% (w/v) of glucose. At the end of experiment, fasted mice were sacrificed and the adipose tissue was dissected. RNA was isolated and reverse transcriptased, followed by quantifying amplification of selected glucose and lipid metabolism mRNA by using qPCR. No significant differences between green tea treatments and control regarding to IR, SREBP1c, PPAR $\gamma$ , and FASN genes expression were seen compared to control. Glut4 and C/EBP $\alpha$  mRNAs were significantly downregulated in mice fed DGTE and GTE supplemented with glucose compared to control. FABP4 mRNA was significantly downregulated in response to all green tea treatments in mice fed normal and glucose rich diet compared to control. Whereas, LPL mRNA was significantly downregulated in response to all green tea treatments in mice fed normal diet only compared to control. Data displayed as relative fold of gene expression which normalised to housekeeping gene. The data presented mean  $\pm$  SEM, n=3.

<b>mRNA</b>	<b>Mice treatment</b>	<b><math>\uparrow\downarrow</math> Fold of control <math>\pm</math> SEM</b>	<b>P value</b>
<b>IR</b>	<b>DGTE</b>	0.8659 ± 0.5984	>0.9999
	<b>DGTE with glucose</b>	0.8246 ± 0.3728	0.9417
	<b>EGCG</b>	9.158 ± 9.032	0.6063
	<b>EGCG with glucose</b>	0.1766 ± 0.04989	0.1252
	<b>GTE</b>	0.5749 ± 0.2741	0.9998
	<b>GTE with glucose</b>	0.327 ± 0.08967	0.2353
<b>Glut4</b>	<b>DGTE</b>	0.3061 ± 0.1698	0.3003
	<b>DGTE with glucose</b>	0.3158 ± 0.1287	0.0124*
	<b>EGCG</b>	0.7082 ± 0.4522	0.8529
	<b>EGCG with glucose</b>	0.5444 ± 0.05545	0.0869
	<b>GTE</b>	0.3038 ± 0.07783	0.2980
	<b>GTE with glucose</b>	0.3415 ± 0.05862	0.0153*

<b>SREBP1c</b>	<b>DGTE</b>	0.5726 ± 0.2813	>0.9999
	<b>DGTE with glucose</b>	0.8144 ± 0.5851	0.9811
	<b>EGCG</b>	30.77 ± 30.5	0.5436
	<b>EGCG with glucose</b>	0.548 ± 0.3507	0.8087
<b>C/EBPα</b>	<b>GTE</b>	0.7828 ± 0.4521	>0.9999
	<b>GTE with glucose</b>	0.194 ± 0.1003	0.4372
	<b>DGTE</b>	0.2149 ± 0.05607	>0.9999
	<b>DGTE with glucose</b>	0.131 ± 0.05096	0.0282*
<b>PPARγ</b>	<b>EGCG</b>	20.8 ± 20.4	0.5483
	<b>EGCG with glucose</b>	0.3115 ± 0.1681	0.0800
	<b>GTE</b>	0.4596 ± 0.1479	>0.9999
	<b>GTE with glucose</b>	0.216 ± 0.09666	0.0459*
<b>FASN</b>	<b>DGTE</b>	2.618 ± 2.458	0.9997
	<b>DGTE with glucose</b>	1.586 ± 0.9036	0.8152
	<b>EGCG</b>	24.73 ± 24.48	0.5541
	<b>EGCG with glucose</b>	0.3629 ± 0.1292	0.7666
<b>FABP4</b>	<b>GTE</b>	1.019 ± 0.8179	>0.9999
	<b>GTE with glucose</b>	0.2375 ± 0.08463	0.6626
	<b>DGTE</b>	0.145 ± 0.0922	0.7984
	<b>DGTE with glucose</b>	0.4961 ± 0.3787	0.9987
<b>LPL</b>	<b>EGCG</b>	2.775 ± 1.284	0.3020
	<b>EGCG with glucose</b>	7.457 ± 4.841	0.3146
	<b>GTE</b>	0.3585 ± 0.1559	0.8996
	<b>GTE with glucose</b>	0.6914 ± 0.444	0.9997
<b>LPL</b>	<b>DGTE</b>	0.2308 ± 0.1077	0.0032*
	<b>DGTE with glucose</b>	0.116 ± 0.07188	0.0098**
	<b>EGCG</b>	0.1476 ± 0.03068	0.0017*
	<b>EGCG with glucose</b>	0.2595 ± 0.06262	0.0252*
<b>LPL</b>	<b>GTE</b>	0.5105 ± 0.1549	0.0386*
	<b>GTE with glucose</b>	0.3369 ± 0.1093	0.0427*
	<b>DGTE</b>	0.1905 ± 0.05939	0.0016**
	<b>DGTE with glucose</b>	0.3443 ± 0.1871	0.1033
<b>LPL</b>	<b>EGCG</b>	0.2129 ± 0.1019	0.0019**
	<b>EGCG with glucose</b>	0.6763 ± 0.1683	0.5679
	<b>GTE</b>	0.538 ± 0.03811	0.0384*
	<b>GTE with glucose</b>	0.7196 ± 0.116	0.6662

#### 4.4 Discussion

Western society's dietary behaviour and increasing consumption of calorie-rich diets are directly involved in dysregulation of glucose and lipid metabolism and thereafter in the global burden of obesity and diabetes, and their related consequences. Using natural compounds could be an additional tool to prevent and ameliorate some disorders related to the impairment of glucose homeostasis. The data presented here suggests that green tea and its active compounds exhibit several beneficial effects in mice; either those fed a normal diet or those fed a high glucose diet. Some previous studies have investigated and confirmed the positive effect of these compounds to regulate glucose homeostasis. In addition to manage body weight and diabetic conditions in rodents (Babu, *et al.*, 2013;Chen, *et al.*, 2011;Roghani and Baluchnejadmojarad, 2010;Snoussi, *et al.*, 2014;Tang, *et al.*, 2013). Therefore, the original plan for this section of the study was to use all of the compounds that had shown any glucoregulatory effects in metabolic cell models in a mouse study. However, due to significant practical and financial issues, this was not possible. An example of this was the insolubility of quercetin, which on the morning of the first set of mouse treatments was discovered to be wholly insoluble in drinking water of mice, even when first dissolved in DMSO or ethanol. Instead DGTE, GTE and EGCG were used because of their solubility. Based on this, the present study attempted to investigate the specific effects of DGTE, EGCG, and whole GTE on several parameters regarding glucose and lipid metabolism, body composition and mass in C57BL/6 mice fed a normal or glucose rich diet (30% glucose) for four weeks.

In this study, the impacts of green tea extracts on glucose regulation during glucose tolerance testing were determined after 28 days in mice fed a normal or glucose-rich diet. Supplemented glucose diet to mice for 28 days did not impaired glucose tolerance as it failed to increase gAUC and reduce glucose disposal compared the data in day 0. Feeding DGTE, EGCG, and GTE to mice either with or without a high glucose supplementation showed no differences in glucose tolerance, as gAUC and glucose clearance after 2h of GTT were not affected (Figure 4.11 andFigure 4.12). These results are consistent with the study of Moreno, *et al.* (2014) in mice fed high fat diet and supplemented with EGCG for 30 days, and the study of Nomura, *et al.* (2015) in diabetic mice. These findings are inconsistent with the results of several studies which have identified that green tea compounds can improve glucose tolerance. This improvement is through reducing the time of glucose clearance, and decreasing gAUC in diabetic and high calorie fed mice (Nishiumi, *et al.*, 2010;Ortsater, *et al.*, 2012;Snoussi, *et al.*, 2014;Tang, *et al.*, 2013;Yan, *et al.*, 2012). These unexpected effects may be due to the difference in treatment or could be related to the route of administration (drinking water), which affects the concentration of treatments based on either individual drinking behaviour or absorption rate. Interestingly, in the present study, administration of glucose solution for 28 days did cause a significant elevation of FBG level compared to day 0 (Figure 4.13 B). Thus, the study suggesting that animals that had consumed high levels of

glucose had impaired fasting glucose, a form of 'pre-diabetes' that in humans significantly increases the risk of developing T2D. This result is in agreement with previously published results that showed consumption of a high-glucose diet can increase FBG (Barros, *et al.*, 2007;Hininger-Favier, *et al.*, 2009;la Fleur, *et al.*, 2011). These increases in the levels of FBG were significantly decreased by the effect of green tea extract and EGCG (Bose, *et al.*, 2008;Ortsater, *et al.*, 2012;Santamarina, *et al.*, 2015;Yan, *et al.*, 2012). These results are in agreement with the present study result that showed DGTE and EGCG significantly reduced FBG (Figure 4.13). This result was associated with an impressive increase in insulin secretion (Figure 4.14 B) and downregulation of expression of Glut4 in adipose tissue (Table 4.3) in response to DGTE and GTE supplementation. High glucose intake could be responsible for impairment of Glut4 expression, as appeared in the present study and as previously reported (Atkinson, *et al.*, 2013;Ritze, *et al.*, 2014). Collectively, the results presented in the present study showed positive effects of selected green tea extracts on FBG in mice fed a glucose-rich diet, therefore suggesting the use of green compounds could be of benefit for individuals who have pre-existing impaired fasting glucose or who are at risk of developing such a condition.

High-energy diet intake can increase body mass and weight gain (Ritze, *et al.*, 2014;Wagoner, *et al.*, 2015;Williams, *et al.*, 2014). Therefore in the present study, the water supply of some groups of mice was supplemented with a 30% (w/v) of glucose solution to challenge energy homeostasis and increase body mass. Alongside that, the effect of DGTE, EGCG, and GTE on body weight and weight gain was investigated. Analysis showed that there were no significant differences in body weight between treatments and control in all groups during the experiment, except GTE fed mice at week one only, which significantly increased body weight in both normal and glucose fed groups (Figure 4.1). This result could be possibly due to individual differences of ingestion behaviour, primary differences in body mass at the start point, and low green tea treatment concentrations associated with limited exposure time. The result is supported by a study which identified that GTE did not change mice body weight (Ortsater, *et al.*, 2012;Tang, *et al.*, 2013). Conversely, several studies have identified that green tea compounds can reduce body mass and weight gain in high calorie fed and diabetic animals (Bose, *et al.*, 2008;Chen, *et al.*, 2011;Santamarina, *et al.*, 2015;Snoussi, *et al.*, 2014). Additionally, weight gain analysis showed no change in weight gain in mice fed a glucose-rich diet and supplemented with green tea extracts (Figure 4.2 B). Significant reductions in weight gain were observed in mice fed a normal diet with DGTE and EGCG (Figure 4.2 A). This result contradicts with some previous findings (Moreno, *et al.*, 2014;Richard, *et al.*, 2009), and partially corresponds with the result of Snoussi, *et al.* (2014). While there is clearly still a lack of clarity regarding the actions of green tea compounds in the management of body mass and weight gain, the present data suggests that consumption of green tea may be a useful tool in the prevention of weight gain in individuals who consume a diet that is not excessively rich in sugar. The observation that this effect is lost in animals that consume excess glucose concerns, as it suggests that in the Western world, where glucose-rich diets are more common (Manzel,

*et al.*, 2014), green tea may not have any impact on the rising incidence of obesity. However, further studies considering treatment concentration, experiment time, and route of administration are needed to clarify this aspect.

Average chow and water intake were measured in all groups. Mice supplied with glucose solution showed decreased food intake and increased water consumption (Figure 4.3 and Figure 4.4). These differences most likely occurred due to the glucose solution stimulating mice to drink more water and decreasing hunger signals which led to reduced consumption of dry food (Bergheim, *et al.*, 2008; Pang, *et al.*, 2014; Ritze, *et al.*, 2014). Administration of DGTE, EGCG, and GTE, in addition to glucose supplementation, did not alter the amount of food and water intake (Figure 4.3 and Figure 4.4 B). This result is possibly due to the sweetened taste of the water which would have masked the taste of green tea compounds. This finding is consistent with several studies that reported unchanged diet and water consumption when experimental animals received green tea extracts (Bose, *et al.*, 2008; Chen, *et al.*, 2011; Li, *et al.*, 2010). In groups that received their treatments without glucose supplemented water, DGTE significantly reduced food and water intake compared to control (Figure 4.3 and Figure 4.4 A). This result may be due to direct interaction with hunger signals, whilst the reduction in water consumption may be attributable to the taste of the water that contained DGTE. This interesting finding suggests that consumption of green tea can regulate feeding behaviour, possibly either by increasing satiety or reducing hunger signals. This observation is in contradiction of several studies that showed green tea compounds have no effect on food consumption in different animal models (Chen, *et al.*, 2011; Li, *et al.*, 2010; Ortsater, *et al.*, 2012). There is, however, some supporting data, where green tea extract reduced food and water intake in diabetic rats (Sundaram, *et al.*, 2013). Similarly, Chen, *et al.* (2009) provided evidence that water intake in rats was decreased in response to GTE and EGCG. The possibility exists therefore that green tea compounds may have a regulatory role in food intake, but further research is needed to clarify the extent of this role.

It has been previously reported that high a calorie diet induces obesity through alteration of adipose tissue mass, particular WAT mass, while green tea extracts have an anti-obesity effect via reduction of body weight and WAT mass (Nishiumi, *et al.*, 2010). In this study, the effect of supplementing DGTE, EGCG, and GTE on body composition mass was determined in mice fed a normal or glucose-rich diet. No significant differences in skeletal muscle mass were seen in all treatment groups (Figure 4.6). Similarly, the hepatic mass was unchanged between most treatment and control groups, and only mice that received EGCG without glucose supplementation showed increased liver mass (Figure 4.5). Supplemented glucose diet to mice for 28 days did not significantly affected fat depots mass except SAT mass was significantly increased compared to day 0 SAT mass. Interestingly, however, mouse adipose tissue depots including WAT and BAT showed marked responses to green tea treatments. DGTE and EGCG consumption significantly increased SAT mass, whilst only EGCG increased VAT mass in mice

that received treatments without glucose (Figure 4.7 and Figure 4.8 A). Significant increases in the mass of these adipose tissue depots were seen in mice fed a glucose diet with DGTE and GTE (Figure 4.7 and Figure 4.8 B). These data suggest that exposure to selected green tea extracts increase the capacity of the body to store nutrients in adipose tissue stores, and is therefore potentially obesogenic agents. Additionally, interesting increases in BAT mass were observed in mice fed a normal diet with EGCG only, while mice supplemented with DGTE and GTE alongside a glucose rich diet significantly increased BAT mass (Figure 4.9). These data are noticeably inconsistent with previously published studies that have investigated the effect of green tea compounds on body anthropometry, particularly concerning WAT and BAT depots (Bose, *et al.*, 2008;Chen, *et al.*, 2009;Li, *et al.*, 2006b). Previous research has shown that mice fed a high-fat diet expressed increases in VAT and BAT mass which were reversed by EGCG (Chen, *et al.*, 2011). A clear difference between these studies and the present study are the methods of introducing a glucos rich diet. The approach taken here to supplement glucose provides a different challenge than increasing lipid deposition. It is, therefore, possible that green tea compounds have cellular and molecular effects that could counteract the challenge of a high-fat diet, but not a high carbohydrate diet. This observation is important as Western diets often include consumption of excess carbohydrates and sugars (Manzel, *et al.*, 2014), and therefore might provide an environment in which green tea is less able to have any anti-obesity effects. Further research in this area might compare the different forms of obesity induction directly to investigate this discrepancy.

The level of circulating insulin is directly related to the level of circulating glucose in healthy individuals. High energy intake, including a high fat or high glucose diet, has been shown to be involved in dysregulation of glucose homeostasis. This impairment, therefore, increase circulating insulin in response to hyperglycaemia associated with increase insulin resistance (Pang, *et al.*, 2016;Zhang, *et al.*, 2015). Green tea extract and some of its active compounds have been reported to have reversible effects on high levels of insulin due to high glucose level (Moreno, *et al.*, 2014;Nomura, *et al.*, 2008;Qin, *et al.*, 2010). In the present study, the levels of insulin in response to DGTE, EGCG, and GTE in mice supplemented without and with a high glucose diet were determined. The results were fascinating, as it appears that EGCG caused a marked and significant increase in insulin level in mice fed a normal or glucose-rich diet, whilst GTE promoted a similar effect on insulin levels in mice that received a high glucose diet only (Figure 4.14). These results were accompanied by significant reduction of FBG in mice that received only DGTE and EGCG with glucose. These findings are in part supported by the study of Sundaram, *et al.* (2013), who identified that green tea could increase the level of circulating insulin in diabetic and high-calorie diet fed rats. Another study by Wolfram, *et al.* (2006) showed that administration of EGCG to db/db mice and diabetic rats for two and ten weeks respectively increased levels of insulin compared to diabetic control. Based on these results together, the study suggests that selected green tea extracts act as non-physiologically insulinotropic agents and could activate beta-cells to secrete high levels of insulin, however further studies are required to determine the role of green tea

on pancreatic beta-cell and glucose stimulated insulin secretion. This finding is important, as factors that can boost insulin secretion are of interest when considered in the context of the increasing levels of insulin resistance seen in many populations.

HOMA is reliable, sensitive, and inexpensive method developed by Matthews which used to determine insulin resistance, sensitivity, and beta cell function in human based on the levels of insulin and glucose in fasting condition. Limited study validated this model to use in the rodent (Antunes, *et al.*, 2016), however still limited due to the metabolic differences and more studies in this regards is needed to validate use in rodents. In this study, the effect of green tea extracts on insulin resistance, sensitivity, and beta cell function was investigated by calculating HOMA-IR, B, and S. Recent results of published studies identified the ability of green tea compounds to ameliorate insulin resistance, increase beta-cell function, and increase insulin sensitivity (Gan, *et al.*, 2015; Jang, *et al.*, 2013a), and therefore in agreement with current study result. Data from the present study suggests that EGCG significantly increased insulin resistance concomitant with increased pancreatic beta-cell function in mice fed a normal diet (Figure 4.15 and Figure 4.16 A), as insulin increased but blood glucose did not decrease equally. This effect of EGCG is, however, consistent with the result of Santana, *et al.* (2015) who found that Swiss mice exhibited insulin resistance when supplemented with EGCG compounds. This result suggests that EGCG is possibly interfering with the traditional glucoregulatory role of insulin under these conditions. Furthermore, all treatments did not change HOMA-IR, HOMA-B, and HOMA-S in mice fed a glucose-rich diet (Figure 4.15, Figure 4.16, and Figure 4.17 B). Why the present study saw such a marked response in insulin secretion to EGCG, and therefore why the HOMA measures were so altered, is difficult to explain. It is clear that EGCG is insulinotropic agent, however, when taking this into account, it still does not explain such a marked increase with no change in glucose levels. This observation suggests that the animals under these conditions were insulin resistant, which contradicts the other published findings above. This could be due to insensitivity of HOMA in the mice as it used in human only, or insulin resistance is developed due to increase adipose depot mass which could secrete FFA and inflammatory cytokines and impaired insulin signalling. It would be interesting to assess the role of EGCG in pancreatic islet insulin secretion to better establish if this effect is irrespective of glucose levels.

Alteration of lipid metabolism including TC, TG, HDL, and LDL in response to excess energy intake has been seen in several studies (Gan, *et al.*, 2015; Zhang, *et al.*, 2015). These alterations can be improved in response to green tea (Jeong, *et al.*, 2012; Qin, *et al.*, 2010; Santana, *et al.*, 2015). The effect of DGTE, EGCG, and GTE on lipid metabolism were, therefore, investigated in mice fed a normal or glucose rich diet in the present study. After 28 days, only DGTE significantly reduced TC concentration in mice fed a normal diet (Figure 4.18 A). All green tea extracts significantly decreased TC levels in mice supplemented with a glucose diet (Figure 4.18 B). This result is consistent with most studies which have

shown green tea, and its active compounds can decrease the high level of TC in diabetic and high fat fed animal models (Bose, *et al.*, 2008;Chen, *et al.*, 2011;Santana, *et al.*, 2015).This impact has been studied in normal, diabetic, and high energy intake animal models. however, no effect of green tea compounds on TC was seen in several studies including Richard, *et al.* (2009) in C57Bl/6 mice, Snoussi, *et al.* (2014) in normal rats, and Sugiura, *et al.* (2012) in mice treated for 30 days. Western lifestyle, liver dysfunction due to alcoholic addiction, and diabetes are risk factors of cardiovascular diseases due to high levels of TC. However, the present study result showed the ability of selected green tea extracts to reduce circulating TC levels. Therefore, regular drinking of green tea might provide protection from cardiovascular diseases through controlling circulating TC levels.

Additionally, the levels of TG in the present study were significantly increased when mice received DGTE and EGCG alone, and EGCG with a high glucose diet (Figure 4.19). This result was accompanied by increases in SAT and VAT mass (Figure 4.7 and Figure 4.8), with no significant change in SREBP1c, PPAR $\gamma$ , and FASN mRNA expression (Table 4.3). in addition, decreased C/EBP $\alpha$  mRNA expression in response to DGTE and GTE in mice fed a glucose-rich diet, downregulation of LPL in mice fed a normal diet in response to all treatments (Table 4.3). Concomitant with significant downregulated FABP4 in all groups in response to all treatments (Table 4.3). These unexpected findings are inconsistent with many studies which have identified that green tea extracts can produce significant decreases in TG level in diabetic or high calorie fed animal models (Hininger-Favier, *et al.*, 2009;Qin, *et al.*, 2010;Roghani and Baluchnejadmojarad, 2010;Wu, *et al.*, 2004a). This decrease in TG and inhibition of lipolysis were reported to be mediated through regulation expression of adipogenic and lipolytic genes, including downregulated PPAR $\gamma$ , SREBP1c, FAS, C/EBP $\alpha$ , FABP4, and LPL (Lee, *et al.*, 2013;Lee, *et al.*, 2009b). Several studies have reported no effect of green tea extract on TG levels (Snoussi, *et al.*, 2014;Sugiura, *et al.*, 2012;Tang, *et al.*, 2013). However, supplementation of EGCG to rats fed a high-fat diet caused significant increase in TG level (Chen, *et al.*, 2009). Alteration of lipid metabolism transcriptional factors like FABP4, SREBP1c, PPAR $\gamma$ , C/EBP $\alpha$ , FASN, and LPL are distinguishing markers of obesity, insulin resistance, and T2D (Guilherme, *et al.*, 2008;Lee, *et al.*, 2009b). Expression of adipogenic factors can increase the level of TG which is then hydrolysed by the activity of LPL to release FFA that are transported in the circulation by FABP4 (Furuhashi, *et al.*, 2014;Wang and Eckel, 2009). These data collectively highlight the lack of a clear picture regarding green tea and TG. As TG is a significant cardiovascular risk factor, it is clearly important to identify factors that can reduce or increase TG, so that the public can be better informed. However, despite the current research provides evidence to prevent increase circulating FFA, more research in this field is required for a clearer view regarding this effect of green tea. Insignificant expression of some of glucose and lipid metabolism genes in the mice adipose tissue is could be nonspecific primer binding (Figure 8.28 to Figure 8.34), or methodological error due to insufficient independent experiment which need to be considered in future study.

In addition to previous results of TC and TG, the levels of HDL and cLDL were measured with no significant differences seen in all mice supplemented with green tea extracts in terms of HDL levels (Figure 4.20). This result is in disagreement with results that have shown green tea compounds can increase the level of HDL in diabetic animals or those with excess energy intake (Jeong, *et al.*, 2012;Roghani and Baluchnejadmojarad, 2010). However, no effect has also been observed as reported by Moreno, *et al.* (2014), Santana, *et al.* (2015), and Snoussi, *et al.* (2014) which is consistent with the present study result. Furthermore, DGTE and EGCG treatments significantly decreased the level of cLDL in mice fed a normal diet, whilst all green tea treatments did reduce the level of cLDL in mice fed a glucose-rich diet (Figure 4.21). This result is consistent with studies that showed green tea can reduce the LDL which is increased in diabetic and high energy diet fed animals (Qin, *et al.*, 2010;Roghani and Baluchnejadmojarad, 2010). However, no effect of green tea on the level of LDL was reported by a study of. As LDL is a key modifiable mediator of cardiovascular risk, these data are of particular interest, as the current strategies clinically focus on drugs like statins which have significant side effect profiles (Golomb and Evans, 2008) so any natural or food based remedies are of interest clinically.

The present study attempted to provide a mechanism for some of the physiological changes seen in green tea-treated mice by investigating the gene expression of the main metabolic genes in tissues taken from mice. Maintaining the normal levels of metabolic mRNA in the main sites of glucose metabolism including liver, skeletal muscles, and adipose tissue are essential to regulate glucose homeostasis (Han, *et al.*, 2016;Rui, 2014;Saltiel and Kahn, 2001). Green tea extract has been shown to have regulatory effects on several genes in relation to glucose metabolism in the liver (Yasui, *et al.*, 2011), adipocytes (Chan, *et al.*, 2011), and skeletal muscle (Ueda, *et al.*, 2008). The result of the present study showed no significant differences between treatments and control in the expression of glucose metabolism genes in the liver, except PEPCK, which was significantly downregulated in EGCG fed mice that received a high glucose diet (Table 4.1). This result is associated with decreased FBG in response to selected green tea compounds in mice supplemented with glucose (Figure 4.13 B). Green tea has ability to maintain glucoregulatory gene expression in mice liver including suppressed G6Pase and PEPCK gene expression, and therefore inhibits glucose output (Collins, *et al.*, 2007;Waltner-Law, *et al.*, 2002;Wolfram, *et al.*, 2006). In addition, increases Glut2 expression and therefore regulate glucose uptake (Cao, *et al.*, 2007). Based on these results together with the published study results, the present study suggests that selected green tea compounds could inhibit hepatic glucose production and is partially involved in the glucose regulation process. As the current study data showed levels of mRNA expression without considering levels of protein activity (due to cost and time limitations), a further study is required to measure protein expression alongside mRNA. The insignificant expression of the most of glucose metabolism genes in the liver is might be unspecific primer binding (Figure 8.28 to Figure 8.34). Second reason could be methodological error and more independent experiment is required to verify this insignificant expression, or mRNA did not expressed rather protein expression.

Similarly, no significant differences in glucose metabolism genes expression were recorded in skeletal muscle, except EGCG and GTE-mediated, which showed significant downregulation of PDK4 in mice supplemented with a glucose diet (Table 4.2). This result is accompanied by a decrease in the level of FBG (Figure 4.13 B). These data are broadly inconsistent with the results of Cao, *et al.* (2007) and Qin, *et al.* (2010) who identified that green tea extract involves regulation of glucose metabolism in muscles through increasing expression of Glut4, Gys1, and PGC1 $\alpha$  mRNA. As the main role of a PDK4 transcriptional factor is regulation of pyruvate dehydrogenase complex (PDC) and utilisation of glucose, increased expression of PDK4 causes decreased PDC activity and impaired glucose utilisation, which can be seen in insulin resistance and diabetic conditions (Kim, *et al.*, 2006b; Lee, 2014). The present study, therefore, suggests that inhibition PDK4 could partially involve regulation of glucose metabolism and modulate many disorders related to that. The insignificant expression of the most of glucose metabolism genes in the mice skeletal muscle is could be unspecific primer binding (Figure 8.28 to Figure 8.34), or insufficient independent experiment, or mRNA was not expression rather protein expression.

In conclusion, a high glucose diet intake could induce dysregulation of some glucose and lipid metabolism markers including elevated levels of FBG and fasting insulin, and induce insulin resistance concomitant with a reduction in functional beta-cells being recorded. Furthermore, glucose supplementation might disturbance of lipid metabolism parameters, increased of SAT mass, and alteration of feeding behaviour. Green tea, including DGTE, EGCG, and GTE, could regulate many of these impairment parameters. Selected extracts improved the impaired FBG in mice fed glucose diet. Additionally, these extracts might be improved some lipid markers including TC and cLDL, however triglyceride levels were increased alongside an increase of fat pad mass (SAT, VAT, and BAT), and suppressed lipolysis through decreasing LPL gene only in normal mice. Surprisingly, some of these extracts increased insulin level without affecting level of glucose during GTT. Total body weight and weight gain were unchanged even with increased fat pad weight, which suggests there is no effect of green tea on weight, however decrease weight gain was seen in normal mice in response to selected extract which suggested that these extract could managed weight gain in individuals that not regularly consumed glucose-rich diet. As a result, green tea could potentially assist in the maintenance of normal glucose homeostasis through regulating glucose and lipid metabolism. Therefore, regular consumption of green tea could help people with existing metabolic disorders to ameliorate impaired glucose and lipid metabolism. However, further research is required, particularly to elucidate the signalling pathway of green tea effects in different conditions.

## **Chapter Five**

# **The effect of active compounds of green tea extract on glucose metabolism in breast cancer cell lines**

## 5.1 Introduction

All tissues in the body normally have a very tightly controlled balance between cellular proliferation and programmed cell death to regulate tissue structure and function (Guo and Hay, 1999). This normal, dynamic process of tissue homeostasis is controlled by several key endocrine and paracrine factors (Medh and Thompson, 2000). Defects in these processes can lead to altered rates of cellular proliferation and/or apoptosis and can lead to serious pathological disorders including various types of cancer, autoimmune diseases, neurodegenerative diseases, and ischemic deterioration (Elmore, 2007). Uncontrolled cellular proliferation accompanied with the improper decrease of cellular deletion can eventually lead to the development of cancer, a leading cause of death globally (WHO, 2014b).

All types of cancer including breast cancer (BC) exhibit the characteristic hallmarks of altered metabolism and migration. BC cells acquire an 'aggressive' phenotype and can disseminate to other organs through a process called metastasis, which begins by the creation of new blood vessels through angiogenic processes, and then the cells undergo local migratory and systemic invasion, and finally specific organ cloning (Kozlowski, *et al.*, 2015). Another hallmark of cancerous cells is an alteration of cellular glucose metabolism towards a high rate of aerobic glycolysis. This alteration is to compensate for the high energy demand for rapid proliferation and survival under the hypoxic condition and is facilitated through consumption of high amounts of glucose concomitant with increased lactate production (Li, *et al.*, 2011a). This metabolic process is called the Warburg phenomenon (Warburg, *et al.*, 1924; Warburg, *et al.*, 1927). Activation of Cori cycle in cancer is another process provides glucose as a source of energy required for proliferation and survival of cancer cells (Goodwin, *et al.*, 2014). This process is generate energy through converting lactate to glucose in the liver (Tisdale, 2009).

Several studies revealed that green tea or its abundant active compounds might have some anti-cancerous effects in a variety of cancer types, including BC. These anti-cancerous effects have reported being mediated via reducing cell viability, activating apoptosis (Hsuuw and Chan, 2007; Thangapazham, *et al.*, 2007) . In addition, suppressing cell growth and promoting cell cycle arrest (Adhami, *et al.*, 2003; Albrecht, *et al.*, 2008; Baliga, *et al.*, 2005; Carvalho, *et al.*, 2010; Thyagarajan, *et al.*, 2007). Furthermore, green tea active compounds are showed to have an inhibitory effect on cancer metastasis including BC (Baliga, *et al.*, 2005; Farabegoli, *et al.*, 2011; Kushima, *et al.*, 2009). Several molecular pathways thought to be involved in green tea mediated anti-cancer and anti-metastasis. These effects including targeting cell signalling and metabolic enzymes like PI3K/Akt, MAPK, JAK/STAT, Wnt, Ras/Raf/MAPK, AP-1, Notch, COX, and NFκB (Shankar, *et al.*, 2007; Singh, *et al.*, 2011).

The aims of the research described in this chapter are

- To identify the effect of green tea active compounds including EGCG, EC, ECG, myricetin, quercetin and a combination of (EGCG, EC, and ECG) on BC cell viability and apoptosis.
- To explore the role of signalling pathways including Akt and AMPK in the effect of green tea compounds on BC cell viability and apoptosis.
- To investigate the relationship between the effects of green tea compounds on BC cell viability via apoptosis and the effect of these compounds on BC cell glucose metabolism.
- To determine the anti-migratory effect of these green tea compounds on BC cells.

## **5.2 Materials and methods**

All materials and methods related to this chapter were previously mentioned in detail in chapter two. The effect of active compounds of green tea extract on cell viability of MCF7 and MDA-MB-231 was performed using two separate reagents and methods including PrestoBlue® and Neutral red to confirm the results. Furthermore, the role of additional of selective Akt and AMPK inhibitors, and sodium pyruvate on BC cell viability and glucose metabolism was investigated using PrestoBlue® cell viability assay. Induce apoptosis was determined by measuring the level of caspase 3/7 activation, and qPCR was used to measure the level of some apoptotic and pro-apoptotic gene expression. In addition, the effect of green tea compounds on glucose metabolism was explored by measuring amount of glucose uptake using fluorescent glucose analogue (2-NBDG) and amount of lactate release using fluorimetric assay kit. Cellular migration of both cell line in response to green tea compounds was investigated using classical microscopic imaging wound healing assay and CellIQ. The role of Akt and AMPK signalling in BC treated with green tea compounds was investigated by measuring the Phosphor-specific expression of Akt and AMPK using Western blotting.

## 5.3 Results

### 5.3.1 Selected green tea compounds reduced MCF7 cell viability measured using PrestoBlue®

The effect of active compounds of green tea on cell viability of MCF7 cells was initially investigated using PrestoBlue®, a resazurin based chemical marker of cell viability. MCF7 cells were treated with 0, 1, 10, 50, 100, and 150µM EGCG, EC, ECG, a combination of these compounds, myricetin, and quercetin, and 30µM etoposide chemotherapy drug (positive control) for 24, 48, and 72 hours, followed by measuring cell viability. The result shows that EGCG, combination, and quercetin significantly decreased MCF7 cell viability compared to control. The decreases were: 12.54%±6.27% (p<0.0001), 28%±8.2% (p<0.0001), 17.44%±2.33% (p<0.0001) for 100 and 150µM EGCG, and 150µM quercetin after 24h respectively (Figure 5.1). After 48h, 100 and 150µM EGCG and combination in addition to 50, 100, and 150µM quercetin significantly decreased viability, with reductions of 16.24%±3.46% (p=0.0014), 18.21%±4% (p<0.0001), 14.22%±1.65% (p=0.0157), 15.86%±2.52% (p=0.0023), 19%±6% (p<0.0001), 35.18%±13.2% (p<0.0001), and 30.17%±10.74% (p<0.0001) respectively (Figure 5.2). The recorded decreases in cell viability after 72h treatment with the same effective compounds and doses after 48h incubation were: 33%±7.75% (p<0.0001), 28.57%±6.68% (p<0.0001), 23.95%±10.75% (p<0.0001), 20.93%±2% (p<0.0001), 15.4%±0.66% (p=0.0286), 18.72%±1.42% (p=0.0009), and 34.67%±13.25% (p<0.0001) respectively (Figure 5.3).

### 5.3.2 Selected green tea compounds reduced MDA-MB-231 cell viability measured using PrestoBlue®

The impact of green tea active compounds on cell viability of MDA-MB-231 cells was assessed after exposed cultured cells to various concentrations of EGCG, EC, ECG, combination of these compounds, myricetin, quercetin, and 30µM etoposide chemotherapy drug (positive control) for 24, 48, and 72h using PrestoBlue® cell viability reagent. EGCG, combination, and quercetin caused significant decreases in MDA-MB-231 cell viability compared to control. 100 and 150µM EGCG and combination of catechins in addition to 150µM quercetin induced significant reductions in viable cells after 24h, and these decreases were: 18%±6.76% (p<0.0001), 21.7%±0.94% (p<0.0001), 11.78%±4.33% (p<0.0001), 13.87%±0.62% (p<0.0001), and 14%±2.3% (p<0.0001) respectively (Figure 5.4). Decreases in cell viability were observed after 48h treatment and the recorded percent were: 38.93%±10.58% (p<0.0001), 34.7%±1% (p<0.0001), 20.67%±4.65% (p<0.0001), 30.6%±0.68% (p<0.0001), 35.19%±13.19% (p<0.0001), and 14%±2.3% (p<0.0001) for 100 and 150µM of EGCG, combination, and quercetin respectively (Figure 5.5). EGCG and combination at 50, 100, 150µM, in addition to 100 and 150µM quercetin reduced cell viability by 16.6%±2% (p=0.0112), 19.14%±5.43% (p=0.0007), 31.57%±2.2% (p<0.0001), 16.9%±2.17% (p=0.0082), 19%±2% (p=0.0008), 24.8%±4.87% (p<0.0001), 18.63%±6.34% (p=0.0016), and 30.67%±9.4% (p<0.0001) respectively after 72h (Figure 5.6).

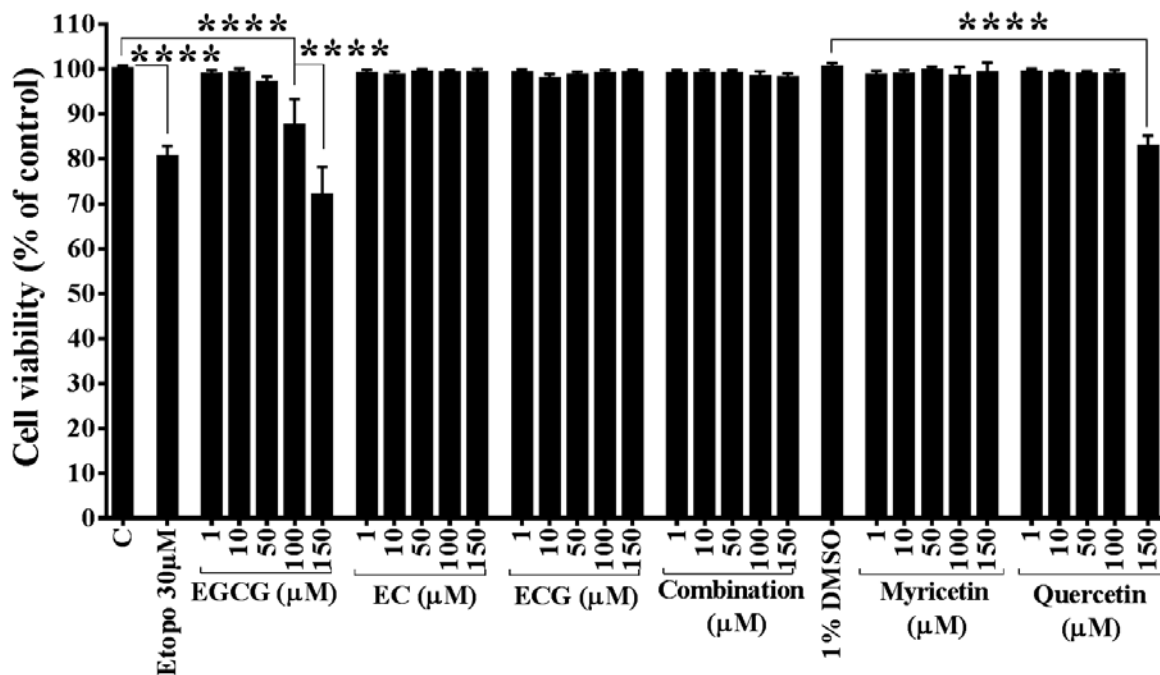


**Figure 5.1 Selected green tea compounds decrease MCF7 cell viability after 24h intervention.**

MCF cells were seeded in 96 well plate at density of 5000/well, and incubated in standard condition for 24h. Cells were exposed to green tea compounds for 24h, and cell viability was investigated using PrestoBlue®. EGCG at 100 and 150µM reduced viable cell compared to control, and 150µM quercetin decreased viable cell compared to DMSO. Data presented mean ± SEM, \*\*\*\*p<0.0001, n=3.

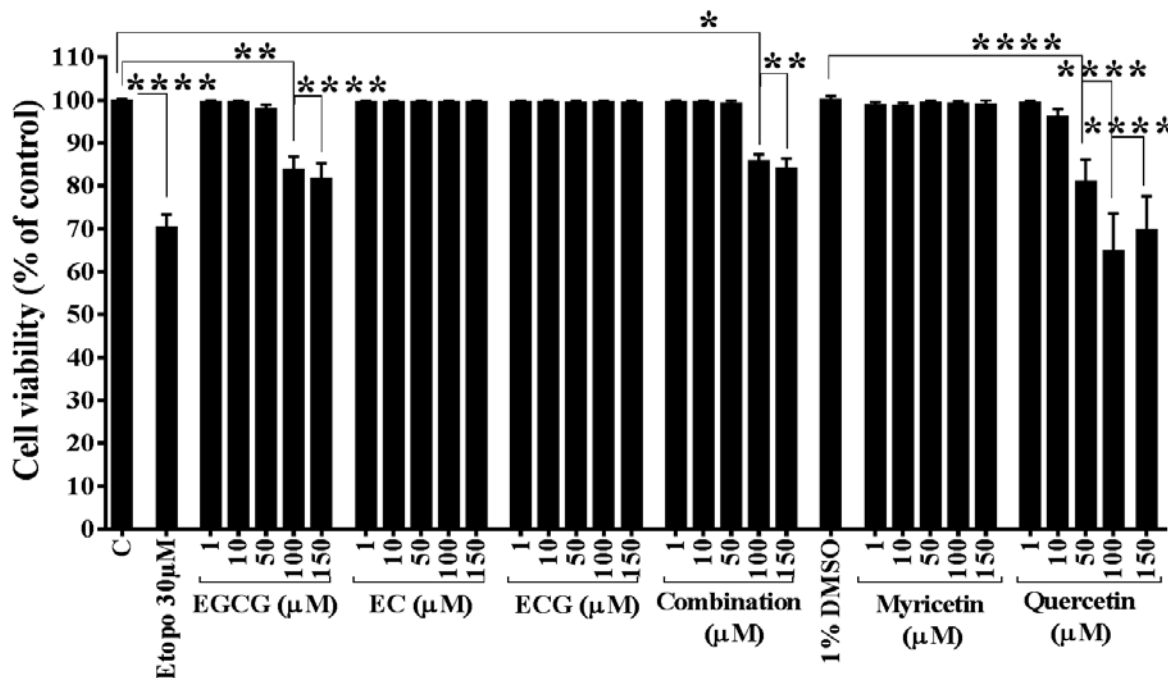


**Figure 5.2 Selected green tea compounds decrease MCF7 cell viability after 48h intervention.**

MCF cells were seeded in 96 well plate at density of 5000/well, and incubated in standard condition for 24h. Cells were exposed to green tea compounds for 48h, and cell viability was investigated using PrestoBlue®. EGCG and catechins combination at 100 and 150µM reduced viable cell compared to control, and 50, 100, and 150µM quercetin decreased viable cell compared to DMSO. Data presented mean ± SEM, \*p<0.05, \*\*p<0.01, \*\*\*\*p<0.0001, n=3.

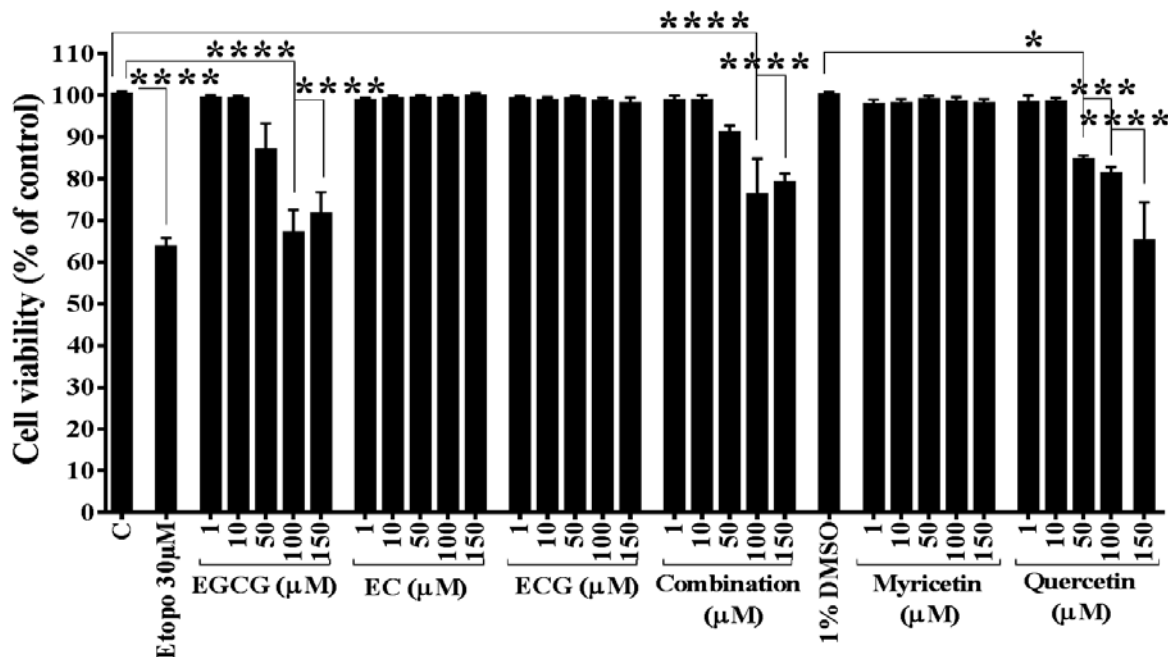


**Figure 5.3 Selected green tea compounds decrease MCF7 cell viability after 72h intervention.**

MCF cells were seeded in 96 well plate at density of 5000/well, and incubated in standard condition for 24h. Cells were exposed to green tea compounds for 72h, and cell viability was investigated using PrestoBlue®. EGCG and catechins combination at 100 and 150µM reduced viable cell compared to control, and 50, 100, and 150µM quercetin decreased viable cell compared to DMSO. Data presented mean ± SEM, \*p<0.05, \*\*\*p<0.001, \*\*\*\*p<0.0001, n=3.

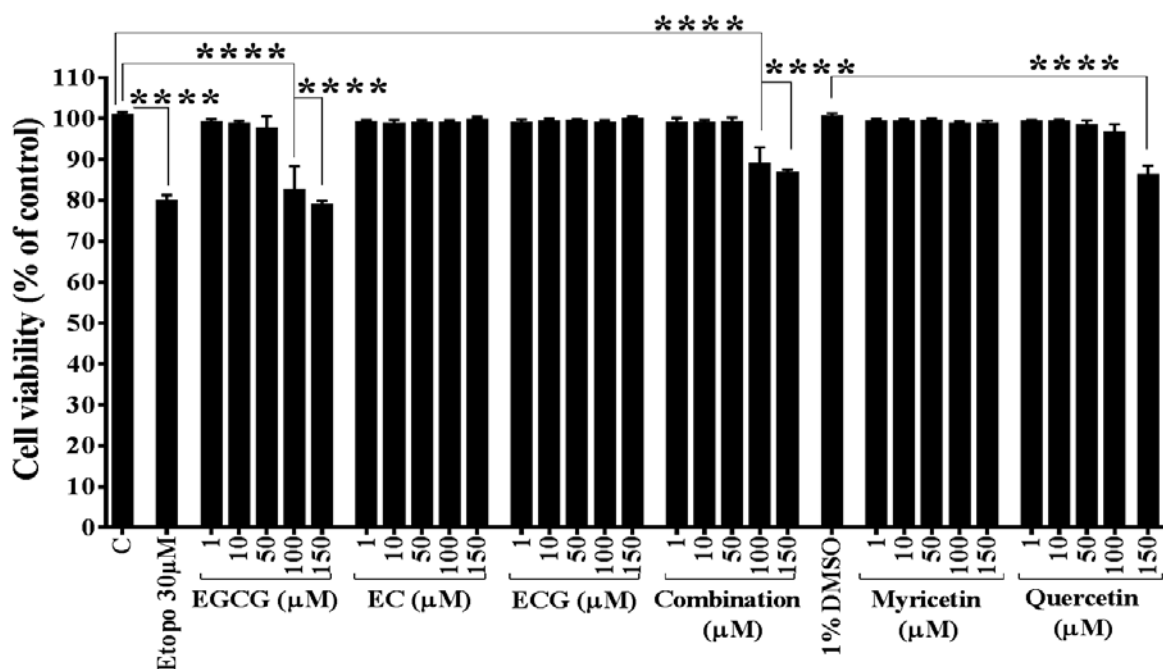


**Figure 5.4 Selected green tea compounds decrease MDA-MB-231 cell viability after 24h intervention.**

MDA-MB-231 cells were seeded in 96 well plate at density of 5000/well, and incubated in standard condition for 24h. Cells were exposed to green tea compounds for 24h, and cell viability was investigated using PrestoBlue®. EGCG and catechins combination at 100 and 150µM reduced viable cell compared to control, and 150µM quercetin decreased viable cell compared to DMSO. Data presented mean ± SEM, \*\*\*\*p<0.0001, n=3.

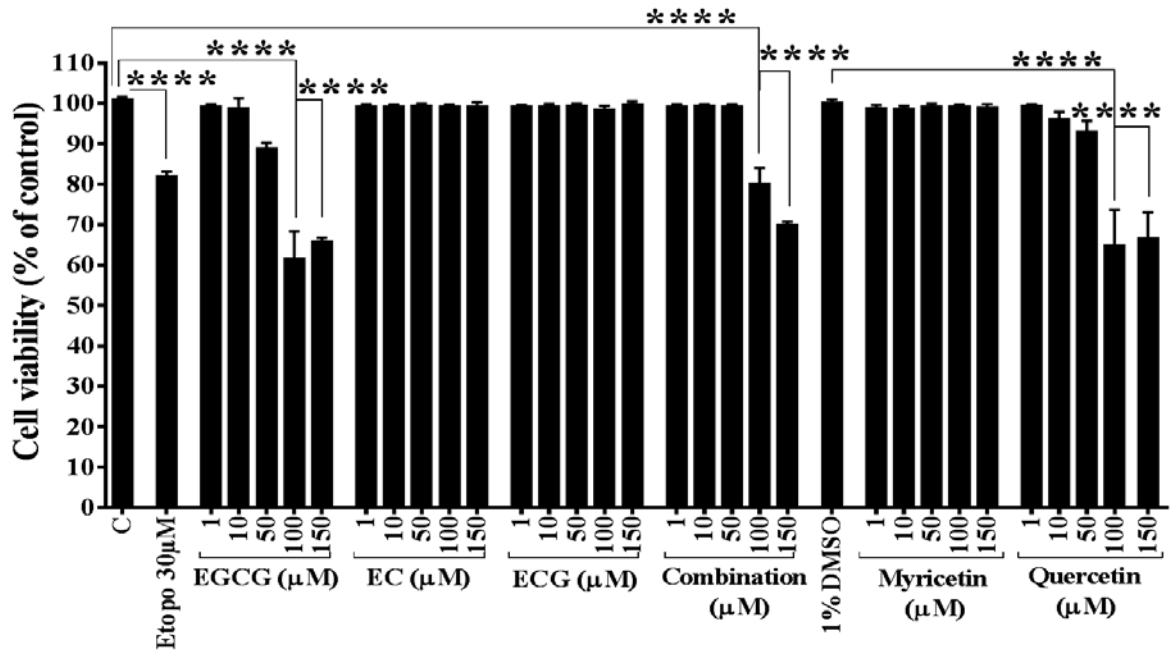


**Figure 5.5 Selected green tea compounds decrease MDA-MB-231 cell viability after 48h intervention.**

MDA-MB-231 cells were seeded in 96 well plate at density of 5000/well, and incubated in standard condition for 24h. Cells were exposed to green tea compounds for 48h, and cell viability was investigated using PrestoBlue<sup>®</sup>. EGCG, catechins combination and quercetin at 100 and 150µM significantly decreased viable cell compared to control and DMSO. Data presented mean ± SEM, \*\*\*\*p<0.0001, n=3.

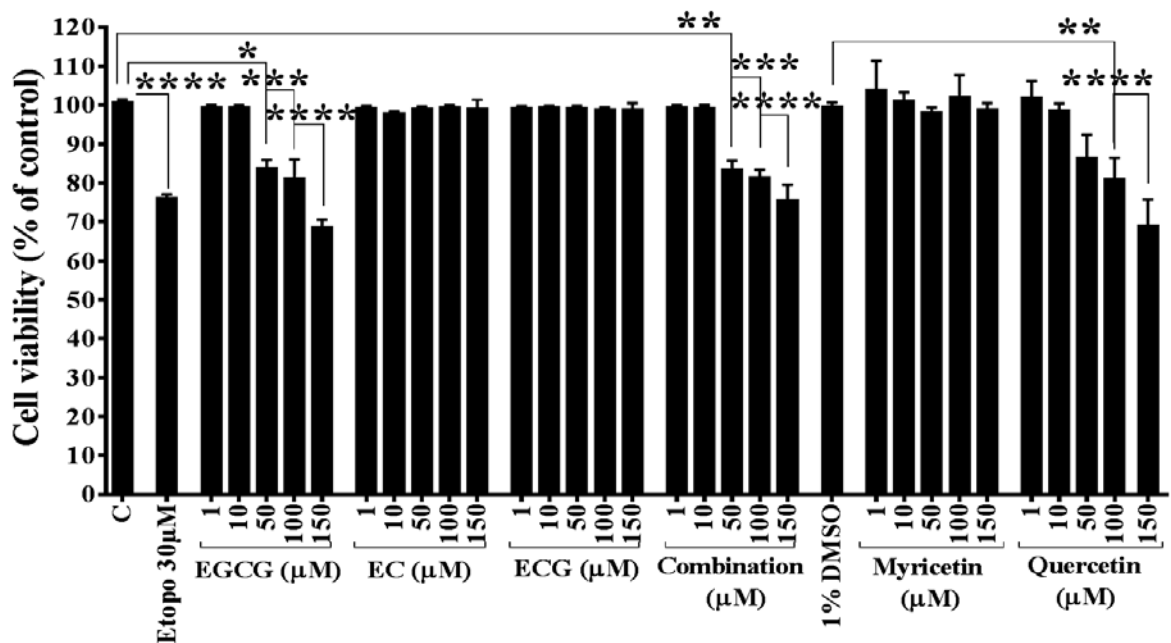


**Figure 5.6 Selected green tea compounds decrease MDA-MB-231 cell viability after 72h intervention.**

MDA-MB-231 cells were seeded in 96 well plate at density of 5000/well, and incubated in standard condition for 24h. Cells were exposed to green tea compounds for 72h, and cell viability was investigated using PrestoBlue<sup>®</sup>. EGCG and catechins combination at 50, 100 and 150µM reduced viable cell compared to control, and 100 and 150µM quercetin decreased viable cell compared to DMSO. Data presented mean ± SEM, \*p<0.05, \*\*p<0.01, \*\*\*p<0.001, and \*\*\*\*p<0.0001, n=3.

### **5.3.3 Selected green tea compounds decreased MCF7 cell viability measured using neutral red**

To confirm the effect of selected ingredients of green tea on MCF7 cell viability that were obtained previously using the PrestoBlue<sup>®</sup> assay, the experiment was repeated using neutral red reagent. Cells were treated with green tea compounds at concentrations and incubation times that previously showed significant decreases in cells viability. Like previous results, MCF7 cells exhibited a significant reduction in cell viability when treated with EGCG, combination, and quercetin (Figure 5.7 to Figure 5.9). The decreases after 24h of 100 and 150 $\mu$ M EGCG and 150 $\mu$ M quercetin were: 41.9% $\pm$ 13.4% (p=0.0010), 45% $\pm$ 17.7% (p=0.0004), and 51.4% $\pm$ 18.5% (p<0.0001) compared to control respectively. Whereas the recorded decreases after 48h of 100 and 150 $\mu$ M EGCG and catechins combination, and 50, 100, 150 $\mu$ M quercetin were: 36% $\pm$ 10.2% (p=0.0345), 54.8% $\pm$ 22.6% (p<0.0001) and 35.4% $\pm$ 13.3% (p=0.0411), 44.3% $\pm$ 13.9% (p=0.0030), and 41% $\pm$ 14% (p=0.0091), 49.3% $\pm$ 17.1% (p=0.0006), and 60.5% $\pm$ 24.7% (p<0.0001) respectively. The decreases in cell viability for the same compounds and concentration at 72h were: 33.4% $\pm$ 3.5% (p=0.0441), 44.25% $\pm$ 12.5% (p=0.0014) and 39.1% $\pm$ 15.6% (p=0.0079), 38.9% $\pm$ 13.2% (p=0.0085), and 34.6% $\pm$ 13.8% (p=0.0299), 35% $\pm$ 12.3% (p=0.0241), and 57% $\pm$ 22.6% (p<0.0001) respectively.

### **5.3.4 Selected green tea compounds decreased MDA-MB-231 cell viability measured using neutral red**

MDA-MB-231 cell viability was investigated using neutral red reagent to confirm the results displayed previously when PrestoBlue<sup>®</sup> cell viability reagent was used. Cells were exposed to green tea compounds that previously caused significant reductions in cell viability for the same incubation periods of 24, 48, and 72h. Results confirmed that EGCG, combination, and quercetin induced significant decreases in cell viability (Figure 5.10 to Figure 5.12). The decreases in cell viability in response to 100 and 150 $\mu$ M EGCG and catechins combination, and 150 $\mu$ M quercetin after 24h were: 46.7% $\pm$ 12.6% (p<0.0001), 69.2% $\pm$ 21.4% (p<0.0001) and 45% $\pm$ 13.4% (p<0.0001), 44.4% $\pm$ 11.9% (p<0.0001), and 55.2% $\pm$ 15.5% (p<0.0001) respectively. Whereas, 100 and 150 $\mu$ M EGCG, catechins combination, and quercetin induced 65.8% $\pm$ 13.8% (p<0.0001), 68.3% $\pm$ 12.3% (p<0.0001) and 37.8% $\pm$ 14.2% (p=0.0007), 53.4% $\pm$ 14.6% (p<0.0001), and 52.8% $\pm$ 18.6% (p<0.0001), and 62.2% $\pm$ 15.5% (p<0.0001) decreases in viable cells after 48h incubation respectively. After 72h 50, 100, and 150 $\mu$ M EGCG and catechins combination, in addition to 100 and 150 $\mu$ M quercetin caused reductions in cell viability of 32.9% $\pm$ 10% (p=0.0242), 65.4% $\pm$ 13.3% (p<0.0001), 64% $\pm$ 17.8% (p<0.0001) and 31.5% $\pm$ 6.7% (p=0.0375), 37.4% $\pm$ 8.4% (p=0.0051), 58.4% $\pm$ 26.6% (p<0.0001) and 40.5% $\pm$ 7.5% (p=0.0032), and 53.9% $\pm$ 11.5% (p<0.0001) respectively.

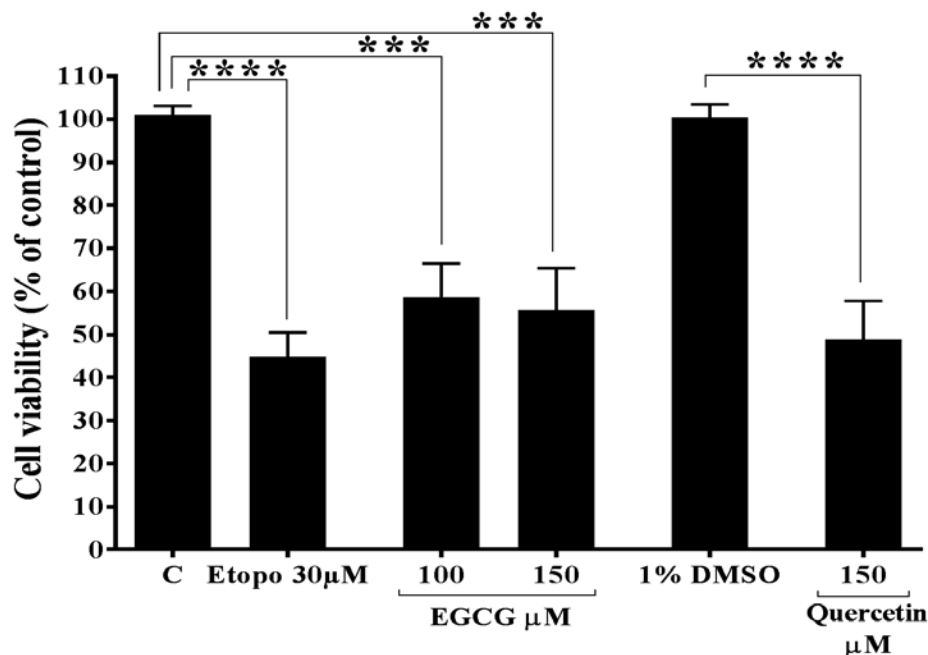


**Figure 5.7 Selected green tea compounds reduce MCF7 cell viability after 24h intervention.**

MCF7 cells were seeded in 96 well plate at density of 5000/well, and incubated in standard condition for 24h. Cells were exposed to green tea compounds for 24h, and cell viability was investigated using Neutral red. 100 and 150µM EGCG reduced viable cell compared to control, and 150µM quercetin reduced viable cell compared to DMSO. Data presented mean ± SEM, \*\*\*p<0.001, and \*\*\*\*p<0.0001, n=3.

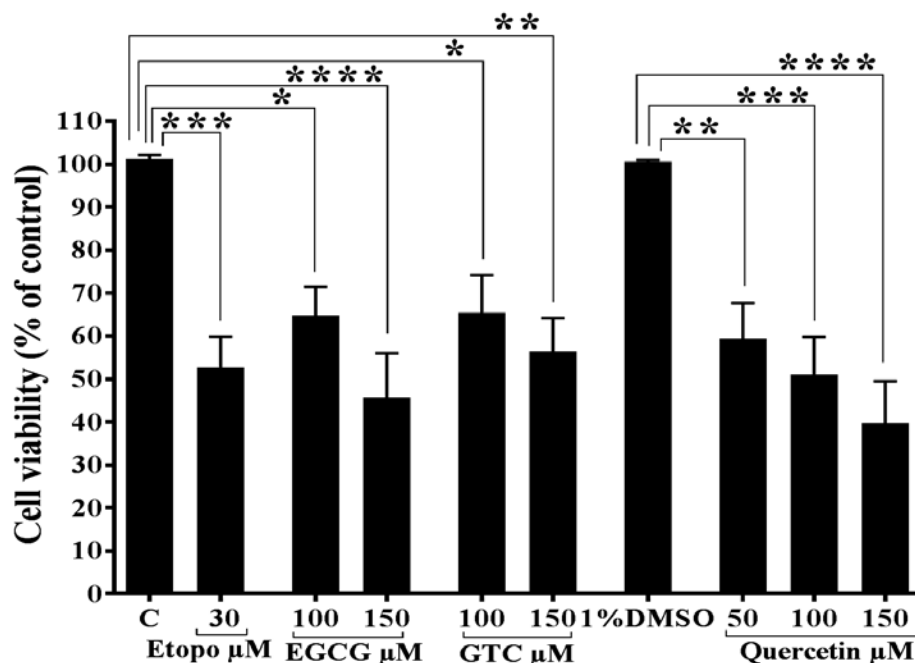


**Figure 5.8 Selected green tea compounds reduce MCF7 cell viability after 48h intervention.**

MCF7 cells were seeded in 96 well plate at density of 5000/well, and incubated in standard condition for 24h. Cells were exposed to green tea compounds for 48h, and cell viability was investigated using Neutral red. 100 and 150µM EGCG and catechins combination reduced viable cell compared to control, and 50, 100, and 150µM quercetin reduced viable cell compared to DMSO. Data presented mean ± SEM, \*p<0.05, \*\*p<0.01, \*\*\*p<0.001, and \*\*\*\*p<0.0001, n=3.

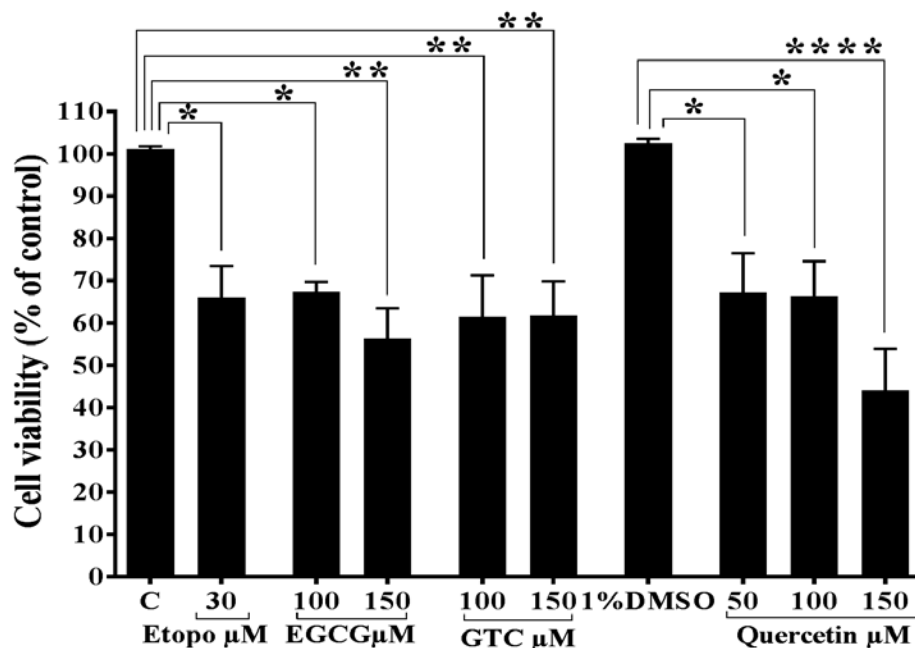


**Figure 5.9 Selected green tea compounds reduce MCF7 cell viability after 72h intervention.**

MCF7 cells were seeded in 96 well plate at density of 5000/well, and incubated in standard condition for 24h. Cells were exposed to green tea compounds for 72h, and cell viability was investigated using Neutral red. 100 and 150μM EGCG and catechins combination reduced viable cell compared to control, and 50, 100, and 150μM quercetin reduced viable cell compared to DMSO. Data presented mean ± SEM, \*p<0.05, \*\*p<0.01, and \*\*\*\*p<0.0001, n=3.

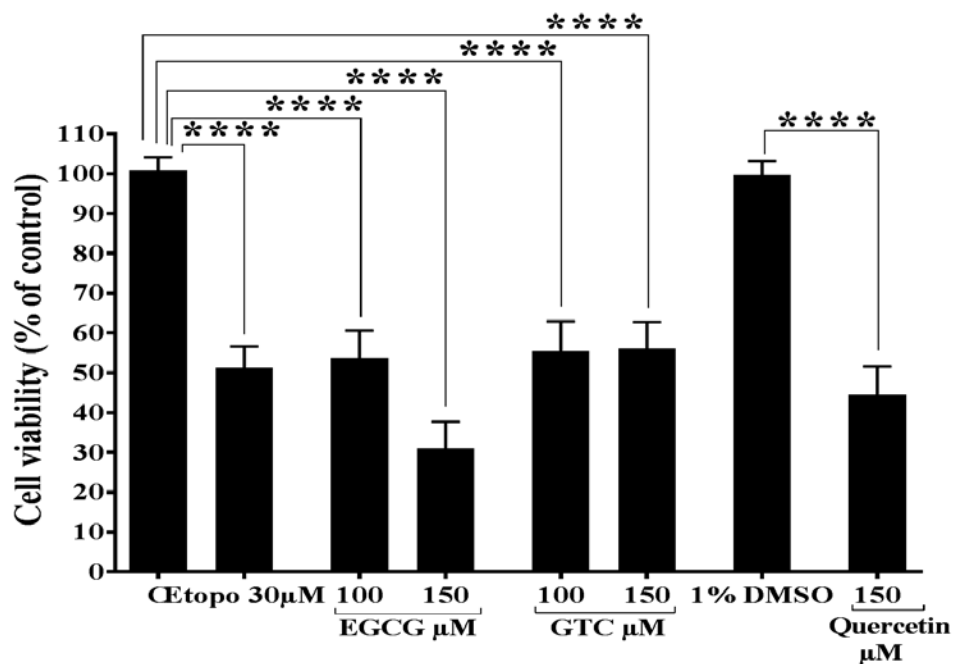


**Figure 5.10 Selected green tea compounds decrease MDA-MB-231 cell viability after 24h intervention.**

MDA-MB-231 cells were seeded in 96 well plate at density of 5000/well, and incubated in standard condition for 24h. Cells were exposed to green tea compounds for 24h, and cell viability was investigated using Neutral red. 100 and 150μM EGCG and catechins combination reduced viable cell compared to control, and 150μM quercetin reduced viable cell compared to DMSO. Data presented mean ± SEM, \*\*\*\*p<0.0001, n=3.

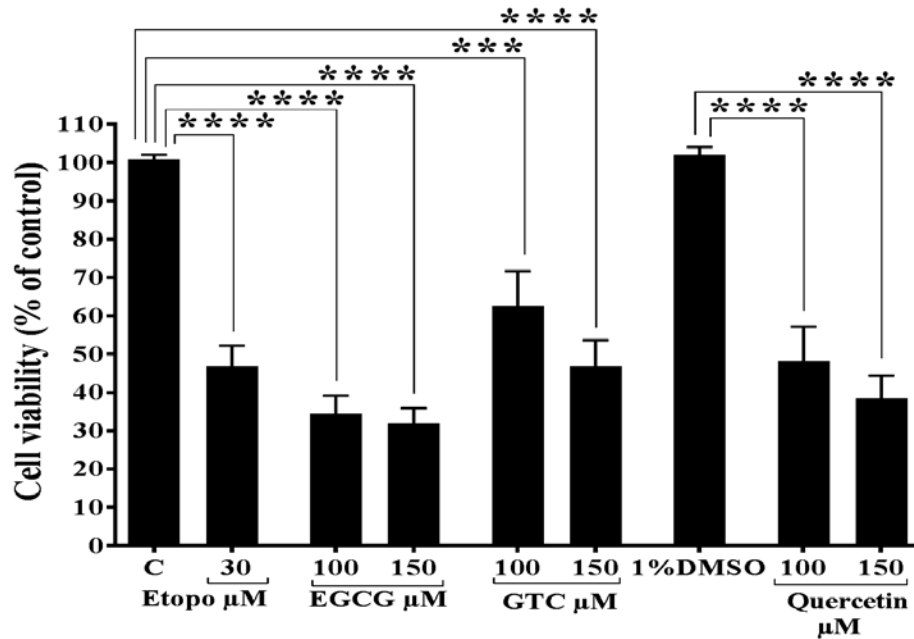


**Figure 5.11 Selected green tea compounds decrease MDA-MB-231 cell viability after 48h intervention.**

MDA-MB-231 cells were seeded in 96 well plate at density of 5000/well, and incubated in standard condition for 24h. Cells were exposed to green tea compounds for 48h, and cell viability was investigated using Neutral red. 100 and 150μM EGCG, catechins combination, and quercetin significantly reduced viable cell compared to control and DMSO. Data presented mean ± SEM, \*\*\*p<0.001, \*\*\*\*p<0.0001, n=3.

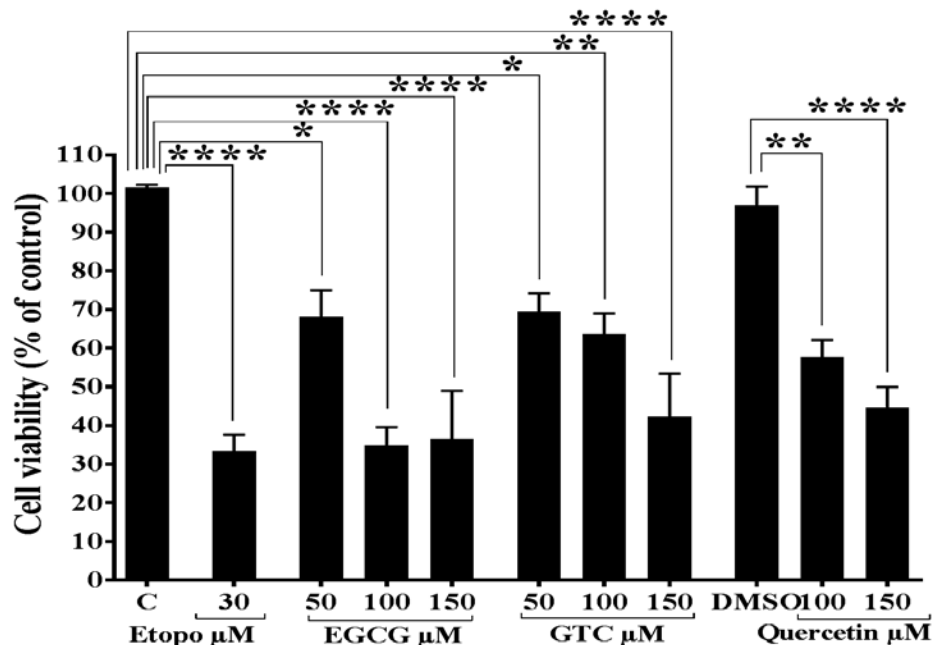


**Figure 5.12 Selected green tea compounds decrease MDA-MB-231 cell viability after 72h intervention.**

MDA-MB-231 cells were seeded in 96 well plate at density of 5000/well, and incubated in standard condition for 24h. Cells were exposed to green tea compounds for 72h, and cell viability was investigated using Neutral red. 50, 100 and 150μM EGCG and catechins combination reduced viable cell compared to control, and 100 and 150μM quercetin reduced viable cell compared to DMSO. Data presented mean ± SEM, \*p<0.05, \*\*p<0.01, \*\*\*p<0.0001, n=3.

### 5.3.5 Selected compounds of green tea does not alter BC cell viability after 6h

To identify the early effect of selected green tea compounds on cell viability, MCF7 and MDA-MB-231 cells were exposed to selected green tea compounds for 6h. PrestoBlue® reagent was used to assess cells viability. No major changes in cell viability were recorded after 6h treatment in both MCF7 and MDA-MB-231 cell lines (Figure 5.13).

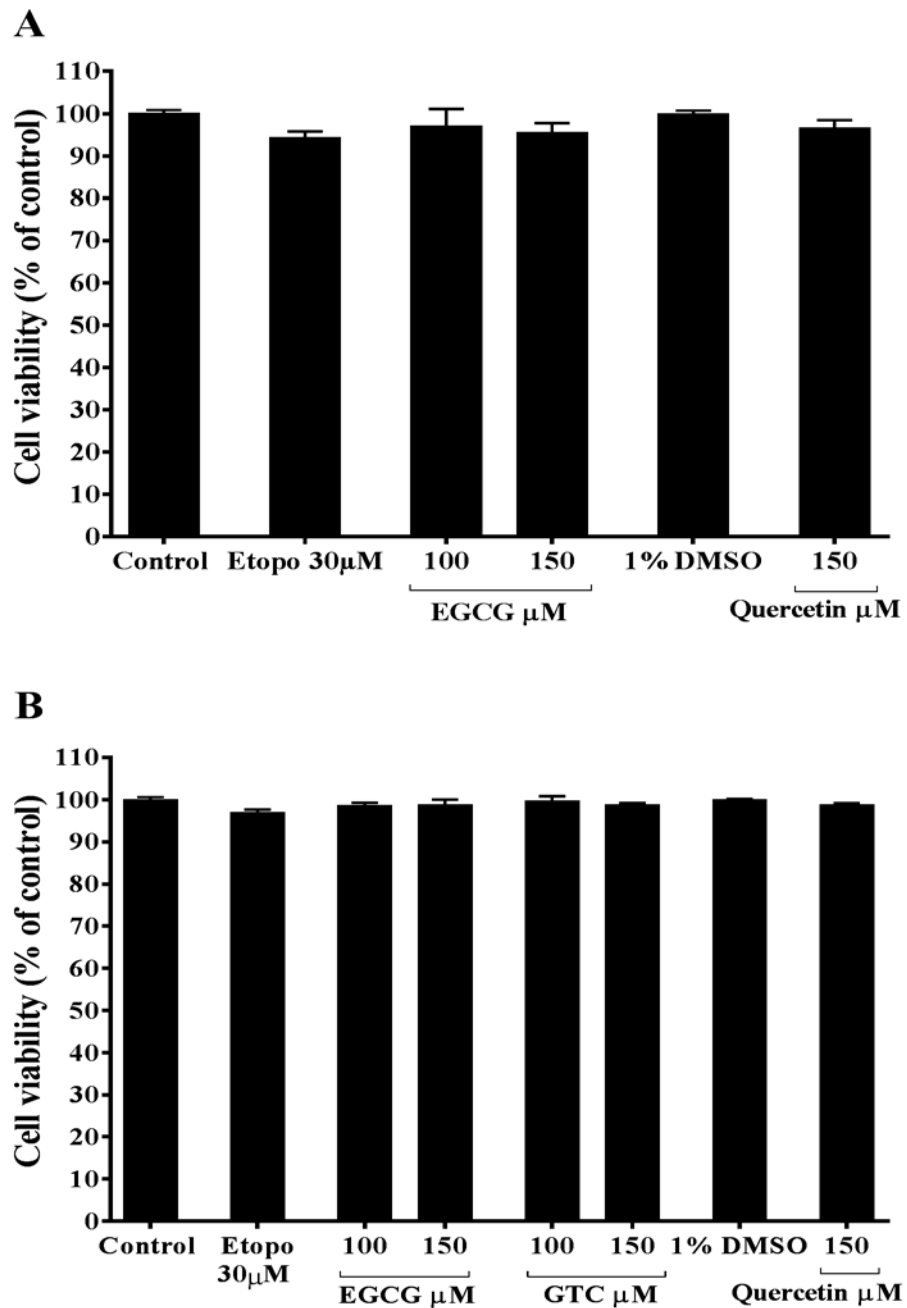


**Figure 5.13 Selected compounds of green tea do not alter BC cell viability after 6h intervention.**

BC cells were seeded in 96 well plate at density of 5000/well, and incubated in standard condition for 24h. Cells were exposed to selected green tea compounds for 6h, and cell viability was investigated using PrestoBlue®. (A) Selected green tea compounds did not change MCF7 cell viability compared to control. (B) Selected green tea compounds did not change MDA-MB-231 cell viability compared to control. Data presented mean  $\pm$  SEM, n=3.

### **5.3.6 Akt inhibition further reduced MCF7 cell viability alongside green tea compounds**

The role of Akt was investigated on decreased MCF7 cell viability as a result of supplementation with selected compounds of green tea. Cells were co-incubated with 10 $\mu$ M of 10-[4'-(N, N-Diethylamino)butyl]-2-chlorophenoxazine hydrochloride (Akt selective inhibitor molecule) in addition to 100 and 150 $\mu$ M EGCG and 150 $\mu$ M quercetin for 24h, cell viability was assessed using PrestoBlue<sup>®</sup> reagent. Results showed that MCF7 exhibited significant decreases in viable cells by 61.2% $\pm$ 3.2% ( $p$ <0.0001) and 89.8% $\pm$ 14.6% ( $p$ <0.0001), and 23.1% $\pm$ 7.3% ( $p$ <0.0001) respectively in response to the green tea compounds mentioned above. Akt inhibition showed further significant decreases in cell viability by 89.4% $\pm$ 22.5% ( $p$ <0.0001) and 39% $\pm$ 8.1% ( $p$ <0.0001) in cells supplemented with 100 $\mu$ M EGCG and 150 $\mu$ M quercetin respectively, compared to cells treated with green tea only (Figure 5.14).

### **5.3.7 AMPK inhibition further reduced MCF7 cell viability alongside green tea compounds**

The role of AMPK on reduced MCF7 cell viability in response to selected compounds of green tea was explored by co-incubating cells with Dorsomorphin dihydrochloride (AMPK selective inhibitor molecule) alongside green tea treatments for 24h. Green tea compounds mentioned above caused significantly reduced cell viability by 17.4% $\pm$ 0.6% ( $p$ <0.0001) and 61.1% $\pm$ 4.1% ( $p$ <0.0001), and 20.5% $\pm$ 0.8% ( $p$ <0.0001) respectively. AMPK inhibition caused an even greater significant reduction of viable cells by 13.8% $\pm$ 1.5% ( $p$ <0.0001) and 34.7% $\pm$ 2.9% ( $p$ <0.0001) respectively in cells incubated with 100 $\mu$ M EGCG and 150 $\mu$ M quercetin, compared to green tea treatments only (Figure 5.15).

### **5.3.8 Sodium pyruvate suppressed reduced MCF7 cell viability induced by green tea compounds**

The effect of sodium pyruvate supplementation on reduced MCF7 cell viability in response to selected compounds of green tea was investigated by co-incubating cells with 1Mm sodium pyruvate alongside green tea treatments for 24h. Selected green tea compounds mentioned above caused 35.9% $\pm$ 12.1% ( $p$ <0.0001) and 47.4% $\pm$ 12% ( $p$ <0.0001), and 20% $\pm$ 1.8% ( $p$ =0.0015) decreases in cell viability respectively. These decreases were significantly suppressed by 53.14% $\pm$ 0.3% ( $p$ <0.0001), 88.3% $\pm$ 0.6% ( $p$ <0.0001), and 22.9% $\pm$ 0.61% ( $p$ <0.0001) respectively in response to supplement sodium pyruvate compared to green tea treatments (Figure 5.16).

### **5.3.9 Akt inhibition further reduced MDA-MB-231 cell viability alongside green tea compounds**

The role of Akt was assessed on reduced MDA-MB-231 cell viability when exposed to selected green tea compounds. Cells were co-cultured with Akt selective inhibitor alongside 100 and 150 $\mu$ M of EGCG and combination of catechins, and 150 $\mu$ M quercetin. Cell viability was examined using

PrestoBlue<sup>®</sup> reagent. Cells exhibited a significant reduction in cell viability in response to these selected green tea compounds. Supplementing Akt inhibitor concomitant with 150 $\mu$ M EGCG and quercetin significantly reduced cell viability by 16.4% $\pm$ 4% ( $p<0.0001$ ) and 35.1% $\pm$ 2.2% ( $p<0.0001$ ) respectively compared to green tea treatments only (Figure 5.17).

#### **5.3.10 AMPK inhibition further reduced MDA-MB-231 cell viability alongside green tea compounds**

An AMPK selective inhibitor was supplemented to cells treated with selected green tea compounds mentioned above for 24h to identify the role of AMPK on reduced cell viability in response to green tea compounds. Co-incubating the cells with AMPK inhibitor alongside 150 $\mu$ M combination catechins and quercetin caused 13.7% $\pm$ 0.6% ( $p=0.0216$ ) and 34.2% $\pm$ 7% ( $p<0.0001$ ) further reduction in cell viability compared to green tea treatments only (Figure 5.18).

#### **5.3.11 Sodium pyruvate suppressed reduced MDA-MB-231 cell viability induced by green tea compounds**

The role of sodium pyruvate supplementation on reduced cell viability in response to green tea was investigated by co-incubating cells with sodium pyruvate combined with selected green tea compounds for 24h. Supplementing 1mM of sodium pyruvate was enough to counter the effect of 100 and 150 $\mu$ M EGCG and combination catechins, and 150 $\mu$ M quercetin on cell viability. Sodium pyruvate promoted significant increased viable cells by 24.8% $\pm$ 0.8% ( $p<0.0001$ ), 27.8% $\pm$ 0.5% ( $p<0.0001$ ) and 14.9% $\pm$ 0.6% ( $p<0.0001$ ), 18.7% $\pm$ 0.9% ( $p<0.0001$ ), and 16% $\pm$ 0.55% ( $p<0.0001$ ) respectively compared to cells treated with green tea compounds only (Figure 5.19).

#### **5.3.12 Impact of green tea compounds on phosphorylation of Akt and AMPK**

The impact of green tea compounds on Akt and AMPK activity in the BC cell lines was investigated. Phosphor-specific Western blotting was performed in response to active compounds of green tea that appeared to show significant effects based on previously obtained results, and the expression levels of pAkt and pAMPK proteins was determined. Unfortunately, due to budget and time limitations, it was not possible to run three independent experiments, and therefore, no statistical test could reliably be applied. The data qualitatively, however, suggests that there were no significant differences in pAkt and pAMPK between green tea compound treatments and control (Figure 5.20 and Figure 5.21), and these data cannot be used to draw firm conclusions, and more independent research is therefore required.

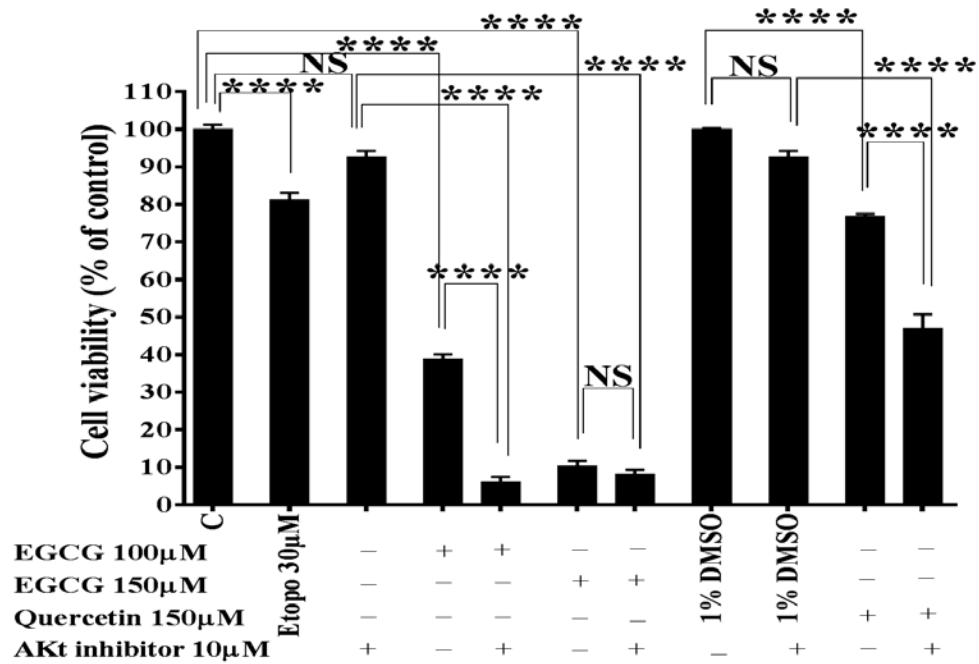


**Figure 5.14 Akt inhibitor increases reduced MCF7 cell viability by green tea compounds.**

MCF7 cells were seeded in 96 well plate at density of 5000/well. Cells were exposed to selected green tea compounds in presence and absence 10µM of Akt inhibitor for 24h, and cell viability was measured using PrestoBlue®. Green tea compound reduced viable cell compared to control, and Akt inhibition selectively further decreased viable cell compared to green tea compounds. Data presented mean ± SEM, \*\*\*\*p<0.0001, n=3.

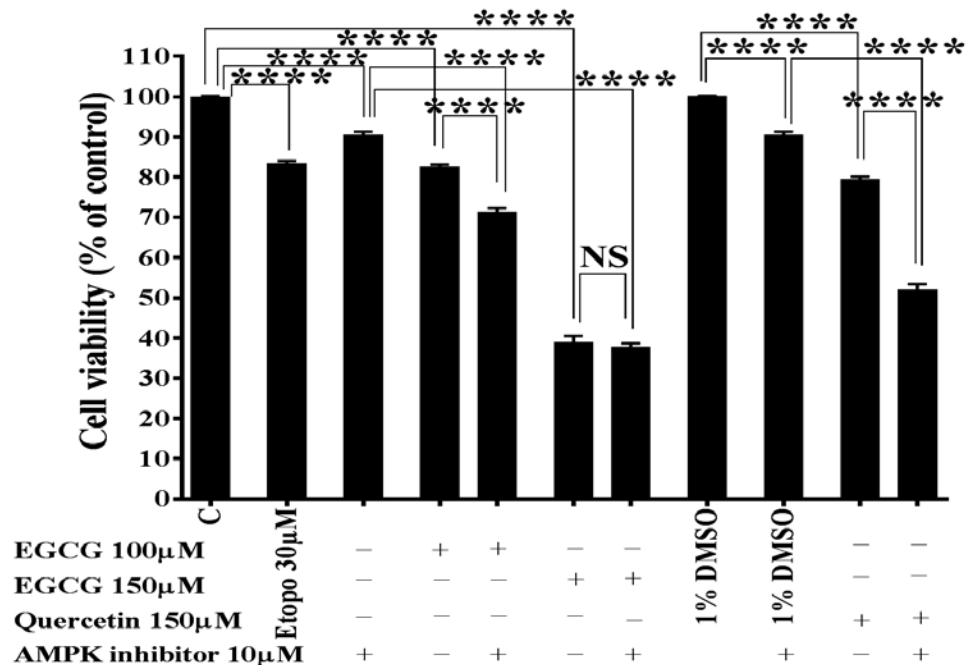


**Figure 5.15 AMPK inhibitor increases reduced MCF7 cell viability by green tea compounds.**

MCF7 cells were seeded in 96 well plate at density of 5000/well. Cells were exposed to selected green tea compounds in presence and absence 10µM of AMPK inhibitor for 24h, and cell viability was measured using PrestoBlue®. Green tea compound reduced viable cell compared to control, and AMPK inhibition selectively further decreased viable cell compared to green tea compounds. Data presented mean ± SEM, \*\*\*\*p<0.0001, n=3.

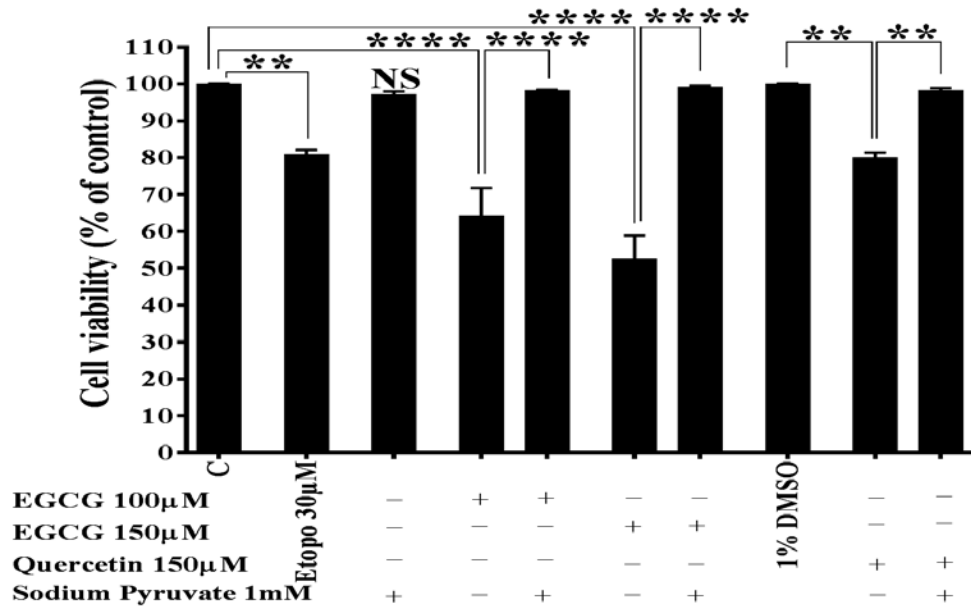


**Figure 5.16 Sodium pyruvate suppresses reduced MCF7 cell viability by green tea compounds.**

MCF7 cells were seeded in 96 well plate at density of 5000/well. Cells were exposed to selected green tea compounds in presence and absence 1mM of sodium pyruvate for 24h, and cell viability was measured using PrestoBlue®. Green tea compound reduced viable cell compared to control, and sodium pyruvate increased viable cell compared to green tea compounds. Data presented mean ± SEM, \*\*p<0.01\*\*\*\*p<0.0001, n=3.

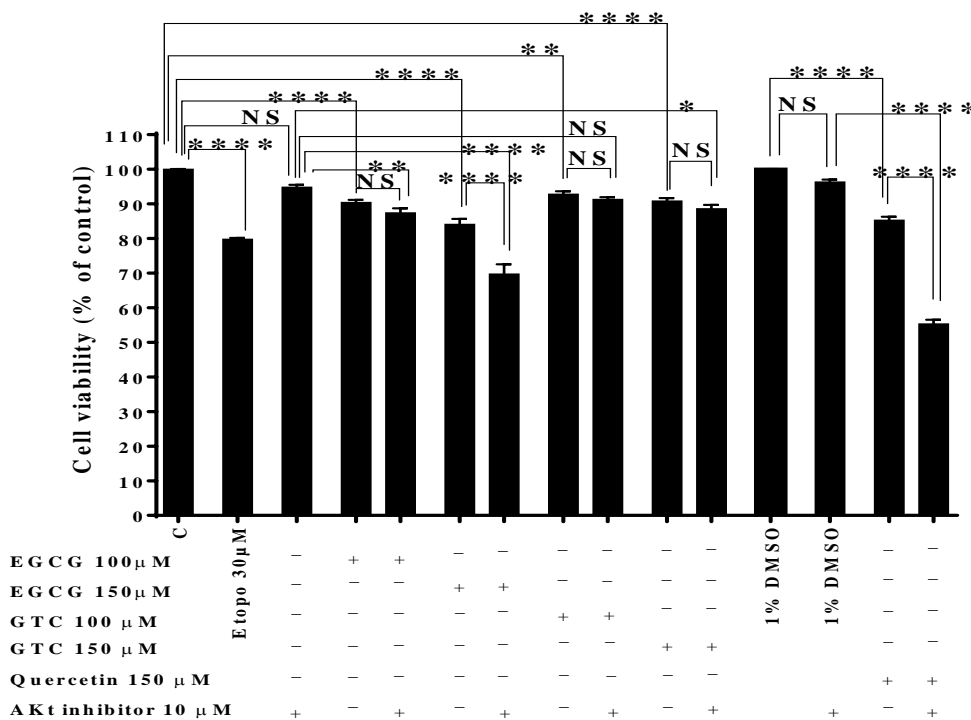


**Figure 5.17 Akt inhibitor increases reduced MDA-MB-231 cell viability by green tea compounds.**

MDA-MB-231 cells were seeded in 96 well plate at density of 5000/well. Cells were exposed to selected green tea compounds in presence and absence 10µM of Akt inhibitor for 24h, and cell viability was measured using PrestoBlue®. Green tea compound reduced viable cell compared to control, and Akt inhibition selectively further decreased viable cell compared to green tea compounds. Data presented mean ± SEM, \*p<0.05. \*\*p<0.01, and \*\*\*\*p<0.00001, n=3.

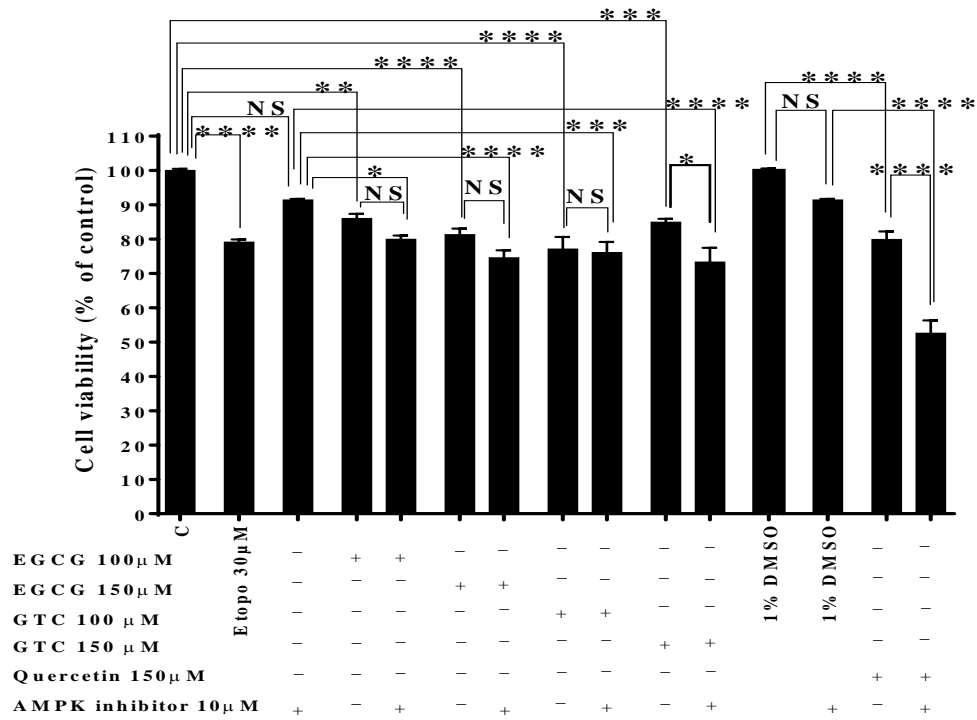


**Figure 5.18 AMPK inhibitor increases reduced MDA-MB-231 cell viability by green tea.**

MCF7 cells (5000/well) of 96 well plate were exposed to green tea compounds with AMPK inhibitor for 24h, and cell viability was measured. AMPK inhibition selectively further decreased viable cell compared to green tea compounds. Data presented mean ± SEM, \*p<0.05, \*\*p<0.01, \*\*\*p<0.001, and \*\*\*\*p<0.0001, n=3.

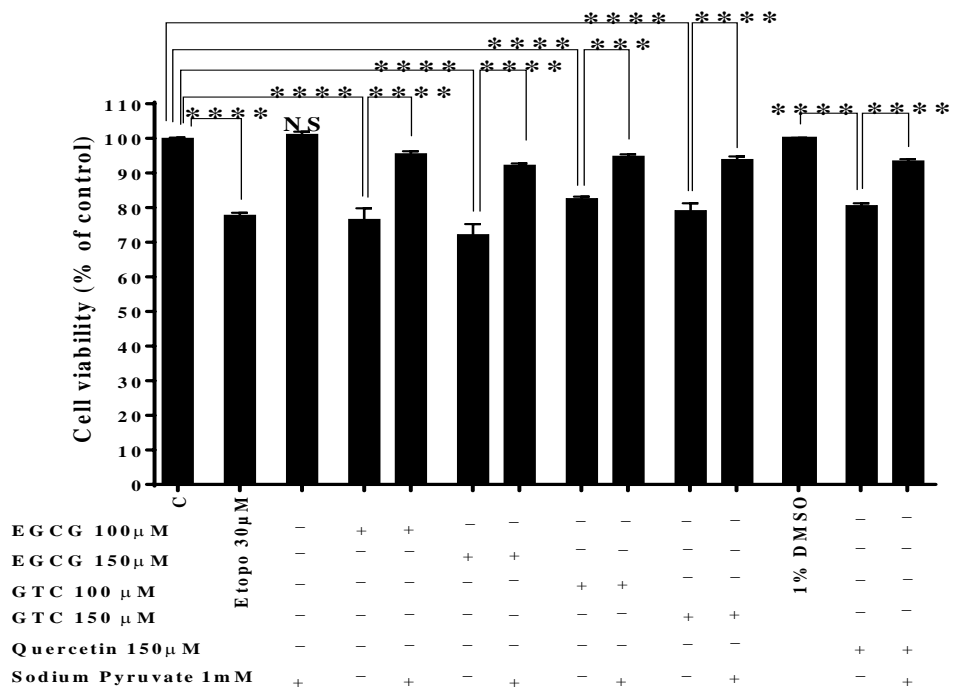


**Figure 5.19 Sodium Pyruvate suppresses reduced MDA-MB-231 cell viability by green tea.**

MDA-MB-231 cells (5000/well) of 96 well plate were exposed to green tea compounds with sodium pyruvate for 24h, and cell viability was measured. Sodium pyruvate increased viable cell compared to green tea compounds. Data presented mean ± SEM, \*\*\*p<0.001 and \*\*\*\*p<0.0001, n=3.

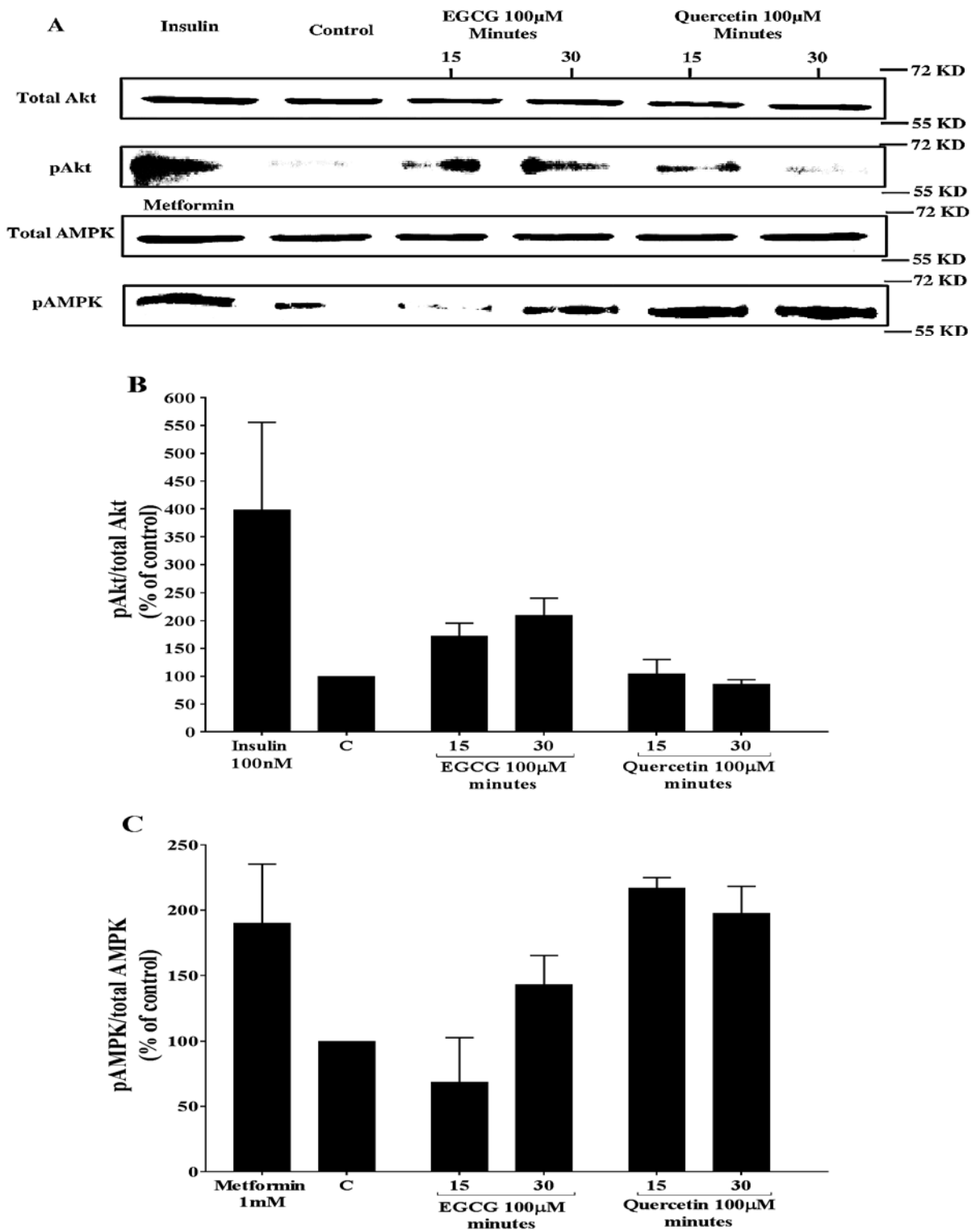


**Figure 5.20 Effect of selected green tea compounds on pAkt & pAMPK expression in MCF7 cell.**

MCF7 cells were seeded in 6 well plate, and incubated in standard conditions until completed confluency. The cells were serum starved for 2h, and then were treated with 100µM of EGCG and quercetin for 15 and 30 minutes. Total protein was isolated and quantified, and phosphor western blotting was performed to identify the leves of pAkt and pAMPK. (A). Total Akt, total AMPK, pAkt, and pAMPK Bands expressed in MCF7 represented one experiment. (B). analysed data of pAkt expression. (C). Analysed data of pAMPK expression. The data displayed as a % of control which normalised to total Akt or AMPK expression. Bands intensity were quantified using Image J software. Data presented as n=2.

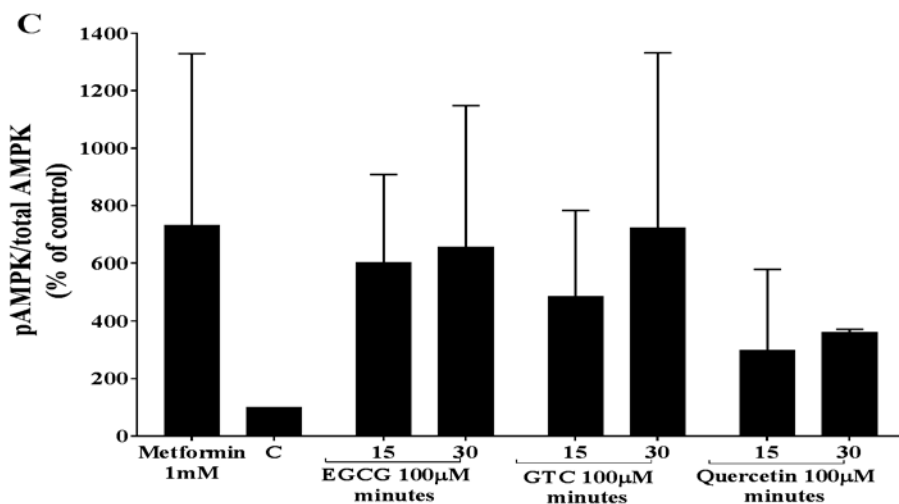
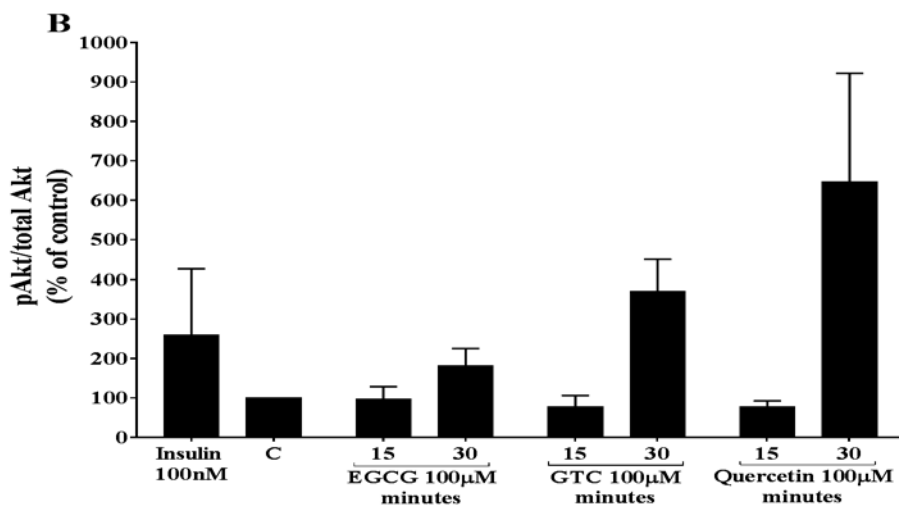
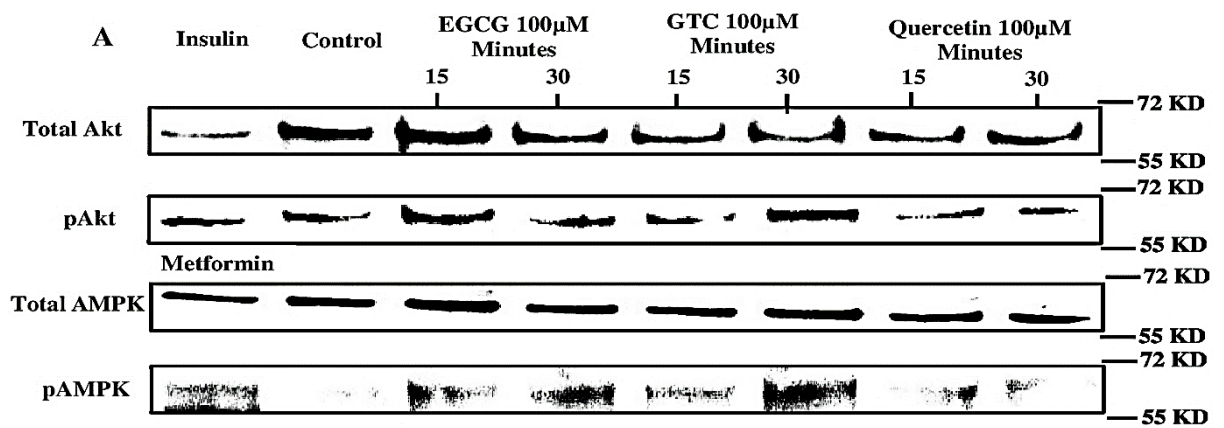


**Figure 5.21 Effect of selected green tea compounds on pAkt & pAMPK expression in MDA-MB-231 cell.**

MDA-MB-231 cells were seeded in 6 well plate, and incubated in standard conditions until completed confluency. The cells were serum starved for 2h, and then were treated with 100 $\mu$ M of EGCG, GTC, and quercetin for 15 and 30 minutes. Total protein was isolated and quantified, and phosphor western blotting was performed to identify the leves of pAkt and pAMPK. (A). Total Akt, total AMPK, pAkt, and pAMPK Bands expressed in MDA-MB-231 cell represented one experiment. (B). analysed data of pAkt expression. (C). Analysed data of pAMPK expression. The data displayed as a % of control which normalised to total Akt or AMPK expression. Bands intensity were quantified using Image J software. Data presented as n=2.

### 5.3.13 Selected green tea compounds induced apoptosis in BC cell lines

As previous results have indicated, cell viability was reduced after exposure to green tea compounds. The effect of these compounds on the levels of cellular apoptosis was investigated in MCF7 and MDA-MB-231 cells. Cells were exposed to previous effective concentrations of green tea compounds and supplemented with or without sodium pyruvate substrate to identify its role in apoptosis. Induction of apoptosis was measured through activation of caspase 3/7. The results show that EGCG at 100 and 150 $\mu$ M, and 150 $\mu$ M quercetin significantly induced apoptosis in MCF7 cells after just 24h incubation compared to control (Figure 5.22 A). The increases in caspase 3/7 activity were 36.55% $\pm$ 1.5% (p=0.0009), 38.40% $\pm$ 2.8% (p=0.0004), 32.11% $\pm$ 3.34% (p=0.0055) respectively. Co-incubating 1mM sodium pyruvate alongside green tea compounds had no significant effect on green tea compounds-induced increases in apoptosis by activation of caspase 3/7. Similarly, EGCG and a combination of catechins at 100 and 150 $\mu$ M, and quercetin at 150 $\mu$ M significantly promoted apoptosis in MDA-MB-231 cells compared to control after 24h treatment (Figure 5.22 B). The data showed increases in caspase 3/7 of 79.87% $\pm$ 3.6% (p=0.0080), 93.35% $\pm$ 5.33% (p=0.0007), 76.77% $\pm$ 8% (p=0.0132), 76.05% $\pm$ 9.22% (p=0.0147), and 86.36% $\pm$ 11.66% (p=0.0026) respectively. Like MCF7 cells, the addition of sodium pyruvate had no significant effect on activation of caspase 3/7 compared to cells treated with green tea active ingredients only.

### 5.3.14 Effect of selected compounds of green tea on BC cell apoptotic gene expression

The impact of active ingredients of green tea that induced apoptosis previously on the expression of some pro-apoptotic and anti-apoptotic gene expression in MCF7 and MDA-MB-231 were assessed by using qRT-PCR. These apoptosis regulatory genes are Bcl2, Bax, P53 and Myc. The obtained  $C_t$  values of targeting genes were normalised using endogenous reference hYWHAZ gene followed by using equation  $2^{-\Delta\Delta C_t}$  to estimate relative gene expression in control and treatment cells. In MCF7, the results showed that EGCG and quercetin did not alter expression of Bcl2, Myc, and P53 (Table 5.1) compared to control. Whereas, EGCG only significantly upregulated Bax gene expression by 0.7 fold (p=0.0335) compared to control (Table 5.1). Different effects of some active compounds of green tea on the apoptotic gene in MDA-MB-231 cells were displayed. Quercetin significantly upregulated Bcl2 expression by 2.9 fold (p=0.0096) compared to control, with no effect of EGCG and GTC (p=0.9863 and >0.9999) (Table 5.2). Significant upregulation of Bax expression was mediated by EGCG and quercetin by 1.75 (p=0.0417), and 1.9 (p=0.0165) fold more than control (Table 5.2). Furthermore, these selected compounds of green tea did not change the expression level of Myc, whereas only quercetin significantly upregulated P53 expression by 0.96 (p=0.0343) fold more than control (Table 5.2).

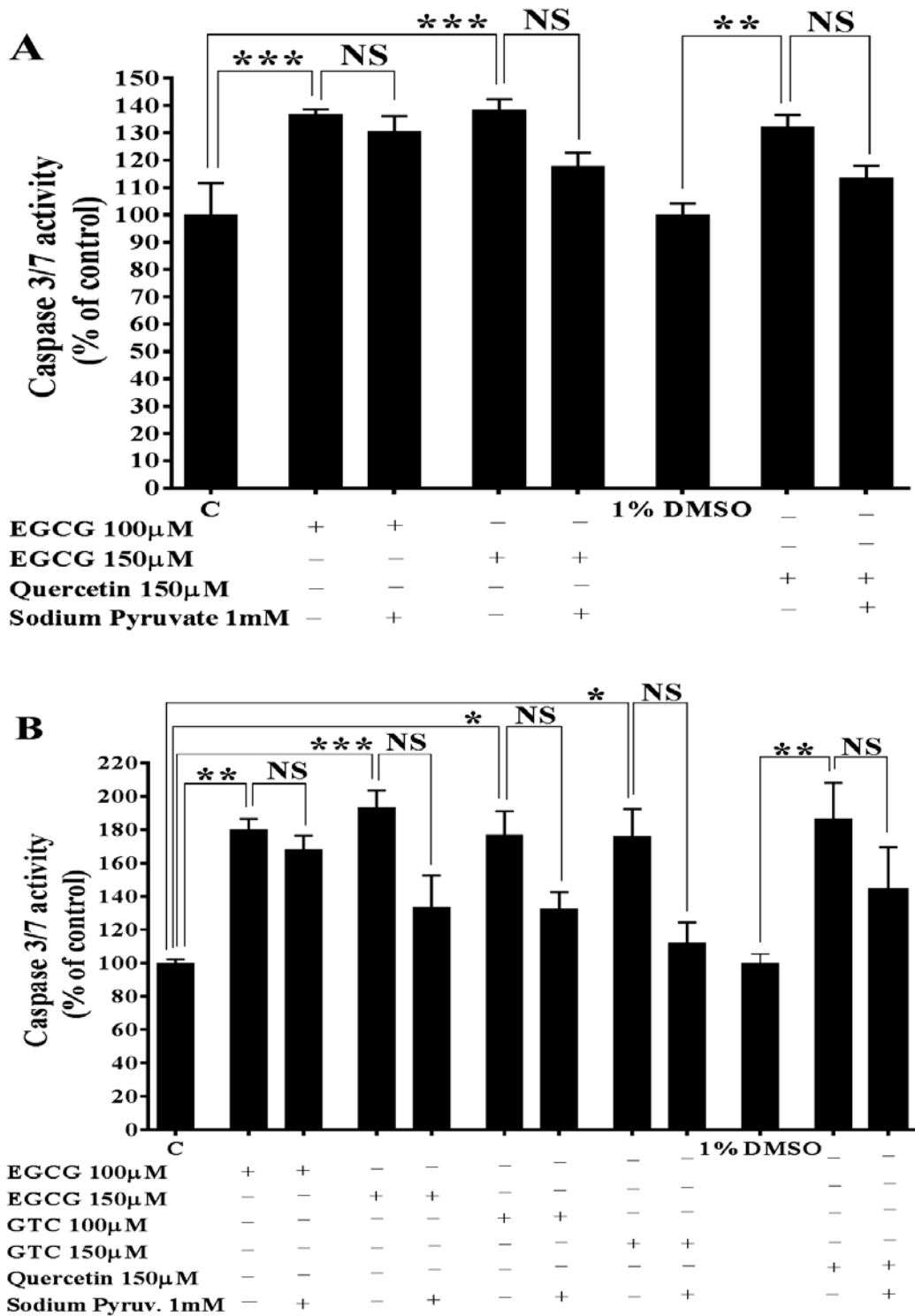


**Figure 5.22 Selected green tea compounds induce apoptosis in BC cell.**

BC cells were seeded in 96 well plate at density of 5000/well. Cells were exposed to selected green tea compounds in presence and absence 1mM of sodium pyruvate for 24h. Apoptosis was investigated by exposing cells to CellEvent® Caspase 3/7 ready Probes® to measure activation of caspase 3/7 for 1h. (A) MCF7 cells exhibited a significant increase in apoptosis in response to green tea compounds compared to control, with no effect of addition sodium pyruvate. (B) MDA-MB-231 cells exhibited a significant increase in apoptosis in respond to green tea compounds compared to control, and sodium pyruvate did not alter apoptosis. Data presented mean  $\pm$  SEM, \* $p$ <0.05, \*\* $p$ <0.01, and \*\*\* $p$ <0.001,  $n$ =3.

**Table 5.1 Effect of green tea compounds on some pro and anti-apoptotic mRNA expression in MCF7 cell.**

MCF7 cells were seeded into 12 well plate, and incubated in standard condition until completed confluency. Cells were serum starved for 2h and then were treated with 100 $\mu$ M of EGCG and quercetin for 24h. RNA was isolated and reverse transcriptased, followed by quantifying amplification of some pro and anti-apoptotic mRNA by using qPCR. No significant differences between green tea treatments and control of all tested genes were seen except EGCG significantly upregulated Bax mRNA leve compared to control. Data displayed as relative fold of gene expression which normalised to housekeeping gene. The data presented mean  $\pm$  SEM, n=3.

mRNA	Treatment	$\uparrow\downarrow$ Fold of control	P value
<b>Bcl2</b>	<b>EGCG</b>	1.62 $\pm$ 0.7712	0.7725
	<b>Quercetin</b>	0.7542 $\pm$ 0.1996	0.9534
<b>Bax</b>	<b>EGCG</b>	1.714 $\pm$ 0.06678	0.0335*
	<b>Quercetin</b>	1.106 $\pm$ 0.1002	0.9722
<b>P53</b>	<b>EGCG</b>	1.433 $\pm$ 0.4236	0.6833
	<b>Quercetin</b>	0.7992 $\pm$ 0.1272	0.9111
<b>Myc</b>	<b>EGCG</b>	2.63 $\pm$ 0.8306	0.1350
	<b>Quercetin</b>	1.315 $\pm$ 0.3704	0.9606

**Table 5.2 Effect of green tea compounds on some pro and anti-apoptotic mRNA expression in MDA-MB-231 cell.**

MDA-MB-231 cells were seeded into 12 well plate, and incubated in standard condition until completed confluency. Cells were serum starved for 2h and then were treated with 100 $\mu$ M of EGCG, GTC, and quercetin for 24h. RNA was isolated and reverse transcriptased, followed by quantifying amplification of some pro and anti-apoptotic mRNA by using qPCR. No significant differences between green tea treatments and control of Myc mRNA was seen. Quercetin significantly upregulated Bcl2, Bax, and P53 mRNA compared to control. Whereas, EGCG significantly upregulated Bax mRNA compared to control. Data displayed as relative fold of gene expression which normalised to housekeeping gene. The data presented mean  $\pm$  SEM, n=3.

mRNA	Treatment	$\uparrow\downarrow$ Fold of control	P value
<b>Bcl2</b>	<b>EGCG</b>	1.411 $\pm$ 0.3615	0.9863
	<b>GTC</b>	0.9905 $\pm$ 0.2471	>0.9999
	<b>Quercetin</b>	3.938 $\pm$ 0.9092	0.0096**
<b>Bax</b>	<b>EGCG</b>	2.753 $\pm$ 0.38	0.0417*
	<b>GTC</b>	1.606 $\pm$ 0.2781	0.8711
	<b>Quercetin</b>	2.907 $\pm$ 0.3345	0.0165*
<b>P53</b>	<b>EGCG</b>	0.949 $\pm$ 0.08675	0.9979
	<b>GTC</b>	1.079 $\pm$ 0.1522	0.9997
	<b>Quercetin</b>	1.966 $\pm$ 0.2795	0.0343*
<b>Myc</b>	<b>EGCG</b>	1.482 $\pm$ 0.1633	0.4537
	<b>GTC</b>	1.609 $\pm$ 0.1385	0.2303
	<b>Quercetin</b>	1.233 $\pm$ 0.1458	0.8714

### **5.3.15 Selected green tea compounds decreased BC cell lactate production after 24h**

The impact of active compounds of green tea on glycolysis in BC cells was investigated by exposing MCF7 and MDA-MB-231 cells to previous effective concentrations of green tea compounds for 24h. The amount of lactate produced from control and green tea-treated cells was measured. EGCG at 100 and 150 $\mu$ M, and quercetin at 150 $\mu$ M, significantly decreased lactate release from MCF7 cells compared to control (Figure 5.23 A). The decreases in lactate were: 50% $\pm$ 20.84% ( $p=0.0073$ ), 52.7% $\pm$ 16.6% ( $p=0.0019$ ), and 34.44% $\pm$ 16% ( $p=0.0441$ ) respectively. Furthermore, MDA-MB-231 cells also exhibited a significant decrease in lactate production when treated with 100 and 150 $\mu$ M of EGCG and combination of catechins, in addition to 150 $\mu$ M of quercetin compared to control (Figure 5.23 B). The reductions in lactate were: 56.9% $\pm$ 12.16% ( $p<0.0001$ ), 45.3% $\pm$ 2% ( $p=0.0003$ ), 40.8% $\pm$ 17.8% ( $p=0.0014$ ), 48% $\pm$ 19.2% ( $p=0.0001$ ), and 38.6% $\pm$ 4.26% ( $p=0.0026$ ) respectively.

### **5.3.16 Sodium pyruvate suppressed green tea reduced BC cell lactate production after 24h**

To study the role of sodium pyruvate substrate on green tea mediated lactate reduction, MCF7 and MDA-MB-231 cells were treated with 150 $\mu$ M of selected green tea compounds that promoted significant decreases in lactate production in presence and absence of 1mM sodium pyruvate. The results showed EGCG and quercetin significantly decreased MCF7 lactate production by 65.3% $\pm$ 3.6% ( $p<0.0001$ ) and 54.8% $\pm$ 5.2% ( $P<0.0001$ ) respectively compared to control. Whereas, the addition of sodium pyruvate significantly restored lactate release by 122% $\pm$ 1.9% ( $p<0.0001$ ), and 33.3% $\pm$ 6.8% ( $p=0.0486$ ) respectively compared to cells treated with green tea compounds (Figure 5.24 A). Like MCF7, EGCG, a combination of catechins, and quercetin significantly reduced of lactate in media by 39.4% $\pm$ 3.3% ( $p<0.0001$ ), 26.7% $\pm$ 3.7% ( $p=0.0001$ ), and 36.9% $\pm$ 3.9% ( $p<0.0001$ ) respectively compared to control. Supplementing cells with sodium pyruvate alongside green tea compounds significantly increased lactate by 32.55% $\pm$ 2% ( $p=0.0031$ ), 22.53% $\pm$ 2% ( $p=0.0147$ ), and 27.6% $\pm$ 6.84% ( $p=0.0118$ ) respectively compared to cells treated with green tea compounds (Figure 5.24 B).

### **5.3.17 Selected compounds of green tea decreased BC cell lactate production after 6h.**

In order to establish whether the changes in glucose homeostasis/glycolysis occur before or after changes in cell viability, the early effects of green tea active compounds on BC cell glycolysis were investigated by measuring the amount of lactate release from cells after just 6h. MCF7 and MDA-MB-231 cell lines were treated with EGCG and quercetin for 6h only. As early as 6h incubation, EGCG and quercetin promoted significant reductions in lactate release from treated MCF7 compared to control (Figure 5.25 A). Percentage decreases were: 10.66% $\pm$ 3.36% ( $p=0.0462$ ) and 10.2% $\pm$ 0.54% ( $p=0.0487$ ) respectively. Similarly, both EGCG and quercetin mediated significant reduced amounts of lactate in MDA-MB-231 cells after just 6h treatment with decreases of 11.43% $\pm$ 2.6% ( $p=0.0015$ ) and 7.44% $\pm$ 0.4% ( $p=0.0143$ ) respectively (Figure 5.25 B).

### **5.3.18 Sodium pyruvate does not alter green tea reduced BC lactate production after 6h**

MCF7 and MDA-MB-231 cells were treated with high concentrations of EGCG and quercetin with and without sodium pyruvate for 6h to identify the early effect on decreased lactate production mediated by green tea compounds. EGCG and quercetin caused significant decreases in MCF7 lactate production by  $20.88\% \pm 2.11\%$  ( $p=0.0040$ ) and  $23\% \pm 4.35\%$  ( $p=0.0044$ ) compared to control without any significant effect of sodium pyruvate to alter these reductions (Figure 5.26 A). Similarly, EGCG and quercetin mediated significant reductions in lactate release in MDA-MB-231 cells with  $11.43\% \pm 2.6\%$  ( $P=0.0015$ ) and  $7.44\% \pm 0.4\%$  ( $P=0.0143$ ) decreases being recorded respectively. These significant decreases in lactate production were unaffected by supplementing sodium pyruvate substrate (Figure 5.26 B).

### **5.3.19 Selected compounds of green tea decreased 2-NBDG uptake in BC cells**

Previous results in the present study indicate that active compounds in green tea have the ability to decrease lactate release from BC cell earlier without affected viable cell. The effect of green tea active ingredients on BC cell glucose uptake were determined in MCF7 and MDA-MB-231 cells post exposure to previous effective compounds of green tea. Cellular glucose uptake was measured using a fluorescent glucose analogue after 4h treatment. Measuring direct cellular glucose uptake using 2-NBDG is accurate, valid and widely used method than measuring amount of glucose remain in the media, as the previous research in this study did (Nowis, *et al.*, 2014). The results showed that 100 and 150 $\mu$ M EGCG and 150 $\mu$ M quercetin significantly reduced 2-NBDG uptake in MCF7 cells compared to control (Figure 5.27 A) with decreases of  $19.67\% \pm 5.4\%$  ( $p<0.0001$ ),  $15.57\% \pm 3.62\%$  ( $p=0.0018$ ), and  $13.34\% \pm 2\%$  ( $p=0.0095$ ) respectively being recorded. A similar effect of green tea compounds on glucose uptake in MDA-MB-231 cells was seen, with EGCG and combination compounds at 100 and 150 $\mu$ M in addition to quercetin at 150 $\mu$ M significantly decreases in glucose uptake compared to control (Figure 5.27 B). The recorded decreases in 2-NBDG uptake were:  $20.44\% \pm 6.2\%$  ( $p=0.0072$ ),  $24.25\% \pm 4.4\%$  ( $p=0.0008$ ),  $20.99\% \pm 2\%$  ( $p=0.0053$ ),  $22.97\% \pm 5.58\%$  ( $p=0.0017$ ), and  $21.80\% \pm 6.3\%$  ( $p=0.0033$ ) respectively.

### **5.3.20 Akt and AMPK inhibition unaltered green tea compounds-induced decrease BC cell 2-NBDG uptake**

The role of Akt and AMPK signalling pathways on glucose uptake was determined through supplementing small molecule inhibitors alongside green tea compounds for 4 and 8h incubations in both MCF7 and MDA-MB-231 cells. Supplementation of Akt or AMPK inhibitor alongside green tea compounds to MCF7 cells did not significantly alter 2-NBDG uptake compared to significant decreases that were promoted by green tea compounds after 4h treatment (Figure 5.28 A). Similarly, MDA-MB-231 cells exposed to Akt or AMPK inhibitor alongside selected green tea compounds did not respond differently regarding 2-NBDG uptake compared to green tea compounds alone after 4h incubation (Figure 5.28 B). Furthermore, no differences were observed in 2-NBDG uptake after 8h of co-incubated cell with Akt or AMPK inhibitor alongside selected green tea compounds in both cell lines (Figure 5.29).

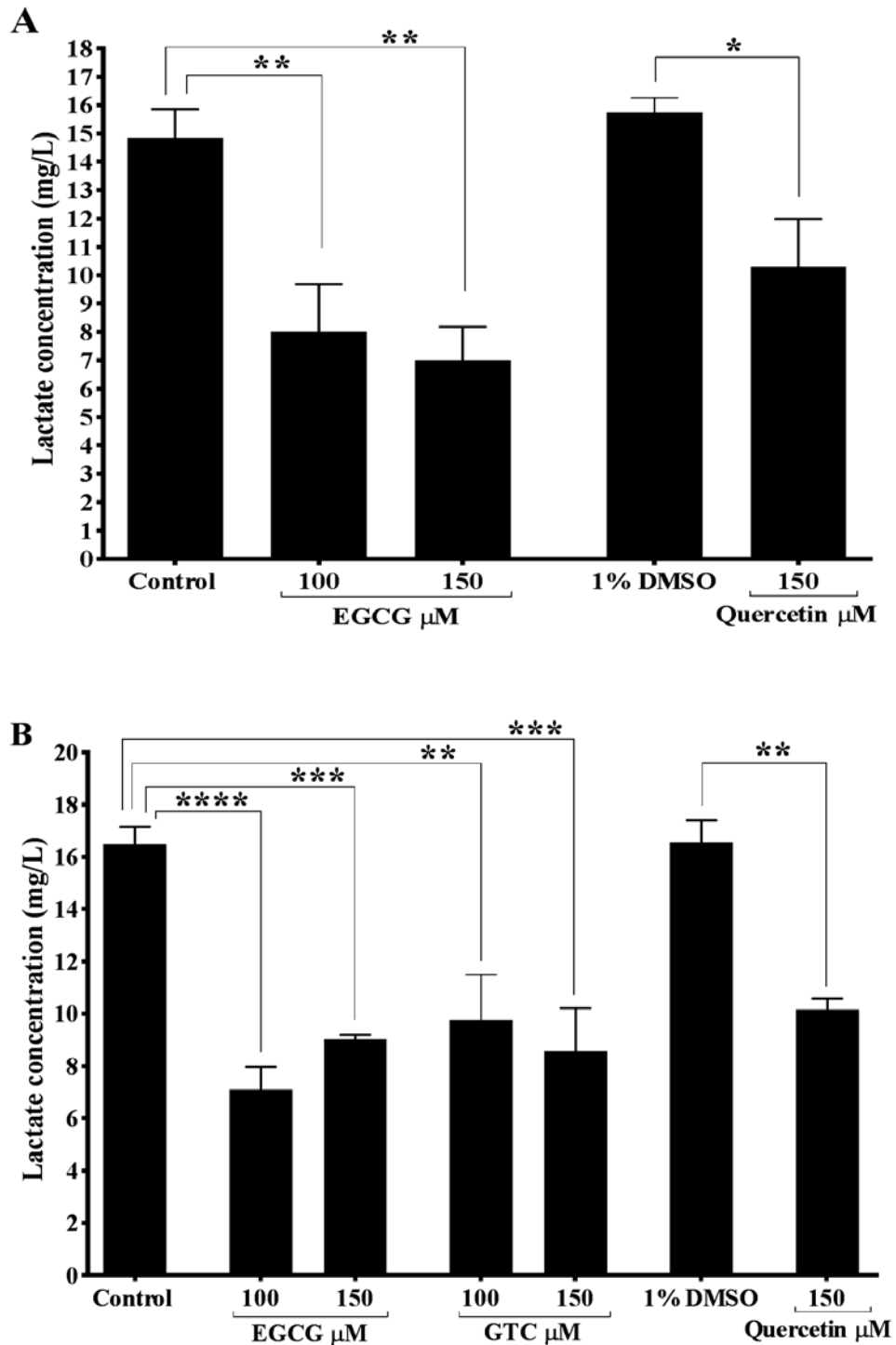


**Figure 5.23 Selected green tea compounds decrease BC cell lactate production after 24h intervention.**

BC cells were seeded into 24 well plate at density of  $3 \times 10^4$ , and incubated in standard condition for 24h. Cells were then exposed to selected green tea compounds for 24h. Culture media were collected, deproteinized, and the level of lactate was measured using fluorimetric L-Lactate assay. (A) MCF7 cells showed significantly decreased in lactate level in response to EGCG and quercetin compared to control. (B) MDA-MB-231 cells showed significantly reduced lactate level in response to EGCG, GTC, and quercetin compared to control and DMSO. Data presented mean  $\pm$  SEM, \* $p < 0.05$ , \*\* $p < 0.01$ , \*\*\* $p < 0.001$ , and \*\*\*\* $p < 0.0001$ ,  $n = 3$ .

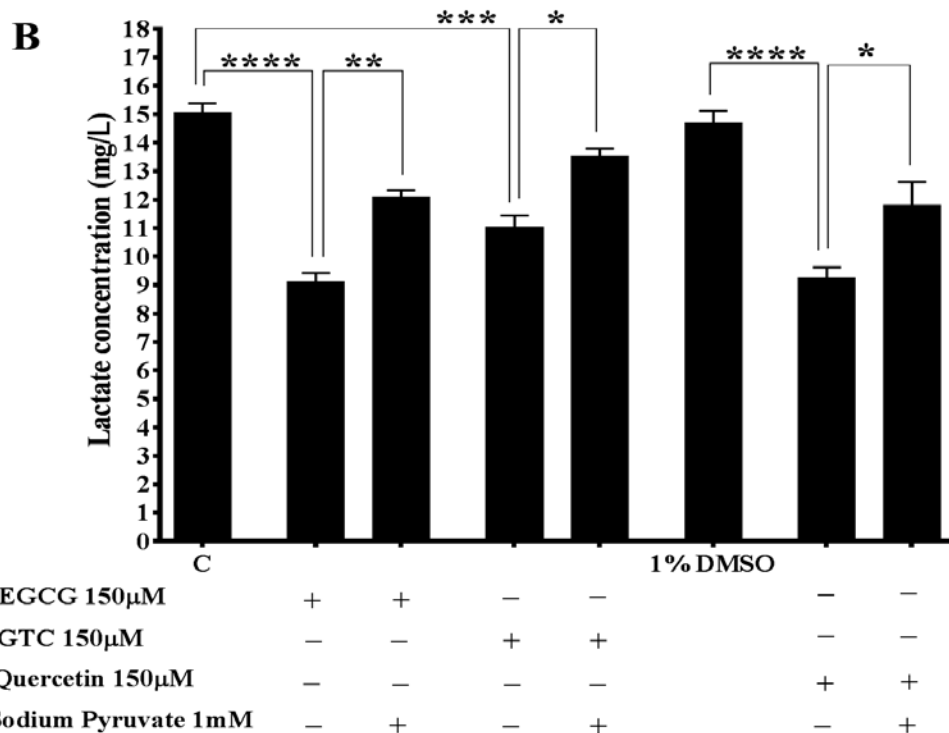
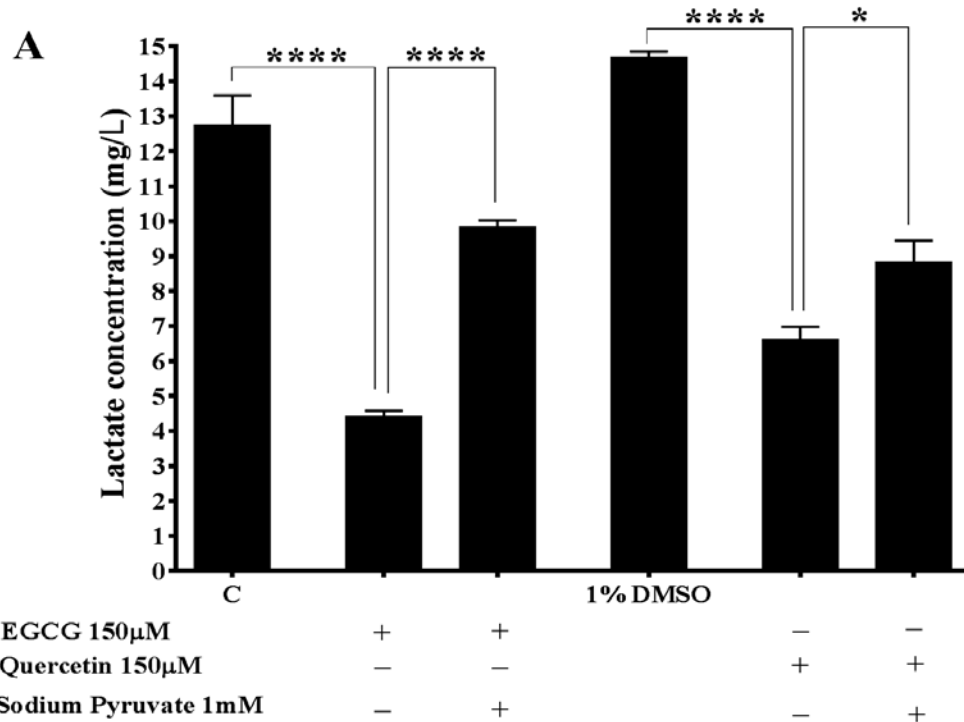


**Figure 5.24 Sodium pyruvate suppresses green tea reduced BC cell lactate release after 24h intervention.**

BC cells were seeded into 24 well plate at density of  $3 \times 10^4$ , and incubated in standard condition for 24h. Cells were then exposed to selected green tea compounds in presence and absence 1mM sodium pyruvate for 24h. Culture media were collected, deproteinised, and the level of lactate was measured using fluorimetric L-Lactate assay. (A) Supplementation of sodium pyruvate significantly increased MCF7 cells lactate production compared to green tea compounds. (B) Supplementation of sodium pyruvate significantly increased MDA-MB-231 cells lactate production compared to green tea compounds. Data presented mean  $\pm$  SEM, \* $p < 0.05$ , \*\* $p < 0.01$ , \*\*\* $p < 0.001$ , and \*\*\*\* $p < 0.0001$ ,  $n = 3$ .

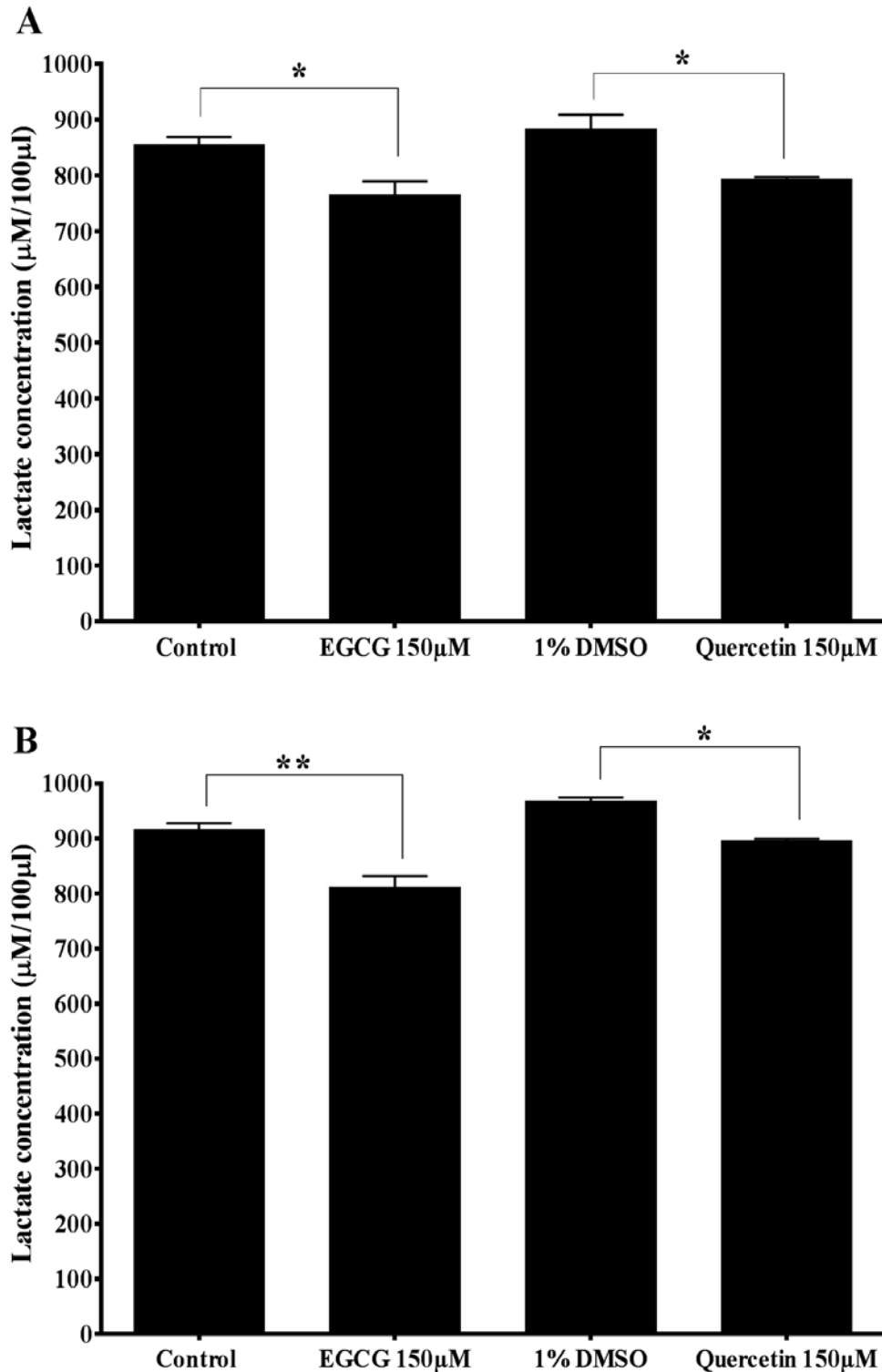


**Figure 5.25 Selected green tea compounds reduce BC cell lactate production after 6h intervention.**

The early effects of selected green tea compounds on BC cell glycolysis were investigated. Cells were seeded into 24 well plate at density of  $3 \times 10^4$ , and incubated in standard condition for 24h. Cells were then exposed to selected green tea compounds for 6h. Culture media were collected, deproteinized, and the level of lactate was measured using fluorimetric L-Lactate assay. (A) MCF7 cells showed a significant decrease of lactate level in response to EGCG and quercetin compared to control and DMSO (B) MDA-MB-231 cells showed significant reduce of lactate level in response to EGCG and quercetin compared to control and DMSO. Data presented mean  $\pm$  SEM, \* $p < 0.05$ , \*\* $p < 0.01$ ,  $n = 3$ .

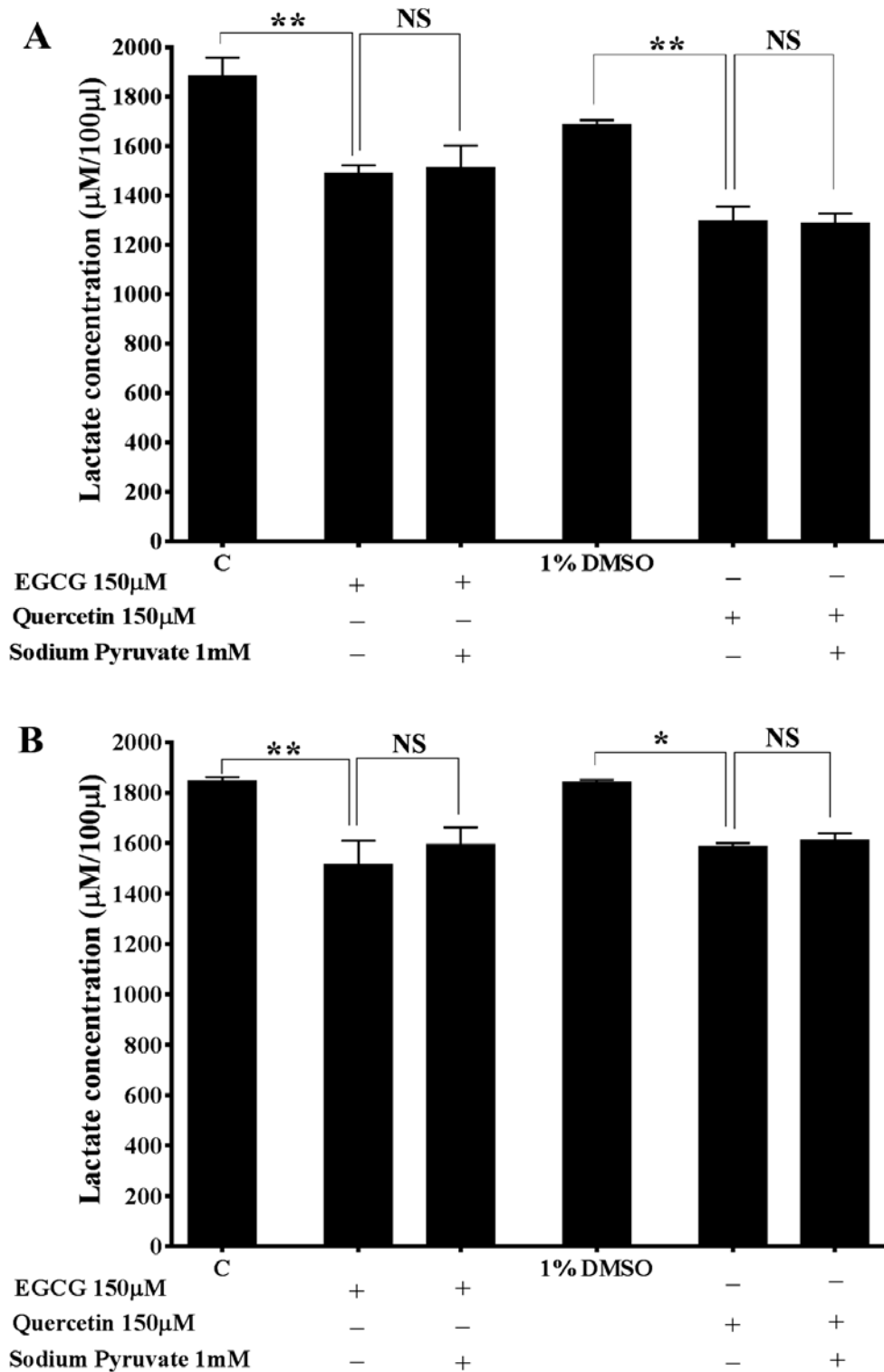


**Figure 5.26 Sodium pyruvate does not alter BC cell lactate release after 6h intervention.**

BC cells were seeded into 24 well plate at density of  $3 \times 10^4$ , and incubated in standard condition for 24h. Cells were then exposed to selected green tea compounds in presence and absence 1mM sodium pyruvate for 6h. Culture media were collected, deproteinised, and the level of lactate was measured using fluorimetric L-Lactate assay. (A) Supplementation of sodium pyruvate did not alter MCF7 cell lactate level compared to green tea compounds. (B) Supplementation of sodium pyruvate did not alter MDA-MB-231 cell lactate level compared to green tea compounds. Data presented mean  $\pm$  SEM, \* $p < 0.05$ , and \*\* $p < 0.01$ ,  $n = 3$ .

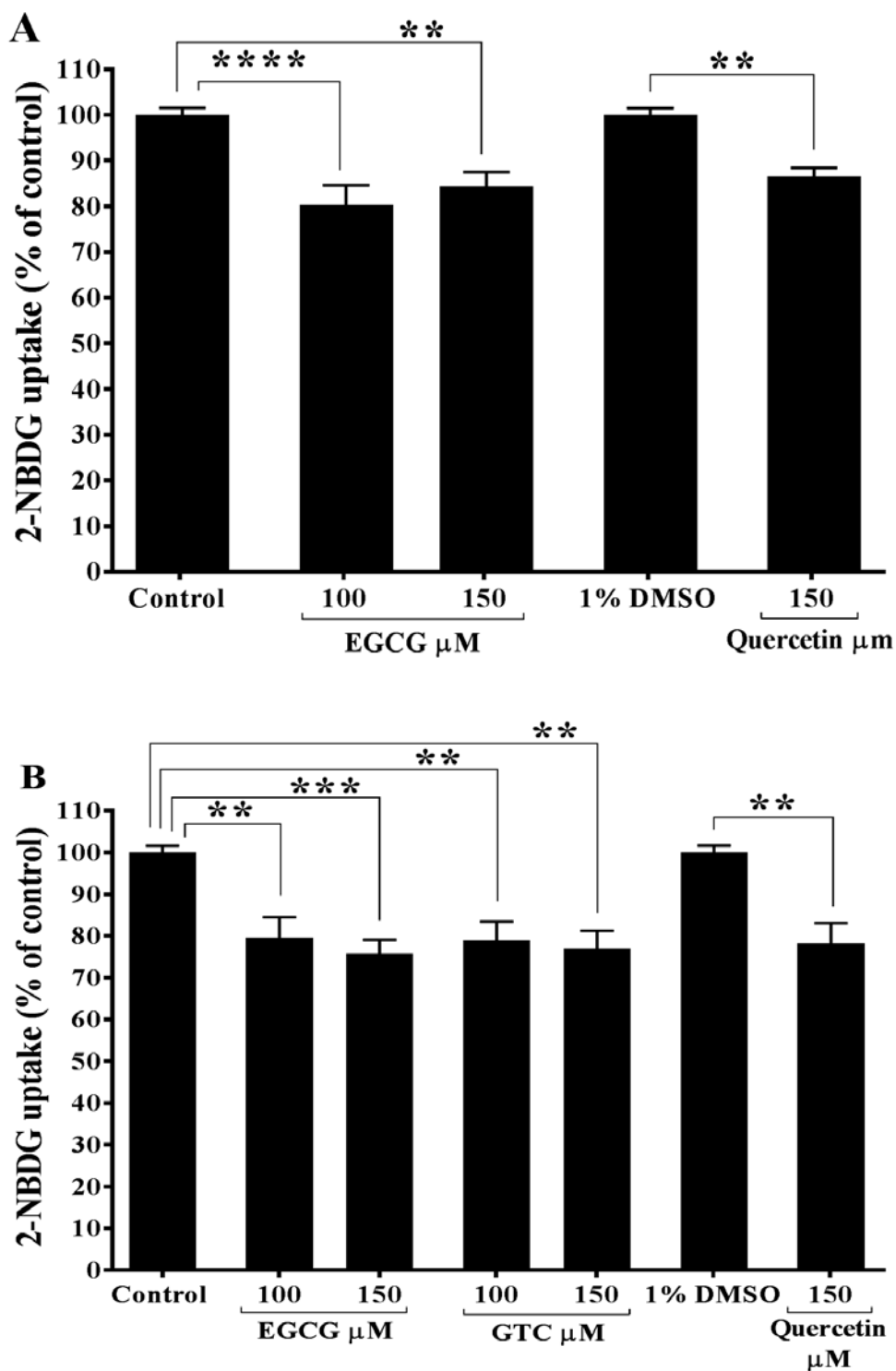


**Figure 5.27 Selected compounds of green tea reduce BC cell 2-NBDG uptake.**

BC cells were seeded into 96 well plate at density of  $10^4$ , and incubated in standard condition for 24h. Cells were then treated with selected green tea compounds in low glucose media containing  $100\mu$ M 2-NBDG for 4h, and amount of fluorescent 2-NBDG uptake was quantified. (A) MCF7 cells showed significantly decreased of 2-NBDG uptake in response to EGCG and quercetin compared to control. (B) MDA-MB-231 cells showed significant decreased of 2-NBDG uptake in response to EGCG, a combination of catechins, and quercetin compared to control. Data presented mean  $\pm$  SEM, \*\* $p$ <0.01, \*\*\* $p$ <0.001, and \*\*\*\* $p$ <0.0001,  $n=3$ .

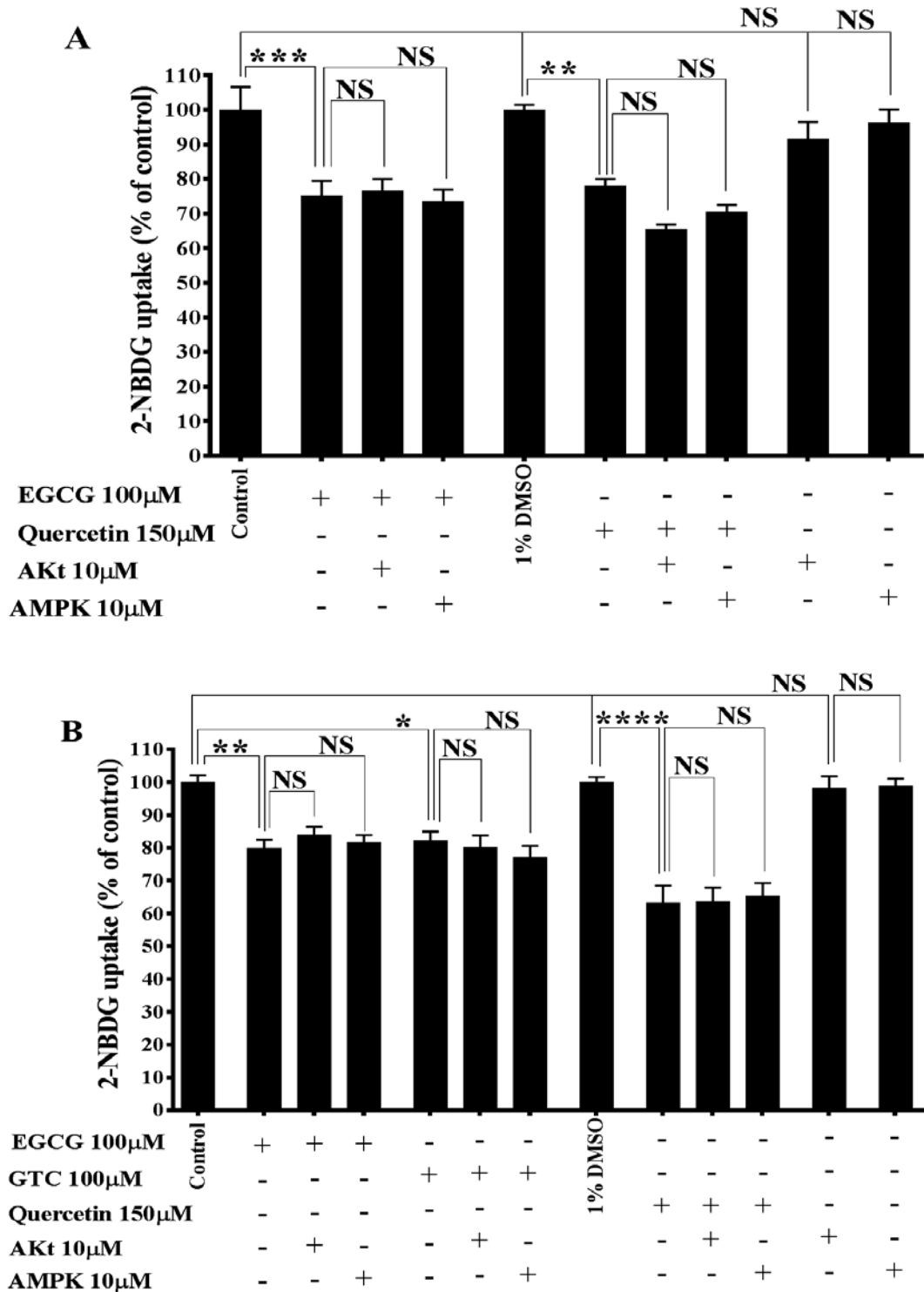


**Figure 5.28 Akt and AMPK inhibitors do not alter green tea reduced BC 2-NBDG uptake after 4h intervention.**

BC cells were seeded into 96 well plate at density of  $10^4$ , and incubated in standard condition for 24h. Cells were then treated with selected green tea compounds in low glucose media containing 100 $\mu$ M 2-NBDG for 4h in presence and absence 10 $\mu$ M of Akt or AMPK inhibitors, and amount of fluorescent 2-NBDG uptake was quantified. (A) Akt or AMPK inhibition did not alter MCF7 cell 2-NBDG uptake compared to green tea compounds. (B) Akt or AMPK inhibition did not alter MDA-MB-231 2-NBDG uptake compared to green tea compounds. Data presented mean  $\pm$  SEM, \* $p$ <0.05, \*\* $p$ <0.01, \*\*\* $p$ <0.001, and \*\*\*\* $p$ <0.0001,  $n$ =3.

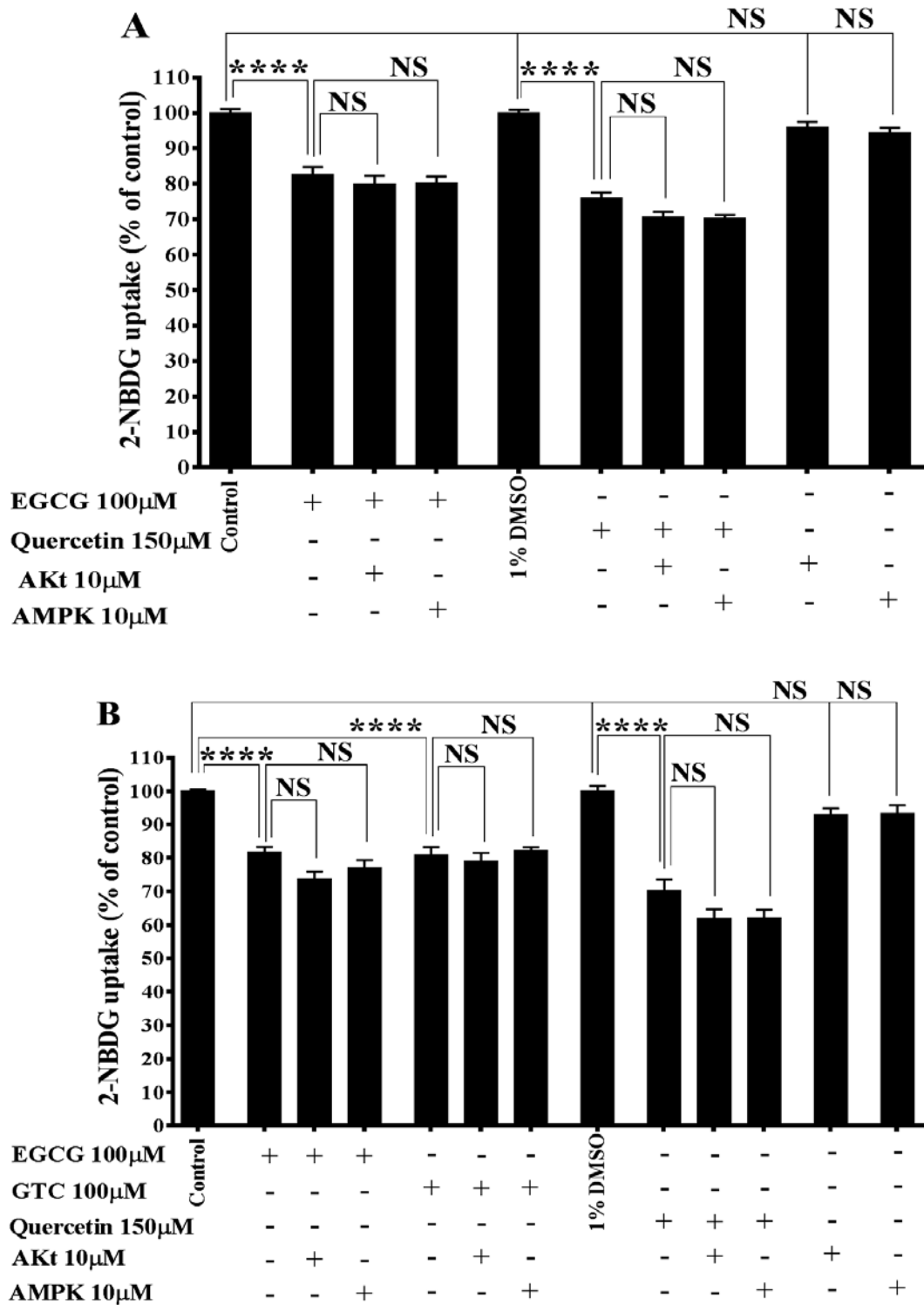


**Figure 5.29 Akt and AMPK inhibitors do not alter green tea reduced BC 2-NBDG uptake after 8h intervention.**

BC cells were seeded into 96 well plate at density of  $10^4$ , and incubated in standard condition for 24h. Cells were then treated with selected green tea compounds in low glucose media containing 100 $\mu$ M 2-NBDG for 8h in presence and absence 10 $\mu$ M of Akt or AMPK inhibitors, and amount of fluorescent 2-NBDG uptake was quantified. (A) Akt or AMPK inhibition did not alter MCF7 cell 2-NBDG uptake compared to green tea compounds. (B) Akt or AMPK inhibition did not alter MDA-MB-231 2-NBDG uptake compared to green tea compounds. Data presented mean  $\pm$  SEM, \*\*\*\*p<0.0001, n=3.

### 5.3.21 Selected compounds of green tea reduced MCF7 cellular migration

The effect of green tea compounds on the cellular migration of BC cell was explored by using two methods based on wound healing to close an artificial scratch. The wound healing assay (scratch) has been widely used to study cellular migration of various type of cancer and drugs screening *in vitro*. This assay is either using microscope for imaging (Arif, 2014;Liu, *et al.*, 2015) and/or live cell automated imaging (CellIQ™) (Arif, 2014;Isherwood, *et al.*, 2011). Artificial scratches were made and the cells treated with 50µM of EGCG and quercetin. Images were captured using (inverted microscope, Figure 5.30) and automated live imaging (CellIQ™, Figure 5.31) at time 0 and 24h. The data were collected, and cellular migration was calculated as a percentage of wound closure, as detailed in chapter two. The results of microscopic imaging of the wound healing assay showed that EGCG and quercetin significantly reduced MCF7 cellular migration after 24h (Figure 5.32 A). The percentage decreases in wound closure were: 46.71%±6.2% (p=0.0001) and 58.87%±13.32% (p=0.0003) compared to control. Similar results were recorded on the measurement of cellular migration in MCF7 cells using the automated cell live imaging system (CellIQ™). Cells exhibited significant decreases of wound closure after 24h treated with EGCG and quercetin compared to control (Figure 5.32 B). Reductions in migration of 28.33%±3.75% (p=0.0001) and 28.82%±6.25% (p=0.0003) respectively were recorded.

### 5.3.22 Selected compounds of green tea reduced MDA-MB-231 cellular migration

Similar to MCF7, the effect of selected compounds of green tea were examined on MDA-MB-231 cellular migration using a standard wound healing assay, and an automated cell lives imaging system (CellIQ™). The artificial scratch was made and the cells treated with 50µM of EGCG, GTC, and quercetin. Images were captured using an inverted microscope (Figure 5.33) and automated live imaging CellIQ™ (Figure 5.34) at time 0 and 24h. The collected data were analysed, and cellular migration was calculated as a percent of wound closure as mentioned in detail in chapter two. The microscopic imaging analysis results showed that EGCG and quercetin significantly decreased wound closure by 40.56%±13.63% (p=0.0076) and 55.70%±15.44% (p<0.0001) compared to control (Figure 5.35 A). The combination of catechins did not significantly alter wound closure (reduction of 29%±11.20%, p=0.1024) compared to control. Like the microscopic imaging result, the CellIQ™ analysed imaging showed that EGCG and quercetin caused significant decreases in the cellular migration of MDA-MB-231 by 34.37%±11% (p=0.0040) and 52.86%±8.61% (p=0.0003) respectively compared to control without significant effect of combination catechins (Figure 5.35 B).

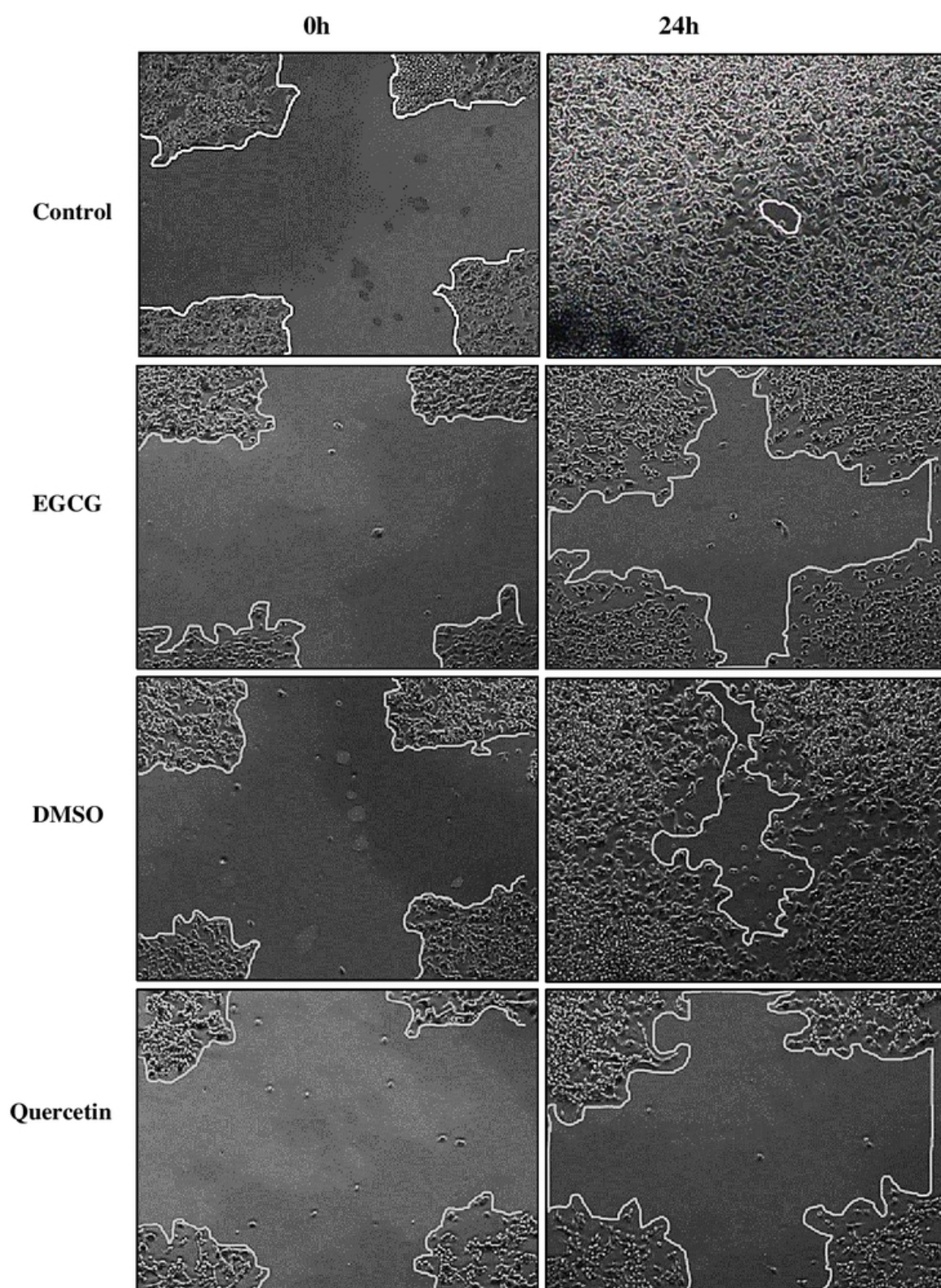


**Figure 5.30 Effect of selected green tea compounds on MCF7 cell migration (microscope images).**

MCF7 cells were seeded into 24 well plate, and incubated in standard condition until completely confluency. Cells were then exposed to  $5\mu\text{g}$  of mitomycin C in serum free media for 2h to inhibit cellular proliferation. Cross artificial scratch was made, and the cells were then washed with HBSS and treated with  $50\mu\text{M}$  of EGCG and quercetin for 24h. Images at day 0 and 24h were captured by using Leica DMI4000 B inversion microscope at 100x magnification and analysed using TScratch software (CSE Lab, ETH, Zurich), the images are representative sample of  $n=3$  shown.

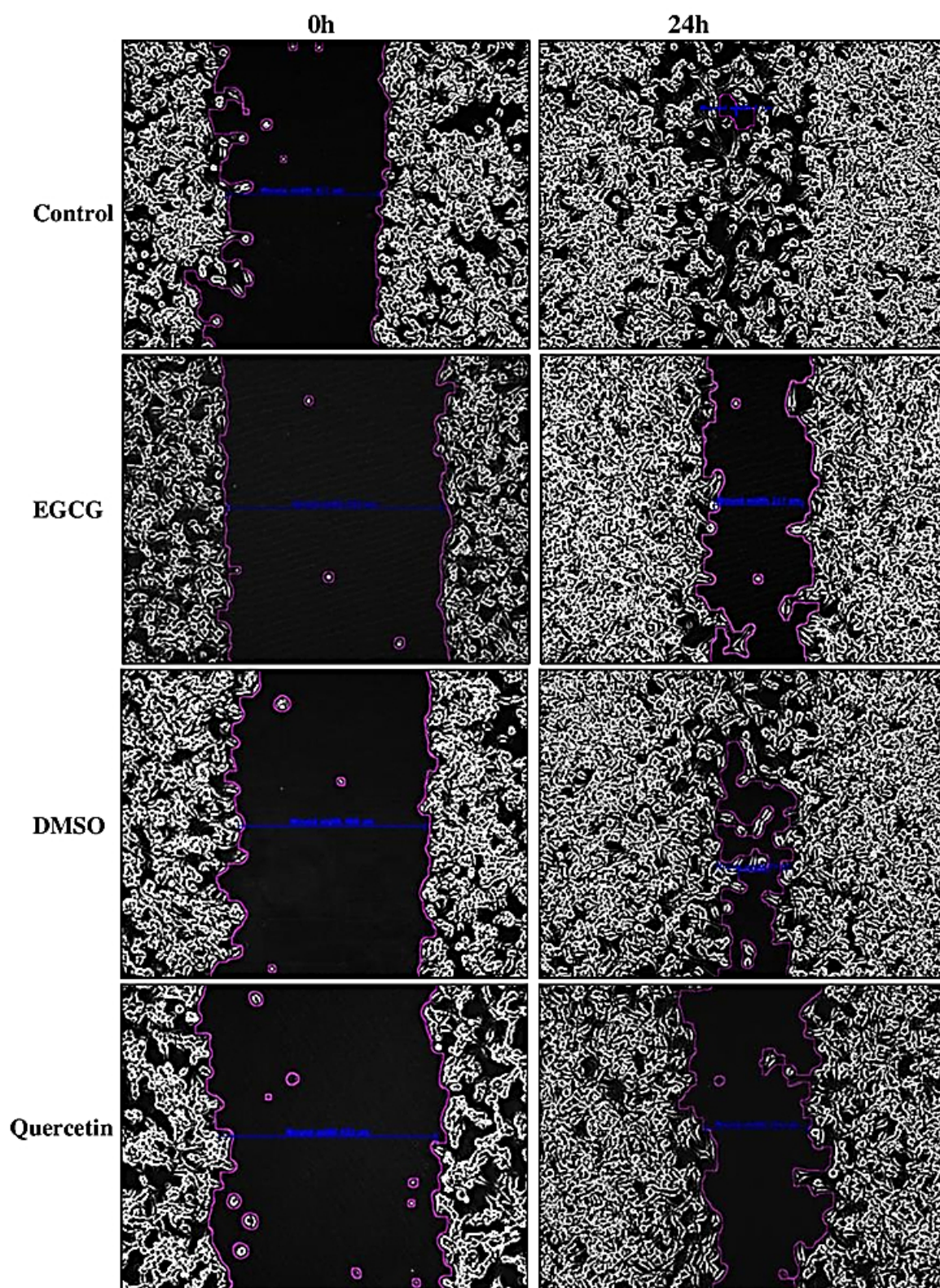


**Figure 5.31** Effect of selected green tea compounds on MCF7 cell migration (CellIQ®) images.

MCF7 cells were seeded into 24 well plate, and incubated in standard condition until completely confluency. Cells were then exposed to 5 $\mu$ g of mitomycin C in serum free media for 2h to inhibit cellular proliferation. Longitudinal artificial scratch was made, and the cells were then washed with HBSS and treated with 50 $\mu$ M of EGCG and quercetin for 24h. Two interested area of each well were chosen, and images at day 0 and 24h were captured by automated live cell imaging system (CellIQ®) and analysed using CellIQ® software, the images are representative sample of n=3 shown.

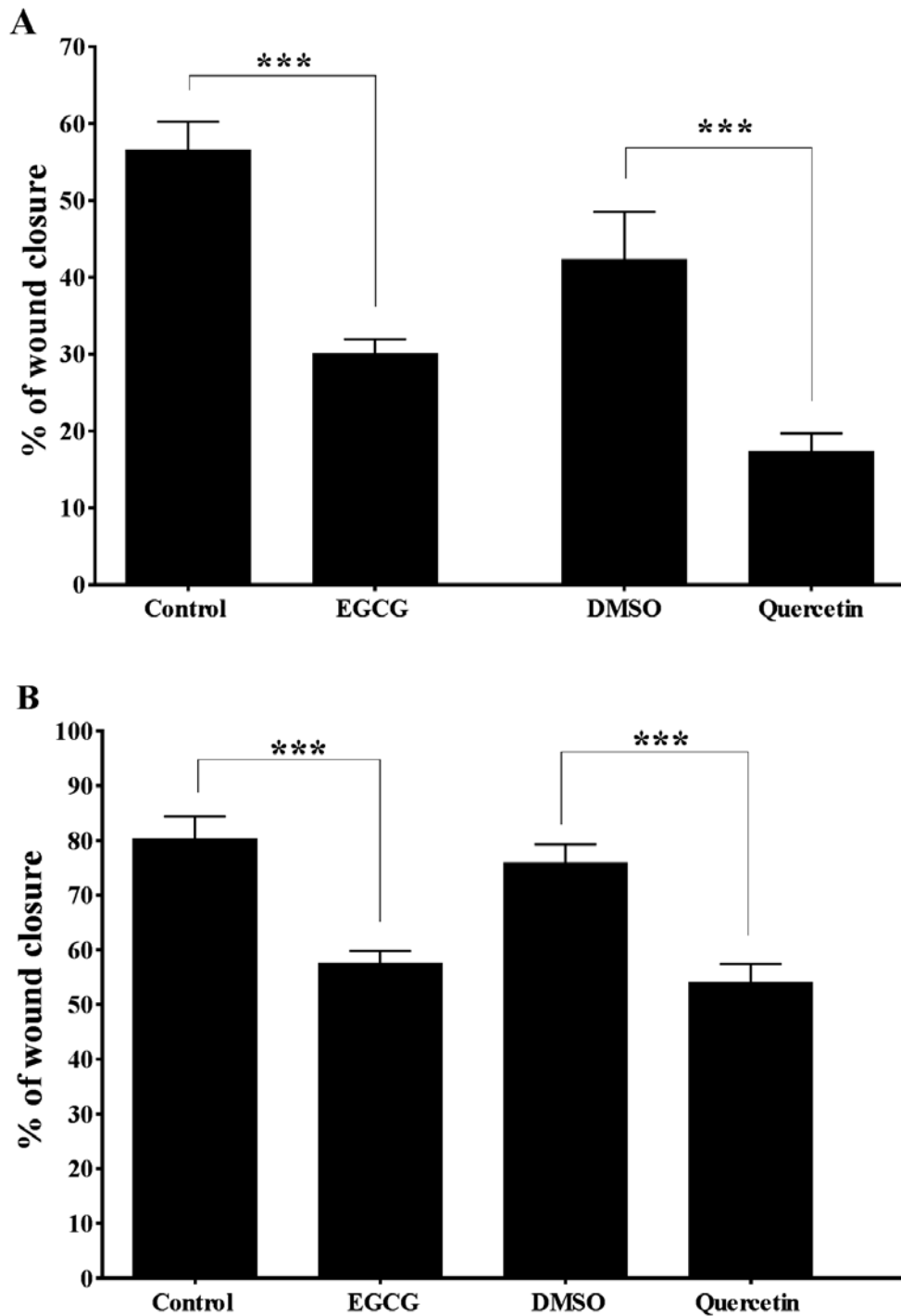


**Figure 5.32 Selected compounds of green tea reduce MCF7 cell migration.**

MCF7 cells were seeded into 24 well plate, and incubated in standard condition until completely confluency. Cells were then exposed to 5 $\mu$ g of mitomycin C in serum free media for 2h to inhibit cellular proliferation. Artificial scratch was made, and the cells were then washed with HBSS and treated with 50 $\mu$ M of EGCG and quercetin for 24h. Cellular migration was monitored, and calculated as a % of wound closure. (A) Microscope images wound healing analysis of MCF7 cells. (B) CellIQ<sup>®</sup> images wound healing analysis of MCF7 cells. Both results showed significantly decreased of wound closure in response to EGCG and quercetin after 24h compared to control. Microscopic data analysed using TScratch software (CSE Lab, ETH, Zurich) and CellIQ<sup>®</sup> data analysed using CellIQ<sup>®</sup> software. Data presented mean  $\pm$  SEM, \*\*\*p<0.001, n=3.

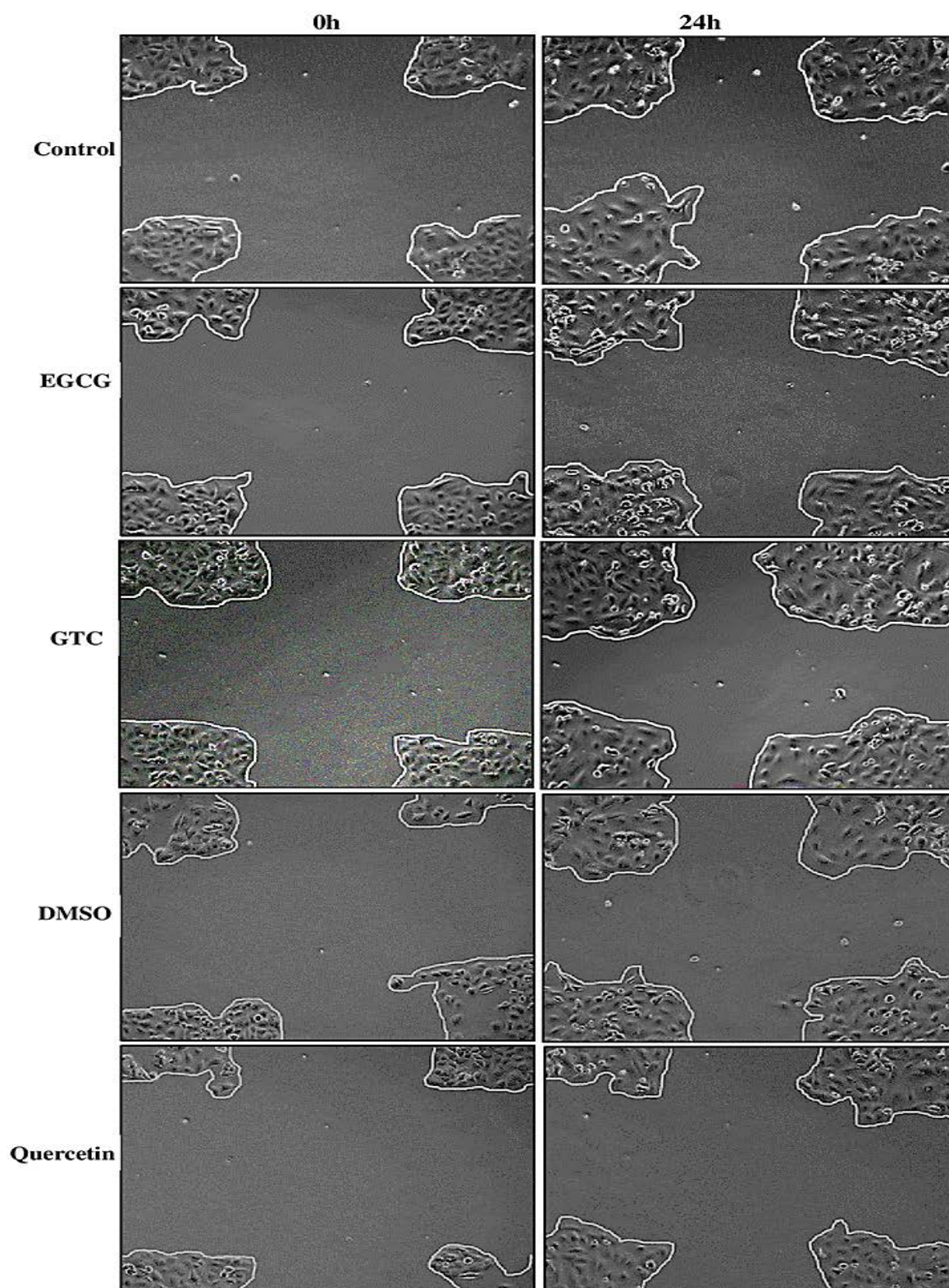


**Figure 5.33** Effect of selected green tea compounds on MDA-MB-231 cell migration (microscope images).

MDA-MB-231 cells were seeded into 24 well plate, and incubated in standard condition until completely confluency. Cells were then exposed to 5 $\mu$ g of mitomycin C in serum free media for 2h to inhibit cellular proliferation. Cross artificial scratch was made, and the cells were then washed with HBSS and treated with 50 $\mu$ M of EGCG, GTC, and quercetin for 24h. Images at day 0 and 24h were captured by using Leica DMI4000 B inversion microscope at 100x magnification and analysed using TScratch software (CSE Lab, ETH, Zurich), the images are representative sample of n=3 shown.

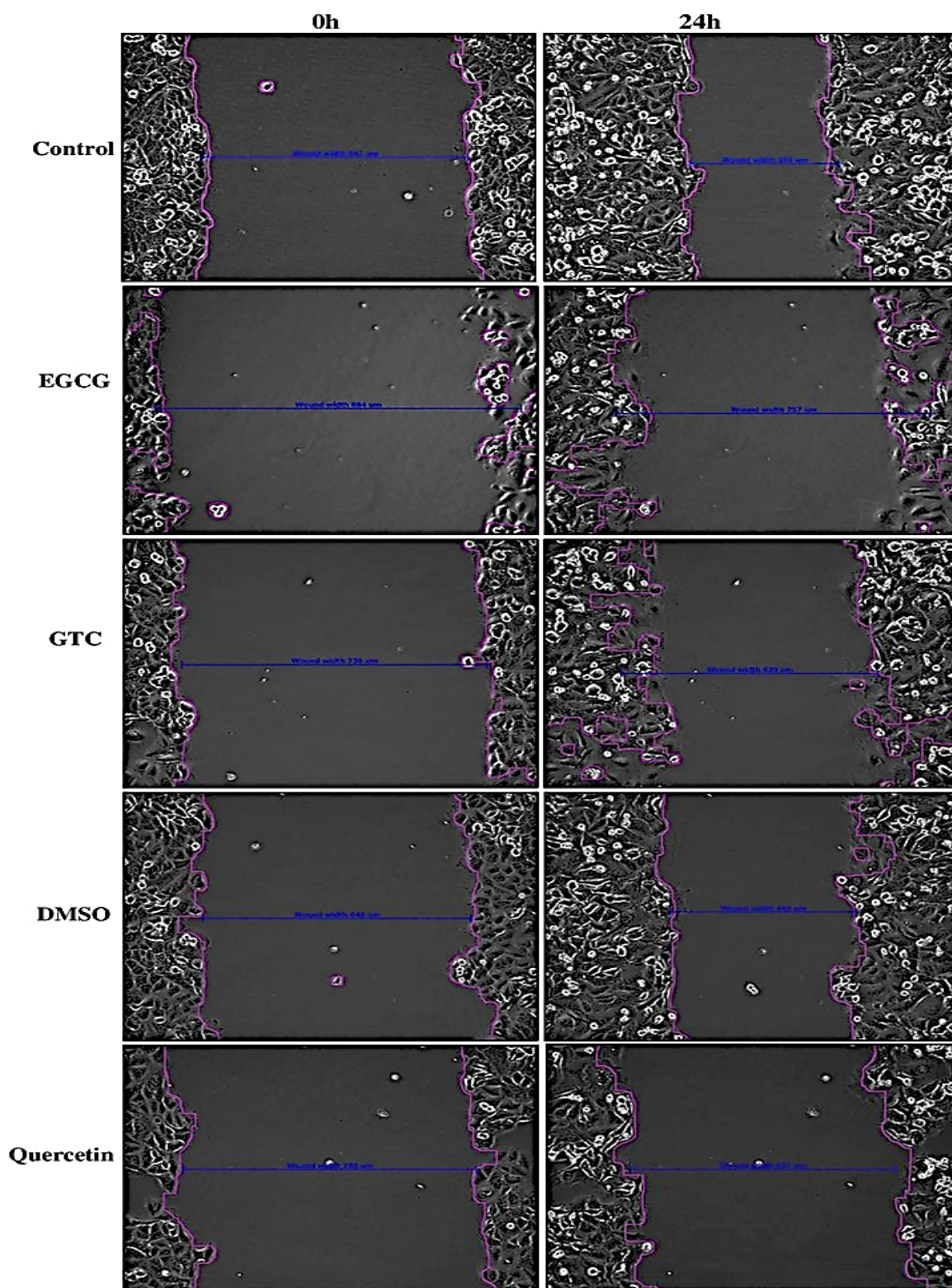


**Figure 5.34** Effect of selected green tea compounds on MDA-MB-231 cell migration (CellIQ®) images.

MDA-MB-231 cells were seeded into 24 well plate, and incubated in standard condition until completely confluency. Cells were then exposed to 5 $\mu$ g of mitomycin C in serum free media for 2h to inhibit cellular proliferation. Longitudinal artificial scratch was made, and the cells were then washed with HBSS and treated with 50 $\mu$ M of EGCG and quercetin for 24h. Two interested area of each well were chosen, and images at day 0 and 24h were captured by automated live cell imaging system (CellIQ®) and analysed using CellIQ® software, the images are representative sample of n=3 shown.

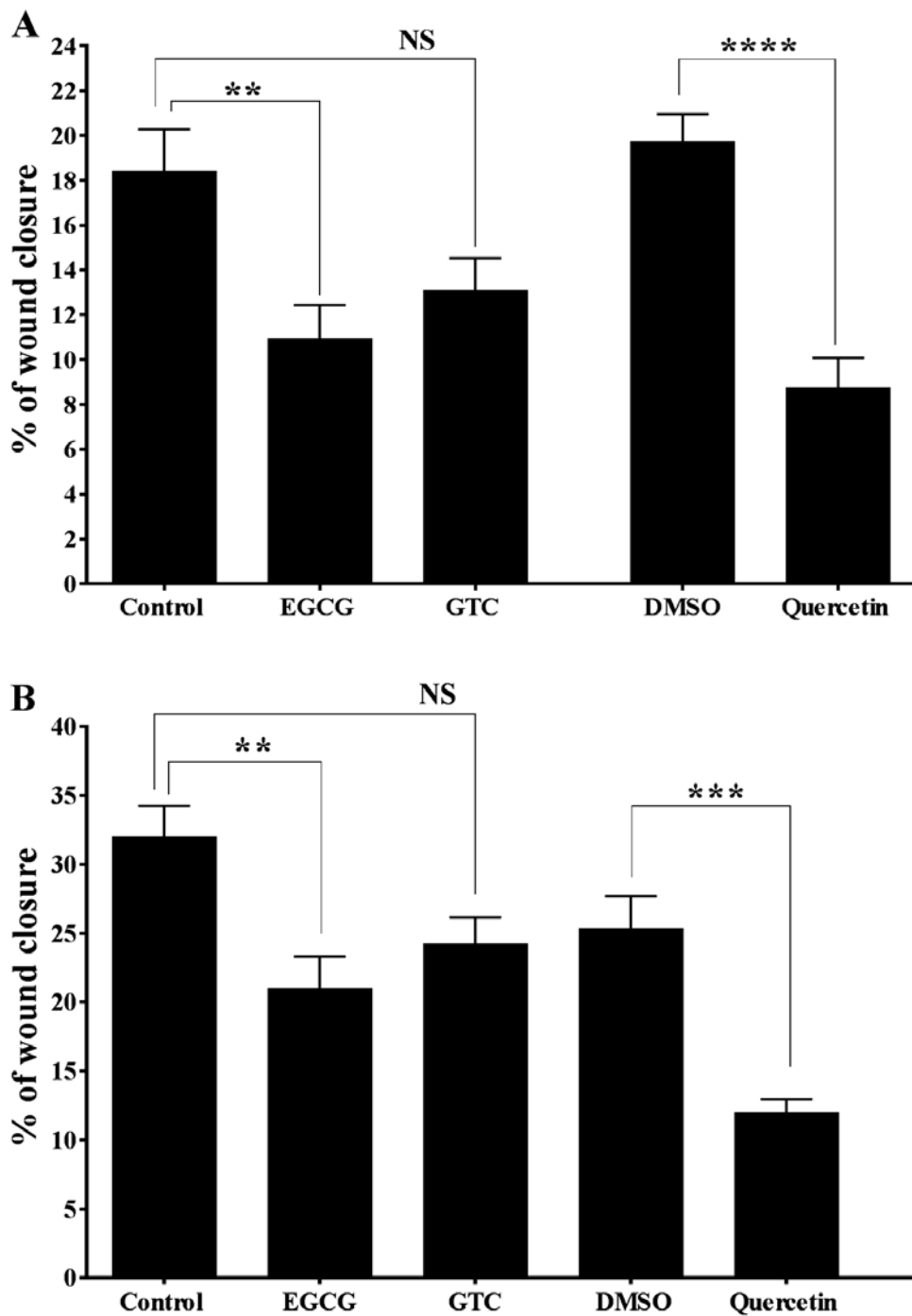


**Figure 5.35 Selected compounds of green tea reduce MDA-MB-231 cell migration.**

MDA-MB-231 cells were seeded into 24 well plate, and incubated in standard condition until completely confluency. Cells were then exposed to 5 $\mu$ g of mitomycin C in serum free media for 2h to inhibit cellular proliferation. Artificial scratch was made, and the cells were then washed with HBSS and treated with 50 $\mu$ M of EGCG, GTC, and quercetin for 24h. Cellular migration was monitored, and calculated as a % of wound closure. (A) Microscope images wound healing analysis of MDA-MB-231 cells. (B) CellIQ<sup>®</sup> images wound healing analysis of MDA-MB-231 cells. Both results showed significant decreased of wound closure in response to EGCG and quercetin but not GTC after 24h compared to control. Microscopic data analysed using TScratch software (CSE Lab, ETH, Zurich) and CellIQ<sup>®</sup> data analysed using CellIQ<sup>®</sup> software. Data presented mean  $\pm$  SEM, \*\*p<0.01, \*\*\*p<0.001, and \*\*\*\*p<0.0001, n=3.

## 5.4 Discussion

The broad aim of this chapter is to investigate the effect of several individual compounds of green tea at set time points, and concentrations on BC cell biology. Initially, experiments determined the ability of these compounds to promote cytotoxic effects to reduce cell viability and induce apoptosis. Secondly, as metastasis is the major factor that is responsible for increasing mortality, the effect of these compounds on BC cellular migration was also explored to reduce the risk of death due to metastasis. Linking all these together with abnormal glucose metabolism in BC cells, a key purpose of this chapter is to investigate the role of green tea compounds on BC glucose metabolism. As a result of considering this approach, targeting BC glucose metabolism by natural compounds is the main purpose of the research described in this chapter.

The effect of several compounds and concentrations of green tea on BC cell viability and activity of caspase 3/7 (apoptosis) was investigated. The results showed that EGCG, a combination of catechins, and quercetin significantly decreased cell viability in MCF7 (Figure 5.1 to Figure 5.6), and in MDA-MB-231 (Figure 5.7 to Figure 5.12). The present study focussed on the role of glucose metabolism in BC biology in response to green tea, the data presented here shows that some green tea compounds decrease cell viability in BC cells; as would be expected from previously published findings. Green tea catechins caused cell cycle arrest and significantly decreased cell viability in different cell lines (Chen, *et al.*, 2014; Geetha and Santhy, 2013; Liang, *et al.*, 1999; Thangapazham, *et al.*, 2007; Wang, *et al.*, 2010b). In line with a wealth of previously published data, this gives a clear indication that the compounds found in green tea exhibit potent cytotoxic effect on BC. This result is substantiated by clinical studies that have shown consumption of green tea can reduce cancer risk or improve prognosis (Wu and Butler, 2011). Therefore, the potential development of new chemotherapeutic agents from green tea exists and needs further exploration.

Additionally, the present study measured apoptosis in MCF7 and MDA-MB-231 cells exposed to selected green tea compounds. As a reduction of BC cell viability by selected compounds of green tea, these compounds could stimulate cancer cells to undergo apoptosis as measured by caspase 3/7 activation. The result showed increased caspase 3/7 activity by EGCG and quercetin in MCF7 cells, whilst increases in caspase 3/7 activity was observed in MDA-MB-231 in response to EGCG, GTC, and quercetin (Figure 5.22). This activation of caspase 3/7 was associated with alteration of some pro-apoptotic and anti-apoptotic gene expression in both cell lines in response to these compounds. Among all genes explored MCF7 cells exhibited increased Bax expression responding to EGCG only (Table 5.1), and quercetin upregulated Bcl2 and P53 expression in MDA-MB-231 cells, concomitant with increased expression of Bax by EGCG and quercetin (Table 5.2). The strategy of chemotherapeutic drugs is based on induction of apoptosis in cancer cells through two distinct pathways which are intrinsic (mitochondrial) and extrinsic (death receptor) (Debatin, 2004; Mukhtar, *et al.*, 2012). However, most

chemotherapeutic drugs have been used to promote their final effect through caspase activation (Debatin, 2004). Studies by Duo, *et al.* (2012) and Hsuuw and Chan (2007) showed that EGCG and quercetin induce apoptosis in MCF7 cells through activation of caspase 3/9 and with an increase in Bax/Bcl2 ratio. This effect was displayed in MDA-MB-468 cells exposed to EGCG (Roy, *et al.*, 2005). Interestingly, a study by Katunuma, *et al.* (2006) reported that green tea and its catechins compound suppressed apoptosis in Hela cells through downregulation of caspase 2/3/7 activity; although this study seems to be almost unique in suggesting this effect. MCF7 cells lack caspase 3 (Jänicke, *et al.*, 1998). Thus apoptotic results of the present study in MCF7 cells responding to green tea compounds refers to caspase 7 activation (Liang, *et al.*, 2001) and an increase in Bax expression. The data from the present study indicates that the decreases in cell viability seen are likely due to increase cellular apoptosis and this fits with previously published findings. However, few studies have investigated the effect of green tea polyphenol, EGCG, and quercetin on cell viability and apoptosis in BC and most studies have used MCF7, with studies in MDA-MB-231 and MDA-MB-468 being even scarcer. These studies have looked at Bax/Bcl2 ratio as an indicator for apoptosis after 48h focusing on low concentrations of treatments. The current study used MCF7 and MDA-MB-231 cells, which exhibited a significant decrease in cell viability in response to high concentrations of EGCG, quercetin, and a combination of catechins just after 24h. These compounds also induced apoptosis just after 24h, mostly through caspase 3/7 activity, in conjugation with upregulated Bax by EGCG only. Therefore, from these results, the present study suggests that these compounds could promote their effect in a complex way and further investigation of this complexity is required. More detailed investigation of the mechanisms is warranted, including protein-based (e.g. Western blotting) analysis of markers of apoptosis.

While there exists evidence of the anti-cancerous effects of green tea, few studies have focussed on the role of glucose metabolism in this process. As the cancer cell exhibits alteration of glucose metabolism, targeting this aspect could provide spectacular therapeutic promise (Chaneton, 2014). Therefore, the present study assessed metabolic markers including glucose uptake and lactate release, and the role of Akt and AMPK in glucose uptake in MCF7 and MDA-MB-231 cells, in response to effective compounds of green tea. The results show selected green tea compounds significantly reduced lactate production in both cell lines after 24h treatment (Figure 5.23), suggesting that they are successfully interfering with glucose metabolism. The addition of sodium pyruvate restored lactate release compared to cells treated with green tea compounds only (Figure 5.24), which suggests this process can be manipulated by adding lactate precursor. As 24h treatment of green tea compounds caused a significant fall in cell viability previously, these decreases in lactate could be due to decreased cell viability. To further clarify this, analysis after 6h was performed. Selected green tea compounds significantly decreased MCF7 and MDA-MB-231 cell lactate production after just 6h of treatment (Figure 5.25), suggesting a rapid decline in glycolysis. This result was not associated with any reduction in cell viability (Figure 5.13), and any effect of supplementing sodium pyruvate (Figure 5.26), which

suggests that this change is not due to cell death. Overall, this result suggests that EGCG, quercetin, and combination of catechins modulate BC glycolysis which finally reduced lactate production. Several natural occurring compounds have been shown to have chemopreventive effects through targeting metabolic events of cancer cells (Dihal, *et al.*, 2008;Jung, *et al.*, 2013). However, few studies have identified the metabolic effect of green tea compounds as anti-cancer therapy. Thus more quantitative and qualitative research is required to elucidate the exact metabolic role of green tea compounds on cancer cells (Lu, *et al.*, 2015;Zhang, *et al.*, 2011). Limited studies have explored the metabolic effect of green tea on BC. Those that have reported inhibition lactate production in response to EGCG and quercetin after 4h (Moreira, *et al.*, 2013) and 24h (Xintaropoulou, *et al.*, 2015). These studies were associated with significant reductions in cell viability which can reduce lactate production. The present study showed that these compounds reduced lactate production in BC cells after 6h without a reduction in cell viability. Interestingly, after 24h treatment, in addition to these compounds, GTC also decreased lactate production in MDA-MB-231 cells. However, this was associated with a decrease in cell viability. As these results are exclusively due to selected compounds of green tea, exploring the effect of more compounds individually and together is required for short and long term incubation to investigate all markers related to glucose metabolism and apoptosis.

The reduction in lactate production could either be due to reduced glucose metabolism or reduced glucose uptake into the cells. The results presented here suggest that green tea compounds significantly suppress glucose uptake in both cell lines (Figure 5.27) and therefore this would appear to be the likely mechanism by which glycolysis is being reduced. By inhibiting the availability of glucose to the cell through blocking its uptake, glycolysis is reduced and therefore the cell has less ATP available to it. This hypothesis is supported by the data presented here; that showed supplementing green tea compounds with pyruvate could block some of the reduction in cell death previously induced by the green tea compounds alone. Further research is needed to elucidate the mechanism of reduced glucose uptake under these conditions. However, it is likely that the active ingredients in green tea may be suppressing expression or trafficking of Gluts, as has been previously reported (Lu, *et al.*, 2015;Moreira, *et al.*, 2013;Xintaropoulou, *et al.*, 2015). As expected, EGCG and quercetin significantly prevent MCF7 and MDA-MB-231 cells uptake of glucose, however this suppression in glucose uptake was induced just after 4h incubation, and for the first time combination of catechins (GTC) induced inhibition of MDA-MB-231 glucose uptake. Four hours is considered an early time point, however reducing the time of incubation and looking for glucose uptake, and expression of markers of glucose trafficking and metabolism would be an excellent study to clarify the relationship between green tea compounds and glucose uptake and metabolism in BC cells. Collectively, these data suggest that green tea contains compounds that can effectively target glucose metabolism in BC cells by direct targeting cellular glucose uptake and glycolytic activity.

PI3K/Akt is a critical pathway to regulate cellular proliferation, differentiation, growth, survival, and metabolism (Fresno Vara, *et al.*, 2004). Accumulating evidence shows that this pathway is involved in the initiation of many pathological conditions including cancer. Accordingly, cancer cells have exhibited the high activity of PI3K/Akt to maintain cellular proliferation and survival (Cantley, 2002; Crowell, *et al.*, 2007; Hidalgo and Rowinsky, 2000; Itoh, *et al.*, 2002). The present study investigated this role of Akt in green tea active compound mediated changes in cell viability and apoptosis in BC cells through inhibition Akt, and measurement of phosphorylation levels of Akt, in response to green tea compounds. The results showed that inhibition of Akt caused significant further decreases of MCF7 and MDA-MB-231 cell viability (Figure 5.14 and Figure 5.17). Furthermore, due to limited phosphor-specific Western blotting performed in the present study, it is difficult to suggest the activation of Akt (Figure 5.20 and Figure 5.21). As both time and resources prohibited repeats these experiments, sufficient time to be able to perform statistical analyses to draw any solid conclusions is difficult. Recently, the anti-cancer effect of green tea polyphenol and/or EGCG has been shown to be mediated through inhibition of PI3K/Akt pathway in human bladder cancer cells (Qin, *et al.*, 2012). Furthermore, in ovarian cancer cells (Spinella, *et al.*, 2006), prostate cancer cells (Siddiqui, *et al.*, 2004), and HeLa and HepG2 cells (Zhang, *et al.*, 2006). Therefore, this study presented, for the first time, data regarding inhibition of Akt alongside selected compounds of green tea that caused more decreases in cell viability in BC cells. However repeated experiments related to pAkt expression are required. Based on previously published data and the results of the present study, it is reasonable to suggest that EGCG and quercetin may interact with the PI3K/Akt pathways to exert their cytotoxic effect in BC cells. This result is the first data presented in BC which suggests targeting PI3K/Akt signalling pathway in cancer conditions by natural compounds like green tea may provide a therapeutic solution for different types of tumour.

AMPK is a conservative energy sensor that has a critical role in the regulation of cellular energy homeostasis, and believed to be involved in many diseases, including tumour progression (Hardie, 2013). As such, activation of AMPK can switch anabolic processes to catabolic, which inhibits cellular proliferation and cell cycle progression, and induces apoptosis of cancer cells (Andrade and de Carvalho, 2014; Kim and He, 2013; Li, *et al.*, 2014). Therefore, neoplastic cells express a low AMPK expression (El-Masry, *et al.*, 2012; Hadad, *et al.*, 2008; Huang, *et al.*, 2008; Kuhajda, 2008). The present study investigated the role of AMPK in reduced BC cell viability by selected compounds of green tea. The study showed that inhibiting AMPK had an additive effect to the cytotoxic effects of green tea compounds in MCF7 and MDA-MB-231 cells (Figure 5.15 and Figure 5.18). The limited Western blotting analysis seemed to suggest that more independent experiments are required, as the experiment was only run twice, and therefore, it is not possible to draw a solid conclusion from these observations. (Figure 5.20 and Figure 5.21). Green tea compounds have shown anti-cancer effects through activation of the AMPK pathway in MDA-MB-231 cells (Chen, *et al.*, 2012), HT-29 cells (Hwang, *et al.*, 2007; Kim, *et al.*, 2010), and HeLa cells (Jung, *et al.*, 2010). As the main role of AMPK is maintaining

ATP levels required for cellular growth, proliferation and survival of cancer cells. This role casts doubt on previous studies that reported anti-cancer effect of green tea compounds through activation of AMPK (Bonini and Gantner, 2013;Chhipa, *et al.*, 2010;Frigo, *et al.*, 2011;Jang, *et al.*, 2011;Jeon and Hay, 2012;Park, *et al.*, 2009). Due to the role of AMPK, the cancer cells therefore expressed activation level of AMPK (Laderoute, *et al.*, 2014). The data presented here is unique in that it shows inhibition of AMPK alongside green tea compounds caused further reduction in BC cell viability, which suggests these compounds of green tea inhibit the activity of AMPK. However, this activity was not confirmed by Western blotting as it was conducted on two occasions only. This was not statistically reasonable, repetition of pAMPK expression in response to green tea compounds is therefore required.

The migration of cancer cell from the original site to the various organs occurs through a multi-step process initiated by local invasion, angiogenesis, systemic invasion, and colonisation of target organs (Fidler, 2003;Friedl and Alexander, 2011;Gupta and Massague, 2006;Kozlowski, *et al.*, 2015). The present study investigated the anti-migration effect of EGCG, quercetin, and the combination of catechins on MCF7 and MDA-MB-231 cells using microscopic and an automated imaging system (CellIQ®). The results showed EGCG and quercetin significantly delayed wound closure in BC cells (Figure 5.32 and Figure 5.35). Green tea compounds have been identified as anti-migratory compounds in oral cancer cells (Lai, *et al.*, 2013), colorectal cancer cells (Maruyama, *et al.*, 2014), prostate and cervical cancer cells (Senthilkumar, *et al.*, 2011;Sharma, *et al.*, 2012), lung cancer cells (Takahashi, *et al.*, 2014), and BC cells (Bigelow and Cardelli, 2006;Ho, *et al.*, 2013;Tao, *et al.*, 2015). Exploring the effect of green tea compounds on the cellular migration of BC cell in this study is essential, as BC cell invasion and migration are often responsible for the high female mortality rate. The result of this study is consistent with previously published results. However, the data presented here is more reliable; firstly two methods were used and secondly the interference of cellular proliferation was inhibited to prevent erroneous result. Therefore, these results suggest that alongside the antiproliferative and proapoptotic effects of green tea compounds there exists a potential anti-migratory property mediated by an inhibitory effect on cell migration. However, signalling pathways of this effect in BC need to be elucidated.

To conclude, some compounds of green tea, particularly EGCG, GTC, and quercetin show promising chemotherapeutic effects against two different BC cell lines. These compounds decreased cell viability and induced apoptosis, whilst also regulating cell migration. The cytotoxic effect of these green tea compounds could mediated through inhibition PI3K and interestingly AMPK which is unlike any other previous published findings. Furthermore, these effects of selected green tea compounds are likely mediated by the impact of these compounds on cellular glucose metabolism that includes decreased glucose uptake, and therefore, modulation of glycolysis due to glucose shortage. Thus, these compounds of green tea could be a therapeutic agent for various types of cancer including BC, but further work is needed to clarify the precise mechanisms involved.

# **Chapter Six**

## **Discussion, conclusion, and future studies**

## 6.1 Discussion

The research questions upon which this project was based encompassed the concept that green tea, and therefore its constituent phytochemicals, may be able to regulate how the body handles glucose at a cellular level. Glucose homeostasis is normally tightly regulated by hormones such as insulin and glucagon, but as modern lifestyles increasingly promote dysregulation of glucose homeostasis, identifying factors that can restore or protect this loss of function is important. Globally, consumption of green tea is increasing as new geographical areas become aware of its potential benefits. These advantages are often suggested to include eliminating a wide variety of diseases and disorders (Chacko, *et al.*, 2010), due to the numerous phenolic compounds contained therein, including catechins and more specifically to its most abundant active compound EGCG (Abdel-Rahman, *et al.*, 2011). There are some physiological and pathological states that glucose has a role in, but the present study focusses on metabolic cell and cancer cell glucose homeostasis. One of the potential beneficial properties of green tea is modulating impaired glucose homeostasis and therefore potentially pre-diabetes and T2D (Babu, *et al.*, 2013;Roghani and Baluchnejadmojarad, 2010). Another potential beneficial effect of green tea is promoting cytotoxic effects and, therefore, possible anti-cancerous actions (Adhami, *et al.*, 2003;Baliga, *et al.*, 2005). Therefore, the present thesis focused on the regulation of glucose homeostasis and metabolism in metabolic cells, mice fed a glucose-rich diet and BC cells. Furthermore, this thesis looked at the mechanism of how green tea compounds act to regulate glucose metabolism in various conditions encompassing three different cellular metabolisms.

Based on the initial aim of the present study, which included determination of glucoregulatory effect of several active compounds in green tea *in vitro*, the effect of green tea compounds to regulate glucose and lipid metabolism was investigated on insulin-sensitive cell lines including C2C12, 3T3-L1, and AML12 cells. The results showed that selected compounds of green tea potently and selectively regulate glucose uptake in these insulin-sensitive cell lines (Figure 3.3 to Figure 3.11, and Figure 3.24 to Figure 3.26). These results are in agreement with previously published work which showed green tea compounds increase glucose uptake in human hepatoma (HepG2) cells (Cordero-Herrera, *et al.*, 2014). In addition to, 3T3-L1 cells (Ueda, *et al.*, 2010;Yan, *et al.*, 2012), and C2C12 and L6 cells (Deng, *et al.*, 2012;Zhang, *et al.*, 2010). These studies reported that these effects were mediated through modulation of Glut2 and Glut4 translocation. Expression of Glut2 and Glut4 mRNA in this study were not affected by exposure to green tea compounds (Table 3.1, Table 3.2, and Table 3.3), and without measuring protein expression or translocation, the present data set is therefore partially inconsistent with previously published results. Thus, specific immunohistochemical and phosphor-western blotting of translocation and phosphorylation levels of Gluts are required in future studies. As the data presented here shows, specific green tea compounds increased glucose uptake differently in insulin-sensitive cell lines. Therefore, the study suggests that green tea compounds selectively promote their effects to regulate

levels of glucose according to cell type. Although a combination of experimental compounds induced effect in AML12 cells, whole green tea extract needs to be assessed in these cell lines by variation of concentration and incubation time.

As a part of exploring signalling pathways of the previously described effects of selected green tea compounds, Akt and AMPK regulators of glucose metabolism were separately inhibited alongside green tea compounds that increased glucose uptake. As selected green tea compounds increased glucose uptake, these increases were significantly suppressed by inhibiting of AMPK in C2C12 cells, and Akt in 3T3-L1 and AML12 cells (Figure 3.12 to Figure 3.23, and Figure 3.27 to Figure 3.29). Based on these results, phosphor-specific Western blotting was performed, but the results were limited as the independent experiment was only carried out on two occasions due to time and budget limitations (Figure 3.35 to Figure 3.37), and thus can only be qualitatively considered and firm conclusions cannot be made. This work, therefore, needs further independent experiments to be considered. In this regard, several studies reported different suggestions based on their final results, and have shown that the green tea compounds regulated glucose metabolism in insulin-sensitive cells by activation of AMPK pathway (Ding, *et al.*, 2012;Li, *et al.*, 2011b;Murase, *et al.*, 2009). Few studies, however, have reported glucoregulatory effect of green tea compounds in these cells through activation of PI3K/Akt pathway (Jung, *et al.*, 2008;Ueda, *et al.*, 2010). The results of these previous studies are based on increased expression of pAkt or pAMPK protein in response to green tea compounds. As above studies did not use AML12 cell and the present study built conclusions based on Akt or AMPK inhibition experiments only, the current study results are not completely in agreement with previous study results. Based on all findings together, the present data suggest that selected green tea compounds mediate their effect on insulin-sensitive cells through triggering different pathways in different cell types. With respect to whole green tea extract, which was not assessed in this study, specific research is needed to determine the role of this extract on regulation glucose homeostasis in these metabolic cells and the molecular mechanism of this role.

The levels of glycogen, glycogenic and gluconeogenic transcriptional factors Gys1, G6Pase and PEPCK were assessed in AML12 cell that previously showed significant glucose uptake in response to selected green tea compounds. Whilst some compounds at specific concentrations and incubation times increased glycogen content (Figure 3.30 and Figure 3.31), none of these selected green tea compounds altered glycogen synthase (Gys1) gene expression, and glucose production (G6Pase and PEPCK) gene (Table 3.3). These results are inconsistent with almost all published study results that identified EGCG and green tea extract can increase the level of glycogen and decreased hepatic glucose production through the activation of GS gene and suppressed activity of G6Pase and PEPCK gene and enzymes (Collins, *et al.*, 2007;Kim, *et al.*, 2013;Sundaram, *et al.*, 2013;Yasui, *et al.*, 2011). Although, the present study data showed the ability of quercetin and ECG to elevate the level of glycogen, which has not been

demonstrated before in AML12 cells, and both EGCG and green tea extract were not considered in these experiments. These unexpected results are possibly due to increase cellular glucose oxidation, which prevents glycogen synthesis, as the cells consume more glucose in response to green tea compounds, and some of this glucose undergoes oxidation which was not investigated in this study. Furthermore, this result might be due to insensitive of the kit used to measure glycogen, and therefore need to consider kit sensitivity in future study. Secondly, poor primer performance might be the reason behind the lack of changes in gene expression seen or methodological error and more independent experiments are required to clarify that. Whilst previous studies have looked at phosphorylation status of protein or enzyme activity in addition to gene expression. The present study measured the mRNA expression only, and a clear indication of the gene product levels or activity was not achievable. Investigating protein phosphorylation is a terrific tool that can show the amount of activation of a signalling molecule. This measurement would have benefited the present study, but due to a neumerous of compounds and cell lines, and multi-targeting of interesting protein, this was not done due to the prohibitive cost. Another reason that could be responsible for all unexpected presented data is using AML12 cell lines which have not used before, and this cell might be less responsive to regulated glucose metabolism than any other cell line like the HepG2 cell line, which was employed in previous studies.

As the adipose tissue plays a key role in glucose regulation and previously selected green tea compounds increased cellular glucose uptake in 3T3-L1 cells, estimation of the amount of triglyceride, the level of glycerol release, and expression level of lipogenesis and lipolysis gene were determined. Analysis showed that selected green tea compounds suppressed triglyceride synthesis and reduced levels of glycerol release (Figure 3.33 and Figure 3.34), without affected adipogenic and lipolytic gene expression (Table 3.2). Most of these results are consistent with previous study results that have shown green tea and EGCG suppresses lipid accumulation and inhibit 3T3-L1 cell differentiation (Hwang, *et al.*, 2005;Lao, *et al.*, 2015;Lee, *et al.*, 2009a). This effect occurs through downregulating C/EBP $\alpha$ , SREBP-1c and PPAR $\gamma$  transcription factors, and inhibit lipolysis by reducing glycerol release (Chan, 2009;Kim, 2014;Lao, *et al.*, 2015). However the data presented here shows in addition to EGCG, both EC and ECG significantly reduced triglyceride and glycerol levels. Nonetheless, previous studies built their results using only primary pre-adipocyte, whereas the present data was obtained using mature adipocytes as the lipid droplets had already formed. Since mature adipose tissue that contains triglyceride being anatomically and physiologically present in the human body, the present results are more relevant to the physiological function of adipose tissue as it exhibits various levels of lipogenesis and lipolysis. Therefore, the study suggests that selected green tea compounds mimicked the effects of insulin in adipocyte, although investigation of lipogenic and lipolytic genes expression did not provide any marked changes and therefore further research is required to clarify this. The latter result could be due to insufficient independent experiments, poor primer performance, incorrect time point selection or simply that the transcriptional levels of these genes are not altered, but rather that there are

translational/post-translational events. It would be particularly interesting to co-incubate insulin with green tea compounds to see if any potentiation or inhibition of insulin occurs. As high NEFA release due to active lipolysis triggers impairment of normal glucose metabolism pathways, and can, therefore, induce insulin resistance, and finally develop T2D. Therefore, downregulating lipolysis in diabetic patients using green tea compounds could help to counter the effect of excessive released of NEFA.

Many people spend most of their time at work and therefore have limited time to prepare their meals. In addition to that, availability and low cost of fast food, therefore, makes their life easy as they regularly consume this type of food and accordingly consume a hypercaloric diet as standard. As part of the common modern lifestyle, this behaviour is also often associated with lack of physical activity (Kuneš, 2014). Thus, taking all these factors into account, some disorders and diseases related to glucose metabolism can emerge such as obesity, insulin resistance, T2D, and their complications. A number of studies have reported beneficial effects of consumption of green tea, or its active compounds, including anti-obesity and anti-diabetes properties (Iso, *et al.*, 2006; Wu, *et al.*, 2003). Furthermore, regulation of glucose and lipid metabolism (Babu, *et al.*, 2013; Roghani and Baluchnejadmojarad, 2010). Thus, linking to the previous work, the present study aimed to explore the effect of green tea extracts on regulation of glucose and lipid metabolism *in vivo*. This experiment used a mouse model, supplementing with or without a glucose rich diet (as a part of western diet) to attempt to extend the *in vitro* results from chapter 3. This study used three different extracts to determine their effect. Firstly, and in contrast to previous work which does not investigate the effect of whole green tea compounds, this study used purified DGTE and commercial GTE in a form that is available for purchase over the internet. Secondly, like previous studies, the effective and abundant compound EGCG was also used. The original design of this study was to use all compounds previously tested in addition to whole green tea extract. However, only a limited range of extracts was used. This limitation was due to some compounds such as EC and ECG being too expensive, and the study budget was limited. Other compounds like myricetin and quercetin are easily dissolved in DMSO but came out of solution when placed in water and therefore had to be excluded from this study, as they could not be administered in the drinking supply. This issue occurred on the first morning of the test so last minute adjustments had to be made to ensure the experiment could continue. Furthermore, the study was designed to investigate the effect of these extracts on mice just for 28 days. This limited time was again due to cost, as 28 days was felt to be enough to have an effect on mice physiologically. Secondly, the number of mice used in this study was 48. Therefore, it was very hard to run the experiments using all mice together. Thus the mice were separated into four groups used in four weeks, which finally extended the experiments one month more than the original design, which extended overall time, and cost of care (such as food costs), which in turn affected the study budget and thus longer treatments could not be used.

Glucose data generated during GTT, including gAUC and glucose clearance (Figure 4.11 and Figure 4.12), reported here in addition to Glut2 and Glut4 mRNA activity in liver and skeletal muscle (Table 3.1 and Table 3.3), showed no significant changes in response to green tea treatments. Whilst, impairment of FBG due to exposure to a calorie rich diet was significantly improved by DGTE and EGCG (Figure 4.13). This result was associated with decreased Glut4 expression in adipose tissue (Table 3.2). However, PEPCK mRNA was reduced by EGCG (Table 3.1). Most of these results are contradictory with the results of many studies in this field which have revealed several green tea compounds can reduce gAUC (Gan, *et al.*, 2015; Santamarina, *et al.*, 2015). In addition, reduce glucose clearance time thereby improving glucose tolerance associated with reduced FBG and increased activity of Glut2 and Glut4 (Ortsater, *et al.*, 2012; Snoussi, *et al.*, 2014; Tang, *et al.*, 2013). As the FBG is the main physiological indicator of the proper level of circulating glucose, high FBG indicates pre-diabetic or diabetic conditions. Glucose rich diet exposure did increase FBG and this impaired glucose uptake and increased glucose output. Although the effects of green tea extracts appear above, data reported here is only related to mRNA expression, so further studies to investigate protein expression of Glut2, Glut4, PEPCK, and G6Pase are needed to draw clear conclusions. DGTE or EGCG might, therefore, help pre-diabetic and diabetic people to maintain FBG levels and inhibit glucose production. Several explanations of differences in GTT results are raised; the relatively short time of treatment (28 days), the low concentration of extracts used (these concentrations were derived from previously published literature) and the route of administration, as the study here administered treatments by the rarely used method of inclusion in drinking water. This latter fact meant that various concentrations could theoretically be taken by different mice within a group, based on individual drinking behaviour, which can affect the results. Instead of this, ideally treatment can be given by oral gavage on one time/day. However, this is very hard to do as the number of mice and treatments used are numerous, but it is not impossible if all divided but again this takes time and is associated with increased costs.

The level of fasting insulin was measured as it is proportional to the level of FBG. Interestingly, the level of fasting insulin was elevated in response to EGCG or both EGCG and GTE in mice fed normal or glucose rich diets respectively (Figure 4.14). Only this effect in mice fed a normal diet was associated with high values of HOMA-IR and HOMA-B (Figure 4.15 and Figure 4.16). These results are unique but contradict with several published studies that have reported green tea, and EGCG are able to reduce high levels of insulin in rats and mice fed excess energy diets (Moreno, *et al.*, 2014; Qin, *et al.*, 2010). An increase in insulin level have been observed in diabetic rats in response to green tea extracts (Sundaram, *et al.*, 2013) and therefore was in agreement with the present results. Furthermore, EGCG reduced insulin resistance, increased insulin sensitivity and beta-cell function in mice fed a high-energy diet (Gan, *et al.*, 2015) which contradicts with the present study result. Therefore, the present study suggests that the selected green tea extracts stimulate insulin secretion independently despite glucose level, this could be due to the stimulating effect of green tea on pancreatic beta-cell biogenesis and

increase insulin secretion. Increased HOMA-IR and B in response to EGCG is likely due to high levels of insulin secreted, which indicates high activity of pancreatic beta-cells. HOMA-IR is not the best way to measure insulin resistance in mice, as it developed and validated to measure insulin sensitivity in human (Chang, *et al.*, 2006). Indeed there are other methods of calculating resistance such as QUICKI (Gutch, *et al.*, 2015) or the gold standard (glucose clamp) (Gutch, *et al.*, 2015). Therefore a specific study is required to investigate the role of these green tea compounds on insulin secretion, action and biogenesis of beta cell *in vitro*. The data presented here, however, does not clearly provide a specific solution to diabetic patients that exhibit markers of insulin resistance but could be potentially involved. A study on diabetic mouse models or human volunteer is therefore needed to clarify the potential effect of drinking green tea by diabetic patients.

Several formulations of green tea have been advertised and used globally to control body weight and weight loss based on recently accumulated evidence of usage (Kozuma, *et al.*, 2005; Wang, *et al.*, 2010a). The results of the present study showed no effect of these compounds on body weight after 28 days, but the collective weight gain in mice fed a normal diet was decreased only in response to DGTE and EGCG (Figure 4.2). This result is inconsistent with most studies that have determined green tea, and EGCG can reduce body mass, and weight gain in mice and rats fed a high fat and normal diet (Bose, *et al.*, 2008; Snoussi, *et al.*, 2014). Therefore, the present study suggests that the selected green tea extracts could be potentially involved in reducing weight and weight gain when drinking is accompanied by calorie restriction. As regular ingestion of a glucose-rich diet can increase body weight and induce obesity, green tea cannot likely counter this effect as long as this behaviour exists. The results observed here could be due to the time limit of 28 days not being enough to make differences, even in mice fed a normal diet. The second reason, as mentioned before, might be due to low concentrations of treatments associated with differences in drinking behaviour as a route of dependent administration. Decreased weight gain in mice fed a normal diet in response to selected compounds of green tea could be due to reduced appetite, which decreased food and water intake. Overall, these extracts could be used as anti-obesity agents, but not alone, and should be associated with physical activity and calorie restriction. Some studies would be required with several modifications in green tea concentration, route of administration and period of treatments to identify any real effect; this was not considered in the present study due to limited funding.

In addition to measurement of body mass and weight gain, metabolic tissue mass including liver, skeletal muscle, SAT, VAT, and BAT were measured. The result of liver and skeletal muscle mass in response to green tea extracts showed that only EGCG fed a normal diet increased liver mass (Figure 4.5 and Figure 4.6). Interestingly SAT pad was significantly increased in response to DGTE and EGCG in mice fed a normal diet, whilst DGTE and GTE were elevated in SAT mass of mice fed a glucose-rich diet (Figure 4.7). Noticeably, these results were associated with significantly increased VAT mass

(Figure 4.8). Astonishingly, all of these results were accompanied by significantly increased BAT mass (Figure 4.9). As increases in fat pad mass were seen without overall changes in body weight, this suggests a significant change in body composition. However, almost all previously published studies showed that green tea compounds reduced body mass and weight gain associated with reducing fat pad mass (Bose, *et al.*, 2008;Chen, *et al.*, 2009;Chen, *et al.*, 2011;Li, *et al.*, 2006b). The results presented here conflict with the results of these studies, which makes it unique data as body weight did not change with increases in fat mass in response to selected green tea extracts. Despite the views that considered increasing peripheral adipose tissue fat (SAT) might or might not be implicated in a number of diseases pathogenesis, an increase of SAT and VAT mass can systemically contribution in several metabolic disorders and diseases like obesity, T2D and cardiovascular disease (CVD). Some of these fat pads could provide a protective effect as the normal physiological function is to store nutrients. The data presented in this study could reflect to this protective effect as the BAT mass was also increased. These increases in SAT and VAT mass could be due to the adipocyte hypertrophy and/or storage of more energy as triglyceride without affected physiological function. Whereas, the reason that could be responsible for increasing BAT mass is the ability of green tea to stimulate BAT growth (proliferation and differentiation) through activating adipogenesis to maintain thermogenesis (Cypess and Kahn, 2010;Dulloo, 2013;Dulloo, *et al.*, 2000). The results presented here are difficult to explain clearly, therefore, ideally further experiments to clarify how these compounds might regulate fat pad mass and how this might relate to metabolic rate are required.

Following previous study results, the effect of green tea extracts on circulating levels of TC, TG, HDL, and LDL were investigated. All green tea extracts reduced TC, and cLDL levels in mice fed a high glucose diet, whilst mice fed a normal diet exhibited a significantly decreased the level of TC by EGCG and cLDL level in response to DGTE and EGCG (Figure 4.18 and Figure 4.21). Interestingly, the level of circulating TG was increased in mice fed a glucose-rich diet alongside EGCG, while DGTE and EGCG elevated TG levels in mice fed a normal diet (Figure 4.19). These results were accompanied with down regulation of FABP4 in all mice and only LPL mRNA expression in mice fed a normal diet (Table 3.2). These results are partially consistent with a number of published study results that have shown some green tea compounds can regulate lipid metabolism through reducing the level of TC (Bose, *et al.*, 2008;Snoussi, *et al.*, 2014), and increasing the level of HDL (Jeong, *et al.*, 2012). Furthermore, reducing the levels of TG and LDL (Qin, *et al.*, 2010;Roghani and Baluchnejadmojarad, 2010). These regulations of lipid metabolism occurred through regulating the adipogenic and lipolytic transcriptional factors, including downregulated PPAR $\gamma$ , SREBP1c, C/EBP $\alpha$ , FAS, FABP4, and LPL (Lee, *et al.*, 2013;Lee, *et al.*, 2009b). Based on the results of all previous studies, the present study showed the ability of some green tea compounds to regulate the levels of TC and cLDL, in normal and glucose fed mice just after 28 days using different low concentrations. The unexpected and interesting result was related to the high level of circulating TG, which may reflect to the increase in SAT and VAT mass. As the

high level of TG is a risk factor for CVD and can be hydrolysed to increase the level of NEFA, all green tea extracts inhibited transcriptional factor FABP4, which is responsible for transporting NEFA. This effect, therefore, reduces the level of circulating NEFA; thought to be involved in many pathogenesis processes. Data presented here is promising and suggestive that the consumption of these green tea extracts could improve impairment in lipid metabolism in obese and diabetic conditions. However, the increased TG level in response to selected green tea extract might be due to excessive storing of TG due to continuous glucose uptake, which could impair metabolism and therefore increase the level of circulating TG. Modulation of this impairment by green tea requires more time than was available in this study to promote this recovery effect and decrease the level of circulating TG.

Dysregulation of glucose and lipid metabolism can increase obesity and eventually T2D, which robustly correlated with initiation of cancer including BC through several mechanisms (Gallagher and LeRoith, 2015; Lipscombe, *et al.*, 2015). As BC is markedly involved in the female death, and a number of side effects are reported when using chemotherapeutic drugs, looking for authentic natural compounds that possess chemotherapeutic property is important. Green tea has been reported previously to have potential anti-cancerous properties (Chen, *et al.*, 2012; Hsuuw and Chan, 2007; Moreira, *et al.*, 2013). In line with previous literature, the present study was designed to identify the effect of several active compounds of green tea on BC using an MCF7 and MDA-MB-231 cell line model with a focus on glucose metabolism.

The initial results of this study showed decreased cell viability in both cell lines in response to EGCG, a combination of catechins, and quercetin (Figure 5.1 to Figure 5.12). This result seemingly appeared due to increased activation of caspase 3/7 which triggered apoptosis process (Figure 5.22). Induction of apoptosis in different cancer cell lines in response to several compounds of green tea have been reported. However, the signalling pathway of this effect still needs to be elucidated (Alshatwi, 2010; Roy, *et al.*, 2005). The results presented here are partially different from some previously published results (Duo, *et al.*, 2012; Hsuuw and Chan, 2007), as some green tea compounds that have not been shown before to induce apoptosis in MDA-MB-231 cells through the activation of caspase 3/7 after just 24h. Reduced cell viability could refer to the status of pro-apoptotic and apoptotic factors which was not verified, as only mRNA level was measured, therefore ideal measurement of protein activity is required for clarification (which was not considered in this study due to cost). Here it seems that the apoptosis in MCF7 was induced by activation of caspase 3/7, since caspase 3 is not exist in the cell (Liang, *et al.*, 2001). Thus caspase 7 could be responsible for this effect. The study, therefore suggests that high concentrations of selected green tea compounds could potentially treat cancer conditions that are not responding favourably to chemotherapy. In addition, could be synergistically uses with chemotherapy drug to treat chemotherapy resistance cancer conditions, however *in vivo* studies are needed to investigate and validate these findings.

With regards to signalling mechanisms, the role of PI3K/Akt and LKB1/AMPK pathways on decreased BC cell viability by green tea compounds were considered. Inhibition of either Akt or AMPK alongside selected green tea compounds caused further reduction in cell viability of BC cell lines, which was restored by supplementing sodium pyruvate (Figure 5.14 to Figure 5.19). A number of studies have revealed that some green tea compounds suppress PI3K/Akt pathways to promote their anti-cancer effect (Qin, *et al.*, 2012;Singh, *et al.*, 2011;Spinella, *et al.*, 2006) which is consistent with the data presented. However, Western blotting analysis of pAkt or pAMPK expression in response to selected green tea compounds was not able to support this finding, as the experiment was repeated on only two occasions and does not allow clear conclusions to be drawn. Although the present study suggests that the green tea compounds could exert their effect on BC cells through inhibiting Akt signalling, further experiments are needed to focus on expression/activation levels of pAkt to validate this theory. Green tea is believed to be an adequate AMPK activator to mediate anti-cancer effects (Hwang, *et al.*, 2007;Kim, *et al.*, 2010) which is in conflict with the data presented here. With respect to this, activation of AMPK could be involved in cancer initiation and progression, which reflected to the main function of AMPK to maintain the level of ATP, that required for cellular proliferation and survival (Bonini and Gantner, 2013;Frigo, *et al.*, 2011). As cancer cells are adapted to metabolic stress, the activation level of AMPK exists in cancer cells to maintain proliferation and survival (Laderoute, *et al.*, 2014;Rios, *et al.*, 2014). This result is in agreement with data presented here regarding inhibition of AMPK which induced a decrease in cell viability regardless of the protein phosphorylation result mentioned above. The current study, therefore, shows conflicting data in this area. However, further study is needed to support these findings. Take all of these conclusions into account, selected green tea compounds could potentially exert anti-cancerous effects by targeting cellular proliferation and survival signalling. Interestingly they could regulate both Akt and AMPK, although a study linking these data with protein activation could provide clearer evidence of the signalling pathway of green tea compounds.

The cancer cells modify glucose metabolism to provide the energy required for rapid growth, proliferation, and invasive properties. Therefore, the effect of green tea compounds on this aspect in BC was explored. The results show that 24h or 6h exposure of BC cells to selected green tea compounds reduced lactate production (Figure 5.23 and Figure 5.25). As a reduction of cell viability was seen after 24h, this effect could be due to decreased cell numbers. Acute exposure is however considered the proper effect as cell viability was unaffected. These decreases in lactate production were accompanied by reduced glucose uptake (Figure 5.27). These results are in agreement with all of the studies that have shown green tea compounds can reduce cancer cell glucose uptake and glycolysis including the study of Xintaropoulou, *et al.* (2015) in breast and ovarian cancer cell lines, the study of Lu, *et al.* (2015) in pancreatic adenocarcinoma MIA PaCa-2 cells. In addition to the study of Moreira, *et al.* (2013) in MCF7 and MDA-MB-231 cell lines . Collectively, these results suggest that some active compounds of green tea successfully interfered with BC metabolism and exert their effect through decreasing glucose uptake,

thereafter reducing glycolysis. The acute result in this study is unique as the selected green tea compounds modified cellular glucose metabolism without affected cell viability. In addition, the combination of green tea compounds for the first time successfully altered MDA-MB-231 cell metabolism after 24h, but unfortunately this was associated with reduce cell viability. Although the current study did not investigate the full BC glucose metabolism modification process in response to selected green tea compounds, several future studies should be considered in this aspect in gathering details from glucose uptake to production of lactate to establish a clear signalling network.

Cancer cell migration is considered a significant predictor of poor prognosis, therefore, inhibition of migratory behaviour of cancerous cells is a substantial tool to provide a better prognosis. The present study investigated the impact of selected green tea compounds on BC migration, and both cell lines reduced their migratory behaviour in response to selected green tea compounds (Figure 5.32 and Figure 5.35). This result was expected, however, in some areas was different from the results of published studies in this field (Ho, *et al.*, 2013; Tao, *et al.*, 2015). The current study used two separate scratched assay methods to confirm the results, in addition to considering cellular proliferation, which was inhibited using mitomycin c. Although the data presented in this study is promising, clarification of the mechanism of this effect was not explored due to the cost, and therefore future specific studies to identify the mechanisms of potential anti-metastatic effects of selected green tea compounds is required. Collectively, this study suggests that early consumption of effective green tea compounds could potentially improve cancer prognosis by inhibiting cellular migration.

In the present study, several limitations were presented which were likely to have affect on the results and should be considered for future research. Most of these constraints arose from funding and lack of time. The results showed the level of gene expression related to glucose and lipid metabolism and pro and anti-apoptotic in response to green tea compounds, but protein expression/activity was therefore not determined, which is important because the level of mRNA is not always indicative of protein expression or activity. Secondly, Gluts translocation in response to green tea compounds that increased glucose uptake in insulin-sensitive cell, and reduced BC cell glucose uptake were not assessed in this study due to the cost. It could have been done, however, using fluorescent immunocytochemistry, which would have provided images that could allow identification of the position of Gluts in the cell. Several methods could be used to detect Gluts translocation, the first method is using flow cytometry to quantify the level of Gluts translocation using specific Gluts antibody tagged with fluorophore dye which bind with the Gluts after translocation to the plasma membrane, or visualised using fluorescent microscope. Another method is to transfect cells with lipofectamine which is the Gluts-4-eGFP fluorescence plasmid, and the latter translocation is then visualised using laser-scanning confocal microscope. Furthermore, the study identified the phosphorylation level of Akt or AMPK in response to selected green tea compounds. Unfortunately, no conclusion can be drawn as the experiment was repeated only twice, as previously

mentioned in the results. This limited measurement was mostly due to the study budget. In addition, identifying the phosphorylation level of downstream signalling proteins that are directly regulated by both Akt and AMPK in response to selected green tea compounds is needed to draw accurate conclusions; it was not considered in the scope of the present study. The other constraint to this research was using high glucose drinking solution instead of a high-fat diet, which again was due to costs as high-fat chow cost £700 per week and was not allocated in the study budget. Furthermore, the low volumes of blood obtained from the tail of mice during GTT was another limitation of the study which only allowed low levels of glucose to be measured, and therefore the research had to exclude measurement of insulin during GTT test and the levels of circulating TC, TG, HDL, and cLDL at the base line before treatments apply. The main reason for this was the route of obtaining blood described in animal licensing, which is allow to obtained blood only from the tail of mice. Instead, many other methods and sites could be used to collect blood from mice, these are from orbital sinus (periorbital, posterior orbital, venous plexus) and cardiac puncture, however the single sample only collected in these both collection sites, with cardiac puncture used only at the end of experiment. As the research required many samples based on the test employ in this study, therefore, tail vein surgical cannulation could be used or surgical cannulation of femoral artery or vein, carotid artery, and jugular vein.

## 6.2 Future studies

This study has added to the existing knowledge in the field and has helped to emphasise the beneficial effects of green tea compounds on glucose and lipid metabolism metabolism and their ability to target cancer cells. Future studies are required to take forward the interesting data reported here to clarify some of the contradictory or controversial findings. Ideally, these studies would be in human volunteers.

*In vitro* studies using human insulin-sensitive primary cell lines to better identify the signalling pathways of green tea extracts would be beneficial. These studies should measure gene and protein activity markers related to glucose and lipid metabolism in these cell lines. These studies are focusing on the effect of green tea extracts on the main glucose regulation pathways PI3K/Akt and AMPK and their up regulators (extracellular growth factors could stimulate cell membrane receptor tyrosine kinases (RTKs), G-protein-coupled receptors (GPCRs), and cytokine receptors, as well as ROS, ATP, and calcium level could involve in activation of LKB1, CaMKK, and TAK1. In addition to, downstream signalling including G6Pase, PEPCK, C/EBP $\alpha$ , PPAR $\gamma$ , SREBP1c, FASN, GS, FABP4, Gluts, PDK4, and more. Furthermore, explore the glucoregulatory effect of decaffeinated green tea extract, commercial green tea extract, and caffeine on these cells to identify the potential effective compounds or extracts. These studies would be valuable research to confirm the mechanism of these compounds so that their actions can be better formulated as therapeutic agents.

Several *in vivo* studies to explore the proper effect of various extracts and/or active compounds of green tea would be a beneficial next step. Primarily, further clarification of the effects of green tea on impaired glucose and lipid metabolism in individuals with pre-diabetes or T2D. The studies could include inclusion of various extracts, formulation (liquid, capsule or caplet, tablet), and oral daily doses during short or long duration. Secondly a more comprehensive study of the effects of green tea on body weight in obese and diabetic subjects. These studies could include other measurements of glucose homeostasis, such as measuring HbA1c or fructosamine in addition to assessing the levels of fasting glucose and insulin, as well as OGTT at the base line and at the end of experiments. Furthermore, measuring body weight, weight gain, body adiposity, and fat free mass in response to these green tea extracts. Moreover, measurement cytokines leptin/adiponectin index, as well as pro and anti-inflammatory biomarkers like chemokine ligand 2 (CCL2), interferon gamma-induced protein 10 (CXCL10), TNF $\alpha$ , IL-6, IL-10, IL-1Ra, and C-reactive protein (CRP). To extent the research, inclusion of green tea could associate with calorie restriction and/or easy to moderate excise to identify the effect of each of these factors alone or agonist effect to regulate glucose and lipid metabolism. Aligned to this, further study of lipid profiles and cardiovascular risk levels of TC, TG, HDL, and LDL before and after treatments would be fascinating. Furthermore, identifying the main signalling pathways of the effect of green tea compounds *in vivo* by focusing on key genes and proteins to confirm the *in vitro* studies would provide interesting data. Examination of several concentrations, compounds and extracts, route of administration (orally or injection), and several different time periods of treatment could comprehensively assess the proper effects and therefore provide a clearer view regarding the regulation of glucose and lipid metabolism, as well as weight loss in overweight, obese, pre-diabetic, and T2D individuals.

Future studies could also assess the role of green tea in animal models of BC, using a nude mouse system, cancer cells could be injected into the tail vein of mice with and without green tea, or cancer cells injected before treatment until cancer formation is confirmed. Various extracts and doses could IV administration for short and long duration, and then the effect of these extract on formed tumour was measured. The measurement including histological study, in addition to size and metastasis properties, as well as radioactive glucose uptake activity. Furthermore, measurement pro and anti-apoptotic gene and protein activity using qPCR and western blotting, these including Bcl2, Bax, P53, and Myc, in addition to caspase 3, 7, and 9. This experiment would give physiologically relevant data regarding the anti-cancerous effects of green tea compounds. Moreover, identify specific changes in the glycolytic activity of BC cells treated with green tea using the seahorse technique that measures the level of oxygen consumption and PH level in surrounding environment would also be a logical next step in future studies. As the present study only showed the effect of purified compounds of green tea on BC cell lines, examination of whole green tea extracts is therefore required to identify the exact effect of this extract.

### 6.3 Conclusions

The current study identified several interesting findings which potentially could be used as a basis for future research. The research observations presented in this study showed that selected compounds of green tea regulated glucose and lipid metabolism in insulin-sensitive cell lines through stimulating cellular glucose uptake, maintaining metabolism, and reducing glycolysis and lipolysis *in vitro*. These effects could be mediated either through activation of PI3/Akt or AMPK signalling pathways, however further research on this approach is required to confirm the signalling pathway of the effect of these selected green tea compounds.

The *in vivo* study presented in this thesis confirmed that consuming of a glucose rich diet might cause deterioration of several markers of glucose and lipid metabolism, which in turn promoted impairment of glucose homeostasis including glucose and lipid metabolism; a distinguished marker of obesity and T2D. Green tea extracts including DGTE, EGCG, and GTE showed the ability to modulate impaired of glucose homeostasis by improving most impaired markers related to glucose and lipid metabolism. This effect was concomitant with interesting increases in adipose depots mass and circulating triglyceride. However, these effects were associated with reduced NEFA release through inhibiting lipolysis. As these extracts are used widely for weight loss, the results presented in this study suggest that these extracts did not affect body weight after four weeks of treatments, although this was a relatively short period.

*In vitro* data also showed that selected green tea compounds, especially EGCG and quercetin, possess cytotoxic effects against BC cell through stimulating apoptosis and decreasing viable cells. These effects could be mediated through inhibiting PI3K/Akt and partially or completely suppressing LBK1/AMPK activation. This effect is likely due to altered cellular glucose metabolism which forces the cells to change their glucose metabolism behaviour by decreasing glucose uptake and lactate production. However, this pathway needs to be further elucidated as it is not completely validated. The study also observed that these green tea compounds could inhibit cellular migration, and therefore could be potential anti-metastatic agents.

# **Chapter Seven**

## **References**

## 7 References

- Abdel-Rahman, A., Anyangwe, N., Carlacci, L., Casper, S., Danam, R. P., Enongene, E., . . . Walker, N. J. (2011). The safety and regulation of natural products used as foods and food ingredients. *Toxicological Sciences*, 123 (2), 333-348.
- Abel, E. D. (2010). Free fatty acid oxidation in insulin resistance and obesity. *Heart Metab*, 48 5-10.
- Abrahamson, P. E., Gammon, M. D., Lund, M. J., Flagg, E. W., Porter, P. L., Stevens, J., . . . Coates, R. J. (2006). General and abdominal obesity and survival among young women with breast cancer. *Cancer Epidemiology Biomarkers & Prevention*, 15 (10), 1871-1877.
- Adam, J., Yang, M., Soga, T. and Pollard, P. J. (2014). Rare insights into cancer biology. *Oncogene*, 33 (20), 2547-2556.
- Adhami, V. M., Ahmad, N. and Mukhtar, H. (2003). Molecular targets for green tea in prostate cancer prevention. *Journal of Nutrition*, 133 (7), 2417s-2424s.
- Ahren, B. (1999). Plasma leptin and insulin in C57BL/6J mice on a high-fat diet: relation to subsequent changes in body weight. *Acta Physiol Scand*, 165 (2), 233-40.
- Air, E. L., Strowski, M. Z., Benoit, S. C., Conarello, S. L., Salituro, G. M., Guan, X. M., . . . Zhang, B. B. (2002). Small molecule insulin mimetics reduce food intake and body weight and prevent development of obesity. *Nat Med*, 8 (2), 179-83.
- Alam, M. A. and Rahman, M. M. (2014). Mitochondrial dysfunction in obesity: potential benefit and mechanism of Co-enzyme Q10 supplementation in metabolic syndrome. *J Diabetes Metab Disord*, 13 60.
- Alam, M. M., Meerza, D. and Naseem, I. (2014). Protective effect of quercetin on hyperglycemia, oxidative stress and DNA damage in alloxan induced type 2 diabetic mice. *Life Sciences*, 109 (1), 8-14.
- Albrecht, D. S., Clubbs, E. A., Ferruzzi, M. and Bomser, J. A. (2008). Epigallocatechin-3-gallate (EGCG) inhibits PC-3 prostate cancer cell proliferation via MEK-independent ERK1/2 activation. *Chemico-Biological Interactions*, 171 (1), 89-95.
- Allred, D. C., Mohsin, S. K. and Fuqua, S. A. (2001). Histological and biological evolution of human premalignant breast disease. *Endocr Relat Cancer*, 8 (1), 47-61.
- Alshatwi, A. A. (2010). Catechin hydrate suppresses MCF-7 proliferation through TP53/Caspase-mediated apoptosis. *Journal of Experimental & Clinical Cancer Research*, 29
- Andrade, B. M. and de Carvalho, D. P. (2014). Perspectives of the AMP-activated kinase (AMPK) signalling pathway in thyroid cancer. *Bioscience Reports*, 34 (2),
- Antunes, L. C., Elkfury, J. L., Jornada, M. N., Foletto, K. C. and Bertoluci, M. C. (2016). Validation of HOMA-IR in a model of insulin-resistance induced by a high-fat diet in Wistar rats. *Archives of Endocrinology and Metabolism*, 60 138-142.
- Arif, M. (2014). The Role of Aquaporin 3 (AQP3) in Breast Cancer. Doctor of Philosophy. Aston University. Birmingham, UK.
- Aronne, L. J., Nelinson, D. S. and Lillo, J. L. (2009). Obesity as a disease state: a new paradigm for diagnosis and treatment. *Clin Cornerstone*, 9 (4), 9-25; discussion 26-9.
- Aronoff, S. L., Berkowitz, K., Shreiner, B. and Want, L. (2004). Glucose Metabolism and Regulation: Beyond Insulin and Glucagon. *Diabetes Spectrum*, 17 (3), 183-190.
- Atkinson, B. J., Griesel, B. A., King, C. D., Josey, M. A. and Olson, A. L. (2013). Moderate GLUT4 Overexpression Improves Insulin Sensitivity and Fasting Triglyceridemia in High-Fat Diet-Fed Transgenic Mice. *Diabetes*, 62 (7), 2249-58.
- Axling, U., Olsson, C., Xu, J., Fernandez, C., Larsson, S., Strom, K., . . . Berger, K. (2012). Green tea powder and *Lactobacillus plantarum* affect gut microbiota, lipid metabolism and inflammation in high-fat fed C57BL/6J mice. *Nutr Metab (Lond)*, 9 (1), 105.
- Babu, P. V., Liu, D. and Gilbert, E. R. (2013). Recent advances in understanding the anti-diabetic actions of dietary flavonoids. *J. Nutr. Biochem.*, 24 (11), 1777-1789.
- Baliga, M. S., Meleth, S. and Kadiyar, S. K. (2005). Growth inhibitory and antimetastatic effect of green tea polyphenols on metastasis-specific mouse mammary carcinoma 4T1 cells in vitro and in vivo systems. *Clinical Cancer Research*, 11 (5), 1918-1927.
- Bano, G. (2013). Glucose homeostasis, obesity and diabetes. *Best Practice & Research Clinical Obstetrics and Gynaecology*, 27 715-726.

- Barbosa-da-Silva, S., Sarmiento, I. B., Lonzezzetti Bargut, T. C., Souza-Mello, V., Aguila, M. B. and Mandarim-de-Lacerda, C. A. (2014). Animal models of nutritional induction of type 2 diabetes mellitus. *Int. J. Morphol*, 32 (1), 279-293.
- Barros, C. M., Lessa, R. Q., Grechi, M. P., Mouco, T. L., Souza, M., Wiernsperger, N. and Bouskela, E. (2007). Substitution of drinking water by fructose solution induces hyperinsulinemia and hyperglycemia in hamsters. *Clinics (Sao Paulo)*, 62 (3), 327-34.
- Barsh, G. S. and Schwartz, M. W. (2002). Genetic approaches to studying energy balance: perception and integration. *Nat Rev Genet*, 3 (8), 589-600.
- Batsis, J. A., Nieto-Martinez, R. E. and Lopez-Jimenez, F. (2007). Metabolic syndrome: from global epidemiology to individualized medicine. *Clin Pharmacol Ther*, 82 (5), 509-24.
- Bays, H. E., Gonzales-Campoy, J. M., Bray, G. A., Kitabechi, A. E., Bergman, D. A., Schorr, A. B., . . . Henry, R. R. (2008). Pathogenic potential of adipose tissue and metabolic consequences of adipocyte hypertrophy and increased visceral adiposity. *Expert Rev. Cardiovasc. Ther*, 6 (3), 343-368.
- Beecher, G. R. (2003). Overview of Dietary Flavonoids: Nomenclature, Occurrence and Intake1. *The Journal of Nutrition*, (133), 3248S-3254S.
- Bensaad, K., Tsuruta, A., Selak, M. A., Vidal, M. N., Nakano, K., Bartrons, R., . . . Vousden, K. H. (2006). TIGAR, a p53-inducible regulator of glycolysis and apoptosis. *Cell*, 126 (1), 107-20.
- Bergheim, I., Weber, S., Vos, M., Krämer, S., Volynets, V., Kaserouni, S., . . . Bischoff, S. C. (2008). Antibiotics protect against fructose-induced hepatic lipid accumulation in mice: Role of endotoxin. *Journal of Hepatology*, 48 (6), 983-992.
- Bianconi, E., Piovesan, A., Facchin, F., Beraudi, A., Casadei, R., Frabetti, F., . . . Canaider, S. (2013). An estimation of the number of cells in the human body. *Annals of Human Biology*, 40 (6), 463-471.
- Bigelow, R. L. and Cardelli, J. A. (2006). The green tea catechins, (-)-Epigallocatechin-3-gallate (EGCG) and (-)-Epicatechin-3-gallate (ECG), inhibit HGF/Met signaling in immortalized and tumorigenic breast epithelial cells. *Oncogene*, 25 (13), 1922-30.
- Birnbaum, M. J. (2005). Activating AMP-activated protein kinase without AMP. *Molecular Cell*, 19 (3), 289-290.
- Bonini, M. G. and Gantner, B. N. (2013). The multifaceted activities of AMPK in tumor progression--why the "one size fits all" definition does not fit at all? *IUBMB Life*, 65 (11), 889-96.
- Bose, M., Lambert, J. D., Ju, J., Reuhl, K. R., Shapses, S. A. and Yang, C. S. (2008). The major green tea polyphenol, (-)-epigallocatechin-3-gallate, inhibits obesity, metabolic syndrome, and fatty liver disease in high-fat-fed mice. *J Nutr*, 138 (9), 1677-83.
- Bowe, J. E., Franklin, Z. J., Hauge-Evans, A. C., King, A. J., Persaud, S. J. and Jones, P. M. (2014). Metabolic phenotyping guidelines: assessing glucose homeostasis in rodent models. *J Endocrinol*, 222 (3), G13-25.
- Bowker, S. L., Richardson, K., Marra, C. A. and Johnson, J. A. (2011). Risk of Breast Cancer After Onset of Type 2 Diabetes Evidence of detection bias in postmenopausal women. *Diabetes Care*, 34 (12), 2542-2544.
- Boyle, P., Boniol, M., Koechlin, A., Robertson, C., Valentini, F., Coppens, K., . . . Autier, P. (2012). Diabetes and breast cancer risk: a meta-analysis. *British Journal of Cancer*, 107 (9), 1608-1617.
- Bray, F., Jemal, A., Grey, N., Ferlay, J. and Forman, D. (2012). Global cancer transitions according to the Human Development Index (2008-2030): a population-based study. *Lancet Oncol*, 13 (8), 790-801.
- Bultot, L., Guigas, B., Von Wilamowitz-Moellendorff, A., Maisin, L., Vertommen, D., Hussain, N., . . . Rider, M. H. (2012). AMP-activated protein kinase phosphorylates and inactivates liver glycogen synthase. *Biochemical Journal*, 443 193-203.
- Buzzi, F., Xu, L. H., Zuellig, R. A., Boller, S. B., Spinass, G. A., Hynx, D., . . . Niessen, M. (2010). Differential Effects of Protein Kinase B/Akt Isoforms on Glucose Homeostasis and Islet Mass. *Molecular and Cellular Biology*, 30 (3), 601-612.
- Cabrera, C., Artacho, R. and Giménez, R. (2006). Beneficial effects of green tea--a review. *J. Am. Coll. Nutr.*, 25 (2), 79-99.
- Cairns, R. A., Harris, I. S. and Mak, T. W. (2011). Regulation of cancer cell metabolism. *Nature Reviews Cancer*, 11 (2), 85-95.

- Calle, E. E., Rodriguez, C., Walker-Thurmond, K. and Thun, M. J. (2003). Overweight, obesity, and mortality from cancer in a prospectively studied cohort of US adults. *New England Journal of Medicine*, 348 (17), 1625-1638.
- Campbell, P., Carlson, M., Hill, J. and Nurjhan, N. (1992). Regulation of free fatty acid metabolism by insulin in humans: role of lipolysis and reesterification. *American J. Physiol. Endocrinol. Metab.*, 263 E1063-E1069.
- Cano, N. (2002). Bench-to-bedside review: Glucose production from the kidney. *Critical Care*, 6 (4), 317-321.
- Cantley, L. C. (2002). The Phosphoinositide 3-Kinase Pathway. *Science*, 296 (5573), 1655-1657.
- Cao, H., Hiniger-Favier, I., Kelly, M. A., Benaraba, R., Dawson, H., Covas, S., . . . Anderson, R. A. (2007). Green Tea Polyphenol Extract Regulates the Expression of Genes Involved in Glucose Uptake and Insulin Signaling in Rats Fed a High Fructose Diet. *J. Agric. Food Chem.*, 55 (15), 6372-6378.
- Carling, D. (2004). The AMP-activated protein kinase cascade - a unifying system for energy control. *Trends in Biochemical Sciences*, 29 (1), 18-24.
- Carling, D. (2005). AMP-activated protein kinase: balancing the scales. *Biochimie*, 87 (1), 87-91.
- Carretero, M., Escamez, M. J., Garcia, M., Duarte, B., Holguin, A., Retamosa, L., . . . Larcher, F. (2008). In vitro and in vivo wound healing-promoting activities of human cathelicidin LL-37. *Journal of Investigative Dermatology*, 128 (1), 223-236.
- Carvalho, M., Jerónimo, C., Valentão, P., Andrade, P. B. and Silva, B. M. (2010). Green tea: A promising anticancer agent for renal cell carcinoma. *Food Chemistry*, 122 (1), 49-54.
- Castro, A. V. B., Kolka, C. M., Kim, S. P. and Bergman, R. N. (2014). Obesity, insulin resistance and comorbidities - Mechanisms of association. *Arquivos Brasileiros De Endocrinologia E Metabologia*, 58 (6), 600-609.
- Cavet, M., Harrington, K., Vollmer, T., Ward, K. and Zhang, J. (2011). Anti-inflammatory and anti-oxidative effects of the green tea polyphenol epigallocatechin gallate in human corneal epithelial cells. *Molecular Vision*, 17 533-542.
- Chacko, S. M., Thambi, P. T., Kuttan, R. and Nishigaki, I. (2010). Beneficial effects of green tea: a literature review. *Chinese Med*, 5 13.
- Chan, C.-y. (2009). Effects of (-)-epigallocatechin gallate in 3T3-L1 adipogenesis. 香港大學學位論文, 1-0.
- Chan, C. Y., Wei, L., Castro-Munozledo, F. and Koo, W. L. (2011). (-)-Epigallocatechin-3-gallate blocks 3T3-L1 adipose conversion by inhibition of cell proliferation and suppression of adipose phenotype expression. *Life Sciences*, 89 (21-22), 779-785.
- Chaneton, B. J. (2014). Targeting cancer cell metabolism as a therapeutic strategy. PhD. University of Glasgow. UK.
- Chang, A. M., Smith, M. J., Bloem, C. J., Galecki, A. T., Halter, J. B. and Supiano, M. A. (2006). Limitation of the Homeostasis Model Assessment to Predict Insulin Resistance and  $\beta$ -Cell Dysfunction in Older People. *The Journal of Clinical Endocrinology & Metabolism*, 91 (2), 629-634.
- Chen, D., Pamu, S., Cui, Q. Z., Chan, T. H. and Dou, Q. P. (2012). Novel epigallocatechin gallate (EGCG) analogs activate AMP-activated protein kinase pathway and target cancer stem cells. *Bioorganic & Medicinal Chemistry*, 20 (9), 3031-3037.
- Chen, N., Bezzina, R., Hinch, E., Lewandowski, P. A., Cameron-Smith, D., Mathai, M. L., . . . Weisinger, R. S. (2009). Green tea, black tea, and epigallocatechin modify body composition, improve glucose tolerance, and differentially alter metabolic gene expression in rats fed a high-fat diet. *Nutr Res*, 29 (11), 784-93.
- Chen, X., Li, Y., Lin, Q., Wang, Y., Sun, H., Wang, J., . . . Dong, X. (2014). Tea polyphenols induced apoptosis of breast cancer cells by suppressing the expression of Survivin. *Scientific Reports*, 4 4416.
- Chen, Y.-K., Cheung, C., Reuhl, K. R., Liu, A. B., Lee, M.-J., Lu, Y.-P. and Yang, C. S. (2011). Effects of Green Tea Polyphenol (-)-Epigallocatechin-3-gallate on Newly Developed High-Fat/Western-Style Diet-Induced Obesity and Metabolic Syndrome in Mice. *Journal of Agricultural and Food Chemistry*, 59 (21), 11862-11871.

- Cheng, T. O. (2004). Will green tea be even better than black tea to increase coronary flow velocity reserve? *Am. J. Cardiol*, 94 (9), 1223.
- Cheng, T. O. (2006). All teas are not created equal: The Chinese green tea and cardiovascular health. *International Journal of Cardiology*, 108 (3), 301-308.
- Chhipa, R. R., Wu, Y., Mohler, J. L. and Ip, C. (2010). Survival advantage of AMPK activation to androgen-independent prostate cancer cells during energy stress. *Cell Signal*, 22 (10), 1554-61.
- Cho, H., Mu, J., Kim, J. K., Thorvaldsen, J. L., Chu, Q. W., Crenshaw, E. B., . . . Birnbaum, M. J. (2001). Insulin resistance and a diabetes mellitus-like syndrome in mice lacking the protein kinase Akt2 (PKB beta). *Science*, 292 (5522), 1728-1731.
- Chung, F., Schwartz, J., Herzog, C. and Yang, Y. (2003). Tea and Cancer Prevention: Studies in Animals and Humans1. *The Journal of Nutrition.*, 133 3268S–3274S.
- Cinti, S. (2009). Transdifferentiation properties of adipocytes in the adipose organ. *Am. J. Physiol. Endocrinol. Metab.*, 297 E977–E986.
- Cohen, D. H. and LeRoith, D. (2012). Obesity, type 2 diabetes, and cancer: the insulin and IGF connection. *Endocrine-Related Cancer*, 19 (5), F27-F45.
- Collins, F. S., Lander, E. S., Rogers, J., Waterston, R. H. and Conso, I. H. G. S. (2004). Finishing the euchromatic sequence of the human genome. *Nature*, 431 (7011), 931-945.
- Collins, Q. F., Liu, H. Y., Pi, J. B., Liu, Z. Q., Quon, M. J. and Cao, W. H. (2007). Epigallocatechin-3-gallate (EGCG), a green tea polyphenol, suppresses hepatic gluconeogenesis through 5'-AMP-activated protein kinase. *Journal of Biological Chemistry*, 282 (41), 30143-30149.
- Cool, B., Zinker, B., Chiou, W., Kifle, L., Cao, N., Perham, M., . . . Frevert, E. (2006). Identification and characterization of a small molecule AMPK activator that treats key components of type 2 diabetes and the metabolic syndrome. *Cell Metabolism*, 3 (6), 403-416.
- Cooper, G. (2000). *The Cell: A Molecular Approach*. 2nd. Sunderland (MA).
- Cordero-Herrera, I., Martin, M. A., Goya, L. and Ramos, S. (2014). Cocoa flavonoids attenuate high glucose-induced insulin signalling blockade and modulate glucose uptake and production in human HepG2 cells. *Food Chem. Toxicol.*, 64 10-9.
- Crowell, J. A., Steele, V. E. and Fay, J. R. (2007). Targeting the AKT protein kinase for cancer chemoprevention. *Mol Cancer Ther*, 6 (8), 2139-48.
- Cunha, C. A., Lira, F. S., Rosa Neto, J. C., Pimentel, G. D., Souza, G. I., da Silva, C. M., . . . Oyama, L. M. (2013). Green tea extract supplementation induces the lipolytic pathway, attenuates obesity, and reduces low-grade inflammation in mice fed a high-fat diet. *Mediators Inflamm*, 2013 635470.
- Cypess, A. M. and Kahn, C. R. (2010). Brown fat as a therapy for obesity and diabetes. *Current opinion in endocrinology, diabetes, and obesity*, 17 (2), 143-149.
- Daling, J. R., Malone, K. E., Doody, D. R., Johnson, L. G., Gralow, J. R. and Porter, P. L. (2001). Relation of body mass index to tumor markers and survival among young women with invasive ductal breast carcinoma. *Cancer*, 92 (4), 720-729.
- Dalluge, J. and Nelson, B. (2000). Determination of tea catechins. *Journal of Chromatography A.*, 881 411–424.
- Dang, C. V. (2013). MYC, Metabolism, Cell Growth, and Tumorigenesis. *Cold Spring Harbor Perspectives in Biology*, 5 (8),
- Dang, C. V., Kim, J.-w., Gao, P. and Yustein, J. (2008). The interplay between MYC and HIF in cancer. *Nat Rev Cancer*, 8 (1), 51-56.
- Daval, M., Diot-Dupuy, F., Bazin, R., Hainault, I., Viollet, B., Vaulont, S., . . . Foufelle, F. (2005). Anti-lipolytic action of AMP-activated protein kinase in rodent adipocytes. *Journal of Biological Chemistry*, 280 (26), 25250-25257.
- Daval, M., Foufelle, F. and Ferre, P. (2006). Functions of AMP-activated protein kinase in adipose tissue. *J Physiol*, 574 (Pt 1), 55-62.
- Dean, D., Dugaard, J. R., Young, M. E., Saha, A., Vavvas, D., Asp, S., . . . Ruderman, N. (2000). Exercise diminishes the activity of acetyl-CoA carboxylase in human muscle. *Diabetes*, 49 (8), 1295-1300.
- Debatin, K. M. (2004). Apoptosis pathways in cancer and cancer therapy. *Cancer Immunol Immunother*, 53 (3), 153-9.
- DeFronzo, R. A. (1988). The triumvirate: beta cell, muscle, liver – a conclusion responsible for NIDDM. *Diabetes.*, 37 (6), 667-684.

- DeFronzo, R. A. and Tripathy, D. (2009). Skeletal Muscle Insulin Resistance Is the Primary Defect in Type 2 Diabetes. *Diabetes Care*, 32 S157-S163.
- Deng, Y. T., Chang, T. W., Lee, M. S. and Lin, J. K. (2012). Suppression of free fatty acid-induced insulin resistance by phytopolyphenols in C2C12 mouse skeletal muscle cells. *J. Agric. Food Chem.*, 60 (4), 1059-66.
- Devi, P. U. (2004). Basis of carcinogenesis. *Health Administrator*, XVII (1), 16-24.
- Dhillon, A. S., Hagan, S., Rath, O. and Kolch, W. (2007). MAP kinase signalling pathways in cancer. *Oncogene*, 26 (22), 3279-3290.
- Dihal, A. A., van der Woude, H., Hendriksen, P. J., Charif, H., Dekker, L. J., Ijsselstijn, L., . . . Stierum, R. H. (2008). Transcriptome and proteome profiling of colon mucosa from quercetin fed F344 rats point to tumor preventive mechanisms, increased mitochondrial fatty acid degradation and decreased glycolysis. *Proteomics*, 8 (1), 45-61.
- Ding, Y., Dai, X. Q., Zhang, Z. F. and Li, Y. (2012). Myricetin attenuates hyperinsulinemia-induced insulin resistance in skeletal muscle cells. *European Food Research and Technology*, 234 (5), 873-881.
- Distefano, J. K. and Watanabe, R. M. (2010). Pharmacogenetics of Anti-Diabetes Drugs. *Pharmaceuticals (Basel)*, 3 (8), 2610-2646.
- Drira, R. and Sakamoto, K. (2013). Modulation of adipogenesis, lipolysis and glucose consumption in 3T3-L1 adipocytes and C2C12 myotubes by hydroxytyrosol acetate: A comparative study. *Biochemical and Biophysical Research Communications*, 440 (4), 576-581.
- Drucker, D. J. (2005). Biologic actions and therapeutic potential of the proglucagon-derived peptides. *Nature Clinical Practice Endocrinology & Metabolism*, 1 (1), 22-31.
- Dulloo, A. G. (2013). Translational issues in targeting brown adipose tissue thermogenesis for human obesity management. *Annals of the New York Academy of Sciences*, 1302 (1), 1-10.
- Dulloo, A. G., Seydoux, J., Girardier, L., Chantre, P. and Vandermader, J. (2000). Green tea and thermogenesis: interactions between catechin-polyphenols, caffeine and sympathetic activity. *Int J Obes Relat Metab Disord*, 24 (2), 252-8.
- Duncan, R. E., Ahmadian, M., Jaworski, K., Sarkadi-Nagy, E. and Sul, H. S. (2007). Regulation of lipolysis in adipocytes. *Annu Rev Nutr*, 27 79-101.
- Dunmore, S. J. and Brown, J. E. (2013). The role of adipokines in beta-cell failure of type 2 diabetes. *J. Endocrinol.*, 216 (1), T37-45.
- Duo, J., Ying, G. G., Wang, G. W. and Zhang, L. (2012). Quercetin inhibits human breast cancer cell proliferation and induces apoptosis via Bcl-2 and Bax regulation. *Mol Med Rep*, 5 (6), 1453-6.
- Edgerton, D. S., Johnson, K. M. and Cherrington, A. D. (2009). Current strategies for the inhibition of hepatic glucose production in type 2 diabetes. *Frontiers in bioscience.*, 14 1169-1181.
- El-Masry, O. S., Brown, B. L. and Dobson, P. R. (2012). Effects of activation of AMPK on human breast cancer cell lines with different genetic backgrounds. *Oncol Lett*, 3 (1), 224-228.
- El-Shahawi, M. S., Hamza, A., Bahaffi, S. O., Al-Sibaai, A. A. and Abduljabbar, T. N. (2012). Analysis of some selected catechins and caffeine in green tea by high performance liquid chromatography. *Food Chem*, 134 (4), 2268-2275.
- Elmore, S. (2007). Apoptosis: a review of programmed cell death. *Toxicol Pathol*, 35 (4), 495-516.
- Elston, C. W. and Ellis, I. O. (1991). Pathological prognostic factors in breast cancer. I. The value of histological grade in breast cancer: experience from a large study with long-term follow-up. *Histopathology*, 19 (5), 403-10.
- Elstrom, R. L., Bauer, D. E., Buzzai, M., Karnauskas, R., Harris, M. H., Plas, D. R., . . . Thompson, C. B. (2004). Akt stimulates aerobic glycolysis in cancer cells. *Cancer Research*, 64 (11), 3892-3899.
- Engelman, J. A., Luo, J. and Cantley, L. C. (2006). The evolution of phosphatidylinositol 3-kinases as regulators of growth and metabolism. *Nature Reviews Genetics*, 7 (8), 606-619.
- Erler, J. T., Bennewith, K. L., Nicolau, M., Dornhofer, N., Kong, C., Le, Q.-T., . . . Giaccia, A. J. (2006). Lysyl oxidase is essential for hypoxia-induced metastasis. *Nature*, 440 (7088), 1222-1226.
- Ezkurdia, I., Juan, D., Rodriguez, J. M., Frankish, A., Diekhans, M., Harrow, J., . . . Tress, M. L. (2014). Multiple evidence strands suggest that there may be as few as 19 000 human protein-coding genes. *Human Molecular Genetics*, 23 (22), 5866-5878.
- Fain, J. N. (2010). Release of inflammatory mediators by human adipose tissue is enhanced in obesity and primarily by the nonfat cells: a review. *Mediators Inflamm.*, 2010 1-20.

- Fain, J. N. (2012). *Effect of Obesity on Circulating Adipokines and Their Expression in Omental Adipose Tissue of Female Bariatric Surgery patients*. In: Huang, C.-K. (2012). Croatia: InTech.
- Fantuzzi, G. (2005). Adipose tissue, adipokines, and inflammation. *J Allergy Clin Immunol*, 115 (5), 911-9; quiz 920.
- Farabegoli, F., Papi, A. and Orlandi, M. (2011). (-)-Epigallocatechin-3-gallate down-regulates EGFR, MMP-2, MMP-9 and EMMPRIN and inhibits the invasion of MCF-7 tamoxifen-resistant cells. *Bioscience Reports*, 31 (2), 99-108.
- Farooqi, I. S. (2005). Genetic and hereditary aspects of childhood obesity. *Best Practice & Research Clinical Endocrinology & Metabolism*, 19 (3), 359-374.
- Fidler, I. J. (2003). The pathogenesis of cancer metastasis: the 'seed and soil' hypothesis revisited. *Nat Rev Cancer*, 3 (6), 453-8.
- Flier, J. S. (2004). Obesity wars: molecular progress confronts an expanding epidemic. *Cell*, 116 (2), 337-50.
- Foster, F. M., Traer, C. J., Abraham, S. M. and Fry, M. J. (2003). The phosphoinositide (PI) 3-kinase family. *Journal of Cell Science*, 116 (15), 3037-3040.
- Fraser, K., Lane, G. A., Otter, D. E., Hemar, Y., Quek, S., Harrison, S. J. and Rasmussen, S. (2013). Analysis of metabolic markers of tea origin by UHPLC and high resolution mass spectrometry. *Food Research International*, 53 (2), 827-835.
- Frayn, K. N. (2003). The glucose-fatty acid cycle: a physiological perspective. *Biochemical Society transactions*, 31 1115-1119.
- Fresno Vara, J. A., Casado, E., de Castro, J., Cejas, P., Belda-Iniesta, C. and Gonzalez-Baron, M. (2004). PI3K/Akt signalling pathway and cancer. *Cancer Treat Rev*, 30 (2), 193-204.
- Friedewald, W. T., Levy, R. I. and Fredrickson, D. S. (1972). Estimation of the Concentration of Low-Density Lipoprotein Cholesterol in Plasma, Without Use of the Preparative Ultracentrifuge. *Clinical Chemistry*, 18 (6), 499.
- Friedl, P. and Alexander, S. (2011). Cancer invasion and the microenvironment: plasticity and reciprocity. *Cell*, 147 (5), 992-1009.
- Friedman, J. M. and Halaas, J. L. (1998). Leptin and the regulation of body weight in mammals. *Nature*, 395 (6704), 763-770.
- Friigo, D. E., Howe, M. K., Wittmann, B. M., Brunner, A. M., Cushman, I., Wang, Q., . . . McDonnell, D. P. (2011). CaM kinase kinase beta-mediated activation of the growth regulatory kinase AMPK is required for androgen-dependent migration of prostate cancer cells. *Cancer Res*, 71 (2), 528-37.
- Frosig, C., Pehmoller, C., Birk, J. B., Richter, E. A. and Wojtaszewski, J. F. P. (2010). Exercise-induced TBC1D1 Ser237 phosphorylation and 14-3-3 protein binding capacity in human skeletal muscle. *Journal of Physiology-London*, 588 (22), 4539-4548.
- Funai, K. and Cartee, G. D. (2009). Inhibition of Contraction-Stimulated AMP-Activated Protein Kinase Inhibits Contraction-Stimulated Increases in PAS-TBC1D1 and Glucose Transport Without Altering PAS-AS160 in Rat Skeletal Muscle. *Diabetes*, 58 (5), 1096-1104.
- Furuhashi, M., Saitoh, S., Shimamoto, K. and Miura, T. (2014). Fatty Acid-Binding Protein 4 (FABP4): Pathophysiological Insights and Potent Clinical Biomarker of Metabolic and Cardiovascular Diseases. *Clinical Medicine Insights. Cardiology*, 8 (Suppl 3), 23-33.
- Gaidhu, M. P., Frontini, A., Hung, S., Pistor, K., Cinti, S. and Ceddia, R. B. (2011). Chronic AMP-kinase activation with AICAR reduces adiposity by remodeling adipocyte metabolism and increasing leptin sensitivity. *J. Lipid Res.*, 52 (9), 1702-1711.
- Gallagher, E. J. and LeRoith, D. (2015). Obesity and Diabetes: The Increased Risk of Cancer and Cancer-Related Mortality. *Physiological Reviews*, 95 (3), 727-748.
- Gan, L., Meng, Z. J., Xiong, R. B., Guo, J. Q., Lu, X. C., Zheng, Z. W., . . . Li, H. (2015). Green tea polyphenol epigallocatechin-3-gallate ameliorates insulin resistance in non-alcoholic fatty liver disease mice. *Acta Pharmacol Sin*, 36 (5), 597-605.
- Ganapathy-Kanniappan, S. and Geschwind, J.-F. H. (2013). Tumor glycolysis as a target for cancer therapy: progress and prospects. *Molecular Cancer*, 12 (1), 1-11.
- Ganguly, D. K. (2003). Tea Consumption on oxidative damage and cancer. *Indian Council of Medicine Research Bulletin*, 33 (4-5), 37-52.
- Gatenby, R. A. and Gillies, R. J. (2004). Why do cancers have high aerobic glycolysis? *Nature Reviews Cancer*, 4 (11), 891-899.

- Geback, T., Schulz, M. M. P., Koumoutsakos, P. and Detmar, M. (2009). TScratch: a novel and simple software tool for automated analysis of monolayer wound healing assays. *Biotechniques*, 46 (4), 265-+.
- Geetha, B. and Santhy, K. S. (2013). Anti-proliferative activity of green tea extract in Human Cervical Cancer Cells (HeLa). *International Journal of Current Microbiology and Applied Sciences*, 2 (9), 341-346.
- Gerich, J. (2000). Physiology of glucose homeostasis. *Diabetes, Obesity and Metabolism.*, 2 345-350.
- Ghose, A., Kundu, R., Toumeh, A., Hornbeck, C. and Mohamed, I. (2015). A Review of Obesity, Insulin Resistance, and the Role of Exercise in Breast Cancer Patients. *Nutrition and Cancer-an International Journal*, 67 (2), 197-202.
- Ginter, E. and Simko, V. (2010). Diabetes type 2 pandemic in 21st century. *Bratisl Lek Listy.*, 111 (3), 134-137.
- Giovannucci, E., Harlan, D. M., Archer, M. C., Bergengal, R. M., Gapstur, S. M., Habel, L. A., . . . Yee, D. (2010). Diabetes and Cancer A consensus report. *Diabetes Care*, 33 (7), 1674-1685.
- Golomb, B. A. and Evans, M. A. (2008). Statin Adverse Effects: A Review of the Literature and Evidence for a Mitochondrial Mechanism. *American journal of cardiovascular drugs : drugs, devices, and other interventions*, 8 (6), 373-418.
- Gong, Z. and Muzumdar, R. H. (2012). Pancreatic function, type 2 diabetes, and metabolism in aging. *Int. J. Endocrinol.*, 2012 1-12.
- Goodwin, M. L., Gladden, L. B., Nijsten, M. W. N. and Jones, K. B. (2014). Lactate and Cancer: Revisiting the Warburg Effect in an Era of Lactate Shuttling. *Frontiers in Nutrition*, 1 27.
- Gortmaker, S. L., Must, A., Sobol, A. M., Peterson, K., Colditz, G. A. and Dietz, W. H. (1996). Television viewing as a cause of increasing obesity among children in the united states, 1986-1990. *Archives of Pediatrics & Adolescent Medicine*, 150 (4), 356-362.
- Gual, P., Le Marchand-Brustel, Y. and Tanti, J. F. (2005). Positive and negative regulation of insulin signaling through IRS-1 phosphorylation. *Biochimie*, 87 (1), 99-109.
- Guilherme, A., Virbasius, J. V., Puri, V. and Czech, M. P. (2008). Adipocyte dysfunctions linking obesity to insulin resistance and type 2 diabetes. *Nature reviews. Molecular cell biology*, 9 (5), 367-377.
- Guo, M. and Hay, B. A. (1999). Cell proliferation and apoptosis. *Current Opinion in Cell Biology*, 11 (6), 745-752.
- Gupta, G. P. and Massague, J. (2006). Cancer metastasis: building a framework. *Cell*, 127 (4), 679-95.
- Gutch, M., Kumar, S., Razi, S. M., Gupta, K. K. and Gupta, A. (2015). Assessment of insulin sensitivity/resistance. *Indian Journal of Endocrinology and Metabolism*, 19 (1), 160-164.
- Gutman, R. and Ryu, B. (1996). Rediscovering Tea: An Exploration of the Scientific Literature. *HerbalGram.*, (37), 33.
- Guyton, A. C. and Hall, J. E. (2006). *textbook of Medical physiology*. 11th. Philadelphia: Elsevier.
- Hadad, S. M., Fleming, S. and Thompson, A. M. (2008). Targeting AMPK: a new therapeutic opportunity in breast cancer. *Crit Rev Oncol Hematol*, 67 (1), 1-7.
- Haidari, F., Shahi, M. M., Zarei, M., Rafiei, H. and Omidian, K. (2012). Effect of green tea extract on body weight, serum glucose and lipid profile in streptozotocin-induced diabetic rats: A dose response study. *Saudi Medical Journal*, 33 (2), 128-133.
- Han, H. S., Kang, G., Kim, J. S., Choi, B. H. and Koo, S. H. (2016). Regulation of glucose metabolism from a liver-centric perspective. *Experimental and Molecular Medicine*, 48
- Hanhineva, K., Torronen, R., Bondia-Pons, I., Pekkinen, J., Kolehmainen, M., Mykkanen, H. and Poutanen, K. (2010). Impact of dietary polyphenols on carbohydrate metabolism. *Int J Mol Sci*, 11 (4), 1365-402.
- Hardefeldt, P. J., Edirimanne, S. and Eslick, G. D. (2012). Diabetes increases the risk of breast cancer: a meta-analysis. *Endocr Relat Cancer*, 19 (6), 793-803.
- Hardie, D. G. (2004). The AMP-activated protein kinase pathway - new players upstream and downstream. *Journal of Cell Science*, 117 (23), 5479-5487.
- Hardie, D. G. (2013). AMPK: a target for drugs and natural products with effects on both diabetes and cancer. *Diabetes*, 62 (7), 2164-72.
- Hardin, J., Bertoni, G., Kleinsmith, L. J. and Becker, W. M. (2012). *Becker's world of the cells*. 8th. Bostin: Benjamin Cummings.

- Harris, A. L. (2002). Hypoxia [mdash] a key regulatory factor in tumour growth. *Nat Rev Cancer*, 2 (1), 38-47.
- Harvey, R. and Ferrier, D. (2011). *Intermediat metabolism: glycolysis*. 5th. In: Harvey, R. (2011). *Lippincott's Illustrated Reviews*. USA: Lippincott Williams & Wilkins. 8.
- Hawley, S. A., Pan, D. A., Mustard, K. J., Ross, L., Bain, J., Edelman, A. M., . . . Hardie, D. G. (2005). Calmodulin-dependent protein kinase kinase-beta is an alternative upstream kinase for AMP-activated protein kinase. *Cell Metabolism*, 2 (1), 9-19.
- Heilbronn, L. K., Gan, S. K., Turner, N., Campbell, L. V. and Chisholm, D. J. (2007). Markers of mitochondrial biogenesis and metabolism are lower in overweight and obese insulin-resistant subjects. *J Clin Endocrinol Metab*, 92 (4), 1467-73.
- Hennessy, B. T., Gonzalez-Angulo, A. M., Stemke-Hale, K., Gilcrease, M. Z., Krishnamurthy, S., Lee, J. S., . . . Mills, G. B. (2009). Characterization of a naturally occurring breast cancer subset enriched in epithelial-to-mesenchymal transition and stem cell characteristics. *Cancer Res*, 69 (10), 4116-24.
- Herrero-Martin, G., Hoyer-Hansen, M., Garcia-Garcia, C., Fumarola, C., Farkas, T., Lopez-Rivas, A. and Jaattela, M. (2009). TAK1 activates AMPK-dependent cytoprotective autophagy in TRAIL-treated epithelial cells (vol 28, pg 677, 2009). *Embo Journal*, 28 (10), 1532-1532.
- Hidalgo, M. and Rowinsky, E. K. (2000). The rapamycin-sensitive signal transduction pathway as a target for cancer therapy. *Oncogene*, 19 (56), 6680-6.
- Hill, J. O., Wyatt, H. R. and Peters, J. C. (2012). Energy Balance and Obesity. *Circulation*, 126 (1), 126-132.
- Hininger-Favier, I., Benaraba, R., Coves, S., Anderson, R. and Roussel, A. (2009). Green Tea Extract Decreases Oxidative Stress and Improves Insulin Sensitivity in an Animal Model of Insulin Resistance, the Fructose-Fed Rat. *Journal of the American College of Nutrition.*, 28 (4), 355-361.
- Ho, J.-N., Choue, R. and Lee, J. (2013). Green tea seed extract inhibits cell migration by suppressing the epithelial-to-mesenchymal transition (EMT) process in breast cancer cells. *Food Science and Biotechnology*, 22 (4), 1125-1129.
- Horike, N., Sakoda, H., Kushiya, A., Ono, H., Fujishiro, M., Kamata, H., . . . Asano, T. (2008). AMP-activated Protein Kinase Activation Increases Phosphorylation of Glycogen Synthase Kinase 3 beta and Thereby Reduces cAMP-responsive Element Transcriptional Activity and Phosphoenolpyruvate Carboxykinase C Gene Expression in the Liver. *Journal of Biological Chemistry*, 283 (49), 33902-33910.
- Hou, J. C., Williams, D., Vicogne, J. and Pessin, J. E. (2009). The glucose transporter 2 undergoes plasma membrane endocytosis and lysosomal degradation in a secretagogue-dependent manner. *Endocrinology.*, 150 (9), 4056-4064.
- Hsu, P. P. and Sabatini, D. M. (2008). Cancer cell metabolism: Warburg and beyond. *Cell*, 134 (5), 703-707.
- Hsuuw, Y. D. and Chan, W. H. (2007). Epigallocatechin gallate dose-dependently induces apoptosis or necrosis in human MCF-7 cells. *Ann N Y Acad Sci*, 1095 428-40.
- Huang, X., Wullschleger, S., Shpiro, N., McGuire, V. A., Sakamoto, K., Woods, Y. L., . . . Alessi, D. R. (2008). Important role of the LKB1-AMPK pathway in suppressing tumorigenesis in PTEN-deficient mice. *Biochem J*, 412 (2), 211-21.
- Hwang, J. T., Ha, J., Park, I. J., Lee, S. K., Baik, H. W., Kim, Y. M. and Park, O. J. (2007). Apoptotic effect of EGCG in HT-29 colon cancer cells via AMPK signal pathway. *Cancer Lett*, 247 (1), 115-21.
- Hwang, J. T., Park, I. J., Shin, J. I., Lee, Y. K., Lee, S. K., Baik, H. W., . . . Park, O. J. (2005). Genistein, EGCG, and capsaicin inhibit adipocyte differentiation process via activating AMP-activated protein kinase. *Biochemical and Biophysical Research Communications*, 338 (2), 694-699.
- IDF. (2006). The metabolic syndrome. [http://www.idf.org/webdata/docs/IDF\\_Meta\\_def\\_final.pdf](http://www.idf.org/webdata/docs/IDF_Meta_def_final.pdf)
- IDF. (2015). *Diabetes: A global emergency*. 7th. Belgium:
- Int Veld, P. and Marichal, M. (2010). *Microscopic Anatomy of the Human Islet of Langerhans*. In: Shahidul Islam, M. (2010). *Advances in Experimental Medicine and Biology*. Springer Netherlands. 1.
- Inzucchi, S. E., Bergenstal, R. M., Buse, J. B., Diamant, M., Ferrannini, E., Nauck, M., . . . Matthews, D. R. (2012). Management of Hyperglycemia in Type 2 Diabetes: A Patient-Centered Approach:

- Position Statement of the American Diabetes Association (ADA) and the European Association for the Study of Diabetes (EASD). *Diabetes Care*, 35 (6), 1364-79.
- Isherwood, B., Timpson, P., McGhee, E. J., Anderson, K. I., Canel, M., Serrels, A., . . . Carragher, N. O. (2011). Live cell in vitro and in vivo imaging applications: accelerating drug discovery. *Pharmaceutics*, 3 (2), 141-70.
- Islam, M. S. and Loots du, T. (2009). Experimental rodent models of type 2 diabetes: a review. *Methods Find Exp Clin Pharmacol*, 31 (4), 249-61.
- Iso, H., Date, C., Wakai, K., Fukui, M. and Tamakoshi, A. (2006). The relationship between green tea and total caffeine intake and risk for self-reported type 2 diabetes among Japanese adults. *Ann Intern Med*, 144 (8), 554-62.
- Item, F. and Konrad, D. (2012). Visceral fat and metabolic inflammation: the portal theory revisited. *Obes. Rev.*, 13 Suppl 2 30-39.
- Itoh, N., Semba, S., Ito, M., Takeda, H., Kawata, S. and Yamakawa, M. (2002). Phosphorylation of Akt/PKB is required for suppression of cancer cell apoptosis and tumor progression in human colorectal carcinoma. *Cancer*, 94 (12), 3127-34.
- Jang, H. J., Ridgeway, S. D. and Kim, J. A. (2013a). Effects of the green tea polyphenol epigallocatechin-3-gallate on high-fat diet-induced insulin resistance and endothelial dysfunction. *Am J Physiol Endocrinol Metab*, 305 (12), E1444-51.
- Jang, M., Kim, S. S. and Lee, J. (2013b). Cancer cell metabolism: implications for therapeutic targets. *Experimental and Molecular Medicine*, 45
- Jang, T., Calaoagan, J. M., Kwon, E., Samuelsson, S., Recht, L. and Laderoute, K. R. (2011). 5'-AMP-activated protein kinase activity is elevated early during primary brain tumor development in the rat. *Int J Cancer*, 128 (9), 2230-9.
- Jänicke, R. U., Sprengart, M. L., Wati, M. R. and Porter, A. G. (1998). Caspase-3 Is Required for DNA Fragmentation and Morphological Changes Associated with Apoptosis. *Journal of Biological Chemistry*, 273 (16), 9357-9360.
- Jeon, S.-M. and Hay, N. (2012). The dark face of AMPK as an essential tumor promoter. *Cellular Logistics*, 2 (4), 197-202.
- Jeong, S. M., Kang, M. J., Choi, H. N., Kim, J. H. and Kim, J. I. (2012). Quercetin ameliorates hyperglycemia and dyslipidemia and improves antioxidant status in type 2 diabetic db/db mice. *Nutrition Research and Practice*, 6 (3), 201-207.
- Jian, L., Xie, L. P., Lee, A. H. and Binns, C. W. (2004). Protective effect of green tea against prostate cancer: a case-control study in southeast China. *Int. J. Cancer*, 108 (1), 130-135.
- Joensuu, K., Leidenius, M., Kero, M., Andersson, L. C., Horwitz, K. B. and Heikkilä, P. (2013). ER, PR, HER2, Ki-67 and CK5 in Early and Late Relapsing Breast Cancer-Reduced CK5 Expression in Metastases. *Breast Cancer (Auckl)*, 7 23-34.
- Jorgensen, S. B., Nielsen, J. N., Birk, J. B., Olsen, G. S., Viollet, B., Andreelli, F., . . . Wojtaszewski, J. F. P. (2004). The alpha 2-5 ' AMP-activated protein kinase is a site 2 glycogen synthase kinase in skeletal muscle and is responsive to glucose loading. *Diabetes*, 53 (12), 3074-3081.
- Joung, K. H., Jeong, J. W. and Ku, B. J. (2015). The association between type 2 diabetes mellitus and women cancer: the epidemiological evidences and putative mechanisms. *Biomed Res Int*, 2015 920618.
- Juge-Aubry, C. E., Somm, E., Giusti, V., Pernin, A., Chicheportiche, R., Verdumo, C., . . . Meier, C. A. (2003). Adipose tissue is a major source of interleukin-1 receptor antagonist - Upregulation in obesity and inflammation. *Diabetes*, 52 (5), 1104-1110.
- Jung, J. H., Lee, J. O., Kim, J. H., Lee, S. K., You, G. Y., Park, S. H., . . . Kim, H. S. (2010). Quercetin suppresses HeLa cell viability via AMPK-induced HSP70 and EGFR down-regulation. *J Cell Physiol*, 223 (2), 408-14.
- Jung, K. H., Choi, H. S., Kim, D. H., Han, M. Y., Chang, U. J., Yim, S. V., . . . Kang, S. A. (2008). Epigallocatechin gallate stimulates glucose uptake through the phosphatidylinositol 3-kinase-mediated pathway in L6 rat skeletal muscle cells. *J. Med. Food*, 11 (3), 429-434.
- Jung, K. H., Lee, J. H., Thien Quach, C. H., Paik, J. Y., Oh, H., Park, J. W., . . . Lee, K. H. (2013). Resveratrol suppresses cancer cell glucose uptake by targeting reactive oxygen species-mediated hypoxia-inducible factor-1alpha activation. *J Nucl Med*, 54 (12), 2161-7.

- Kahn, B. B., Alquier, T., Carling, D. and Hardie, D. G. (2005). AMP-activated protein kinase: ancient energy gauge provides clues to modern understanding of metabolism. *Cell Metab*, 1 (1), 15-25.
- Kahn, S. E., Hull, R. L. and Utzschneider, K. M. (2006). Mechanisms linking obesity to insulin resistance and type 2 diabetes. *Nature*, 444 (7121), 840-846.
- Katunuma, N., Ohashi, A., Sano, E., Ishimaru, N., Hayashi, Y. and Murata, E. (2006). Catechin derivatives: specific inhibitor for caspases-3, 7 and 2, and the prevention of apoptosis at the cell and animal levels. *FEBS Lett*, 580 (3), 741-6.
- Kelly, B., Hattersley, L., King, L. and Flood, V. (2008). Persuasive food marketing to children: use of cartoons and competitions in Australian commercial television advertisements. *Health Promot Int*, 23 (4), 337-44.
- Kemp, B. E., Stapleton, D., Campbell, D. J., Chen, Z. P., Murthy, S., Walter, M., . . . Witters, L. A. (2003). AMP-activated protein kinase, super metabolic regulator. *Biochemical Society Transactions*, 31 162-168.
- Kennecke, H., Yerushalmi, R., Woods, R., Cheang, M. C., Voduc, D., Speers, C. H., . . . Gelmon, K. (2010). Metastatic behavior of breast cancer subtypes. *J Clin Oncol*, 28 (20), 3271-7.
- Khan, A. H. and Pessin, J. E. (2002). Insulin regulation of glucose uptake: A complex interplay of intracellular signalling pathways. *Diabetologia*, 45 (11), 1475-1483.
- Kim, E. K. and Choi, E. J. (2010). Pathological roles of MAPK signaling pathways in human diseases. *Biochimica Et Biophysica Acta-Molecular Basis of Disease*, 1802 (4), 396-405.
- Kim, H. J., Kim, S. K., Kim, B. S., Lee, S. H., Park, Y. S., Park, B. K., . . . Jung, J. Y. (2010). Apoptotic effect of quercetin on HT-29 colon cancer cells via the AMPK signaling pathway. *J Agric Food Chem*, 58 (15), 8643-50.
- Kim, I. and He, Y. Y. (2013). Targeting the AMP-Activated Protein Kinase for Cancer Prevention and Therapy. *Front Oncol*, 3 175.
- Kim, J.-w., Tchernyshyov, I., Semenza, G. L. and Dang, C. V. (2006a). HIF-1-mediated expression of pyruvate dehydrogenase kinase: A metabolic switch required for cellular adaptation to hypoxia. *Cell Metabolism*, 3 (3), 177-185.
- Kim, J. J., Tan, Y., Xiao, L., Sun, Y. L. and Qu, X. (2013). Green tea polyphenol epigallocatechin-3-gallate enhance glycogen synthesis and inhibit lipogenesis in hepatocytes. *Biomed. Res. Int.*, 2013 1-8.
- Kim, J. J. Y. (2014). Green tea polyphenols a natural therapeutic approach for metabolic syndrome and diabetes prevention. PhD thesis. University of Technology Sydney. Sydney, Australia.
- Kim, J. W., Gao, P., Liu, Y. C., Semenza, G. L. and Dang, C. V. (2007). Hypoxia-inducible factor I and dysregulated c-myc cooperatively induce vascular endothelial growth factor and metabolic switches hexokinase 2 and pyruvate dehydrogenase kinase 1. *Molecular and Cellular Biology*, 27 (21), 7381-7393.
- Kim, Y. I., Lee, F. N., Choi, W. S., Lee, S. and Youn, J. H. (2006b). Insulin regulation of skeletal muscle PDK4 mRNA expression is impaired in acute insulin-resistant states. *Diabetes*, 55 (8), 2311-7.
- King, A. J. F. (2012). The use of animal models in diabetes research. *British Journal of Pharmacology*, 166 (3), 877-894.
- Klaus, S., Pultz, S., Thone-Reineke, C. and Wolfram, S. (2005). Epigallocatechin gallate attenuates diet-induced obesity in mice by decreasing energy absorption and increasing fat oxidation. *Int J Obes (Lond)*, 29 (6), 615-23.
- Klein, C. A. (2009). Parallel progression of primary tumours and metastases. *Nat Rev Cancer*, 9 (4), 302-312.
- Knopfholz, J., Disslerol, C. C., Pierin, A. J., Schirr, F. L., Streisky, L., Takito, L. L., . . . Bandeira, A. M. (2014). Validation of the friedewald formula in patients with metabolic syndrome. *Cholesterol*, 2014 261878.
- Kohno, D., Gao, H. Z., Muroya, S., Kikuyama, S. and Yada, T. (2003). Ghrelin directly interacts with neuropeptide-Y-containing neurons in the rat arcuate nucleus Ca<sup>2+</sup> signalling via protein kinase A and N-type channel-dependent mechanisms and cross-talk with leptin and orexin. *Diabetes*, 52 (4), 948-956.
- Koo, M. and Cho, C. (2004). Pharmacological effects of green tea on the gastrointestinal system. *Eur. J. Pharmacol.*, 500 (1-3), 177-185.

- Koppenol, W. H., Bounds, P. L. and Dang, C. V. (2011). Otto Warburg's contributions to current concepts of cancer metabolism (vol 11, pg 325, 2011). *Nature Reviews Cancer*, 11 (8), 618-618.
- Kozłowski, J., Kozłowska, A. and Kocki, J. (2015). Breast cancer metastasis - insight into selected molecular mechanisms of the phenomenon. *Postępy Hig Med Dosw (Online)*, 69 447-51.
- Kozuma, K., Chikama, A., Hoshino, E., Kataoka, K., Mori, K., Hase, T., . . . Nakamura, H. (2005). Effect of Intake of a Beverage Containing 540 mg Catechins on the Body Composition of Obese Women and Men. *Progress in Medicine*, 25 (7), 1945-1957.
- Krafts, K. P. (2010). Tissue repair The hidden drama. *Organogenesis*, 6 (4), 225-233.
- Kroemer, G. (2006). Mitochondria in cancer. *Oncogene*, 25 (34), 4630-2.
- Kuhajda, F. P. (2008). AMP-activated protein kinase and human cancer: cancer metabolism revisited. *Int J Obes (Lond)*, 32 Suppl 4 S36-41.
- Kumar, v., Abbas, A., Fausto, N. and Aster, J. (2010). *Tissue renewal, regeneration and repair*. 8th. In: Robbins, S. L. and Cotran, R. S. (2010). *Pathologic basis of disease*. Philadelphia: Elsevier. 3.
- Kuneš, J. (2014). Western diet and/or lifestyle: is this a big health problem? *Experimental Physiology*, 99 (9), 1180-1181.
- Kushima, Y., Iida, K., Nagaoka, Y., Kawaratani, Y., Shirahama, T., Sakaguchi, M., . . . Uesato, S. (2009). Inhibitory Effect of (-)-Epigallocatechin and (-)-Epigallocatechin Gallate against Heregulin beta 1-Induced Migration/Invasion of the MCF-7 Breast Carcinoma Cell Line. *Biological & Pharmaceutical Bulletin*, 32 (5), 899-904.
- la Fleur, S. E., Luijendijk, M. C., van Rozen, A. J., Kalsbeek, A. and Adan, R. A. (2011). A free-choice high-fat high-sugar diet induces glucose intolerance and insulin unresponsiveness to a glucose load not explained by obesity. *Int J Obes (Lond)*, 35 (4), 595-604.
- Laderoute, K. R., Calaoagan, J. M., Chao, W. R., Dinh, D., Denko, N., Duellman, S., . . . Boros, L. G. (2014). 5'-AMP-activated protein kinase (AMPK) supports the growth of aggressive experimental human breast cancer tumors. *J Biol Chem*, 289 (33), 22850-64.
- Lai, W. W., Hsu, S. C., Chueh, F. S., Chen, Y. Y., Yang, J. S., Lin, J. P., . . . Chung, J. G. (2013). Quercetin inhibits migration and invasion of SAS human oral cancer cells through inhibition of NF-kappaB and matrix metalloproteinase-2/-9 signaling pathways. *Anticancer Res*, 33 (5), 1941-50.
- Landau, B. R., Wahren, J., Chandramouli, V., Schumann, W. C., Ekberg, K. and Kalhan, S. C. (1996). Contributions of gluconeogenesis to glucose production in the fasted state. *Journal of Clinical Investigation*, 98 (2), 378-385.
- Lander, E. S., Consortium, I. H. G. S., Linton, L. M., Birren, B., Nusbaum, C., Zody, M. C., . . . Conso, I. H. G. S. (2001). Initial sequencing and analysis of the human genome. *Nature*, 409 (6822), 860-921.
- Lann, D. and LeRoith, D. (2008). The Role of Endocrine Insulin-Like Growth Factor-I and Insulin in Breast Cancer. *Journal of Mammary Gland Biology and Neoplasia*, 13 (4), 371-379.
- Lanner, J. T., Katz, A., Tavi, P., Sandstrom, M. E., Zhang, S. J., Wretman, C., . . . Westerblad, H. (2006). The role of Ca<sup>2+</sup> influx for insulin-mediated glucose uptake in skeletal muscle. *Diabetes*, 55 (7), 2077-2083.
- Lao, W., Tan, Y., Jin, X., Xiao, L., Kim, J. J. Y. and Qu, X. (2015). Comparison of Cytotoxicity and the Anti-Adipogenic Effect of Green Tea Polyphenols with Epigallocatechin-3-Gallate in 3T3-L1 Preadipocytes. *The American Journal of Chinese Medicine*, 43 (06), 1177-1190.
- Laron, Z. (2001). Insulin-like growth factor 1 (IGF-1): a growth hormone. *Journal of Clinical Pathology-Molecular Pathology*, 54 (5), 311-316.
- Larsson, S. C., Mantzoros, C. S. and Wolk, A. (2007). Diabetes mellitus and risk of breast cancer: a meta-analysis. *Int J Cancer*, 121 (4), 856-62.
- Lebovitz, H. E. (2006). Insulin resistance--a common link between type 2 diabetes and cardiovascular disease. *Diabetes Obes Metab*, 8 (3), 237-49.
- Lee, H., Bae, S. and Yoon, Y. (2013). The anti-adipogenic effects of (-)-epigallocatechin gallate are dependent on the WNT/beta-catenin pathway. *Journal of Nutritional Biochemistry*, 24 (7), 1232-1240.
- Lee, I.-K. (2014). The Role of Pyruvate Dehydrogenase Kinase in Diabetes and Obesity. *Diabetes & Metabolism Journal*, 38 (3), 181-186.

- Lee, M. S., Kim, C. T., Kim, I. H. and Kim, Y. (2009a). Inhibitory effects of green tea catechin on the lipid accumulation in 3T3-L1 adipocytes. *Phytother Res*, 23 (8), 1088-91.
- Lee, M. S., Kim, C. T. and Kim, Y. (2009b). Green tea (-)-epigallocatechin-3-gallate reduces body weight with regulation of multiple genes expression in adipose tissue of diet-induced obese mice. *Ann Nutr Metab*, 54 (2), 151-7.
- Leney, S. E. and Tavaré, J. M. (2009). The molecular basis of insulin-stimulated glucose uptake: signalling, trafficking and potential drug targets. *Journal of Endocrinology*, 203 (1), 1-18.
- Leong, A. S. and Zhuang, Z. (2011). The changing role of pathology in breast cancer diagnosis and treatment. *Pathobiology*, 78 (2), 99-114.
- Li, C., Liu, V. W., Chiu, P. M., Yao, K.-M., Ngan, H. Y. and Chan, D. W. (2014). Reduced expression of AMPK- $\beta$ 1 during tumor progression enhances the oncogenic capacity of advanced ovarian cancer. *Molecular Cancer*, 13 (1), 1-12.
- Li, C. I., Malone, K. E., Saltzman, B. S. and Daling, J. R. (2006a). Risk of invasive breast carcinoma among women diagnosed with ductal carcinoma in situ and lobular carcinoma in situ, 1988-2001. *Cancer*, 106 (10), 2104-12.
- Li, N., Tan, W., Li, N., Li, P., Lee, S., Wang, Y. and Gong, Y. (2011a). Glucose Metabolism in Breast Cancer and its Implication in Cancer Therapy. *International Journal of Clinical Medicine*, Vol.02No.02 18.
- Li, Q. O., Zhao, H. F., Zhao, M., Zhang, Z. F. and Li, Y. (2010). Chronic green tea catechins administration prevents oxidative stress-related brain aging in C57BL/6J mice. *Brain Research*, 1353 28-35.
- Li, R. W., Douglas, T. D., Maiyoh, G. K., Adeli, K. and Theriault, A. G. (2006b). Green tea leaf extract improves lipid and glucose homeostasis in a fructose-fed insulin-resistant hamster model. *Journal of Ethnopharmacology*, 104 (1-2), 24-31.
- Li, Y., Zhao, S., Zhang, W., Zhao, P., He, B., Wu, N. and Han, P. (2011b). Epigallocatechin-3-O-gallate (EGCG) attenuates FFAs-induced peripheral insulin resistance through AMPK pathway and insulin signaling pathway in vivo. *Diabetes Res Clin Pract*, 93 (2), 205-14.
- Liang, C. C., Park, A. Y. and Guan, J. L. (2007). In vitro scratch assay: a convenient and inexpensive method for analysis of cell migration in vitro. *Nature Protocols*, 2 (2), 329-333.
- Liang, Y., Yan, C. and Schor, N. F. (2001). Apoptosis in the absence of caspase 3. *Oncogene*, 20 (45), 6570-8.
- Liang, Y. C., Lin-Shiau, S. Y., Chen, C. F. and Lin, J. K. (1999). Inhibition of cyclin-dependent kinases 2 and 4 activities as well as induction of Cdk inhibitors p21 and p27 during growth arrest of human breast carcinoma cells by (-)-epigallocatechin-3-gallate. *Journal of Cellular Biochemistry*, 75 (1), 1-12.
- Liao, S. C., Li, J. X., Wei, W., Wang, L. J., Zhang, Y. M., Li, J. J., . . . Sun, S. R. (2011). Association between Diabetes Mellitus and Breast Cancer Risk: a Meta-analysis of the Literature. *Asian Pacific Journal of Cancer Prevention*, 12 (4), 1061-1065.
- Lim, J. S., Mietus-Snyder, M., Valente, A., Schwarz, J.-M. and Lustig, R. H. (2010). The role of fructose in the pathogenesis of NAFLD and the metabolic syndrome. *Nat Rev Gastroenterol Hepatol*, 7 (5), 251-264.
- Lipscombe, L. L., Fischer, H. D., Austin, P. C., Fu, L. D., Jaakkimainen, R. L., Ginsburg, O., . . . Paszat, L. (2015). The association between diabetes and breast cancer stage at diagnosis: a population-based study. *Breast Cancer Research and Treatment*, 150 (3), 613-620.
- Liu, B., Chen, Y. M. and Clair, D. K. S. (2008a). ROS and p53: A versatile partnership. *Free Radical Biology and Medicine*, 44 (8), 1529-1535.
- Liu, C. H., Tang, W. C., Sia, P., Huang, C. C., Yang, P. M., Wu, M. H., . . . Lee, K. H. (2015). Berberine Inhibits the Metastatic Ability of Prostate Cancer Cells by Suppressing Epithelial-to-Mesenchymal Transition (EMT)-Associated Genes with Predictive and Prognostic Relevance. *International Journal of Medical Sciences*, 12 (1), 63-71.
- Liu, Y., Dentin, R., Chen, D., Hedrick, S., Ravnskjaer, K., Schenk, S., . . . Montminy, M. (2008b). A fasting inducible switch modulates gluconeogenesis via activator/coactivator exchange. *Nature*, 456 (7219), 269-U74.
- Livak, K. J. and Schmittgen, T. D. (2001). Analysis of relative gene expression data using real-time quantitative PCR and the 2(-Delta Delta C(T)) Method. *Methods*, 25 (4), 402-8.

- Lizcano, J. M., Goransson, O., Toth, R., Deak, M., Morrice, N. A., Boudeau, J., . . . Alessi, D. R. (2004). LKB1 is a master kinase that activates 13 kinases of the AMPK subfamily, including MARK/PAR-1. *Embo Journal*, 23 (4), 833-843.
- Llewellyn, C. H., van Jaarsveld, C. H. M., Boniface, D., Carnell, S. and Wardle, J. (2008). Eating rate is a heritable phenotype related to weight in children. *American Journal of Clinical Nutrition*, 88 (6), 1560-1566.
- Lorusso, G. and Ruegg, C. (2012). New insights into the mechanisms of organ-specific breast cancer metastasis. *Semin Cancer Biol*, 22 (3), 226-33.
- Lu, Q. Y., Zhang, L., Yee, J. K., Go, V. W. and Lee, W. N. (2015). Metabolic Consequences of LDHA inhibition by Epigallocatechin Gallate and Oxamate in MIA PaCa-2 Pancreatic Cancer Cells. *Metabolomics*, 11 (1), 71-80.
- Lunt, S. Y. and Vander Heiden, M. G. (2011). Aerobic glycolysis: meeting the metabolic requirements of cell proliferation. *Annu Rev Cell Dev Biol*, 27 441-64.
- Mackenzie, T., Leary, L. and Brooks, W. B. (2007). The effect of an extract of green and black tea on glucose control in adults with type 2 diabetes mellitus: double-blind randomized study. *Metabolism*, 56 (10), 1340-4.
- Maffeis, C. (2000). Aetiology of overweight and obesity in children and adolescents. *European Journal of Pediatrics*, 159 S35-S44.
- Mahlapuu, M., Johansson, C., Lindgren, K., Hjalm, G., Barnes, B. R., Krook, A., . . . Marklund, S. (2004). Expression profiling of the gamma-subunit isoforms of AMP-activated protein kinase suggests a major role for gamma 3 in white skeletal muscle. *American Journal of Physiology-Endocrinology and Metabolism*, 286 (2), E194-E200.
- Mak, J. C. (2012). Potential role of green tea catechins in various disease therapies: progress and promise. *Clin. Exp. Pharmacol. Physiol.*, 39 (3), 265-273.
- Makki, K., Froguel, P. and Wolowczuk, I. (2013). Adipose tissue in obesity-related inflammation and insulin resistance: cells, cytokines, and chemokines. *ISRN Inflamm*, 2013 139239.
- Mandel, S., Maor, G. and Youdim, M. H. (2004). Iron and  $\alpha$ -synuclein in the substantia nigra of MPTP-treated mice. *Journal of Molecular Neuroscience*, 24 (3), 401-416.
- Manning, B. D. and Cantley, L. C. (2007). AKT/PKB signaling: Navigating downstream. *Cell*, 129 (7), 1261-1274.
- Manzel, A., Muller, D. N., Hafler, D. A., Erdman, S. E., Linker, R. A. and Kleinewietfeld, M. (2014). Role of “Western Diet” in Inflammatory Autoimmune Diseases. *Current allergy and asthma reports*, 14 (1), 404-404.
- Martín-Timón, I., Sevillano-Collantes, C., Segura-Galindo, A. and del Cañizo-Gómez, F. J. (2014). Type 2 diabetes and cardiovascular disease: Have all risk factors the same strength? *World J Diabetes*, 5 (4), 444-70.
- Maruyama, T., Murata, S., Nakayama, K., Sano, N., Ogawa, K., Nowatari, T., . . . Ohkohchi, N. (2014). (-)-Epigallocatechin-3-gallate suppresses liver metastasis of human colorectal cancer. *Oncol Rep*, 31 (2), 625-33.
- Matoba, S., Kang, J. G., Patino, W. D., Wragg, A., Boehm, M., Gavrilova, O., . . . Hwang, P. M. (2006). p53 regulates mitochondrial respiration. *Science*, 312 (5780), 1650-3.
- Mayo, K. E., Miller, L. J., Bataille, D., Dalle, S., Goke, B., Thorens, B. and Drucker, D. J. (2003). International union of pharmacology. XXXV. The glucagon receptor family. *Pharmacological Reviews*, 55 (1), 167-194.
- McArdle, M. A., Finucane, O. M., Connaughton, R. M., McMorrow, A. M. and Roche, H. M. (2013). Mechanisms of obesity-induced inflammation and insulin resistance: insights into the emerging role of nutritional strategies. *Front Endocrinol (Lausanne)*, 4 52.
- McBride, A., Ghilagaber, S., Nikolaev, A. and Hardie, D. G. (2009). The Glycogen-Binding Domain on the AMPK beta Subunit Allows the Kinase to Act as a Glycogen Sensor. *Cell Metabolism*, 9 (1), 23-34.
- McKay, D. and Blumberg, J. (2002). The Role of Tea in Human Health: An Update. *Journal of the American College of Nutrition.*, 21 (1), 1-13.
- Mckee, T. and Mckee, J. (2013). *Biochemistry: The molecular basis of life*. 5th.USA: Oxford University Press.

- Medh, R. D. and Thompson, E. B. (2000). Hormonal regulation of physiological cell turnover and apoptosis. *Cell Tissue Res*, 301 (1), 101-24.
- Mochizuki, M. and Hasegawa, N. (2004). Effects of green tea catechin-induced lipolysis on cytosol glycerol content in differentiated 3T3-L1 cells. *Phytother Res*, 18 (11), 945-6.
- Mogensen, M. and Sahlin, K. (2005). Mitochondrial efficiency in rat skeletal muscle: influence of respiration rate, substrate and muscle type. *Acta Physiologica Scandinavica*, 185 (3), 229-236.
- Montgomery, M. K. and Turner, N. (2015). Mitochondrial dysfunction and insulin resistance: an update. *Endocr Connect*, 4 (1), R1-R15.
- Moreira, L., Araujo, I., Costa, T., Correia-Branco, A., Faria, A., Martel, F. and Keating, E. (2013). Quercetin and epigallocatechin gallate inhibit glucose uptake and metabolism by breast cancer cells by an estrogen receptor-independent mechanism. *Experimental Cell Research*, 319 (12), 1784-1795.
- Moreno, M. F., De Laquila, R., Okuda, M. H., Lira, F. S., de Souza, G. I. d. M. H., de Souza, C. T., . . . Oyama, L. M. (2014). Metabolic profile response to administration of epigallocatechin-3-gallate in high-fat-fed mice. *Diabetology & Metabolic Syndrome*, 6 (1), 84.
- Morino, K., Petersen, K. F. and Shulman, G. I. (2006). Molecular mechanisms of insulin resistance in humans and their potential links with mitochondrial dysfunction. *Diabetes*, 55 S9-S15.
- Mu, J., Barton, E. R. and Birnbaum, M. J. (2003). Selective suppression of AMP-activated protein kinase in skeletal muscle: update on 'lazy mice'. *Biochem Soc Trans*, 31 (Pt 1), 236-41.
- Mukhtar, E., Adhami, V. M., Khan, N. and Mukhtar, H. (2012). Apoptosis and autophagy induction as mechanism of cancer prevention by naturally occurring dietary agents. *Curr Drug Targets*, 13 (14), 1831-41.
- Muoio, D. M. and Newgard, C. B. (2008). Molecular and metabolic mechanisms of insulin resistance and [beta]-cell failure in type 2 diabetes. *Nat Rev Mol Cell Biol*, 9 (3), 193-205.
- Murase, T., Misawa, K., Haramizu, S. and Hase, T. (2009). Catechin-induced activation of the LKB1/AMP-activated protein kinase pathway. *Biochem. Pharmacol.*, 78 (1), 78-84.
- Nathan, D. M., Buse, J. B., Davidson, M. B., Ferrannini, E., Holman, R. R., Sherwin, R. and Zinman, B. (2009). Medical Management of Hyperglycemia in Type 2 Diabetes: A Consensus Algorithm for the Initiation and Adjustment of Therapy: A consensus statement of the American Diabetes Association and the European Association for the Study of Diabetes. *Diabetes Care*, 32 (1), 193-203.
- Nishiumi, S., Bessyo, H., Kubo, M., Aoki, Y., Tanaka, A., Yoshida, K. and Ashida, H. (2010). Green and black tea suppress hyperglycemia and insulin resistance by retaining the expression of glucose transporter 4 in muscle of high-fat diet-fed C57BL/6J mice. *J Agric Food Chem*, 58 (24), 12916-23.
- Nomura, S., Ichinose, T., Jinde, M., Kawashima, Y., Tachlyashiki, K. and Imaizumi, K. (2008). Tea catechins enhance the mRNA expression of uncoupling protein 1 in rat brown adipose tissue. *Journal of Nutritional Biochemistry*, 19 (12), 840-847.
- Nomura, S., Monobe, M., Ema, K., Matsunaga, A., Yamamoto, M. and Hideki, H. (2015). Effects of flavonol-rich green tea (*Camellia sinensis* L. cv. Sofu) on blood glucose and insulin levels in diabetic mice. *Integr Obesity Diabetes*, 1 (5), 109-111.
- Nowis, D., Malenda, A., Furs, K., Oleszczak, B., Sadowski, R., Chlebowska, J., . . . Golab, J. (2014). Statins impair glucose uptake in human cells. *BMJ. Open Diabetes Research and Care*, 2 1-11.
- O'Neil, R. G., Wu, L. and Mullani, N. (2005). Uptake of a fluorescent deoxyglucose analog (2-NBDG) in tumor cells. *Mol Imaging Biol*, 7 (6), 388-92.
- O-Sullivan, I., Zhang, W., Wasserman, D. H., Liew, C. W., Liu, J., Paik, J., . . . Unterman, T. G. (2015). FoxO1 integrates direct and indirect effects of insulin on hepatic glucose production and glucose utilization. *Nat Commun*, 6
- Ohtsubo, K., Takamatsu, S., Minowa, M. T., Yoshida, A., Takeuchi, M. and Marth, J. (2005). Dietary and genetic control of glucose transporter 2 glycosylation promotes insulin secretion in suppressing diabetes. *Cell*, 123 (7), 1307-1321.
- Orci, L., Cook, W. S., Ravazzola, M., Wang, M. Y., Park, B. H., Montesano, R. and Unger, R. H. (2004). Rapid transformation of white adipocytes into fat-oxidizing machines. *Proceedings of the National Academy of Sciences of the United States of America*, 101 (7), 2058-2063.

- Ortsater, H., Grankvist, N., Wolfram, S., Kuehn, N. and Sjöholm, A. (2012). Diet supplementation with green tea extract epigallocatechin gallate prevents progression to glucose intolerance in db/db mice. *Nutr Metab (Lond)*, 9 11.
- Paget, S. (1989). The distribution of secondary growths in cancer of the breast. 1889. *Cancer Metastasis Rev*, 8 (2), 98-101.
- Pallottini, V., Montanari, L., Cavallini, G., Bergamini, E., Gori, Z. and Trentalance, A. (2004). Mechanisms underlying the impaired regulation of 3-hydroxy-3-methylglutaryl coenzyme A reductase in aged rat liver. *Mechanisms of Ageing and Development*, 125 (9), 633-639.
- Pang, G., Xie, J., Chen, Q. and Hu, Z. (2014). Energy intake, metabolic homeostasis, and human health. *Food Science and Human Wellness*, 3 (3-4), 89-103.
- Pang, J., Xi, C., Huang, X. Q., Cui, J., Gong, H. and Zhang, T. M. (2016). Effects of Excess Energy Intake on Glucose and Lipid Metabolism in C57BL/6 Mice. *Plos One*, 11 (1),
- Pantel, K. and Brakenhoff, R. H. (2004). Dissecting the metastatic cascade. *Nat Rev Cancer*, 4 (6), 448-56.
- Papandreou, I., Cairns, R. A., Fontana, L., Lim, A. L. and Denko, N. C. (2006). HIF-1 mediates adaptation to hypoxia by actively downregulating mitochondrial oxygen consumption. *Cell Metabolism*, 3 (3), 187-197.
- Papas, M. A., Alberg, A. J., Ewing, R., Helzlsouer, K. J., Gary, T. L. and Klassen, A. C. (2007). The built environment and obesity. *Epidemiol Rev*, 29 129-43.
- Parise, C. A. and Caggiano, V. (2014). Breast Cancer Survival Defined by the ER/PR/HER2 Subtypes and a Surrogate Classification according to Tumor Grade and Immunohistochemical Biomarkers. *J Cancer Epidemiol*, 2014 469251.
- Park, H., DiNatale, D., Chung, M., Park, Y., Lee, J., Koo, S., . . . Bruno, R. (2011). Green tea extract attenuates hepatic steatosis by decreasing adipose lipogenesis and enhancing hepatic antioxidant defenses in ob/ob mice. *J. Nutr. Biochem.*, 22 (4), 393-400.
- Park, H. U., Suy, S., Danner, M., Dailey, V., Zhang, Y., Li, H., . . . Collins, S. P. (2009). AMP-activated protein kinase promotes human prostate cancer cell growth and survival. *Mol Cancer Ther*, 8 (4), 733-41.
- Park, J., Morley, T. S., Kim, M., Clegg, D. J. and Scherer, P. E. (2014). Obesity and cancer-mechanisms underlying tumour progression and recurrence. *Nature Reviews Endocrinology*, 10 (8), 455-465.
- Peres, R., Tonin, F., Tavares, M. and Rodriguez-Amaya, D. (2011). Determination of catechins in green tea infusions by reduced flow micellar electrokinetic chromatography. *Food Chem*, 127 (2), 651-655.
- Perou, C. M., Sorlie, T., Eisen, M. B., van de Rijn, M., Jeffrey, S. S., Rees, C. A., . . . Botstein, D. (2000). Molecular portraits of human breast tumours. *Nature*, 406 (6797), 747-52.
- Persaud, S. J., Liu, B. and Jones, P. M. (2012). *Functional Analysis of Human Islets of Langerhans Maintained in Culture*. In: Mitry, R. R. and Hughes, R. D. (2012). Totowa, NJ: Humana Press.
- Pessin, J. E. and Saltiel, a. A. R. (2000). Signaling pathways in insulin action: molecular targets of insulin resistance. *The Journal of Clinical Investigation*, 106 (2), 165-169.
- Petersen, K. F. and Shulman, G. I. (2006). Etiology of insulin resistance. *American Journal of Medicine*, 119 (5), 10s-16s.
- Piris, A. and Mihm, M. C., Jr. (2007). Mechanisms of metastasis: seed and soil. *Cancer Treat Res*, 135 119-27.
- Qin, B., Polansky, M., Harry, D. and Anderson, R. (2010). Green tea polyphenols improve cardiac muscle mRNA and protein levels of signal pathways related to insulin and lipid metabolism and inflammation in insulin-resistant rats. *Mol. Nutr. Food Res.*, 54 Suppl 1 S14-23.
- Qin, J., Wang, Y., Bai, Y., Yang, K., Mao, Q., Lin, Y., . . . Xie, L. (2012). Epigallocatechin-3-gallate inhibits bladder cancer cell invasion via suppression of NF-kappaB-mediated matrix metalloproteinase-9 expression. *Mol Med Rep*, 6 (5), 1040-4.
- Rains, T., Agarwal, S. and Maki, K. (2011). Antiobesity effects of green tea catechins: a mechanistic review. *J. Nutr. Biochem.*, 22 (1), 1-7.
- Rameh, L. E. and Cantley, L. C. (1999). The role of phosphoinositide 3-kinase lipid products in cell function. *Journal of Biological Chemistry*, 274 (13), 8347-8350.
- Rasouli, N. and Kern, P. (2008). Adipocytokines and the metabolic complications of obesity. *J. Clin. Endocrinol. Metab.*, 93 (11 Suppl 1), S64-73.

- Reeves, G. K., Pirie, K., Beral, V., Green, J., Spencer, E., Bull, D. and Million Women Study, C. (2007). Cancer incidence and mortality in relation to body mass index in the Million Women Study: cohort study. *BMJ*, 335 (7630), 1134.
- Reynolds, A. R. (2010). Potential Relevance of Bell-Shaped and U-Shaped Dose-Responses for the Therapeutic Targeting of Angiogenesis in Cancer. *Dose-Response*, 8 (3), 253-284.
- Richard, D., Kefi, K., Barbe, U., Poli, A., Bausero, P. and Visioli, F. (2009). Weight and plasma lipid control by decaffeinated green tea. *Pharmacol. Res.*, 59 (5), 351-354.
- Rios, M., Foretz, M., Viollet, B., Prieto, A., Fraga, M., Garcia-Caballero, T., . . . Senaris, R. (2014). Lipoprotein internalisation induced by oncogenic AMPK activation is essential to maintain glioblastoma cell growth. *Eur J Cancer*, 50 (18), 3187-97.
- Ritov, V. B., Menshikova, E. V., He, J., Ferrell, R. E., Goodpaster, B. H. and Kelley, D. E. (2005). Deficiency of subsarcolemmal mitochondria in obesity and type 2 diabetes. *Diabetes*, 54 (1), 8-14.
- Ritze, Y., Bardos, G., D'Haese, J. G., Ernst, B., Thurnheer, M., Schultes, B. and Bischoff, S. C. (2014). Effect of High Sugar Intake on Glucose Transporter and Weight Regulating Hormones in Mice and Humans. *Plos One*, 9 (7),
- Robey, R. B. and Hay, N. (2009). Is Akt the "Warburg kinase"?-Akt-energy metabolism interactions and oncogenesis. *Seminars in Cancer Biology*, 19 (1), 25-31.
- Robinson, T. N. (2001). Television viewing and childhood obesity. *Pediatric Clinics of North America*, 48 (4), 1017-+.
- Roghani, M. and Baluchnejadmojarad, T. (2010). Hypoglycemic and hypolipidemic effect and antioxidant activity of chronic epigallocatechin-gallate in streptozotocin-diabetic rats. *Pathophysiology.*, 17 (1), 55-59.
- Rosa, M. (2015). Advances in the Molecular Analysis of Breast Cancer: Pathway Toward Personalized Medicine. *Cancer Control*, 22 (2), 211-9.
- Rose, D. P. and Vona-Davis, L. (2012). The cellular and molecular mechanisms by which insulin influences breast cancer risk and progression. *Endocr Relat Cancer*, 19 (6), R225-41.
- Rossner, S. (2002). Obesity: the disease of the twenty-first century. *Int J Obes Relat Metab Disord*, 26 Suppl 4 S2-4.
- Roy, A. M., Baliga, M. S. and Katiyar, S. K. (2005). Epigallocatechin-3-gallate induces apoptosis in estrogen receptor-negative human breast carcinoma cells via modulation in protein expression of p53 and Bax and caspase-3 activation. *Molecular Cancer Therapeutics*, 4 (1), 81-90.
- Rui, L. Y. (2014). Energy Metabolism in the Liver. *Comprehensive Physiology*, 4 (1), 177-197.
- Saha, A. K. and Ruderman, N. B. (2003). Malonyl-CoA and AMP-activated protein kinase: An expanding partnership. *Molecular and Cellular Biochemistry*, 253 (1-2), 65-70.
- Saltiel, A. and Kahn, C. (2001). Insulin signalling and the regulation of glucose and lipid metabolism. *Nature.*, 414 799-806.
- Santamarina, A. B., Carvalho-Silva, M., Gomes, L. M., Okuda, M. H., Santana, A. A., Streck, E. L., . . . Oyama, L. M. (2015). Decaffeinated green tea extract rich in epigallocatechin-3-gallate prevents fatty liver disease by increased activities of mitochondrial respiratory chain complexes in diet-induced obesity mice. *The Journal of Nutritional Biochemistry*, 26 (11), 1348-1356.
- Santana, A., Santamarina, A., Souza, G., Mennitti, L., Okuda, M., Venancio, D., . . . Oyama, L. (2015). Decaffeinated green tea extract rich in epigallocatechin-3-gallate improves insulin resistance and metabolic profiles in normolipidic diet-but not high-fat diet-fed mice. *Journal of Nutritional Biochemistry*, 26 (9), 893-902.
- Santarpia, L., Lippman, S. M. and El-Naggar, A. K. (2012). Targeting the MAPK-RAS-RAF signaling pathway in cancer therapy. *Expert Opin Ther Targets*, 16 (1), 103-19.
- Savage, D. B., Petersen, K. F. and Shulman, G. I. (2005). Mechanisms of insulin resistance in humans and possible links with inflammation. *Hypertension*, 45 (5), 828-33.
- Schenk, S., Saberi, M. and Olefsky, J. M. (2008). Insulin sensitivity: modulation by nutrients and inflammation. *Journal of Clinical Investigation*, 118 (9), 2992-3002.
- Schnitt, S. J. (2010). Classification and prognosis of invasive breast cancer: from morphology to molecular taxonomy. *Mod Pathol*, 23 Suppl 2 S60-4.
- Schultz, A., Neil, D., Aguila, M. B. and Mandarim-de-Lacerda, C. A. (2013). Hepatic adverse effects of fructose consumption independent of overweight/obesity. *Int J Mol Sci*, 14 (11), 21873-86.

- Schultze, S. M., Hemmings, B. A., Niessen, M. and Tschopp, O. (2012). PI3K/AKT, MAPK and AMPK signalling: protein kinases in glucose homeostasis. *Expert Reviews in Molecular Medicine*, 14
- Schultze, S. M., Jensen, J., Hemmings, B. A., Tschopp, O. and Niessen, M. (2011). Promiscuous affairs of PKB/AKT isoforms in metabolism. *Arch Physiol Biochem*, 117 (2), 70-7.
- Semenza, G. L. (2010). HIF-1: upstream and downstream of cancer metabolism. *Current Opinion in Genetics & Development*, 20 (1), 51-56.
- Senanayake, N. (2013). Green tea extract: Chemistry, antioxidant properties and food applications – A review. *Journal of Functional Foods*, 5 (4), 1529-1541.
- Senthilkumar, K., Arunkumar, R., Elumalai, P., Sharmila, G., Gunadharini, D. N., Banudevi, S., . . . Arunakaran, J. (2011). Quercetin inhibits invasion, migration and signalling molecules involved in cell survival and proliferation of prostate cancer cell line (PC-3). *Cell Biochem Funct*, 29 (2), 87-95.
- Seo, M., Crochet, R. B. and Lee, a. Y.-H. (2014). *Metabolic alteration in cancer*. 2nd. In: Neidle, S. (2014). USA: Academic Press. 14.
- Sesti, G. (2006). Pathophysiology of insulin resistance. *Best Practice & Research Clinical Endocrinology & Metabolism*, 20 (4), 665-679.
- Sesti, G., Federici, M., Hribal, M. L., Lauro, D., Sbraccia, P. and Lauro, R. (2001). Defects of the insulin receptor substrate (IRS) system in human metabolic disorders. *Faseb Journal*, 15 (12), 2099-2111.
- Shakya, A., Cooksey, R., Cox, J. E., Wang, V., McClain, D. A. and Tantin, D. (2009). Oct1 loss of function induces a coordinate metabolic shift that opposes tumorigenicity. *Nature Cell Biology*, 11 (3), 320-U204.
- Shankar, S., Ganapathy, S. and Srivastava, R. K. (2007). Green tea polyphenols: biology and therapeutic implications in cancer. *Front Biosci*, 12 4881-99.
- Sharma, C., Nusri Qel, A., Begum, S., Javed, E., Rizvi, T. A. and Hussain, A. (2012). (-)-Epigallocatechin-3-gallate induces apoptosis and inhibits invasion and migration of human cervical cancer cells. *Asian Pac J Cancer Prev*, 13 (9), 4815-22.
- Siddiqui, I. A., Adhami, V. M., Afaq, F., Ahmad, N. and Mukhtar, H. (2004). Modulation of phosphatidylinositol-3-kinase/protein kinase B- and mitogen-activated protein kinase-pathways by tea polyphenols in human prostate cancer cells. *J Cell Biochem*, 91 (2), 232-42.
- Siegel, R., Desantis, C. and Jemal, A. (2014). Colorectal cancer statistics, 2014. *CA Cancer J Clin*, 64 (2), 104-17.
- Singh, B. N., Shankar, S. and Srivastava, R. K. (2011). Green tea catechin, epigallocatechin-3-gallate (EGCG): mechanisms, perspectives and clinical applications. *Biochem Pharmacol*, 82 (12), 1807-21.
- Snel, M., Jonker, J. T., Schoones, J., Lamb, H., de Roos, A., Pijl, H., . . . Jazet, I. M. (2012). Ectopic Fat and Insulin Resistance: Pathophysiology and Effect of Diet and Lifestyle Interventions. *International Journal of Endocrinology*, Artn 98381410.1155/2012/983814
- Snoussi, C., Ducroc, R., Hamdaoui, M. H., Dhaouadi, K., Abaidi, H., Cluzeaud, F., . . . Bado, A. (2014). Green tea decoction improves glucose tolerance and reduces weight gain of rats fed normal and high-fat diet. *Journal of Nutritional Biochemistry*, 25 (5), 557-564.
- Sorlie, T., Tibshirani, R., Parker, J., Hastie, T., Marron, J. S., Nobel, A., . . . Botstein, D. (2003). Repeated observation of breast tumor subtypes in independent gene expression data sets. *Proc Natl Acad Sci U S A*, 100 (14), 8418-23.
- Spanoa, D., Heckc, C., Antonellisa, P. D., Christofori, G. and Zolloa, a. M. (2012). Molecular networks that regulate cancer metastasis. *Seminars in Cancer Biology* 22 234– 249.
- Spinella, F., Rosano, L., Di Castro, V., Decandia, S., Albin, A., Nicotra, M. R., . . . Bagnato, A. (2006). Green tea polyphenol epigallocatechin-3-gallate inhibits the endothelin axis and downstream signaling pathways in ovarian carcinoma. *Mol Cancer Ther*, 5 (6), 1483-92.
- Stambolic, V., MacPherson, D., Sas, D., Lin, Y., Snow, B., Jang, Y., . . . Mak, T. W. (2001). Regulation of PTEN transcription by p53. *Molecular Cell*, 8 (2), 317-325.
- Stephenson, G. D. and Rose, D. P. (2003). Breast cancer and obesity: an update. *Nutr Cancer*, 45 (1), 1-16.
- Steward, B. W. and Wild, C. P. (2014). *World cancer report*. 3rd. France: IARC.
- Sudhakar, A. (2009). History of Cancer, Ancient and Modern Treatment Methods. *J Cancer Sci Ther*, 1 (2), 1-4.

- Sugiura, C., Nishimatsu, S., Moriyama, T., Ozasa, S., Kawada, T. and Sayama, K. (2012). Catechins and Caffeine Inhibit Fat Accumulation in Mice through the Improvement of Hepatic Lipid Metabolism. *Journal of Obesity*, 2012 10.
- Suliburska, J., Bogdanski, P., Szulinska, M., Stepien, M., Pupek-Musialik, D. and Jablęcka, A. (2012). Effects of Green Tea Supplementation on Elements, Total Antioxidants, Lipids, and Glucose Values in the Serum of Obese Patients. *Biological Trace Element Research*, 149 (3), 315-322.
- Sumiyoshi, M., Sakanaka, M. and Kimura, Y. (2006). Chronic intake of high-fat and high-sucrose diets differentially affects glucose intolerance in mice. *J Nutr*, 136 (3), 582-7.
- Sundaram, R., Naresh, R., Shanthi, P. and Sachdanandam, P. (2013). Modulatory effect of green tea extract on hepatic key enzymes of glucose metabolism in streptozotocin and high fat diet induced diabetic rats. *Phytomedicine*, 20 (7), 577-584.
- Surwit, R. S., Kuhn, C. M., Cochrane, C., McCubbin, J. A. and Feinglos, M. N. (1988). Diet-Induced Type II Diabetes in C57BL/6J Mice. *Diabetes*, 37 (9), 1163-1167.
- Swinburn, B. A., Caterson, I., Seidell, J. C. and James, W. P. (2004). Diet, nutrition and the prevention of excess weight gain and obesity. *Public Health Nutr*, 7 (1A), 123-46.
- Szablewski, L. (2011). *Glucose Homeostasis – Mechanism and Defects*. In: Rigobelo, E. (2011). Croatia: InTech.
- Taherian-Fard, A., Srihari, S. and Ragan, M. A. (2015). Breast cancer classification: linking molecular mechanisms to disease prognosis. *Brief Bioinform*, 16 (3), 461-74.
- Takahashi, A., Watanabe, T., Mondal, A., Suzuki, K., Kurusu-Kanno, M., Li, Z., . . . Suganuma, M. (2014). Mechanism-based inhibition of cancer metastasis with (-)-epigallocatechin gallate. *Biochemical and Biophysical Research Communications*, 443 (1), 1-6.
- Tang, W., Li, S., Liu, Y., Huang, M.-T. and Ho, C.-T. (2013). Anti-diabetic activity of chemically profiled green tea and black tea extracts in a type 2 diabetes mice model via different mechanisms. *Journal of Functional Foods*, 5 (4), 1784-1793.
- Tao, S. F., He, H. F. and Chen, Q. (2015). Quercetin inhibits proliferation and invasion acts by up-regulating miR-146a in human breast cancer cells. *Mol Cell Biochem*, 402 (1-2), 93-100.
- Thangapazham, R. L., Passi, N. and Maheshwari, R. K. (2007). Green tea polyphenol and epigallocatechin gallate induce apoptosis and inhibit invasion in human breast cancer cells. *Cancer Biology & Therapy*, 6 (12), 1938-1943.
- Thorens, B. and Mueckler, M. (2010). Glucose transporters in the 21st Century. *Am. J. Physiol. Endocrinol. Metab*, 298 (2), E141-E145.
- Thyagarajan, A., Zhu, J. S. and Sliva, D. (2007). Combined effect of green tea and Ganoderma lucidum on invasive behavior of breast cancer cells. *International Journal of Oncology*, 30 (4), 963-969.
- Tisdale, M. J. (2009). Mechanisms of Cancer Cachexia. *Physiological Reviews*, 89 (2), 381.
- Tran, L. T., Yuen, V. G. and McNeill, J. H. (2009). The fructose-fed rat: a review on the mechanisms of fructose-induced insulin resistance and hypertension. *Molecular and Cellular Biochemistry*, 332 (1), 145-159.
- Trayhurn, P., Bing, C. and Wood, I. S. (2006). Adipose tissue and adipokines--energy regulation from the human perspective. *J Nutr*, 136 (7 Suppl), 1935s-1939s.
- Tremblay, F., Dubois, M. and Marette, A. (2003). Regulation of GLUT4 traffic and function by insulin and contraction in skeletal muscle. *Frontiers in bioscience a journal and virtual library.*, 8 d1072-d1084.
- Tse, J. C. and Kalluri, R. (2007). Mechanisms of metastasis: epithelial-to-mesenchymal transition and contribution of tumor microenvironment. *J Cell Biochem*, 101 (4), 816-29.
- Tsilidis, K. K., Kasimis, J. C., Lopez, D. S., Ntzani, E. E. and Ioannidis, J. P. A. (2015). Type 2 diabetes and cancer: umbrella review of meta-analyses of observational studies. *BMJ*, 350
- Tsuneki, H., Ishizuka, M., Terasawa, M., Wu, J.-B., Sasaoka, T. and Kimura, I. (2004). Effect of green tea on blood glucose levels and serum proteomic patterns in diabetic (db/db) mice and on glucose metabolism in healthy humans. *BMC Pharmacology*, 4 18-18.
- Turner, N. and Heilbronn, L. K. (2008). Is mitochondrial dysfunction a cause of insulin resistance? *Trends in Endocrinology and Metabolism*, 19 (9), 324-330.
- Ueda, M., Furuyashiki, T., Yamada, K., Aoki, Y., Sakane, I., Fukuda, I., . . . Ashida, H. (2010). Tea catechins modulate the glucose transport system in 3T3-L1 adipocytes. *Food Funct*, 1 (2), 167-73.

- Ueda, M., Nishiumi, S., Nagayasu, H., Fukuda, I., Yoshida, K. and Ashida, H. (2008). Epigallocatechin gallate promotes GLUT4 translocation in skeletal muscle. *Biochemical and Biophysical Research Communications*, 377 (1), 286-290.
- van Kruijsdijk, R. C., van der Wall, E. and Visseren, F. L. (2009). Obesity and cancer: the role of dysfunctional adipose tissue. *Cancer Epidemiol Biomarkers Prev*, 18 (10), 2569-78.
- Vander Heiden, M. G., Cantley, L. C. and Thompson, C. B. (2009). Understanding the Warburg effect: the metabolic requirements of cell proliferation. *Science*, 324 (5930), 1029-33.
- Vanhaesebroeck, B., Guillermet-Guibert, J., Graupera, M. and Bilanges, B. (2010). The emerging mechanisms of isoform-specific PI3K signalling. *Nature Reviews Molecular Cell Biology*, 11 (5), 329-341.
- Venables, M. C., Hulston, C. J., Cox, H. R. and Jeukendrup, A. E. (2008). Green tea extract ingestion, fat oxidation, and glucose tolerance in healthy humans. *Am J Clin Nutr*, 87 (3), 778-84.
- Vidal-Alabró, A., Méndez-Lucas, A., Semakova, J., Gómez-Valadés, A. and Perales, J. C. (2012). *Liver Glucokinase and Lipid Metabolism*. In: Kelishadi, R. (2012). Croatia: InTech.
- Visvader, J. E. (2009). Keeping abreast of the mammary epithelial hierarchy and breast tumorigenesis. *Genes Dev*, 23 (22), 2563-77.
- Vousden, K. H. and Ryan, K. M. (2009). p53 and metabolism. *Nat Rev Cancer*, 9 (10), 691-700.
- Vuong, Q., Golding, J., Nguyen, M. and Rand oach, P. (2010). Extraction and isolation of catechins from tea. *J. Sep. Sci.*, 33 (21), 3415-3428.
- Vuong, Q. V. (2014). Epidemiological evidence linking tea consumption to human health: a review. *Crit. Rev. Food Sci. Nutr.*, 54 (4), 523-536.
- Wagoner, J., Felzien, E., Vetter, C., Johnson, K. and Rodriguez, A. (2015). Development of a Mouse Model of Obesity via High Sucrose Consumption. *2015 NCUR*,
- Wallace, D. C. (2012). Mitochondria and cancer. *Nat Rev Cancer*, 12 (10), 685-98.
- Walley, A. J., Blakemore, A. I. and Froguel, P. (2006). Genetics of obesity and the prediction of risk for health. *Hum Mol Genet*, 15 Spec No 2 R124-30.
- Waltner-Law, M., Wang, X., Law, B., Hall, R., Nawano, M. and Granner, D. (2002). Epigallocatechin gallate, a constituent of green tea, represses hepatic glucose production. *J. Biol. Chem.*, 277 (38), 34933-34940.
- Wang, H. and Eckel, R. H. (2009). Lipoprotein lipase: from gene to obesity. *American Journal of Physiology - Endocrinology And Metabolism*, 297 (2), E271-E288.
- Wang, H. and Helliwell, K. (2000). Determination of flavonols in green and black tea leaves and green tea infusions by high-performance liquid chromatography. *Food Research International*, (34), 223-227.
- Wang, H., Wen, Y., Du, Y., Yan, X., Guo, H., Rycroft, J. A., . . . Mela, D. J. (2010a). Effects of Catechin Enriched Green Tea on Body Composition. *Obesity*, 18 (4), 773-779.
- Wang, P. W., Henning, S. M. and Heber, D. (2010b). Limitations of MTT and MTS-Based Assays for Measurement of Antiproliferative Activity of Green Tea Polyphenols. *Plos One*, 5 (4),
- Wang, R. N., Dillon, C. P., Shi, L. Z., Milasta, S., Carter, R., Finkelstein, D., . . . Green, D. R. (2011). The Transcription Factor Myc Controls Metabolic Reprogramming upon T Lymphocyte Activation. *Immunity*, 35 (6), 871-882.
- Warburg, O., Posener, K. and Negelein, E. (1924). Über den Stoffwechsel der Carcinomzelle. *Biochem. Zeitschr*, 152 309-344.
- Warburg, O., Wind, F. and Negelein, E. (1927). THE METABOLISM OF TUMORS IN THE BODY. *J Gen Physiol*, 8 (6), 519-30.
- Weigelt, B., Geyer, F. C. and Reis-Filho, J. S. (2010). Histological types of breast cancer: how special are they? *Mol Oncol*, 4 (3), 192-208.
- Weigelt, B., Peterse, J. L. and van 't Veer, L. J. (2005). Breast cancer metastasis: markers and models. *Nat Rev Cancer*, 5 (8), 591-602.
- Weinhouse, S. (1976). The Warburg hypothesis fifty years later. *Z Krebsforsch Klin Onkol Cancer Res Clin Oncol*, 87 (2), 115-26.
- Whiteman, E. L., Cho, H. , and Birnbaum, M.J. (2002). Role of Akt/protein kinase B in metabolism. *Endocrinology and Metabolism*, 13 (10), 444-451.

- Williams, L. M., Campbell, F. M., Drew, J. E., Koch, C., Hoggard, N., Rees, W. D., . . . Tups, A. (2014). The Development of Diet-Induced Obesity and Glucose Intolerance in C57Bl/6 Mice on a High-Fat Diet Consists of Distinct Phases. *Plos One*, 9 (8),
- Willson, K. C. (1999). *Coffee, cocoa and tea*. Oxon; New York: CABI.
- Winzell, M. S. and Ahren, B. (2004). The high-fat diet-fed mouse: a model for studying mechanisms and treatment of impaired glucose tolerance and type 2 diabetes. *Diabetes*, 53 Suppl 3 S215-9.
- Wolfram, S., Raederstorff, D., Preller, M., Wang, Y., Teixeira, S. R., Riegger, C. and Weber, P. (2006). Epigallocatechin gallate supplementation alleviates diabetes in rodents. *Journal of Nutrition*, 136 (10), 2512-2518.
- Wolfram, S., Raederstorff, D., Wang, Y., Teixeira, S. R., Elste, V. and Weber, P. (2005). TEAVIGO (epigallocatechin gallate) supplementation prevents obesity in rodents by reducing adipose tissue mass. *Ann Nutr Metab*, 49 (1), 54-63.
- Wong, K. A. and Lodish, H. F. (2006). A revised model for AMP-activated protein kinase structure - The alpha-subunit binds to both the beta- and gamma-subunits although there is no direct binding between the beta- and gamma-subunits. *Journal of Biological Chemistry*, 281 (47), 36434-36442.
- Woods, A., Dickerson, K., Heath, R., Hong, S. P., Momcilovic, M., Johnstone, S. R., . . . Carling, D. (2005). Ca<sup>2+</sup>/calmodulin-dependent protein kinase kinase-beta acts upstream of AMP-activated protein kinase in mammalian cells. *Cell Metabolism*, 2 (1), 21-33.
- Woods, A., Johnstone, S. R., Dickerson, K., Leiper, F. C., Fryer, L. G. D., Neumann, D., . . . Carling, D. (2003). LKB1 is the upstream kinase in the AMP-activated protein kinase cascade. *Current Biology*, 13 (22), 2004-2008.
- Wright, D. C., Geiger, P. C., Holloszy, J. O. and Han, D. H. (2005). Contraction- and hypoxia-stimulated glucose transport is mediated by a Ca<sup>2+</sup>-dependent mechanism in slow-twitch rat soleus muscle. *American Journal of Physiology-Endocrinology and Metabolism*, 288 (6), E1062-E1066.
- Wu, A. H. and Butler, L. M. (2011). Green tea and breast cancer. *Molecular Nutrition & Food Research*, 55 (6), 921-930.
- Wu, C. H., Lu, F. H., Chang, C. S., Chang, T. C., Wang, R. H. and Chang, C. J. (2003). Relationship among habitual tea consumption, percent body fat, and body fat distribution. *Obes Res*, 11 (9), 1088-95.
- Wu, L. Y., Juan, C. C., Ho, L. T., Hsu, Y. P. and Hwang, L. S. (2004a). Effect of green tea supplementation on insulin sensitivity in Sprague-Dawley rats. *J Agric Food Chem*, 52 (3), 643-8.
- Wu, L. Y., Juan, C. C., Hwang, L. S., Hsu, Y. P., Ho, P. H. and Ho, L. T. (2004b). Green tea supplementation ameliorates insulin resistance and increases glucose transporter IV content in a fructose-fed rat model. *Eur J Nutr*, 43 (2), 116-24.
- Xintaropoulou, C., Ward, C., Wise, A., Marston, H., Turnbull, A. and Langdon, S. P. (2015). A comparative analysis of inhibitors of the glycolysis pathway in breast and ovarian cancer cell line models. *Oncotarget*, 6 (28), 25677-95.
- Xu, B. J., Goulding, E. H., Zang, K. L., Cepoi, D., Cone, R. D., Jones, K. R., . . . Reichardt, L. F. (2003). Brain-derived neurotrophic factor regulates energy balance downstream of melanocortin-4 receptor. *Nature Neuroscience*, 6 (7), 736-742.
- Yan, J., Zhao, Y., Suo, S., Liu, Y. and Zhao, B. (2012). Green tea catechins ameliorate adipose insulin resistance by improving oxidative stress. *Free Radic Biol Med*, 52 (9), 1648-57.
- Yang, Z. Z., Tschopp, O., Hemmings-Mieszczyk, M., Feng, J. H., Brodbeck, D., Perentes, E. and Hemmings, B. A. (2003). Protein kinase B alpha/Akt1 regulates placental development and fetal growth. *Journal of Biological Chemistry*, 278 (34), 32124-32131.
- Yarrow, J. C., Perlman, Z. E., Westwood, N. J. and Mitchison, T. J. (2004). A high-throughput cell migration assay using scratch wound healing, a comparison of image-based readout methods. *Bmc Biotechnology*, 4
- Yasui, K., Miyoshi, N., Tanabe, H., Ishigami, Y., Fukutomi, R., Imai, S. and Isemura, M. (2011). Effects of a catechin-free fraction derived from green tea on gene expression of gluconeogenic enzymes in rat hepatoma H4IIE cells and in the mouse liver. *Biomedical Research-Tokyo*, 32 (2), 119-125.
- Zhang, L., Pang, E., Loo, R. R., Rao, J., Go, V. L., Loo, J. A. and Lu, Q. Y. (2011). Concomitant inhibition of HSP90, its mitochondrial localized homologue TRAP1 and HSP27 by green tea in pancreatic cancer HPAF-II cells. *Proteomics*, 11 (24), 4638-47.

- Zhang, Q., Ramracheya, R., Lahmann, C., Tarasov, A., Bengtsson, M., Braha, O., . . . Rorsman, P. (2013a). Role of KATP channels in glucose-regulated glucagon secretion and impaired counterregulation in type 2 diabetes. *Cell Metab*, 18 (6), 871-82.
- Zhang, Q. Z., Tang, X. D., Lu, Q. Y., Zhang, Z. F., Rao, J. Y. and Le, A. D. (2006). Green tea extract and (-)-epigallocatechin-3-gallate inhibit hypoxia- and serum-induced HIF-1 alpha protein accumulation and VEGF expression in human cervical carcinoma and hepatoma cells. *Molecular Cancer Therapeutics*, 5 (5), 1227-1238.
- Zhang, Y., Li, Q., Xing, H., Lu, Zhao, L., Qu, K. and Bi, K. (2013b). Evaluation of antioxidant activity of ten compounds in different tea samples by means of an on-line HPLC–DPPH assay. *Food Research International.*, 53 (2), 847-856.
- Zhang, Y., Yu, Y., Li, X., Meguro, S., Hayashi, S., Katashima, M., . . . Li, K. (2012). Effects of catechin-enriched green tea beverage on visceral fat loss in adults with a high proportion of visceral fat: A double-blind, placebo-controlled, randomized trial. *Journal of Functional Foods*, 4 (1), 315-322.
- Zhang, Z. F., Li, Q., Liang, J., Dai, X. Q., Ding, Y., Wang, J. B. and Li, Y. (2010). Epigallocatechin-3-O-gallate (EGCG) protects the insulin sensitivity in rat L6 muscle cells exposed to dexamethasone condition. *Phytomedicine*, 17 (1), 14-18.
- Zhang, Z. H., Wang, Z. Q., Yang, Z., Niu, Y. X., Zhang, W. W., Li, X. Y., . . . Su, Q. (2015). A novel mice model of metabolic syndrome: the high-fat-high-fructose diet-fed ICR mice. *Experimental Animals*, 64 (4), 435-442.
- Zhao, F. Q. and Keating, A. F. (2007). Functional properties and genomics of glucose transporters. *Current Genomics*, 8 (2), 113-128.
- Zheng, X., Xu, Y., Li, S., Liu, X., Hui, R. and Huang, X. (2011). Green tea intake lowers fasting serum total and LDL cholesterol in adults: a meta-analysis of 14 randomized controlled trials. *Am. J. Clin. Nutr.*, 94 (2), 601-610.
- Zhou, G., Myers, R., Li, Y., Chen, Y., Shen, X., Fenyk-Melody, J., . . . Moller, D. E. (2001). Role of AMP-activated protein kinase in mechanism of metformin action. *J Clin Invest*, 108 (8), 1167-74.
- Zuo, Y., Chen, H. and Deng, Y. (2002). Simultaneous determination of catechins, caffeine and gallic acids in green, Oolong, black and pu-erh teas using HPLC with a photodiode array detector. *Talanta*, 57 (2), 307-16.

# Appendices

## 8.1 Appendix 1; Amplification and disassociation curves of glucose and lipid metabolism gene expression in insulin-sensitive cell lines

### 8.1.1 Amplification and disassociation curves of glucose metabolism gene expression in C2C12 cells

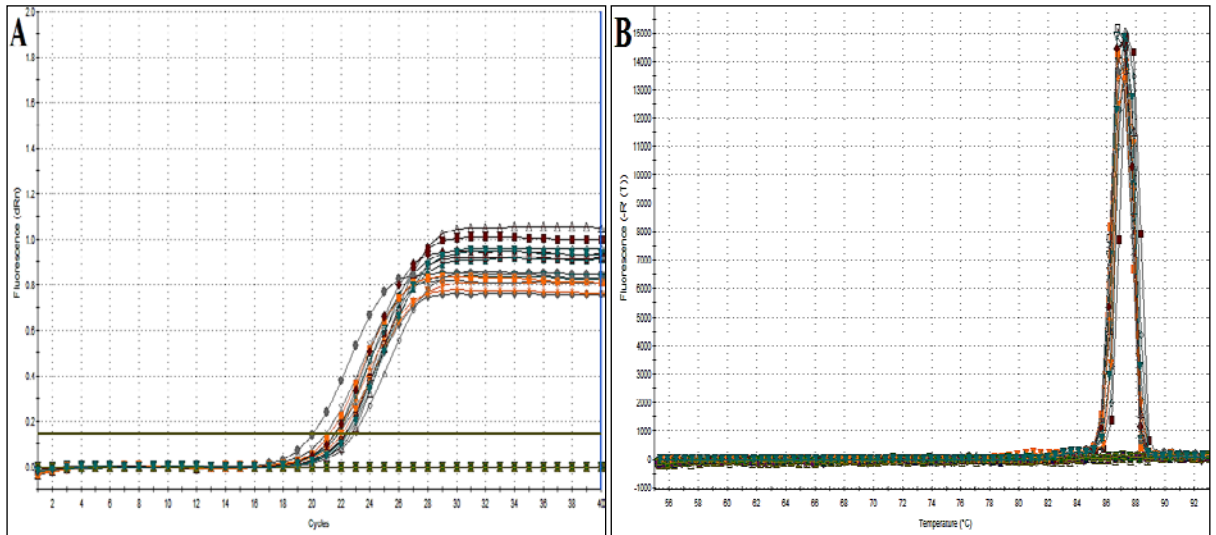


**Figure 8.1 C2C12 SYBR<sup>®</sup> Green Rt. PCR analysis of actin gene expression.**

Actin gene expression was determined in C2C12 cDNA samples. (A) Amplification curves displayed the mean  $C_t$  value of actin was 22.020. (B) Dissociation curve showed one peak which dissociated approximately at 87°C suggestion excellent primer specificity, n=3.

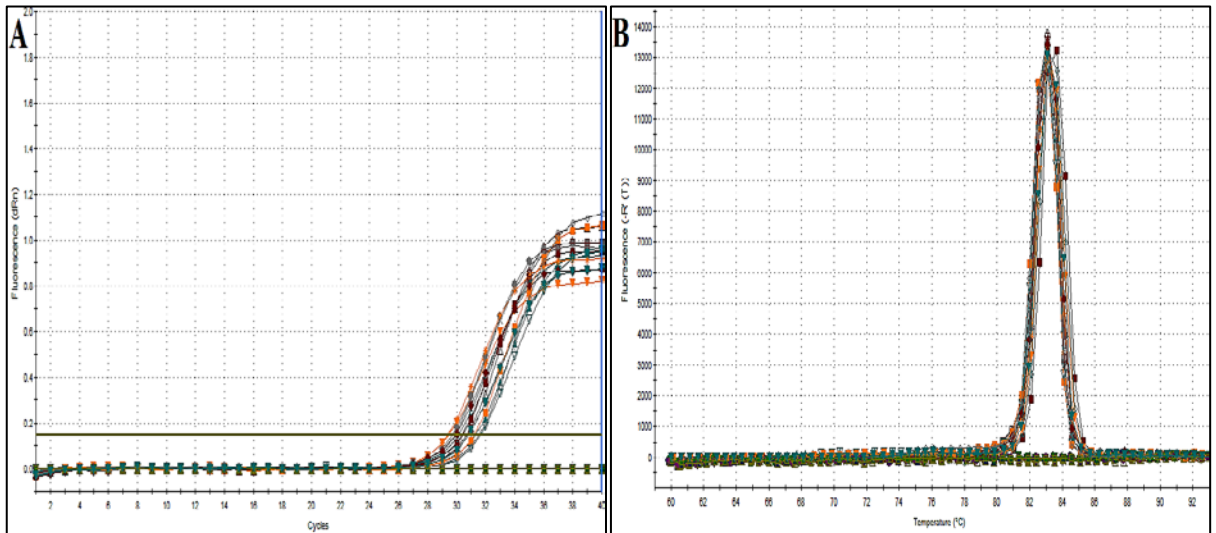


**Figure 8.2 C2C12 SYBR<sup>®</sup> Green Rt. PCR analysis of IR gene expression.**

Insulin receptor gene expression was determined in control and treated C2C12 cDNA samples. (A) Amplification curves displayed that the mean  $C_t$  value of IR gene was 29.845. (B) Dissociation curve showed one peak which dissociated approximately at 83°C suggestion excellent primer specificity, n=3.

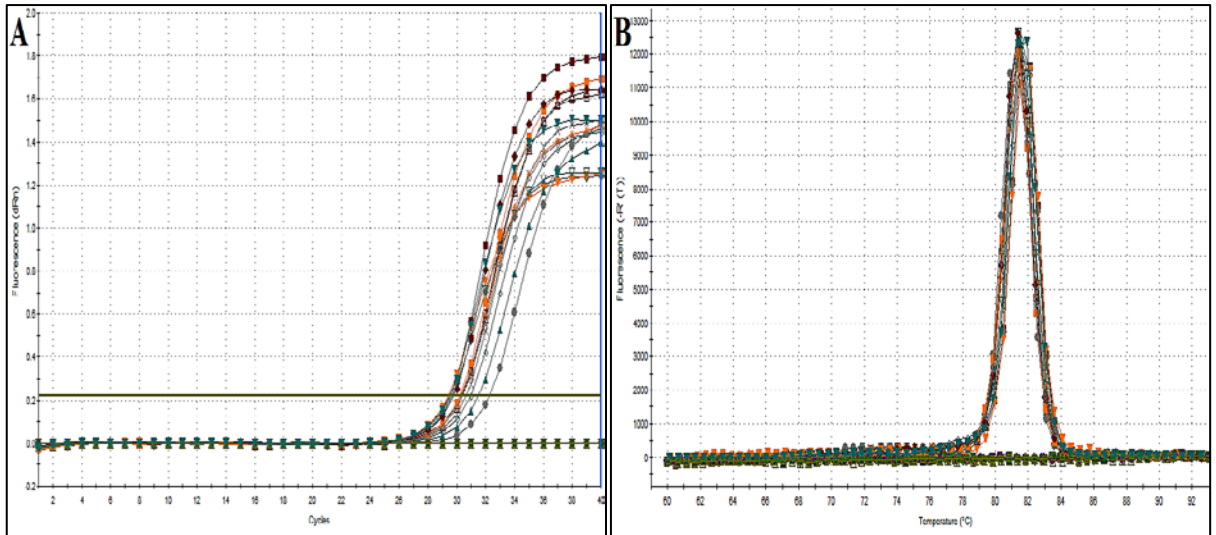


**Figure 8.3 C2C12 SYBR<sup>®</sup> Green Rt. PCR analysis of HK1 gene expression.**

HK1 gene expression was determined in control and treated C2C12 cDNA samples. (A) Amplification curves displayed that the mean  $C_t$  value of HK1 gene was 30.426. (B) Dissociation curve showed one peak which dissociated approximately at 81°C suggesting excellent primer specificity, n=3.

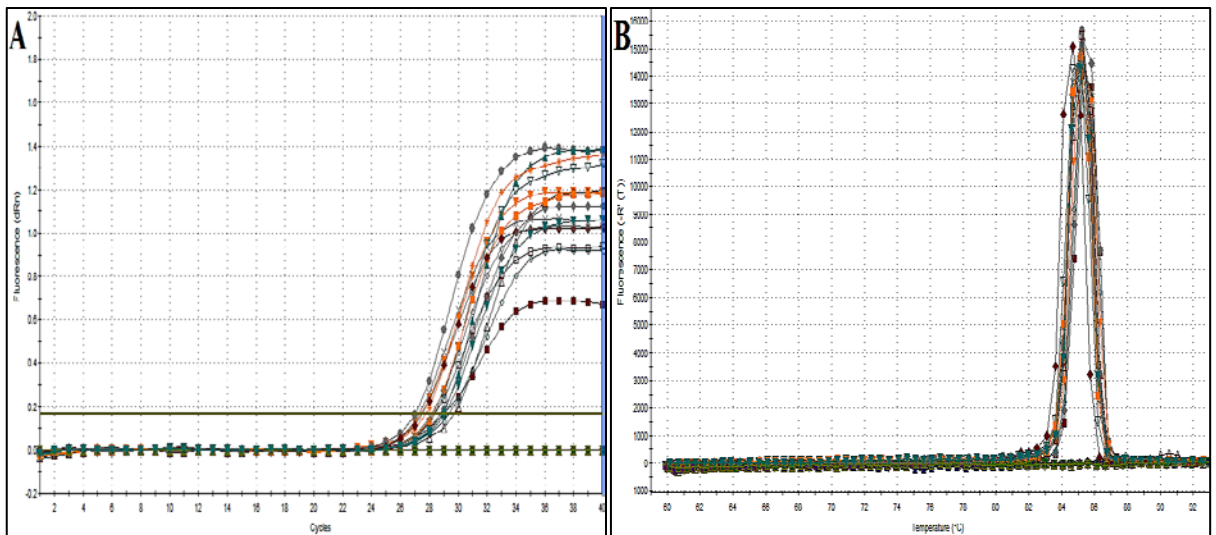


**Figure 8.4 C2C12 SYBR<sup>®</sup> Green Rt. PCR analysis of Glut4 gene expression**

Glut4 gene expression was determined in control and treated C2C12 cDNA samples. (A) Amplification curves displayed that the mean  $C_t$  value of Glut4 gene was 28.454. (B) Dissociation curve showed one peak which dissociated approximately at 85°C suggesting excellent primer specificity, n=3.

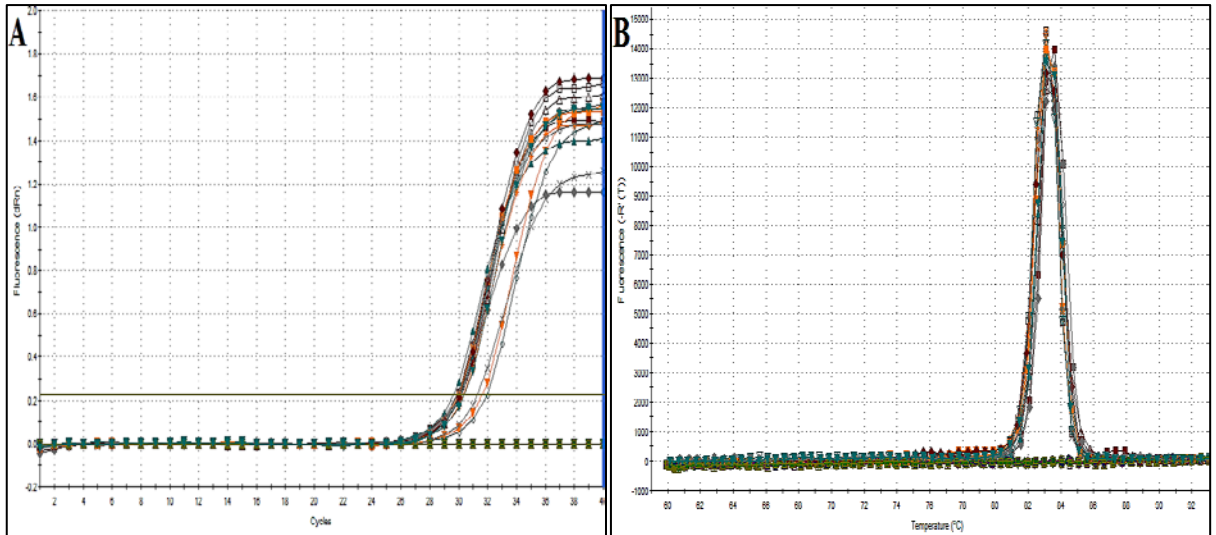


**Figure 8.5 C2C12 SYBR® Green Rt. PCR analysis of PDK4 gene expression.**

PDK4 gene expression was determined in control and treated C2C12 cDNA samples. (A) Amplification curves displayed that the mean  $C_t$  value of PDK4 gene was 30.277. (B) Dissociation curve showed one peak which dissociated approximately at 83°C suggestion excellent primer specificity,  $n=3$ .

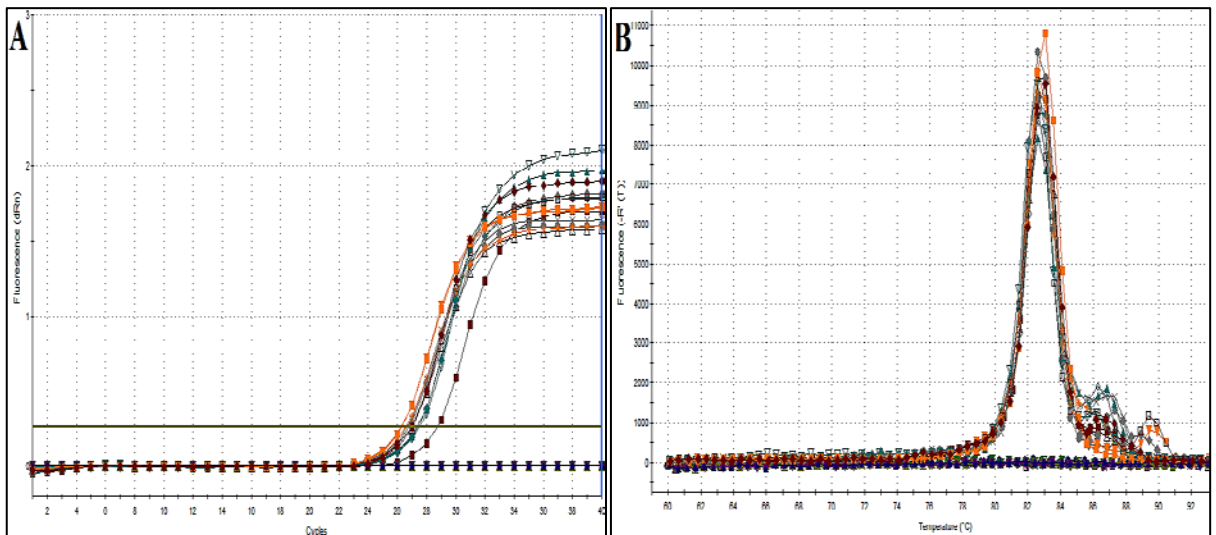


**Figure 8.6 C2C12 SYBR® Green Rt. PCR analysis of PGC1 $\alpha$  gene expression.**

PGC1 $\alpha$  gene expression was determined in control and treated C2C12 cDNA samples. (A) Amplification curves displayed that the mean  $C_t$  value of PGC1 $\alpha$  gene was 26.991. (B) Dissociation curve showed one peak with minor shouldering which dissociated approximately at 83°C suggestion very good primer specificity,  $n=3$ .

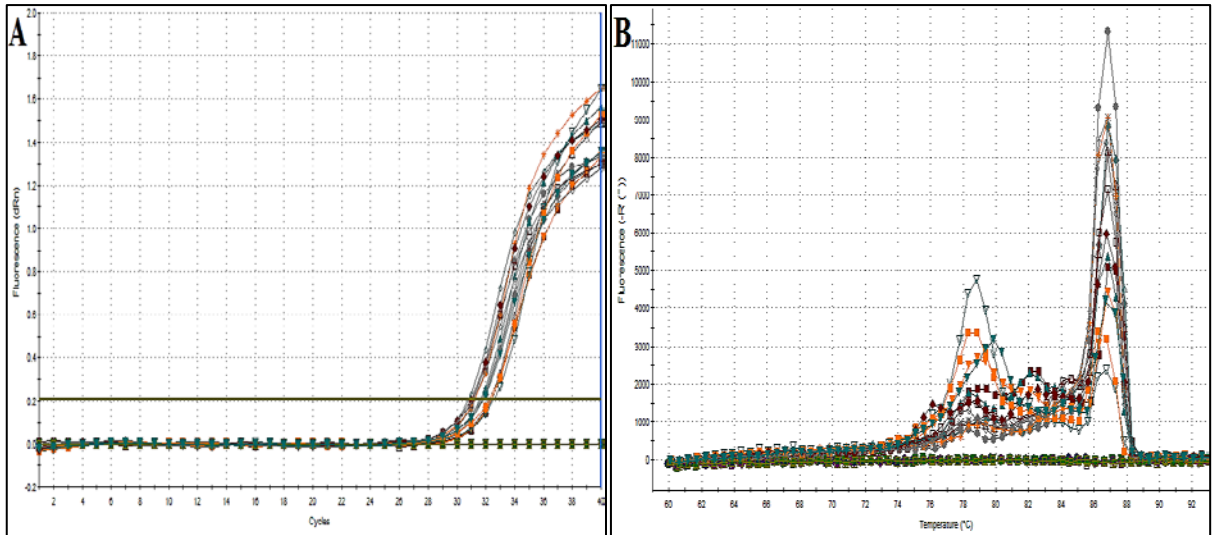


**Figure 8.7 C2C12 SYBR® Green Rt. PCR analysis of Gys1 gene expression.**

Gys1 gene expression was determined in control and treated C2C12 cDNA samples. (A) Amplification curves displayed that the mean  $C_t$  value of Gys1 gene was 31.999. (B) Dissociation curve showed two peaks which dissociated at two temperatures suggestion some nonspecific primer binding,  $n=3$ .

### 8.1.2 Amplification and disassociation curves of glucose and lipid metabolism gene expression in 3T3L1 cells

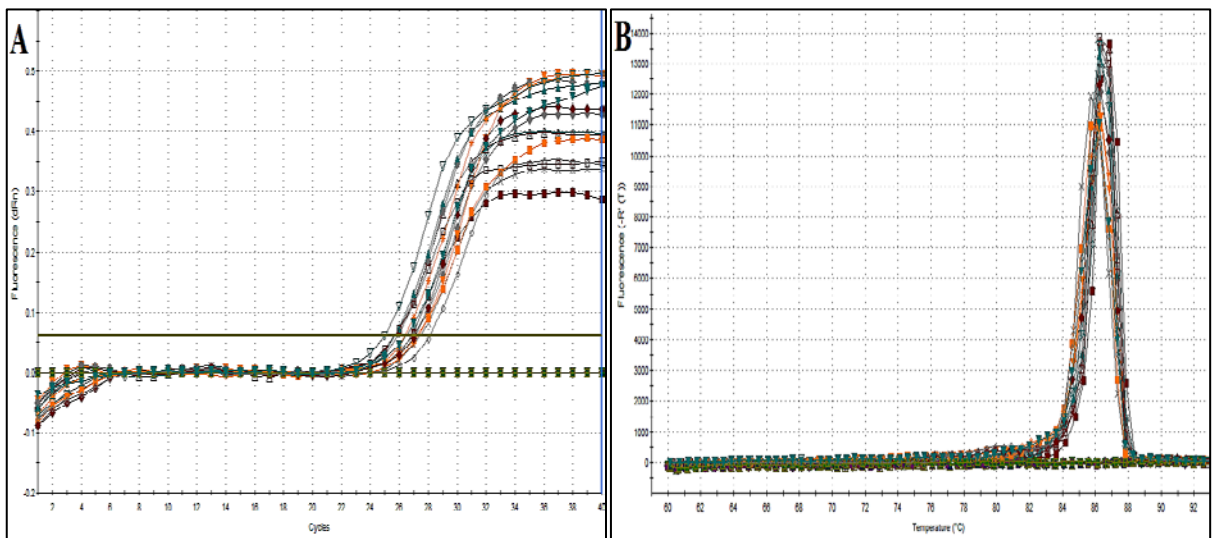


**Figure 8.8 3T3-L1 SYBR® Green Rt. PCR analysis of actin gene expression.**

Actin gene expression was determined in 3T3-L1 cDNA samples. (A) Amplification curves displayed the mean  $C_t$  value of actin was 27.674. (B) Dissociation curve showed one peak which dissociated approximately at 86.5°C suggesting excellent primer specificity,  $n=3$ .

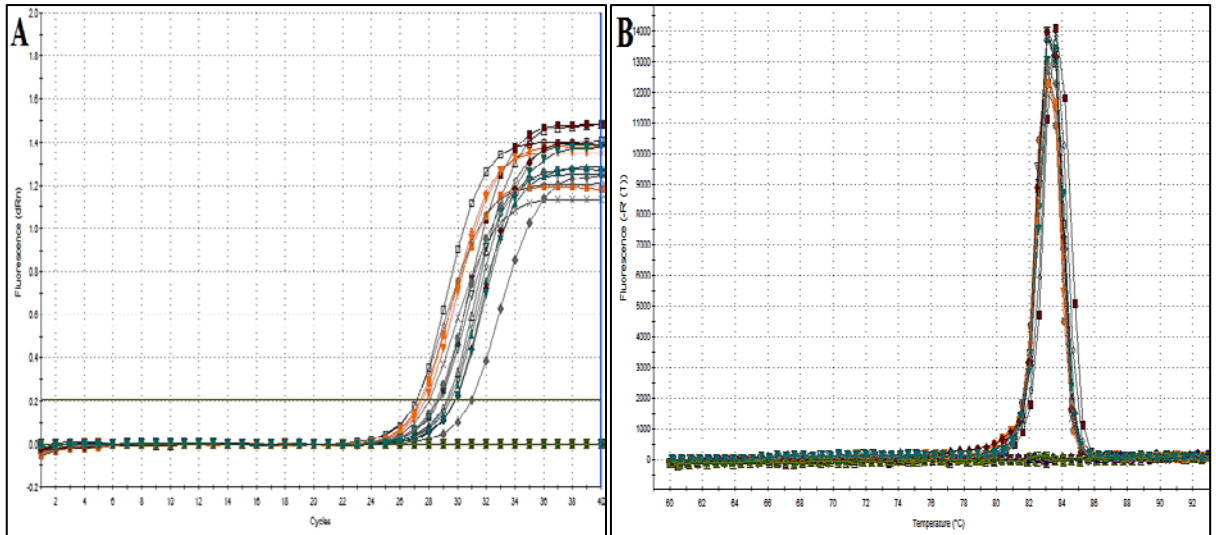


**Figure 8.9 3T3-L1 SYBR® Green Rt. PCR analysis of IR gene expression.**

IR gene expression was determined in control and treated 3T3-L1 cDNA samples. (A) Amplification curves displayed that the mean  $C_t$  value of IR gene was 27.897. (B) Dissociation curve showed one peak which dissociated approximately at 83°C suggesting excellent primer specificity, n=3.

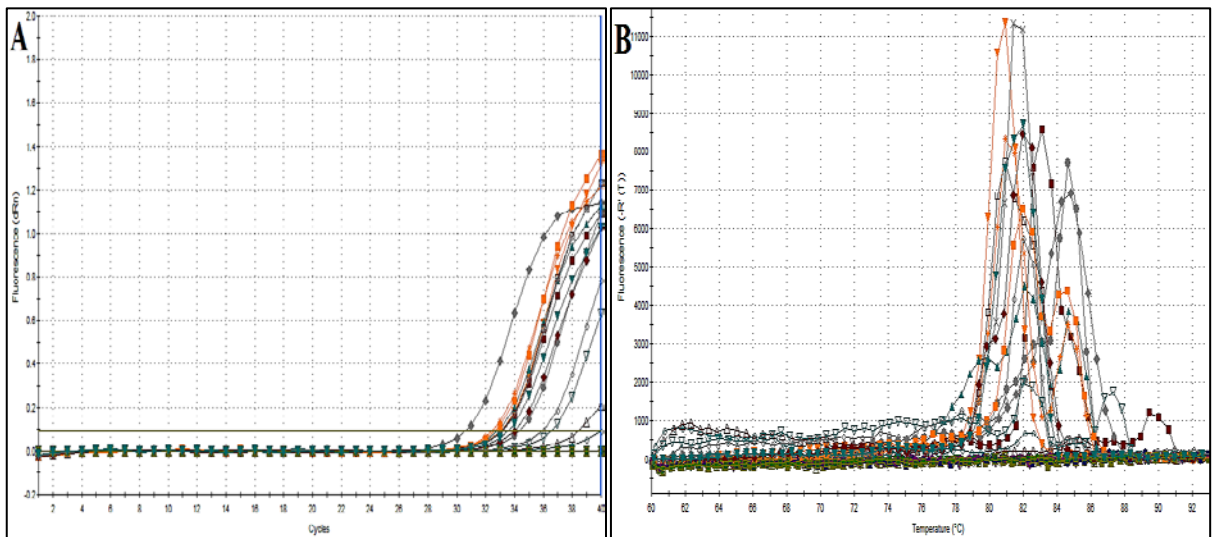


**Figure 8.10 3T3-L1 SYBR® Green Rt. PCR analysis of HK1 gene expression.**

HK1 gene expression was determined in control and treated 3T3-L1 cDNA samples. (A) Amplification curves displayed that the mean  $C_t$  value of HK1 gene was 32.331. (B) Dissociation curve showed multiple peaks which dissociated at different temperatures suggestion poor specificity of primer binding. n=3.

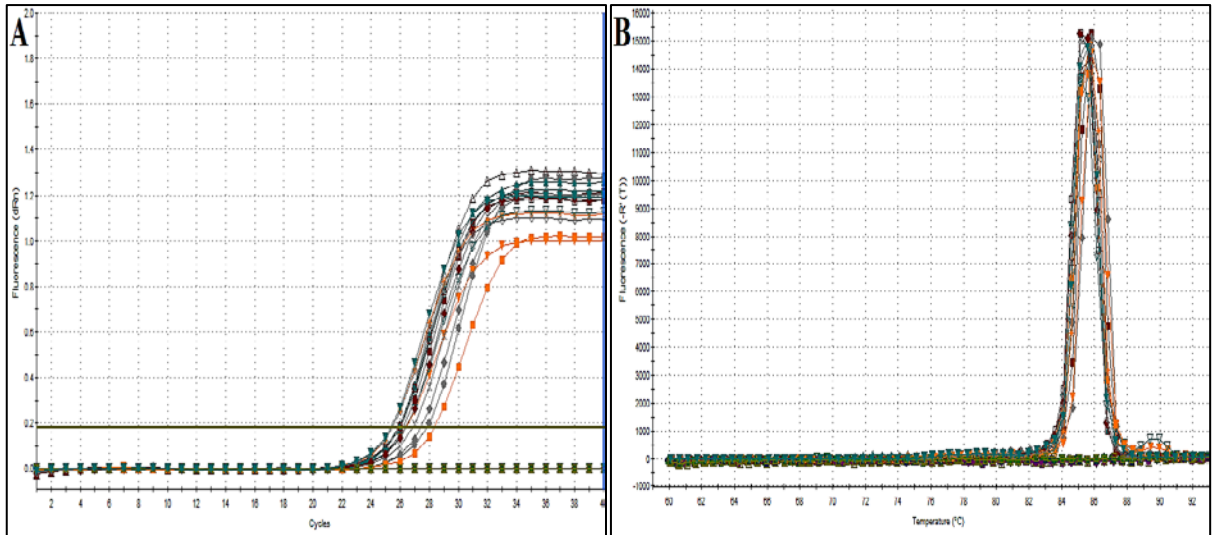


**Figure 8.11 3T3-L1 SYBR<sup>®</sup> Green Rt. PCR analysis of Glut4 gene expression.**

Glut4 gene expression was determined in control and treated 3T3-L1 cDNA samples. (A) Amplification curves displayed that the mean  $C_t$  value of Glut4 gene was 25.339. (B) Dissociation curve showed one peak which dissociated approximately at 85.5°C suggesting excellent primer specificity,  $n=3$ .

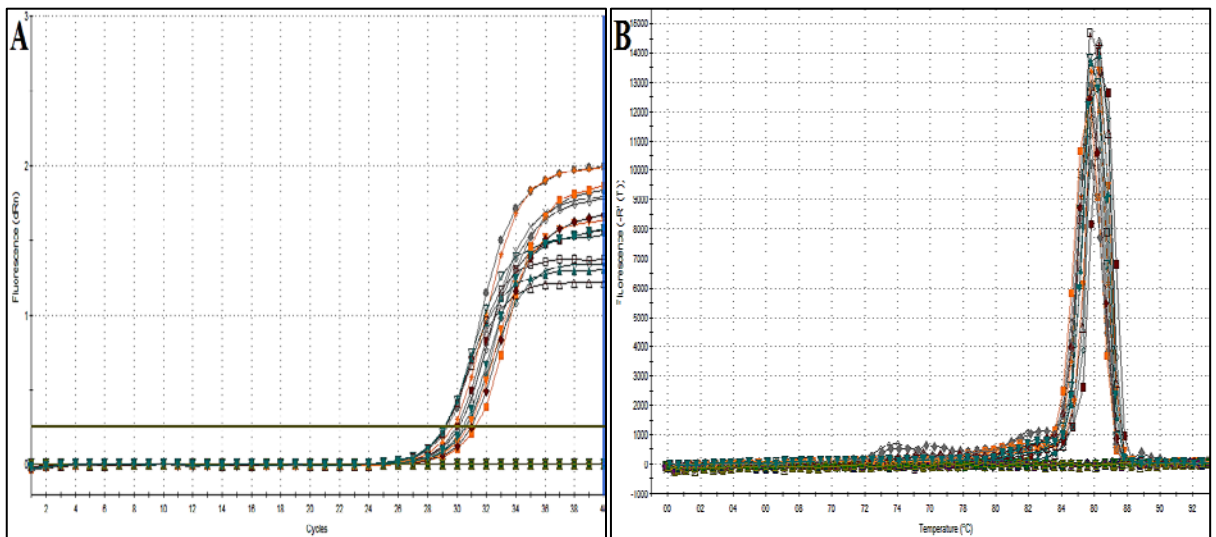


**Figure 8.12 3T3-L1 SYBR<sup>®</sup> Green Rt. PCR analysis of C/EBP $\alpha$  gene expression.**

C/EBP $\alpha$  gene expression was determined in control and treated 3T3-L1 cDNA samples. (A) Amplification curves displayed that the mean  $C_t$  value of C/EBP $\alpha$  gene was 29.886. (B) Dissociation curve showed one peak which dissociated approximately at 86°C suggesting excellent primer specificity,  $n=3$ .

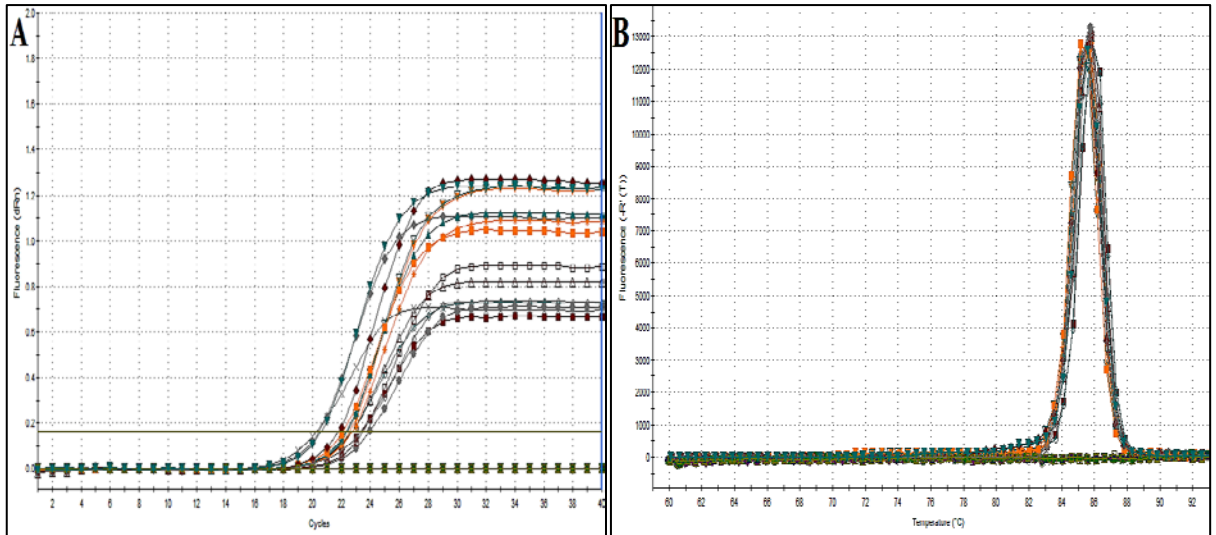


**Figure 8.13 3T3-L1 SYBR® Green Rt. PCR analysis of LPL gene expression.**

LPL gene expression was determined in control and treated 3T3-L1 cDNA samples. (A) Amplification curves displayed that the mean  $C_t$  value of LPL gene was 21.443. (B) Dissociation curve showed one peak which dissociated approximately at 85.75°C suggesting excellent primer specificity,  $n=3$ .

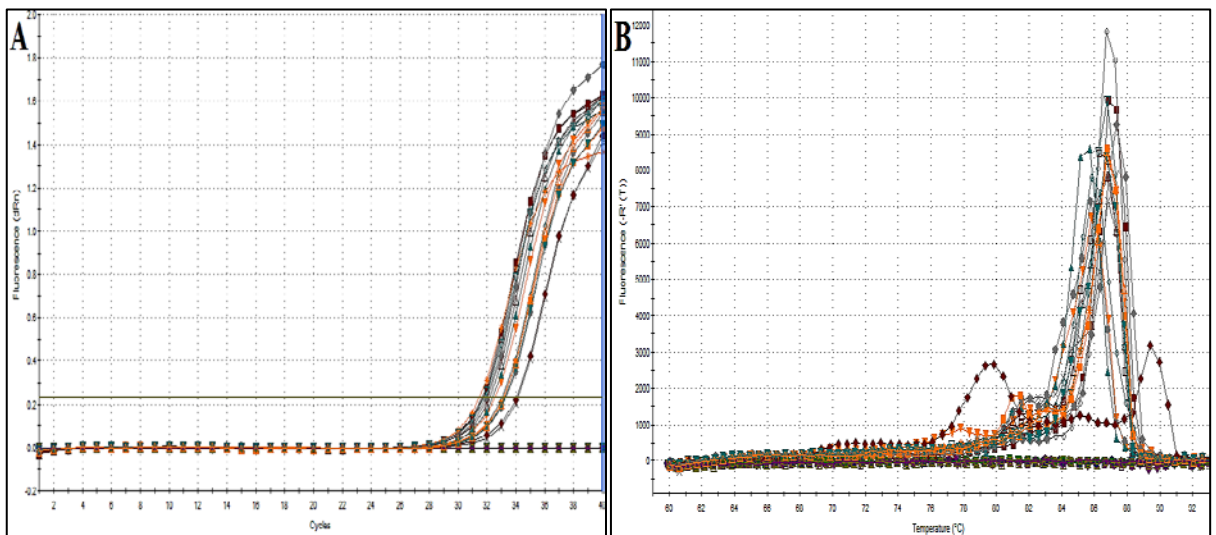


**Figure 8.14 3T3-L1 SYBR® Green Rt. PCR analysis of FASN gene expression.**

FASN gene expression was determined in control and treated 3T3-L1 cDNA samples. (A) Amplification curves displayed that the mean  $C_t$  value of FASN gene was 32.6. (B) Dissociation curve showed one peak which dissociated approximately at 86°C suggestion mixed primer specificity,  $n=3$ .

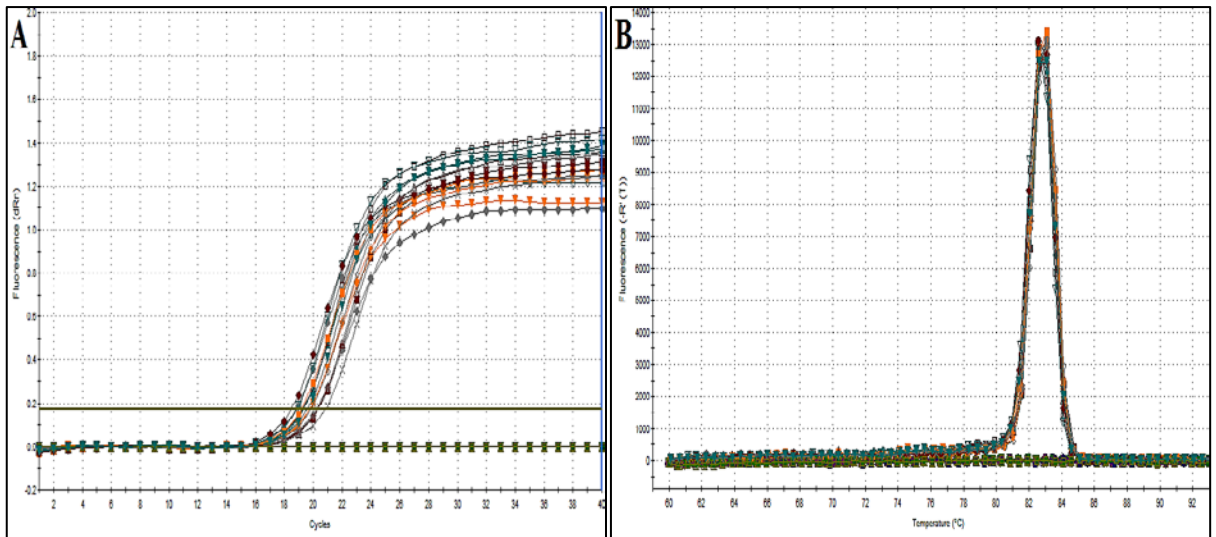


**Figure 8.15 3T3-L1 SYBR<sup>®</sup> Green Rt. PCR analysis of FABP4 gene expression.**

FABP4 gene expression was determined in control and treated 3T3-L1 cDNA samples. (A) Amplification curves displayed that the mean  $C_t$  value of FABP4 gene was 20.007. (B) Dissociation curve showed one peak which dissociated approximately at 83°C suggesting excellent primer specificity,  $n=3$ .

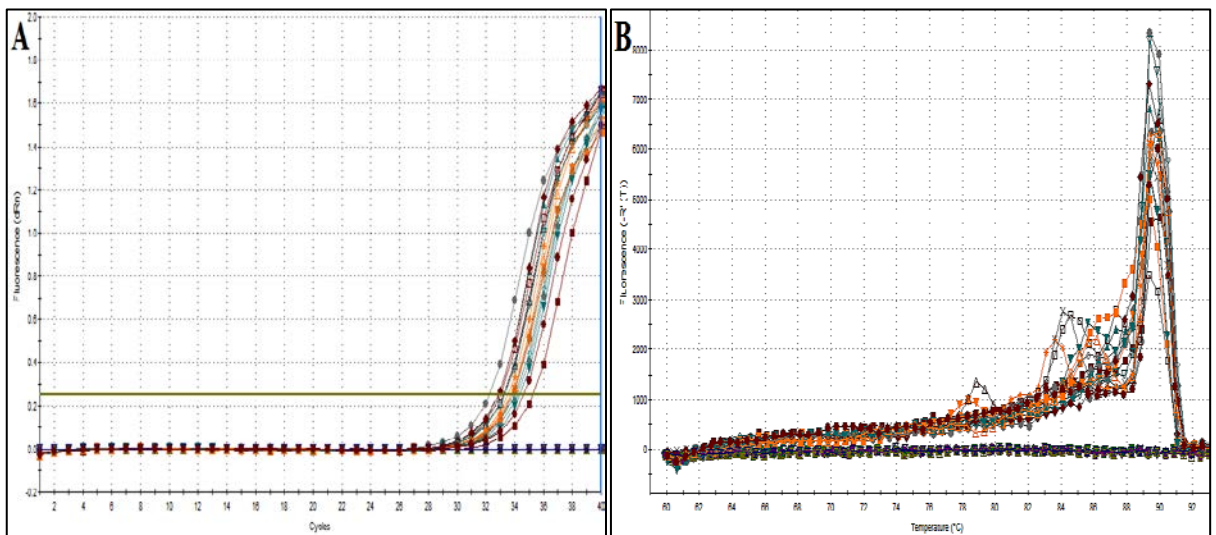


**Figure 8.16 3T3-L1 SYBR<sup>®</sup> Green Rt. PCR analysis of SREBP1c gene expression.**

SREBP1c gene expression was determined in control and treated 3T3-L1 cDNA samples. (A) Amplification curves displayed that the mean  $C_t$  value of SREBP1c gene was 33.265. (B) Dissociation curve showed one peak with shouldering which dissociated approximately at 89.5°C suggesting poor primer specificity,  $n=3$ .

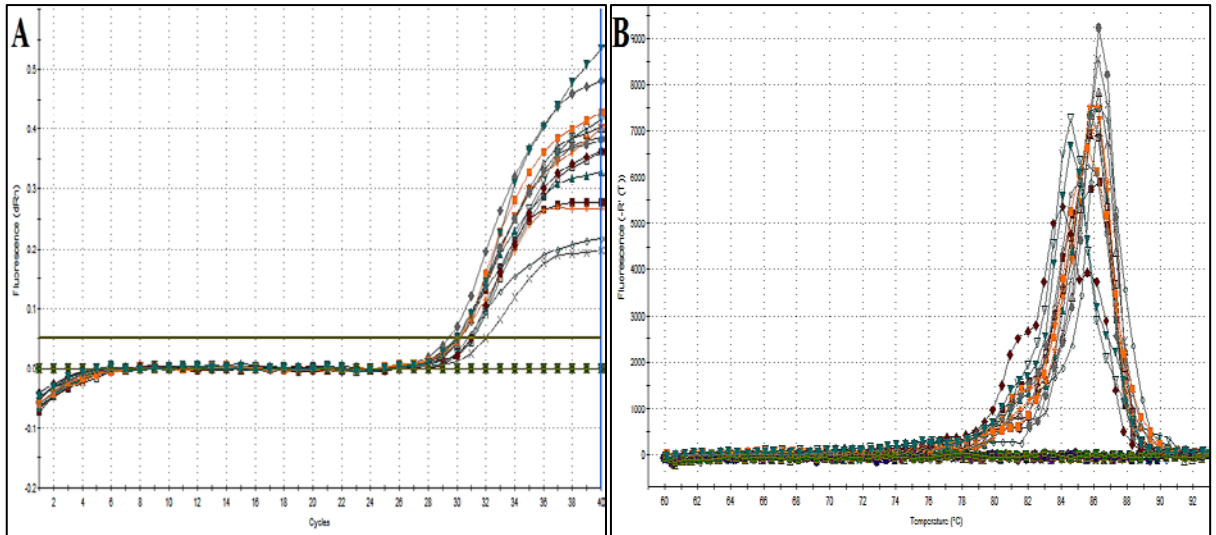


**Figure 8.17 3T3-L1 SYBR<sup>®</sup> Green Rt. PCR analysis of PPAR $\gamma$  gene expression.**

PPAR $\gamma$  gene expression was determined in control and treated 3T3-L1 cDNA samples. (A) Amplification curves displayed that the mean  $C_t$  value of PPAR $\gamma$  gene was 31.038. (B) Dissociation curve showed one peak which dissociated approximately at 86°C suggesting adequate primer specificity,  $n=3$ .

### 8.1.3 Amplification and disassociation curves of glucose metabolism gene expression in AML12 cells

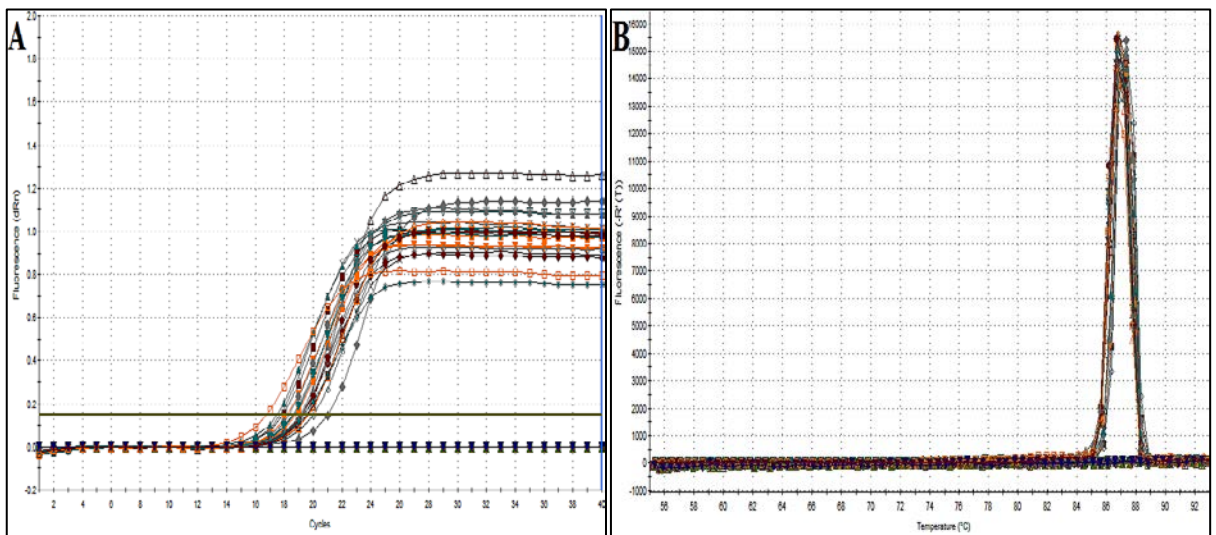


**Figure 8.18 AML12 SYBR<sup>®</sup> Green Rt. PCR analysis of actin gene expression.**

Actin gene expression was determined in control and treated AML12 cDNA samples. (A) Amplification curves displayed that the mean  $C_t$  value of actin gene was 19.008. (B) Dissociation curve showed one peak which dissociated approximately at 87°C suggesting excellent primer specificity,  $n=3$ .

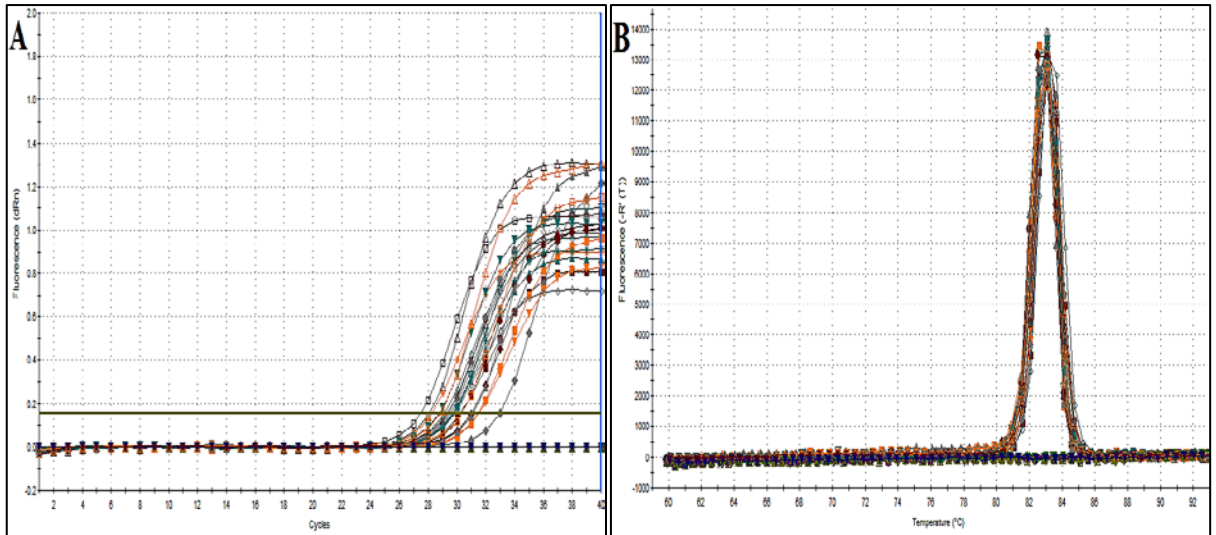


**Figure 8.19 AML12 SYBR® Green Rt. PCR analysis of IR gene expression.**

IR gene expression was determined in control and treated AML12 cDNA samples. (A) Amplification curves displayed that the mean  $C_t$  value of IR gene was 29.127. (B) Dissociation curve showed one peak which dissociated approximately at 83°C suggesting excellent primer specificity,  $n=3$ .

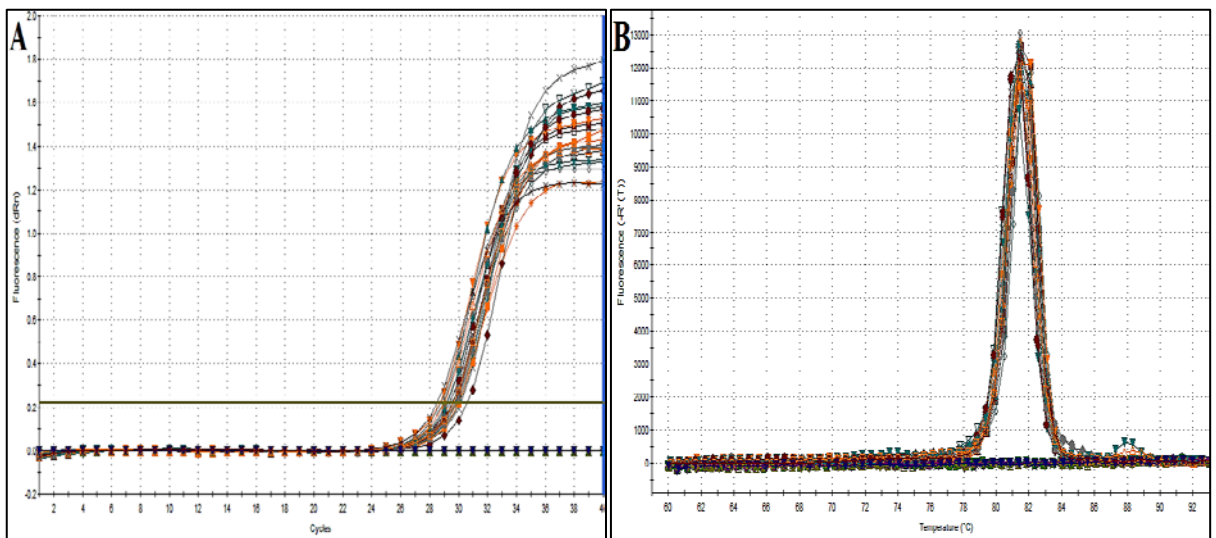


**Figure 8.20 AML12 SYBR® Green Rt. PCR analysis of HK1 gene expression.**

HK1 gene expression was determined in control and treated AML12 cDNA samples. (A) Amplification curves displayed that the mean  $C_t$  value of HK1 gene was 29.603. (B) Dissociation curve showed one peak which dissociated approximately at 81°C suggesting excellent primer specificity,  $n=3$ .

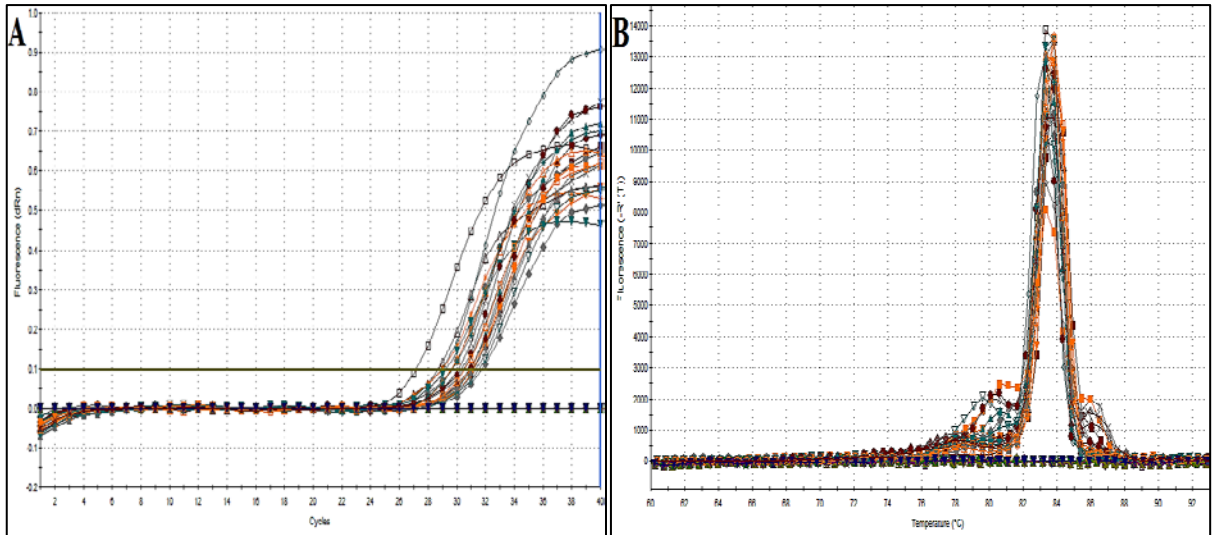


**Figure 8.21 AML12 SYBR® Green Rt. PCR analysis of Glut2 gene expression.**

Glut2 gene expression was determined in control and treated AML12 cDNA samples. (A) Amplification curves displayed that the mean  $C_t$  value of Glut2 gene was 30.88. (B) Dissociation curve showed one peak with minor shouldering which dissociated approximately at 83°C suggestion good primer specificity, n=3.

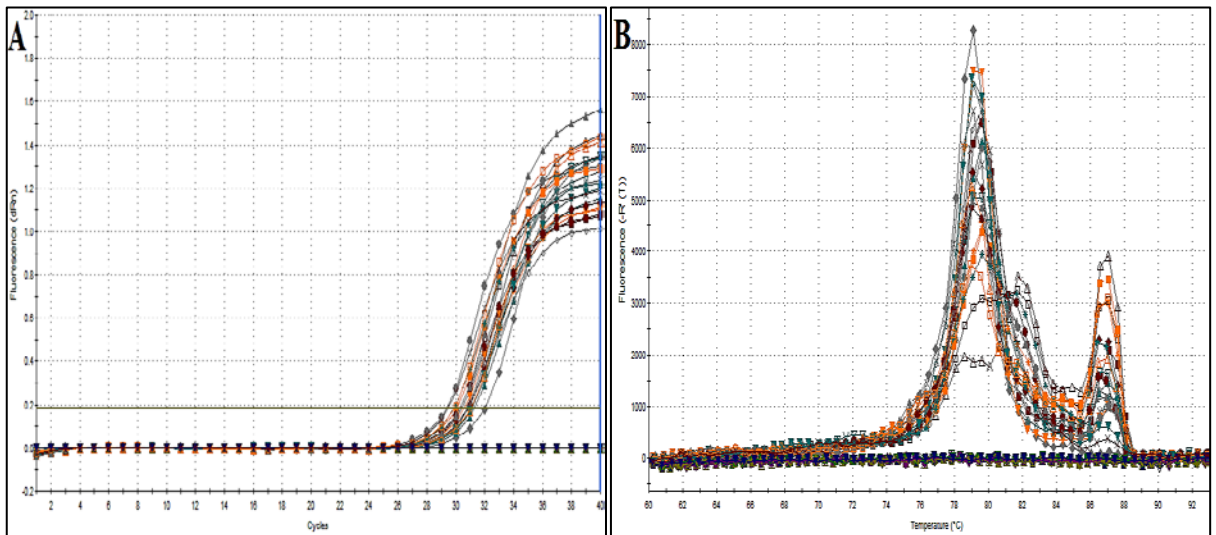


**Figure 8.22 AML12 SYBR® Green Rt. PCR analysis of Gys1 gene expression.**

Gys1 gene expression was determined in control and treated AML12 cDNA samples. (A) Amplification curves displayed that the mean  $C_t$  value of Gys1 gene was 30.391. (B) Dissociation curve showed two peaks which dissociated at different temperatures suggestion nonspecific primer binding, n=3.

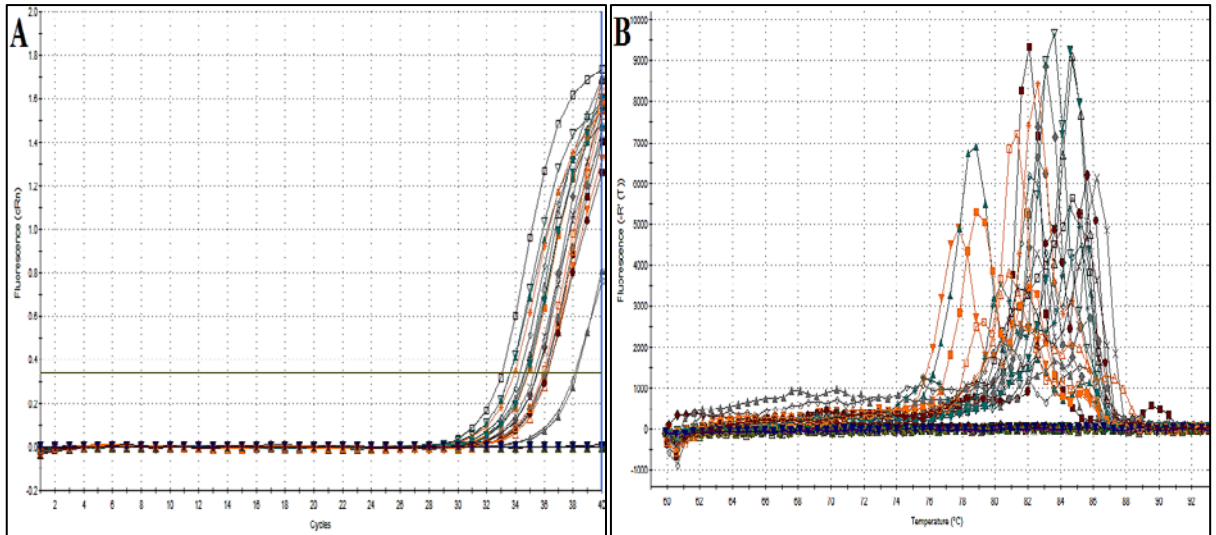


**Figure 8.23 AML12 SYBR® Green Rt. PCR analysis of G6Pase gene expression.**

G6Pase gene expression was determined in control and treated AML12 cDNA samples. (A) Amplification curves displayed that the mean  $C_t$  value of G6Pase gene was 33.4. (B) Dissociation curve showed multiple peaks which dissociated at different temperatures suggestion nonspecific primer binding,  $n=3$ .

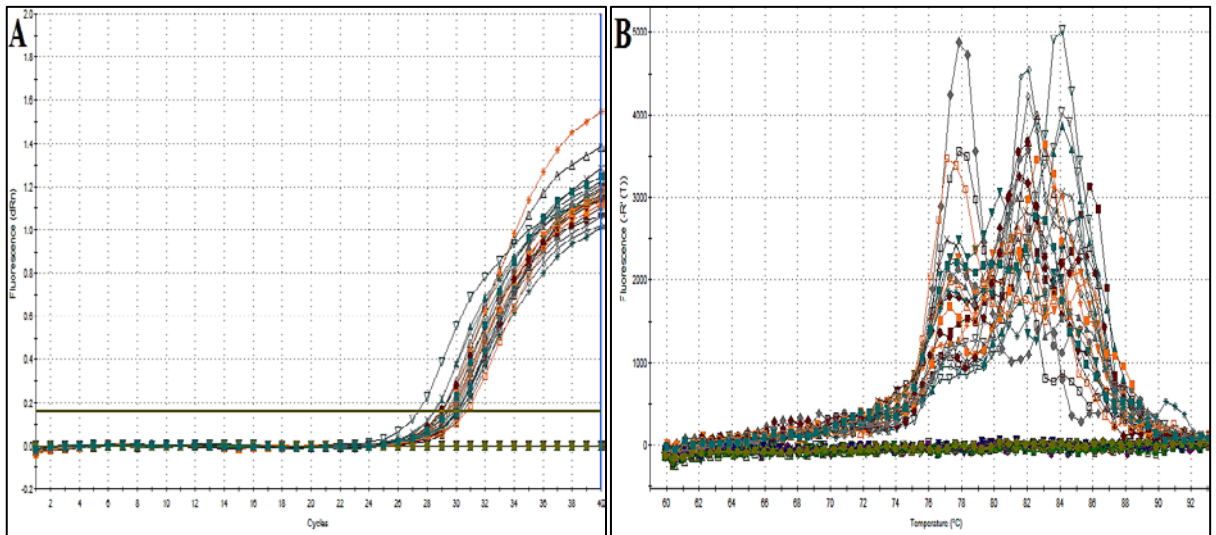


**Figure 8.24 AML12 SYBR® Green Rt. PCR analysis of PEPCK gene expression.**

PEPCK gene expression was determined in control and treated AML12 cDNA samples. (A) Amplification curves displayed that the mean  $C_t$  value of PEPCK gene was 28.490. (B) Dissociation curve showed multiple peaks which dissociated at different temperatures suggestion nonspecific primer binding,  $n=3$ .

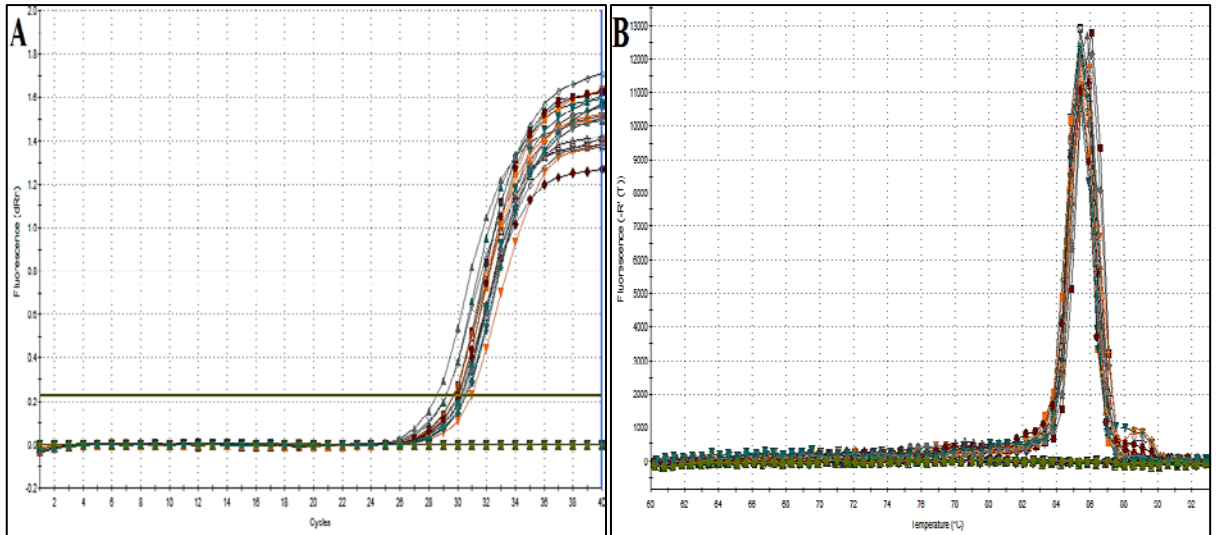


**Figure 8.25 AML12 SYBR® Green Rt. PCR analysis of CPT1 $\alpha$  gene expression.**

CPT1 $\alpha$  gene expression was determined in control and treated AML12 cDNA samples. (A) Amplification curves displayed that the mean  $C_t$  value of CPT1 $\alpha$  gene was 29.327. (B) Dissociation curve showed one peak which dissociated approximately at 83.5°C suggesting excellent primer specificity,  $n=3$ .

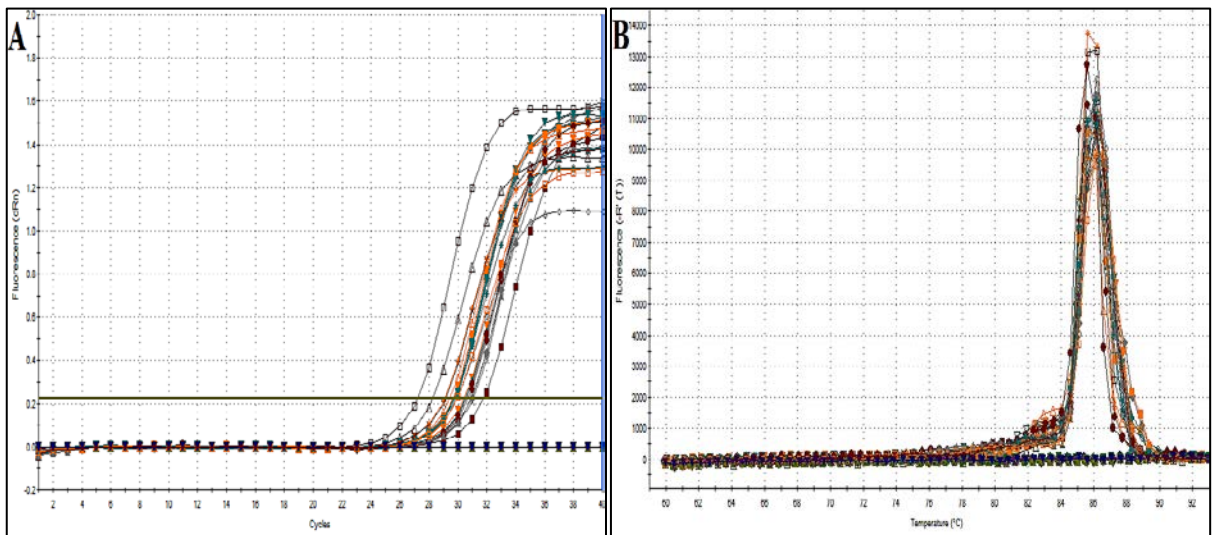


**Figure 8.26 AML12 SYBR® Green Rt. PCR analysis of ACSL gene expression.**

ACSL gene expression was determined in control and treated AML12 cDNA samples. (A) Amplification curves displayed that the mean  $C_t$  value of ACSL gene was 28.400. (B) Dissociation curve showed one peak which dissociated approximately at 86°C suggesting excellent primer specificity,  $n=3$ .

## 8.2 Appendix 2; Amplification and disassociation curves of glucose and lipid metabolism gene expression in mice insulin-sensitive tissues

### 8.2.1 Amplification and disassociation curves of glucose metabolism gene expression in mice liver

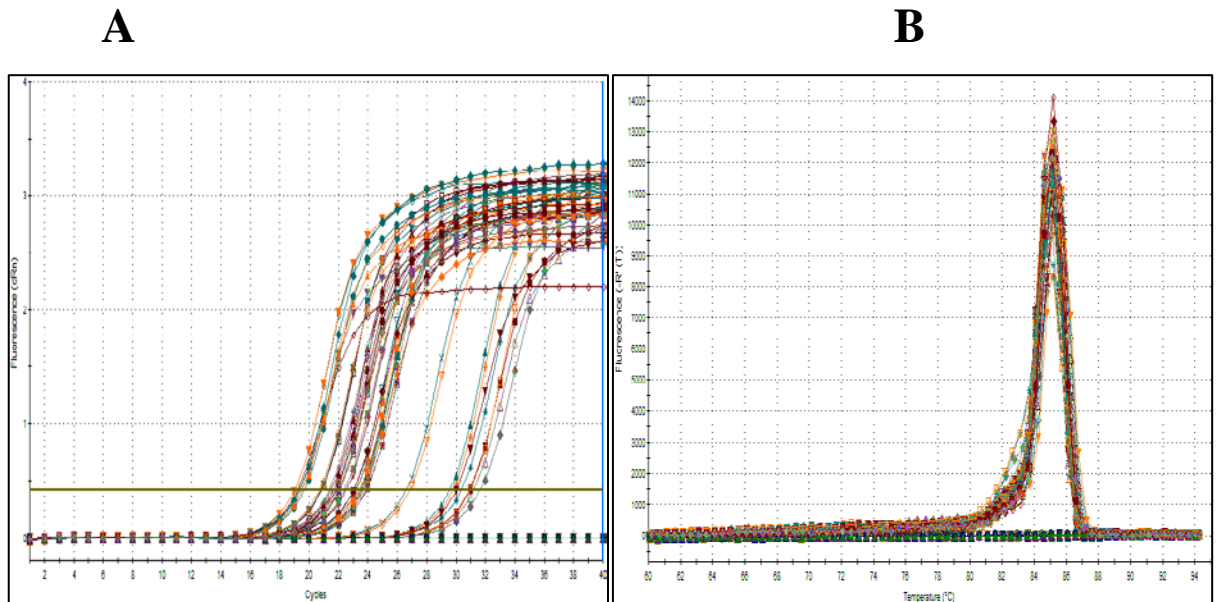


**Figure 8.27 Liver SYBR® Green Rt. PCR analysis of actin gene expression.**

Actin gene expression was determined in treated and control mice liver cDNA samples. (A) Amplification curves displayed the mean  $C_t$  value of actin was 23.16. (B) Dissociation curve showed one peak which dissociated approximately at 85°C suggestion excellent primer specificity,  $n=3$ .

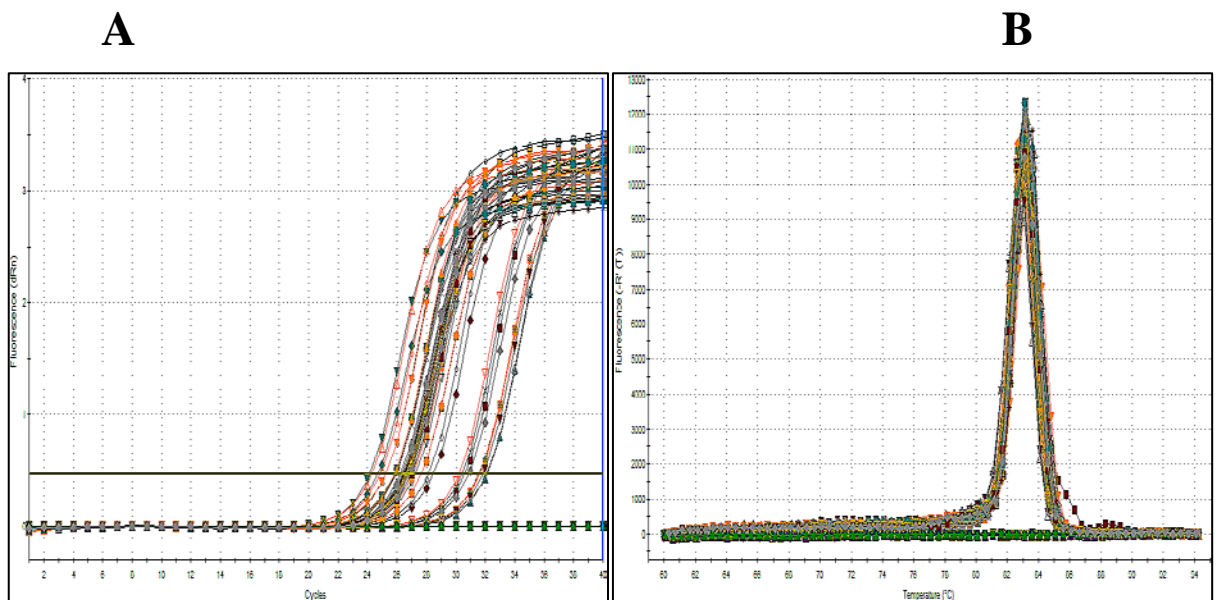


**Figure 8.28 Liver SYBR® Green Rt. PCR analysis of IR gene expression.**

Insulin receptor gene expression was determined in treated and control mice liver cDNA samples. (A) Amplification curves displayed that the mean  $C_t$  value of IR gene was 27.08. (B) Dissociation curve showed one peak which dissociated approximately at 83°C suggestion excellent primer specificity,  $n=3$ .

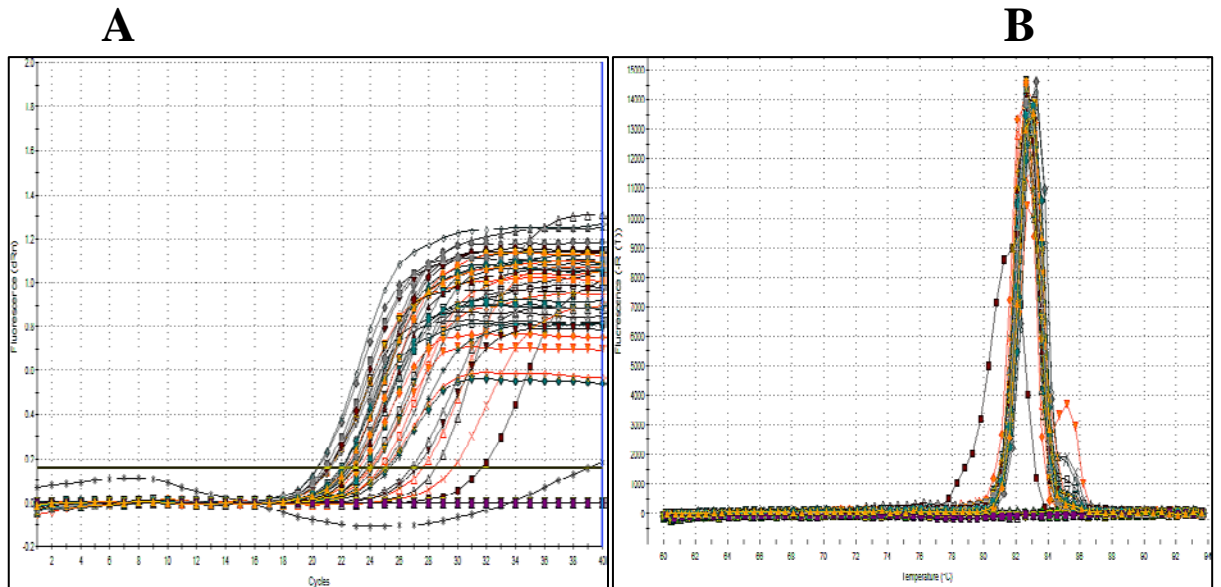


**Figure 8.29 Liver SYBR® Green Rt. PCR analysis of Glut2 gene expression.**

Glut2 gene expression was determined in treated and control mice liver cDNA samples. (A) Amplification curves displayed that the mean  $C_t$  value of Glut2 gene was 23.987. (B) Dissociation curve showed one peak which dissociated approximately at 83°C suggestion good primer specificity, n=3.

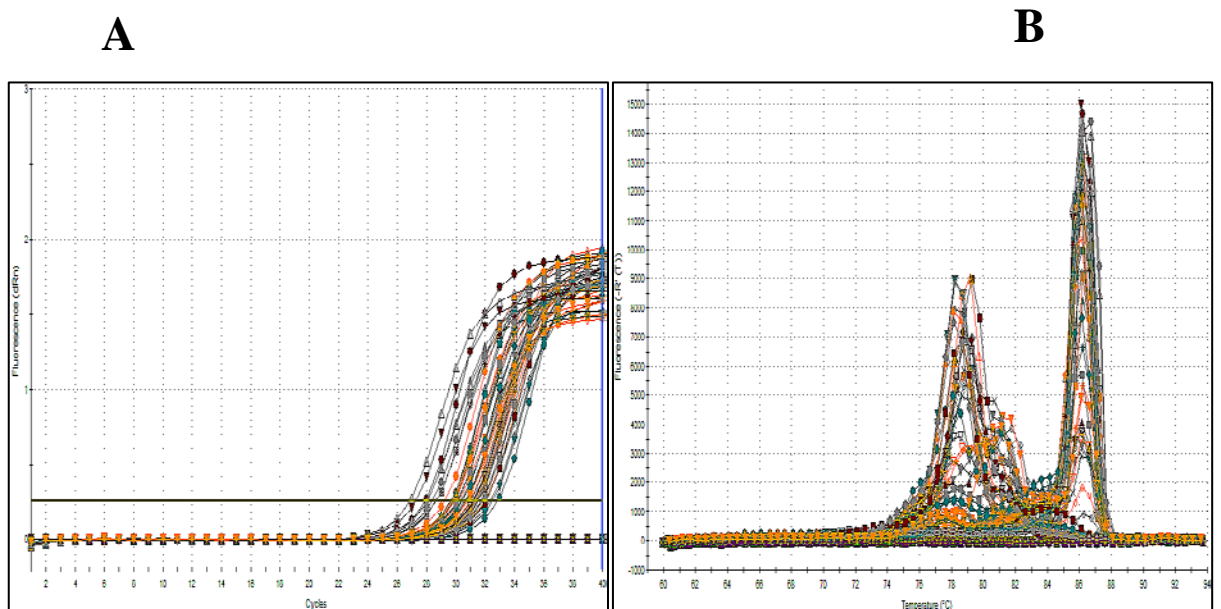


**Figure 8.30 Liver SYBR® Green Rt. PCR analysis of Gys1 gene expression.**

Gys1 gene expression was determined in treated and control mice liver cDNA samples. (A) Amplification curves displayed that the mean  $C_t$  value of Gys1 gene was 30.2. (B) Dissociation curve showed more than one peak which dissociated approximately at different temperatures which suggestion nonspecific primer binding, n=3.

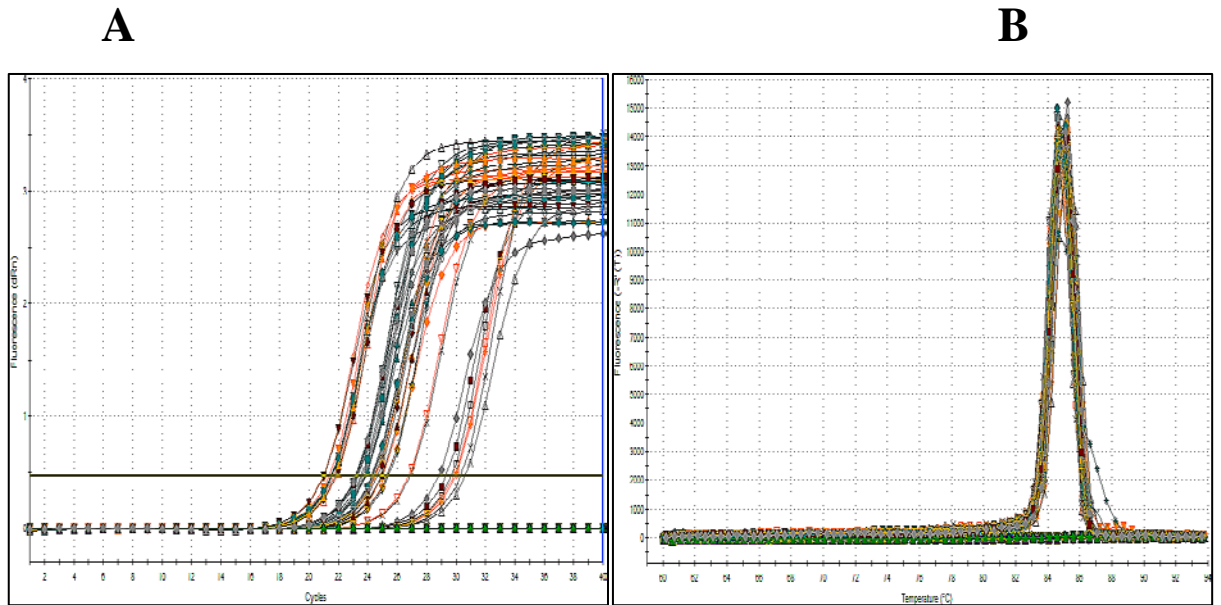


**Figure 8.31 Liver SYBR® Green Rt. PCR analysis of G6Pase gene expression.**

G6Pase gene expression was determined in treated and control mice liver cDNA samples. (A) Amplification curves displayed that the mean  $C_t$  value of G6Pase gene was 24.892. (B) Dissociation curve showed one peak which dissociated approximately at 85°C suggestion excellent primer specificity,  $n=3$ .

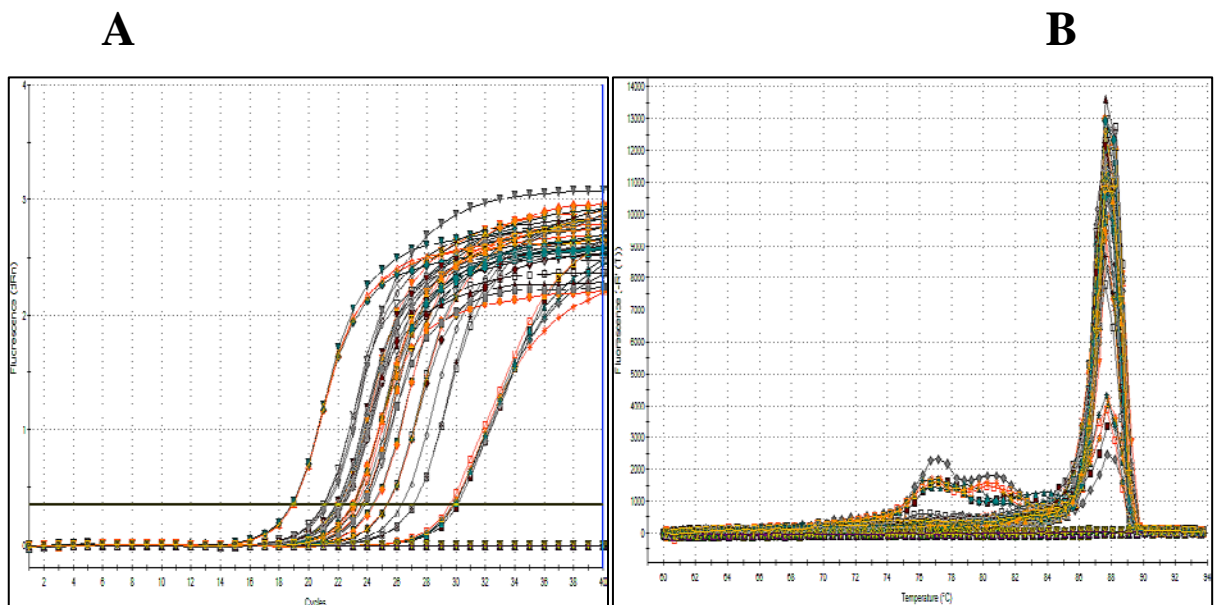


**Figure 8.32 Liver SYBR® Green Rt. PCR analysis of PEPCK gene expression.**

PEPCK gene expression was determined in treated and control mice liver cDNA samples. (A) Amplification curves displayed that the mean  $C_t$  value of PEPCK gene was 24.454. (B) Dissociation curve showed one major peak which dissociated approximately at 88°C suggestion acceptable primer specificity,  $n=3$ .

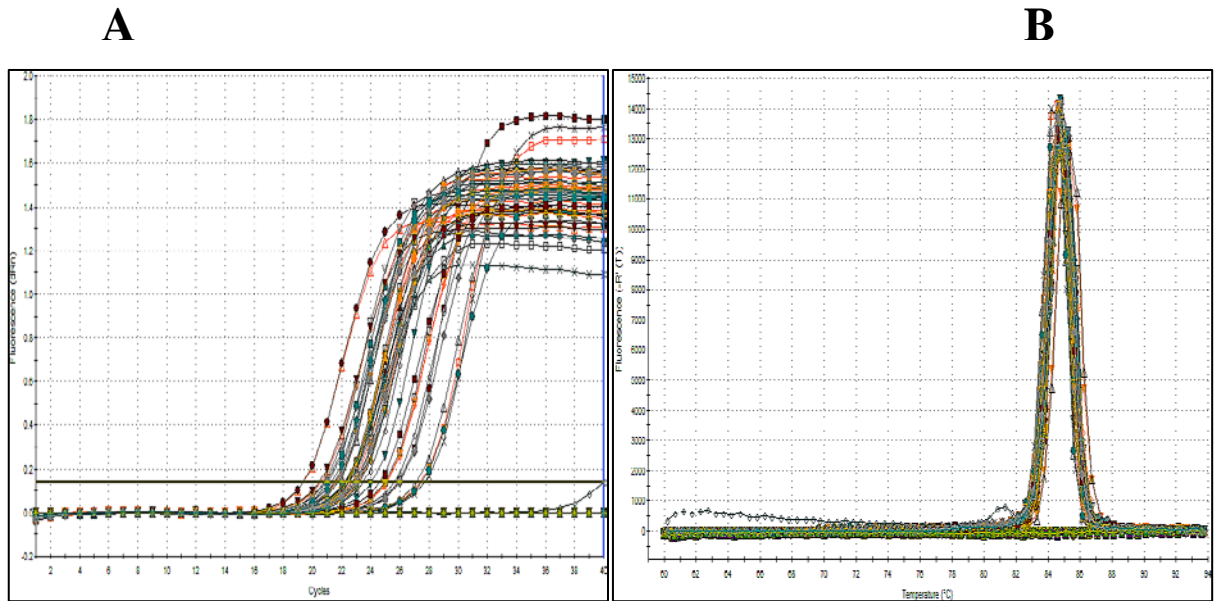


**Figure 8.33 Liver SYBR® Green Rt. PCR analysis of CPT1 $\alpha$  gene expression.**

CPT1 $\alpha$  gene expression was determined in treated and control mice liver cDNA samples. (A) Amplification curves displayed that the mean  $C_t$  value of CPT1 $\alpha$  gene was 23.461. (B) Dissociation curve showed one peak which dissociated approximately at 85°C suggestion excellent primer specificity, n=3.

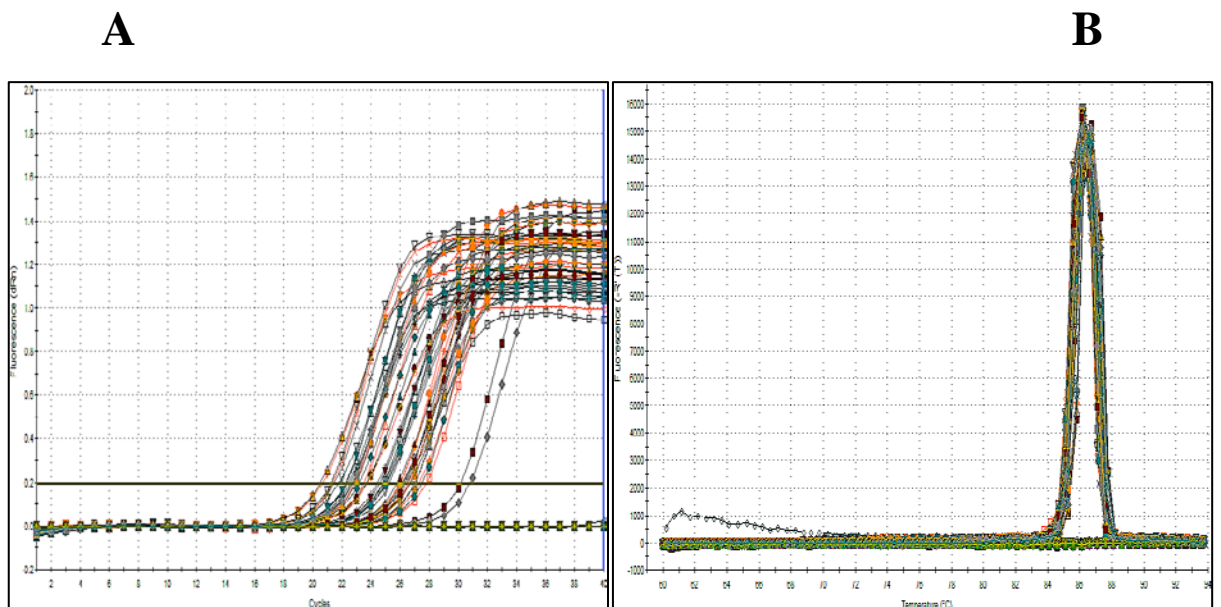


**Figure 8.34 Liver SYBR® Green Rt. PCR analysis of FASN gene expression.**

FASN gene expression was determined in treated and control mice liver cDNA samples. (A) Amplification curves displayed that the mean  $C_t$  value of FASN gene was 25.231. (B) Dissociation curve showed one peak which dissociated approximately at 87°C suggestion excellent primer specificity, n=3.

## 8.2.2 Amplification and dissociation curves of glucose metabolism gene expression in mice skeletal muscle

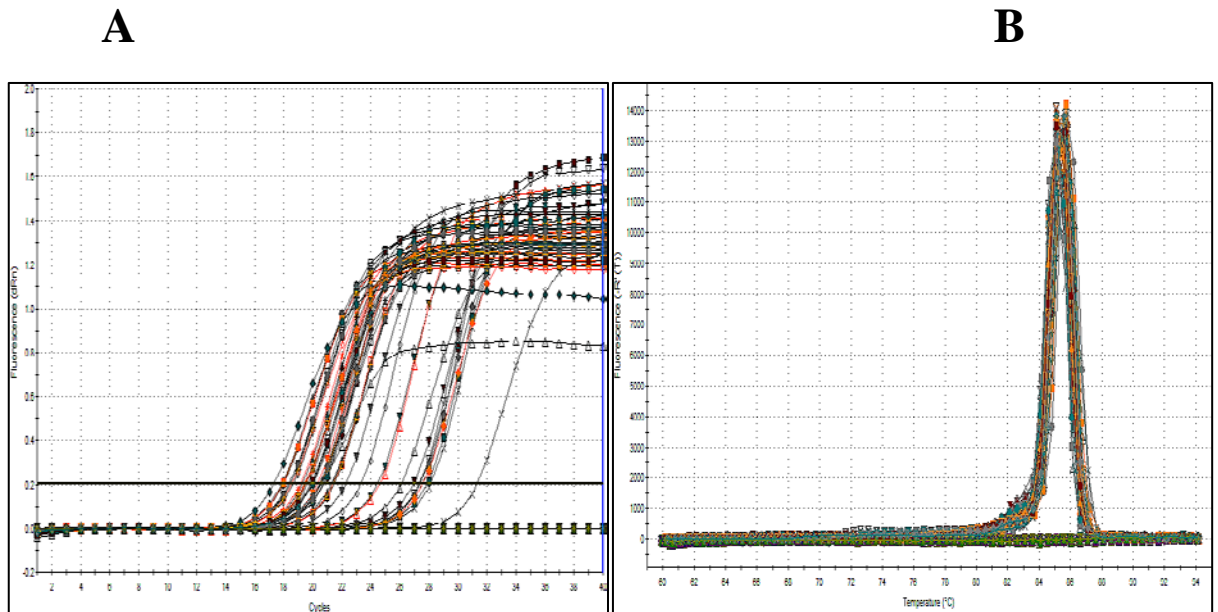


**Figure 8.35** Skeletal muscle SYBR® Green Rt. PCR analysis of actin gene expression.

Actin gene expression was determined in treated and control mice skeletal muscle cDNA samples. (A) Amplification curves displayed the mean  $C_t$  value of actin was 21.786. (B) Dissociation curve showed one peak which dissociated approximately at 85°C suggestion excellent primer specificity,  $n=3$ .

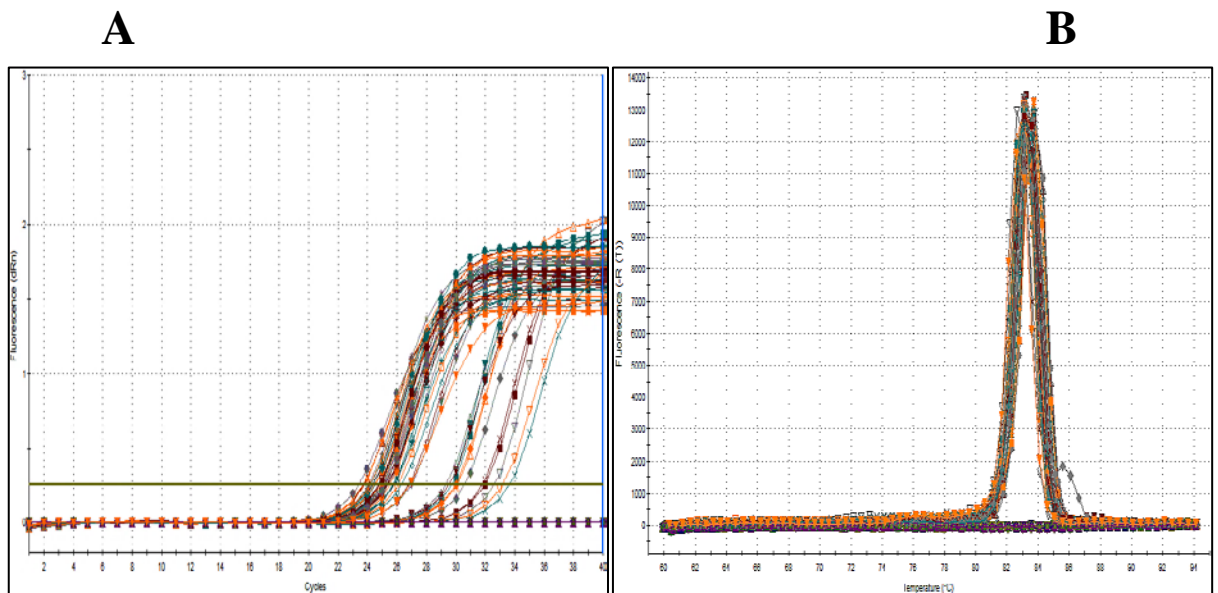


**Figure 8.36** Skeletal muscle SYBR® Green Rt. PCR analysis of IR gene expression.

Insulin receptor gene expression was determined in treated and control mice skeletal muscle cDNA samples. (A) Amplification curves displayed that the mean  $C_t$  value of IR gene was 26.202. (B) Dissociation curve showed one peak which dissociated approximately at 83°C suggestion excellent primer specificity,  $n=3$ .

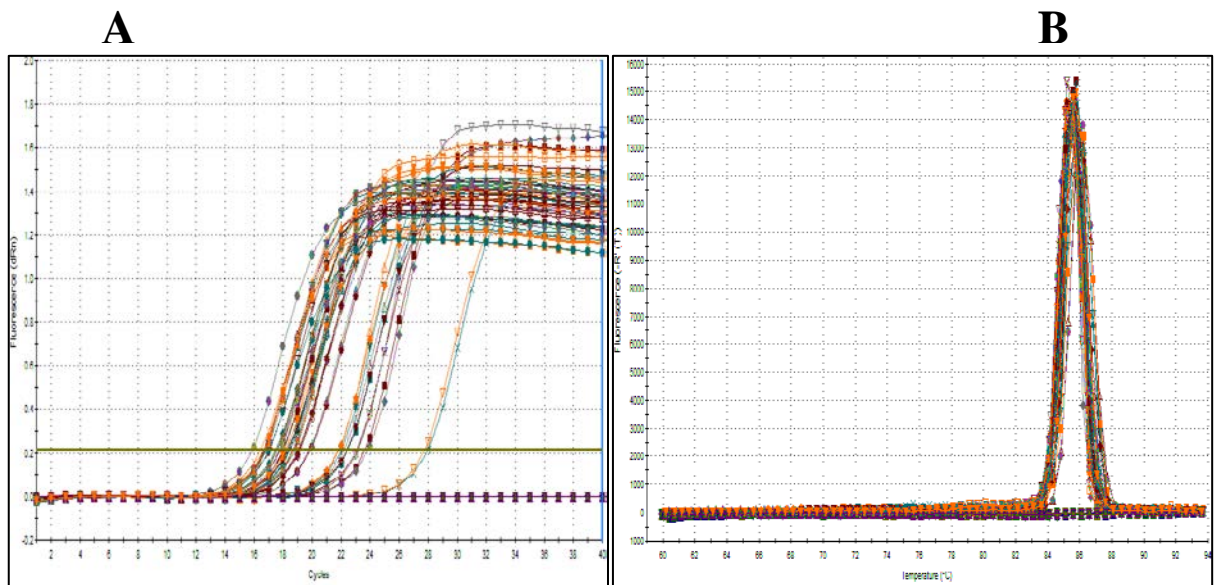


**Figure 8.37** Skeletal muscle SYBR® Green Rt. PCR analysis of Glut4 gene expression.

Glut4 gene expression was determined in treated and control mice skeletal muscle cDNA samples. (A) Amplification curves displayed that the mean  $C_t$  value of Glut4 gene was 19.272. (B) Dissociation curve showed one peak which dissociated approximately at 86°C suggestion excellent primer specificity, n=3.

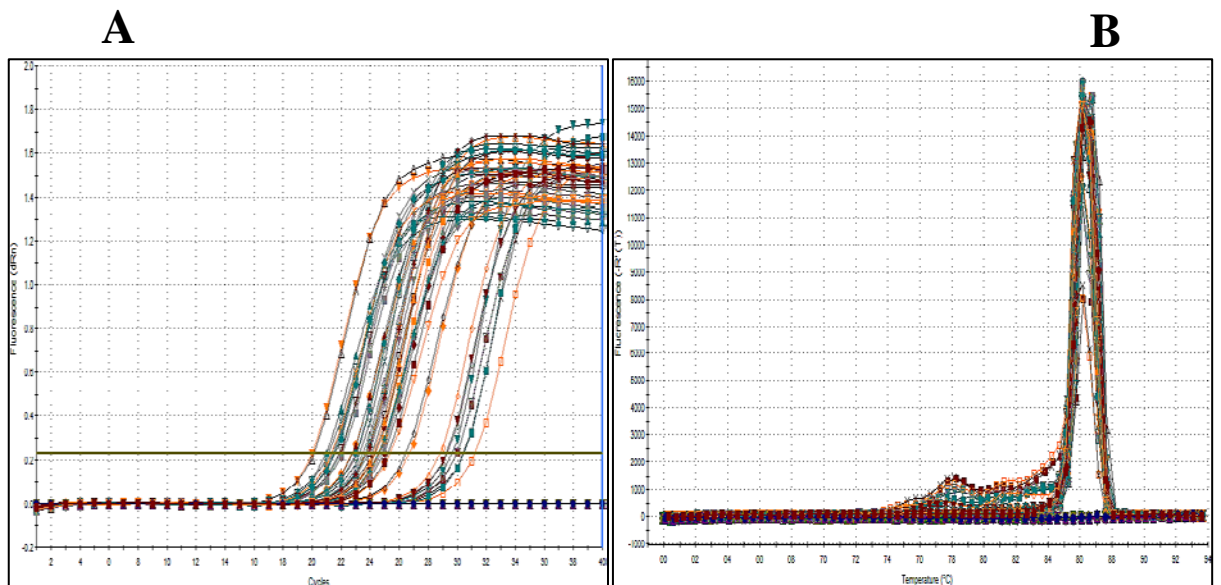


**Figure 8.38** Skeletal muscle SYBR® Green Rt. PCR analysis of Gys1 gene expression.

Gys1 gene expression was determined in treated and control mice skeletal muscle cDNA samples. (A) Amplification curves displayed that the mean  $C_t$  value of Gys1 gene was 24.793. (B) Dissociation curve showed one peak which dissociated approximately at 86.5°C suggestion excellent primer specificity, n=3.

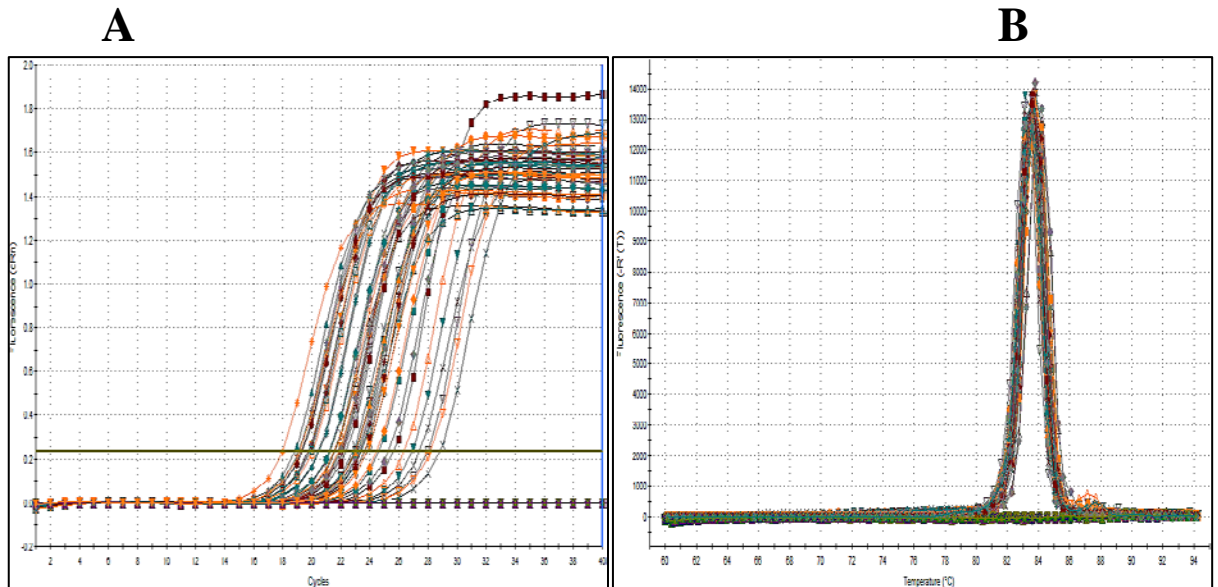


**Figure 8.39** Skeletal muscle SYBR® Green Rt. PCR analysis of PDK4 gene expression.

PDK4 gene expression was determined in treated and control mice skeletal muscle cDNA samples. (A) Amplification curves displayed that the mean  $C_t$  value of PDK4 gene was 22.346. (B) Dissociation curve showed one peak which dissociated approximately at 83.5°C suggestion excellent primer specificity,  $n=3$ .

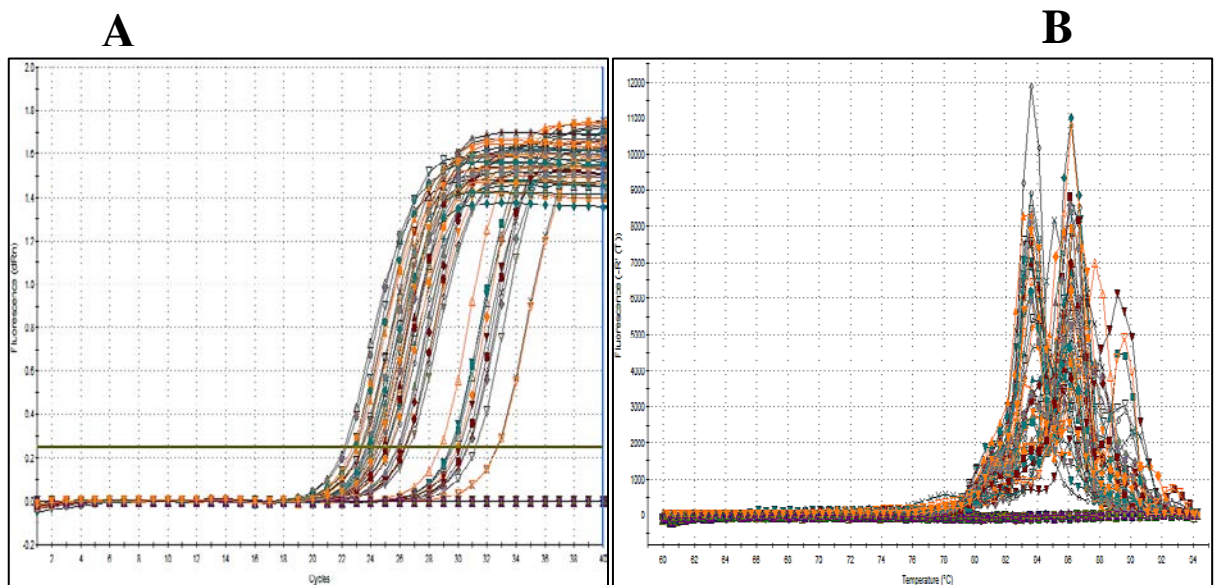


**Figure 8.40** Skeletal muscle SYBR® Green Rt. PCR analysis of PGC1 $\alpha$  gene expression.

PGC1 $\alpha$  gene expression was determined in treated and control mice liver cDNA samples. (A) Amplification curves displayed that the mean  $C_t$  value of PGC1 $\alpha$  gene was 25.771. (B) Dissociation curve showed more than one peak which dissociated approximately at different temperatures which suggestion nonspecific primer binding,  $n=3$ .

### 8.2.3 Amplification and dissociation curves of glucose and lipid metabolism gene expression in mice adipose tissue

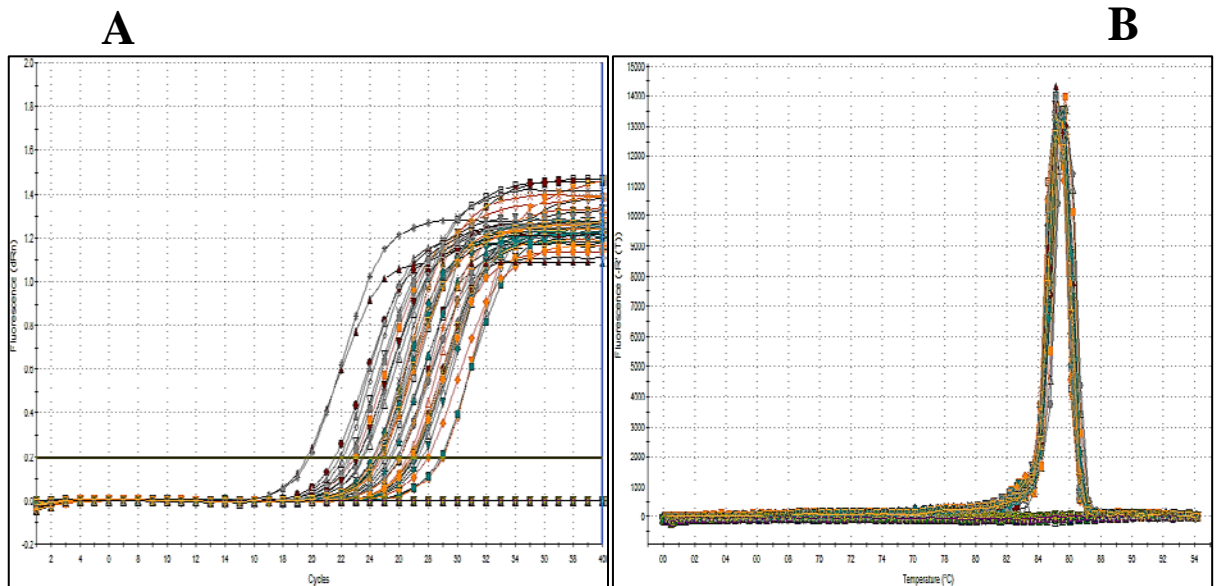


**Figure 8.41 Adipose tissue SYBR® Green Rt. PCR analysis of Actin gene expression.**

Actin gene expression was determined in treated and control mice adipose tissue cDNA samples. (A) Amplification curves displayed the mean  $C_t$  value of actin was 25.611. (B) Dissociation curve showed one peak which dissociated approximately at 85°C suggestion excellent primer specificity,  $n=3$ .

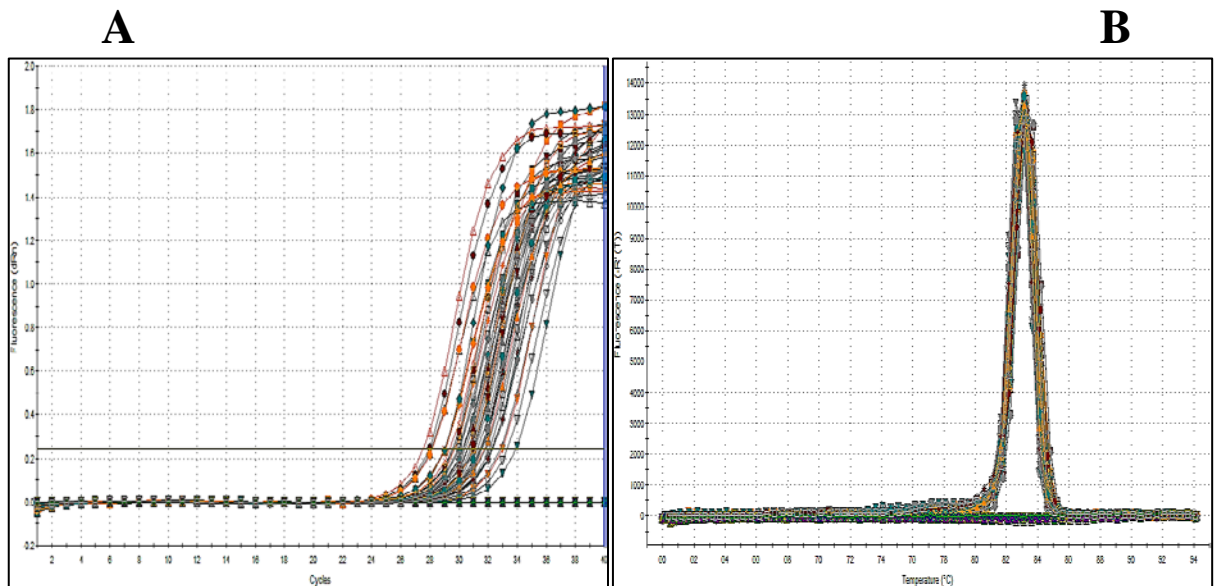


**Figure 8.42 Adipose tissue SYBR® Green Rt. PCR analysis of IR gene expression.**

IR gene expression was determined in treated and control mice adipose tissue cDNA samples. (A) Amplification curves displayed that the mean  $C_t$  value of IR gene was 30.739. (B) Dissociation curve showed one peak which dissociated approximately at 83°C suggestion excellent primer specificity,  $n=3$ .

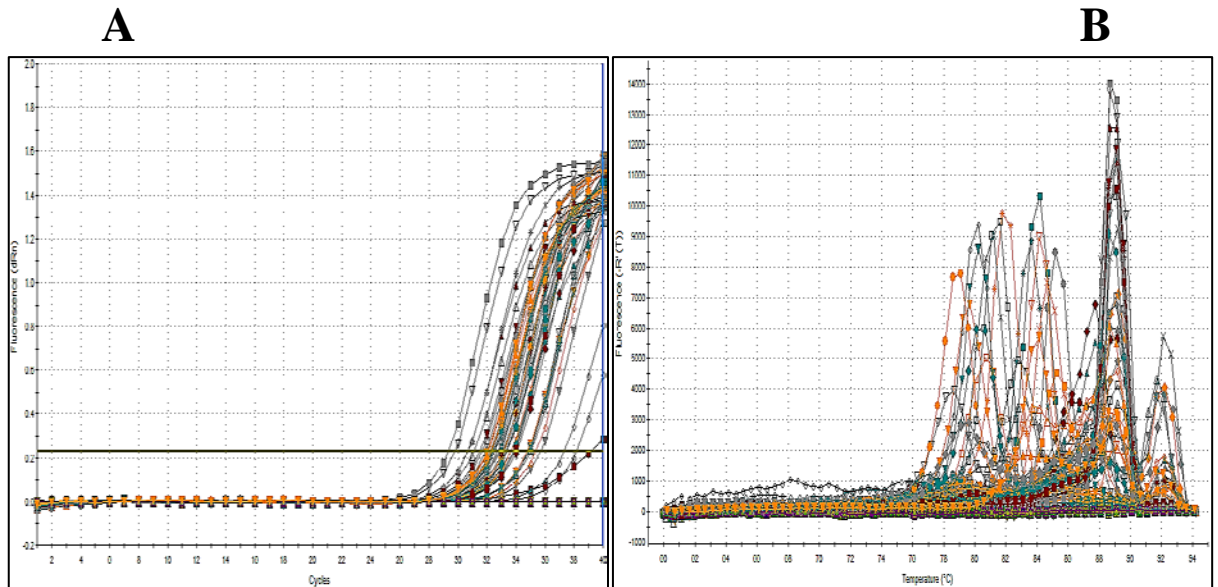


**Figure 8.43 Adipose tissue SYBR® Green Rt. PCR analysis of SREBP1c gene expression.**

SREBP1c gene expression was determined in treated and control mice adipose tissue cDNA samples. (A) Amplification curves displayed that the mean  $C_t$  value of SREBP1c gene was 33.002. (B) Dissociation curve showed more than one peak which dissociated approximately at different temperatures which suggestion nonspecific primer binding,  $n=3$ .

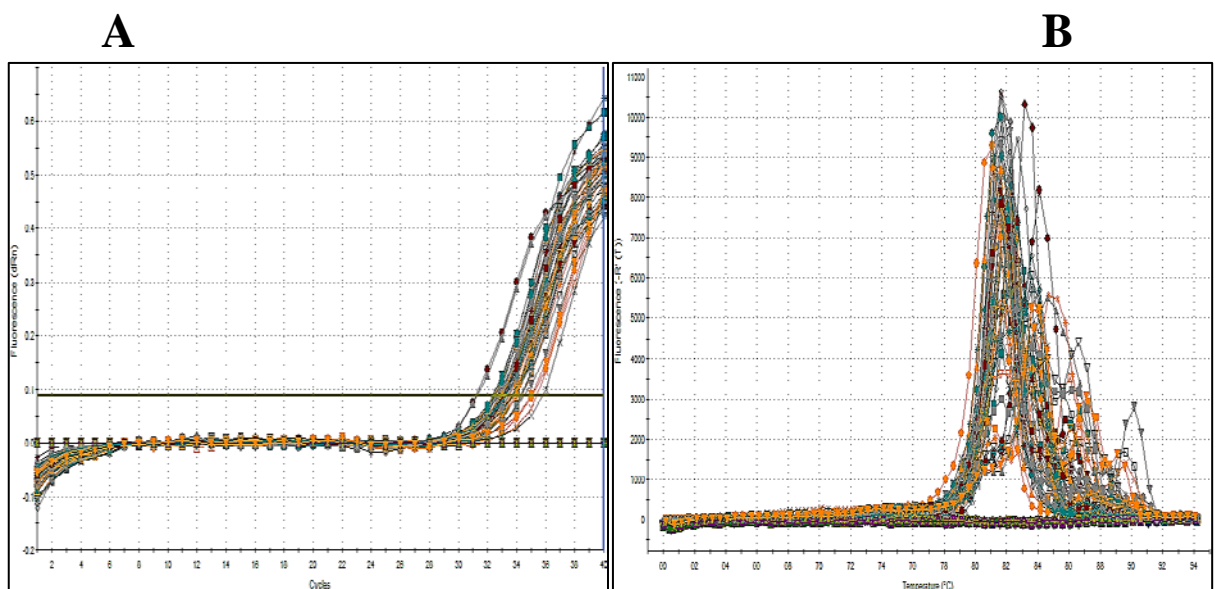


**Figure 8.44 Adipose tissue SYBR® Green Rt. PCR analysis of PPAR $\gamma$  gene expression.**

PPAR $\gamma$  gene expression was determined in treated and control mice adipose tissue cDNA samples. (A) Amplification curves displayed that the mean  $C_t$  value of PPAR $\gamma$  gene was 35.041. (B) Dissociation curve showed more than one peak which dissociated approximately at different temperatures which suggestion nonspecific primer binding,  $n=3$ .

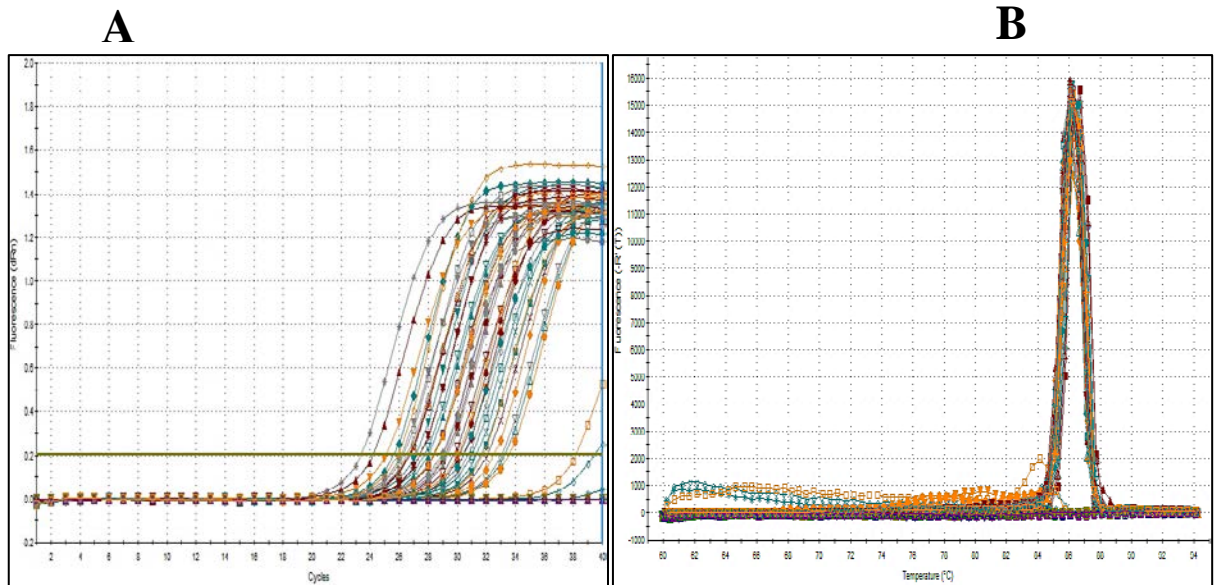


**Figure 8.45 Adipose tissue SYBR® Green Rt. PCR analysis of FASN gene expression.**

FASN gene expression was determined in treated and control mice adipose tissue cDNA samples. (A) Amplification curves displayed that the mean  $C_t$  value of FASN gene was 29.682. (B) Dissociation curve showed one peak which dissociated approximately at 86.5°C suggestion excellent primer specificity, n=3.

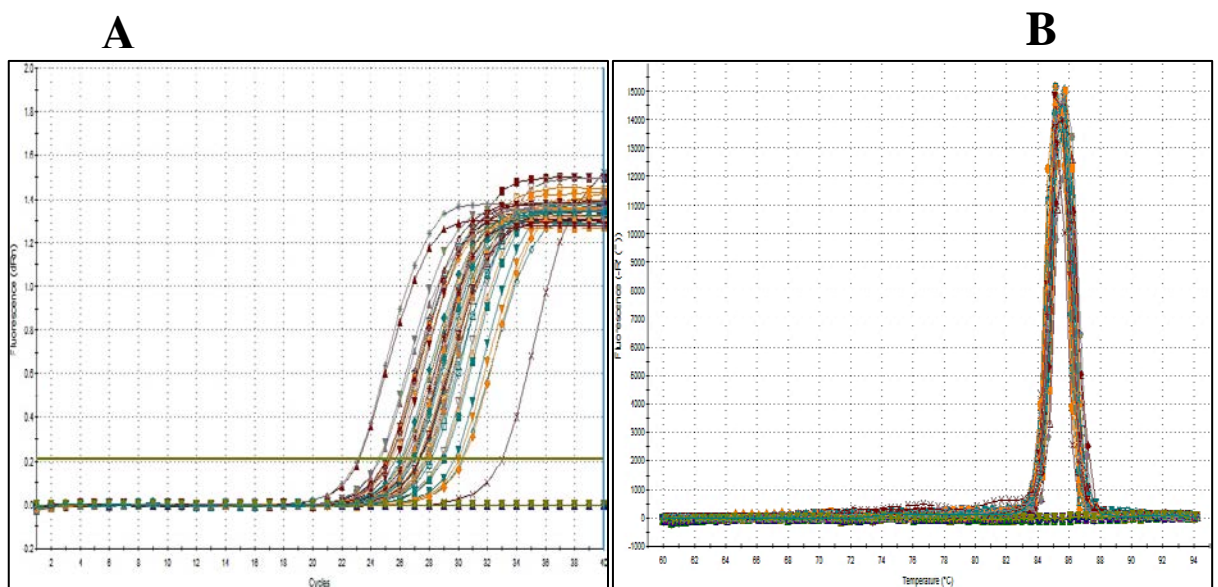


**Figure 8.46 Adipose tissue SYBR® Green Rt. PCR analysis of Glut4 gene expression.**

Glut4 gene expression was determined in treated and control mice adipose tissue cDNA samples. (A) Amplification curves displayed that the mean  $C_t$  value of Glut4 gene was 27.558. (B) Dissociation curve showed one peak which dissociated approximately at 85°C suggestion excellent primer specificity, n=3.

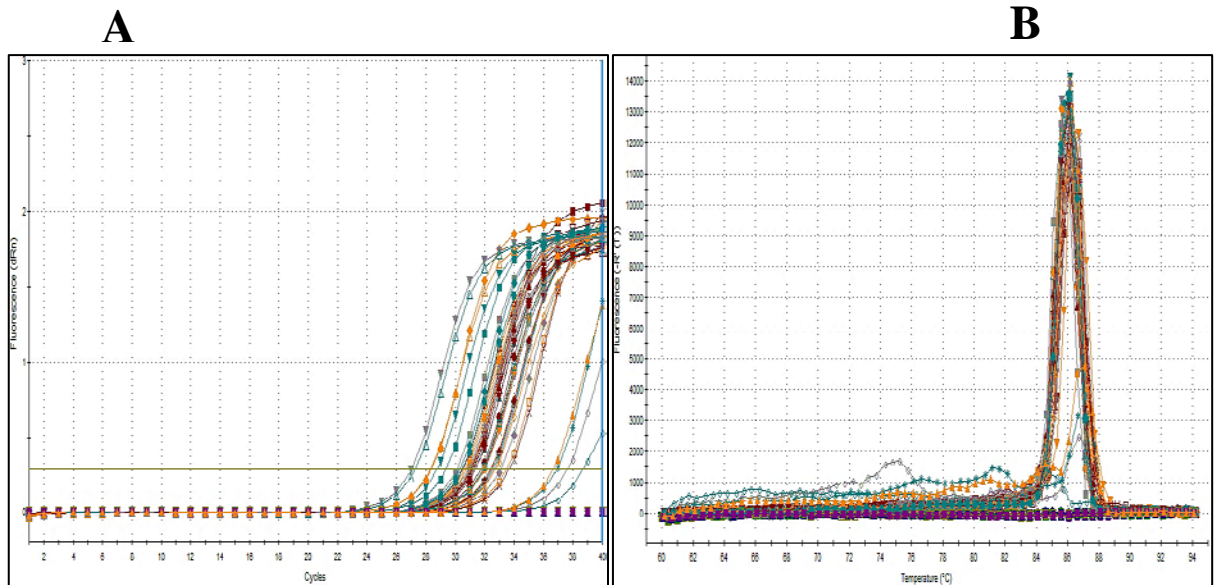


**Figure 8.47 Adipose tissue SYBR® Green Rt. PCR analysis of C/EBP $\alpha$  gene expression.**

C/EBP $\alpha$  gene expression was determined in treated and control mice adipose tissue cDNA samples. (A) Amplification curves displayed that the mean  $C_t$  value of C/EBP $\alpha$  gene was 31.689. (B) Dissociation curve showed one peak which dissociated approximately at 86°C suggestion good primer specificity, n=3.

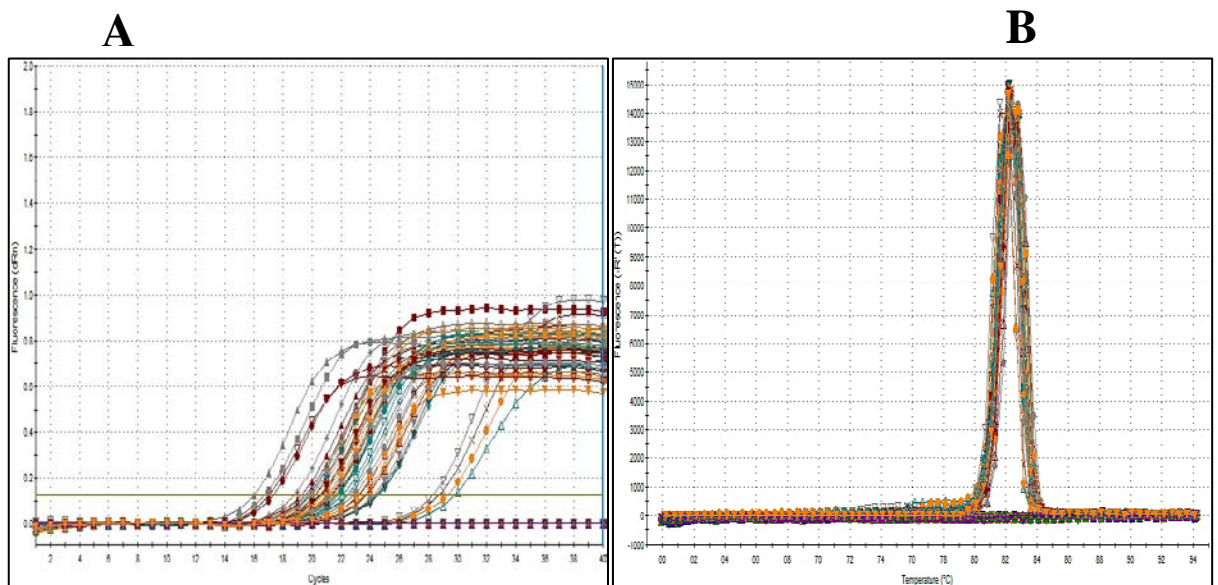


**Figure 8.48 Adipose tissue SYBR® Green Rt. PCR analysis of FABP4 gene expression.**

FABP4 gene expression was determined in treated and control mice adipose tissue cDNA samples. (A) Amplification curves displayed that the mean  $C_t$  value of FABP4 gene was 22.292. (B) Dissociation curve showed one peak which dissociated approximately at 82.5°C suggestion excellent primer specificity, n=3.

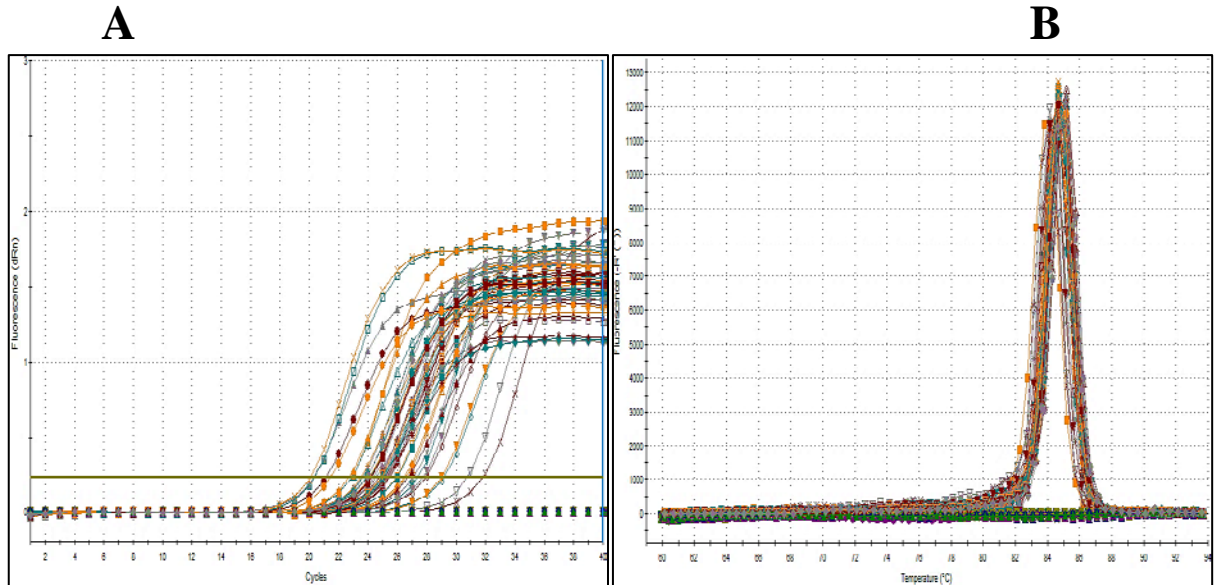


**Figure 8.49 Adipose tissue SYBR® Green Rt. PCR analysis of LPL gene expression.**

LPL gene expression was determined in treated and control mice adipose tissue cDNA samples. (A) Amplification curves displayed that the mean  $C_t$  value of LPL gene was 25.575. (B) Dissociation curve showed one peak which dissociated approximately at 84.5°C suggestion excellent primer specificity,  $n=3$ .

### 8.3 Appendix 3; Amplification and disassociation curves of pro and anti-apoptotic gene expression in BC cells

#### 8.3.1 Amplification and disassociation curves of pro and anti-apoptotic gene expression in MCF7 cell

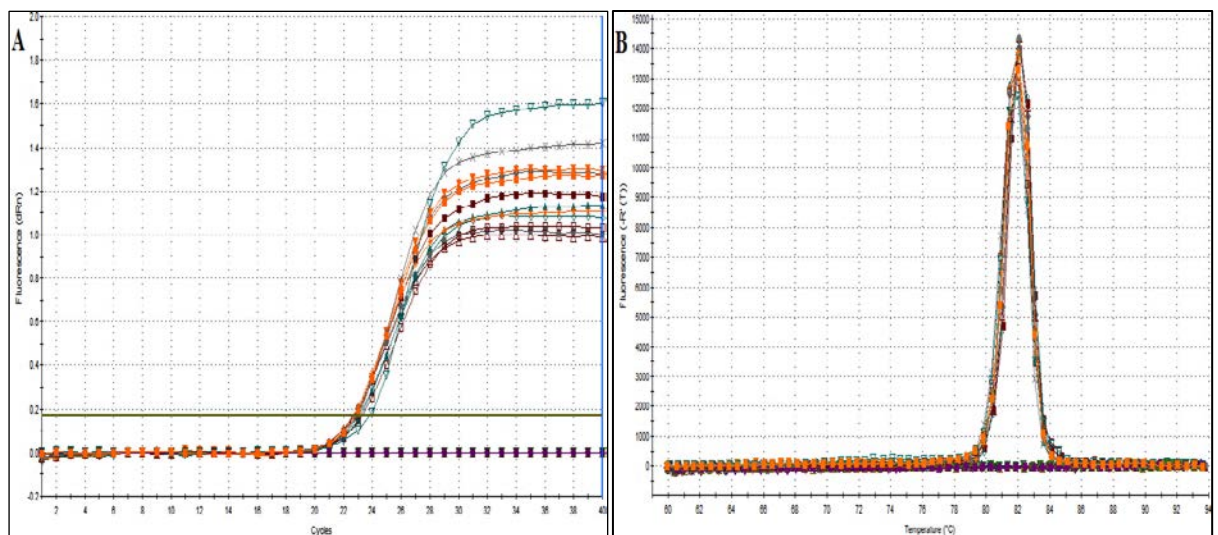


**Figure 8.50 MCF7 SYBR® Green Rt. PCR analysis of hYWHAZ gene expression.**

Housekeeping hYWHAZ gene expression was determined in treated MCF7 cell cDNA samples. (A) Amplification curves displayed the mean  $C_t$  value of actin was 23.44625. (B) Dissociation curve showed one peak which dissociated approximately at 82°C suggestion excellent primer specificity,  $n=3$ .

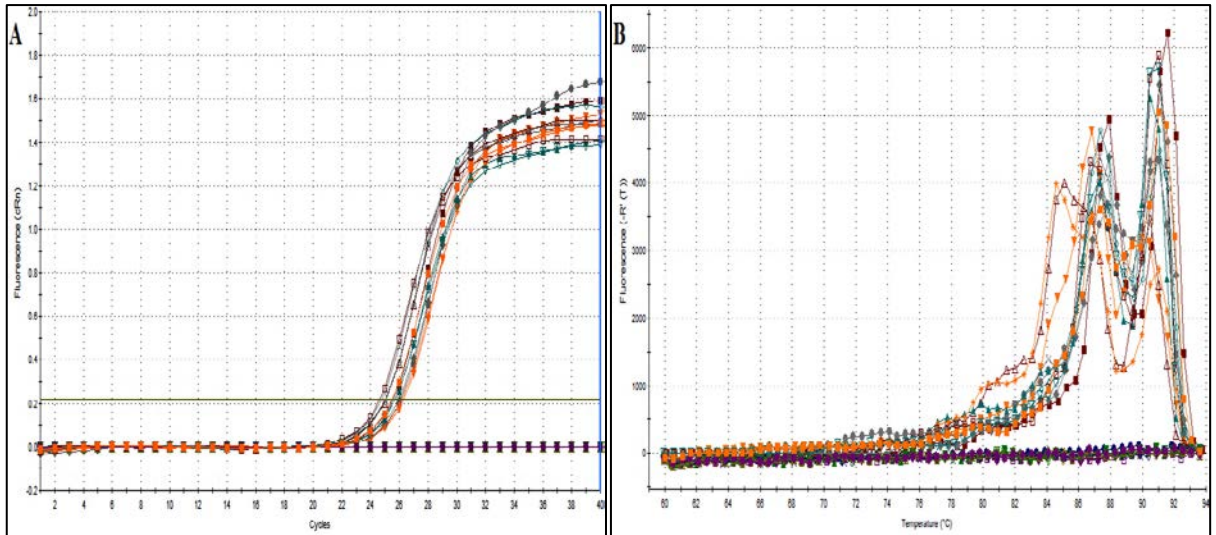


**Figure 8.51 MCF7 SYBR® Green Rt. PCR analysis of Bcl2 gene expression.**

Bcl2 gene expression was determined in treated MCF7 cell cDNA samples. (A) Amplification curves displayed that the mean  $C_t$  value of Bcl2 gene was 25.637. (B) Dissociation curve showed many peaks which dissociated at temperatures suggestion nonspecific primer binding,  $n=3$ .

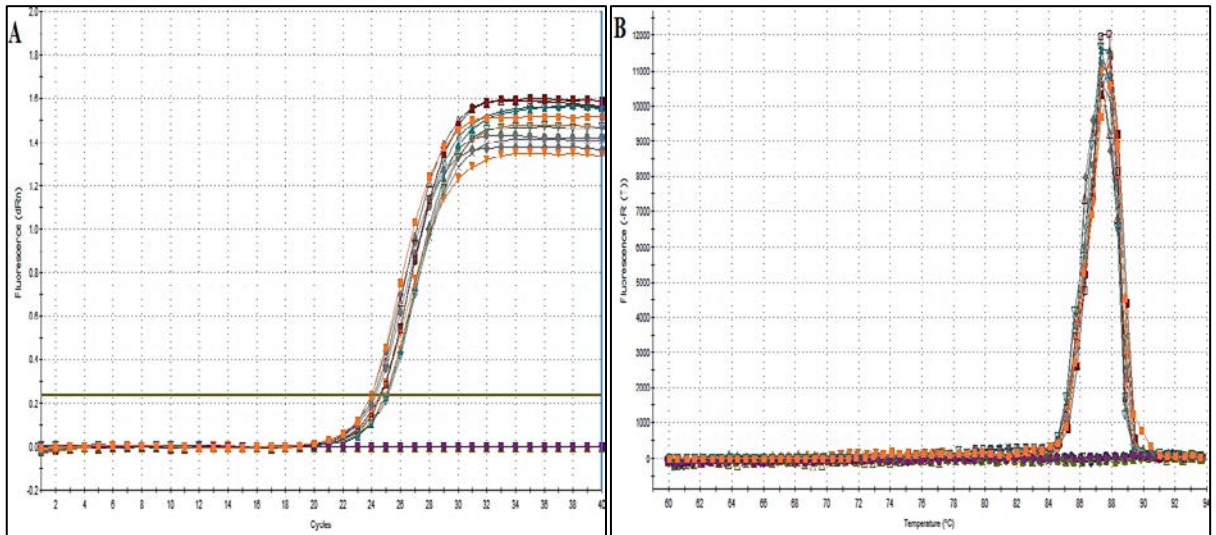


**Figure 8.52 MCF7 SYBR® Green Rt. PCR analysis of Bax gene expression.**

Bax gene expression was determined in treated MCF7 cell cDNA samples. (A) Amplification curves displayed that the mean  $C_t$  value of Bax gene was 24.501. (B) Dissociation curve showed one peak which dissociated approximately at 87°C suggestion excellent primer specificity,  $n=3$ .

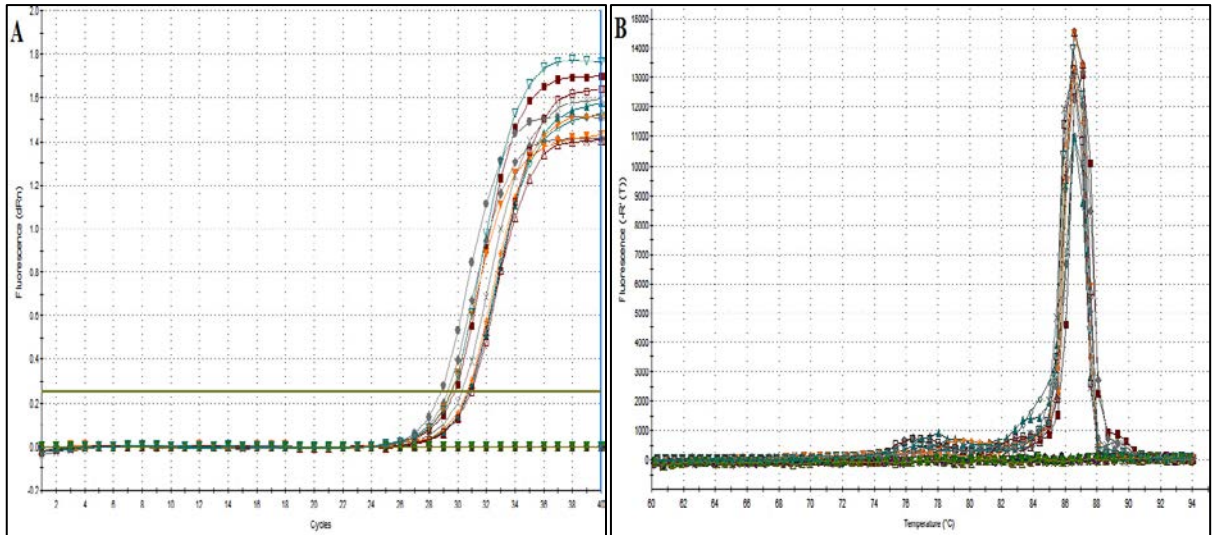


**Figure 8.53 MCF7 SYBR® Green Rt. PCR analysis of Myc gene expression.**

Myc gene expression was determined in treated MCF7 cell cDNA samples. (A) Amplification curves displayed that the mean  $C_t$  value of Myc gene was 29.895. (B) Dissociation curve showed one peak which dissociated approximately at 89°C suggestion excellent primer specificity, n=3.

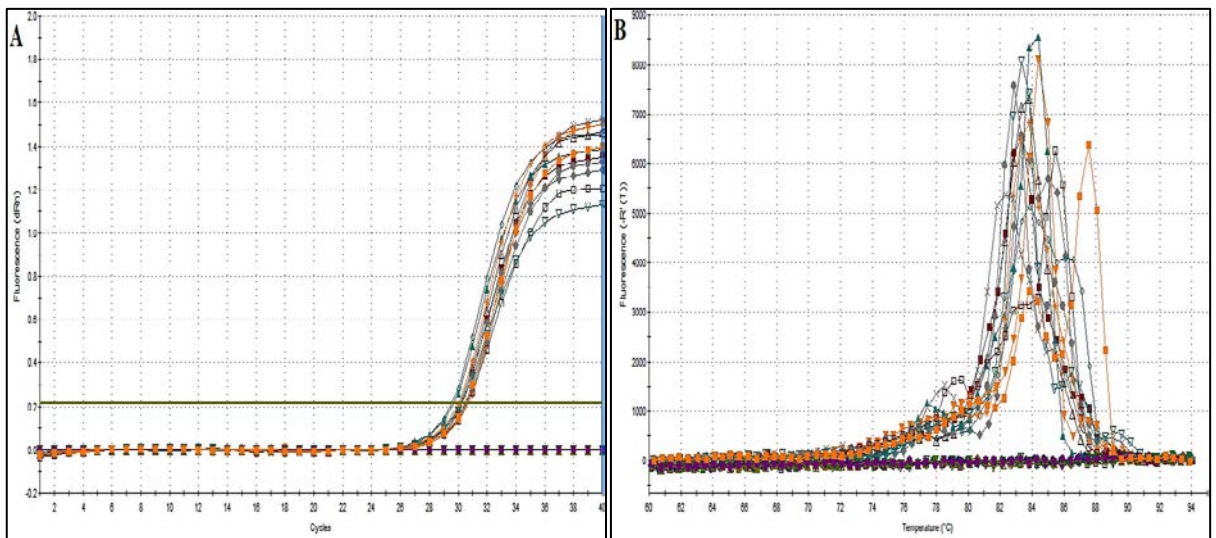


**Figure 8.54 MCF7 SYBR® Green Rt. PCR analysis of P53 gene expression.**

P53 gene expression was determined in treated MCF7 cell cDNA samples. (A) Amplification curves displayed that the mean  $C_t$  value of P53 gene was 30.343. (B) Dissociation curve showed many peaks which dissociated at temperatures suggestion nonspecific primer binding, n=3.

### 8.3.2 Amplification and disassociation curves of pro and anti-apoptotic gene expression in MDA-MB-231 cell

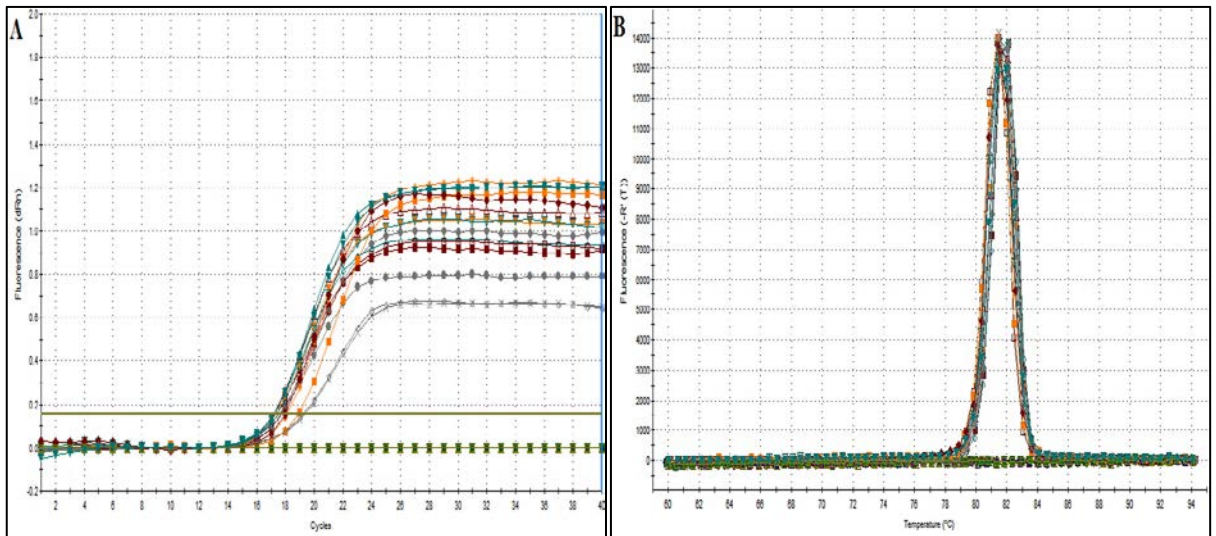


**Figure 8.55** MDA-MB-231 SYBR<sup>®</sup> Green Rt. PCR analysis of hYWHAZ gene expression.

Housekeeping hYWHAZ gene expression was determined in treated MDA-MB-231 cell cDNA samples. (A) Amplification curves displayed the mean  $C_t$  value of actin was 18.404. (B) Dissociation curve showed one peak which dissociated approximately at 81.5°C suggestion excellent primer specificity, n=3.

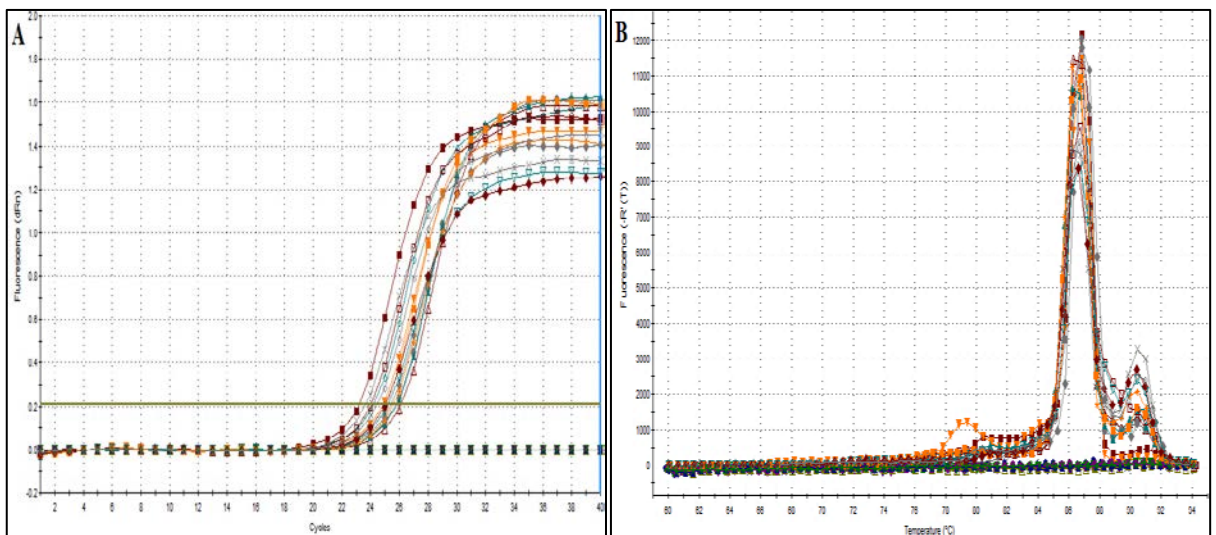


**Figure 8.56** MDA-MB-231 SYBR<sup>®</sup> Green Rt. PCR analysis of Bcl2 gene expression.

Bcl2 gene expression was determined in treated MDA-MB-231 cell cDNA samples. (A) Amplification curves displayed that the mean  $C_t$  value of Bcl2 gene was 24.997. (B) Dissociation curve showed one peak which dissociated approximately at 87°C suggestion adequate primer specificity, n=3.

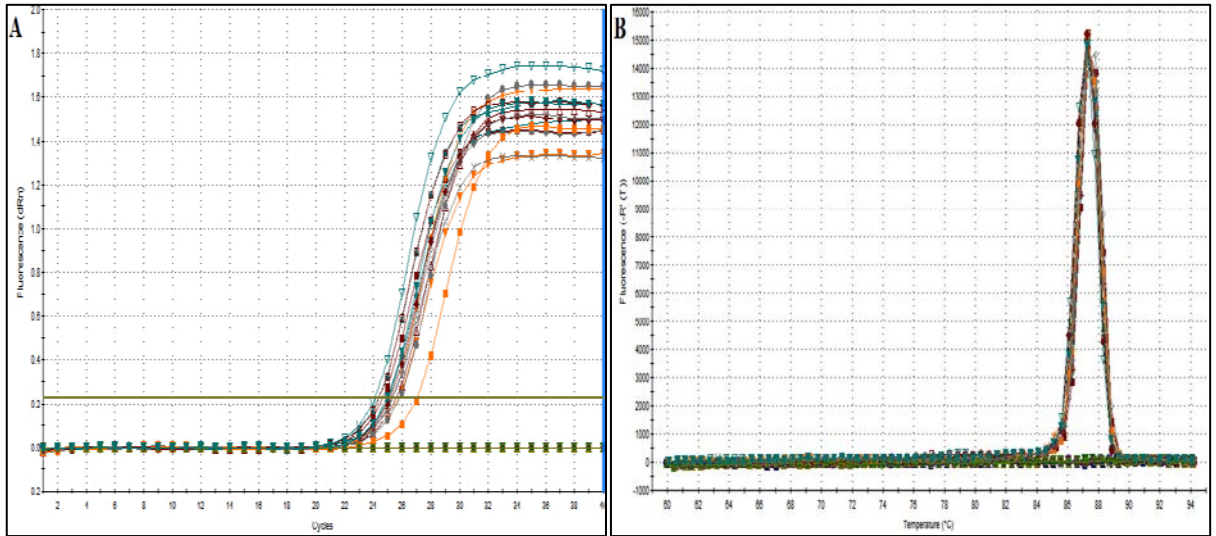


**Figure 8.57 MDA-MB-231 SYBR® Green Rt. PCR analysis of Bax gene expression.**

Bax gene expression was determined in treated MDA-MB-231 cell cDNA samples. (A) Amplification curves displayed that the mean  $C_t$  value of Bax gene was 25.121. (B) Dissociation curve showed one peak which dissociated approximately at 87°C suggestion excellent primer specificity, n=3.

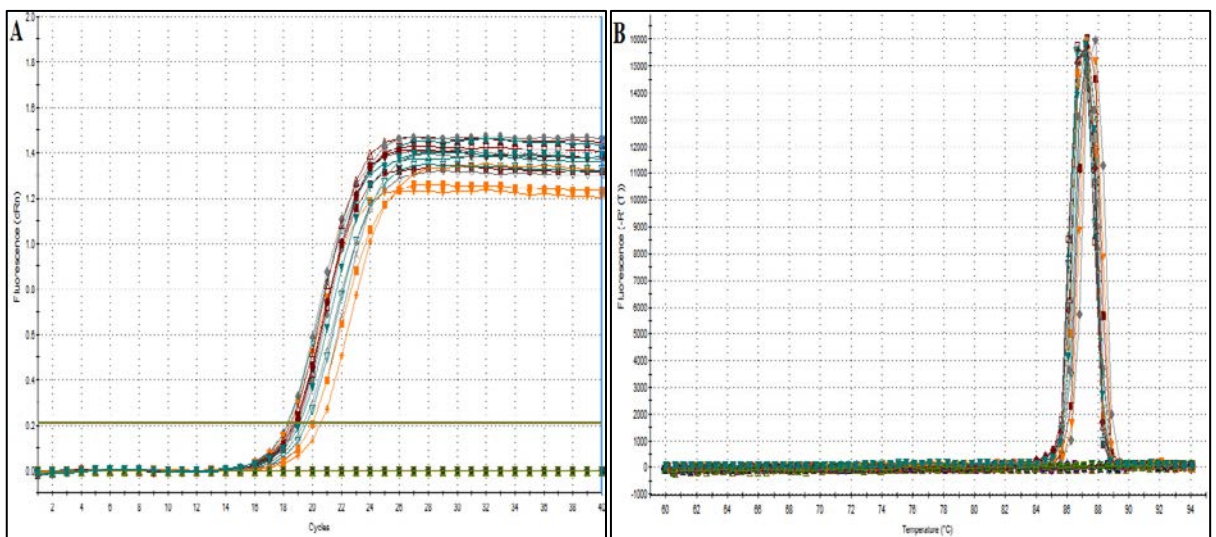


**Figure 8.58 MDA-MB-231 SYBR® Green Rt. PCR analysis of Myc gene expression.**

Myc gene expression was determined in treated MDA-MB-231 cell cDNA samples. (A) Amplification curves displayed that the mean  $C_t$  value of Myc gene was 18.875. (B) Dissociation curve showed one peak which dissociated approximately at 85°C suggestion excellent primer specificity, n=3.

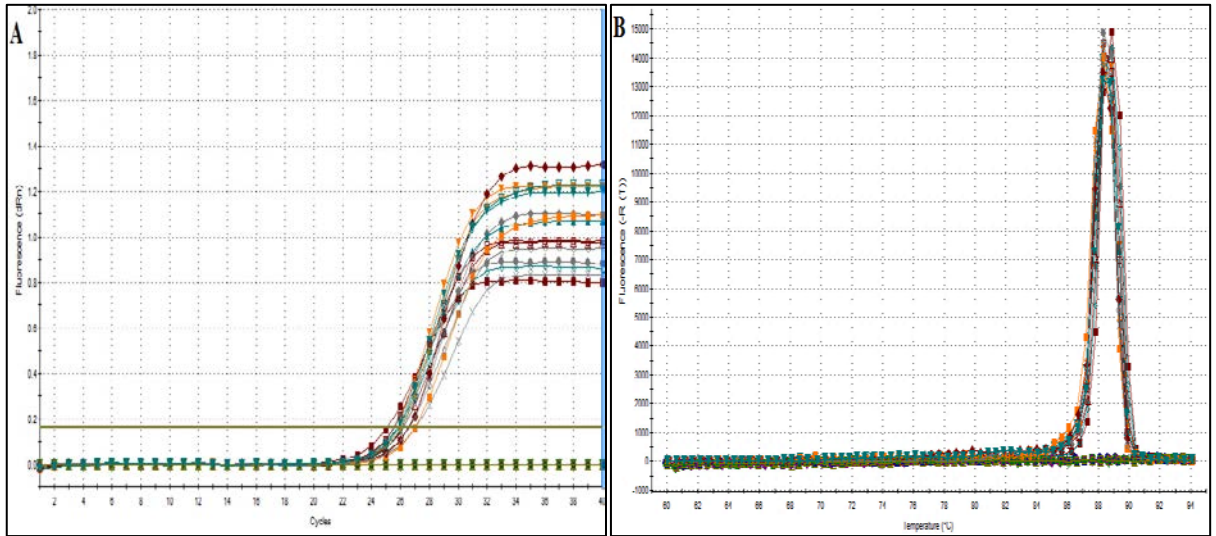


**Figure 8.59 MDA-MB-231 SYBR® Green Rt. PCR analysis of P53 gene expression.**

P53 gene expression was determined in treated MDA-MB-231 cell cDNA samples. (A) Amplification curves displayed that the mean  $C_t$  value of P53 gene was 26.254. (B) Dissociation curve showed one peak which dissociated approximately at 89°C suggestion excellent primer specificity, n=3.